

I. Stereoselective Synthesis of 1,3-Diamino-2-ols *via* Allene Oxidation.
II. Tunable, Chemoselective Silver(I)-Catalyzed Nitrene Transfer Reactions: Development and Mechanistic Study.

By Cale Daniel Weatherly

A dissertation submitted in partial fulfillment
of the requirements for the degree of

Doctor of Philosophy
(Chemistry)

at the
University of Wisconsin-Madison
2015

Date of final oral examination: 05/18/15

The dissertation is approved by the following members of the Final Oral Committee:

Jennifer M. Schomaker, Associate Professor, Chemistry

Steven D. Burke, Professor, Chemistry

Ive Hermans, Associate Professor, Chemistry

Shannon S. Stahl, Professor, Chemistry

Tehshik P. Yoon, Professor, Chemistry

I. Stereoselective Synthesis of 1,3-Diamino-2-ols *via* Allene Oxidation.**II. Tunable, Chemoselective Silver(I)-Catalyzed Nitrene Transfer Reactions: Development and Mechanistic Study.**

By Cale Daniel Weatherly

Under the supervision of Professor Jennifer M. Schomaker
at the University of Wisconsin-Madison

Abstract

Stereodefined carbon-nitrogen bonds are ubiquitous in pharmaceuticals and biologically active natural products, but their construction is often a difficult task, especially when these bonds are part of complex stereochemical arrays. The work described in this thesis addresses two aspects of chemo- and stereoselective carbon-nitrogen bond formation. Chapters 1 and 2 describe two methods for the transformation of homoallylic carbamates to 1,3-diamino-2-ols, motifs found in a number of important biologically active compounds. Each method utilizes catalytic nitrene transfer to access a bicyclic methylene aziridine, which possesses a carbon-carbon double bond capable of further functionalization. Chapter 3 addresses the nitrene transfer reaction directly, describing the development of a chemoselective silver(I)-catalyzed method for aziridination, first applied to the synthesis of bicyclic methylene aziridines. Further investigations demonstrated that simple changes in ligand:metal ratio altered the chemoselectivity of the transformation in favor of allenic C-H amination. These conditions were applied to the aziridination and C-H amination of homoallylic carbamates with equal efficacy. Chapter 4 presents a selective review of mechanistic literature on metal-catalyzed nitrene transfer reactions, emphasizing common

experimental probes of these reactions and their interpretation. Chapter 5 describes mechanistic study of our own silver(I)-catalyzed nitrene transfer reaction, including spectroscopic analysis, mechanistic probe experiments, and kinetic profiling. The experiments suggest that two distinct catalytic species are responsible for the aziridination and C-H amination reactions, and that chemoselectivity is governed primarily by the different steric environments provided by the two catalysts. Finally, Chapter 6 describes effort to render the intramolecular silver(I)-catalyzed aziridination of alkenes enantioselective. The use of accessible bisoxazoline ligands provides high yields and $ee > 80\%$ for both *cis*- and *trans*-substituted alkenes. Simple modifications to current ligands are suggested for further improvements to the system. These improvements could render the system among the most accessible and selective methods of asymmetric intramolecular aziridination.

Acknowledgements

The stereotype of the solitary scientist is as false as it is persistent. The work described in this thesis has been a collective effort, and the other members of the Schomaker group deserve my foremost thanks. In particular; Dr. Jared Rigoli for his vision in carrying out several of the projects described herein; Dr. R. David Grigg for endless scientific bull sessions in the lab and over beer (never at the same time!); Prof. John Hershberger and Dr. Daniel Wherritt (Reich group, honorary Schomaker group member) for lending experience and wisdom to the group in its early days; Julie Alderson and Minsoo Ju for their contributions to this research and continued efforts to complete these projects; and Michael Freidberg, my undergraduate mentee, for his efforts in research. Seeing Michael progress as a scientist has been one of my greatest pleasures in graduate school, and I wish him the best in his own graduate studies.

Other members of the department also deserve my thanks: Profs. Steven Burke, Ivo Hermans, Shannon Stahl and Tehshik Yoon, not only for serving on my thesis committee, but for their roles in fostering intellectual community in the department, and their helpful comments on research throughout my time at UW-Madison. I thank Prof. John Berry for his work on computational modeling of the silver chemistry, and Prof. Jason Hein (UC-Merced) for his guidance in performing kinetic studies of the same. I am indebted to the department's instrumentation staff, especially Drs. Charlie Fry, Martha Vestling, and Ilia Guzei, for their assistance with difficult experiments and continuous upkeep of the instrumentation facilities. I am also grateful that I was able to TA under Ieva Reich during her final year as an instructor. TAing for her was as important for my intellectual growth as many of the official program requirements, and she is the most effective teacher I have encountered in any setting.

Of course, my interest in science began many years before I considered graduate school. Some of the teachers who are responsible: Mrs. Stewart, Mrs. Richardson, Mr. Lazar, Mr. Lerch, Mr. Grunder, Mr. Martin, Mrs. Cantey, Mr. Chughtai. Few were science teachers, but they were all academic hedonists, and their pleasure in learning is mine by osmosis. Prof. Thomas Smith, my undergraduate advisor, gave me my first research experience in synthetic organic chemistry, and will always have my thanks. Only now do I realize the magnitude of ambition required to attempt natural product syntheses with undergraduates. Profs. David Richardson and Christopher Goh also made significant contributions to my interest in organic and organometallic chemistry.

I have been blessed with many friendships in graduate school, and three have been especially crucial, so I thank David Grigg (again), Ryan Van Hoveln, and Mary Van Vleet for their camaraderie. I also thank the members of Geneva Campus Church and the UW-Madison graduate chapter of Intervarsity Christian Fellowship for the communities they provide. For their unending love and support, I thank my parents, Jon and Tammie, my sister Allison, and my spouse-to-be, Laurie Wood. They are worth more than is printable in an academic document.

Finally, I thank my advisor, Prof. Jennifer Schomaker. When I had first arrived at UW and was deciding which group to join, Jen's excitement, creativity, and relentlessness won me over. She promised that working in her group would be difficult, which it was, and that the difficulty would be worthwhile, and I believe it has been. Jen is particularly good at adapting her advising style to individual students and to different periods of their time in her lab. She has always placed expectations ever-so-slightly higher than my capability, which is the only way to inspire improvement. I am deeply grateful that she has allowed me to work on the research projects that seemed most interesting to me, and has supported my personal and professional

decisions. Even as I leave her group, I look forward to future friendship and advice from Jen, and to following the group's research for many years to come.

Table of Contents

Abstract.....	ii
Acknowledgements.....	iv
Chapter 1. Stereoselective Synthesis of 1,3-Diamino-2-ols via Rearrangement of 1,4-Diazaspiro[2.2]pentanes.....	2
1.1. Allenes as Templates for Stereotriad Construction	3
1.2. Prevalence of 1,3-diamino-2-ols in Biologically Active Products.	6
1.3. Synthesis of 1,3-Diaminated Compounds.....	7
1.4. Conversion of 1,4-Diazaspiro-[2.2]-pentanes to 1,3-diaminoketones.	8
1.5. Stereoselective Reduction of 1,3-diamino-2-ones to 1,3-diamino-2-ols.	13
1.6. Possible mechanism of rearrangement of DASPs.	15
1.7. Conclusions.....	16
1.8. Notes and References.....	17
1.9. Experimental Details and Characterization.	18
1.9.1. General Experimental Information.	18
1.9.2. Synthesis of 1,4-Diazaspiro[2.2]pentane Substrates.....	20
1.9.3. Synthesis of Ring-Opened DASPs.	22
1.9.4. Rearrangements of Ring-Opened DASPs to 1,3-Diaminated Ketones.....	23

1.9.5. Verification of the Transfer of Axial Chirality from the DASP 1.36 to the 1,3-Diaminated Compound 1.37.....	29
1.9.6. Reductions of 1,3-Diaminated Ketones.....	30
Chapter 2. Stereoselective Synthesis of 1,3-Diamino-2-ols <i>via</i> Aminohydroxylation of Bicyclic Methylene Aziridines.....	34
2.1. Basic synthetic strategy.....	35
2.2. Catalytic aminohydroxylation of olefins.	35
2.3. Optimization of aminohydroxylation of bicyclic methylene aziridines.	37
2.4. Optimization of aminohydroxylation of aryl-substituted methylene aziridines.	40
2.5. Scope of Aminohydroxylation/Reduction Sequence.....	41
2.6. Conclusions.....	45
2.7. References.....	45
2.8. Experimental Details and Characterization.	46
2.8.1. Preparation of Homoallenic Carbamates.	46
2.8.2. Synthesis of Bicyclic Methylene Aziridines.....	49
2.8.3. Synthesis of 1,3-Diaminated Ketones by Aminohydroxylation of Methylene Aziridines.	52
2.8.4. Synthesis of 1,3-Diamino-2-ols.	58
Chapter 3. Development of Dynamic, Chemoselective Silver(I)-Catalyzed Intramolecular Aminations of Allenes and Alkenes.	

3.1 Overview of Chemoselective, Ag(I)-Catalyzed Amination.....	65
3.2. Development of silver-catalyzed aziridination of homoallylic carbamates.....	66
3.3. Scope of Ag(I)-catalyzed aziridination.....	68
3.4. Chemoselective C-H insertion in homoallylic and homoallylic carbamate substrates.....	72
3.5. Scope of Ag(I)-catalyzed aziridination.....	75
3.6. Conclusions.....	78
3.7. References.....	79
3.8. Experimental Details and Characterization.....	80
3.8.1 Preparation of homoallylic carbamates.....	80
3.8.2. Ag(I)-catalyzed methylene aziridination.....	84
3.8.3. Synthesis of C-H insertion products.....	91
3.8.4. Synthesis of Homoallylic Carbamates.....	95
3.8.5. Synthesis of Aziridines.....	96
3.8.6. Synthesis of Allylic C-H Insertion Products.....	99
Chapter 4. Review: Mechanistic Studies of Metal-Catalyzed Nitrene Transfer.....	102
4.1. Introduction to Mechanistic Aspects of Nitrene Transfer.....	103
4.2. Early Studies of Metal-catalyzed Nitrene Transfer.....	104
4.3 Evidence for the Intermediacy of Metal Nitrenes.....	107

4.3. Assessing the mechanism of C-N bond formation: concerted or stepwise?	113
4.4. Kinetic Studies	121
4.6. Computational studies of nitrene transfer	124
4.7. Conclusions	126
4.8. References	127
Chapter 5. Mechanistic Studies of Dynamic, Chemoselective, Silver(I)-Catalyzed Aziridination and C-H Amination	129
5.1. Introduction	130
5.2. Solution-state behavior of silver complexes	130
5.3. Experiments to assess the nature of the aziridination and C-H amination steps.	133
5.4. Kinetic analysis of dynamic silver catalysis	141
5.6. Notes and References	156
5.7 Experimental Details and Characterization.	157
5.7.1. Synthesis of probe substrates	157
5.7.2. Characterization of amination products	167
5.7.3. Kinetic Analysis of Amination Reactions	182
5.7.4. Rate law for aziridination reaction	191
Chapter 6. Development of Enantioselective Silver (I)-Catalyzed Intramolecular Aziridinations.	197

6.1 Introduction.....	198
6.2. Highly enantioselective methods of alkene aziridination <i>via</i> nitrene transfer.....	198
6.3. Development of silver(I)-catalyzed asymmetric aziridination.	201
6.4. Conclusions.....	207
6.5. Notes and References.....	207
6.6. Experimental Details and Characterization.	209
Appendix A. ^1H -NMR and ^{13}C -NMR spectra of new compounds.....	214
Appendix B. X-ray Crystallographic Data.....	460
Appendix C. Select HPLC Traces for Enantioselective Aziridination.	519

List of Schemes

Scheme 1.1. Complementary strategies for stereotriad construction.	3
Scheme 1.2. Spirodiepoxide strategy for accessing complex natural products.	4
Scheme 1.3. Methylene aziridine strategies for stereotriad synthesis.	6
Scheme 1.4. Approaches to the synthesis of 1,3-diamines.	8
Scheme 1.5. Scope of Rearrangement.	11
Scheme 1.6. One-pot conversion of homoallylic carbamates to 1,3-diamino-2-ones.	12
Scheme 1.7. Maintenance of enantioenrichment in rearrangement.	13
Scheme 1.8. Stereoselective reduction of the 1,3-diamino-2-one	14
Scheme 1.9. Reduction of 1,3-diamino-2-ones to provide 1,3-diamino-2-ols.	14
Scheme 1.10. Proposed mechanism for rearrangement of acetate-opened DASPs to 1,3-diamino-2-ones.	16
Scheme 2.1. Difunctionalizations of bicyclic methylene aziridines.	35
Scheme 2.2. Proposed mechanism of asymmetric aminohydroxylation.	37
Scheme 2.3. Aminohydroxylation and reduction of a methylene aziridine lacking geminal dimethyl groups.	42
Scheme 3.1. Chemoselectivity in Rh-catalyzed aziridination of homoallylic carbamates.	66
Scheme 3.2. Dynamic behavior of Ag complexes demonstrated by <i>in situ</i> control of catalyst.	78
Scheme 4.1. Mechanism of transition-metal-catalyzed nitrene transfer.	104

Scheme 4.2. Early proposal for the mechanism of metal-nitrene formation.	105
Scheme 4.3. Isolable iminoiodinanes as reactive intermediates for metal-catalyzed nitrene transfer.	106
Scheme 4.4. Radical mechanisms for aziridination and C-H amination.	107
Scheme 4.5. Ru-imido complexes as NTs-transfer reagents and presumed catalytic intermediates.	108
Scheme 4.6. Isolation of a presumed intermediate in Fe-catalyzed amination.	109
Scheme 4.7. Di-copper complexes bridged by a nitrene.	111
Scheme 4.8. Isolation of Cu- and Ag-nitrene complexes.	112
Scheme 4.9. Metal-nitrene formation <i>via</i> proton-coupled electron transfer.	112
Scheme 4.10. Possible mechanisms for C-H amination and aziridination steps.	114
Scheme 4.11. Isomerization in the Cu-catalyzed aziridination of alkenes.	115
Scheme 4.12. Opening of radical clock substrates.	116
Scheme 4.13. Hammett effects used to elucidate mechanisms of N-tosyl transfer from Ru-diimido complexes.	117
Scheme 4.14. Hammett effects in Ru-porphyrin-catalyzed benzylic C-H amination.	118
Scheme 4.15. Hammett data in Rh- and Ru-catalyzed C-H amination.	120
Scheme 4.16. Intramolecular competition to assess intramolecular KIEs.	120
Scheme 4.17. Kinetic study of Cu-diimine-catalyzed aziridination.	121

Scheme 4.18. Formation of iminoiodinane as rate-limiting step.	122
Scheme 4.19. Kim and Chang's proposal for Cu-catalyzed aziridination.	123
Scheme 4.20. Kinetic analysis for decomposition of bridged dicopper nitrenes.	123
Scheme 4.21. Computed spin-crossover in Ag-catalyzed aziridination.	125
Scheme 4.22. Computed singlet, stepwise pathway for Rh-catalyzed C-H amination.	126
Scheme 5.1. Performance of AgL and AgL ₂ systems in aziridination.	135
Scheme 5.2. Benzylic amination with AgLOTf and AgL ₂ ⁺ .	136
Scheme 5.3. Isomerization probes for aziridination and C-H amination.	136
Scheme 5.4. Stereochemical probes for C-H insertion.	137
Scheme 5.5. Radical inhibition studies.	137
Scheme 5.6. Amination of a radical clock substrate.	138
Scheme 5.7. Hammett studies of Ag-catalyzed C-H amination.	139
Scheme 5.8. Ag-catalyzed aziridination of styrenes.	139
Scheme 5.9. Intrinsic KIE measurement.	140
Scheme 5.10. Metal-nitrene formation and reaction in the presence of either catalyst.	141
Scheme 5.11. Intermolecular competition to determine KIE.	148
Scheme 5.12. Possible decomposition of iminoiodinane intermediate.	150
Scheme 5.13. Iminoiodinane consumption.	151
Scheme 5.14. Mechanisms of Ag-catalyzed C-H amination and aziridination.	154

Scheme 6.1. Intermolecular aziridination with chiral copper catalysts.	199
Scheme 6.2. Intermolecular aziridinations using azides as nitrogen sources.	200
Scheme 6.3. Copper-catalyzed enantioselective intramolecular aziridinations.	201
Scheme 6.4. Synthesis of novel amino alcohols.	207

List of Figures

Figure 1.1. Selected 1,3-diamino-2-ols in biologically active molecules.	7
Figure 1.2. Felkin-Anh model applied to reduction of 1,3-diamino-2-ones.	15
Figure 2.1. Electronic rationale for unreactive substrates.	44
Figure 3.1. Examples of catalysts for chemoselective nitrene transfer.	65
Figure 3.2. A dynamic approach to chemoselective amination.	72
Figure 4.1. EPR characterization of a Co-bound iminoradical.	110
Figure 5.1. Binding modes and coordination geometries of bidentate nitrogenated ligands with Ag.	131
Figure 5.2. Spectroscopic study of Ag complexes in solution. a) NMR titration using 4,4'-di- <i>tert</i> -butylbipyridine. b) DOSY NMR experiments to assess the nuclearity of Ag complexes.	134
Figure 5.3. Kinetic profiles of a) aziridination and b) C-H amination under standard conditions.	142
Figure 5.4. a) Aziridination at varied ligand loadings. b) C-H amination at varied ligand loadings.	143
Figure 5.5. Starting material consumption at varied AgOTf loadings at a) 1:1.25 Ag:ligand and b) 1:3 Ag:ligand.	144
Figure 5.6. Normalized starting material consumption at varied initial concentrations under a) aziridination conditions b) C-H amination conditions.	146

- Figure 5.7.** Effect of the oxidant on the chemoselectivity. a) Aziridination with (^tBubipy)AgOTf.
b) C-H amination with (^tBubipy)₂AgOTf. 147
- Figure 5.8.** Independent rate measurement of labelled and unlabelled substrates. 153
- Figure 5.9** Pre-stir of oxidant and substrate obviates induction period. 155

List of Tables.

Table 1.1. Rearrangement of acetate-opened DASP.	9
Table 1.2. Optimization and investigation of rearrangement.	10
Table 2.1. Optimization of aminohydroxylation of methylene aziridines.	38
Table 2.2. Solvent effects in the reduction of 1,3-diamino-2-ones.	39
Table 2.3. Optimization of aminohydroxylation of aryl substituted methylene aziridines.	40
Table 2.4. Re-optimization of the reduction of aryl-substituted ketones.	41
Table 2.5. Scope of aminohydroxylation/reduction of bicyclic methylene aziridines.	43
Table 3.1. Examination of catalyst for allene aziridination.	68
Table 3.2. Aziridination of α,α' -disubstituted homoallenic carbamates.	70
Table 3.3. Chemoselective Aziridination of Homoallenic Carbamates Using Ag(I) Catalysis.	71
Table 3.4. Effect of Ag:phen Stoichiometry on the Aziridination/Insertion Ratio.	73
Table 3.5. Tunable, chemoselective amination of homoallenic carbamates.	76
Table 3.6. Amination of homoallylic carbamate.	77
Table 6.1. Bisphosphine ligands as potential catalysts for Ag(I)-catalyzed aziridination.	202
Table 6.2. Optimization of aziridination conditions using (<i>R</i>)-BINAPINE.	203
Table 6.3. Examination of chiral bidentate nitrogen-containing ligands.	204
Table 6.4. Bisoxazoline scaffold modifications.	205

Table 6.5. Further optimization of enantioselective intramolecular aziridination.

206

For Laurie

Chapter 1. Stereoselective Synthesis of 1,3-Diamino-2-ols via Rearrangement of 1,4-Diazaspiro[2.2]pentanes.

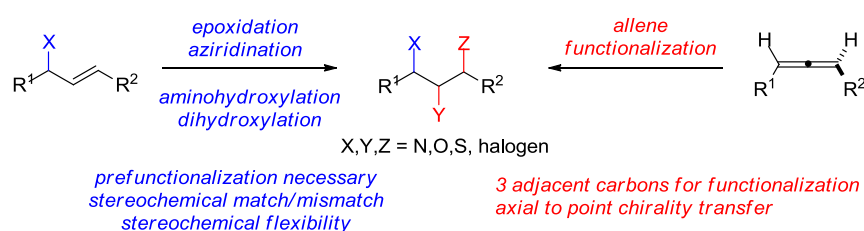
This chapter is adapted from work published previously:

Weatherly, C. D.; Rigoli, J. W.; Schomaker, J. M. *Org. Lett.* **2012**, *14*, 1704.

1.1. Allenes as Templates for Stereotriad Construction

The development of enantioselective methods for the oxidation of alkenes is among the most significant advances in organic chemistry in the late twentieth and early twenty-first centuries, as attested by the awarding of a half share of the 2001 Nobel Prize in Chemistry to K. Barry Sharpless for his trio of enantioselective alkene functionalizations: epoxidation, dihydroxylation, and aminohydroxylation.¹ These and other stereoselective methods of alkene functionalization have seen powerful deployment in the synthesis of complex natural products, and are now standard techniques for the synthesis of adjacent heteroatom-bearing stereocenters. However, many biologically active natural products and pharmaceutical compounds contain arrays of three or more contiguous carbon-heteroatom stereocenters. Use of enantioselective alkene functionalization to construct these moieties is a popular and viable strategy, but it often requires other challenging methods for establishing an allylic stereocenter, which may cause problems of matching and mismatching in subsequent alkene functionalization (Scheme 1.1).²

Scheme 1.1. Complementary strategies for stereotriad construction.

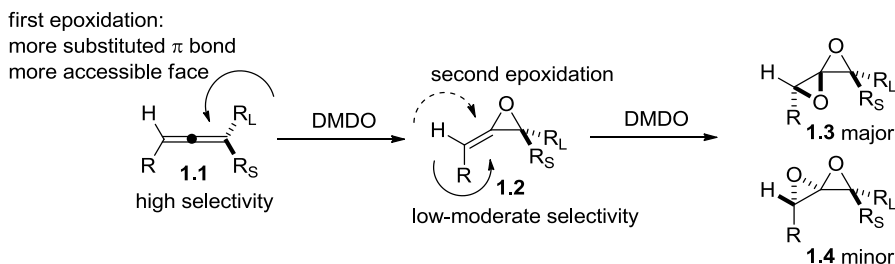


An alternative strategy for the synthesis of arrays of three contiguous carbon-heteroatom bonds (“stereotriads”) is oxidative allene functionalization. Several features of allenes make them attractive templates for stereotriad construction: they are easily synthesized, contain two nucleophilic carbon-carbon double bonds, and often possess axial chirality that may be transferred to point chirality. In 1968, the groups of Crandall and Greene simultaneously

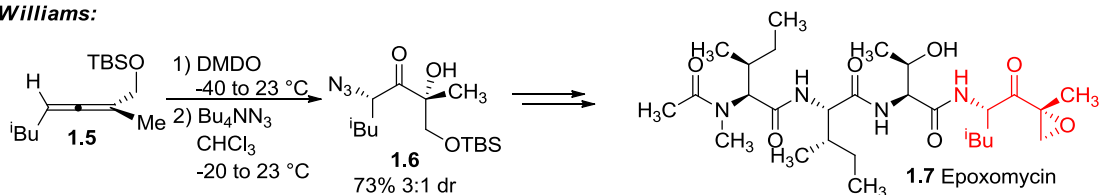
described the isolation of allene oxide and spirodiepoxide products obtained *via* treatment of allenes with peracids.^{3,4} Crandall later showed that the milder DMDO (dimethyldioxirane) was a superior oxidant for the transformation and proposed a simple stereochemical model for its regio- and stereoselectivity (Scheme 1.2).⁵ In this model, the more substituted, electronic rich π bond undergoes a first epoxidation with high selectivity for the less hindered face of the allene, providing allene oxide intermediate **1.2**. A faster second epoxidation occurs with low to moderate selectivity for the less hindered face of the allene oxide (**1.3** and **1.4**). The Williams group has used allene-derived spirodiepoxides to obtain complex stereochemical intermediates *en route* to several biologically active natural products, including epoxomycin and stereochemical analogs (Scheme 1.2).^{6,7}

Scheme 1.2. Spirodiepoxide strategy for accessing complex natural products.

Crandall:



Williams:



The inherent drawbacks of the spirodiepoxide tactic are the limited stereocontrol in the second epoxidation, and the limited regiocontrol in subsequent epoxide-opening. Additionally, the higher rate of the second epoxidation prevents direct functionalization of the allene oxide

with other heteroatoms. What selectivity is obtained is determined almost exclusively by steric features of the substrate. Our group has developed a modified strategy allene oxidation strategy to access nitrogen-containing stereotriads. Intramolecular aziridination using a homoallylic carbamate or sulfamate **1.8** gives rise to a bicyclic methylene aziridine **1.9** with complete regioselectivity, and transfers the axial chirality of the allene to point chirality in the product.⁸

From this intermediate, at least three complementary patterns of reactivity can be envisioned. The bicyclic methylene aziridine could undergo ring opening to form an enecarbamate, which could then react with an electrophile to provide an imine intermediate. Reaction of the imine with a second nucleophile would provide a stereotriad of the form C-Y/C-N/C-E **1.10** (Scheme 1.3, left).⁹ Alternatively, the methylene aziridine could react directly with an electrophile to provide a strained spiro intermediate, which could undergo further ring-opening to give a stereotriad of the form C-N/C-N/C-Y **1.11** (Scheme 1.3, right).¹⁰ Hydrolysis of the *N,N*-aminal could provide opportunities for further functionalization. Finally, oxidative 1,2-difunctionalization of the methylene aziridine, followed by reduction, would provide a stereotriad of the form C-Z/C-O/C-N **1.12** (Scheme 1.3, center).¹¹ To date, all three strategies have been successfully deployed to synthesize a functionally and stereochemically diverse collection of stereotriads.

1.2 Prevalence of 1,3-diamino-2-ols in Biologically Active Products.

The 1,3-diamino-2-ol was chosen as an early target motif for the second strategy. Compounds containing 1,3-diamino-2-ol stereotriads are prevalent in a variety of biologically active natural products and pharmaceuticals (Figure 1.1). These include a potent BACE-1 inhibitor developed by Merck,¹² mipralden, a small molecule modulator of protein-protein interactions,¹³ substituted cyclohexyl components of streptomycin and other antibiotics,¹⁴ and the hydroxyenduracidine components of the mannopeptimycin family of antibiotics.¹⁵ Perhaps most significantly, 1,3-diamino-2-ol appears in six of the twelve FDA-approved HIV-protease inhibitors, including Darunavir, with the 1,4-diamino-2-ol appearing in two others.¹⁶

Scheme 1.3. Methylene aziridine strategies for stereotriad synthesis.

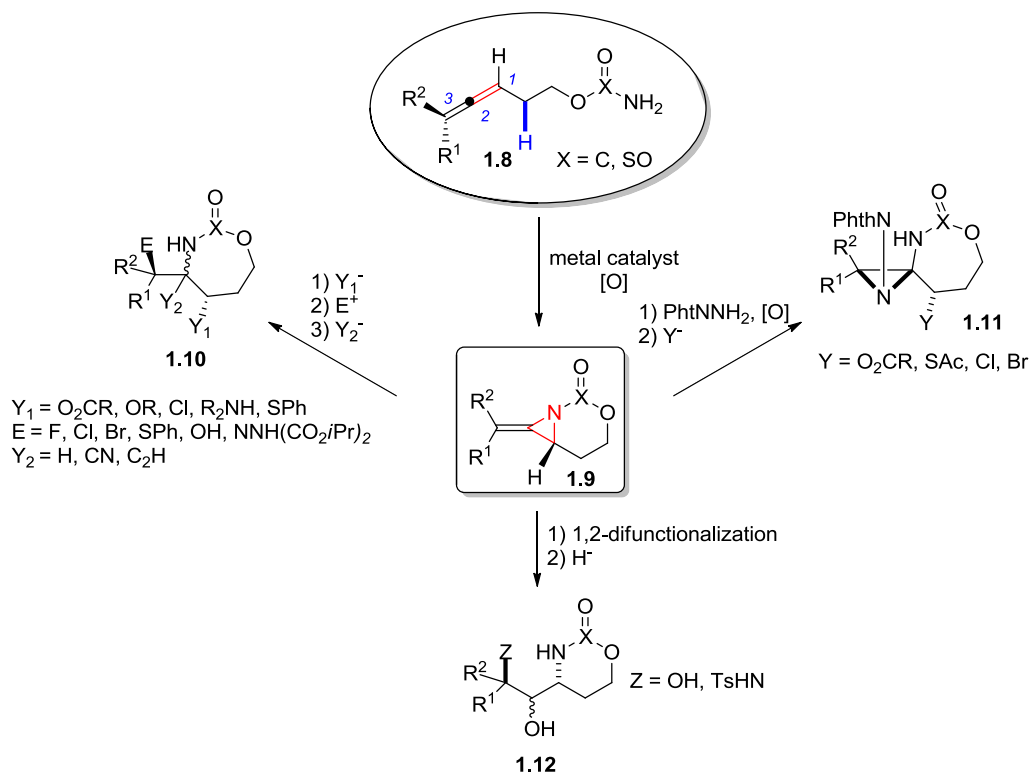
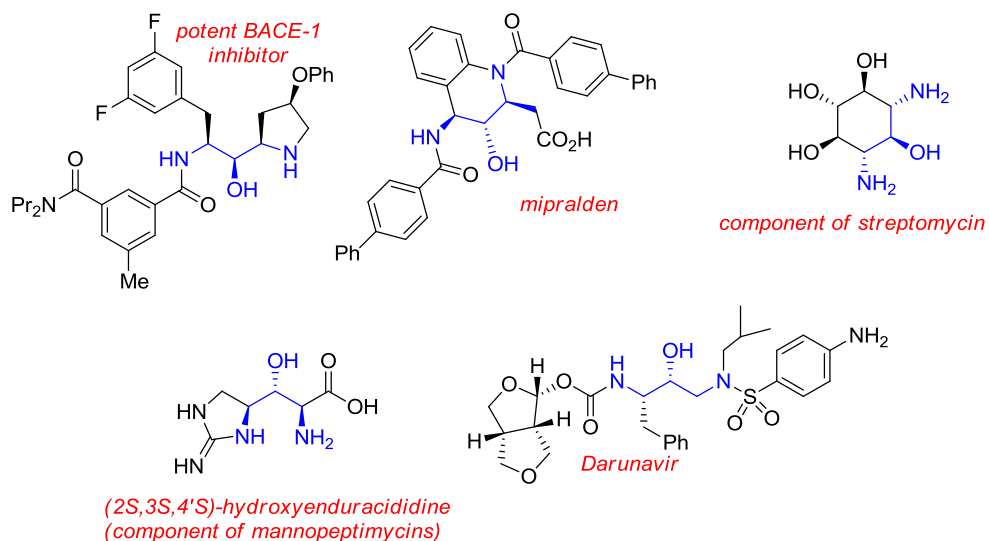


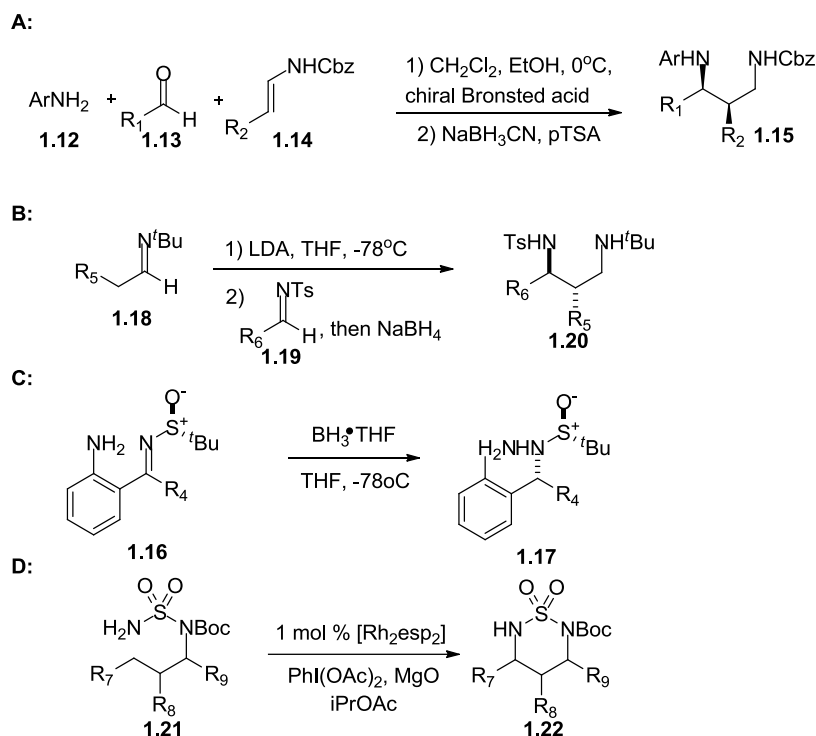
Figure 1.1. Selected 1,3-diamino-2-ols in biologically active molecules.



1.3. Synthesis of 1,3-Diaminated Compounds.

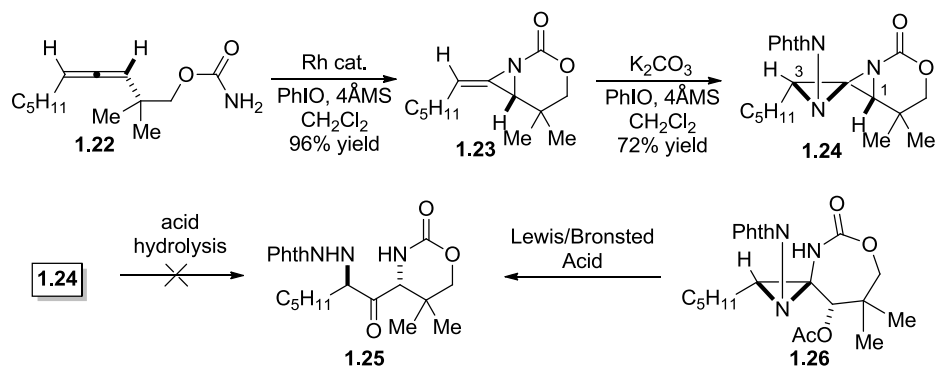
Several general approaches to 1,3-diamines have been described. Most are transformations of imines, including: the addition of enecarbamates to imines to yield *anti* 1,3-diamines (Scheme 1.4A),¹⁷ the addition of the α -carbanion of imines to *N*-protected imines (Scheme 1.4B),¹⁸ and the diastereoselective reduction of ketimines (Scheme 1.4C).¹⁹ Additionally, transition-metal catalyzed C-H amination can provide 1,3-diamines (Scheme 1.4D).²⁰ However, access to complex functionalized 1,3-diaminated compounds of the form C-N/C-X/C-N using well-established methodology is much more limited.

Scheme 1.4. Approaches to the synthesis of 1,3-diamines.



1.4. Conversion of 1,4-Diazaspiro-[2.2]-pentanes to 1,3-diaminoketones.

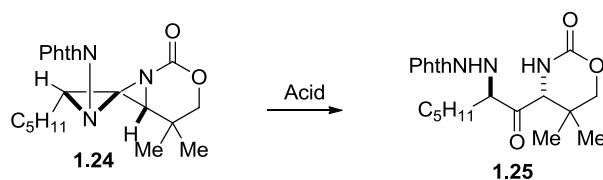
Previous work in the Schomaker group had established a reliable sequence for the synthesis of 1,4-diazaspiro-[2.2]-pentanes (DASPs). Rh-catalyzed aziridination of an allenic carbamate **1.23**, followed by a second aziridination using *N*-aminophthalimide, potassium carbonate and iodosylbenzene, provide DASP **1.24** in good yield and excellent diastereoselectivity (Table 1.1). We initially envisioned **1.24** as a 1,3-diaminated ketone “protected” as an *N,N*-aminal, and would yield ketone **1.25** upon hydrolysis. However, a variety of Lewis and Bronsted acids failed to promote the rearrangement irrespective of the presence or absence of water. In the case of mild acids, the DASP did not react or underwent ring opening at C1. The use of stronger acids generally resulted in intractable mixtures of products.

Table 1.1. Rearrangement of acetate-opened DASP.

entry	additives ^a	conversion	entry	additives ^a	conversion
1	CeCl ₃ •7H ₂ O	0%	7	Sc(OTf) ₃	100% ^b
2	NiCl ₂ •6H ₂ O	0%	8	BF ₃ OEt ₂	100%
3	Ti(O ⁱ Pr) ₄	0%	9	TsOH	100%
4	ZnCl ₂	0%	10	Bi(OTf) ₃	96% ^c
5	Cu(OTf) ₂	100% ^b	11	Bi(OTf) ₃ (0.2 equiv)	100%
6	InCl ₃	33%	12	Bi(OTf) ₃ (0.05 equiv)	100%

^a 1.0 equiv unless otherwise indicated. ^b Complete conversion with several side products. ^c Isolated yield.

We postulated that the recalcitrance of the DASP to undergo hydrolysis might be a consequence of inability of the nitrogen atoms to provide resonance stabilization to an intermediate carbocation at C2. The relief of ring strain might render the heteroatoms better able to stabilize this carbocation, thus facilitating the desired reaction. In this vein, the acetate-opened DASP **1.26** was treated with a series of Lewis and Bronsted acids (Table 1.1). Weak Lewis acids, including CeCl₃, Ti(OⁱPr)₄, and ZnCl₂ (entries 1-4), gave no reaction, and the starting material was recovered unchanged. InCl₃ (entry 6) gave slow conversion to the desired product, while Cu(OTf)₂ and Sc(OTf)₃ (entries 5 and 7) yielded unidentified mixtures of products. BF₃OEt₂, TsOH, and Bi(OTf)₃ (entries 8-12) all gave complete conversion of the starting material, with Bi(OTf)₃ resulting in a 96% isolated yield of **1.25**. Full conversion to the desired products was subsequently observed with 0.2 and 0.05 equivalents of Bi(OTf)₃.

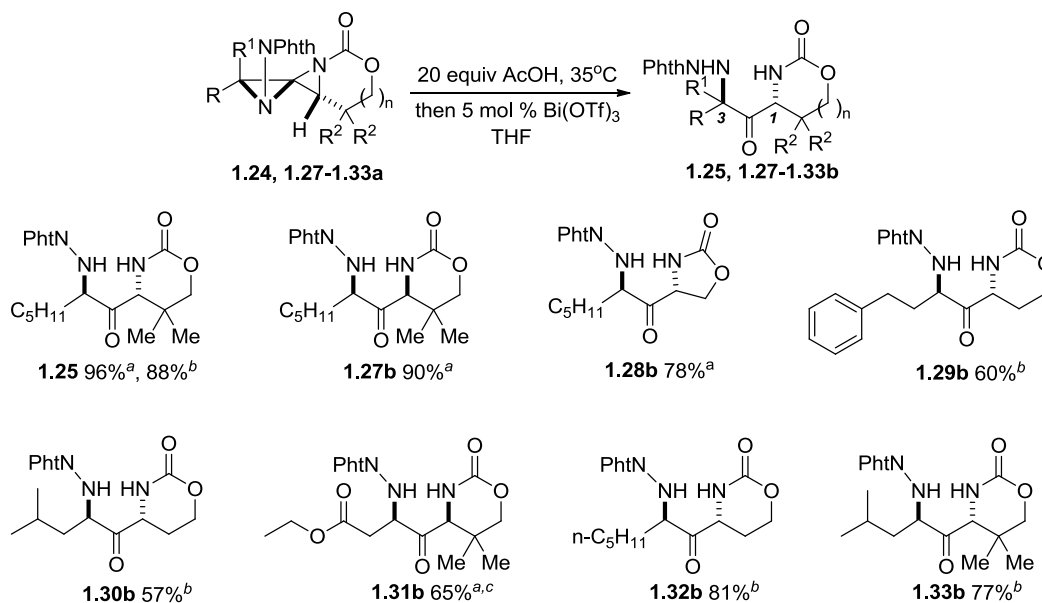
Table 1.2. Optimization and investigation of rearrangement.

entry	conditions	conversion
1	Bi(OTf) ₃ (1.0 equiv)	0%
2	AcOH, then Bi(OTf) ₃ (0.05 equiv) ^a	100%
3	TMSCl, then Bi(OTf) ₃ (0.05 equiv) ^b	0%
4	AcSH, then Bi(OTf) ₃ (0.05 equiv) ^b	0%
5	ClCH ₂ CO ₂ H, then Bi(OTf) ₃ (0.05 equiv)	100%
6	AcOH, then cat. TfOH	100%
7	AcOH at 35 °C, then Bi(OTf) ₃ (0.05 equiv)	100% (88%) ^{c,d}

^a 40 h reaction time. ^b The product was the ring-opened DASP.
^c 12 h reaction time. ^d Isolated yield.

Bi(OTf)₃ was chosen to further optimize the conversion of the DASP **1.24** directly to **1.25** (Table 1.2). The addition of Bi(OTf)₃ to the DASP directly (entry 1) did not promote the desired reaction. Treatment of the DASP with AcOH, followed by addition of 5 mol % Bi(OTf)₃ (entry 2), gave complete conversion of the DASP to **1.25**; however the ring-opening with AcOH was slow. Ring-opening of **1.24** with TMSCl, followed by treatment with the Lewis acid (entry 3), gave only the chloride-opened product and none of the desired rearrangement product. The same result was observed when thioacetic acid (entry 4) was employed as the nucleophile to open **1.24**. These results suggested that the ester was playing an important role in promoting the rearrangement, and indeed, treatment of **1.24** with chloroacetic acid and Bi(OTf)₃ also promoted the desired rearrangement (entry 5). We suspected that the role of Bi(OTf)₃ might be simply to generate small amounts of TfOH, and the addition of a catalytic amount of TfOH to **1.26** did promote the desired rearrangement. In order to decrease the reaction time, the acetate-opening reaction was conducted at 35°C, followed by the introduction of Bi(OTf)₃ at room temperature (entry 7) to give ketone **1.24** in 88% isolated yield over the one-pot, two-step reaction.

Scheme 1.5. Scope of Rearrangement.



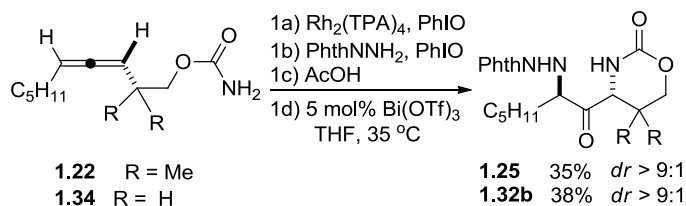
^aStarting material was acetate-opened DASP. ^bStarting material was DASP.

^c*dr* was 86:12; >95:5 in all other cases.

A variety of DASPs were converted to the corresponding 1,3-diaminated ketone products (Scheme 1.5) using optimized reaction conditions. There was only a slight difference in yield between the use of the DASP **1.24** or the ring-opened DASP **1.26**. DASPs formed from *Z* bicyclic methylene aziridines also underwent the desired rearrangement with high stereoselectivity. The stereospecificity of the reaction is illustrated by a comparison of the 1,3-diaminated ketone **1.25**, obtained in 88% yield from the rearrangement of a DASP **1.24** derived from an *E*-methylene aziridine, with the distinct product ketone **1.27b**, obtained in 90% yield from the rearrangement of a DASP formed from a *Z*-methylene aziridine. The rearrangement was not affected by the absence of alkyl substitution in the tether (**1.29b-1.30b**, **1.32b**) or limited to the formation of six-membered rings, as a five-membered ring product **1.28b** was obtained in 78% yield. The *dr* of the two nitrogen-bearing stereocenter was greater than 19:1 in most cases.

Not surprisingly, if the product was allowed to remain under the acidic conditions for extended periods of time, significant isomerization to a mixture of diastereomers did occur.

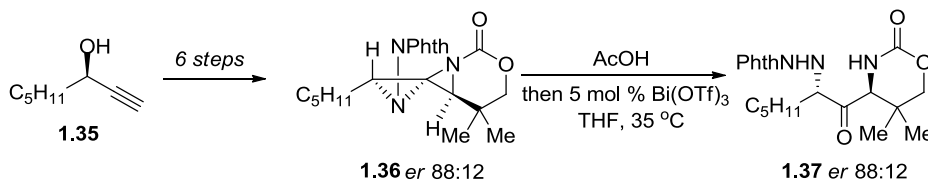
Scheme 1.6. One-pot conversion of homoallenic carbamates to 1,3-diamino-2-ones.



We were pleased to find that the conversion of allenic carbamates **1.22** and **1.34** to the resulting 1,3-diaminated ketones could be achieved in a single pot (Scheme 1.6). Although the yields were only moderate (approximately 80% per chemical step), the reaction introduces significant complexity into a simple, easily accessed substrate. The major loss in yield occurs in the first allene aziridination, where the formation of the *Z*-methylene aziridine competes with that of the desired *E* methylene aziridine. The *Z*-methylene aziridine reacts much more slowly in the subsequent reactions and can be easily separated from the final desired product. The diastereoselectivity of the isolated products in the one-pot process was greater than 19:1, comparable to the *dr* observed in the stepwise conversion of the isolated DASPs to ketones **1.25** and **1.32b**.

One convenient advantage of this methodology arises as a result of the ability to transfer the axial chirality of an enantioenriched allene to the 1,3-diaminated products. To test the fidelity of this transfer, an enantioenriched DASP **1.36** was synthesized in six steps from the commercially available enantioenriched propargyl alcohol **1.35**. The enantioenriched DASP **1.36** was subjected to the reaction conditions for the rearrangement to **1.37** (Scheme 1.7). No degradation of the enantiopurity was indicated by chiral HPLC.

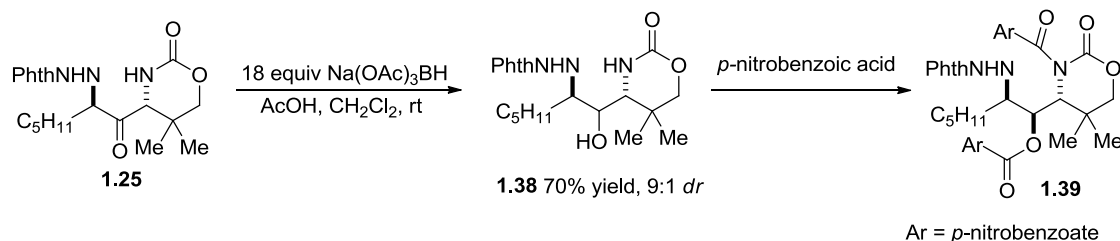
Scheme 1.7. Maintenance of enantioenrichment in rearrangement.



1.5. Stereoselective Reduction of 1,3-diamino-2-ones to 1,3-diamino-2-ols.

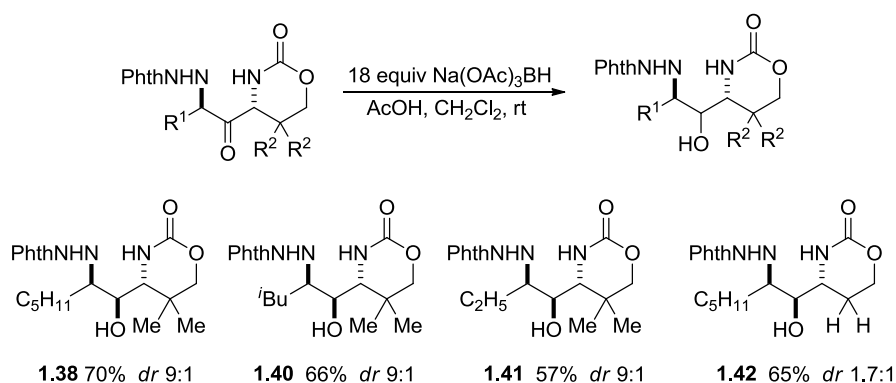
The next challenge was to develop a stereocontrolled reduction of the ketone (Scheme 1.8). This task presented two difficulties. First, the phthalimide moiety was also sensitive to reduction conditions. Secondly, the two stereocenters flanking the ketone might exert competing influence on the stereochemistry of ketone reduction. Several conditions for the reduction were examined. Not surprisingly, NaBH_3CN failed to reduce the ketone, while $\text{Zn}(\text{BH}_4)_2$, NaBH_4 and LiAlH_4 gave complex mixtures of products, presumably due to reduction of the phthalimide and/or carbamate moieties. Gratifyingly, the portionwise addition of sodium triacetoxyborohydride over 18 hours to a solution of the ketone in CH_2Cl_2 gave the 1,3-diamino-2-ol **1.38** in 70% yield and 9:1 *dr*. Performing the reduction in THF gave a 70% yield of product, but only a 3:1 *dr*.

Scheme 1.8. Stereoselective reduction of the 1,3-diamino-2-one.



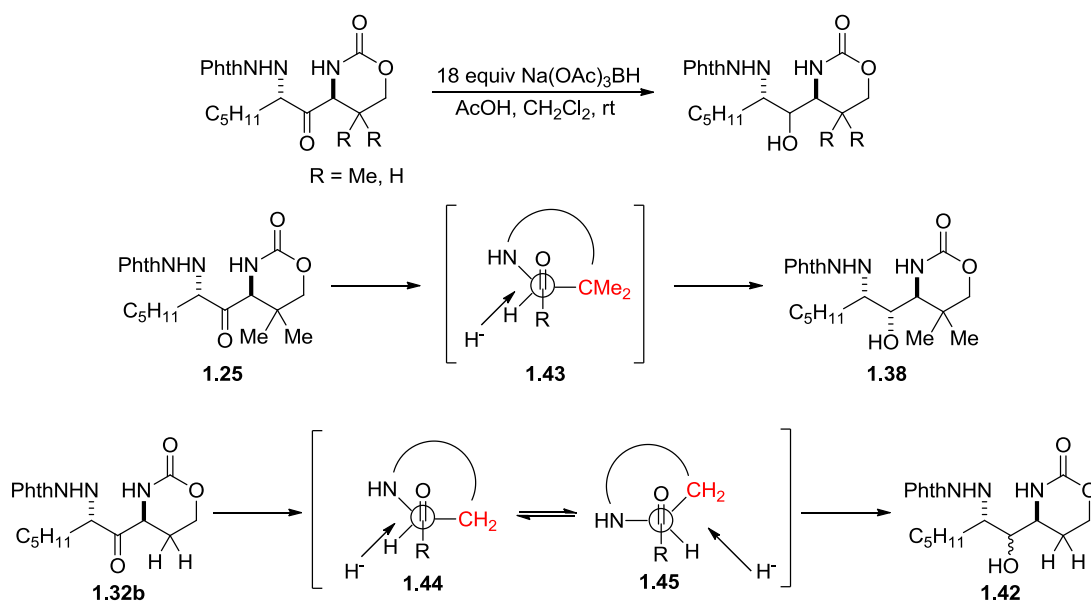
To establish the relative stereochemistry of the stereotriad, the 1,3-diamino-2-ol was treated with an excess of *p*-nitrobenzoyl chloride to give crystalline **1.39**. X-ray crystallography of this compound unambiguously demonstrated a 1,2-*anti*/2,3-*syn* relationship among the substituents. It was not clear on this basis which aspects of substrate structure controlled the diastereoselectivity of the reduction, so several related compounds were investigated (Scheme 1.9). Reduction of ketones with varied alkyl substituents at C3 gave similarly high diastereoselectivity, with *dr* of 9:1 (**1.40**, **1.41**). However, when a substrate lacking geminal dimethyl groups in the ring was subjected to the reduction conditions, a *dr* of only 1.7:1 was observed (**1.42**).

Scheme 1.9. Reduction of 1,3-diamino-2-ones to provide 1,3-diamino-2-ols.



This result suggests that the C1 stereocenter is the primary controlling element in the stereoselectivity of the reduction, and is easily rationalized with a Felkin-Anh model. When geminal dimethyl groups are present in the carbamate ring, the large steric difference between the quaternary carbon and the nitrogen of the carbamate likely favors conformation **1.42** (Figure **1.2**), leading to high diastereoselectivity. In contrast, when the dimethyl groups are removed, there is little steric differentiation between the two substituents. Therefore, conformations **1.43** and **1.44** are similar in energy, and little selectivity is observed. The observed selectivity is also consistent with Cram-type chelation involving the C1-bound nitrogen. However, more electron-rich C3 nitrogen would likely be a stronger chelator, and is predicted to give the opposite stereochemical outcome.

Figure 1.2. Felkin-Anh model applied to reduction of 1,3-diamino-2-ones.

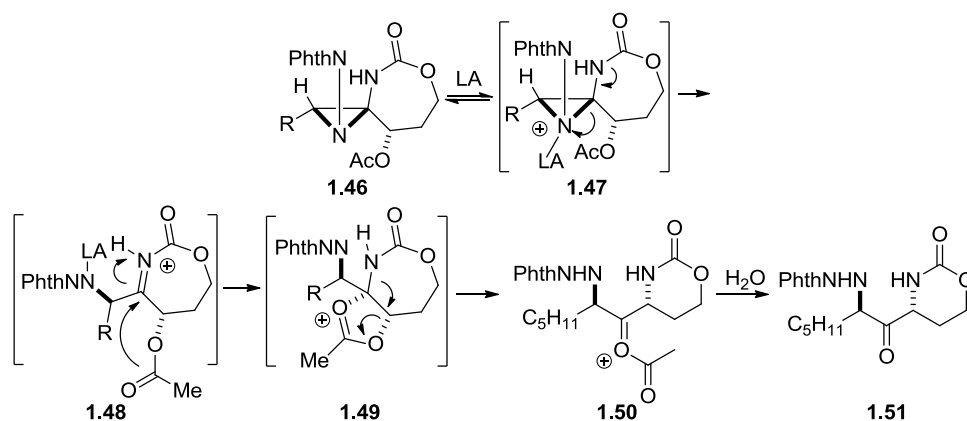


1.6. Possible mechanism of rearrangement of DASPs.

While detailed mechanistic studies of the rearrangement were not undertaken, a mechanism consistent with the observed stereochemical outcome of the reaction is easily

envisioned (Scheme 1.10). In the proposed mechanism, Lewis acid binding to the more electron-rich of the two nitrogens (**1.47**) leads to ring-opening of that aziridine to give iminium intermediate **1.48**. Attack of the lone pair electrons of the carbonyl oxygen provides a cyclic *N,O*-aminal **1.49**, which undergo 1,2-migration of the nitrogen atom to give an oxocarbenium intermediate suitable for hydrolysis. This mechanism accounts for both the observed stereochemical outcome and the necessity of using an acetate-opened DASP for the rearrangement.

Scheme 1.10. Proposed mechanism for rearrangement of acetate-opened DASPs to 1,3-diamino-2-ones.



1.7 Conclusions.

A stereoselective method for the synthesis of 1,3-diamino-2-ols from homoallylic carbamates has been developed, serving as the first example of the “electrophile/nucleophile” strategy for the functionalization of bicyclic methylene aziridines. Ring opening of a 1,4-diazaspiro-[2.2]-pentane, followed by $\text{Bi}(\text{OTf})_3$ -catalyzed rearrangement, yields a 1,3-diamine, which can undergo stereoselective reduction to provide a 1,2-*anti*/2,3-*syn* relationship among the substituents. Substrate control of the stereoselectivity of the reduction limits the scope of the

methodology, but also provides insight into the means of stereocontrol. While application of this methodology to the synthesis of biologically active targets was considered, the substrate requirements for attaining high diastereoselectivity and the presence of the recalcitrant *N*-aminophthalimide moiety dissuaded us from these pursuits. Instead, the limitations of this methodology and the desire to access the desired motifs more directly led to the development of a second generation synthesis.

1.8 Notes and References.

1. Nobelprize.org. http://www.nobelprize.org/nobel_prizes/chemistry/laureates/2001/press.html (accessed Apr 30, 2015).
2. For selected reviews on oxidations applied to chiral alkenes, see: a) Cardona, F.; Goti, A. *Nat. Chem.* **2009**, *1*, 269. b) Chemler, S. R. *Org. Biomol. Chem.* **2009**, *7*, 3009. c) de Figueiredo, R. M. *Angew. Chem. Int. Ed.* **2009**, *48*, 1190. d) Du, H. F.; Yuan, W. C.; Zhao, B. G.; Shi, Y. *J. Am. Chem. Soc.* **2007**, *129*, 7496. e) Trost, B. M.; Malhotra, S.; Olson, D. E.; Maruniak, A.; Du Bois, J. *J. Am. Chem. Soc.* **2009**, *131*, 4190. f) Donohoe, T. J.; Callens, C. K. A.; Flores, A.; Lacy, A. R.; Rath, A. H. *Chem. Eur. J.* **2011**, *17*, 58. (g) Johnson, R. A.; Sharpless, K. B. in *Catalytic Asymmetric Synthesis*, Ojima, I., Ed.; VCH: New York, 1993, pp. 103-158. h) De Jong, S. Nosal, D. G.; Wardrop, D. J. *Tetrahedron* **2012**, *68*, 4067.
3. Crandall, J. K.; Machleder, W. H. *J. Am. Chem. Soc.* **1968**, *90*, 7292.
4. Camp, R. L.; Greene, F. D. *J. Am. Chem. Soc.* **1968**, *90*, 7349.
5. Crandall, J. K.; Batal, D. J. *J. Org. Chem.* **1988**, *53*, 1340.
6. a) Lotesta, S. D.; Hou, Y.; Williams, L. J. *Org. Lett.* **2007**, *9*, 869. b) Kolakowski, R.; Williams, L. J. *Tetrahedron Lett.* **2007**, *48*, 4761. c) Shangguan, N.; Kiren, S.; Williams, L. J. *Org. Lett.* **2007**, *9*, 1093. d) Ghosh, P.; Zhang, Y.; Emge, T. J.; Williams, L. J. *Org. Lett.* **2009**, *11*, 4402. e) Liu, K.; Kim, H.; Ghosh, P.; Akhmedov, N. G.; Williams, L. J. *J. Am. Chem. Soc.* **2011**, *133*, 14968.
7. For a review of oxidative allene functionalizations, see: Adams, C. S.; Weatherly, C. D.; Burke, E. G.; Schomaker, J. M. *Chem. Soc. Rev.* **2014**, *43*, 3136.
8. Boralsky, L. A.; Martston, D.; Grigg, R. D.; Hershberger, J. C.; Schomaker, J. M. *Org. Lett.* **2011**, *13*, 1924.
9. a) Adams, C.; Boralsky, L. A.; Guzei, I. A.; Schomaker, J. M. *J. Am. Chem. Soc.* **2012**, *134*, 10807. b) Adams, C. S.; Grigg, R. D.; Schomaker, J. M. *Tetrahedron* **2014**, *70*, 4128. c) Adams, C. S.; Grigg, R. D.; Schomaker, J. M. *Chem. Sci.* **2014**, *5*, 3046.
10. Rigoli, J. W.; Boralsky, L. A.; Hershberger, J. C.; Meis, A. R.; Marston, D.; Guzei, I. A.; Schomaker, J. M. *J. Org. Chem.* **2012**, *77*, 2446.
11. Rigoli, J. W.; Guzei, I. A.; Schomaker, J. M. *Org. Lett.* **2014**, *16*, 1696.
12. Iserloh, U.; Wu, Y.; Cumming, J. N.; Pan, J.; Wang, L. Y.; Stamford, A. W.; Kennedy, M. E.; Kuvelkar, R.; Chen, X.; Parker, E. M.; Strickland, C.; Viogt, J. *Bioorg. Med. Chem. Lett.* **2007**, 414.

13. Prakesch, M.; Denisov, A. Y.; Naim, M.; Gehring, K.; Arya, P. *Bioorg. Med. Chem.* **2008**, *16*, 7443.
14. *Aminoglycoside Antibiotics*; Arya, D. P., Ed.; John Wiley & Sons; Hoboken, NJ, 2007.
15. He, H.; Williamson, R. T.; Shen, B.; Graziani, E. I.; Yang, H. Y.; Sakya, S. M.; Petersen, P. J.; Carter, G. T. *J. Am. Chem. Soc.* **2002**, *124*, 9729.
16. *Rang and Dale's Pharmacology (6th ed.)*; Rang, H. P.; Dale, M. M.; Ritter, J. M.; Flower, R. J.; Churchill Livingstone Elsevier; Philadelphia, PA, 2007.
17. a) Dagousset, G.; Drouet, F.; Masson, G.; Zhu, J. *Org. Lett.* **2009**, *11* 5546. b) Vesely, J.; Ibrahim, I.; Rios, R.; Zhao, G.; Xu, Y.; Cordova, A. *Tetrahedron Lett.* **2007**, *48*, 2193. c) Zhao, C.; Liu, L.; Wang, D.; Chen, Y. *Eur. J. Org. Chem.* **2006**, *13*, 2977. d) Merla, B.; Risch, N. *Synthesis* **2002**, *10*, 1365. e) Wu, P.; Lin, D.; Lu, X.; Zhou, L.; Sun, J. *Tetrahedron Lett.* **2009**, *50* 7249. f) Matsubara, R.; Kobayashi, S. *Acc. Chem. Res.* **2010**, *41*, 292. G) Robak, M. T.; Herbage, M. A.; Ellman, J. A. *Chem. Rev.* **2010**, *110*, 3600. h) Lanter, J. C.; Chen, H.; Zhang, X.; Sui, Z. *Org. Lett.* **2005**, *7*, 5905.
18. Martjuga, M.; Belyakov, S.; Liepinsh, E.; Suna, E. *J. Org. Chem.* **2011**, *76*, 3635 and references therein.
19. a) Hou, X.; Luo, Y.; Yuan, K.; Dai, L.; *J. Chem. Soc., Perkin, Tans. 1* **2002**, *12*, 1487. b) Kiss, L.; Mangelinckx, S.; Sillanpaae, R.; Fueleop, F.; DeKimpe, N. *J. Org. Chem.* **2007**, *72*, 7199.
20. For selected references, see: a) Espino, C. G.; When, P. M.; Chow, J.; Du Bois, J. *J. Am. Chem. Soc.* **2001**, *123*, 6935. b) Kurokawa, T.; Kim, M.; Du Bois, J. *Angew. Chem. Int. Ed.* **2009**, *48*, 2777. c) Liang, C.; Robert-Peillard, F.; Fruit, C.; Mueller, P.; Dodd, R. H.; Dauban, P. *Angew. Chem. Int. Ed.* **2006**, *45*, 4641.
21. Armarego, W.L.F.; Chai, C.L.L. *Purification of Laboratory Chemicals* 6th ed., Elsevier: Burlington, MA, 2009.
22. Still, W. C.; Kahn, M.; Mitra, A. *J. Org. Chem.* **1978**, *43*, 2923.

1.9 Experimental Details and Characterization.

1.9.1. General Experimental Information.

All glassware was either oven-dried overnight at 130 °C or flame-dried under a stream of dry nitrogen prior to use. Unless otherwise specified, reagents were used as obtained from the vendor without further purification. Tetrahydrofuran and diethyl ether were freshly distilled from purple Na/benzophenone ketyl. Dichloromethane, acetonitrile and toluene were dried over CaH₂ and freshly distilled prior to use. All other solvents were purified in accordance with "Purification of Laboratory Chemicals".²¹ Analytical thin layer chromatography (TLC) was performed utilizing pre-coated silica gel 60 F₂₅₄ plates containing a fluorescent indicator, while preparative chromatography was performed using SilicaFlash P60 silica gel (230-400 mesh) via

Still's method.²² Unless otherwise stated, the mobile phases for column chromatography were mixtures of hexanes/ethyl acetate. Columns were typically run using a gradient method, beginning with 100% hexanes and gradually increasing the polarity using ethyl acetate. Various stains were used to visualize reaction products, including *p*-anisaldehyde, KMnO₄, ceric ammonium nitrate and phosphomolybdic acid in ethanol stain.

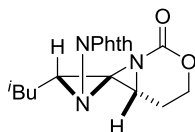
¹H NMR and ¹³C NMR spectra were obtained using Bruker-300, Varian Inova-500, Varian Unity-500 or Varian Inova-600 NMR spectrometers. For ¹H NMR, chemical shifts are reported relative to residual protiated solvent peaks (δ 7.26, 2.49, 7.15 and 4.80 ppm for CDCl₃, (CD₃)₂SO, C₆D₆ and CD₃OD respectively). ¹³C NMR spectra were measured at either 125 MHz or 150 MHz on the same instruments noted above for recording ¹H NMR spectra. Chemical shifts were again reported in accordance to residual protiated solvent peaks (δ 77.0, 39.5, 128.0 and 49.0 ppm for CDCl₃, (CD₃)₂SO, C₆D₆, and CD₃OD, respectively). IR spectral data were obtained using a Bruker Vector 22 spectrometer using either a thin film or an ATR adapter. Melting points were obtained with a Mel-Temp II (Laboratory Devices, Inc.) melting point apparatus. High-pressure liquid chromatography (HPLC) analyses were performed at 224 and 254 nm using Shimadzu HPLC, Model LC-20AB. An AD-H column (4.6 μ m diameter x 258 mm) at a temperature of 40 °C was employed, using a flow rate of 1 mL/min and a gradient starting at 10% isopropanol in hexanes for 10 min and increasing to 30% isopropanol in hexanes. The eluant was then held at 30% isopropanol in hexanes until the run was completed. Accurate mass measurements were acquired at the University of Wisconsin, Madison using a Micromass LCT (electrospray ionization, time-of-flight analyzer or electron impact methods). The NMR and Mass Spectrometry facilities are funded by the NSF (CHE-9974839, CHE-9304546, CHE-9208463, CHE-9629688) and the University of Wisconsin, as well as the NIH (RR08389-01).

1.9.2. Synthesis of 1,4-Diazaspiro[2.2]pentane Substrates.

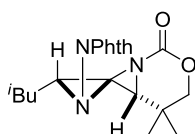
The following compounds were prepared according to procedures reported in a previous publication: **1.22**, **1.23**, **1.24**, **1.26**, **1.27a**, **1.29a**, **1.31a**, **1.32a**.¹⁰

General Procedure. To a mixture of the allenic carbamate (1.0 mmol, 1.0 equiv), Rh₂(TPA)₄ or Rh₂esp₂ catalyst (0.025 mmol, 0.025 equiv) and 4Å molecular sieves (500 mg), 10 mL of dry dichloromethane was added. The solution was allowed to stir 10 min to achieve uniformity and PhIO (2.0 mmol, 2.0 equiv) was added in a single portion. The solution was monitored by TLC until complete consumption of the carbamate starting material was indicated, typically 2-4 h. The mixture was then cooled to 0 °C and treated with *N*-aminophthalimide (1.5 mmol, 1.5 equiv) and dry potassium carbonate (3.5 mmol, 3.5 equiv), followed by PhIO as the oxidant (1.6 mmol, 1.6 equiv). The resulting light yellow slurry was allowed to warm slowly to rt and monitored carefully by TLC. When reaction was complete, the dichloromethane was removed under reduced pressure on a vacuum line, the residue diluted with EtOAc and the organics decanted. The residual salts were washed two more times with EtOAc and the volatiles removed under reduced pressure on a vacuum line. A silica gel column was packed using 99.5:0.5 hexanes/triethylamine, followed by flushing with four column volumes of hexanes prior to loading the sample onto the column to improve the separation and prevent the decomposition of sensitive DASPs. The residue was loaded onto the column and eluted using a hexanes/ethyl acetate gradient. Phenyl iodide eluted first from the column, followed by unreacted MA (if present), then the desired 1,4-diazaspiro[2.2]pentane(s) and finally, *N*-aminophthalimide/hydrolysis products and/or products arising from DASP ring-opening. The DASPs were stored in a freezer at -20 °C. It was best to run NMRs in deuterated benzene if the

sample was to be recovered, as any residual acid in the CDCl_3 caused decomposition of the product.



Compound 1.30a. The product was isolated in 20% overall yield as an off-white solid from the corresponding allenic carbamate. The crude reaction mixture included C-H amination products and unreacted *Z* methylene aziridine. $^1\text{H-NMR}$: (499.9 MHz, CDCl_3) δ 7.78 (dd, $J = 5.7, 3.1$ Hz, 2H), 7.69 (dd, $J = 5.7, 3.1$ Hz, 1H), 4.59 (ddd, $J = 13.4, 11.1, 1.6$ Hz, 1H), 4.40 (ddd, $J = 10.5, 3.8, 1.6$ Hz, 1H), 4.02 (ddd, $J = 8.6, 4.8, 0.6$ Hz, 1H), 3.88 (dd, $J = 9.1, 6.8$ Hz, 1H), 2.45 (ddt, $J = 14.7, 6.7, 2.2$ Hz, 1H), 2.13 (sep, $J = 6.8$ Hz, 1H), 1.74-1.62 (overlapping signals, 3H), 1.13 (d, $J = 6.5$ Hz, 3H), 1.05 (d, $J = 6.5$ Hz, 3H). $^{13}\text{C-NMR}$: (125.7 MHz, acetone- d_6) δ 164.58, 157.22, 134.35, 130.48, 122.84, 68.96, 66.73, 43.76, 42.34, 38.19, 26.19, 22.44, 22.17, 21.79. HRMS (ESI) m/z calculated for $\text{C}_{18}\text{H}_{19}\text{N}_3\text{O}_4$ $[\text{M} + \text{H}]^+$ 342.1449, found 342.1455.

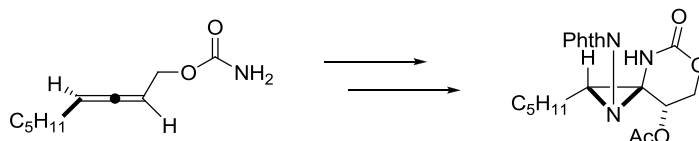


Compound 1.32a. The product was obtained in 31% overall yield as an off-white solid from the corresponding allenic carbamate. Much of the remaining mass was unreacted *Z* methylene aziridine. $^1\text{H-NMR}$: (499.9 MHz, CDCl_3) δ 7.78 (dd, $J = 5.4, 3.1$ Hz, 2H), 7.69 (dd, $J = 5.5, 3.0$ Hz, 2H), 4.37 (d, $J = 10.6$ Hz, 1H), 4.26 (dd, $J = 10.6, 3.2$ Hz, 1H), 3.82 (d, $J = 10.6$ Hz, 1H), 3.70 (s, 1H), 2.27 (sep of t, $J = 6.7, 2.1$ Hz, 1H), 1.68 (ddd, $J = 14.2, 8.6, 2.9$ Hz, 1H), 1.50 (ddd, $J = 14.5, 10.5, 4.3$ Hz, 1H), 1.32 (s, 3H), 1.19 (d, $J = 6.6$ Hz, 3H), 1.06 (d, $J = 6.6$ Hz, 3H), 0.97 (s, 3H); $^{13}\text{C-NMR}$: (125.7 MHz, CDCl_3) δ 167.97, 160.11, 136.97, 136.76, 133.14, 126.25, 125.87,

80.68, 79.95, 79.69, 79.44, 67.67, 53.91, 47.32, 43.44, 32.29, 28.57, 26.76, 26.11, 24.72, 23.86; HRMS (ESI) m/z calculated for $C_{20}H_{23}N_3O_4Na$ $[M + Na]^+$ 392.1581, found 392.1589.

1.9.3. Synthesis of Ring-Opened DASPs.

General Procedure for Acetic Acid DASP Ring Openings: The DASP was dissolved in enough THF to prepare a 0.1 M solution and cooled to 0 °C. Glacial acetic acid (20.0-25.0 equivalents) was added dropwise to the reaction mixture over 2 min, ensuring that the reaction temperature remained at 0 °C. The reaction was warmed to room temperature and monitored by TLC until complete (24-36 h). After complete consumption of the starting material was indicated by TLC, the reaction mixture was concentrated under reduced pressure and purified *via* column chromatography (hexanes/ethyl acetate gradient) to afford the desired ring-opened DASP as white solids.



Compound S1.1. To a mixture of the allenic carbamate⁸ (1.0 mmol, 1.0 equiv), $Rh_2(TPA)_4$ or Rh_2esp_2 catalyst (0.025 mmol, 0.025 equiv) and 4Å molecular sieves (500 mg), 10 mL of dry dichloromethane was added. The solution was allowed to stir 10 min to achieve uniformity and PhIO (2.0 mmol, 2.0 equiv) was added in a single portion. The mixture was allowed to stir four hours to ensure complete the methylene aziridine formation, then cooled to 0 °C. PhthNNH₂ was added, followed by $PhI(OAc)_2$ and K_2CO_3 . The mixture was stirred for 19 h and then was concentrated under reduced pressure. The mixture was redissolved in EtOAc and decanted. The residual salts were washed two more times with EtOAc, and the volatiles were removed under reduced pressure. The residue was loaded onto a silica gel column and eluted using a

hexanes/ethyl acetate gradient. The *N, N*-aminal **12** was obtained in 15% overall yield as a white solid from the corresponding allenic carbamate (estimated 38% yield methylene aziridine formation, 39% diaziridine formation and ring-opening). ¹H-NMR: (500.2 MHz, CDCl₃) δ 7.82 (dd, *J* = 5.4, 3.2 Hz, 2H), 7.75 (dd, *J* = 5.4, 3.2 Hz, 2H), 6.47 (s, 1H), 4.63 (dd, *J* = 9.2, 3.0 Hz, 1H), 4.44 (t, *J* = 8.6 Hz, 1H), 3.88 (dd, *J* = 8.4, 3.0 Hz, 1H), 3.66 (t, *J* = 6.5 Hz, 1H), 1.99 (s, 3H), 1.78-1.59 (m, 4H), 1.44-1.34 (m, 4H), 0.93 (t, *J* = 6.8 Hz, 3H). ¹³C-NMR: (125.7 MHz, CDCl₃) δ 170.33, 165.69, 159.73, 134.70, 130.21, 123.67, 74.74, 65.66, 56.25, 53.43, 31.64, 28.93, 26.22, 22.59, 20.84, 14.17. HRMS (ESI) *m/z* calculated for C₂₀H₂₃N₃O₆ [M + Na]⁺ 424.1480, found 424.1495.

1.9.4. Rearrangements of Ring-Opened DASPs to 1,3-Diaminated Ketones.

General Procedure for Rearrangements of Ring-Opened DASPs to 1,3-Diaminated

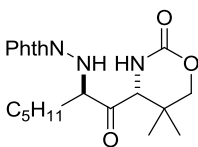
Ketones: The ring-opened DASP was dissolved in enough THF to prepare a 0.1 M solution and 0.05 equivalents of Bi(OTf)₃ were added. The reaction was monitored by TLC and was generally completed in 3-4 h. The reaction was quenched with deionized H₂O and the mixture was extracted with EtOAc, dried over Na₂SO₄, concentrated under reduced pressure and immediately purified via column chromatography to afford the desired 1,3-diaminated ketones as white solids.

General Procedure for One-pot Ring-Opening/Rearrangements of DASPs to 1,3-

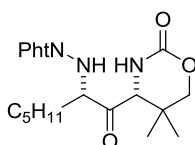
Diaminated Ketones. Procedure A: The DASP was dissolved in enough THF to prepare a 0.1 M solution and cooled to 0 °C. Glacial acetic acid (20.0-25.0 equiv) was added dropwise to the reaction mixture over 2 min, ensuring that the reaction temperature remained at 0 °C. The reaction was warmed to room temperature and brought to reflux at 35 °C. For some substrates, a DASP decomposition product was formed upon heating and reactions were conducted at room temperature. Reactions were monitored by TLC and, upon completion, the reaction was cooled

to room temperature and 0.05 equiv $\text{Bi}(\text{OTf})_3$ was added to the mixture. The reaction was monitored by TLC and was generally completed in 3-4 h. The reaction was quenched with deionized H_2O and the mixture was extracted with EtOAc, dried over Na_2SO_4 , concentrated under reduced pressure and immediately purified via column chromatography to afford the desired 1,3-diaminated ketones as white solids.

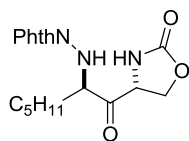
Procedure B: For some substrates, a mixture of diastereomers was observed when rearrangements were conducted in the presence of acetic acid. The DASP was dissolved in enough THF to prepare a 0.1 M solution and cooled to 0 °C. Glacial acetic acid (20.0-25.0 equiv) was added dropwise to the reaction mixture over 2 min, ensuring that the reaction temperature remained at 0 °C. The reaction was warmed to room temperature and brought to reflux at 35 °C. For some substrates, a DASP decomposition product was formed upon heating and reactions were conducted at room temperature. Reactions were monitored by TLC and, upon completion, were cooled to room temperature and quenched with NaHCO_3 . The resulting mixture was extracted with EtOAc, washed with H_2O , dried over Na_2SO_4 and concentrated under reduced pressure. The resulting mixture was redissolved in enough THF to form a 0.1 M solution, and 0.05 equivalents $\text{Bi}(\text{OTf})_3$ were added. The reaction was monitored by TLC and was generally completed in 3-4 h. The reaction was quenched with deionized H_2O and the reaction mixture was extracted with EtOAc, dried over Na_2SO_4 , concentrated under reduced pressure and immediately purified *via* column chromatography to afford the desired 1,3-diaminated ketones as white solids.



Compound 1.25. The product was obtained in 96% yield as a white solid from the ring-opened DASP **1.26** using general procedure A.¹⁰ ¹H-NMR: (300.1 MHz, acetone-d₆) δ 7.89-7.83 (m, 4H), 6.71 (br s, 1H), 5.72 (d, *J* = 4.8 Hz, 1H), 4.43 (d, *J* = 2.4 Hz, 1H), 4.20 (q, *J* = 5.4 Hz, 1H), 4.04 (d, *J* = 11.4 Hz, 1H), 3.89 (d, *J* = 11.4 Hz, 1H), 1.86-1.71 (m, 1H), 1.68-1.54 (m, 1H), 1.54-1.42 (m, 1H), 1.38-1.24 (overlapping multiplet and singlet, 8H), 1.04 (s, 3H), 0.92-0.85 (m, 3H). ¹³C-NMR: (125.7 MHz, CDCl₃) δ 206.15, 166.68, 152.97, 134.60, 129.88, 123.71, 77.31, 77.16, 77.06, 76.80, 75.22, 66.37, 65.63, 31.71, 31.69, 29.55, 26.48, 25.34, 23.43, 22.38, 19.29, 13.95. HRMS (ESI) *m/z* calculated for [C₂₁H₂₇N₃O₅ + Na⁺] 424.1843, found 424.1843.

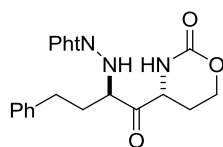


Compound 1.27b. The product was obtained in 90% yield (average of two runs) from DASP **1.27a** general procedure A. ¹H-NMR: (499.9 MHz, CDCl₃) δ 7.83 (dd, *J* = 5.4, 3.0 Hz, 2H), 7.76 (dd, *J* = 5.4, 3.0 Hz, 2H), 6.17 (br s, 1H), 5.06 (br s, 1H), 4.66 (d, *J* = 1.7 Hz, 1H), 4.00 (d, *J* = 10.9 Hz, 1H), 3.90 (d, *J* = 10.9 Hz, 1H), 3.65 (td, *J* = 6.7, 5.0 Hz, 1H), 1.80-1.57 (m, 2H), 1.40-1.24 (overlapping singlet and multiplets, 9H), 0.99 (s, 3H), 0.89 (t, *J* = 6.9 Hz, 3H). ¹³C-NMR: (125.7 MHz, CDCl₃) δ 206.10, 166.92, 134.93, 129.96, 124.05, 74.39, 68.28, 65.26, 31.88, 31.59, 28.25, 26.06, 24.73, 22.61, 20.39, 14.15. HRMS (ESI) *m/z* calculated for [C₂₁H₂₇N₃O₅ + Na⁺] 402.2024, found 402.2030.

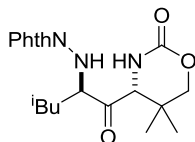


Compound 1.28b. The product was obtained in 78% yield from ring-opened DASP **S1.1** using general procedure B. ¹H-NMR: (500.2 MHz, CDCl₃) δ 7.85 (dd, *J* = 5.6, 3.1 Hz, 2H), 7.77 (dd, *J*

= 5.6, 3.1 Hz, 2H), 7.05 (s, 1H), 5.01 (dd, $J = 9.5, 5.6$ Hz, 1H), 4.95 (d, $J = 5.6$ Hz, 1H), 4.62 (t, $J = 9.5$ Hz, 1H), 4.47 (dd, $J = 9.5, 5.6$ Hz, 1H), 3.83 (q, $J = 6.4$ Hz, 1H), 1.80-1.70 (m, 2H), 1.42-1.28 (m, 6H), 0.91-0.86 (m, 3H). $^{13}\text{C-NMR}$: (125.7 MHz, CDCl_3) δ 208.93, 169.35, 161.58, 137.48, 132.39, 126.55, 69.99, 68.89, 59.71, 34.23, 32.07, 27.92, 25.00, 16.57. HRMS (ESI) m/z calculated for $\text{C}_{18}\text{H}_{21}\text{N}_3\text{O}_5$ [$\text{M}+\text{H}^+$] 360.1554, found 360.1549.

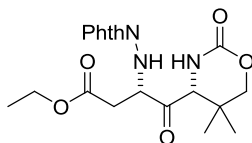


Compound 1.29b. Obtained in 60% yield from DASP **1.29a** as an off-white solid using general procedure B. $^1\text{H-NMR}$: (499.9 MHz, CDCl_3) δ 7.85 (dd, $J = 5.5, 3.1$ Hz, 2H), 7.77 (dd, $J = 5.5, 3.1$ Hz, 2H), 7.31-7.27 (m, 2H), 7.22-7.18 (m, 3H), 6.25 (br s, 1H), 5.06 (d, $J = 6.2$ Hz, 1H), 4.56 (ddd, $J = 7.5, 6.0, 1.9$ Hz, 1H), 4.26 (ddd, $J = 7.1, 3.9, 2.6$ Hz, 2H), 3.97 (q, $J = 6.2$ Hz, 1H), 2.82 (t, $J = 7.7$ Hz, 2H), 2.25 (m, 1H) 2.16-1.99 (m, 3H), $^{13}\text{C-NMR}$: (125.7 MHz, CDCl_3) δ 208.87, 169.21, 137.41, 132.45, 131.38, 131.22, 129.21, 126.51, 79.93, 79.68, 79.42, 79.20, 79.10, 68.08, 67.40, 59.05, 34.85, 34.42, 32.98, 26.17. HRMS (ESI) m/z calculated for $\text{C}_{22}\text{H}_{21}\text{N}_3\text{O}_5$ [$\text{M}+\text{H}^+$] 408.1554, found 408.1554.

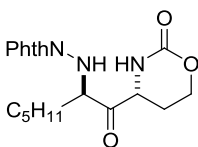


Compound 1.30b. The product was obtained in 77% yield from DASP **1.20a** as a white solid using general procedure A. $^1\text{H-NMR}$: (499.9 MHz, CDCl_3) δ 7.84 (dd, $J = 5.5, 3.0$ Hz, 2H), 7.76 (dd, $J = 5.5, 3.0$ Hz, 2H), 6.91 (br s, 1H), 5.11 (d, $J = 4.9$ Hz, 1H), 4.24 (d, $J = 1.3$ Hz, 1H), 4.10 (ddd, $J = 10.8, 6.0, 5.1$ Hz, 1H), 3.98 (s, 2H), 1.87 (sep, $J = 6.6$ Hz, 1H), 1.55 (ddd, $J = 14.1, 7.0, 6.3$ Hz, 1H), 1.50 (ddd, $J = 14.1, 7.0, 6.3$ Hz, 1H), 1.21 (s, 3H), 1.00 (s, 3H), 0.96 (d, $J = 6.6$ Hz,

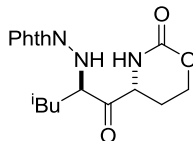
6H). $^{13}\text{C-NMR}$: (125.7 MHz, CDCl_3) δ 208.82, 169.32, 155.44, 137.33, 132.48, 126.46, 79.93, 79.89, 79.68, 79.42, 78.05, 73.28, 68.42, 67.10, 40.98, 34.42, 27.08, 25.96, 25.51, 24.96, 21.93. HRMS (ESI) m/z calculated for $\text{C}_{20}\text{H}_{25}\text{N}_3\text{O}_5$ $[\text{M}+\text{H}^+]$ 390.2024, found 390.2032.



Compound 1.31b. The product was obtained in 65% yield as a yellow solid from ring opened DASP **1.31a** using general procedure B. $^1\text{H-NMR}$: (299.9 MHz, acetone- d_6) δ 7.89 (s, 4H), 6.13 (d, $J = 6.2$ Hz, 1H), 6.04 (br s, 1H), 5.22 (dd, $J = 2.2, 0.7$ Hz, 1H), 4.38 (ddd, $J = 11.1, 6.2, 4.9$ Hz, 1H), 4.08 (q, $J = 7.1$ Hz, 2H), 4.01 (d, $J = 11.0$ Hz, 1H), 3.90 (d, $J = 11.0$ Hz, 1H), 3.00-2.82 (m, 2H), 1.38 (s, 3H), 1.20 (t, $J = 7.1$ Hz, 3H), 1.05 (s, 3H). $^{13}\text{C-NMR}$ (75.4 MHz, acetone- d_6) δ 206.83, 171.19, 167.35, 152.19, 134.88, 130.50, 123.49, 73.79, 64.29, 62.76, 60.47, 33.21, 31.05, 23.74, 19.30, 13.75. HRMS (ESI) m/z calculated for $\text{C}_{20}\text{H}_{23}\text{N}_3\text{O}_7$ $[\text{M}+\text{Na}^+]$ 440.1429, found 440.1440.



Compound 1.32b. The product was obtained in 89% yield from the corresponding ring-opened DASP¹⁰ and in 81% from the DASP **1.32a** as a white solid using general procedure A. $^1\text{H-NMR}$ (300 MHz, CDCl_3), δ 7.86 (m, 4H), 6.39 (br s, 1H), 4.90 (d, $J = 4.7$ Hz, 1H), 4.76 (ddd, $J = 7.5, 5.5, 1.8$ Hz, 1H), 4.33 (dd, $J = 5.5, 5.5$ Hz, 2H), 3.90 (m, 1H), 2.39 (m, 1H), 2.05 (m, 1H), 1.74 (m, 2H), 1.33 (m, 6H), 0.90 (m, 3H). $^{13}\text{C-NMR}$ (75.4 MHz, CDCl_3) δ 206.55, 166.77, 153.46, 134.86, 129.99, 123.95, 66.88, 65.00, 56.14, 31.73, 30.69, 25.65, 23.72, 22.54, 14.12. HRMS (ESI) m/z calculated for $\text{C}_{19}\text{H}_{23}\text{N}_3\text{O}_5$ $[\text{M}+\text{H}^+]$ 374.1711, found 374.1711.

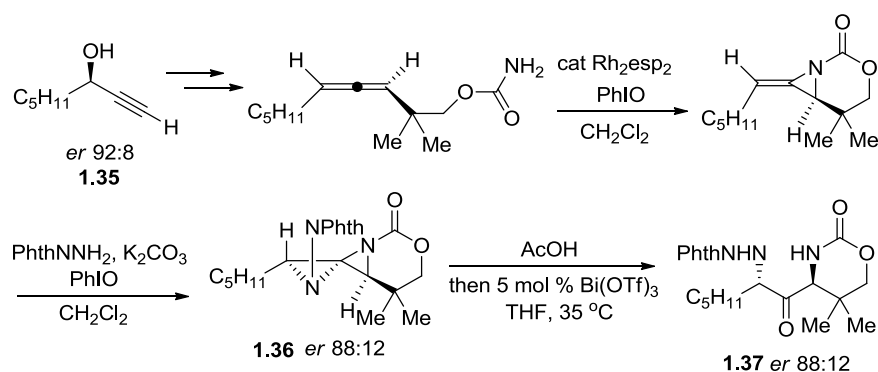


Compound 1.33b. The product was obtained in 57% yield from DASP **1.33a** as a white solid using general procedure B. $^1\text{H-NMR}$: (499.9 MHz, CDCl_3) δ 7.85 (dd, $J = 5.5, 3.4$ Hz, 2H), 7.78 (dd, $J = 5.5, 3.4$ Hz, 2H), 6.27 (br s, 1H), 4.87 (d, $J = 3.9$ Hz, 1H), 4.83 (ddd, $J = 7.7, 5.6, 1.8$ Hz, 1H), 4.38-4.29 (m, 2H), 3.96 (td, $J = 7.5, 3.1$ Hz, 1H), 2.42 (dtd, $J = 13.9, 5.6, 4.5$ Hz, 1H), 2.07-1.99 (m, 1H), 1.85 (sep, $J = 6.9$ Hz, 1H), 1.66-1.55 (m, 2H), 0.99 (d, $J = 6.7$ Hz, 3H), 0.98 (d, $J = 6.7$ Hz, 3H). $^{13}\text{C-NMR}$: (125.7 MHz, CDCl_3) δ 206.62, 166.46, 153.00, 134.75, 129.74, 123.84, 77.25, 76.99, 76.74, 76.50, 65.61, 64.73, 55.62, 39.63, 25.00, 23.92, 22.75, 22.16, -0.04. HRMS (ESI) m/z calculated for $\text{C}_{18}\text{H}_{21}\text{N}_3\text{O}_5$ [$\text{M}+\text{Na}^+$] 382.1374, found 382.1374.

General Procedure for the One-Pot Oxidation of Allenes to 1,3-Diaminated Ketones: To a mixture of the allenic carbamate (1.0 mmol, 1.0 equiv), $\text{Rh}_2(\text{TPA})_4$ or Rh_2esp_2 catalyst (0.025 mmol, 0.025 equiv) and 4\AA molecular sieves (500 mg), 10 mL of dry dichloromethane was added. The solution was allowed to stir 10 min to achieve uniformity and PhIO (2.0 mmol, 2.0 equiv) was added in a single portion. The solution was monitored by TLC until consumption of the carbamate starting material, typically 2-4 h. The mixture was then cooled to $0\text{ }^\circ\text{C}$ and treated with *N*-aminophthalimide (1.5 mmol, 1.5 equiv) and dry potassium carbonate (3.5 mmol, 3.5 equiv), followed by PhIO as the oxidant (1.6 mmol, 1.6 equiv). The resulting light yellow slurry was allowed to warm slowly to rt and monitored carefully by TLC. When reaction was complete, the dichloromethane was removed under reduced pressure on a vacuum line, the residue diluted with EtOAc and the organics decanted. The residual salts were washed two more times with EtOAc and the volatiles removed under reduced pressure on a vacuum line. The mixture was dissolved in enough THF to prepare a 0.1 M solution and cooled to $0\text{ }^\circ\text{C}$. Glacial acetic acid

(20.0-25.0 equivalents) was added dropwise to the reaction mixture over 2 min, ensuring that the reaction temperature remained at 0 °C. The reaction was warmed to room temperature. The reaction was monitored by TLC and, upon completion, was quenched with NaHCO₃. The resulting mixture was extracted with EtOAc, washed with H₂O dried over Na₂SO₄, and concentrated under reduced pressure. The resulting mixture was redissolved in enough THF to form a 0.1 M solution, and 0.05 equivalents Bi(OTf)₃ were added. The reaction was monitored by TLC and was generally completed in 3-4 h. The reaction was quenched with deionized H₂O and the reaction mixture was extracted with EtOAc, dried over Na₂SO₄, concentrated under reduced pressure and immediately purified via column chromatography (hexanes/ethyl acetate gradient) to afford the desired 1,3-diaminated ketones as white solids.

1.9.5. Verification of the Transfer of Axial Chirality from the DASP 1.36 to the 1,3-Diaminated Compound 1.37. The enantioenriched DASP **1.36** was prepared according to literature procedure.¹⁰

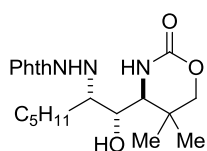


The enantioenriched propargyl alcohol was prepared according to literature procedure.⁴ The same procedure previously reported for the synthesis of racemic DASPs was used to prepare the enantioenriched sample. High-pressure liquid chromatography (HPLC) analyses were performed at 224 and 254 nm using Shimadzu HPLC, Model LC-20AB. An AD-H column (4.6 μm

diameter x 258 mm) at a temperature of 40 °C was employed, using a flow rate of 1 mL/min and a gradient starting at 10% isopropanol in hexanes for 10 min and increasing to 30% isopropanol in hexanes. The eluant was then held at 30% isopropanol in hexanes until the run was completed. The reaction for the conversion of **1.36** to **1.37** followed the general procedure and the HPLC was run in the same manner as described above.

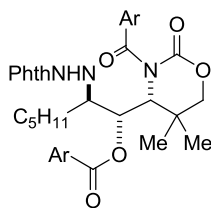
1.9.6. Reductions of 1,3-Diaminated Ketones.

General Procedure: The 1,3-diaminated ketone was dissolved in enough dichloromethane to make a 0.01 M solution. Glacial acetic acid (5.0 equiv) was added and the mixture was allowed to stir for 30 min. Portions of Na(OAc)₃BH (3.0 equiv) were added at hourly intervals, and the reaction was sonicated for 30 min after each addition. Typically, 6-7 portions were required to bring the reaction near completion, while further additions had little effect on yield. The reaction mixture was quenched with saturated NaHCO₃, extracted with dichloromethane, and purified via column chromatography (hexanes/ethyl acetate gradient) to yield the desired 1,3-diaminated alcohol.

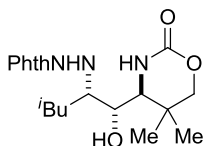


Compound 1.38. Obtained as a white powder from diaminoketone **1.25** in 70% yield as a 9:1 mixture of diastereomers. ¹H-NMR: (499.9 MHz, acetone-d₆) δ 7.88 (s, 4H), 7.09 (s, 1H), 5.13 (d, *J* = 8.5 Hz, 1H), 4.31 (d, *J* = 6.9 Hz, 1H), 3.91 (d, *J* = 11.4 Hz, 1H), 3.88 (ddd, *J* = 8.7, 6.8, 2.0 Hz, 1H), 3.81 (d, *J* = 11.4 Hz, 1H), 3.46 (dd, *J* = 9.0, 2.1 Hz, 1H), 3.25 (tdd, *J* = 8.4, 5.5, 2.0 Hz, 1H), 1.84-1.75 (m, 1H), 1.61 (m, 1H), 1.51-1.42 (m, 1H), 1.38-1.22 (m, 5H), 1.20 (s, 3H), 1.15 (s, 3H), 0.85-0.81 (t, 3H). ¹³C-NMR: (125.7 MHz, acetone-d₆) δ 208.06, 207.90, 207.75,

169.35, 154.87, 137.11, 133.15, 125.77, 76.74, 72.67, 64.56, 63.37, 34.61, 33.48, 32.16, 32.07, 32.01, 31.92, 31.86, 31.76, 31.61, 31.45, 31.30, 31.15, 28.34, 26.91, 25.00, 21.80, 16.04. HRMS (ESI) m/z calculated for $C_{21}H_{29}N_3O_5$ $[M+H]^+$ 404.2180, found 404.2175.

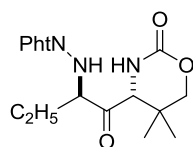


Compound 1.39. The alcohol **1.38** (10.0 mg, 0.025 mmol, 1 equiv) was dissolved in 0.5 mL of dichloromethane and treated with *p*-nitrobenzoyl chloride (91.6 mg, 0.50 mmol, 20 equiv) and triethylamine (0.50 mmol, 20 equiv). The reaction mixture was stirred at rt for 48 h, then quenched with 15% NaOH solution. The mixture was extracted with portions of dichloromethane, the combined organics washed with brine, dried over Na_2SO_4 and the volatiles removed under reduced pressure. The residue was purified twice by column chromatography (hexanes/ethyl acetate gradient). The resulting solid was dissolved in a minimum amount of ethyl acetate in a vial. The vial was placed inside a larger vial containing pentane; vapor diffusion provided X-ray quality crystals of **1.39**. The structure was verified by X-ray crystallography (see below).

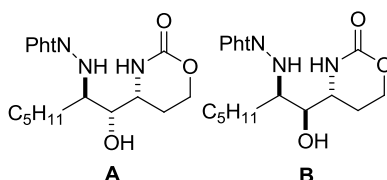


Compound 1.40. The product was obtained as a white powder from the 1,3-diamino-2-one **1.33b** in 66% yield as a 9:1 mixture of diastereomers. 1H -NMR: (499.9 MHz, $CDCl_3$) δ 7.88 (dd, $J = 5.5, 3.1$ Hz, 2H), 7.76 (dd, $J = 5.5, 3.1$ Hz, 2H), 7.17 (br s, 1H), 4.70 (d, $J = 8.8$ Hz, 1H), 3.90 (d, $J = 11.0$ Hz, 1H), 3.83 (d, $J = 11.0$ Hz, 1H), 3.71 (ddd, $J = 8.3, 5.9, 1.7$ Hz, 1H), 3.41 (dd, $J =$

8.9, 2.4 Hz, 1H), 3.33-3.26 (m, 1H), 1.95 (d, $J = 6.0$ Hz, 1H), 1.71-1.58 (m, 2H), 1.46-1.38 (m, 1H), 1.25 (s, 3H), 1.15 (s, 3H), 0.95 (d, $J = 6.5$ Hz, 3H), 0.83 (dd, $J = 6.5$ Hz, 3H). ^{13}C -NMR: (125.7 MHz, CDCl_3) δ 169.51, 137.23, 132.68, 126.52, 79.93, 79.67, 79.42, 79.06, 78.97, 78.86, 78.05, 76.97, 73.99, 63.42, 61.75, 41.47, 33.64, 27.70, 27.54, 26.12, 24.72, 22.67. HRMS (ESI) m/z calculated for $[\text{C}_{21}\text{H}_{27}\text{N}_3\text{O}_5+\text{H}^+]$ 404.2180, found 404.2175.



Compound S1.2. Obtained as a white powder from the corresponding ring-opened DASP in 57% yield. ^1H -NMR: (299.9 MHz, CDCl_3) δ 7.85 (m, 2H), 7.76 (m, 2H), 6.81 (br s, 1H), 5.08 (d, 1H), 4.21 (d, 1H), 4.03 – 3.94 (overlapping multiplets, 3H), 1.89-1.65 (overlapping multiplets, 2H), 1.23 (s, 3H), 1.04 (s, 3H), 1.02 (t, 3H); ^{13}C NMR: (125.8 MHz, CDCl_3) δ 205.79, 166.85, 152.90, 134.89, 130.06, 124.01, 75.68, 67.81, 66.29, 32.12, 26.73, 23.51, 22.94, 19.39; HRMS (ESI) m/z calculated for $\text{C}_{18}\text{H}_{21}\text{N}_3\text{O}_5$ $[\text{M}+\text{Na}^+]$ 382.1374, found 382.1371.



Compound 1.41. Obtained as an inseparable 1.7:1 mixture of diastereomers from compound **1.32b** in 65% yield. ^1H -MR: (500.2 MHz, CDCl_3) δ 7.90-7.86 (m, 2H, **B**), 7.85-7.81 (m, 2H, **A**), 7.81-7.77 (m, 2H, **B**), 7.76-7.71 (m, 2H, **A**), 6.97 (d, $J = 2.7$ Hz, 1H, **A**), 6.04 (br s, 1H, **B**), 4.95 (d, $J = 8.4$ Hz, 1H, **A**), 4.57 (d, $J = 3.2$ Hz, 1H, **B**), 4.36-4.25 (m, 2H **A**, 2H **B**), 4.18 (td, $J = 12.1$, 1.9 Hz, 1H, **A**), 3.99 (d, $J = 1.9$ Hz, 1H, **B**), 3.89-3.84 (m, 1H, **A**), 3.65-3.54 (m, 1H, **A**, 1H, **B**), 3.29 (d, $J = 8.3$ Hz, 1H, **B**), 3.19 (tdd, $J = 3.0$, 5.1, 8.1 Hz, 1H, **A**), 3.10 (dq, $J = 3.0$, 8.3 Hz, 1H, **B**), 2.19-2.13 (m, 1H **A**, 1H **B**), 1.87-1.17 (m, 9H, **A**, 9H, **B**), 0.93 (t, $J = 7.4$ Hz, 3H, **B**), 0.83 (t,

$J = 5.9$ Hz, 3H, **A**); ^{13}C NMR: (125.8 MHz, CDCl_3) δ 167.69, 167.22, 154.90, 153.92, 135.01, 134.65, 130.27, 130.01, 124.11, 123.85, 73.42, 72.49, 65.26, 64.51, 60.94, 60.37, 52.07, 51.85, 32.16, 31.99, 30.09, 26.52, 25.91, 25.86, 23.87, 23.30, 22.72, 14.21, 14.17; HRMS (ESI) m/z calculated for $\text{C}_{19}\text{H}_{25}\text{N}_3\text{O}_5$ $[\text{M}+\text{H}^+]$ 376.1867, found 376.1874.

**Chapter 2. Stereoselective Synthesis of 1,3-Diamino-2-ols *via* Aminohydroxylation of
Bicyclic Methylene Aziridines.**

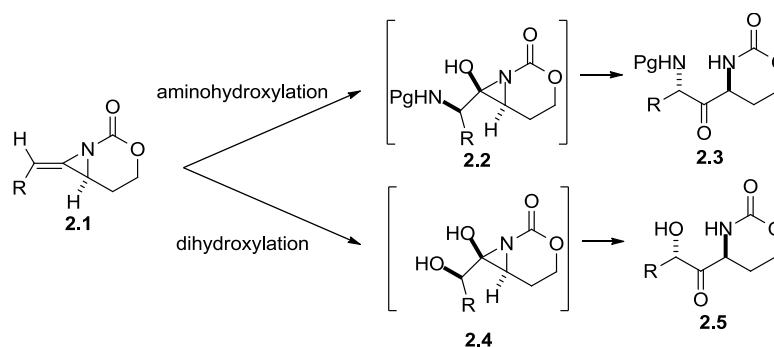
This chapter is adapted from work published previously:

Weatherly, C. D.; Guzei, I. A.; Schomaker, J. M. *Eur. J. Org. Chem.* **2013**, 3667.

2.1. Basic synthetic strategy.

To address the limitations inherent in the first generation synthesis, the direct aminohydroxylation of bicyclic methylene aziridines was investigated as a route to N/O/N stereotriads. This strategy required achieving a stereo- and regioselective aminohydroxylation to form an *N,O*-aminal intermediate capable of selective rearrangement to a 1,3-diamino-2-one **2.3** (Scheme 2.1, top). Our previous reports demonstrated that the convexity of the bicyclic methylene aziridine **2.1** structure rendered transformations of the exocyclic olefin highly diastereoselective. Concurrent with the work described in this chapter, other group members worked toward the development of diastereoselective dihydroxylation of bicyclic methylene aziridines (Scheme 2.1, bottom); their early success in developing this transformation offered further validation of the aminohydroxylation strategy.¹

Scheme 2.1. Difunctionalizations of bicyclic methylene aziridines.

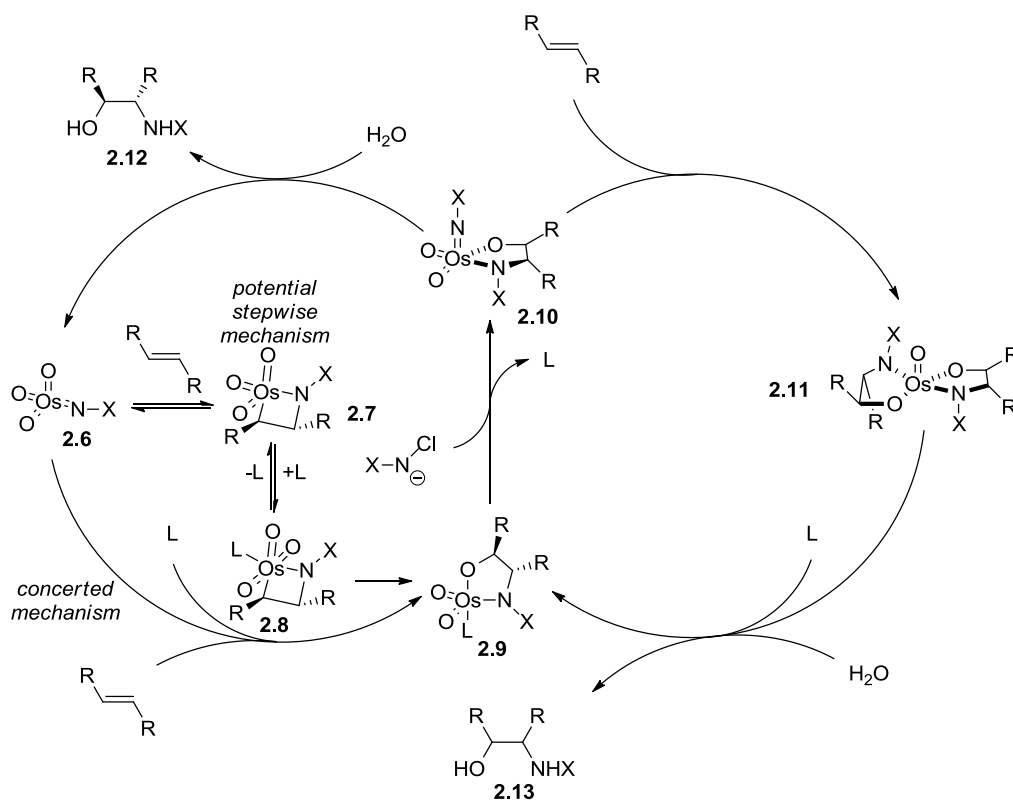


2.2. Catalytic aminohydroxylation of olefins.

Achieving catalytic aminohydroxylation or oxyamination of olefins requires overcoming inherent difficulties in entropy, diastereoselectivity, and regioselectivity. A suitable method for oxyamination of methylene aziridines would deliver both the oxygen and nitrogen atoms intermolecularly, and would provide the oxygen atom as an unprotected hydroxyl group. Though

many oxyaminations of alkenes have been reported,² only the Sharpless method of aminohydroxylation met these important criteria.^{3,4}

First disclosed in 1976, this method uses an osmium catalyst and chloramine salt in the presence of water to transform an olefin to an *N*-protected amino alcohol. Several modifications in procedure were subsequently reported, improving the scope of nitrogen sources and operational efficiency. With the disclosure of the asymmetric variant, a mechanistic proposal was offered for the transformation, based on analogy to the mechanism of the asymmetric dihydroxylation reaction. In this proposal, two distinct catalytic cycles are thought to be simultaneously operable, with the first cycle providing high enantioselectivity (Scheme 2.2, left), and the second cycle providing low enantioselectivity (Scheme 2.2, right).^{2f} In the first cycle, an imidoosmium species **2.6** reacts with an olefin in a direct, formal [3+2] cycloaddition, or in a formal [2+2] cycloaddition, followed by [1,2]-migration;^{2g} each process yields osmium(VI) azaglycolate **2.9**. Reoxidation by a chloramine provides imidiotrioosmium (VIII) glycolate **2.10**. Hydrolysis by water yields the aminohydroxylation product **2.12** and regenerates imidoosmium species **2.6**. Alternatively, addition of a second equivalent of the olefin leads into the second, unselective cycle, forming bisazaosmium (VI) glycolate **2.11**. Hydrolysis of this intermediate, reported to be slow, also yields the aminohydroxylation product **2.13** with poor enantioselectivity, and regenerates the osmium(VI) azaglycolate **2.9**.

Scheme 2.2. Proposed mechanism of asymmetric aminohydroxylation.**2.3. Optimization of aminohydroxylation of bicyclic methylene aziridines.**

It was envisioned that the racemic version of the aminohydroxylation could be applied to allene-derived bicyclic methylene aziridines, with the convexity of the substrate promoting a highly diastereoselective transformation. Due to its long-term stability and ease of synthesis, methylene aziridine **2.14** was chosen as the primary substrate for the development of the aminohydroxylation. Early experiments investigated the four major sets of conditions initially disclosed by Sharpless. Using H_2O , and either $t\text{BuOH}$ or CH_3CN as co-solvents gave low yields of the desired ketone and significant byproduct formation (entries 1 and 2). Switching the solvent to benzene and employing BnEt_3NBr as a phase transfer catalyst (PTC) gave low conversion, but mainly to the desired product (entry 3). Increasing the temperature of the reaction gave 70%

conversion, but only 25% yield of **2.15** (entry 4). Changing the solvent to chloroform gave the product in both moderate conversion and yield (entry 5). This system was further optimized by increasing the loading of the catalyst from 5 to 7.5 mol % to give full conversion of **2.14** and 81% yield **2.15** (entry 6). The PTC was paramount to the success of the reaction, as its absence (entries 7 and 8) gave no conversion to **2.15**.

Table 2.1. Optimization of aminohydroxylation of methylene aziridines.

Reaction scheme showing the aminohydroxylation of methylene aziridine **2.14** to product **2.15, 2.15a**. Reagents: cat. $K_2OsO_2(OH)_4$, phase transfer catalyst, 3 equiv Chloramine T or B, solvent: H_2O (1:1), heat, 20 h. Product **2.15, 2.15a** has Ar = Tol, Ph.

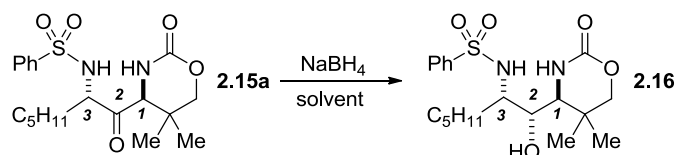
entry	mol% cat.	additive	Chloramine	solvent	temp (°C)	conversion	yield ^a
1	5	none	T	<i>t</i> BuOH	55	100%	0%
2	5	none	T	CH ₃ CN	23	70%	18%
3	5	BnEt ₃ NBr	T	benzene	30	15%	12%
4	5	BnEt ₃ NBr	T	benzene	45	70%	25%
5	5	BnEt ₃ NBr	T	CHCl ₃	33	66%	60%
6	7.5	BnEt₃NBr	T	CHCl₃	33	100%	81%
7	7.5	none	T	CHCl ₃	33	50%	0%
8	7.5	(DHDQ) ₂ PHAL	T	CHCl ₃	33	0%	0%
9	7.5	(DHDQ) ₂ PHAL, BnEt ₃ NBr	T	CHCl ₃	33	100%	43% ^b
10	7.5	BnEt₃NBr	B	CHCl₃	33	100%	74%
11	7.5	BnEt₃NCl	B	CHCl₃	33	100%	79%
12	7.5	BnEt ₃ NCl, 15 mol % pyridine	B	CHCl ₃	33	NA	0%
13	7.5	BnEt ₃ NCl, 15 mol% TMEDA	B	CHCl ₃	33	NA	0%
14	7.5	BnEt ₃ NCl, 8 mol% TMEDA	B	CHCl ₃	33	NA	0%
15	7.5	BnEt ₃ NCl	BocNNaCl	CHCl ₃	33	50%	33%

^a*dr* was > 19:1 unless noted. ^b*dr* was 3:1.

Further improvements to the reaction were investigated. Chloramine B could be used as the nitrogen source to provide **2.15a** in 74 and 79% yield (entries 10 and 11), to provide a product possessing a more labile protecting group. Additionally, BnEt₃Cl could be employed as

the PTC with minimal effect on yield. This additive was somewhat easier to handle than the corresponding bromide salt, and was used in subsequent transformations. Attempts to enhance the reaction rate by using amine additives, including hydroquinidine 1,4-phthalazinediyl diether [(DHDQ)₂PHAL], pyridine, and *N,N,N',N'*-tetramethyl-1,2-ethylenediamine (TMEDA), were unsuccessful (Entries 8, 9, 12-14). The use of BocNNaCl as the nitrogen source (entry 15) resulted in decreased conversion and yield.

Table 2.2. Solvent effects in the reduction of 1,3-diamino-2-ones.



entry	solvent	yield	<i>dr</i>
1 ^[a]	CH ₂ Cl ₂	83%	10:1
2 ^[b]	CHCl ₃	94%	10:1
3 ^[b]	THF	91%	5:1
4 ^[b]	MeOH	87%	1:1

[a] Isolated yield. [b] NMR yield using a mesitylene internal standard.

With these conditions in hand, stereocontrol in the reduction of 1,3-diamino-2-one was investigated. Whereas the previously synthesized diaminoketones possessed a sensitive phthalimide moiety, limiting the possible conditions for reducing the ketone, these second generation substrates could tolerate stronger reducing conditions. Indeed, reduction of **2.15a** with NaBH₄ in CH₂Cl₂ gave 1,3-diamino-2-ol **2.16** in excellent yield and diastereoselectivity (Table 2.2, entry 1). Attempts to conduct the aminohydroxylation and reduction in a single pot gave a comparable overall yield, but a significant decrease in the *dr* (5:1 *dr* single pot, 10:1 *dr* two pots). A series of reduction in solvents of differing polarities (entries 2-4) demonstrated that a greater *dr* was obtained in less polar solvents. The relative 1,2-*anti*/2,3-*syn* stereochemistry of **2.16** was confirmed by X-ray crystallography of a derivative synthesized by condensation of

2.16 with *p*-bromobenzoic acid in the presence of dicyclohexycarbodiimide (DCC) (see Experimental Details below). As in the first generation synthesis, this stereochemistry, as well as the observed solvent effects, are consistent with Felkin-Ahn control of the reduction by the C1 carbon.⁵

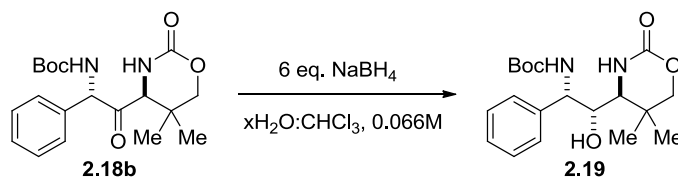
Table 2.3. Optimization of aminohydroxylation of aryl substituted methylene aziridines.

entry	Chloramine	temp (°C)	CHCl ₃ :H ₂ O	yield
1	Chloramine B	22	1:1	28% 2.18a
2	BocNNaCl	22	1:1	28% (37% brsm) ^[a] 2.18b
3	BocNNaCl	30	1:1	47% 2.18b
4	CbzNNaCl	30	1:1	unidentified product
5	BocNNaCl	30	4:1	55% 2.18b

[a] Based on recovered starting material.

2.4. Optimization of aminohydroxylation of aryl-substituted methylene aziridines.

Further optimization of the reaction conditions was required for aminohydroxylation of aryl-substituted methylene aziridines. When methylene aziridine **2.17** was subjected to the aminohydroxylation conditions at room temperature with Chloramine B as the nitrogen source, only 28% of the desired ketone product was obtained (Table 2.3, entry 1). The use of carbamate-derived chloramine salt BocNaCl, common employed for the aminohydroxylation of styrenes, slowed conversion, (Table 2.3, entry 2), giving 28% yield and 37% yield based on recovered starting material at room temperature. Increasing the temperature to 30°C gave full conversion and 47% yield of product (entry 3), while the use of CbzNaCl at 30°C gave full conversion to an unidentified product. Adjustment of the solvent volume ratio to 4:1 CHCl₃:H₂O gave 55% yield of ketone **2.18b**. Less than 10% of the dihydroxylation products were observed; the remaining mass balance consisting of decomposition products.

Table 2.4. Re-optimization of the reduction of aryl-substituted ketones.

entry	H ₂ O:CHCl ₃	conversion ^b	yield
1 ^a	0:100	100%	64%
2	1:10	28%	25%
3	1:4	62%	42%
4	1:1	84%	64%
5 ^c	1:1	100%	88%

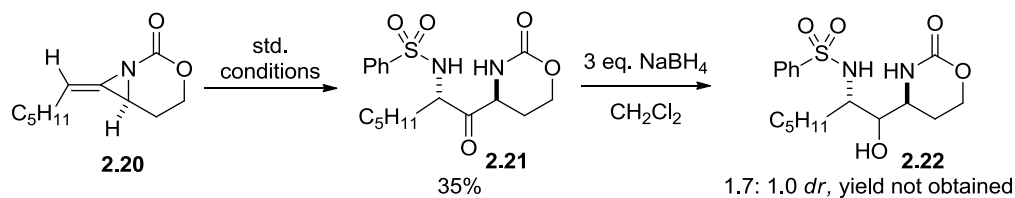
^aResult was not reproducible. ^bConversion and yield after 6 hours. ^cReaction was sonicated.

Reduction of the resulting ketone also required re-optimization. Initially, the standard conditions for reduction of **2.16** were applied, giving the product in 64% yield; however, these results were irreproducible, giving no conversion of starting material in several attempts. It was conjectured that the presence of water during workup might facilitate the reduction, as NaBH₄ is minimally soluble in CHCl₃. The reduction was therefore performed in biphasic mixtures of CHCl₃ and H₂O (Table 2.4). A 10:1 mixture of CHCl₃:H₂O gave 25% yield of the alcohol and 28% conversion after 6 hours. Increasing the amount of H₂O improved conversion (entries 2-4). Finally, sonication of the reaction mixture in 1:1 CHCl₃:H₂O for 6 hours gave the desired product in 88% yield with >19:1 *dr*.

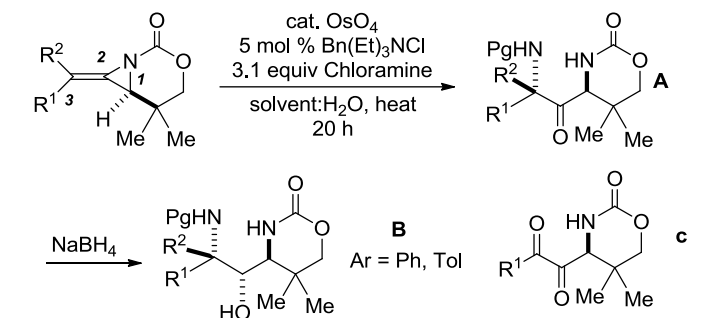
2.5. Scope of Aminohydroxylation/Reduction Sequence.

An important goal in developing this methodology was to successfully transform substrates lacking the geminal dimethyl groups required for stereoselective reduction of first generation substrates. However, difficulty in applying the aminohydroxylation stifled this

Scheme 2.3. Aminohydroxylation and reduction of a methylene aziridine lacking geminal dimethyl groups.



investigation. When the standard aminohydroxylation conditions were applied to methylene aziridine **2.20**, only a 35% yield of product was obtained, with much of the remaining mass balance unidentifiable, possibly due to ring-opening by water (Scheme 2.3). Because of this low yield, conditions for stereoselective reduction were not extensively investigated. Treatment of ketone **2.21** with NaBH_4 in CH_2Cl_2 gave the alcohol **2.22** with only 1.7:1 *dr*. This result is again consistent with the Felkin-Anh control of reduction described for the first generation synthesis.

Table 2.5. Scope of aminohydroxylation/reduction of bicyclic methylene aziridines.

entry	R ¹ , R ²	Cond.	yield A ^a	yield B
1	C ₅ H ₁₁ , H	2.14 A	79%	2.15 83%, 10:1 <i>dr</i> 2.16
2	H, C ₅ H ₁₁	2.23 A	60%	2.31a 83%, 10:1 <i>dr</i> 2.31b
3	<i>i</i> Bu, H	2.24 B	57% ^b	2.32a 94%, 10:1 <i>dr</i> 2.32b
4	TIPSO(CH ₂) ₂ , H	2.25 B	50% ^{b,c}	2.33a 94%, 10:1 <i>dr</i> 2.33b
5	Ph(CH ₂) ₂ , H	2.26 B	57%	2.34a 88%, 10:1 <i>dr</i> 2.34b
6	EtOC(O)CH ₂ , H	2.27 B	< 5% ^d	--- 2.35b
7	Ph, H (Table 3)	2.17 C	55% ^b	2.18b 88%, >19:1 <i>dr</i> 2.19
8	<i>p</i> -MePh, H	2.28 C	53% ^b	2.36a 88%, >19:1 <i>dr</i> 2.36b
9	<i>p</i> -FPh, H	2.29 C	52% ^b	2.37a 92%, >19:1 <i>dr</i> 2.37b
10	<i>p</i> -OMePh, H	2.30 C	< 5% ^d	--- 2.38b

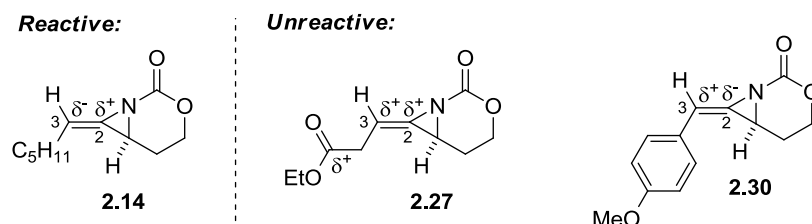
Condition **A**: aminohydroxylation: 7.5 mol % K₂OsO₂(OH)₄, Chloramine T, 33 °C; reduction: NaBH₄ in CH₂Cl₂. Condition **B**: aminohydroxylation: 10 mol % OsO₄, Chloramine B, 37 °C; reduction: NaBH₄ in CH₂Cl₂. Condition **C**: aminohydroxylation: 7.5 mol % OsO₄, BocNNaCl, 30 °C; reduction: NaBH₄ in 1:1 CHCl₃:H₂O with sonication. ^a *dr* >19:1 for all substrates. ^b <10% dihydroxylation product observed. ^c 60% based on recovered starting material. ^d No reaction upon heating to 50 °C.

The scope of the aminohydroxylation/reduction of bicyclic methylene aziridines to 1,3-diamino-2-ols was investigated for *gem*-dimethyl substituted substrates (Table 2.5). The reaction was highly stereoselective and stereospecific, as *E* methylene aziridine **2.14** (Table 2.5, entry 1) and *Z* isomer **2.23** (Table 2.5, entry 2) were shown to yield 1,3-diamino-2-ols **2.16** and **2.31b**, epimeric at C3. This relative stereochemistry of **2.31b** was confirmed by X-ray crystallography of a derivative, synthesized in the manner described above. The transformation tolerated branching in the C3 alkyl group, silyl-protected alcohols, and remote aryl groups (entries 3-6). Portionwise addition of the catalyst over several hours was found to improve the conversion and yields of these reactions. For more electron-rich methylene aziridines (entries 3 and 4), trace

amounts of overoxidized products **c** were observed. Application of the conditions optimized for phenyl-substituted substrate **2.17** to other aryl-substituted methylene aziridines gave moderate yields of the desired products (Table 2.5, entries 4-9), although electron-rich **2.30** did not react, even at increased temperature. The moderate yields of these reactions were offset by the high yields and diastereoselectivity of the reduction, leading to rapid increases in stereochemical complexity.

The excellent regioselectivity of the aminohydroxylation may be attributed to the preference of the chloramine nitrogen atom to bind to the less substituted and/or more electron-rich carbon atom of the methylene aziridine,⁶ as the carbamate of the substrate likely serves as an inductively electron-withdrawing group. The failure of two substrates, β -carboxyethyl-substituted **2.27** and *p*-MeO-phenyl-substituted **2.30**, to react in the aminohydroxylation supports electronic control of both reactivity and regioselectivity (Figure 2.1). The former withdraws electron density from the less-substituted C3 carbon atom of the reactive site, whereas the latter donates electron density to the more substituted C2 position. In comparison, reactive methylene aziridine **2.14** features a small partial positive charge at C2, and a small partial negative charge at C3.

Figure 2.1. Electronic rationale for unreactive substrates.



2.6. Conclusions.

A second generation synthesis of 1,3-diamino-2-ols has been developed, employing an Os-catalyzed aminohydroxylation of bicyclic methylene aziridines, and *in situ* rearrangement to provide 1,3-diaminated ketones in moderate to good yields. Subsequent reduction of the ketones with NaBH₄ provides the 1,3-diamino-2-ols in excellent yield and diastereoselectivity. While this methodology presents an improvement over the first generation synthesis in step efficiency, the method continues to suffer limitations in substrate scope, requiring *gem*-dimethyl substitution in the tether of the carbamate in order to attain good yields and stereoselectivities. Nevertheless, this method serves as an important validation of the 1,2-difunctionalization strategy for allene functionalization discussed in Chapter 1. Additionally, many of the compounds synthesized in developing this methodology have been submitted to the UW Small Molecule Screening Facility as part of the development of a library of novel compounds from University of Wisconsin-Madison labs and are currently undergoing biological assay.

2.7. References.

1. Rigoli, J. W.; Guzei, I. A.; Schomaker, J. M. *Org. Lett.* **2014**, *16*, 1696.
2. For selected references on oxyaminations involving intramolecular delivery of the nitrogen atom, see: a) Alexanian, E. J., Lee, C., and Sorensen, E. J. *J. Am. Chem. Soc.* **2005**, *127*, 7690. b) Szolcsányi, P. and Gracza, T. *Chem. Commun.* **2005**, 3948. c) Liu, G. and Stahl, S. S. *J. Am. Chem. Soc.* **2006**, *128*, 7179. d) Desai, L. V. and Sanford, M. S. *Angew. Chem., Int. Ed.* **2007**, *46*, 5737. e) Noack, M. and Göttlich, R. *Chem. Commun.* **2002**, 536. f) Fuller, P. H., Kim, J.-W., and Chemler, S. R. *J. Am. Chem. Soc.* **2008**, *130*, 17638. g) Sherman, E. S. and Chemler, S. R. *Adv. Synth. Catal.* **2009**, *351*, 467. h) Paderes, M. C. and Chemler, S. R. *Org. Lett.* **2009**, *11*, 1915. i) Michaelis, D. J.; Shaffer, C. J.; Yoon, T. P. *J. Am. Chem. Soc.* **2007**, *129*, 1866. j) Michaelis, D. J.; Ischay, M. A.; Yoon, T. P. *J. Am. Chem. Soc.* **2008**, *130*, 6610. k) Michaelis, D. J.; Williamson, K. S.; Yoon, T. P. *Tetrahedron* **2009**, *65*, 5118. l) Benkovics, T.; Du, J.; Guzei, I. A.; Yoon, T. P. *J. Org. Chem.* **2009**, *74*, 5545. m) Williamson, K. S.; Yoon, T. P. *J. Am. Chem. Soc.* **2010**, *132*, 4570. n) Williamson, K. S.; Yoon, T. P. *J. Am. Chem. Soc.* **2012**, *134*, 12370.

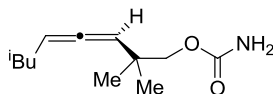
3. For key references on the Sharpless aminohydroxylation, see: a) Sharpless, K. B.; Chon, A. O.; Oshima, K. *J. Org. Chem.* **1976**, *41*, 177. b) Herranz, E.; Sharpless, K. B. *J. Org. Chem.* **1978**, *43*, 2544. c) Heranz, E.; Biller, S. A.; Sharpless, K. B. *J. Am. Chem. Soc.* **1978**, *100*, 3596. d) Herranz, E.; Sharpless, K. B. *J. Org. Chem.* **1980**, *45*, 2710. e) Li, G.; Chang, H.-T.; Sharpless, K. *Angew. Chem. Int. Ed.* **1996**, *35*, 451. f) Rudolph, J.; Sennhenn, P. C.; Vlaar, C. P.; Sharpless, K. B. *Angew. Chem. Int. Ed.* **1996**, *35*, 2810. g) Lohray, B. B.; Bhushan, V.; Reddy, G. J.; Reddy, A. S. *Indian J. Chem., Sect. B* **2002**, *41B*, 161.
4. For recent reviews on the aminohydroxylation of alkenes, see: a) Donohoe, T. J.; Callens, C. K. A.; Flores, A. R.; Lacy, A. R.; Rathi, A. H. *Chem. Eur. J.* **2011**, *17*, 58. b) Niolv, D.; Reiser, O. *Adv. Synth. Catal.* **2002**, *344*, 1169. c) Muniz, K. *Chem. Soc. Rev.* **2004**, *33*, 166.
5. a) Anh, N. T.; Eisenstein, O. *Nouv. J. Chim.* **1997**, *1*, 61. b) Anh, N. T.; Eisenstein, O.; Lefour, J.-M.; Dau, M.-E. *J. Am. Chem. Soc.* **1973**, *95*, 6146.
6. Kurti, L.; Czako, B. Eds. *Sharpless Asymmetric Aminohydroxylation. Strategic Applications of Named Reactions in Organic Synthesis* Elsevier, Amsterdam, **2005**.

2.8. Experimental Details and Characterization.

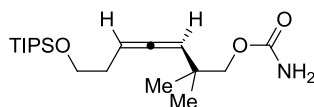
2.8.1. Preparation of Homoallenic Carbamates.

General procedure for the synthesis of homoallenic carbamates. The homoallenic alcohol (between 0.5 g and 3.0 g, 1 equiv) was dissolved in dichloromethane (0.3 M) and placed in an ice bath. Trichloroacetylisocyanate (1.2 equiv) was slowly added dropwise. The ice bath was removed and the reaction stirred until TLC indicated complete consumption of the starting material. The solvent was then removed and the crude reaction was dissolved in methanol (0.4 M). Potassium carbonate (0.5 equiv) was then added to the reaction and stirred at room temperature until TLC indicated complete consumption of the starting material. Water was added to the reaction and the mixture was extracted with three portions of dichloromethane. The organic phase was dried with sodium sulfate and concentrated under reduced pressure. The crude products were purified by silica gel column chromatography (0 → 30% EtOAc in hexanes,

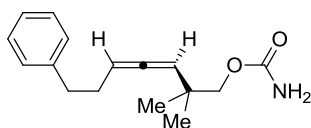
6% increments). All allenes were stored in a freezer prior to use. Other homoallenic carbamates were prepared from their corresponding alcohols according to literature procedures.³



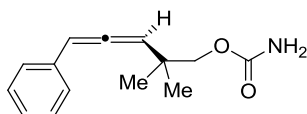
Compound S2.1. Obtained from the corresponding homoallenic alcohol as a clear oil in 86% yield. ¹H-NMR (500.0 MHz, CDCl₃) δ 5.15 (q, *J* = 6.5 Hz, 1H), 5.05 (dt, *J* = 6.5, 2.3 Hz, 1H), 4.64 (br s, 2H), 3.86 (overlapping d, 2H), 1.98-1.82 (m, 2H), 1.66 (sep, *J* = 6.6 Hz, 1H), 1.04 (s, 6H), 0.92 (d, *J* = 6.6 Hz, 6H). ¹³C-NMR δ 125.7 MHz, CDCl₃) δ 202.85, 157.04, 97.60, 92.04, 73.26, 38.67, 35.42, 28.61, 24.95, 24.90, 22.37, 22.30. HRMS (ESI) *m/z* calculated for C₁₂H₂₁NO₂ [M+H⁺] 212.1646, found 212.1640. IR (cm⁻¹) 3539, 3428, 2963, 2899, 2873, 1961, 1733, 1590, 1467, 1403, 1379, 1332, 1107, 1069.



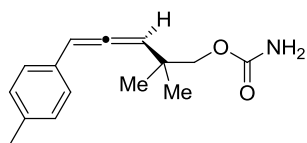
Compound S2.2. Obtained as a clear oil from the corresponding homoallenic alcohol in 49% yield. ¹H-NMR: (300.1 MHz, CDCl₃) δ 5.24 (q, *J* = 6.4 Hz, 1H), 5.07 (dt, *J* = 6.4, 3.1 Hz, 1H), 4.68-4.50 (br s, 2H), 3.86 (s, 2H), 3.74 (t, *J* = 7.0 Hz, 2H), 2.26 (qd, *J* = 7.0, 3.1 Hz, 2H), 1.14-0.99 (m, 27H); ¹³C-NMR: (75.4 MHz, CDCl₃) δ 203.21, 157.20, 98.37, 90.13, 73.39, 63.47, 35.55, 33.11, 25.04, 18.24, 12.23; HRMS (ESI) *m/z* calculated for C₁₉H₃₇NO₃Si [M+H⁺] 356.2616, found 356.2622. IR: in CH₂Cl₂: 3535, 3424, 2968, 1728, 1585, 1454, 1399, 1378, 1331, 1271, 1068 cm⁻¹.



Compound S2.3. Obtained from the corresponding homoallenenic alcohol as a clear, colorless oil in 75% yield. $^1\text{H-NMR}$: (299.9 MHz, CDCl_3) δ 7.32-7.23 (m, 2H), 7.22-7.14 (m, 3H), 5.25 (q, $J = 6.1$ Hz, 1H), 5.09 (dt, $J = 6.1, 3.1$ Hz, 1H), 4.83-4.64 (br s, 2H), 3.84 (s, 2H), 2.72 (t, $J = 7.4$ Hz, 2H), 2.40-2.25 (m, 2H), 1.01 (s, 6H); $^{13}\text{C-NMR}$: (75.4 MHz, CDCl_3) δ 157.29, 141.96, 128.65, 128.52, 126.07, 99.07, 92.92, 73.31, 35.60, 30.87, 25.04; HRMS (ESI) m/z calculated for $\text{C}_{16}\text{H}_{21}\text{NO}_2$ [$\text{M}+\text{H}^+$] 260.1646, found 260.1656. IR: in CH_2Cl_2 3537, 3426, 2949, 1732, 1602, 1589, 1464, 1404, 1382, 1332, 1101 cm^{-1} .

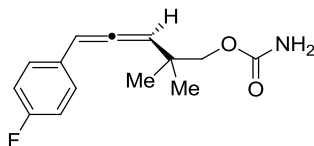


Compound S2.4. Obtained from the corresponding homoallenenic alcohol as a yellow oil in 74% yield. $^1\text{H NMR}$ (500.0 MHz, CDCl_3) δ 7.32-7.27 (m, 4H), 7.22-7.16 (m, 1H), 6.23 (d, $J = 6.3$ Hz, 1H), 5.55 (d, $J = 6.3$ Hz, 1H), 4.72 (br s, 2H), 3.95 (s, 2H), 1.13 (s, 6H). $^{13}\text{C NMR}$ (125.7 MHz, CDCl_3) δ 203.79, 157.11, 134.72, 128.62, 126.91, 126.58, 102.37, 96.65, 72.94, 36.46, 24.98, 24.94. HRMS (ESI) m/z calculated for $\text{C}_{14}\text{H}_{17}\text{NO}_2$ [$\text{M}+\text{NH}_4^+$] 249.1598, found 249.1593. IR (cm^{-1}) 3534, 3424, 2971, 2931, 2873, 1949, 1734, 1584, 1510, 1403, 1378, 1333, 1108, 1071.



Compound S2.5. Obtained from the corresponding homoallenenic alcohol as a yellow oil in 72% yield. $^1\text{H NMR}$ (500.0 MHz, CDCl_3) δ 7.22 (d, $J = 7.7$ Hz, 2H), 7.13 (d, $J = 7.7$ Hz, 2H), 6.23 (d, $J = 6.2$ Hz, 1H), 5.56 (d, $J = 6.2$ Hz, 1H), 4.91 (br s, 2H), 3.96 (s, 2H), 2.35 (s, 3H), 1.15 (s, 6H). $^{13}\text{C NMR}$ (125.7 MHz, CDCl_3) δ 203.50, 157.35, 136.69, 131.71, 129.36, 126.48, 102.26, 96.47, 72.97, 36.46, 24.98, 24.92, 21.19. HRMS (ESI) m/z calculated for $\text{C}_{15}\text{H}_{19}\text{NO}_2$ [$\text{M}+\text{NH}_4^+$]

263.1755, found 263.1765. IR (cm⁻¹) 3537, 3424, 2971, 2933, 2873, 1950, 1735, 1605, 1585, 1516, 1473, 1403, 1381, 1331, 1109, 1071.



Compound S2.6. Obtained from the corresponding homoallylic alcohol as a yellow oil in 78% yield. ¹H NMR (299.9 MHz) δ 7.29-7.21 (m, 2H), 7.03-6.93 (m, 2H), 6.20 (d, *J* = 6.3 Hz, 1H), 5.55 (d, *J* = 6.3 Hz, 1H), 4.89 (br s, 2H), 3.94 (s, 2H), 1.12 (s, 6H). ¹³C NMR (75.4 MHz, CDCl₃) δ 204.33, 164.32, 161.05, 158.01, 131.47, 128.79, 116.48, 103.42, 96.50, 73.69, 37.26, 25.75. HRMS (ESI) *m/z* calculated for C₁₄H₁₆FNO₂ [M+H⁺] 250.1238, found 250.1233.

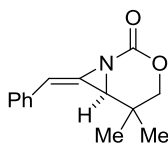
2.8.2. Synthesis of Bicyclic Methylene Aziridines

The following methylene aziridines were prepared according to procedures described in chapter 1: **2.14, 2.23, 2.27.**

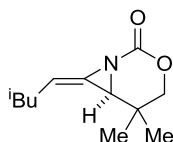
General Procedure A for the Synthesis of Methylene Aziridines: A round-bottomed flask was charged with AgOTf (0.20 equiv), 1,10-phenanthroline (0.25 equiv) and dry dichloromethane. The mixture was allowed to stir 30 minutes, then an equal volume of a dichloromethane solution of the allenic carbamate (1 equiv) was added to yield a solution that was 0.1 M in substrate. A portion of 4 Å powdered molecular sieves was added (four times the mass of substrate), and the mixture stirred for 10 min. PhIO (2 equiv) was added and the reaction was monitored by TLC. After full consumption of the starting material (2-4 h), the reaction was filtered through a sintered glass funnel and concentrated under reduced pressure. The crude mixture was purified via column chromatography (100 g SiO₂/1 g crude material, hexanes/EtOAc) to give the individual isomers of the desired product.

General Procedure B for the Synthesis of Methylene Aziridines:

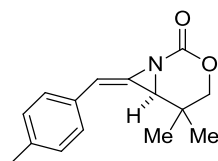
To a mixture of the allenic carbamate (1.0 equiv), $\text{Rh}_2(\text{TPA})_4$ or Rh_2esp_2 catalyst (0.025 equiv) and 4Å molecular sieves (1.1 times the mass of PhIO used), dry dichloromethane was added to give a solution 0.1M in substrate. The solution was allowed to stir 10 min to achieve uniformity and PhIO (2.0 equiv) was added in a single portion. The solution was monitored by TLC until complete consumption of the carbamate starting material was indicated, typically 2-4 h. The crude mixture was then purified via column chromatography (100 g SiO_2 /1 g crude material, hexanes/EtOAc) to give individual isomers of the desired product.



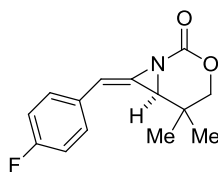
Compound 2.17. Obtained as an off-white solid from the corresponding allenic carbamate using general procedure B in 51% yield as a single diastereomer. Mp 82-84 °C. ^1H NMR (300.1 MHz, C_6D_6) δ 7.10-7.05 (overlapping m, 4H), 7.04-6.96 (m, 1H), 6.56 (d, $J = 0.7$ Hz, 1H), 3.52 (d, $J = 10.6$ Hz, 1H), 3.07 (d, $J = 10.6$ Hz, 1H), 2.66 (s, 1H), 0.46 (s, 6H). ^{13}C -NMR (75.4 MHz, C_6D_6) δ 154.74, 131.42, 126.14, 116.46, 103.87, 101.18, 78.17, 48.67, 29.85, 23.66, 19.79. HRMS (ESI) m/z calculated for $\text{C}_{14}\text{H}_{15}\text{NO}_2$ [$\text{M}+\text{NH}_4^+$] 247.1442, found 247.1443. IR (cm^{-1}) 2975, 2940, 2899, 2881, 1771, 1736, 1598, 1581, 1496, 1473, 1458, 1408, 1379, 1227, 1172, 1122, 1046, 1011.



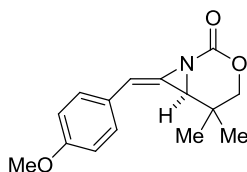
Compound 2.24. The product was synthesized using General Procedure A to give the methylene aziridine in 85% yield and 2.5:1 *E*:*Z* mixture of isomers as a clear oil. *E* isomer: ^1H NMR (500.2 MHz, CDCl_3) δ 5.62 (t, $J = 7.8$ Hz, 1H), 4.25 (d, $J = 10.5$ Hz, 1H), 3.84 (d, $J = 10.5$ Hz, 1H), 3.15 (s, 1H), 2.08-1.96 (m, 2H), 1.72 (sep, $J = 6.9$ Hz, 1H), 1.27 (s, 3H), 0.93 (d, $J = 6.9$ Hz, 3H), 0.92 (d, $J = 6.9$ Hz, 3H), 0.90 (s, 3H). ^{13}C NMR (125.8 MHz, CDCl_3) δ 156.35, 124.11, 103.24, 77.97, 48.85, 38.01, 29.77, 28.81, 24.29, 22.62, 22.32, 20.97. HRMS (ESI) m/z calculated for $\text{C}_{12}\text{H}_{19}\text{NO}_2$ $[\text{M}+\text{NH}_4^+]$ 210.1489, found 210.1479. IR (cm^{-1}) 3535, 3426, 2962, 2898, 2872, 2843, 1793, 1731, 1586, 1474, 1404, 1378, 1334, 1319, 1296, 1231, 1213, 1171, 1124, 1062.



Compound 2.28. Obtained from the corresponding allenic carbamate using general procedure B in 54% yield as a single diastereomer as an off-white solid. Mp 85-86 °C. ^1H NMR (299.9 MHz, CDCl_3) δ 7.24 (d, $J = 8.0$ Hz, 2H), 7.15 (d, $J = 8.0$ Hz, 2H), 6.56 (s, 1H), 4.38 (d, $J = 9.8$ Hz, 1H), 3.87 (d, $J = 9.8$ Hz, 1H), 3.45 (s, 1H), 2.35 (s, 3H), 1.36 (s, 3H), 0.86 (s, 3H). ^{13}C NMR (75.4 MHz, CDCl_3) δ 155.73, 137.64, 131.42, 129.79, 126.21, 124.35, 105.19, 78.56, 49.06, 30.33, 24.18, 21.40, 19.99. HRMS (ESI) m/z calculated for $\text{C}_{15}\text{H}_{17}\text{NO}_2$ $[\text{M}+\text{H}^+]$ 244.1333, found 244.1336. IR (cm^{-1}) 2958, 2929, 2874, 1736, 1516, 1473, 1407, 1377, 1325, 1215, 1200, 1170, 1122, 1043, 1024.



Compound 2.29. Obtained as an off-white solid from the corresponding allenic carbamate using general procedure B in 71% yield as a single diastereomer. ^1H NMR (300.1 MHz, C_6D_6) δ 6.89-6.81 (m, 2H), 6.72 (tt, $J = 8.7, 1.7$ Hz, 2H), 6.43 (s, 1H), 3.55 (d, $J = 10.6$ Hz, 1H), 3.10 (d, $J = 10.6$ Hz, 1H), 2.64 (s, 1H), 0.46 (s, 3H), 0.42 (s, 3H). ^{13}C NMR (75.4 MHz, C_6D_6) δ 163.86, 160.60, 154.19, 130.91, 125.59, 115.90, 115.61, 103.31, 77.61, 29.30, 23.11, 19.23. HRMS (ESI) m/z calculated for $\text{C}_{14}\text{H}_{14}\text{NO}_2$ [$\text{M}+\text{NH}_4^+$] 248.1082, found 248.1082.



Compound 2.30. Obtained as an off-white solid from the corresponding homoallenic carbamate using general procedure B in 60% yield as a single diastereomer. ^1H NMR (299.9 MHz) δ 7.07 (dt, $J = 8.9, 2.3$ Hz, 2H), 6.73 (dt, $J = 8.9, 2.3$ Hz, 2H), 6.59 (s, 1H), 3.65 (d, $J = 10.5$ Hz, 1H), 3.31 (s, 3H), 3.18 (d, $J = 10.5$ Hz, 1H), 2.80 (s, 1H), 0.58 (s, 3H), 0.53 (s, 3H). ^{13}C NMR (75.4 MHz, C_6D_6) δ 159.93, 155.36, 127.81, 124.70, 115.00, 104.67, 78.22, 55.24, 48.87, 30.02, 23.71, 19.87. HRMS (ESI) m/z calculated for $\text{C}_{15}\text{H}_{17}\text{NO}_3$ [$\text{M}+\text{H}^+$] 260.1282, found 260.1276.

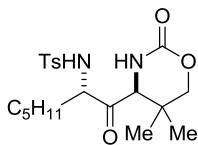
2.8.3. Synthesis of 1,3-Diaminated Ketones by Aminohydroxylation of Methylene

Aziridines.

General Procedure A: CHCl_3 was added to a round-bottom flask containing the methylene aziridine (1 equiv) and potassium osmate (0.075 equiv) under N_2 to give a final substrate concentration of 0.05 M. An equal volume of an aqueous solution of the chloramine salt (3.1 equiv) and the phase transfer catalyst (0.05 equiv) was then added. The flask was fitted with a reflux condenser and the mixture was heated to 33 $^\circ\text{C}$ or 37 $^\circ\text{C}$ using an oil bath. In order to achieve reproducible good yields and conversions, it was critical that the reflux condenser was

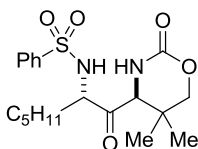
well-greased and that the oil level exceeded that of the liquid in the flask. After 20 h, the reaction mixture was cooled to room temperature and poured into a separatory funnel. The aqueous layer was extracted with three portions of CH_2Cl_2 and the combined organic washings were dried over Na_2SO_4 and concentrated under reduced pressure. The residue was purified via flash chromatography to give the ketone products.

General Procedure B: CHCl_3 was added to a round-bottom flask containing the methylene aziridine (1 equiv) under N_2 to give a total substrate concentration of 0.05 M. An equal volume of an aqueous solution of the chloramine salt (3.1 equiv) and the phase transfer catalyst (0.05 equiv) was then added, followed by an aqueous solution of 2% (w/v) OsO_4 (0.05 equiv). The flask was fitted with a reflux condenser and the mixture was heated to 33 °C or 37 °C in an oil bath. In order to obtain reproducible good yields and conversions, it was critical that the reflux condenser was well-greased, and that the oil level exceeded that of the liquid in the flask. Two further portions of 2% (w/v) OsO_4 solution (0.025 equiv) were added at 4 h intervals. After 20 h, the reaction was cooled to room temperature and poured into a separatory funnel. The aqueous layer was extracted with CH_2Cl_2 , the combined organic washings were dried over Na_2SO_4 and the volatiles removed under reduced pressure. The residue was purified via flash chromatography to give the ketone products.

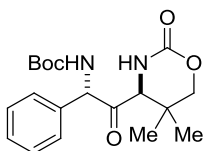


Compound 2.15. Synthesized from methylene aziridine **2.14** using General Procedure A with Chloramine T at 33 °C in 81% yield as a white powder. Mp 155-156 °C. ^1H NMR (500.0 MHz, CDCl_3) δ 7.74 (d, $J = 8.1$ Hz, 2H), 7.30 (d, $J = 8.1$ Hz, 2H), 5.71 (d, $J = 7.9$ Hz, 1H), 5.59 (s,

1H), 4.15-4.07 (m, 2H), 3.91 (d, $J = 11.6$ Hz, 1H), 3.86 (d, $J = 11.6$ Hz, 1H), 2.41 (s, 3H), 1.77-1.69 (m, 1H), 1.51-1.41 (m, 1H), 1.19 (s, 3H), 1.24-1.05 (m, 6H), 0.82 (t, $J = 7.4$ Hz, 3H), 0.63 (s, 3H). ^{13}C -NMR (125.7 MHz, CDCl_3) δ 205.97, 152.49, 144.07, 137.06, 129.80, 127.27, 74.73, 63.73, 61.27, 32.66, 31.17, 31.09, 24.56, 23.76, 22.30, 21.50, 18.72, 13.84. HRMS (ESI) m/z calculated for $\text{C}_{20}\text{H}_{30}\text{N}_2\text{O}_5\text{S}$ [$\text{M}+\text{NH}_4^+$] 433.1768, found 433.1768. IR (cm^{-1}) 3417, 3346, 3066, 2963, 2931, 2876, 2861, 1718, 1598, 1476, 1341, 1166, 1125, 1093, 1077.

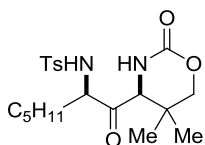


Compound 2.15a. Synthesized from methylene aziridine **2.14** using General Procedure A with Chloramine B at 33 °C in 79% yield as a white powder. Mp 185-187 °C. ^1H NMR (299.9 MHz, CDCl_3) δ 7.87 (dd, $J = 8.1, 0.7$ Hz, 2H), 7.62-7.46 (overlapping m, 3H), 6.20 (d, $J = 7.8$ Hz, 1H), 6.11 (s, 1H), 4.15-4.07 (overlapping m, 2H), 3.92 (d, $J = 11.0$ Hz, 1H), 3.85 (d, $J = 11.0$ Hz, 1H), 1.80-1.69 (m, 1H), 1.53-1.41 (m, 1H), 1.22-1.02 (s + m, 9H), 0.80 (t, $J = 6.8$ Hz, 3H), 0.66 (s, 3H). ^{13}C NMR (100.6 MHz, CDCl_3) δ 206.76, 152.78, 140.20, 133.09, 129.22, 127.21, 75.00, 63.85, 60.13, 41.39, 31.30, 29.72, 24.54, 23.65, 23.21, 20.85. HRMS (ESI) m/z calculated for $\text{C}_{19}\text{H}_{28}\text{N}_2\text{O}_5\text{S}$ [$\text{M}+\text{H}^+$] 397.1792, found 397.1792. IR (cm^{-1}) 3419, 3346, 3054, 2983, 2931, 2688, 2519, 2408, 1724, 1552, 1476, 1420, 1166, 1092, 1075.

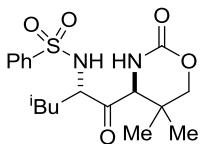


Compound 2.18. Obtained using general procedure B with BocNNaCl at 30 °C to give the ketone in 55% yield from methylene aziridine **2.17** as an off-white solid. Mp 159-161 °C. ^1H

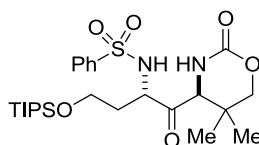
NMR (400.2 MHz, CDCl₃) δ 7.46-7.36 (m, 3H), 7.30-7.27 (m, 2H), 5.61 (d, $J = 7.8$ Hz, 1H), 5.48 (d, $J = 7.8$ Hz, 1H), 5.20 (s, 1H), 4.03 (d, $J = 11.7$ Hz, 1H), 3.89 (s, $J = 11.7$ Hz, 1H), 1.41 (s, 9H), 1.31 (s, 3H), 1.04 (s, 3H). ¹³C NMR (100.6 MHz, CDCl₃) δ 204.62, 152.56, 134.20, 129.94, 129.54, 128.42, 80.56, 74.39, 64.24, 31.36, 28.26, 24.33, 20.66, 19.74; HRMS (ESI) m/z calculated for C₁₉H₂₅N₂O₅ [M+H⁺] 363.1915, found 363.1914. IR: 3425, 3066, 2982, 2933, 1716, 1492, 1477, 1454, 1423, 1395, 1369, 1296, 1171, 1127, 1066.



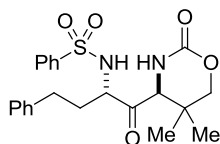
Compound 2.31a. Synthesized from methylene aziridine **2.23** using General Procedure A with Chloramine T at 33 °C in 61% yield as a white powder. Mp 155-156 °C. ¹H NMR (499.9 MHz, CDCl₃) δ 7.77 (d, $J = 8.1$ Hz, 2H), 7.33 (d, $J = 8.1$ Hz, 2H), 6.40 (d, $J = 3.3$ Hz, 1H), 6.28 (d, $J = 9.2$ Hz, 1H), 4.24 (d, $J = 11.0$ Hz, 1H), 4.19 (dd, $J = 2.8, 0.9$ Hz, 1H), 3.88 (td, $J = 7.4, 6.4$ Hz, 1H), 3.76 (d, $J = 11.0$ Hz, 1H), 2.43 (s, 3H), 1.69-1.59 (m, 1H), 1.39-1.29 (m, 1H), 1.19 (s, 3H), 1.15-1.00 (m, 6H), 0.92 (s, 3H), 0.77 (t, $J = 6.8$ Hz, 3H). ¹³C NMR (125.7 MHz, CDCl₃) δ 203.74, 151.98, 142.75, 136.33, 128.89, 126.22, 74.22, 62.27, 61.61, 32.40, 31.96, 31.67, 26.35, 26.13, 23.69, 22.97, 21.62, 15.44. HRMS (ESI) m/z calculated for C₂₀H₃₀N₂O₅S [M+H⁺] 411.1949, found 411.1942. IR (cm⁻¹) 3417, 3346, 3066, 2963, 2931, 2876, 2861, 1718, 1706, 1598, 1476, 1341, 1165, 1124, 1092.



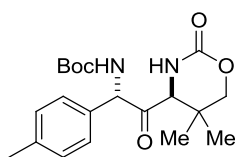
Compound 2.32a. Synthesized from methylene aziridine **2.24** using General Procedure A with Chloramine B at 37 °C in 57% yield as a white powder. Mp 195-196°C. ¹H-NMR (400.2 MHz, CDCl₃) δ 7.87 (d, *J* = 7.2 Hz, 2H), 7.65-7.54 (m, 1H), 7.51 (t, *J* = 7.2 Hz, 2H), 5.98 (d, *J* = 8.7 Hz, 1H), 5.71 (s, 1H), 4.18-4.10 (overlapping m, 2H), 3.89 (s, 2H), 1.75-1.64 (m, 1H), 1.46-1.33 (m, 2H), 1.22 (s, 3H), 0.86 (d, *J* = 6.6 Hz, 3H), 0.76 (d, *J* = 6.6 Hz, 3H), 0.70 (s, 3H). ¹³C-NMR (100.6 MHz, CDCl₃) δ 206.76, 152.78, 140.20, 133.09, 129.22, 127.21, 75.00, 63.85, 60.13, 41.39, 31.30, 29.72, 24.54, 23.65, 23.21, 20.85. HRMS (ESI) *m/z* calculated for C₁₈H₂₆N₂O₅S [M+H⁺] 383.1636, found 383.1628. IR (cm⁻¹) 3339, 2963, 2935, 2873, 1721, 1702, 1560, 1473, 1340, 1167, 1096, 1077.



Compound 2.33a. Synthesized from methylene aziridine **2.25** using General Procedure B with Chloramine B at 37 °C in 50% yield (60% based on recovered starting material) as an off-white powder. Mp 184-185 °C. ¹H NMR (500.2 MHz, CDCl₃) δ 7.89-7.85 (m, 2H), 7.57 (tt, *J* = 7.3, 1.5 Hz, 1H), 7.52-7.47 (m, 2H), 6.47 (d, *J* = 7.4 Hz, 1H), 5.74 (s, 1H), 4.29 (d, *J* = 1.8 Hz, 1H), 4.25 (td, *J* = 7.0, 4.6 Hz, 1H), 3.95 (d, *J* = 10.9 Hz, 1H), 3.83 (s, *J* = 10.9 Hz, 1H), 3.75-3.66 (m, 1H), 1.97 (ddt, *J* = 14.6, 8.9, 3.2 Hz, 1H), 1.83 (ddt, *J* = 15.2, 5.7, 3.2 Hz, 1H), 1.19 (s, 3H), 1.10-0.97 (m, 21H), 0.69 (s, 3H). ¹³C NMR (125.8 MHz, CDCl₃) δ 206.76, 152.93, 140.24, 133.17, 129.43, 127.34, 74.82, 63.10, 60.00, 59.38, 35.27, 31.29, 24.12, 19.26, 18.19, 12.02. HRMS (ESI) *m/z* calculated for C₂₅H₄₂N₂O₆SSi [M+NH₄⁺] 544.2872, found 544.2894. IR (cm⁻¹) 3425, 3341, 3063, 2949, 2870, 1724, 1479, 1449, 1420, 1350, 1169, 1093, 1076.

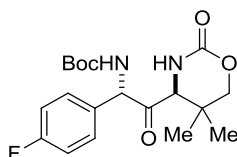


Compound 2.34a. Synthesized using General Procedure B with Chloramine B at 33 °C from methylene aziridine **2.25** to give the 1,3-diaminated ketone in 57% yield as an off-white powder. Mp 188-190 °C. ^1H NMR (500.2 MHz, CDCl_3) δ 7.91-7.87 (m, 2H), 7.58 (tt, $J = 7.6, 2.2$ Hz, 1H), 7.54-7.49 (m, 2H), 7.27 (tt, $J = 7.1, 1.3$ Hz, 2H), 7.22 (tt, $J = 7.6, 2.8$ Hz, 1H), 7.00 (d, $J = 7.0$ Hz, 1H), 6.27 (d, $J = 9.1$ Hz, 1H), 5.36 (s, 1H), 4.05 (td, $J = 8.4, 4.0$ Hz, 1H), 3.85 (d, $J = 1.5$ Hz, 1H), 3.75 (d, $J = 10.9$ Hz, 1H), 3.72 (d, $J = 10.9$ Hz, 1H), 2.69 (dt, $J = 14.5, 7.2$ Hz, 1H), 2.58 (dt, $J = 14.5, 6.8$ Hz, 1H), 2.10 (dtd, $J = 14.9, 8.1, 4.8$ Hz, 1H), 1.85 (m, $J = 1.89$ -1.80 Hz, 2H), 0.93 (s, 3H), 0.52 (s, 3H). ^{13}C NMR (125.8 MHz, CDCl_3) δ 206.21, 152.91, 140.49, 139.71, 133.28, 129.47, 129.03, 128.22, 127.84, 127.44, 74.85, 63.72, 60.95, 34.36, 31.23, 31.12, 23.57, 18.88. HRMS (ESI) m/z calculated for $\text{C}_{22}\text{H}_{26}\text{N}_2\text{O}_4\text{S}$ $[\text{M}+\text{H}^+]$ 431.1636, found 431.1648. IR (cm^{-1}) 3421, 3346, 2963, 2930, 2860, 1728, 1684, 1560, 1509, 1475, 1341, 1167, 1126, 1092, 1080.



Compound 2.35a. Obtained as an off-white powder from methylene aziridine **2.28** in 53% yield using general procedure B with BocNNaCl as the chloramine at 30 °C. Mp 183-186 °C. ^1H NMR (300.1 MHz) δ 7.22 (d, $J = 8.0$ Hz, 2H), 7.15 (d, $J = 8.0$ Hz, 2H), 5.58 (d, $J = 7.1$ Hz, 1H), 5.44 (d, $J = 7.1$ Hz, 1H), 5.02 (s, 1H), 4.04 (d, $J = 11.2$ Hz, 1H), 3.88 (s, 1H), 3.81 (d, $J = 11.2$ Hz, 1H), 2.36 (s, 3H), 1.42 (s, 9H), 1.30 (s, 3H), 1.04 (s, 3H); ^{13}C NMR (75.4 MHz, CDCl_3) δ 204.82, 155.10, 152.68, 139.76, 130.77, 128.47, 80.60, 74.59, 64.28, 31.50, 28.44, 24.50, 21.36,

19.88; HRMS (ESI) m/z calculated for $C_{20}H_{28}N_2O_5$ $[M+H^+]$ 377.2071, found 377.2079. IR (cm^{-1}) 3423, 2972, 2932, 2874, 1950, 1732, 1720, 1585, 1507, 1492, 1404, 1382, 1334, 1166, 1111, 1069.

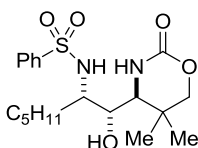


Compound 2.36a. Obtained as an off-white powder from methylene aziridine **2.29** in 52% yield using general procedure B with BocNNaCl as the chloramine at 30°C. Mp 187-190 °C. 1H NMR (400.2 MHz, $CDCl_3$) δ 7.28 (dd, $J = 8.5, 5.0$ Hz, 2H), 7.11 (t, $J = 8.5$ Hz, 2H), 5.63 (d, $J = 6.0$ Hz, 1H), 5.48 (d, $J = 6.0$ Hz, 1H), 5.42 (br s, 1H), 4.00 (d, $J = 11.4$ Hz, 1H), 3.89 (s, 1H), 3.83 (d, $J = 11.4$ Hz, 1H), 1.41 (s, 9H), 1.30 (s, 3H), 1.02 (s, 3H). ^{13}C NMR (100.6 MHz, $CDCl_3$) δ 204.61, 164.42, 154.87, 152.55, 130.28, 117.09, 116.87, 74.38, 64.47, 63.08, 31.38, 28.25, 24.29, 19.77. HRMS (ESI) m/z calculated for $C_{19}H_{25}N_2O_5F$ $[M+H^+]$ 381.1821, found 381.1831. IR (cm^{-1}) 3422, 2982, 2934, 1718, 1687, 1606, 1509, 1492, 1478, 1397, 1371, 1230, 1164, 1125, 1064.

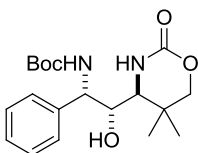
2.8.4. Synthesis of 1,3-Diamino-2-ols.

General Procedure A: $NaBH_4$ (6 equiv) was added to either a flask or a vial containing the ketone substrate, followed by enough CH_2Cl_2 to yield a solution 0.066 M in substrate. The mixture was allowed to stir for 12 h, and then quenched with NH_4Cl . The layers were separated and the aqueous layer extracted with three portions of CH_2Cl_2 . The combined organic layers were then dried over Na_2SO_4 , concentrated *in vacuo* and purified via flash chromatography (hexanes/ethyl acetate) to give the diaminated alcohol products.

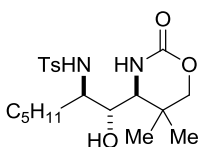
General Procedure B: NaBH₄ (6 equiv) was added to either a flask or a vial containing the ketone substrate. CH₂Cl₂ was then added to yield a solution that was 0.066 M in the substrate. An equal volume of deionized water was added and the mixture sonicated until TLC indicated consumption of the starting material, typically 5-7 h. The layers were separated and the aqueous layer was extracted with three portions of CH₂Cl₂. The combined organic layers were dried over Na₂SO₄, concentrated *in vacuo* and purified via flash chromatography (hexanes/ethyl acetate) to give the diaminated alcohol products.



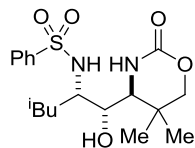
Compound 2.16. Synthesized from ketone **2.15** using General Procedure A in 83% yield and 10:1 *dr* as a white powder. Mp 143-146 °C. ¹H NMR (299.9 MHz, CDCl₃) δ 7.95 (d, *J* = 7.2 Hz, 2H), 7.58 (tt, *J* = 7.2, 2.4 Hz, 1H), 7.55-7.48 (m, 2H), 6.45 (d, *J* = 3.0 Hz, 1H), 5.90 (d, *J* = 9.8 Hz, 1H), 3.89 (d, *J* = 11.1 Hz, 1H), 3.80 (d, *J* = 11.1 Hz, 1H), 3.61-3.45 (m, 2H), 3.32 (dd, *J* = 9.8, 2.0 Hz, 1H), 3.27-3.16 (br s, 1H), 1.93-1.78 (br s, 1H), 1.50-1.36 (m, 1H), 1.15 (s, 3H), 1.14 (s, 3H), 1.01-0.76 (m, 6H), 0.69 (t, *J* = 6.4 Hz, 3H). ¹³C NMR (75.4 MHz, CDCl₃) δ 154.49, 141.07, 133.08, 129.43, 127.31, 75.22, 73.32, 59.44, 55.24, 32.38, 31.59, 31.28, 25.78, 25.20, 22.39, 20.39, 14.02. HRMS (ESI) *m/z* calculated for C₁₉H₃₀N₂O₅S [M+Na⁺] 421.1768, found 421.1764. IR (cm⁻¹) 3533, 3423, 3370, 2969, 2935, 2874, 1733, 1719, 1585, 1507, 1473, 1381, 1332, 1164, 1115, 1072.



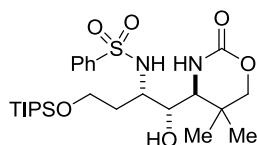
Compound 2.19. Synthesized from ketone **2.18** using General Procedure B in 88% yield and >19:1 *dr* as an off-white powder. Mp 148-150 °C. ¹H NMR (500.0 MHz, CDCl₃) δ 7.41 (t, *J* = 7.8 Hz, 2H), 7.36-7.28 (m, 3H), 6.23 (s, 1H), 5.39 (d, *J* = 10.6 Hz, 1H), 5.11 (d, *J* = 8.8 Hz, 1H), 3.88 (d, *J* = 11.1 Hz, 1H), 3.86 (d, *J* = 11.1 Hz, 1H), 3.80-3.72 (m, 1H), 3.11 (d, *J* = 10.0 Hz, 1H), 1.87 (d, *J* = 4.1 Hz, 1H), 1.46 (s, 9H), 1.20 (s, 3H), 1.11 (s, 3H). ¹³C NMR (125.7 MHz, CDCl₃) δ 156.25, 153.43, 138.87, 129.16, 128.06, 126.47, 80.90, 75.67, 74.92, 60.00, 55.01, 31.06, 29.61, 28.26, 24.91, 19.79. HRMS (ESI) *m/z* calculated for C₁₉H₂₈N₂O₅ [M+Na⁺] 387.1891, found 387.1891. IR (cm⁻¹) 3582, 3435, 3317, 3063, 3035, 2986, 2945, 2885, 1716, 1700, 1607, 1588, 1498, 1481, 1457, 1429, 1394, 1372, 1172, 1123, 1071, 1025.



Compound 2.31b. Synthesized from ketone **2.31a** using General Procedure A in 83% yield and 10:1 *dr* as a white powder. Mp 145-146 °C. ¹H NMR (299.9 MHz, CDCl₃) δ 7.78 (d, *J* = 7.4 Hz, 2H), 7.32 (d, *J* = 7.4 Hz, 2H), 6.17-6.10 (overlapping d and s, 2H), 3.86 (d, *J* = 10.1 Hz, 1H), 3.81 (d, *J* = 10.1 Hz, 1H), 3.55 (td, *J* = 7.9, 1.5 Hz, 1H), 3.45 (d, *J* = 7.6 Hz, 1H), 3.34-3.25 (m, 1H), 3.20 (dd, *J* = 9.1, 2.5 Hz, 1H), 2.42 (s, 3H), 1.55-1.39 (m, 1H), 1.37-1.25 (m, 1H), 1.16 (s, 3H), 1.08 (s, 3H), 1.06-0.86 (m, 6H), 0.71 (t, *J* = 6.0 Hz, 3H). ¹³C NMR (125.7 MHz, CDCl₃) δ 203.74, 151.98, 142.75, 136.33, 128.89, 126.22, 74.22, 62.27, 61.61, 32.40, 31.96, 31.67, 26.35, 26.13, 23.69, 22.97, 21.62, 15.44. HRMS (ESI) *m/z* calculated for C₂₀H₃₂N₂O₅S [M+H⁺] 413.2105, found 413.2111. IR (cm⁻¹) 3276, 2958, 2934, 2873, 1695, 1595, 1451, 1397, 1324, 1289, 1162, 1128, 1093.

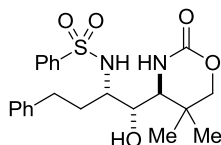


Compound 2.32b. Synthesized from ketone **2.32a** using General Procedure A in 94% yield and 10:1 *dr* as a white powder. Mp 155-156 °C. ¹H NMR (299.9 MHz, CDCl₃) δ 7.94 (d, *J* = 6.8 Hz, 2H), 7.61 (tt, *J* = 6.8, 1.9 Hz, 1H), 7.57-7.50 (m, 2H), 6.32 (d, *J* = 3.1 Hz, 1H), 5.42 (d, *J* = 9.5 Hz, 1H), 3.90 (d, *J* = 11.2 Hz, 1H), 3.81 (d, *J* = 11.2 Hz, 1H), 3.60 (qd, *J* = 8.3, 1.4 Hz, 1H), 3.48 (t, *J* = 8.8 Hz, 1H), 3.27 (dd, *J* = 9.7, 3.1 Hz, 1H), 2.60 (d, *J* = 8.6 Hz, 1H), 1.45-1.04 (overlapping m, 3H), 1.18 (s, 3H), 1.14 (s, 3H), 0.62 (d, *J* = 6.5 Hz, 3H), 0.60 (d, *J* = 6.5 Hz, 3H). ¹³C NMR (75.4 MHz, CDCl₃) δ 153.96, 140.74, 133.24, 129.49, 127.36, 74.97, 73.05, 59.55, 53.03, 41.29, 31.33, 25.34, 24.54, 22.92, 22.26, 20.53. HRMS (ESI) *m/z* calculated for C₁₈H₂₈N₂O₅S [M+H⁺] 385.1792, found 385.1784. IR (cm⁻¹) 3364, 2961, 2928, 2858, 1715, 1481, 1452, 1329, 1163, 1116, 1095.

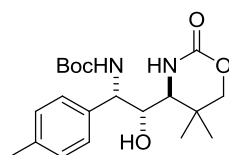


Compound 2.33b. Synthesized from ketone **2.33a** using General Procedure A in 94% yield and 10:1 *dr* as an off-white powder. Mp 156-158 °C. ¹H NMR (500.2 MHz, CDCl₃) δ 7.93-7.88 (m, 2H), 7.62 (tt, *J* = 7.5, 2.0 Hz, 1H), 7.57-7.52 (m, 2H), 5.57 (d, *J* = 2.7 Hz, 1H), 5.40 (d, *J* = 9.3 Hz, 1H), 4.36 (d, *J* = 4.0 Hz, 1H), 3.80 (d, *J* = 11.1 Hz, 1H), 3.73 (d, *J* = 11.1 Hz, 1H), 3.78-3.72 (m, 1H), 3.70-3.59 (m, 1H), 3.55 (dd, *J* = 9.6, 4.0 Hz, 1H), 3.00 (dd, *J* = 9.1, 2.6 Hz, 1H), 1.66-1.50 (m, 2H), 1.15 (s, 3H), 1.07 (s, 3H), 1.10-0.98 (m, 21H). ¹³C NMR (125.8 MHz, CDCl₃) δ 153.57, 140.83, 133.34, 129.65, 127.17, 75.39, 73.76, 59.07, 59.00, 52.36, 36.29, 31.29, 25.14, 19.77, 18.17, 11.81. HRMS (ESI) *m/z* calculated for C₂₅H₄₄N₂O₆SSi [M+H⁺] 529.2763, found

529.2776. IR (cm⁻¹) 3367, 3063, 2949, 2893, 2870, 1712, 1481, 1449, 1423, 1394, 1335, 1166, 1122, 1090, 1055, 1011.

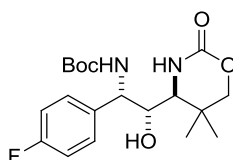


Compound 2.34b. Synthesized from ketone **2.34a** using General Procedure A in 88% yield and 10:1 *dr* as an off-white powder. Mp 195-198 °C. ¹H NMR (500.2 MHz, CDCl₃) δ 7.94-7.89 (m, 2H), 7.58 (t, *J* = 7.3 Hz, 1H), 7.51 (t, *J* = 6.7 Hz, 2H), 7.19 (t, *J* = 8.5 Hz, 2H), 7.13 (t, *J* = 7.3 Hz, 1H), 6.86 (d, *J* = 7.3 Hz, 2H), 6.30 (s, 1H), 3.82 (d, *J* = 10.9 Hz, 1H), 3.74 (d, *J* = 10.9 Hz, 1H), 3.65 (q, *J* = 8.0 Hz, 1H), 3.52 (t, *J* = 8.0 Hz, 1H), 3.26 (dd, *J* = 9.0, 3.3 Hz, 1H), 2.74-2.67 (m, 1H), 2.32-2.17 (m, 2H), 1.85-1.75 (m, 1H), 1.45-1.36 (m, 1H), 1.12 (s, 3H), 1.08 (s, 3H). ¹³C NMR (125.8 MHz, CDCl₃) δ 154.24, 140.86, 133.24, 129.61, 128.74, 127.28, 126.36, 75.01, 72.99, 59.40, 54.91, 34.04, 32.39, 31.21, 25.18, 20.44. HRMS (ESI) *m/z* calculated for C₂₂H₂₈N₂O₅S [M+H⁺] 433.1792, found 433.1082. IR (cm⁻¹) 3685, 3607, 3370, 3066, 2931, 1765, 1712, 1607, 1484, 1449, 1329, 1163, 1119, 1093.



Compound 2.35b. Synthesized from ketone **2.35a** using General Procedure B in 88% yield and >19:1 *dr* as an off-white powder. Mp 148-150 °C. ¹H NMR (500.0 MHz, CDCl₃) δ 7.21 (d, *J* = 8.1 Hz, 2H), 7.18 (d, *J* = 8.1 Hz, 2H), 6.28 (s, 1H), 5.42 (d, *J* = 9.5 Hz, 1H), 5.05 (d, *J* = 10.1 Hz, 1H), 3.87 (d, *J* = 10.7 Hz, 1H), 3.85 (d, *J* = 10.7 Hz, 1H), 3.78-3.67 (m, 1H), 3.10 (d, *J* = 10.1 Hz, 1H), 2.35 (s, 3H), 2.08 (d, *J* = 3.7 Hz, 1H), 1.45 (s, 9H), 1.19 (s, 3H), 1.10 (s, 3H). ¹³C

NMR (125.7 MHz, CDCl₃) δ 153.62, 137.79, 135.76, 129.77, 126.37, 80.77, 75.64, 75.03, 60.02, 54.83, 31.18, 29.66, 28.27, 25.05, 21.03, 19.78. HRMS (ESI) m/z calculated for C₂₀H₃₀N₂O₅ [M+Na⁺] 401.2047, found 401.2047. IR (cm⁻¹) 3580, 3435, 3312, 3141, 3062, 3047, 3008, 2983, 2945, 2891, 1714, 1698, 1502, 1479, 1397, 1369, 1170, 1121, 1069.



Compound 2.36b. Synthesized from ketone **2.36aa** using General Procedure B to give alcohol in 92% yield and >19:1 *dr* as an off-white powder. Mp 148-150 °C. ¹H NMR (500.0 MHz, CDCl₃) δ 7.30 (dd, J = 8.4, 5.9 Hz, 2H), 7.09 (t, J = 8.4 Hz, 2H), 6.30 (s, 1H), 5.48 (d, J = 9.8 Hz, 1H), 5.05 (d, J = 9.1 Hz, 1H), 3.88 (d, J = 10.3 Hz, 1H), 3.86 (d, J = 10.3 Hz, 1H), 3.79-3.72 (m, 1H), 3.11 (d, J = 9.5 Hz, 1H), 2.31 (d, J = 4.9 Hz, 1H), 1.46 (s, 9H), 1.20 (s, 3H), 1.12 (s, 3H). ¹³C NMR (125.7 MHz, CDCl₃) δ 163.40, 161.39, 156.41, 153.62, 134.84, 128.31, 115.81, 80.91, 75.40, 74.96, 60.16, 54.46, 31.06, 28.09, 24.93, 19.88. HRMS (ESI) m/z calculated for C₁₉H₂₇N₂O₅F [M+H⁺] 383.1977, found 383.1991. IR (cm⁻¹) 3585, 3318, 3-64, 2986, 2941, 2894, 1715, 1699, 1610, 1511, 1503, 1484, 1456, 1429, 1395, 1372, 1160, 1120, 1171, 1026.

Chapter 3. Development of Dynamic, Chemoselective Silver(I)-Catalyzed Intramolecular Aminations of Allenes and Alkenes.

This chapter is adapted from work published previously:

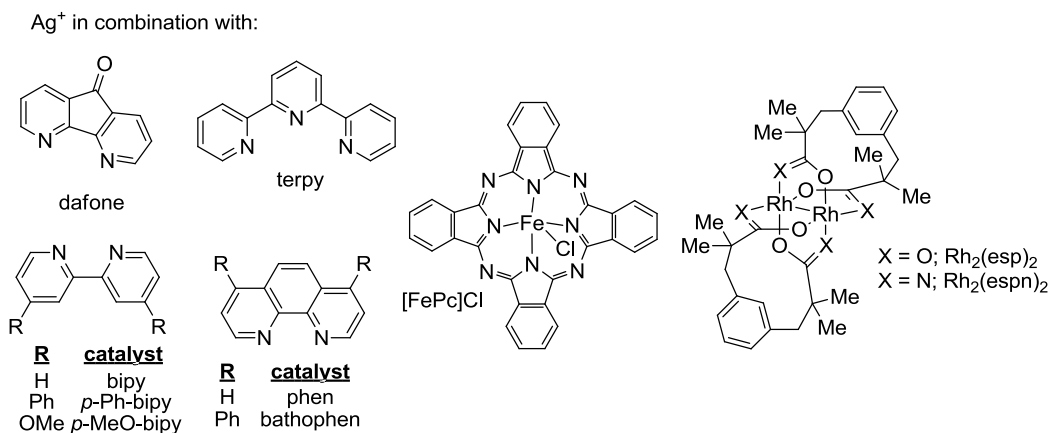
Rigoli, J. W.; Weatherly, C. D.; Vo, B. T.; Neale, S.; Meis, A. R.; Schomaker, J. M. *Org. Lett.* **2013**, *15*, 290.

Rigoli, J. W.; Weatherly, C. D.; Alderson, J. M.; Vo, B. T.; Schomaker, J. M. *J. Am. Chem. Soc.* **2013**, *135*, 17238.

3.1 Overview of Chemoselective, Ag(I)-Catalyzed Amination.

A central challenge in contemporary catalysis is the development of methods for the oxidation of complex organic substrates that are *selective* for single reactive sites, *controlled* by the catalyst system rather than by directing groups, and *tunable* for different reactive sites. Several transition metals, including Rh, Cu, Ru, Fe, Co, Au, and Ag, are known to promote C–N bond formation via presumed nitrene intermediates (Figure 3.1).¹⁻⁸ Recent studies have shown that changing the identity of the metal in the catalyst can control whether predominantly aziridination or C–H amination is observed when both C–H and π -bonds are present.^{9,10} A common challenge in the application of these catalysts is attaining chemo- and site-selectivity in substrates possessing multiple reactive functionalities.

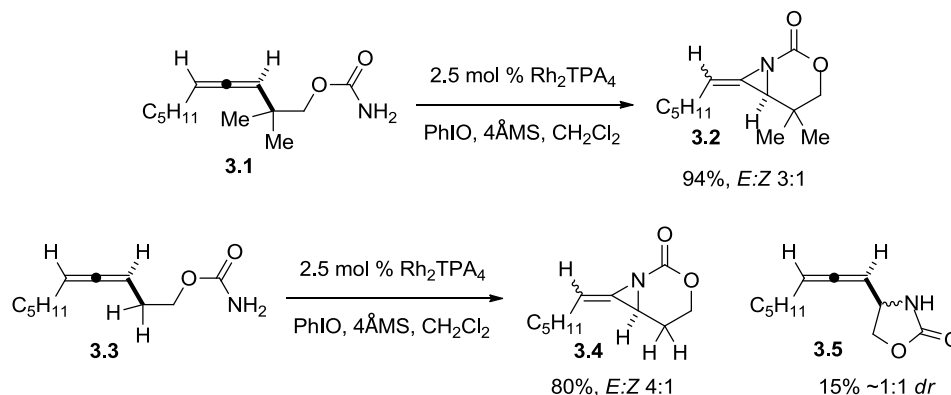
Figure 3.1. Examples of catalysts for chemoselective nitrene transfer.



Construction of the methylene aziridines described in Chapters 1 and 2 was enabled by transition-metal-catalyzed intramolecular nitrene transfer using homoallylic carbamate substrates. For substrates such as **3.1**, which lack allenic protons, the aziridination reaction proceeds in nearly quantitative yield under Rh-catalyzed conditions.¹ However, when allenic protons are present, as in **3.3**, both aziridination and allenic C–H insertion products are obtained

from the reaction (Scheme 3.1). While synthetically useful selectivities are obtained for **3.3**, selectivity in this transformation is highly substrate-dependent, and even small changes in the substrate can greatly reduce the chemoselectivity. In this chapter, efforts to improve the chemoselectivity of allenic aziridination are described, culminating in the development of a silver-catalyzed system capable of providing high selectivity for either aziridination or C-H insertion products based on simple changes in the ligand/metal ratio.

Scheme 3.1. Chemoselectivity in Rh-catalyzed aziridination of homoallenic carbamates.



3.2. Development of silver-catalyzed aziridination of homoallenic carbamates.

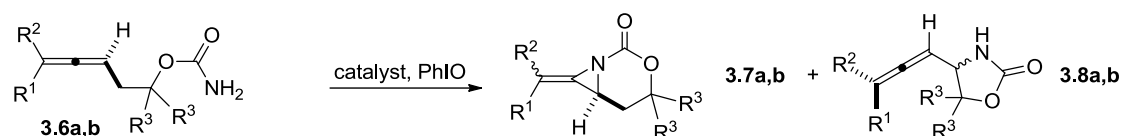
We focused on two substrates, **3.6a** and **3.6b**, that gave poor chemoselectivity in Rh-catalyzed aziridination (Table 3.1). Treatment of **3.6a** with $\text{Rh}_2(\text{esp})_2$ ($\text{esp} = \alpha, \alpha, \alpha', \alpha'$ -tetramethyl-1,3-benzene-dipropionic acid, Table 1, entry 1) gave only a 35% yield of **3.7a** and significant C–H insertion to **3.8a**. $\text{Rh}_2(\text{espn})_2\text{Cl}$ (entry 2) performed better, yet further attempts to improve the chemoselectivity by changing the nature of the carboxylate ligands on the Rh were unsuccessful.¹¹ A series of Cu catalysts gave poor reactivity, and attempts to isolate the iodine prior to amination were unsuccessful. However, $\text{Cu}(\text{MeCN})_4\text{PF}_6$ (entry 5) could be induced to give low yields of amination products by premixing **3.7a** with PhIO before the addition of

catalyst. However, this did not improve the results using Ru- and Fe-based catalysts, even when 20 mol % of the metal was employed (entries 6–7).^{3c,4a,5e} While treatment of **3.6a** with AgOTf in the presence of PhIO gave very little **3.7a** (entry 8), the addition of dafone (4,5-diazafluoren-9-one, entry 9) improved the conversion and, encouragingly, yielded >20:1 chemoselectivity for aziridination over C–H insertion. A series of bipyridine (bipy) ligands (entries 10–12) also gave excellent chemoselectivity for aziridination with good yields.^{8a–8d} Phen (entry 13) increased the yield to 79%, but the additional bulk in bathophen (entry 14) was not necessary. To our surprise, switching to a terpyridine ligand (terpy, entry 15) reversed the chemoselectivity in favor of **3.8a**.^{8a} The nature of the Ag counteranion also had a significant impact on the reaction. Substitution of AgOTf with AgOAc (entry 16) or AgO₂CCF₃ (entry 17) gave almost exclusively C–H insertion **3.8a**, although the reactivity of the catalyst was diminished, as these anions can bind tightly to the metal.

The allenic carbamate **3.6b** was also a challenging substrate for aziridination. When Rh₂(esp)₂ was employed as the catalyst, an 80% yield of **3.8b** was obtained (entry 18),¹² highlighting the impact of substrate structure on the chemoselectivity of Rh-catalyzed C–N bond formation. Neither Rh₂(espn)₂ (entry 19) nor Cu-, Fe-, or Ru-based catalysts (entries 20–22) improved the outcome. However, employing a dafone ligand in the presence of AgOTf (entry 24) reversed the chemoselectivity to 2.7:1 in favor of aziridination. Bipyridine ligands (entries 25–27) improved the chemoselectivity further, resulting in good yields of the aziridine **3.7b** and A:I selectivities ranging from 3.1:1 to 6.4:1. Phen and bathophen (entries 28–29) gave comparable yields, in contrast to the aziridination of the more sterically demanding **3.6a** (entries 13–14). As in the case of **3.6a**, a 2,2':6',2''-terpyridine ligand (entry 30) resulted in a reversal of the chemoselectivity, providing a **3.7b**:**3.8b** ratio of 1:6.6. To our knowledge, these results

represent the first examples of reagent-controlled amination of unsaturated substrates with Ag(I) catalysis.

Table 3.1. Examination of catalyst for allene aziridination.



3.6a-3.8a: R¹=R²=Me, R³=H
3.6b-3.8b: R¹=C₆H₁₁, R²=H, R³=Me

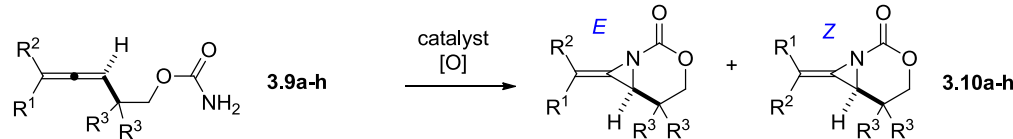
entry	catalyst ^a	A:I ^b	yield 3.7a (3.8a) ^c	entry	catalyst ^a	<i>E:Z</i>	A:I ^b	yield 3.7b (3.8b) ^c
1	Rh ₂ (esp) ₂	2:1	35% (17%)	18	Rh ₂ (esp) ₂	2:1	1:17	5% (80%)
2	Rh ₂ (espn) ₂ Cl	2.7:1	40% (15%)	19	Rh ₂ (espn) ₂ Cl	3:1	1:4.7	9% (42%)
3	Cu(MeCN) ₄ PF ₆	---	0% (0%)	20	Cu(MeCN) ₄ PF ₆	---	---	0%
4	Cu(OTf) ₂ /phen	---	0% (0%)	21	[Ru ₂ (hp) ₄ Cl]	---	---	0%
5	Cu(MeCN) ₄ PF ₆	3.3:1	13% (4%)	22	[FePc]Cl	---	---	0%
6	[Ru ₂ (hp) ₄ Cl]	---	0%	23	AgOTf	nd	---	2% (0%) ^d
7	[FePc]Cl	---	0% (0%)	24	AgOTf/dafone	2.3:1	2.7:1	59% (22%)
8	AgOTf	> 20:1	6% (0%) ^d	25	AgOTf/bipy	2.4:1	6.4:1	68% (11%)
9	AgOTf/dafone	> 20:1	32%	26	AgOTf/ <i>p</i> -Ph-bipy	2.3:1	3.1:1	62% (20%)
10	AgOTf/bipy	> 20:1	60%	27	AgOTf/ <i>p</i> -MeO-bipy	2.2:1	6.4:1	73% (11%)
11	AgOTf/ <i>p</i> -Ph-bipy	> 20:1	66%	28	AgOTf/phen	2.2:1	5.9:1	80% (14%)
12	AgOTf/ <i>p</i> -MeO-bipy	> 20:1	72%	29	AgOTf/bathophen	1.9:1	7:1	84% (12%)
13	AgOTf/phen	> 20:1	79%	30	AgOTf/terpy	2.3:1	1:6.6	9% (61%)
14	AgOTf/bathophen	20:1	57%					
15	AgOTf/terpy	1:1.3	27% (35%)					
16	AgOAc/phen	1:14.6	0% (29%) ^e					
17	AgO ₂ CCF ₃ /phen	1:20	0% (40%) ^f					

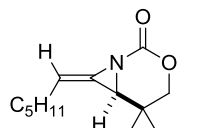
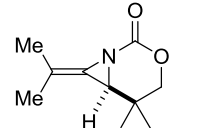
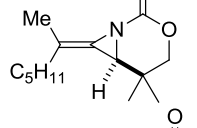
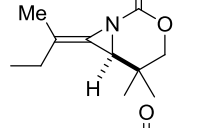
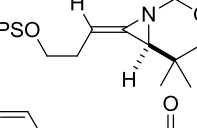
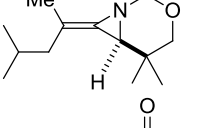
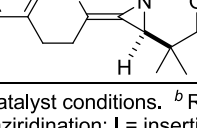
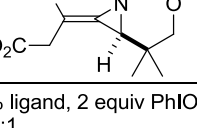
^a Rh catalysis: 5 mol % Rh₂(esp)₂, 2.0 equiv PhIO, CH₂Cl₂, rt. Ag catalysis: 20 mol % AgOTf, 25 mol % ligand, 4 Å MS, 2.0 equiv PhIO, CH₂Cl₂. Entries 1-17 use **3.6a** as the substrate; entries use **3.6b** as the substrate. ^b A = aziridination **3.7a,b**; I = insertion **3.8a,b**. ^c NMR yields using mesitylene as the internal standard. ^d significant decomposition of the carbamate occurred. ^e 45% conversion. ^f 60% conversion.

3.3. Scope of Ag(I)-catalyzed aziridination.

A series of allenes containing α,α -dimethyl groups (Table 3.2) were investigated with Ag(I) catalysts as an attractive alternative to Rh catalysts. Gratifyingly, treatment of **3.9a** with AgOTf/phen gave an excellent yield of **3.10a** (entry 1), which compared well with our previous results using Rh₂TPA₄ (TPA = triphenylacetate). Interestingly, the *E:Z* ratio was not greatly affected by the nature of the catalyst. AgOTf/phen performed similarly to Rh when a 1,3,3-trisubstituted homoallenic carbamate was employed (entry 2), and other 1,3-disubstituted allene

carbamates (entries 3–4, 8) gave good to excellent yields of the methylene aziridines **3.10c**, **3.10d**, and **3.10h**. The presence of a polar carboxyethyl group in **3.10h** (entry 8) resulted in very different behavior depending on whether a Rh- or Ag-based catalyst was employed. While Ag gave the *E* methylene aziridine as the expected stereoisomer, Rh₂(esp)₂ unexpectedly yielded the *Z* isomer as the major product. In addition to the 1,3,3-trisubstituted homoallenic carbamate **3.9b**, other highly substituted allenes bearing α,α -dimethyl branching (entries 5–7) gave good yields of methylene aziridines **3.10e–g**.

Table 3.2. Aziridination of α,α' -disubstituted homoallylic carbamates.


entry	desired product	catalyst ^{a,b}	<i>E</i> : <i>Z</i>	yield	entry	desired product	catalyst	<i>E</i> : <i>Z</i>	yield
1		3.10a Rh ₂ TPA ₄ AgOTf/phen	4:1 4:1	92% 88%	5		3.10e AgOTf/phen	---	98%
2		3.10b Rh ₂ (esp) ₂ AgOTf/phen	2.3:1 2.3:1	88% 81%	6		3.10f AgOTf/phen	3:1	90%
3		3.10c AgOTf/phen	3:1	87%	7		3.10g AgOTf/phen	2.3:1	97%
4		3.10d AgOTf/phen	2.6:1	83%	8		3.10h Rh ₂ (esp) ₂ AgOTf/phen	1:2.8 2.2:1	86% 85%

^a Rh catalyst conditions. ^b Reaction conditions: 20 mol% AgOTf, 25 mol% ligand, 2 equiv PhIO, 4 Å MS, CH₂Cl₂, rt.
^c A = aziridination; I = insertion. ^d 73% conversion. ^e *dr E* = 1:1; *dr Z* = 3:1.

When 1,3-disubstituted allenes **3.3** and **3.11a** were employed (entries 1–2), AgOTf in the presence of bipyridine and phenanthroline ligands gave comparable to slightly improved yields of bicyclic methylene aziridines. The benefit of substituting Ag catalysts for Rh became apparent when substitution was present in the tether between the allene and the carbamate (entries 3–4). Employing these conditions for **3.6b** improved the A:I ratio of 1:17 to 5.9:1 (entry 4). Surprisingly, the 1,3,3-trisubstituted allene carbamates **3.6a** and **3.12c,d** (entries 5–7) exhibited much greater chemoselectivity for aziridination using AgOTf/phen catalysts compared to conventional Rh catalysts. This was counterintuitive, as we expected the increased steric

Table 3.3. Chemoselective Aziridination of Homoallenic Carbamates Using Ag(I) Catalysis.

entry	desired product	catalyst	<i>E:Z</i>	<i>A:I</i> ^c	yield
1		3.4 Rh ₂ TPA ₄	4:1	4:1	80%
		Rh ₂ (esp) ₂	3:1	4:1	66%
		AgOTf/bipy	3:1	4:1	72%
2		Rh ₂ (esp) ₂	>99:1	2:1	49%
		3.12a AgOTf/phen	>99:1	1:1	40% ^d
		AgOTf/by	>99:1	3.7:1	67%
3		3.12b Rh ₂ (esp) ₂	---	1:1	34%
		AgOTf/phen	4.8:1	9:1	80% ^e
4		3.6b Rh ₂ (esp) ₂	2:1	1:17	5%
		AgOTf/phen	1.9:1	5.9:1	70%
5		3.7a Rh ₂ (esp) ₂	---	2:1	35%
		AgOTf/phen	---	>20:1	79%
6		3.12c Rh ₂ (esp) ₂	2.3:1	1:1.3	34%
		AgOTf/phen	2.6:1	11.5:1	87%
7		3.12d Rh ₂ (esp) ₂	---	1.1:1	32%
		AgOTf/phen	2.3:1	19:1	70%

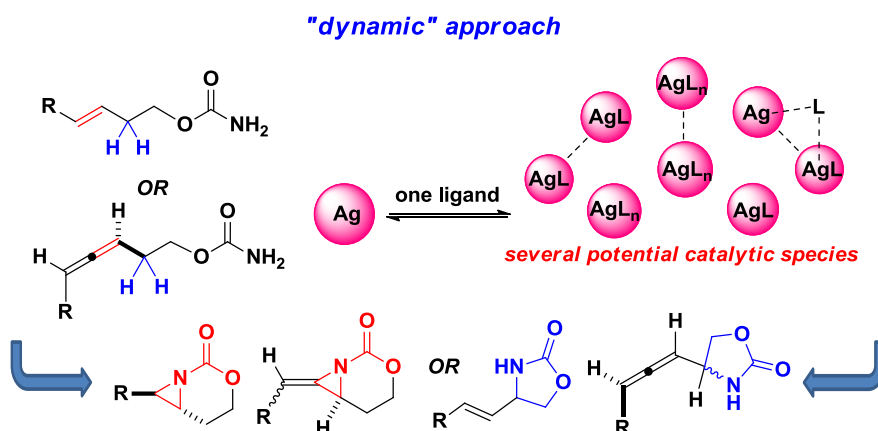
^a Rh catalyst conditions. ^b Reaction conditions: 20 mol% AgOTf, 25 mol% ligand, 2 equiv PhIO, 4 Å MS, CH₂Cl₂, rt. ^c A = aziridination; I = insertion. ^d 73% conversion. ^e *dr E* = 1:1; *dr Z* = 3:1.

congestion around the allene to favor more of the C–H insertion product. The ability to prepare such highly substituted bicyclic methylene aziridines represents a valuable step forward in our ability to prepare densely functionalized and complex nitrogen-containing stereotriads using these reactive scaffolds.

3.4. Chemoselective C-H insertion in homoallylic and homoallylic carbamate substrates.

In the above investigations, we noted that using a tridentate ligand for Ag-catalyzed nitrene transfer reversed selectivity in favor of allenic C-H amination. A deeper look into the literature showed that Ag has the unique ability to change coordination geometry in response to changes in the Ag counteranion, the ligand identity, or the metal/ligand ratio.¹³ If these changes in the coordination geometries of the Ag catalysts were indeed responsible for inducing divergent chemoselectivity, a ‘dynamic approach’ to catalytic amination could be envisioned (Figure 3.2). In this scenario, treatment of a single Ag salt with a single ligand would yield a mixture of several potential catalytic species. Simple perturbation of the equilibrium of this mixture could give different catalytic species capable of promoting divergent amination.

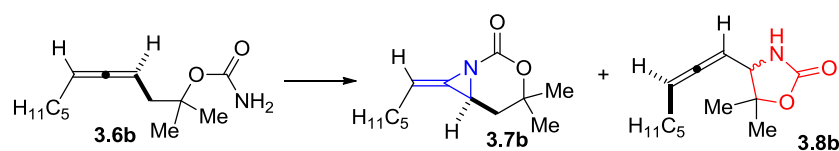
Figure 3.2. A dynamic approach to chemoselective amination.



In order to test the potential for developing a dynamic catalyst system, the metal:ligand stoichiometry of a AgOTf:phen catalyst system was varied to determine the effect on chemoselectivity. To our delight, a clear impact on the amination of **3.6a** was observed (Table 3.4). AgOTf:phen ratios close to 1:1 (entries 1–4) promoted aziridination to **3.7a** as the major

reaction pathway, while increasing the amount of phen gave C–H insertion to **3.8a** as the dominant mode of reactivity (entries 5, 6). The dramatic reversal in the reaction outcome suggests that an equilibrium between Ag(phen)OTf and Ag(phen)₂OTf exists and that each complex favors a different mode of reactivity.

Table 3.4. Effect of Ag:phen Stoichiometry on the Aziridination/Insertion Ratio.



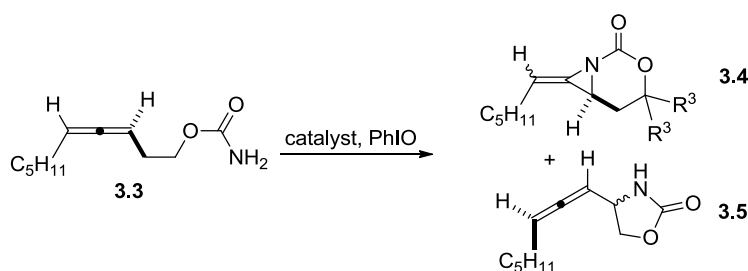
entry ^a	equiv AgOTf/phen	3.7b:3.8b (A:I)	3.7b (3.8b)^b
1	0.2 / 0.1	5.6:1	60% (12%)
2	0.2 / 0.2	5.8:1	75% (13%)
3	0.2 / 0.25	5.9:1	80% (13%)
4	0.2 / 0.3	5.6:1	70% (12%)
5	0.2 / 0.4	1:4	18% (72%)
6	0.2 / 0.6	1:38	2% (76%)

a: Reactions were carried out at 0.125 M **3.6b** in CH₂Cl₂, 2 equiv PhIO, AgOTf/phen, rt. b: NMR yields with mesitylene as the internal standard.

Further experiments were required to optimize the allenic C–H amination reaction for other substrates. The 1,3-disubstituted homoallylic carbamate **3.3**, which showed high selectivity for aziridination under both Rh- and Ag- catalyzed conditions, was chosen for optimization of the C–H amination chemistry. In an effort to show how a single ligand and metal could be used to attain different chemoselectivities, we confined our optimization efforts to 1,10-phenanthroline. Using a 2:1 ligand:metal ratio provided gave moderate yield of the C–H insertion product and excellent chemoselectivity, but incomplete conversion (Table 3.4, entry 1). Increasing the ligand:metal ratio slightly improved the yield and conversion (entry 2). Increasing the temperature to 35°C failed to improve conversion and decreased the overall yield (entry 3). Silver salts with more coordinating counterions such as Ag₂CO₃ and AgNO₃ reduced conversion, while use of the non-coordinating ion SbF₆[−] decreased the yield (entries 4–6). Notably, CH₂Cl₂

was a uniquely suitable solvent for the reaction, as Et₂O, PhCH₃, THF, and CHCl₃ failed to provide any conversion (entries 7-10). The reaction was not affected by use of an inert atmosphere (entry 11). Increasing the concentration of the reaction failed to improve conversion and led to decreased yield (entry 12).

Table 3.4. Optimization of allenic amination for 1,3-disubstituted allenes.



entry ^a	Ag/phen	Ag salt	solvent	cat. loading	equiv. PhIO	% conv.	% yield 3.5 (3.4)
1	1:2	AgOTf	CH ₂ Cl ₂	20 mol %	2.0	86	48 (2)
2	1:3	AgOTf	CH ₂ Cl ₂	20 mol %	2.0	89	55 (2)
3 ^b	1:3	AgOTf	CH ₂ Cl ₂	20 mol %	2.0	86	43 (0)
4	1:3	Ag ₂ CO ₃	CH ₂ Cl ₂	20 mol %	2.0	45	45 (0)
5	1:3	AgNO ₃	CH ₂ Cl ₂	20 mol %	2.0	<5	0 (0)
6	1:3	AgSbF ₆	CH ₂ Cl ₂	20 mol %	2.0	76	45 (0)
7	1:3	AgOTf	THF	20 mol %	2.0	<5	0 (0)
8	1:3	AgOTf	PhCH ₃	20 mol %	2.0	<5	0 (0)
9	1:3	AgOTf	CHCl ₃	20 mol %	2.0	<5	0 (0)
10	1:3	AgOTf	Et ₂ O	20 mol %	2.0	<5	0 (0)
11 ^c	1:3	AgOTf	CH ₂ Cl ₂	20 mol %	2.0	84	54 (0)
12 ^d	1:3	AgOTf	CH ₂ Cl ₂	20 mol %	2.0	16	49 (0)
13	1:3	AgOTf	CH ₂ Cl ₂	20 mol %	3.5	89	67 (2)
14	1:3	AgOTf	CH ₂ Cl ₂	33 mol %	3.5	70	55 (2)
15	1:3	AgOTf	CH ₂ Cl ₂	10 mol %	3.5	80	61 (4)
16	1:3	AgOTf	CH ₂ Cl ₂	20 mol %	5.0	93	57 (4)
17	1:3	AgOTf	CH ₂ Cl ₂	10 mol %	5.0	94	71 (5)
18 ^e	1:3	AgOTf	CH ₂ Cl ₂	10 mol %	5.0	100	68 (<1)
19 ^e	1:1.25	AgOTf	CH ₂ Cl ₂	20 mol %	2.0	83	50 (9)

^aUnless otherwise specified, reactions were conducted at 0.1M initial substrate concentration, at 23°C under air in the presence of 1g/mmol 4Å MS for 20 hours. ^bConducted at 35°C. ^cRun under atmosphere of N₂. ^dInitial starting material concentration of 0.3 M. ^e0.1 equivalents BHT added at reaction outset.

Altering reaction stoichiometry was key to attaining higher yields and conversion. Increasing the oxidant loading to 3.5 equivalents increased the product yield to 67% (entry 13), while increasing the catalyst loading to 33 mol% actually led to decreased conversion (entry 14). A slight decrease in yield was observed when the catalyst loading was lowered to 10 mol %

(entry 15). Because the catalyst was not completely soluble in the reaction solvent, it is likely that higher catalyst loadings did significantly affect the solution concentration of the catalyst. Increasing the oxidant loading to 5.0 equivalents provided even higher yield and conversion (entry 16, 17). To our surprise, the addition of 10 mol % BHT (butylatedhydroxytoluene), intended to probe the formation of radicals in the reaction pathway, provided full conversion and a high yield of product (entry 18). Moreover, the reaction time was reduced from 20 to 8 hours in the presence of BHT. Additionally, the addition of 10 mol % BHT to a 1:1.25 mixture of Ag:phen also reversed the selectivity to favor C-H amination. Two possible explanations for this surprising behavior are that the BHT affects the equilibrium between catalyst species in favor of AgL_2 complex, or that it helps to make the catalyst more soluble.

3.5. Scope of Ag(I)-catalyzed aziridination.

With these conditions in hand, the amination systems were applied to ten homoallenic carbamates (Table 3.5). In all cases, a 1:1.25 ratio of AgOTf:phen favored aziridination, while a 1:3 ratio of AgOTf:phen yielded mainly C-H insertion. Trisubstituted allenes (entries 1, 6–7) exhibited good selectivity under both conditions, while less substituted allenes (entries 2–5, 8) usually gave better selectivity under C-H insertion conditions. In 1,3-disubstituted allenes, the addition of 10 mol % BHT led to improved yields and selectivities (entries 4, 8-10).

Table 3.5. Tunable, chemoselective amination of homoallenic carbamates.

Reaction scheme: A homoallenic carbamate with substituents R¹ and R² reacts with a catalyst and PhIO to form two products: an insertion product (I) and an aziridination product (A).

entry	allene	AgOTf:phen ^{a,b}	I:A ^d	yield I (A or SM)
1		1:1.25 1:3 Rh ₂ (esp) ₂	1:20 100:0 1:2	< 4% (79%) 81% 17% (35%)
2		1:1.25 1:3	1:5.9 76:1	13% (79%) 76% (1%)
3		1:1.25 1:3 Rh ₂ (esp) ₂	1:9 100:0 1:1	9% (80%) 76% 34% (34%)
4		1:1.25 1:3 1:3 ^e	1:4 13:1 100:1	18% (72%) 65% (11% 3.3) 71%
5		1:1.25 ^c 1:3	1:3.7 100:0	18% (67%) 83%
6		1:1.25 1:3 Rh ₂ (esp) ₂	1:11.5 100:0 1.3:1	7% (87%) 88% 44% (34%)
7		1:1.25 1:3	1:19 100:0	4% (70%) 78%
8		1:1.25 1:3 1:3 ^e	1:4.8 19:1 100:1	12% (57%) 74% (10% 3.13b) 68%
9		1:1.25 1:3 1:3 ^e	0:100 24:1 100:1	61% 74% (6% 3.13c) 71%
10		1:1.25 1:3 1:3 ^e	0:100 100:0 30:1	58% 36% (15% 3.13d) 62% (3% 3.13d)

a: Aziridination: 20 mol% AgOTf, 25 mol% phen, 2 equiv PhIO, 4 Å MS, CH₂Cl₂. b: C-H insertion: 10 mol% AgOTf, 30 mol% phen, 3.5 equiv PhIO, 4 Å MS, CH₂Cl₂. c: 2,2'-bipyridine ligand. d: I = insertion, A = aziridination. e: 10 mol% BHT added.

Table 3.6. Amination of homoallylic carbamate.

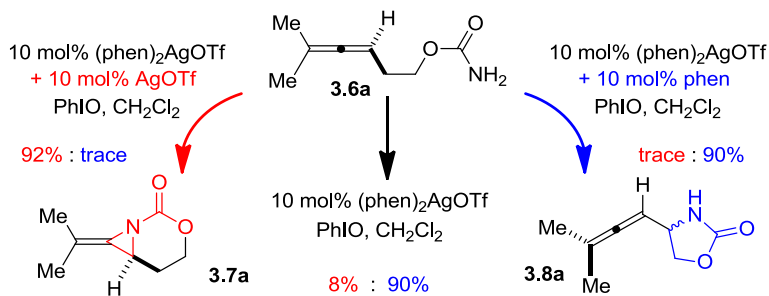
entry	substrate	catalyst ^{a,b,c}	A:I	yield	dr
1	 3.15a	Rh ₂ (OAc) ₄	3.2:1	58% 3.16a	<i>cis</i>
		1:1.25 AgOTf:phen	15.7:1	67% 3.16a	
		1:3 AgOTf:phen	0:100	93% 3.17a	
2	 3.15b	Rh ₂ (esp) ₂	1.8:1	45% 3.16b (25% 3.17b) ^d	nd
		1:1.25 AgOTf:phen	9:1	89% 3.16b	3.2:1
		1:3 AgOTf:phen	1:20	87% 3.17b	3:1
3	 3.15c	Rh ₂ (OAc) ₄	4.9:1	68% 3.16c	<i>trans</i>
		1:1.25 AgOTf:phen	24:1	88% 3.16c	
		1:3 AgOTf:phen	1:6.6	73% 3.17c	
4	 3.15d	Rh ₂ (OAc) ₄	7:1	35% 3.16d	---
		1:1.25 AgOTf:phen	99:1	85% 3.16d	---
		1:3 AgOTf:phen	1:2.9	66% 3.17d	---
5	 3.15e	Rh ₂ (esp) ₂	1.2:1	25% 3.16e (21% 3.17e) ^d	nd
		1:1.25 AgOTf:phen	1.4:1	54% 3.16e (39% 3.17e) ^d	nd
		1:3 AgOTf:phen	0:100	68% 3.17e	2.4:1

a: Rh cat: 3 mol%, 2 equiv PhIO, 4 Å MS, CH₂Cl₂. b: Aziridination: 20 mol% AgOTf, 25 mol% phen, 2 equiv PhIO, 4 Å MS, CH₂Cl₂. c: C-H insertion: 10 mol% AgOTf, 30 mol% phen, 3.5 equiv PhIO, 4 Å MS, CH₂Cl₂. d: NMR yields, mesitylene internal standard.

Simple changes in the AgOTf:phen stoichiometry also provided good chemoselectivity in the amination of homoallylic carbamates (Table 3.6). The *cis*-disubstituted **3.15a** showed increased selectivity for aziridination in switching from Rh₂(OAc)₄ to 1:1.25 AgOTf:phen (entry 1), while changing the AgOTf:phen ratio to 1:3 promoted exclusive insertion. This trend held for both the *cis*-disubstituted **3.15b** (entry 2) containing substitution in the tether and the *trans*-disubstituted **3.15c** (entry 3). The stereochemistry of the olefin was transferred to the resulting aziridines and allylic amines with no detectable isomerization. The 1,1'-disubstituted **3.15d** gave better selectivity and yield for aziridination compared to Rh₂(OAc)₄, although the C–H insertion was moderate. Substrate **3.15e** gave poor results using aziridination conditions, but good selectivity under insertion conditions.

Attempts to isolate Ag complexes from solutions of AgOTf and phenanthroline resulted in the recovery of only Ag(phen)₂OTf. Nonetheless, Ag(phen)₂OTf was capable of producing two distinct catalytic species capable of divergent amination (Scheme 3.2). Reaction of **3.6a** with the preformed Ag(phen)₂OTf gave a 90:8 mixture of products in favor of the C–H insertion, consistent with the results described in Table 3.4. Addition of 10 mol % AgOTf to the initial Ag(phen)₂OTf complex *completely reversed* the chemoselectivity to provide **3.7a** in 92% yield, while an extra 10 mol % of phen shut down the competing aziridination pathway, giving **3.8a** in 90% yield. This experiment suggested that the predominant catalytic species in solution was not solely a function of initial reaction conditions, but could be controlled *in situ* by altering ligand:metal ratios.

Scheme 3.2. Dynamic behavior of Ag complexes demonstrated by *in situ* control of catalyst.



3.6. Conclusions.

We have developed a simple Ag-based catalyst system that represents the only method to date capable of employing the same metal and the same ligand to accomplish *either* aziridination *or* C–H insertion in good yields. The ability for Ag to readily adopt multiple coordination geometries provides a new approach to identify catalysts that can promote other types of chemoselective amination, including choosing between two different C–H bonds. In addition, the

ease with which this methodology can be implemented and hopefully extended to other chemoselective C–heteroatom and C–C bond formations opens a potential gateway in reaction discovery.

3.7. References.

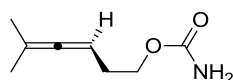
1. Boralsky, L. A.; Marston, D. M.; Grigg, R. D.; Hershberger, J. C.; Schomaker, J. M. *Org. Lett.* **2011**, *13*, 1924-1927.
2. For selected references on Rh-catalyzed amination, see: a) Espino, C. G.; Du Bois, J. *Angew. Chem., Int. Ed.* **2001**, *40*, 598. b) Espino, C. G.; Wehn, P. M.; Chow, J.; Du Bois, J. *J. Am. Chem. Soc.* **2001**, *123*, 6935. c) Padwa, A.; Flick, A. C.; Leverett, C. A.; Stengel, T. *J. Org. Chem.* **2004**, *69*, 6377. d) Espino, C. G.; Fiori, K. W.; Kim, M.; Du Bois, J. *J. Am. Chem. Soc.* **2004**, *126*, 15378. e) Fiori, K. W.; Du Bois, J. *J. Am. Chem. Soc.* **2007**, *129*, 562.
3. For selected references on Cu-catalyzed amination, see: a) Nakanishi, M.; Salit, A.; Bolm, C. *Adv. Synth. Catal.* **2008**, *350*, 1835. b) Han, H.; Park, S. B.; Kim, S. K.; Chang, S. *J. Org. Chem.* **2008**, *73*, 2862. c) Duran, F.; Leman, L.; Ghini, A.; Burton, G.; Dauban, P.; Dodd, R. H. *Org. Lett.* **2002**, *4*, 2481. d) Lebel, H.; Lectard, S.; Parmentier, M. *Org. Lett.* **2007**, *9*, 4797. e) Liu, R. M.; Herron, S. R.; Fleming, S. A. *J. Org. Chem.* **2007**, *72*, 5587. f) Gephart, R. T.; Warren, T. H. *Organometallics* **2012**, *31*, 7728.
4. Harvey, M. E.; Musaev, D. G.; Du Bois, J. *J. Am. Chem. Soc.* **2011**, *133*, 17207, and references therein.
5. For selected references on Fe-catalyzed amination, see: a) Jung, N.; Bräse, S. *Angew. Chem., Int. Ed.* **2012**, *51*, 5538. b) Cramer, S. A.; Jenkins, D. M. *J. Am. Chem. Soc.* **2011**, *133*, 19342. c) Klotz, K. L.; Slominski, L. M.; Riemer, M. E.; Phillips, J. A.; Halfen, J. A. *Inorg. Chem.* **2009**, *48*, 801. d) Mahy, J.; Battioni, P.; Mansuy, D. *J. Am. Chem. Soc.* **1986**, *108*, 1079. e) Paradine, S. M.; White, M. C. *J. Am. Chem. Soc.* **2012**, *134*, 2036.
6. Gao, G.; Harden, J. D.; Zhang, X. P. *Org. Lett.* **2005**, *7*, 3191.
7. Li, Z.; Ding, X.; He, C. *J. Org. Chem.* **2006**, *71*, 5876.
8. For selected references on Ag-catalyzed amination, see: a) Cui, Y.; He, C. *J. Am. Chem. Soc.* **2003**, *125*, 16202. b) Cui, Y.; He, C. *Angew. Chem. Int. Ed.* **2004**, *43*, 4210. c) Li, Z.; Capretto, D. A.; Rahaman, R. H.; He, C. *Angew. Chem., Int. Ed.* **2007**, *46*, 5184. d) Li, Z.; He, C. *Eur. J. Org. Chem.* **2006**, *19*, 4313. e) Kumar, K. A.; Rai, L. K. M.; Umesha, K. B. *Tetrahedron Lett.* **2001**, *57*, 6993. f) Minakaa, S.; Kano, D.; Fukuoka, R.; Oderaotoshi, Y.; Komatsu, M. *Heterocycles* **2003**, *60*, 289. g) Gomez-Emeterio, B. P.; Urbano, J.; Diaz-Requejo, M. M.; Perez, P. J. *Organometallics* **2008**, *27*, 4126. h) Llaveria, J.; Beltrán, A.; Mar Díaz-Requejo, M.; Matheu, M. I.; Castellón, S.; Pérez, P. J. *Angew. Chem. Int. Ed.* **2010**, *122*, 7246.

9. For selected examples of tuning the chemoselectivity of amination using Rh and Ru catalysis, see: a) Hayes, C. J.; Beavis, P. W.; Humphries, L. A. *Chem. Commun.* **2006**, 4501. b) Fiori, K. W.; Du Bois, J. *J. Am. Chem. Soc.* **2007**, *129*, 562. c) Kornecki, K. P.; Berry, J. F. *Eur. J. Inorg. Chem.* **2012**, *3*, 562.
10. Control of chemoselectivity in carbene chemistry is well-developed. (a) Davies, H. M. L.; Morton, D. *Chem. Soc. Rev.* **2011**, *40*, 1857. (b) Nadeau, E.; Ventura, D. L.; Brekan, J. A.; Davies, H. M. L. *J. Org. Chem.* **2010**, *75*, 1927.
11. Kornecki, K. P.; Berry, J. F. *Chem. Commun.* **2012**, *48*, 12097.
12. Grigg, R. D.; Schomaker, J. M.; Timokhin, V. *Tetrahedron* **2011**, *67*, 4318.
13. a) Hung-Low, F.; Renz, A.; Klausmeyer, K. K. *Polyhedron* **2009**, *28*, 407. b) Hung-Low, F.; Renz, A.; Klausmeyer, K. K. *J. Chem. Cryst.* **2011**, *41*, 1174. c) Du, J.-L.; Hu, T.-L.; Zhang, S.-M.; Zeng, Y.-F.; Bu, X.-H. *CrystEngComm.* **2008**, *10*, 1866. d) Zhang, H.; Chen, L.; Song, H.; Zi, G. *Inorg. Chim. Acta.* **2011**, *366*, 320. e) Hung-Low, F.; Renz, A.; Klausmeyer, K. K. *J. Chem. Cryst.* **2009**, *39*, 438. f) Levason, W.; Spicer, M. D. *Coord. Chem. Rev.* **1987**, *76*, 45. g) Leschke, M.; Rheinwald, G.; Lang, H. Z. *Anorg. Allg. Chem.* **2002**, *628*, 2470.

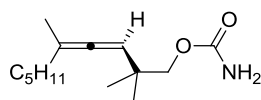
3.8. Experimental Details and Characterization.

3.8.1 Preparation of homoallenic carbamates.

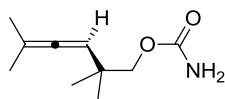
Homoallenic carbamates were prepared according to the general procedures described in chapters 1 and 2. The following homoallenic carbamates were not reported previously:



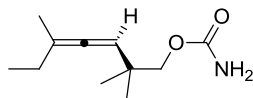
Compound 3.6a. Obtained in 53% yield as a thick oil. ^1H NMR (300 MHz, CDCl_3) δ 4.94 (m, 1H), 4.58 (br s, 2H), 4.11 (t, $J = 6.8$ Hz, 2H), 2.27 (q, $J = 6.6$ Hz, 2H), 1.68 (d, $J = 2.9$ Hz, 6H). ^{13}C NMR (75 MHz, CDCl_3) δ 202.66, 157.48, 96.06, 84.56, 64.65, 28.98, 20.72. HRMS (ESI) m/z calculated for $\text{C}_8\text{H}_{13}\text{NO}_2$ [$\text{M}+\text{Na}^+$] 178.0839, found 178.0842. IR: in CH_2Cl_2 3537, 3424, 2987, 1730, 1585, 1422, 1337, 1265 1159, 1093.



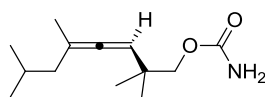
Compound 3.9b. Obtained in 76% yield as an oil. ^1H NMR (400 MHz, CDCl_3) δ 4.97 (m, 1H), 4.72 (s, 2H), 3.84 (s, 2H) 1.92 (ddd, $J = 8.9, 6.2, 2.7$ Hz, 2H), 1.68 (d, $J = 2.9$ Hz, 3H), 1.47-1.22 (m, 6H), 1.02 (s, 6H), 0.89 (t, $J = 6.8$ Hz, 3H) ^{13}C NMR (100 MHz, CDCl_3) δ 199.61, 101.99, 97.52, 73.33, 35.74, 33.98, 31.62, 27.30, 25.02, 25.00, 22.57, 19.38, 14.10. HRMS (ESI) m/z calculated for $\text{C}_{12}\text{H}_{21}\text{NO}_5\text{S}$ [$\text{M}+\text{NH}_4^+$] 309.1479, found 309.1493. IR: in CH_2Cl_2 3530, 3420, 2931, 1731, 1584, 1468, 1397, 1377, 1331, 1271, 1068.



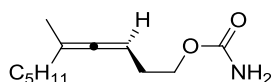
Compound 3.9e. Obtained in 72% yield as a white solid. ^1H NMR (300 MHz, CDCl_3) δ 4.90 (m, 1H), 4.65 (br s, 2H), 3.84 (s, 2H), 1.69 (d, $J = 2.9$ Hz, 6H), 1.02 (s, 6H) ^{13}C NMR (75 MHz, CDCl_3) δ 200.46, 157.30, 97.57, 96.44, 73.45, 35.95, 25.19, 20.90. HRMS (ESI) m/z calculated for $\text{C}_{10}\text{H}_{17}\text{NO}_2$ [$\text{M}-\text{H}^+$] 182.1176, found 182.1169. IR: in CH_2Cl_2 3535, 3422, 2969, 1731, 1584, 1377, 1331, 1270, 1261, 1068.



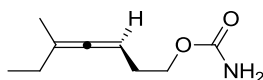
Compound 3.9f. Obtained in 68% yield as a white solid. ^1H NMR (300 MHz, CDCl_3) δ 4.98 (m, 1H), 4.52 (s, 2H), 3.81 (s, 2H), 1.90 (qd, $J = 7.4, 3.3$ Hz, 2H), 1.65 (d, $J = 2.9$ Hz, 3H), 0.98 (s, 6H), 0.95 (t, $J = 7.5, 3\text{H}$) ^{13}C NMR (75 MHz, CDCl_3) δ 199.46, 157.56, 103.85, 98.48, 73.48, 35.90, 27.06, 25.20, 19.53, 12.44. HRMS (ESI) m/z calculated for $\text{C}_{11}\text{H}_{19}\text{NO}_2$ [M^+] 197.1411, found 197.1412. IR: in CH_2Cl_2 3533, 3425, 2968, 1733, 1583, 1459, 1399, 1378, 1328, 1065.



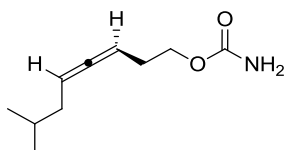
Compound 3.9g. Obtained in 67% yield as a thick oil. ^1H NMR (400 MHz, CDCl_3) δ 5.23-4.57 (m, 3H), 3.84 (s, 2H), 1.93-1.68 (m, 3H), 1.65 (d, $J = 2.9$ Hz, 3H), 1.02 (s, 1H), 0.90 (dd, $J = 6.4$, 1.7 Hz, 1H) ^{13}C NMR (100 MHz, CDCl_3) δ 200.39, 157.39, 100.61, 96.77, 73.31, 43.86, 35.80, 26.36, 25.05, 24.99, 22.72, 22.57, 19.28. HRMS (ESI) m/z calculated for $\text{C}_{13}\text{H}_{23}\text{NO}_2$ [$\text{M}+\text{H}^+$] 226.1802, found 226.1804. IR: in CH_2Cl_2 3536, 3425, 2963, 2879, 1728, 1584, 1465, 1397, 1378, 1323, 1071 cm^{-1} .



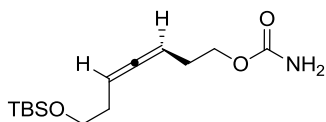
Compound 3.11c. Obtained in 78% yield as an oil. ^1H NMR (400 MHz, CDCl_3) δ 5.03-4.94 (m, 1H), 4.81 (br s, 2H), 4.10 (t, $J = 6.8$ Hz, 2H), 2.28 (q, $J = 6.8$ Hz, 2H), 1.91 (td, $J = 7.5$, 3.0 Hz, 2H), 1.66 (d, $J = 2.9$ Hz, 3H), 1.47-1.20 (m, 6H), 0.89 (t, $J = 6.9$ Hz, 3H) ^{13}C NMR (100 MHz, CDCl_3) δ 202.00, 157.11, 100.38, 85.63, 64.63, 33.87, 31.52, 29.01, 27.17, 22.56, 19.17, 14.11. HRMS (ESI) m/z calculated for $\text{C}_8\text{H}_{13}\text{NO}_2$ [$\text{M}+\text{Na}^+$] 178.0839, found 178.0842. IR: in CH_2Cl_2 3538, 3424, 2987, 1730, 1585, 1422, 1337, 1265, 1115, 1093 cm^{-1} .



Compound 3.11d. Obtained in 69% yield as a thick oil. ^1H NMR (300 MHz, CDCl_3) δ 5.03 (m, 1H), 4.96 (br s, 2H), 4.10 (t, $J = 6.9$ Hz, 2H), 2.28 (q, $J = 6.9$ Hz, 2H), 1.93 (qd, $J = 7.3$, 3.0 Hz, 2H), 1.68 (d, $J = 2.8$ Hz, 3H), 0.99 (t, $J = 7.3$ Hz, 3H) ^{13}C NMR (75 MHz, CDCl_3) δ 201.73, 157.46, 102.35, 86.58, 64.73, 29.16, 27.01, 19.28, 12.36. HRMS (ESI) m/z calculated for $\text{C}_9\text{H}_{15}\text{NO}_2$ [$\text{M}+\text{Na}^+$] 192.0995, found 192.0999. IR: in CH_2Cl_2 3537, 3424, 2987, 1730, 1585, 1422, 1398, 1337, 1265, 1160, 1093 cm^{-1} .



Compound 3.14a. The product was purified by column chromatography using a 0 \rightarrow 20% gradient of EtOAc in hexanes with 5% increments. The resulting colorless oil was obtained in 90% yield from the corresponding homoallylic alcohol. ^1H NMR (500 MHz, CDCl_3) δ 5.12-5.01 (m, 2H), 4.79 (br s, 2H), 4.12 (t, $J = 6.8$ Hz, 2H), 2.31 (qd, $J = 6.8, 2.9$ Hz, 2H), 1.91 (ddd, $J = 14.1, 6.8, 2.7$ Hz, 1H), 1.86 (ddd, $J = 14.1, 6.8, 2.7$ Hz, 1H), 1.65 (non, $J = 6.8$ Hz, 1H), 0.91 (d, $J = 6.8$ Hz, 6H). ^{13}C NMR (125.7 MHz, CDCl_3) δ 205.2, 157.1, 90.3, 85.9, 64.5, 38.3, 28.7, 28.4, 22.2, 22.1. HRMS (ESI) m/z calculated for $\text{C}_{10}\text{H}_{17}\text{NO}_2$ [$\text{M}+\text{Na}^+$] 206.1152, found 206.1156.

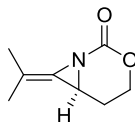


Compound 3.14c. The product was purified by column chromatography using a 0 \rightarrow 25% gradient of EtOAc in hexanes with 5% increments. The resulting colorless oil was obtained in 85% yield from the corresponding homoallylic alcohol. ^1H NMR (500 MHz, CDCl_3) δ 5.14 (qt, $J = 6.9, 2.8$ Hz, 1H), 5.07 (qt, $J = 6.9, 2.8$ Hz, 1H), 4.78 (br s, 2H), 4.11 (t, $J = 6.8$ Hz, 2H), 3.67 (t, $J = 6.9$ Hz, 2H), 2.31 (qd, $J = 6.9, 2.8$ Hz, 2H), 2.21 (qd, $J = 6.8, 2.8$ Hz, 2H), 0.90 (s, 9H), 0.06 (s, 6H). ^{13}C NMR (125.7 MHz, CDCl_3) δ 205.5, 157.2, 88.5, 86.7, 64.5, 63.1, 32.7, 28.7, 26.1, 18.5, -5.1. HRMS (ESI) m/z calculated for $\text{C}_{14}\text{H}_{27}\text{NO}_3\text{Si}$ [$\text{M}+\text{NH}_4^+$] 303.2099, found 303.2090.

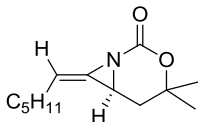
3.9.2. Ag(I)-catalyzed methylene aziridination.

For best results, the silver to ligand ratio needs to be exact. Both silver triflate and phenanthroline are highly hygroscopic and will not give good results if they are not completely dry. Silver reagents should be stored in a glove box and phenanthroline in a standard dessicator. Alternatively, the reaction can be carried out in a glove box, although this is not necessary as long as the quality of the reagents is properly maintained.

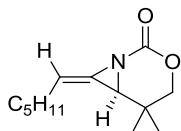
General procedure for Ag catalyzed methylene aziridination. Silver triflate (26 mg, 0.1 mmol, 0.2 eq) and phenanthroline (23 mg, 0.125 mmol, 0.25 eq) were charged into a pre-dried reaction flask. Dichloromethane (1 mL) was added to the flask. The mixture was stirred vigorously for 30 minutes. Then a solution of allene carbamate (0.5 mmol, 1 eq) in dichloromethane (1 mL) was added to the reaction flask followed by 3A or 4A molecular sieves (1 mmol substrate / g of sieves or 0.25 mmol substrate / g of sieves). Iodosobenzene (220 mg, 1 mmol, 2 eq) was then added in one portion and the reaction were to stir at room temperature until complete by TLC (~14 hours). The reaction mixture was then filtered through a glass frit and the filtrate was concentrated via vacuum. The crude products were then purified by silica gel column chromatography (0 → 30% EtOAc in hexanes, 6% increments).



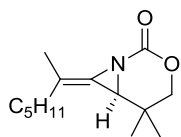
Compound 3.7a. Obtained in 79% yield as an oil. ^1H NMR (300 MHz, CDCl_3) δ 4.50 (m, 1H), 4.33 (m, 1H), 3.38 (t, $J = 7.4$ Hz, 1H), 2.35 (m, 1H), 1.98 (s, 3H), 1.80 (s, 3H), 1.60 (m, 1H) ^{13}C NMR (75 MHz, CDCl_3) δ 156.84, 120.37, 108.25, 68.52, 40.05, 24.36, 19.76, 18.53. HRMS (ESI) m/z calculated for $\text{C}_8\text{H}_{11}\text{NO}_2$ [$\text{M}+\text{H}^+$] 154.0863, found 154.0858. IR: in CH_2Cl_2 2983, 2904, 1793, 1718, 1471, 1384, 1094 cm^{-1} .



Compound 3.8a. Obtained in 80% yield as an oil. The identity of this product was verified by comparison of NMR spectra with reported literature.¹²

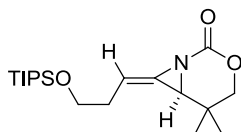


Compound 3.10a. Obtained in 88% yield as an oil. The identity of this product was verified by comparison of NMR spectra with reported literature.¹

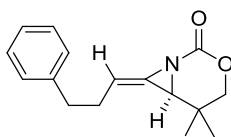


Compound 3.10b. Obtained in a 81% yield as a mixture of *E* and *Z* isomers *E* isomer: ¹H NMR (300 MHz, C₆D₆) δ 3.56 (d, *J* = 9.8 Hz, 1H), 3.19 (d, *J* = 9.8 Hz, 1H), 2.61 (s, 1H), 2.08 (s, 3H), 1.88 (m, 2H), 1.24 (m, 6H), 0.86 (t, *J* = 6.8 Hz, 3H), 0.54 (s, 3H), 0.51 (s, 3H). ¹³C NMR (125 MHz, C₆D₆) δ 155.93, 119.55, 112.54, 77.46, 49.35, 34.82, 32.26, 29.71, 27.58, 23.75, 23.19, 20.58, 17.10, 14.55. HRMS (ESI) *m/z* calculated for C₁₄H₂₃NO₂ [M+H⁺] 238.1802, found 238.1805. *Z* isomer: ¹H NMR (300 MHz, C₆D₆) δ 3.52 (d, *J* = 10.4 Hz, 1H), 3.17 (d, *J* = 10.4 Hz, 1H), 2.59 (m, 1H), 2.53 (s, 1H), 1.88 (m, 1H), 1.53 (s, 3H), 1.23 (m, 6H), 0.91 (t, *J* = 6.8 Hz, 3H), 0.51 (s, 3H), 0.49 (s, 3H). ¹³C NMR (125 MHz, C₆D₆) δ 155.80, 119.79, 112.04, 77.32, 48.73, 33.02, 32.19, 29.57, 28.23, 23.81, 23.31, 20.46, 17.85, 14.67. HRMS (ESI) *m/z* calculated

for $C_{14}H_{23}NO_2$ $[M+H^+]$ 238.1802, found 238.1805. IR: in CH_2Cl_2 2987, 1730, 1422, 1378, 1334, 1265, 1155, 1110 cm^{-1} .

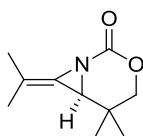


Compound 3.10c. Obtained in 87% yield and 3:1 *E:Z* mixture of isomers as a clear oil. *E* isomer: 1H -NMR: (300.1 MHz, C_6D_6) δ 5.58 (t, $J = 7.5$ Hz, 1H), 3.61-3.49 (m, 3H), 3.15 (d, $J = 10.9$ Hz, 1H), 2.56 (s, 1H), 2.33-2.10 (m, 2H), 1.14-0.98 (m, 21H), 0.53 (s, 3H), 0.46 (s, 3H); ^{13}C NMR: (75.4 MHz, C_6D_6) δ 155.19, 126.06, 100.16, 77.71, 63.53, 48.48, 33.42, 29.32, 23.76, 20.79, 18.61, 12.66; HRMS (ESI) m/z calculated for $C_{19}H_{35}NO_3Si$ $[M+H^+]$ 354.2459, found 354.2457. IR: in DCM 2971, 1727, 1586, 1406, 1377, 1332, 1270, 1070 cm^{-1} *Z* isomer: 1H NMR: (299.9 MHz, C_6D_6) δ 5.49 (t, $J = 7.6$ Hz, 1H), 3.79 (dt, $J = 9.8, 6.0$ Hz, 1H), 3.73 (ddd, $J = 9.8, 6.7, 5.5$ Hz, 1H), 3.48 (d, $J = 10.6$ Hz, 1H), 3.14 (d, $J = 10.6$ Hz, 1H), 2.98-2.79 (m, 2H), 2.54 (s, 1H), 1.15-1.06 (m, 21H), 0.52 (s, 3H), 0.41 (s, 3H); ^{13}C NMR: (75.4 MHz, C_6D_6) δ 155.09, 125.17, 101.98, 77.31, 64.20, 48.73, 31.97, 28.99, 23.62, 20.66, 18.64, 12.68; HRMS (ESI) m/z calculated for $C_{19}H_{35}NO_3Si$ $[M+H^+]$ 354.2459, found 354.2457. IR: in CH_2Cl_2 : 2971, 1731, 1592, 1502, 1382, 1331, 1070 cm^{-1} .

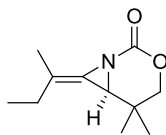


Compound 3.10d. Obtained in 83% yield as a 2.8:1 *E:Z* mixture of diastereomers. *E* isomer: 1H NMR: (300.1 MHz, C_6D_6) δ 7.12 (d, $J = 7.8$ Hz, 2H), 7.08-7.01 (m, 1H), 6.95 (d, $J = 7.4$ Hz, 1H), 5.52 (t, $J = 7.0$ Hz, 1H), 3.45 (d, $J = 10.5$ Hz, 1H), 3.07 (d, $J = 10.5$ Hz, 1H), 2.42 (t, $J = 7.3$ Hz, 2H), 2.37 (s, 1H), 2.10 (non, $J = 7.3$ Hz, 2H), 0.41 (s, 3H), 0.39 (s, 3H) ^{13}C -NMR: (125.8

MHz, CDCl₃) δ 154.24, 140.86, 133.24, 129.61, 126.36, 75.01, 72.99, 59.40, 54.91, 34.04, 32.39, 31.21, 25.18, 20.44; HRMS (ESI) m/z calculated for C₁₆H₁₉NO₂ [M+H⁺] 258.1489, found 258.1494. IR in DCM: 2971, 1728, 1589, 1402, 1380, 1344, 1070. *Z* isomer: ¹H NMR: (299.9 MHz, C₆D₆) δ 7.15-7.10 (m, 4H), 7.09-7.00 (m, 1H), 4.99 (t, J = 7.2 Hz, 1H), 3.42 (d, J = 10.4 Hz, 1H), 3.05 (d, J = 10.4 Hz, 1H), 2.93 (dq, J = 14.4, 7.2 Hz, 1H), 2.77 (dq, J = 14.4, 7.2 Hz, 1H), 2.67 (t, J = 7.2 Hz, 1H), 2.43 (s, 1H), 0.39 (s, 3H), 0.38 (s, 3H); ¹³C NMR: (75.4 MHz, C₆D₆) δ 155.06, 142.06, 129.40, 129.05, 126.59, 124.72, 103.69, 77.18, 48.62, 36.87, 29.78, 28.90, 23.64, 20.56; HRMS (ESI) m/z calculated for C₁₆H₁₉NO₂ [M+NH₄⁺] 275.1755, found 275.1747. IR in CH₂Cl₂: 2971, 1731, 1592, 1502, 1382, 1331, 1070 cm⁻¹.

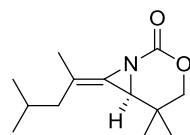


Compound 3.10e. Obtained in a 98% yield as an oil. ¹H NMR (300 MHz, CDCl₃) δ 4.20 (d, J = 10.6 Hz, 1H), 3.81 (d, J = 10.6 Hz, 1H), 3.11 (s, 1H), 1.99 (s, 3H), 1.79 (s, 3H), 1.25 (s, 3H), 0.88 (s, 3H) ¹³C NMR (75 MHz, CDCl₃) δ 156.58, 118.66, 108.95, 77.42, 49.40, 29.76, 24.11, 20.54, 20.08, 18.47. HRMS (ESI) m/z calculated for C₁₀H₁₅NO₂ [M+H⁺] 182.1176, found 182.1173. IR: in CH₂Cl₂ 2975, 1730, 1472, 1404, 1375, 1345, 1298, 1265, 1216, 1185, 1093, 1018 cm⁻¹.

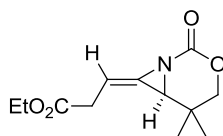


Compound 3.10f. Obtained in a 90% yield as a mixture of *E* and *Z* isomers. *E* isomer: ¹H NMR (300 MHz, CDCl₃) δ 4.22 (d, J = 10.7 Hz, 1H), 3.81 (d, J = 10.7 Hz, 1H), 3.13 (s, 1H), 2.14 (m, 2H), 1.99 (s, 3H), 1.24 (s, 3H), 1.07 (t, J = 7.5 Hz, 3H), 0.87 (s, 3H). ¹³C NMR (75 MHz, CDCl₃) δ 156.17, 117.53, 114.18, 77.22, 49.12, 29.41, 27.10, 23.55, 20.11, 16.09, 11.69. HRMS (ESI)

m/z calculated for $C_{11}H_{17}NO_2$ $[M+H^+]$ 196.1333, found 196.1330. *Z* isomer: 1H NMR (300 MHz, $CDCl_3$) δ 4.20 (d, $J = 10.7$ Hz, 1H), 3.81 (d, $J = 10.7$ Hz, 1H), 3.09 (s, 1H), 2.43 (m, 2H), 1.78 (s, 3H), 1.25 (s, 3H), 1.09 (t, $J = 7.6$ Hz, 3H), 0.88 (s, 3H) ^{13}C NMR (75 MHz, $CDCl_3$) δ 156.17, 117.59, 113.86, 77.00, 48.55, 29.35, 25.51, 23.70, 20.05, 16.89, 12.36. HRMS (ESI) m/z calculated for $C_{11}H_{17}NO_2$ $[M+H^+]$ 196.1333, found 196.1330. IR: in CH_2Cl_2 2972, 1728, 1472, 1404, 1376, 1297, 1245, 1215, 1157, 1096 cm^{-1} .

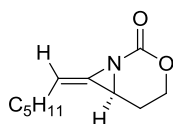


Compound 3.10g. Obtained in a 97% yield as a mixture of *E* and *Z* isomers. *E* isomer: 1H NMR (300 MHz, $CDCl_3$) δ 4.20 (d, $J = 10.6$ Hz, 1H), 3.82 (d, $J = 10.6$ Hz, 1H), 3.10 (s, 1H), 1.98 (m, 2H), 1.96 (s, 3H), 1.88 (m, 1H), 1.25 (m, 3H), 0.89 (m, 9H). ^{13}C NMR (75 MHz, $CDCl_3$) δ 156.55, 119.34, 112.48, 77.40, 49.64, 43.57, 29.82, 26.00, 24.11, 22.93, 22.22, 20.70, 16.49. HRMS (ESI) m/z calculated for $C_{13}H_{21}NO_2$ $[M+H^+]$ 224.1646, found 224.1649. *Z* isomer: 1H NMR (300 MHz, $CDCl_3$) δ 4.19 (d, $J = 10.6$ Hz, 1H), 3.82 (d, $J = 10.6$ Hz, 1H), 3.10 (s, 1H), 2.29 (d, $J = 7.5$ Hz, 2H), 1.88 (m, 1H), 1.75 (s, 3H), 1.26 (s, 3H), 0.89 (m, 9H) ^{13}C NMR (75 MHz, $CDCl_3$) δ 156.32, 119.26, 112.04, 77.34, 49.05, 41.35, 29.67, 26.07, 24.11, 22.54, 22.22, 20.66, 17.82. HRMS (ESI) m/z calculated for $C_{13}H_{21}NO_2$ $[M+H^+]$ 224.1646, found 224.1649. IR: in CH_2Cl_2 2962, 1730, 1472, 1404, 1377, 1341, 1299, 1265, 1214, 1159 cm^{-1} .

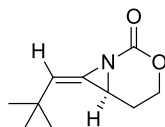


Compound 3.10h. Obtained in 86% yield as a 2.2:1 *E*:*Z* mixture of diastereomers. The *Z* isomer was previously characterized. *E* isomer: 1H -NMR: (300.1 MHz) δ 5.67 (t, $J = 6.7$ Hz, 1H), 3.87 (q, $J = 7.4$ Hz, 2H), 3.49 (d, $J = 10.0$ Hz, 1H), 3.16 (d, $J = 10.0$ Hz, 1H), 2.72 (qd, $J = 16.9, 7.8$

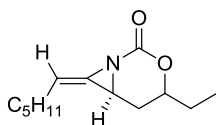
Hz, 2H), 2.50 (s, 1H), 0.90 (t, $J = 7.4$ Hz, 3H), 0.50 (s, 3H), 0.46 (s, 3H); $^{13}\text{C-NMR}$: (75.4 MHz, C_6D_6) δ 170.42, 154.83, 127.46, 96.27, 61.00, 48.55, 34.62, 29.26, 23.56, 20.52, 14.47; HRMS (ESI) m/z calculated for $\text{C}_{12}\text{H}_{17}\text{NO}_4$ $[\text{M}+\text{H}^+]$ 240.1231, found 240.1223. IR in CH_2Cl_2 : 2968, 1728, 1580, 1402, 1380, 1332, 1071 cm^{-1} .



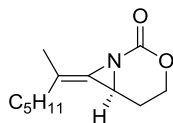
Compound 3.4. Bipyridine was used as the ligand instead of phenanthroline. Obtained in 72% yield as an oil. The identity of this product was verified by comparison of NMR spectra with reported literature.¹



Compound 3.12a. Bipyridine was used as the ligand instead of phenanthroline. Obtained in 67% yield as a white solid. The identity of this product was verified by comparison of NMR spectra with reported literature.¹

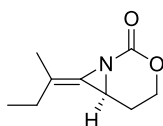


Compound 3.12b. Obtained in 80% yield as an oil. The identity of this product was verified by comparison of NMR spectra with reported literature.¹²

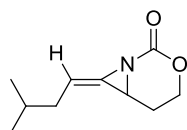


Compound 3.12c. Obtained in a 87% yield as a mixture of *E* and *Z* isomers. *E* isomer: ^1H NMR (300 MHz, CDCl_3) δ 4.50 (ddd, $J = 11.6, 10.7, 2.2$ Hz, 1H), 4.33 (ddd, $J = 10.8, 3.9, 2.7$

Hz, 1H), 3.38 (dd, $J = 8.3, 6.1$ Hz, 1H), 2.35 (dddd, $J = 14.4, 6.1, 2.8, 2.2$ Hz, 1H), 2.16-2.06 (m, 2H), 1.97 (s, 3H), 1.68-1.39 (m, 4H), 1.29 (m, 4H), 0.90 (m, 3H). ^{13}C NMR (75 MHz, CDCl_3) δ 156.86, 120.29, 112.48, 68.44, 40.30, 34.29, 31.81, 26.99, 24.71, 22.64, 16.86, 14.18. HRMS (ESI) m/z calculated for $\text{C}_{12}\text{H}_{19}\text{NO}_2$ [$\text{M}+\text{H}^+$] 210.1489, found 210.1479.

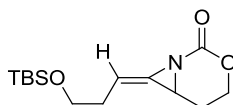


Compound 3.12d. Obtained in a 70% yield as a mixture of *E* and *Z* isomers. *E* isomer: ^1H NMR (300 MHz, CDCl_3) δ 4.51 (m, 1H), 4.34 (m, 1H), 3.38 (m, 1H), 2.38 (m, 1H), 2.15 (m, 2H), 1.98 (s, 3H), 1.62 (m, 1H), 1.07 (t, $J = 7.4$ Hz, 3H) ^{13}C NMR (75 MHz, CDCl_3) δ 156.79, 119.94, 113.86, 68.45, 40.42, 27.42, 24.79, 16.98, 12.14. HRMS (ESI) m/z calculated for $\text{C}_{11}\text{H}_{17}\text{NO}_2$ [$\text{M}+\text{H}^+$] 196.1333, found 196.1330. *Z* isomer: ^1H NMR (300 MHz, CDCl_3) δ 4.51 (m, 1H), 4.34 (m, 1H), 3.38 (m, 1H), 2.38 (m, 3H), 1.98 (s, 3H), 1.62 (m, 1H), 1.07 (t, $J = 7.4$ Hz, 3H) ^{13}C NMR (75 MHz, CDCl_3) δ 156.74, 130.29, 113.44, 68.49, 39.68, 25.81, 24.39, 16.87, 12.63. HRMS (ESI) m/z calculated for $\text{C}_{11}\text{H}_{17}\text{NO}_2$ [$\text{M}+\text{H}^+$] 196.1333, found 196.1330. IR: in CH_2Cl_2 2971, 1728, 1475, 1390, 1265, 1164, 1092, 1002 cm^{-1} .



Compound 3.14aA. The product was purified by column chromatography using a 0 \rightarrow 20% gradient of EtOAc in hexanes with 5% increments. The resulting product was obtained in 57% yield as a 2.5:1 mixture of diastereomers. *E* diastereomer: ^1H NMR (500 MHz, CDCl_3) δ 5.48 (t, $J = 8.0$ Hz, 1H), 3.57 (td, $J = 11.5, 2.0$ Hz, 1H), 3.41 (dt, $J = 10.5, 3.0$ Hz, 1H), 2.59 (dd, $J = 8.4, 6.9$ Hz, 1H), 1.84-1.76 (m, 1H), 1.76-1.69 (m, 1H), 1.42 (sep, $J = 6.8$ Hz, 1H), 1.06-1.00 (m,

1H), 0.89-0.83 (m, 1H), 0.76 (d, $J = 6.8$ Hz, 3H), 0.74 (d, $J = 6.8$ Hz, 3H); ^{13}C NMR (125.7 MHz, CDCl_3) δ 154.9, 126.9, 100.6, 67.9, 38.5, 37.4, 28.3, 23.5, 22.0, 21.9; HRMS (ESI) m/z calculated for $\text{C}_{10}\text{H}_{15}\text{NO}_2$ [M^+] 181.1098, found 181.1088.

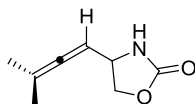


Compound 3.14bA. The product was purified by column chromatography using a 0 \rightarrow 30% gradient of EtOAc in hexanes with 6% increments. The product was obtained in 58% yield as a 1.7:1 mixture of diastereomers. ^1H NMR (500 MHz, CDCl_3) δ 5.47 (t, $J = 7.4$ Hz, 1H), 3.54 (t, $J = 11.1$ Hz, 1H), 3.45-3.37 (m, 3H), 2.60 (dd, $J = 8.3, 6.7$ Hz, 1H), 2.11 (q, $J = 7.4$ Hz, 2H) 1.08-0.99 (m, 1H), 0.95 (s, 9H), 0.88-0.80 (m, 1H), 0.02 (s, 6H); ^{13}C NMR (125.7 MHz, CDCl_3) δ 153.5, 97.4, 66.7, 61.3, 37.4, 30.8, 24.8, 22.3, 17.0, -0.06, -1.46, -6.6; HRMS (ESI) m/z calculated for $\text{C}_{14}\text{H}_{25}\text{NO}_3\text{Si}$ [$\text{M}+\text{H}^+$] 284.1677, found 284.1678.

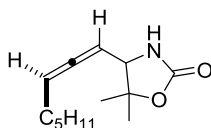
3.9.4. Synthesis of C-H insertion products.

General procedure for Ag-catalyzed allenic C-H Insertion. A pre-dried reaction flask was charged with silver triflate (13.0 mg, 0.5 mmol, 0.1 equiv) and phenanthroline (26.0 mg, 0.15 mmol, 0.3 equiv). Dichloromethane (3 mL) was added to the flask and the mixture was stirred vigorously for 30 min. A solution of the homoallenic carbamate (0.5 mmol, 1 equiv) in dichloromethane (3 mL) was added to the reaction flask, followed by 3Å or 4Å molecular sieves (1 mmol substrate/g of sieves or 0.25 mmol substrate/g of sieves). Iodosobenzene (392 mg, 1.75 mmol, 3.5 equiv) was added in one portion and the reaction mixture was allowed to stir at room temperature until TLC indicated complete consumption of the starting material (~14-16 h). The reaction mixture was filtered through a glass frit and the filtrate concentrated under reduced

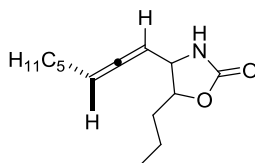
pressure. The crude products were purified by silica gel column chromatography using a hexanes/EtOAc gradient.



Compound 3.8a. The product was purified by column chromatography using a 0 \rightarrow 50% gradient of EtOAc in hexanes with 10% increments. The product was obtained in 81% yield. The proton and carbon NMRs matched reported literature values.⁶ ^1H NMR (300 MHz, CDCl_3) δ 5.72 (s, 1H), 5.02 (m, 1H), 4.52 (t, $J = 8.3$, 1H), 4.32 (m, 1H), 4.15 (dd, $J = 8.4, 5.7$, 1H), 1.72 (m, 6H).

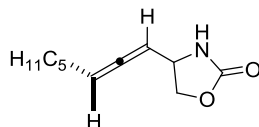


Compound 3.8b. The product was purified by column chromatography using a 0 \rightarrow 30% gradient of EtOAc in hexanes with 6% increments. The product was obtained in 96% yield. The proton and carbon NMRs matched reported literature values.⁶ ^1H NMR (300 MHz, CDCl_3) δ 5.35 (qt, $J = 7.4, 2.2$ Hz, 2H), 5.12 – 5.01 (m, 1H), 4.03 – 3.94 (m, 1H), 2.02 (qdd, $J = 7.4, 4.6, 3.0$ Hz, 2H), 1.48 (s, 3H), 1.45 – 1.23 (m, 9H), 0.89 (t, $J = 6.7$ Hz, 3H).

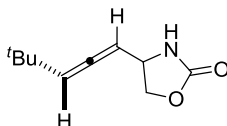


Compound 3.13b. The product was purified by column chromatography using a 0 \rightarrow 50% gradient of EtOAc in hexanes with 10% increments. The product was obtained in 76% yield. The proton and carbon NMRs matched reported literature values.⁵ ^1H NMR (300 MHz, CDCl_3)

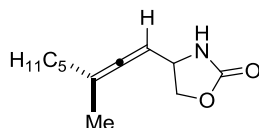
δ 5.54 (s, 1H), 5.52 (s, 1H), 5.34 (m, 1H), 5.10 (m, 1H), 4.63 minor isomer (m, 1H), 4.28 (m, 1H), 3.94 (m, 1H), 2.02 (m, 2H), 1.35 (m, 10H), 0.97 (t, $J = 7.5$ Hz, 3H), 0.88 (t, $J = 6.8$ Hz, 3H).



Compound 3.5. The product was purified by column chromatography using a 0 \rightarrow 30% gradient of EtOAc in hexanes with 6% increments. The product was obtained in 71% yield. The proton and carbon NMRs matched reported literature values.⁴ ^1H NMR (500 MHz, CDCl_3) δ 6.10-6.00 (two br s, 1H), 5.37 (app pd, $J = 6.3, 1.3$ Hz, 1H), 5.16 (m, 1H), 4.54 (t, $J = 8.3$ Hz, 1H), 4.38 (qd, $J = 6.0, 2.0$ Hz, 1H), 4.18 (dd, $J = 8.6, 5.7$ Hz, 1H), 2.02 (pd, $J = 7.4, 2.7$ Hz, 2H), 1.44-1.26 (m, 8H), 0.89 (t, $J = 6.8$ Hz, 3H).

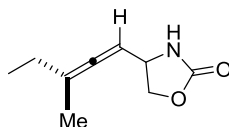


Compound 3.13a. The product was purified by column chromatography using a 0 \rightarrow 50% gradient of EtOAc in hexanes with 10% increments. The product was obtained in 83% yield. The proton and carbon NMRs matched reported literature values.⁴ ^1H NMR (300 MHz, CDCl_3) δ 5.66 (br, 1H), 5.40 (dt, $J = 6.2, 1.9$ Hz, 1H), 5.24 (m, 1H), 4.53 (td, $J = 8.3, 1.8$ Hz, 1H), 4.36 (m, 1H), 4.19 (ddd, $J = 8.5, 5.4, 3.2$ Hz, 1H), 1.05 (d, $J = 0.6$ Hz, 9H).

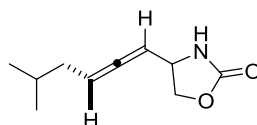


Compound 3.13c. The product was purified by column chromatography using a 0 \rightarrow 50% gradient of EtOAc in hexanes with 10% increments. The product was obtained in 88% yield. The proton and carbon NMRs matched reported literature values.⁶ ^1H NMR (300 MHz, CDCl_3)

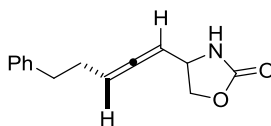
δ 5.68 (br, 1H), 5.08 (m, 1H), 4.52 (td, $J = 8.3, 2.7$ Hz, 1H), 4.32 (m, 1H), 4.15 (ddd, $J = 8.4, 5.7, 1.8$ Hz, 1H), 1.95 (m, 2H), 1.70 (t, $J = 2.6$ Hz, 3H), 1.33 (m, 6H), 0.89 (m, 3H).



Compound 3.13d. The product was purified by column chromatography using a 0 \rightarrow 50% gradient of EtOAc in hexanes with 10% increments. The product was obtained in 78% yield. The proton and carbon NMRs matched reported literature values.⁶ ^1H NMR (300 MHz, CDCl_3) δ 5.60 (s, 1H), 5.13 (dq, $J = 6.1$ Hz, 1H), 4.52 (td, $J = 8.2, 2.6$ Hz, 1H), 4.32 (m, 1H), 4.16 (m, 1H), 1.98 (m, 2H), 1.72 (m, 3H), 0.98 (td, $J = 7.4, 5.3$ Hz, 3H).

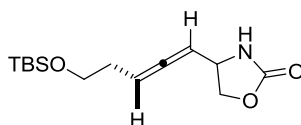


Compound 3.14aI. The product was purified by column chromatography using a 0 \rightarrow 30% gradient of EtOAc in hexanes with 6% increments. The product was obtained in 74% yield. ^1H NMR (500 MHz, CDCl_3) δ 6.14-5.99 (br s, 1H), 5.32 (pd, $J = 7.2, 1.5$ Hz, 1H), 5.14 (qd, $J = 6.4, 2.5$ Hz, 1H), 4.54 (t, $J = 8.5$ Hz, 1H), 4.38 (q, $J = 6.8$ Hz, 1H), 4.18 (dd, $J = 8.5, 5.8$ Hz, 1H), 1.93 (qd, $J = 6.8, 2.5$ Hz, 2H), 1.67 (non of d, $J = 6.8, 2.1$ Hz, 1H), 0.92 (d, $J = 2.1$ Hz, 3H), 0.91 (d, $J = 2.1$ Hz, 3H). ^{13}C NMR (125.7 MHz, CDCl_3) δ 204.4, 204.3, 159.7, 159.7, 93.9, 93.8, 90.5, 90.5, 70.4, 52.3, 52.2, 37.9, 37.8, 28.3, 22.1. HRMS (ESI) m/z calculated for $\text{C}_{10}\text{H}_{15}\text{NO}_2$ $[\text{M}+\text{H}^+]$ 182.1176, found 182.1169.



Compound 3.14bI. The product was purified by column chromatography using a 0 \rightarrow 30% gradient of EtOAc in hexanes with 6% increments. The product was obtained in 74% yield as a

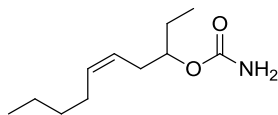
1:1 mixture of diastereomers. The proton NMR matches literature values.⁶ ¹H NMR (500 MHz, CDCl₃) δ 7.30 (td, *J* = 7.0, 2.3 Hz, 2H), 7.24-7.16 (m, 3H), 5.60-5.50 (2 br s, 1H), 5.37 (p, *J* = 7.4 Hz, 1H), 5.12-5.07 (m, 1H), 4.41 (t, *J* = 8.4 Hz, 0.5H), 4.36 (t, *J* = 8.4 Hz, 0.5H), 4.12 (p, *J* = 6.2 Hz, 1H), 4.02 (ddd, *J* = 13.1, 8.4, 5.6 Hz, 1H), 2.81-2.67 (m, 2H), 2.46-2.28 (m, 2H).



Compound 3.14cI. The product was purified by column chromatography using a 0 → 40% gradient of EtOAc in hexanes with 8% increments. The product was obtained in 62% yield as a 1:1 mixture of diastereomers. ¹H NMR (500 MHz, CDCl₃) δ 6.07 (br s, 0.5H), 5.95 (br s, 0.5H), 5.34 (dq, *J* = 10.4, 6.3, 1.7 Hz, 1H), 5.11 (tt, *J* = 6.3, 2.7 Hz, 1H), 4.46 (td, *J* = 8.4, 1.5 Hz, 1H), 4.34-4.27 (m, 1H), 4.11 (dt, *J* = 8.4, 5.4 Hz, 1H), 3.66-3.58 (m, 2H), 2.18 (sd, *J* = 6.9, 2.7 Hz, 2H), 0.84 (d, *J* = 1.8 Hz, 9H), 0.01 (m, 6H). ¹³C NMR (125.7 MHz, CDCl₃) δ 204.4, 159.5, 92.4, 91.1, 70.3, 62.4, 52.0, 32.2, 25.9, 18.4, 18.3, -5.4. HRMS (ESI) *m/z* calculated for C₁₄H₂₅NO₃Si [M+H⁺] 284.1677, found 284.1686.

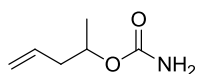
3.9.5. Synthesis of Homoallylic Carbamates.

Compounds **3.15a,c, d** were synthesized according to published procedures.^{9a} The synthesis of the homoallylic carbamates was carried out according to the general procedure described for homoallylic carbamates.



Compound 3.15b. The product was purified by column chromatography using a 0 → 25% gradient of EtOAc in hexanes with 5% increments. The product was obtained in 90% yield as a

waxy solid. ^1H NMR (300 MHz, CDCl_3) δ 5.57 – 5.41 (m, 1H), 5.41 – 5.29 (m, 1H), 4.83 (s, 2H), 4.69 (dt, $J = 11.8, 6.1, 6.1$ Hz, 1H), 2.31 (t, $J = 6.7, 6.7$ Hz, 3H), 2.04 (q, $J = 6.3, 6.3, 6.0$ Hz, 2H), 1.69 – 1.44 (m, 2H), 1.40 – 1.25 (m, 4H), 0.97 – 0.82 (m, 6H). ^{13}C NMR (75 MHz, CDCl_3) δ 157.3, 132.8, 124.3, 76.2, 31.9, 31.7, 27.2, 26.8, 22.5, 14.2, 9.8. HRMS (ESI) m/z calculated for $\text{C}_{11}\text{H}_{21}\text{NO}_2$ [$\text{M}+\text{NH}_4^+$] 217.1911, found 217.1909.

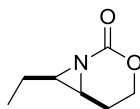


Compound 3.15e. The product was purified by column chromatography using a 0 \rightarrow 25% gradient of EtOAc in hexanes with 5% increments. The product was obtained in 91% yield as a white solid. ^1H NMR (500 MHz, CDCl_3) δ 5.78 (ddt, 1H, $J = 17.2, 10.3, 7.0$ Hz), 5.16–5.03 (m, 2H), 4.84 (appt p, 1H, $J = 6.3$ Hz), 4.81–4.64 (m, 2H), 2.41–2.31 (m, 1H), 2.31–2.23 (m, 1H), 1.23 (d, 3H, $J = 6.3$ Hz). ^{13}C NMR (126 MHz, CDCl_3) δ 156.7, 133.7, 117.7, 70.9, 40.4, 19.7. HRMS (EI) m/z calculated for $\text{C}_6\text{H}_{11}\text{NO}_2$ [M^+] 129.0785, found 129.0782.

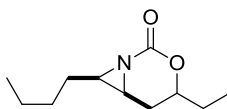
3.9.6. Synthesis of Aziridines.

General procedure. A pre-dried reaction flask was charged with silver triflate (26.0 mg, 0.1 mmol, 0.2 equiv) and phenanthroline (23.0 mg, 0.125 mmol, 0.25 equiv). Dichloromethane (1 mL) was added to the flask and the mixture stirred vigorously for 30 min. A solution of the homoallylic carbamate (0.5 mmol, 1 equiv) in dichloromethane (1 mL) was added to the reaction flask, followed by 3Å or 4Å molecular sieves (1 mmol substrate/g of sieves or 0.25 mmol substrate/g of sieves). Iodosobenzene (220.0 mg, 1 mmol, 2 equiv) was added in one portion and the reaction mixture was allowed to stir at room temperature until TLC indicated complete consumption of the starting material (~14 h). The reaction mixture was filtered through a glass

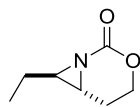
frit and the filtrate was concentrated under reduced pressure. The crude products were purified by silica gel column chromatography using a hexanes/EtOAc gradient.



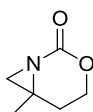
Compound 3.16a. The product was purified by column chromatography using a 0 \rightarrow 50% gradient of EtOAc in hexanes with 10% increments. The product was obtained in 67% yield and the proton NMR matched the reported literature values.^{12a} ^1H NMR (300 MHz, CDCl_3) δ 4.36 (m, 2H), 2.87 (ddd, $J = 9.7, 6.9, 4.9$ Hz, 1H), 2.61 (dt, $J = 8.3, 5.1$ Hz, 1H), 2.19 (ddt, $J = 14.6, 6.9, 2.0$ Hz, 1H), 1.87 (dq, $J = 13.8, 7.0, 6.6, 5.3$ Hz, 1H), 1.48 (dddd, $J = 14.4, 11.8, 9.0, 5.6$ Hz, 1H), 1.23 (m, 1H), 1.11 (m, 3H).



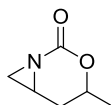
Compound 3.16b. The product was purified by column chromatography using a 0 \rightarrow 2% gradient of MeOH in dichloromethane with 0.5% increments. The product was obtained in 89% yield. ^1H NMR (300 MHz, CDCl_3) δ 4.38 (m, 1H), 2.83 (m, 1H), 2.65 (dt, $J = 9.1, 5.1$ Hz, 1H), 2.18 (m, 1H), 2.06 (m, minor isomer), 1.73 (m, 4H), 1.38 (d, $J = 5.3$ Hz, 3H), 1.15 (m, 2H), 1.04 (t, $J = 9.3$ Hz, 3H), 0.93 (t, $J = 6.6$ Hz, 3H). Major Isomer: ^{13}C NMR (126 MHz, CDCl_3) δ 159.5, 80.9, 43.7, 37.3, 28.9, 28.0, 25.2, 24.4, 22.6, 14.1, 9.4. Minor Isomer: ^{13}C NMR (126 MHz, CDCl_3) δ 158.7, 81.0, 78.0, 43.5, 34.8, 28.8, 26.9, 24.9, 22.6, 21.5, 14.1. HRMS (ESI) m/z calculated for $\text{C}_{11}\text{H}_{19}\text{NO}_2$ $[\text{M}+\text{H}^+]$ 198.1489, found 198.1494.



Compound 3.16c. The product was purified by column chromatography using a 0 → 100% gradient of EtOAc in hexanes with 20% increments. The product was obtained in 88% yield and the proton NMR matched the reported literature values.^{12a} ¹H NMR (300 MHz, CDCl₃) δ 4.48 – 4.33 (m, 1H), 4.36 – 4.23 (m, 1H), 2.61 (ddd, *J* = 8.9, 6.3, 3.3 Hz, 1H), 2.37 (ddt, *J* = 14.6, 6.2, 1.9, Hz, 1H), 2.24 (td, *J* = 6.0, 3.3 Hz, 2H), 1.63 (p, *J* = 6.8 Hz, 2H), 1.40 (dddd, *J* = 14.5, 12.6, 8.7, 4.3 Hz, 1H), 1.06 (t, *J* = 7.4, 3H).



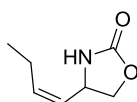
Compound 3.16d. The product was purified by column chromatography using a 0 → 50% gradient of EtOAc in hexanes with 10% increments. The product was obtained in 85% yield and the proton NMR matched the reported literature values.^{12a} ¹H NMR (300 MHz,) δ 4.45 (ddd, *J* = 12.4, 10.8, 1.9 Hz, 1H), 4.31 (ddd, *J* = 10.7, 4.1, 2.0 Hz, 1H), 2.39 (s, 1H), 2.19 (s, 1H), 2.12 (dt, *J* = 14.5, 1.9 Hz, 1H), 1.49 (m, 1H), 1.38 (s, 3H).



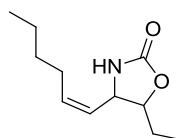
Compound 3.16e. The product was purified by column chromatography using a 0 → 50% gradient of EtOAc in hexanes with 10% increments. The aziridine was obtained in 51% yield, while the C-H insertion product was obtained in 19% yield. ¹H NMR (300 MHz, CDCl₃) δ 4.64 (dq, *J* = 11.0, 6.3, 6.3, 1.9 Hz, 1H), 2.76 (m, 1H), 2.56 (d, *J* = 4.3 Hz, 1H), 2.41 (ddd, *J* = 14.4, 6.1, 1.8 Hz, 1H), 2.07 (d, *J* = 3.7 Hz, 1H), 1.37 (d, *J* = 6.3 Hz, 3H), 1.05 (ddd, *J* = 14.4, 11.1, 8.7 Hz, 1H). ¹³C NMR (126 MHz, CDCl₃) δ 161.4, 76.1, 36.0, 33.7, 32.5, 20.6. HRMS (EI) *m/z* calculated for C₆H₉NO₂ [M+H⁺] 128.0705, found 128.0705.

3.9.7. Synthesis of Allylic C-H Insertion Products.

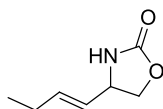
General procedure for Ag-catalyzed allylic C-H insertion. A pre-dried reaction flask was charged with silver triflate (13.0 mg, 0.5 mmol, 0.1 equiv) and phenanthroline (26.0 mg, 0.15 mmol, 0.3 equiv). Dichloromethane (3 mL) was added to the flask and the mixture was stirred vigorously for 30 min. A solution of the homoallylic carbamate (0.5 mmol, 1 equiv) in dichloromethane (3 mL) was added to the reaction flask, followed by 3Å or 4Å molecular sieves (1 mmol substrate/g of sieves or 0.25 mmol substrate/g of sieves). Iodosobenzene (392 mg, 1.75 mmol, 3.5 equiv) was added in one portion and the reaction mixture was allowed to stir at room temperature until TLC indicated complete consumption of the starting material (~14-16 h). The reaction mixture was filtered through a glass frit and the filtrate concentrated under reduced pressure. The crude products were purified by silica gel column chromatography using a hexanes/EtOAc gradient.



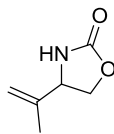
Compound 3.17a. The product was purified by column chromatography using a 0 → 50% gradient of EtOAc in hexanes with 10% increments. The product was obtained in 97% yield and the proton NMR matched the reported literature values.⁸ ¹H NMR (300 MHz, CDCl₃) δ 5.82 (br, 1H), 5.64 (dtd, *J* = 10.9, 7.5, 1.1 Hz, 1H), 5.38 (ddt, *J* = 10.6, 8.9, 1.6 Hz, 1H), 4.74 (m, 1H), 4.52 (t, *J* = 8.5 Hz, 1H), 4.00 (dd, *J* = 8.5, 7.3 Hz, 1H), 2.08 (dddd, *J* = 11.9, 7.4, 5.7, 3.5 Hz, 2H), 0.99 (t, *J* = 7.5 Hz, 3H).



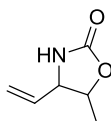
Compound 3.17b. The product was purified by column chromatography using a 0 → 50% gradient of EtOAc in hexanes with 10% increments. The product was obtained in 86% yield. ¹H NMR (300 MHz, CDCl₃) δ 5.65 (m, 1H), 5.36 (m, 2H), minor 4.62 (dd, *J* = 9.7, 7.8 Hz, 1H), minor 4.52 (td, *J* = 8.3, 8.1, 4.7 Hz, 1H), major 4.32 (m, 1H), major 4.12 (td, *J* = 7.0, 5.6 Hz, 1H), 2.07 (m, 2H), 1.72 (m, 2H), 1.33 (m, 4H), 1.02 (m, 3H), 0.90 (m, 3H). Major isomer: ¹³C NMR (75 MHz, CDCl₃) δ 159.2, 136.0, 127.4, 84.3, 54.9, 31.8, 27.5, 26.9, 22.5, 14.1, 9.5. Minor isomer: ¹³C NMR (75 MHz, CDCl₃) δ 159.6, 136.1, 124.6, 81.9, 52.6, 31.8, 27.4, 23.7, 22.5, 14.1, 10.4. HRMS (EI) *m/z* calculated for C₁₁H₁₉NO₂ [M⁺] 197.1411, found 197.1402.



Compound 3.17c. The product was purified by column chromatography using a 0→25% gradient of EtOAc in hexanes with 5% increments. Obtained in 84% yield combined. Proton matched reported literature values.⁸ ¹H NMR (300 MHz, CDCl₃) δ 5.78 (dtd, *J* = 15.3, 6.3, 0.8 Hz, 1H), 5.66 (s, 1H), 5.41 (ddt, *J* = 15.3, 7.9, 1.6 Hz, 1H), 4.51 (t, *J* = 8.4 Hz, 1H), 4.35 (q, *J* = 7.6 Hz, 1H), 4.03 (dd, *J* = 8.4, 6.9 Hz, 1H), 2.02-2.12 (m, 2H), 1.00 (t, *J* = 7.4 Hz, 3H).



Compound 3.17d. The product was purified by column chromatography using a 0 → 50% gradient of EtOAc in hexanes with 10% increments. The product was obtained in 66% yield and the proton NMR matched the reported literature values.⁸ ¹H NMR (300 MHz, CDCl₃) δ 6.10 (s, 1H), 5.03 (bd, *J* = 0.9 Hz, 1H), 4.95 (bs, 1H), 4.54 (t, *J* = 8.7 Hz, 1H), 4.38 (dd, *J* = 8.8, 6.0 Hz, 1H), 4.09 (dd, *J* = 8.4, 6.0 Hz, 1H), 1.76 (s, 3H).



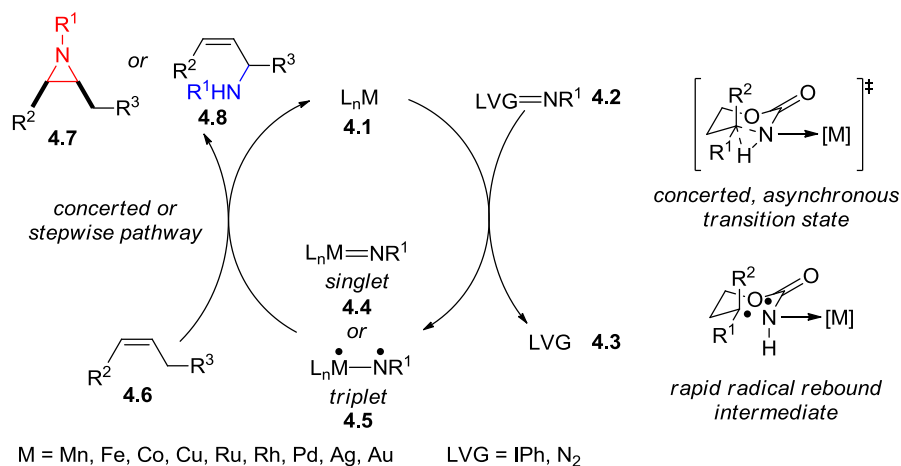
Compound 3.17e. The product was purified by column chromatography using a 0 \rightarrow 50% gradient of EtOAc in hexanes with 10% increments. The product was obtained in 68% yield. An analytical sample of the major isomer was obtained as it eluted prior to mixture of isomers. Major: ^1H NMR (300 MHz, CDCl_3) δ 5.92 (s, 1H), 5.79 (ddd, $J = 17.3, 10.1, 7.5$ Hz, 1H), 5.33 (dt, $J = 17.1, 1.0$ Hz, 1H), 5.26 (dt, $J = 10.2, 0.9$ Hz, 1H), 4.33 (dq, $J = 7.4, 6.3$ Hz, 1H), 3.90 (tq, $J = 7.4, 1.0$ Hz, 1H), 1.44 (d, $J = 6.3$ Hz, 3H). ^{13}C NMR (126 MHz, CDCl_3) δ 159.0, 135.2, 119.1, 78.8, 62.9, 18.9. Minor: ^1H NMR (300 MHz, CDCl_3) δ 5.80 (m, 2H), 5.34 (m, 2H), 4.83 (m, 1H), 4.31 (m, 1H), 1.31 (d, $J = 6.7$ Hz, 3H). ^{13}C NMR (126 MHz, CDCl_3) δ 159.3, 133.0, 119.4, 76.3, 58.5, 16.0. HRMS (EI) m/z calculated for $\text{C}_6\text{H}_9\text{NO}_2$ [M^+] 127.0628, found 127.0624.

Chapter 4. Review: Mechanistic Studies of Metal-Catalyzed Nitrene Transfer.

4.1. Introduction to Mechanistic Aspects of Nitrene Transfer.

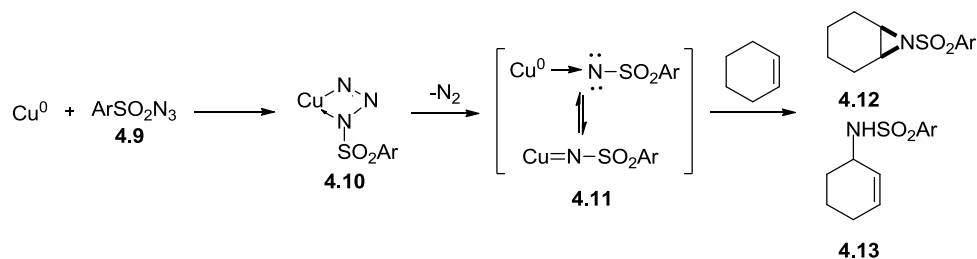
Essential mechanistic features of metal-catalyzed nitrene-transfer have been described as early as Kwart's seminal report on the copper-promoted decomposition of benzenesulfonyl azide.^{1a,b} Formal experimental and computational studies of these processes continue to reveal insight into the nature of metal-nitrene formation, the mechanism of nitrene transfer, and chemoselectivity, supporting a mechanistic scheme common to diverse catalyst systems (Scheme 4.1). An electrophilic metal-nitrene is formed by attack of metal catalyst **4.1** on an iminoiodinane species or azide **4.2**, with subsequent departure of an iodoarene or molecular nitrogen, respectively. The metal-nitrene (**4.4** or **4.5**) then carries out an amination step to provide either aziridine or C-H amination products (**4.7**, **4.8**) and regenerate the catalyst. This chapter will provide a detailed overview of these studies, describing evidence for the existence and reactivity of metal-nitrenes, experiments to probe the nature of nitrene transfer to the organic substrate, and insight obtained by kinetic study of these reactions. Particular attention is given to catalytic systems that attain high chemoselectivity in substrates containing multiple reactive sites and to correlations between mechanistic features and chemoselectivity of individual catalyst systems.

Scheme 4.1. Mechanism of transition-metal-catalyzed nitrene transfer.



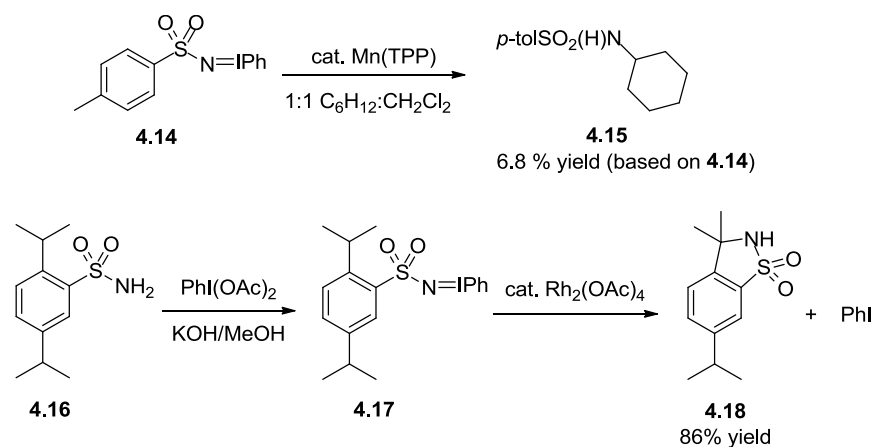
4.2. Early Studies of Metal-catalyzed Nitrene Transfer.

Kwart and Khan's early description of the copper-catalyzed decomposition of benzenesulfonyl azide contains a proposal for the mechanism of the transformation whose general features are still accepted.^{1a,b} It was suggested that the reaction of copper and a sulfonyl azide **4.9** led to coordination of sulfonamide nitrogen atom to copper (**4.10**), followed by the extrusion of molecular nitrogen, and the formation of a copper-nitrene **4.11** (Scheme 4.2). This intermediate could then undergo nitrene insertion to form aziridines **4.12** or allylic amines **4.13** in the presence of cyclohexene. However, the mechanisms of nitrene insertion were not discussed in these communications.

Scheme 4.2. Early proposal for the mechanism of metal-nitrene formation.

Breslow and Gellman's reports on metal-catalyzed amidations demonstrated that iminodiazanes could serve as nitrene precursors.^{2a,b} The first report described the tosylamidation of cyclohexane promoted by $\text{Mn}^{\text{III}}(\text{TPP})$ (TPP = tetraphenylporphyrin), or $\text{Fe}^{\text{III}}(\text{TPP})$, using (tosyliminoiodo)-benzene **4.14** as the nitrogen source (Scheme 4.3). Subsequently, they described the formation of a second isolable iminodiazane **4.17**, which performed intramolecular C-H insertion in the presence of several transition metal catalysts, including the lantern complex $\text{Rh}_2(\text{OAc})_4$, which has served as a model for the design of further high-performing nitrene-transfer catalysts.³ While neither publication provided significant mechanistic detail, iminodiazanes are now assumed to be reactive intermediates in metal-catalyzed nitrene-transfers involving hypervalent iodide reagents.

Scheme 4.3. Isolable iminoiodinanes as reactive intermediates for metal-catalyzed nitrene transfer.

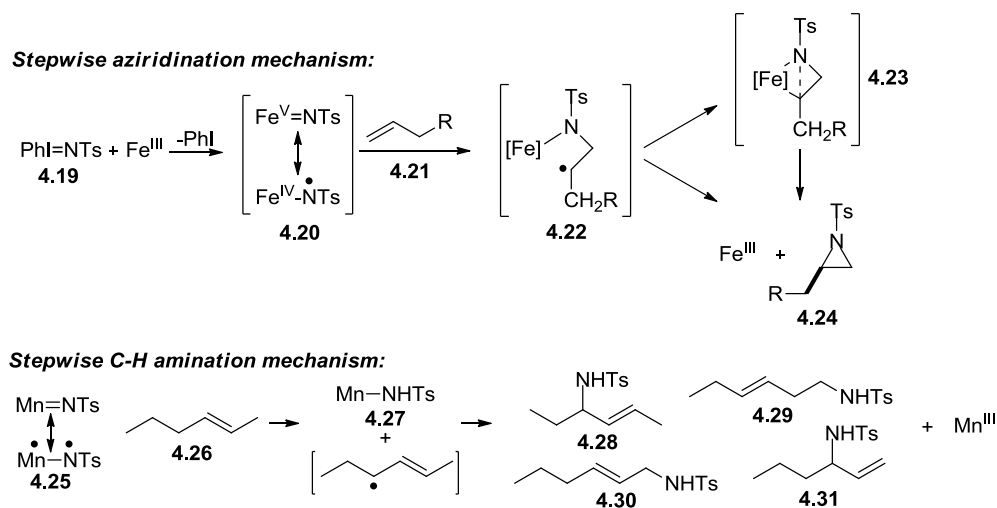


Mansuy and co-workers offered an important contribution to mechanistic understanding of nitrene transfer by invoking a radical mechanism for both aziridination and C-H amination to rationalize the product distributions obtained in the amidation of hydrocarbons with Mn and Fe porphyrin catalysts.^{4a,b} Noting, for example, that *trans*-hex-2-ene **4.19** gave a 10:1 mixture of *trans*:*cis* aziridines in Fe-catalyzed aziridination, they described potential resonance structures for a metal nitrene intermediate that would give this complex radical character. Such an intermediate would react with the alkene in stepwise fashion, potentially proceeding through metallacycle **4.23** (Scheme 4.4). Similarly, Mansuy described an H-atom abstraction mechanism to rationalize stereochemical scrambling in Mn-catalyzed allylic amination (Scheme 4.4, bottom).

With the development of Rh-catalyzed intermolecular nitrene transfer, Mueller and co-workers offered additional proposals for the mechanisms of these transformations.⁵ Based on the stereospecificities of aziridinations and C-H insertions attained with Rh catalysts, as well as other physical organic experiments (*vide infra*), Mueller proposed that the mechanism for transfer of

the nitrogen from the metal-nitrene to the organic substrate was concerted, but did not describe such a mechanism in any detail. In interpreting the results of these experiments, he astutely pointed out that while such experiments can provide strong evidence in favor of stepwise pathways, they cannot easily rule out the involvement of short-lived radical species. Though later studies of nitrene transfer have augmented understanding of these reactions, mechanistic discussion tends to follow the contours established in this early work.

Scheme 4.4. Radical mechanisms for aziridination and C-H amination.

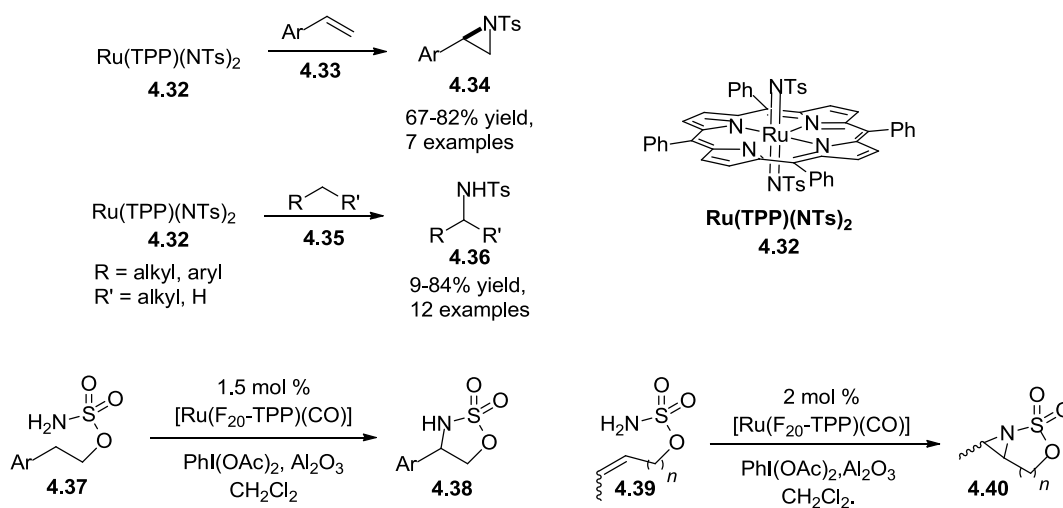


4.3 Evidence for the Intermediacy of Metal Nitrenes.

Though metal-nitrenes are assumed to be intermediates in many oxidative amination reactions, their high reactivity makes isolation or observation of such species extremely difficult. While many metal-imido complexes have been isolated, few of these species show group transfer activity.⁶ The distinction between metal-nitrene and metal-imido species is based upon the M-NR bond order, and correspondingly, the oxidation state of the metal. In a metal-imido complex, the M-NR bond order is approximately two, and the nitrogen ligand possesses strong dianionic character, giving the metal an oxidation state of +2. In a metal-nitrene complex, the M-NR

species is significantly bent such that the bond order is closer to one, and the ligand is treated as neutral. Late transition metal-imido complexes are typically electrophilic at the nitrogen atom, while metal-nitrene complexes that show enhanced reactivity may be termed superelectrophilic.⁷ This section will highlight key examples of isolated metal-imido and metal-nitrene complexes from the recent literature. The activity of these isolated species supports the intermediacy of metal-nitrenes in catalysis.

Scheme 4.5. Ru-imido complexes as NTs-transfer reagents and presumed catalytic intermediates.

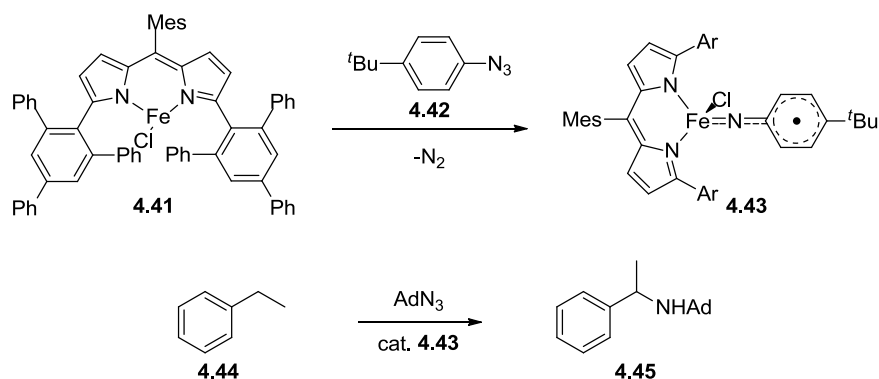


In 1983, Groves and Takahashi reported a well-defined Mn(V)-imido complex, along with a single example of its activity in aziridination.⁸ In 1997, Che and co-workers reported stoichiometric aziridinations with the isolable complex [Ru^{VI}-(TPP)(NTs)₂] **4.32** and attained good yields for several substrates (Scheme 4.5).^{9a} The complex also provided good yields in the amination of activated C-H bonds and was the subject of detailed physical organic study (*vide infra*).^{9b} The group used analogous complexes for catalytic intramolecular aziridination and C-H

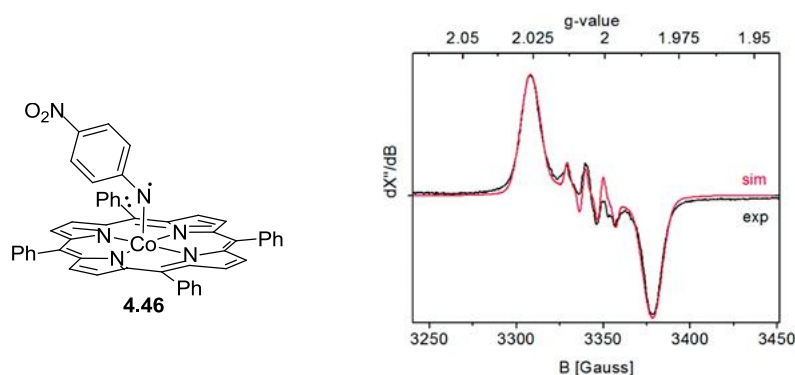
amination reactions.^{9c} The similarity between the two reactive systems provides key evidence for the involvement of metal-nitrenes in this and other catalytic reactions.

Betley and co-workers have described a series of pyrromethene iron complexes that show catalytic activity in C-H amination and aziridination and isolated the putative iron-imido intermediates (Scheme 4.6).^{10a} Treating **4.41** with *p*-*tert*-butylphenyl azide affords mononuclear imido complex **4.43**. This complex provided modest yields in the benzylic amination of toluene. X-ray crystallography and Mössbauer spectroscopy indicated that the complex featured antiferromagnetic coupling of an Fe^{III} center to an imido radical (**4.45**). This complex provided modest yields in the benzylic amination of toluene, suggesting its intermediacy in catalysis.

Scheme 4.6. Isolation of a presumed intermediate in Fe-catalyzed amination.

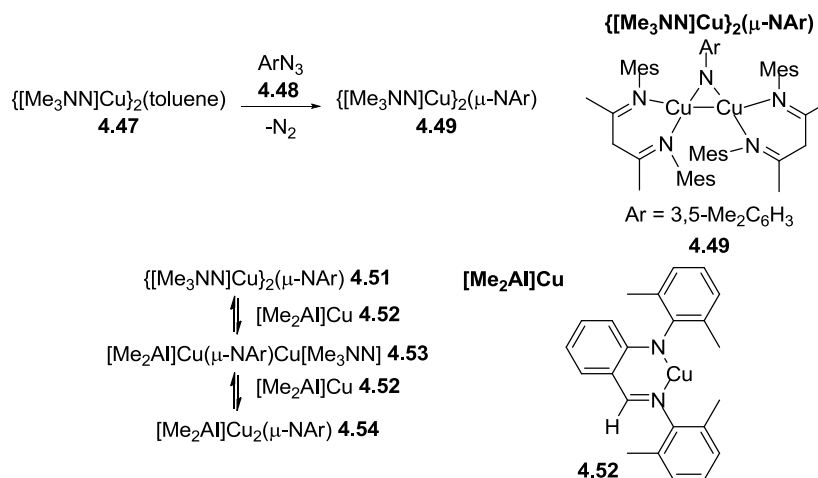


In a related study, Zhang and de Bruin have described the EPR characterization of Co-porphyrin nitrene complexes (**4.46**), which reveal these intermediates to be nitrogen centered radicals (Figure 4.1).^{11a} These results are consistent with DFT calculations of these species, and with experimental evidence for a stepwise C-H amination pathway. The electronic character of the observed species was similar for when either *p*-NO₂C₆H₄SO₂N₃ or TrocN₃ (Troc = 2,2,2-trichloroethoxycarbonyl) was used as the nitrene precursor. The Co complexes involved are known as active catalysts for nitrene transfer.^{11c-d}

Figure 4.1. EPR characterization of a Co-bound iminoradical.

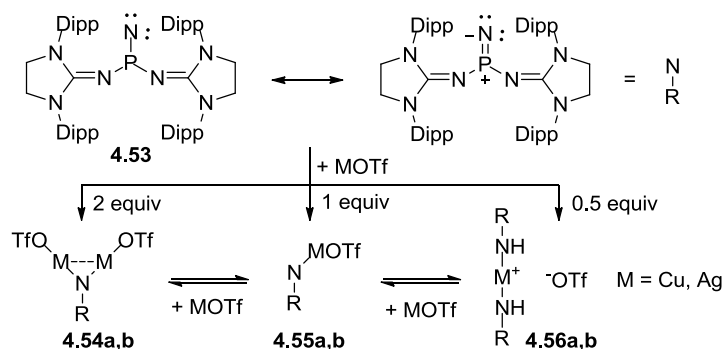
Several nitrene-bridged dicopper species have been isolated and characterized by Warren and co-workers. While $[\text{Me}_2\text{NN}]\text{Cu}(2,4\text{-lutidine})$, a competent aziridination catalyst, showed provided no isolable products when treated with organoazides, the related complex $\{[\text{Me}_3\text{NN}]\text{Cu}\}_2(\text{toluene})$ **4.47** reacted with an aryl azide **4.48** to provide the nitrene-bridged complex $\{[\text{Me}_3\text{NN}]\text{Cu}\}_2(\mu\text{-NAr})$ **4.50**, which was isolated and characterized by X-ray analysis (Scheme 4.6).^{12a} Exchange of Cu-nuclei was observed when **4.51** was treated with the analogous $\{[\text{Me}_2\text{AI}]\text{Cu}\}_2$ **4.52**, which is best explained by the intermediacy of a $[\text{Me}_3\text{NN}]\text{Cu}=\text{NAr}$ species. Related complexes were developed for catalytic C-H amination.^{12b} Kinetic analysis of C-H amination performed by these complexes provided support for the intermediacy of a mononuclear Cu-nitrene in catalysis (*vide infra*).^{12c} Ray and co-workers have also isolated a mononuclear copper-nitrene species by trapping with $\text{Sc}(\text{OTf})_3$ at -90°C . This complex displayed some reactivity in the C-H amination of hydrocarbon substrates.¹³

Scheme 4.7. Di-copper complexes bridged by a nitrene.

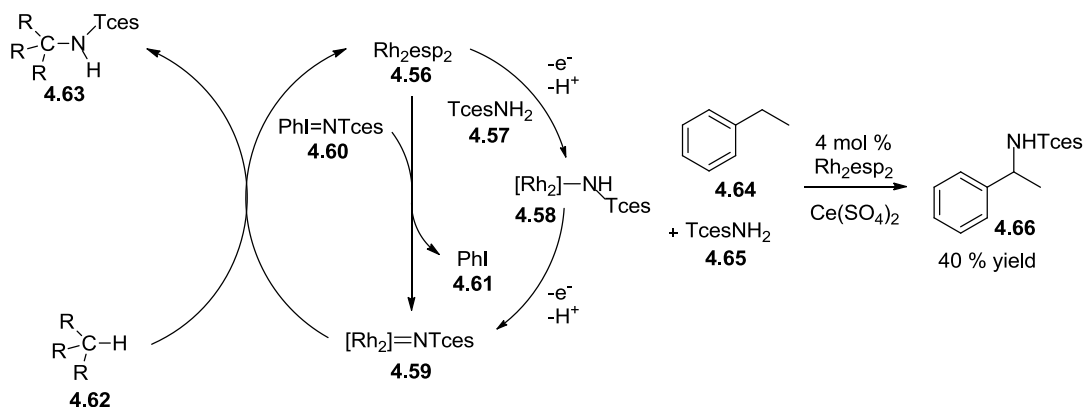


Recently, Bertrand and co-workers have reported the isolation of metal-nitrene complexes with Ag and Cu centers.¹⁴ These studies differed from previous work by employing a stable phosphinonitrene **4.53**, rather than a nitrene precursor, for the synthesis of the coordination complexes. Nevertheless, the major species isolated were bimetallic complexes similar to those obtained by Warren (Scheme 4.8). All attempts to isolate terminal imido complexes **4.55a,b** gave only mixtures of bridged bimetallic complexes **4.54a,b** and diimido complexes **4.56a,b**. This result underscores the difficulty of isolating metal-nitrene species, as even stable nitrenes do not provide complexes of the type invoked as catalytic intermediates. To date, no singlet metal-nitrene complexes have successfully been isolated.

An oft-neglected aspect of catalytic nitrene transfer is the mechanism of metal-nitrene formation. Commonly, mechanistic schemes depict direct reaction of an iminoiodane precursor, usually an azide or iminoiodane, with the metal catalyst, with concomitant extrusion

Scheme 4.8. Isolation of Cu- and Ag-nitrene complexes.

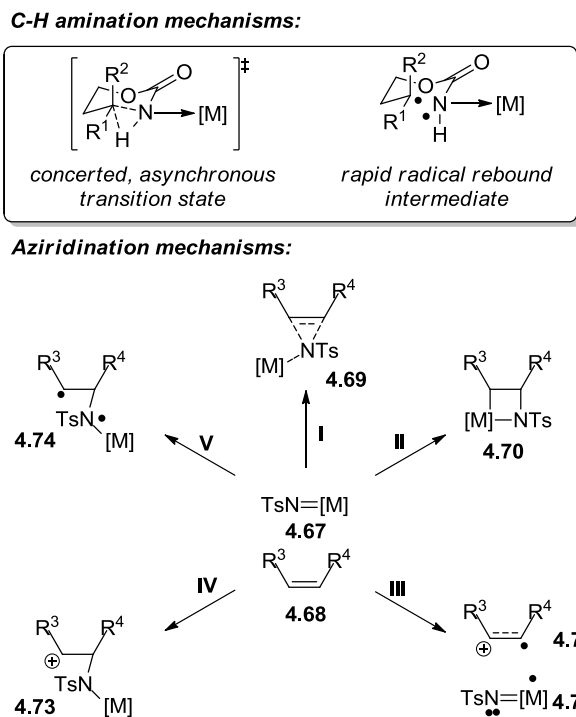
of an iodoarene or molecular nitrogen. Kornecki and Berry observed species $[\text{Rh}_2(\text{esp})_2]\text{NHTces}$ **4.58** and provided strong electrochemical evidence for its intermediacy in a two-step, proton-coupled electron transfer process for formation of the metal nitrene in Rh-catalyzed intermolecular C-H amination chemistry (Scheme 4.9).¹⁵ This proposal does not supplant a mechanism involving direct formation of the metal nitrene from the catalyst and iminoiodinane, but indicates that both pathways could proceed simultaneously. Recognition of this pathway allowed the use of the one-electron oxidant $\text{Ce}(\text{SO}_4)_2$ for intramolecular benzylic C-H amination, albeit in reduced yield.

Scheme 4.9. Metal-nitrene formation *via* proton-coupled electron transfer.

4.3. Assessing the mechanism of C-N bond formation: concerted or stepwise?

Much of the mechanistic literature on catalytic nitrene transfer is concerned with the steps directly involved in C-N bond formation. The most common proposed mechanisms are stepwise processes involving radical formation and recombination and concerted asynchronous processes.¹⁶ For C-H amination reactions, these can be represented by two limiting cases, one in which a nitrogen-centered radical carries out complete hydrogen atom abstraction, which is followed by radical recombination, and one in which the nitrene inserts directly into a C-H bond (Scheme 4.10).

Scheme 4.10. Possible mechanisms for C-H amination and aziridination steps.

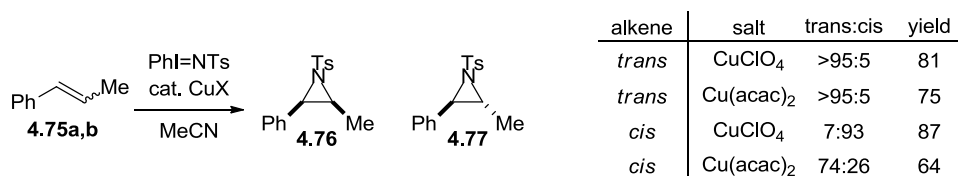


For aziridination reactions, a greater variety of processes and intermediates can be envisioned, including: concerted nitrene insertion into a C=C bond **I**, azametallacyclobutane formation and reductive elimination **II**, or formation of: an alkene radical cation **III**, a

carbocation **IV**, or a carboradical **V** (Scheme 4.10).^{9b} These processes are typically correlated to the electronic structure of the metal-nitrene. Triplet nitrenes are thought to proceed by stepwise aziridination and C-H amination mechanisms, whereas singlet nitrenes are thought to engage in concerted processes, though recent computational studies have complicated these interpretations (*vide infra*). This section will discuss common physical organic probes of these mechanisms, highlighting their use in key mechanistic studies.

Alkene isomerization. The clearest evidence of stepwise pathways in C-H amination and aziridination pathways is the isomerization of alkene substrates; indeed this observation led Mansuy to propose a stepwise pathway for these reactions.^{4b} However, isomerization is often highly substrate-dependent, even with a single catalyst system. For example, Evans and co-workers observed isomerization in Cu-catalyzed aziridination for *cis*-styrenes, but not for *trans*-styrenes or alkyl-substituted alkenes (Scheme 4.11).¹⁷ Similarly, Perez and co-workers observed isomerization in intermolecular aziridination with CuTp complexes only in the aziridination of allylic alcohols.¹⁸ Occasionally, isomerization is nearly complete, as observed by Nicholas and co-workers in intramolecular aziridinations and C-H aminations catalyzed by Cu-diimine complexes.¹⁹ However, radical recombination is expected to be a rapid process and may outcompete isomerization. Hence, isomerization can provide strong evidence in favor of a stepwise process but cannot rule out such a mechanism. Similarly, isomerization of tertiary chiral centers may provide evidence for or against a stepwise mechanism.^{5a, 20, 21}

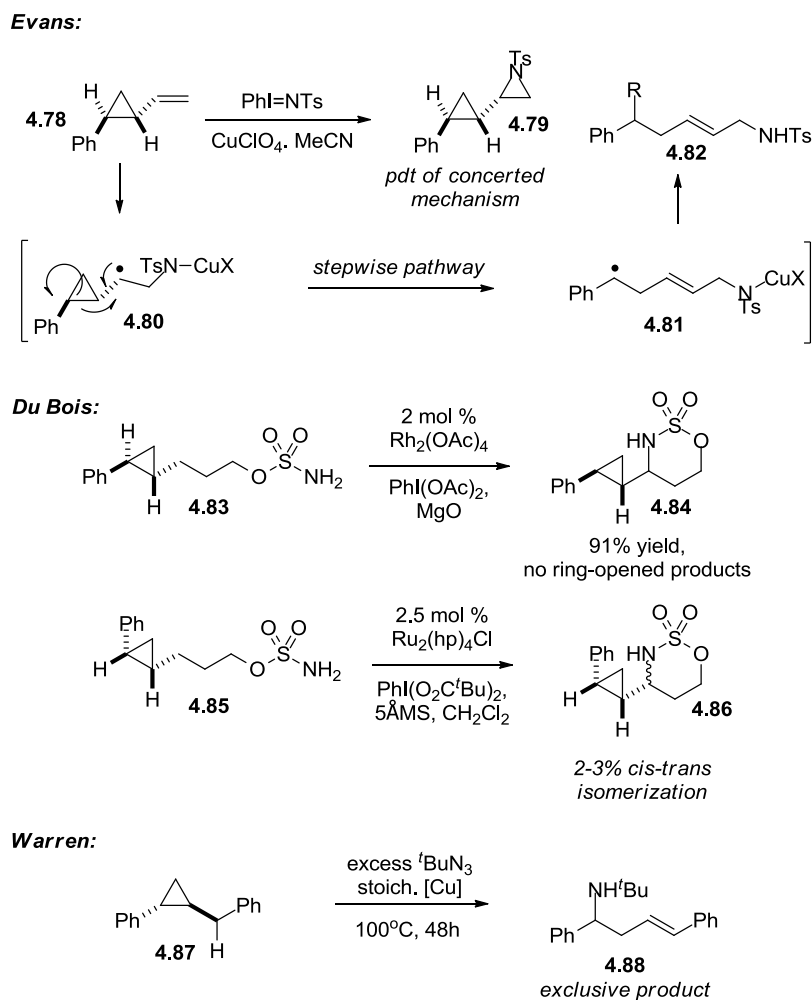
Scheme 4.11. Isomerization in the Cu-catalyzed aziridination of alkenes.



Radical inhibitors. Reactions may be performed in the presence of radical inhibitors such as BHT (butylhydroxytoluene), TEMPO ((2,2,6,6-tetramethylpiperidin-1-yl)oxyl), and DHA (9,10-dihydroanthracene) and the results compared to those obtained under standard conditions. A decrease in yield may correspond to interception of a radical species by the inhibitor. Perez has demonstrated the inhibitory effects of BHT in Cu-catalyzed aziridination.¹⁸ However, these species may have other effects on a reaction, and so these experiments must be interpreted in the broader context of a mechanistic study.

Radical clock substrates. Adopting a technique from the study of epoxidation chemistry,^{22a,b} Evans and co-workers examined the aziridination of *trans*-2-phenyl-1-vinylcyclopropane as a test for the involvement of radicals.¹⁷ Whereas a concerted process would be expected to give only aziridine products, a stepwise process involving radical formation could lead to rearrangement to form a benzyl radical. In this particular case, no such product was formed, supporting a concerted mechanism (Scheme 4.12). Similar probes are common in mechanistic investigations of C-H amination processes. Du Bois and co-workers found no ring opening in the Rh₂(OAc)₄-catalyzed amination of cyclopropyl substrates,²⁰ while Warren and co-workers have shown that amination occurs only with ring-opening in a copper-promoted reaction.^{12c} Stereodefined cyclopropyl substrates may also undergo isomerization, providing evidence for the involvement of radical species in Ru-catalyzed C-H amination.²³

Scheme 4.12. Opening of radical clock substrates.

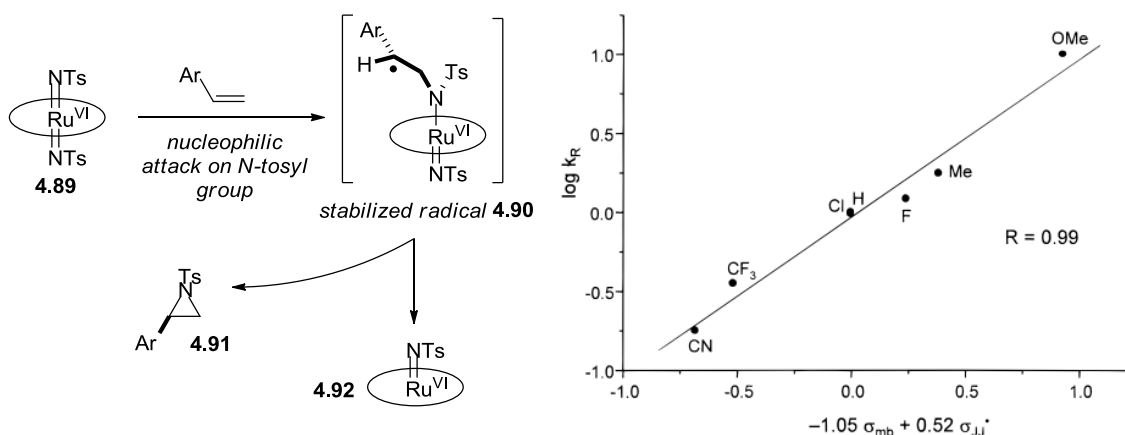


Hammett analysis. While the above experiments often require the detection of small byproducts arising from short-lived radical intermediates, Hammett studies of benzylic C-H amination and styrene aziridination instead examine the rates of formation of major products and hence may provide more detailed information about the mechanism of C-H amination. Here, five cases are considered, which illustrate a range of conclusions that may be drawn from such studies.

Mueller and co-workers determined a ρ value of -0.90 for the Rh-catalyzed intermolecular amination of ethylbenzenes and a higher, unreported value for the same system when applied to aziridination reactions.^{5b} This value is consistent with a concerted, asynchronous

mechanism with significant positive charge buildup in the transition state of the reaction. Du Bois and co-workers obtained a lower ρ value of -0.55 in intramolecular benzylic aminations catalyzed by Rh_2esp_2 .²⁰

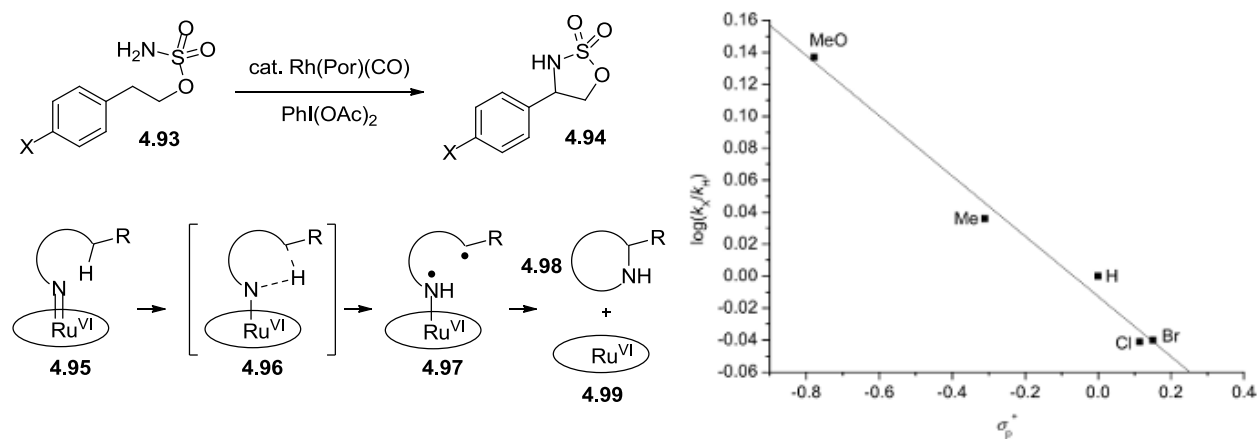
Scheme 4.13. Hammett effects used to elucidate mechanisms of N-tosyl transfer from Ru-diimido complexes.



Che and co-workers observed more complicated effects in stoichiometry aziridinations and C-H aminations by bis(tosylimido)ruthenium(VI) porphyrins.^{9b} Hammett analysis of styrene aziridination showed high linearity when both polar and radical contributions to transition state stabilization were considered (Scheme 4.13). These effects, in conjunction with other experiments, were most consistent with the carboradical aziridination mechanism **V** (Scheme 4.10), depicted above. In this mechanism, both the rate of nucleophilic attack of the styrene on the metal-bound nitrogen and the formation of a carboradical are expected to contribute to the reaction rate, consistent with the observed effects. When the Ru-imido complexes were used for the tosylation of para-substituted ethylbenzenes, a high correlation was observed between the dissociation energy of the benzylic C-H bonds and reaction rate, strongly implicating an H-atom abstraction mechanism.^{12b}

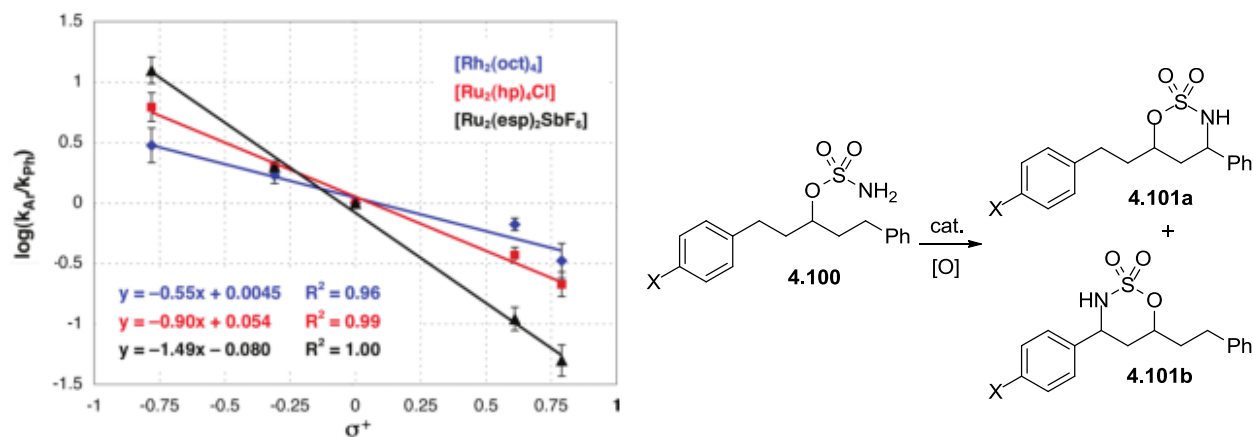
An interesting comparison can be made between these interpretations and those presented for an analogous catalytic system for intramolecular C-H amination using sulfamate nitrene precursors **7.93**.^{12c} For this system, a very small substituent effect was observed, with $\rho = -0.16$ when resonance polar effects were considered exclusively, consistent with a concerted mechanism involving minimal positive charge buildup in the transition state, but somewhat more difficult to reconcile with a radical mechanism. For the same catalyst, high correlation between BDE and reaction rate was observed for intermolecular hydrocarbon amination using TcesNH₂ as the nitrogen source. While this and previous results again point to an H-atom abstraction mechanism for intermolecular C-H amination, the implications for the intermolecular reaction are not as clear, and raise the intriguing possibility that inter- and intramolecular C-H amination occur by different mechanisms, even with the same catalyst system. This possibility also cautions against making strong mechanistic comparisons across nitrene transfer systems.

Scheme 4.14. Hammett effects in Ru-porphyrin-catalyzed benzylic C-H amination.

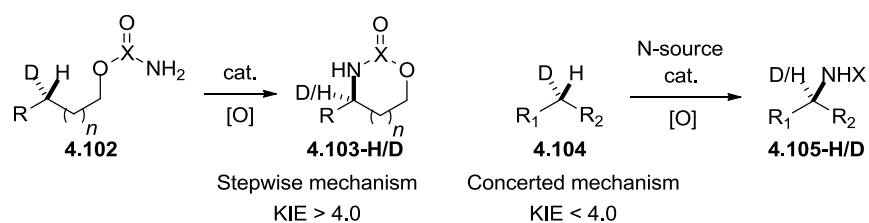


Alternatively, different catalysts can show high linearity with a single Hammett parameter but give divergent ρ values. Du Bois and co-workers have described such an effect in

the study of allylic and benzylic C-H amination catalyzed by diruthenium paddlewheel complexes.²³ In this study, high correlation was observed between $\log(k_{Ar}/k_{Ph})$ and the resonance parameter σ^+ for different catalysts, but with very different ρ values: -0.99 for $\text{Ru}_2(\text{hp})_4\text{Cl}$ and -1.49 for $\text{Ru}_2(\text{esp})_2\text{SbF}_6$ (Scheme 4.15). By comparison, the σ^+ value obtained with $\text{Rh}_2(\text{oct})_4$ is -0.55. The large difference between these values points to a potential change in mechanism from a concerted to a stepwise pathway, involving homo- or heterolytic C-H bond cleavage. Though computational data are offered in support of an H-atom abstraction mechanism, these and other mechanistic data are perhaps easier to reconcile with a pathway involving heterolytic bond cleavage and significant cationic character in the transition state. The high chemoselectivity of the system is attributed to its high propensity for hydride or H-atom abstraction. The complexity of these results underscores the need for a full range of mechanistic experiments to be carried out in assessing nitrene transfer mechanisms.

Scheme 4.15. Hammett data in Rh- and Ru-catalyzed C-H amination.

Kinetic Isotope Effects. Intramolecular competition experiments allow measurement of the full magnitude of kinetic isotope effects without requiring knowledge of a reaction's rate-determining step (Scheme 4.16). A KIE greater than four is thought to correspond to a stepwise mechanism involving a high degree of C-H bond cleavage in the transition state,¹² while smaller KIEs are indicative of concerted mechanisms.²⁰

Scheme 4.16. Intramolecular competition to assess intramolecular KIEs.

Again, there are cases in which the magnitude of observed KIEs is not easily reconciled with other results. For example, Huard and Lebel obtained a KIE of 5.0 in an intermolecular competition experiment involving the Rh-catalyzed amination of cyclohexane, but they posit a concerted mechanism on the basis of other results.²⁴ In contrast, Paradine and White observed a small KIE of 2.5 for intramolecular Fe-porphyrin-catalyzed C-H amination, but they attribute the

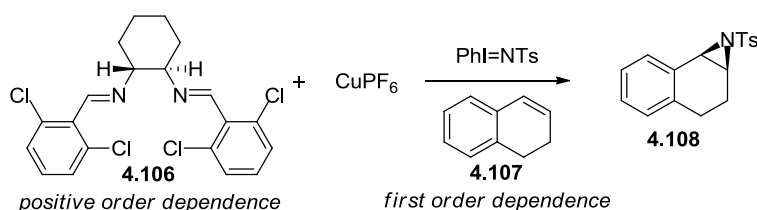
system's high selectivity for allylic amination to its H-atom abstraction ability.²⁵ Again, care is required in interpreting any single mechanistic experiment, and a full series of mechanistic probes should be conducted before conclusions about the nature of the amination pathways are drawn. A summary of expected results and mechanistic implications is provided below.

4.4. Kinetic Studies.

Perhaps due to the intense interest in the the mechanism of C-N bond formation, which may be invisible to steady-state rate laws, kinetic studies of catalytic nitrene transfer reaction are limited to a few examples. Che,⁹ Warren,¹² and Nicholas²⁶ have each described kinetic investigations of stoichiometric nitrene transfer reactions, though limitations in the scope of the methodology or the operational details of the reactions prevented analysis of catalytic systems.

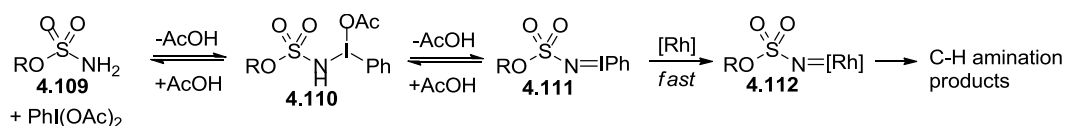
Jacobsen and co-workers have reported a detailed kinetic study of enantioselective Cu-diimine-catalyzed aziridination (Scheme 4.17).²⁷ At constant loading of the Cu salt, the rate showed a first order dependence on starting material. The rate was also found to increase asymptotically in the presence of ligand, indicating that the Cu-diimine complex was a faster catalyst than the unligated Cu. Enantioselectivity could therefore be enhanced by increasing ligand concentration.

Scheme 4.17. Kinetic study of Cu-diimine-catalyzed aziridination.



DuBois and co-workers have also performed kinetic studies on $\text{Rh}_2(\text{O}_2\text{C}^t\text{Bu})_4$ -catalyzed intramolecular C-H amination, establishing first order dependence on substrate and oxidant concentration, and zero-order dependence on catalyst concentration.²⁰ This surprising result indicates that the rate-determining step of the reaction is the formation of the iminoiodinane intermediate, which then undergoes fast interaction with the catalyst to form the active metal-nitrene intermediate (Scheme 4.18). The reaction did show rate dependence on catalyst concentration in later stages, indicating possible catalyst decomposition. Further studies suggest that the related Rh_2esp_2 catalyst undergoes reversible oxidation to form catalytically inactive mixed valence $\text{Rh}^{2+}/\text{Rh}^{3+}$ dimers.²⁸

Scheme 4.18. Formation of iminoiodinane as rate-limiting step.

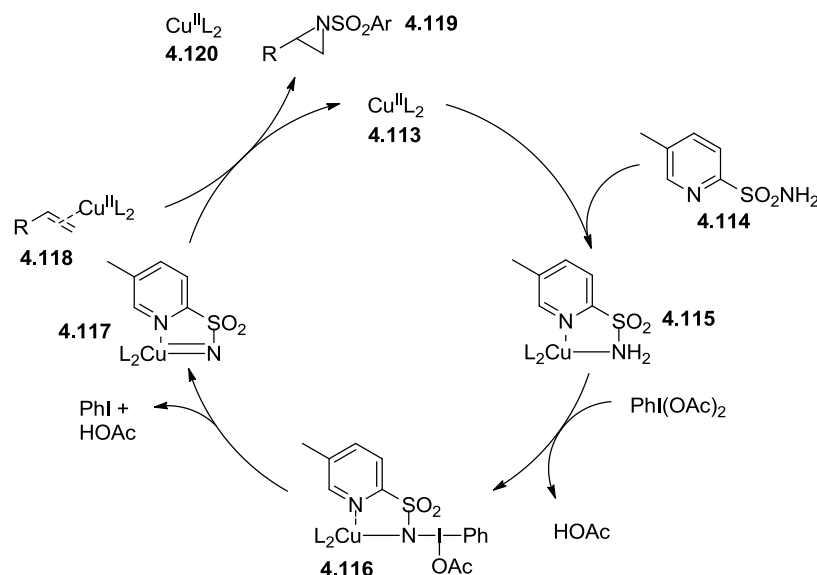


A recent study of Cu-catalyzed aziridination by Kim, Chang and co-workers showed first order dependence on olefin concentration, and second order in Cu catalyst.²⁹ This dependence is explained by the coordination of one equivalent of copper to the olefin substrate prior to aziridination (Scheme 4.19). This explanation is at least counterintuitive, as the olefin is presumed to be a nucleophilic species in these transformations, and it is not clear how the copper activates the olefin. Another possibility that is not considered is the involvement of a dimeric copper catalyst that is formed reversibly.

Though a stoichiometric study, Warren's kinetic study of copper-nitrenes warrants mention for its elegance and for the mechanistic insight provided.^{12c} Stoichiometric amination of

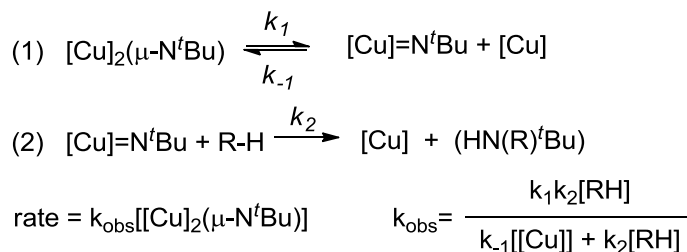
ethylbenzene demonstrated saturation dependence on the concentration of the copper nitrene and inverse dependence on

Scheme 4.19. Kim and Chang's proposal for Cu-catalyzed aziridination.



the concentration of added copper (Scheme 4.20). As the nitrogen source in the reaction is a nitrene-bridged copper dimer, the inverse dependence on copper is best explained by the reversible formation of a mononuclear copper-nitrene species, which is the active oxidant in the transformation.

Scheme 4.20. Kinetic analysis for decomposition of bridged dicopper nitrenes.

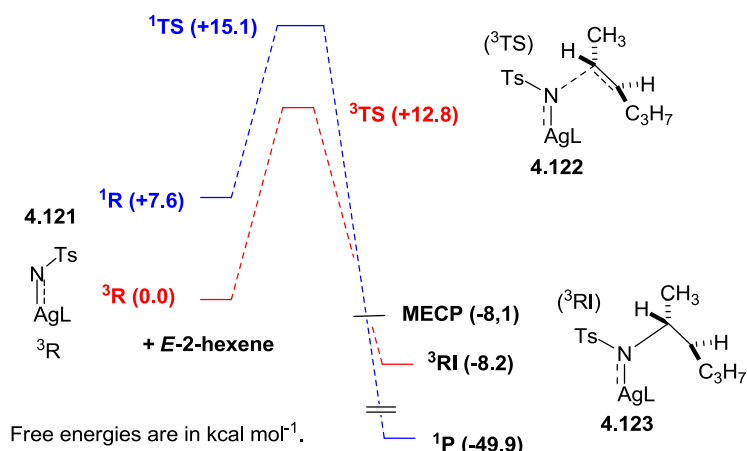


Given the large number of catalytic systems that have been developed for nitrene transfer, it is surprising that so few kinetic studies of these reactions have been reported. Further investigations of catalytic nitrene transfer may afford greater insight into processes such as catalyst activation and death, product acceleration and inhibition and changes in chemoselectivity throughout reactions.

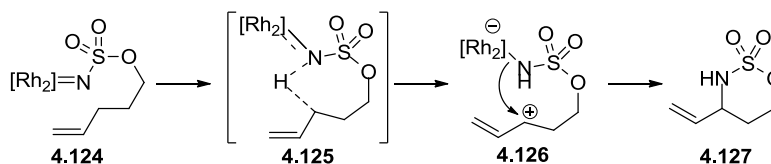
4.6. Computational studies of nitrene transfer.

Computational studies of nitrene transfer reactions support overall mechanistic pathways like those described above. While a full description of the computational literature on nitrene transfer is beyond the scope of this thesis, two recent studies deserve comment. Perez's computational investigations of Ag- and Cu-catalyzed aziridinations is worth noting in the present context because it illustrates some of the complexities associated with distinguishing singlet and triplet pathways.¹⁷ In a computed profile for the Ag-catalyzed reaction, the triplet metal-nitrene species is found to be lower in energy by 7.6 kcal mol⁻¹, and the lowest energy transition state for aziridination is also computed to be in the triplet state. However, no radical intermediate is formed due to spin crossing between the triplet and closed-shell singlet energy profiles after the transition state of the product-forming step. This mechanism is therefore best described as concerted, despite the involvement of a triplet metal-nitrene intermediate. Importantly, Perez notes that the results obtained computationally were highly dependent on the theoretical approach employed.

Scheme 4.21. Computed spin-crossover in Ag-catalyzed aziridination.



Zhao and co-workers have investigated competitive aziridination and C-H insertion by di-Rh catalysts,^{29a,b} with intentions to accurately predict the selectivities of these reactions. From these studies, electron-donating catalyst Rh₂(NCH₃CHO)₄ is thought to proceed through a singlet, stepwise pathway involving a formal hydride migration and carbocation formation for C-H amination (Scheme 4.22). This mechanism is correlated to this catalyst's high selectivity for C-H amination. Other, less electron-donating dirhodium catalysts were found to proceed through more traditional, singlet, concerted, asynchronous pathways. Nevertheless, Zhao humbly writes, "Theoretical descriptions of the dirhodium-nitrene promoted C-H amination and alkene aziridination are largely less than their experimental counterparts," indicating that new theoretical approaches may overturn current results. These two examples illustrate the further complexities entailed by computational approaches to nitrene transfer mechanisms.

Scheme 4.22. Computed singlet, stepwise pathway for Rh-catalyzed C-H amination.

4.7. Conclusions.

Despite the high number of metal-catalyzed nitrene transfer reactions that have been developed and studied, many important questions about the mechanisms of these reactions remain unanswered. Mononuclear metal-nitrenes of the type thought to be active in catalysis have not yet been isolated or directly observed, such that important aspects of metal-ligand bonding in these species have not been investigated. While a common set of physical organic experiments is now regularly applied to investigate these reactions, contrasting or even conflicting results may be observed. Computational results suggest that simple correlations between singlet and triplet nitrene structures and concerted and stepwise mechanisms may require revision. Kinetic studies of catalytic nitrene transfer show diverse behavior across catalyst systems and point to complicating factors such as substrate oxidation, catalyst coordination to substrates, and catalyst death in determining overall reaction rates. These complexities indicate that, despite the mechanistic similarities among nitrene transfer reactions, study of individual systems can still yield new insight, and may play a crucial role in the development of efficient, chemoselective catalysts.

4.8. References.

1. a) Kwart, H.; Kahn, A.A. *J. Am. Chem. Soc.* **1967**, *89*, 1950. b) Kwart, H.; Kahn, A.A. *J. Am. Chem. Soc.* **1967**, *89*, 1951.
2. (a) Breslow, R.; Gellman, S.H. *J. Chem. Soc. Chem. Comm.*, **1982**, 1400. b) Breslow, R.; Gellman, S.H. *J. Am. Chem. Soc.* **1983**, *105*, 6728.
3. Roizen, J.L.; Harvey, M.E.; Du Bois, J. *Accts. Chem. Res.* **2012**, *45*, 911, and references therein.
4. a) Mahy, J.-P.; Bedi, G.; Battioni, P.; Mansuy, D. *J. Chem. Soc., Perkin Trans. 2*, **1988**, 1517. b) Mahy, J.-P.; Bedi, G.; Battioni, P.; Mansuy, D. *Tetrahedron Lett.* **1988**, *29*, 1927.
5. (a) Nageli, I.; Baud, C.; Bernardinelli, G.; Jacquier, Y.; Moran, M.; Mueller, P. *Helv. Chim. Acta*, **1997**, *80*, 1087. b) Mueller, P.; Baud, C.; Naegeli, I. *J. Phys. Org. Chem.* **1998**, *11*, 597.
6. For examples of isolated metal-imido species, see: for Fe: a) Kuppuswamy, S.; Powers, T. M.; Johnson, B. M.; Bezpalko, M. W.; Brozek, C. K.; Foxman, B. M.; Berben, L. A.; Thomas, C.M. *Inorg. Chem.* **2013**, *52*, 4802. b) Bowman, A. C.; Milsmann, C.; Bill, E.; Turner, Z. R.; Lobkovsky, E.; DeBeer, S.; Wieghardt, K.; Chirik, P. J. *J. Am. Chem. Soc.* **2011**, *133*, 17353. For Ru: c) Takaoka, A.; Moret, M.-E.; Peters, J. C. *J. Am. Chem. Soc.* **2012**, *134*, 6695. d) Takaoka, A.; Gerber, L. C. H.; Peters, J. C. *Angew. Chem. Int. Ed.* **2010**, *49*, 4088. e) Fantauzzi, S.; Gallo, E.; Caselli, A.; Ragaini, F.; Casati, N.; Macchic, P.; Cenini, S. *Chem. Commun.* **2009**, 3952. For Os, see: f) Lutz, C. M.; Wilson, S. R.; Shapley, P.A. *Organometallics* **2005**, *24*, 3350. g) Muniz, K.; Nieger, M.; Mansikkamäki, H. *Angew. Chem. Int. Ed.* **2003**, *42*, 5958. For Co, see: h) Lyaskovskyy, V.; Suarez, A. I. O.; Lu, H.; Jiang, H.; Zhang, X. P.; Bruin, B. d. *J. Am. Chem. Soc.* **2011**, *133*, 12264. i) King, E. R.; Sazama, G. T.; Betley, T. A. *J. Am. Chem. Soc.* **2012**, *134*, 17858. j) Jones, C.; Schulten, C.; Rose, R. P.; Stasch, A.; Aldridge, S.; Woodul, W. D.; Murray, K. S.; Moubaraki, B.; Brynda, M.; Macchia, G. L.; Gagliardi, L. *Angew. Chem. Int. Ed.* **2009**, *48*, 7406. For Ir, see: k) Kimura, T.; Koiso, N.; Ishiwata, K.; Kuwata, S.; Ikariya, T. *J. Am. Chem. Soc.* **2011**, *133*, 8880. l) Schau-Magnussen, M.; Malcho, P.; Herbst, K.; Brorsona, M.; Bendix, J. *Dalton Trans.* **2011**, *40*, 4212. m) Glueck, D. S.; Wu, J.; Hollander, F. J.; Bergman, R. G. *J. Am. Chem. Soc.* **1991**, *113*, 2041. n) Waterman, R.; Hillhouse, G. L. *J. Am. Chem. Soc.* **2008**, *130*, 12628. For Ni, see: o) Iluc, V. M.; Miller, A. J. M.; Anderson, J. S.; Monreal, M. J.; Mehn, M. P.; Hillhouse, G. L. *J. Am. Chem. Soc.* **2011**, *133*, 13055. p) Laskowski, C. A.; Miller, A. J. M.; Hillhouse, G. L.; Cundari, T. R. *J. Am. Chem. Soc.* **2011**, *133*, 771.
7. Berry, J.F. *Comments Inorg. Chem.* **2009**, *30*, 28.
8. Groves, J. T.; Takahashi, T. *J. Am. Chem. Soc.* **1983**, *105*, 2073.
9. a) Au, S.-M.; Zhang, S.-B.; Fung, W.-H.; Yu, W.-Y.; Che, C.-M.; Cheung, K.-K. *Chem. Commun.* **1998**, 2677. b) Au, S.-M.; Huang, J.-S.; Yu, W.-Y.; Fung, W.-H.; Che, C.-M. *J. Am. Chem. Soc.* **1999**, *121*, 9120. c) Liang, J.;-L.; Yuan, S.-X.; Hunag, J.-S.; Che, C.-M. *J. Org. Chem.* **2004**, *69*, 3610.
10. King, E.R.; Hennessy, E.T.; Betley, T.A. *J. Am. Chem. Soc.* **2011**, *133* 4917.
11. a) Lyaskovskyy, V.; Suarez, A.I.O.; Lu, H.; Jiang, H.; Zhang, X. P.; de Bruin, B. *J. Am. Chem. Soc.* **2011**, *133*, 12264. b) Gao, G.-Y.; Jones, J. E.; Vyas, R.; Harden, J. D.; Zhang, X. P. *J. Org. Chem.* **2006**, *71*, 6655. c) Ruppel, J. V.; Jones, J. E.; Huff, C.A.; Kamble,

- R.M.; Chen, Y.; Zhang, X.P. *Org. Lett.* **2008**, *10*, 1995. d) Lu, H.-J.; Li, C.-Q.; Jiang, H.-L.; Lizardi, C.L.; Zhang, X.P. *Angew. Chem. Int. Ed.* **2014**, *53*, 7028.
12. a) Badiei, Y.M.; Krishnaswamy, A.; Melzer, M.M.; Warren, T.H. *J. Am. Chem. Soc.* **2006**, *128*, 15056. b) Badiei, Y. M.; Dinescu, A.; Dai, X.; Palomino, R. M.; Heinemann, F. W.; Cundari, T. R.; Warren, T. H. *Angew. Chem. Int. Ed.* **2008**, *47*, 9961. c) Aguila, M. J. B.; Badiei, Y. M.; Warren, T. H. *J. Am. Chem. Soc.* **2013**, *135*, 9399.
13. Kundu, S.; Miceli, E.; Farquhar, E.; Pfaff, F. F.; Kuhlmann, U.; Hildebrandt, P.; Braun, B.; Greco, C.; Ray, K. *J. Am. Chem. Soc.* **2012**, *134*, 14710.
14. Dielmann, F.; Andrada, D. M.; Frenking, G.; Bertrand, G. *J. Am. Chem. Soc.* **2014**, *136*, 3800.
15. Kornecki, K. P.; Berry, J. F. *Chem. Eur. J.* **2011**, *17*, 5827.
16. Sweeney, J.B. Synthesis of Aziridines. In *Aziridines and Epoxides in Organic Synthesis*; Yudin, A.K., Ed.; Wiley: Weinheim, **2006**, pp. 117-144.
17. Evans, D. A.; Faul, M. M.; Bilodeau, M. T. *J. Am. Chem. Soc.* **1994**, *116*, 2742.
18. Maestre, L.; Sameera, W. M. C.; Diaz-Requejo, M. M.; Maseras, F.; Perez, P. J. *J. Am. Chem. Soc.* **2013**, *135*, 1338.
19. Barman, D. N.; Nicholas, K. M. *Eur. J. Org. Chem.* **2011**, *5*, 908.
20. Fiori, K.W.; Espino, C.G.; Brodsky, B.H.; Du Bois, J. *Tetrahedron* **2009**, *65*, 3042.
21. Collet, F.; Lescot, C.; Liang, C.G.; Dauban, P. *Dalton Trans.* **2010**, *39*, 10401.
22. a) He, G.-X.; Bruice, T. C. *J. Am. Chem. Soc.* **1991**, *113*, 2747. b) Newcomb, M.; Manek, M. B. *J. Am. Chem. Soc.* **1990**, *112*, 9662.
23. Harvey, M.E.; Musaev, D.G.; Du Bois, J. *J. Am. Chem. Soc.* **2011**, *133*, 17207.
24. Huard, K.; Lebel, H. *Chem. Eur. J.* **2008**, *14*, 6222.
25. Paradine, S.M.; White, M.C. *J. Am. Chem. Soc.* **2012**, *134*, 2036.
26. Srivastava, R.S.; Tarver, N.R.; Nicholas, K.M. *J. Am. Chem. Soc.* **2007**, *129*, 15250.
27. Li, Z.; Quan, R. W.; Jacobsen, E. N. *J. Am. Chem. Soc.* **1995**, *117*, 5889.
28. Zalatan, D. N.; Du Bois, J. *J. Am. Chem. Soc.* **2009**, *131*, 7558.
29. Han, H.; Park, S. B.; Kim, S. K.; Chang, S. *J. Org. Chem.* **2008**, *73*, 2862.
30. a) Zhang, X.; Ke, Z.; DeYonker, N. J.; Xu, H.; Li, Z.-F.; Xu, X.; Zhang, X.; Su, C.-Y.; Phillips, D. L.; Zhao, C. *J. Org. Chem.* **2013**, *78*, 12460. b) Zhang, X.; Xu, H.; Zhao, C. *J. Org. Chem.* **2014**, *79*, 9799.

**Chapter 5. Mechanistic Studies of Dynamic, Chemoselective, Silver(I)-Catalyzed
Aziridination and C-H Amination.**

5.1. Introduction.

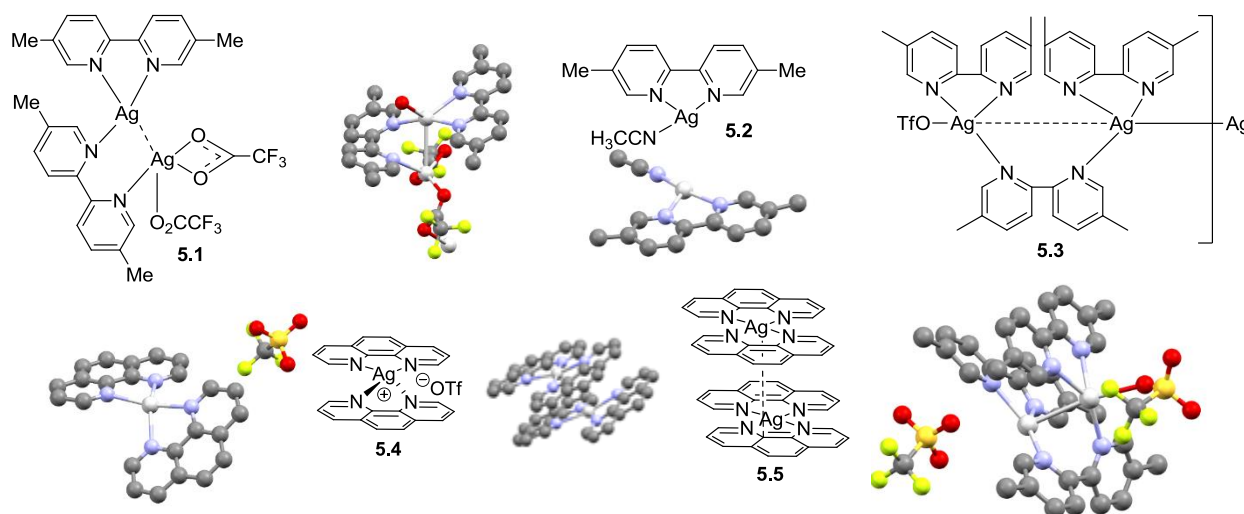
Discovery of the dynamic behavior of our silver catalyst system presented the possibility that variation of ligand:metal ratio could tune chemoselectivity in other systems. In order to better understand the factors underlying the chemoselectivity of the Ag-catalyzed amination reactions described in Chapter 3, we have undertaken mechanistic studies of these reactions, including: spectroscopic examination of the silver catalysts, mechanistic probe experiments, and kinetic studies. Spectroscopic experiments indicate that the active catalyst species in the reaction are $\text{Ag}(\text{phen})\text{OTf}$ and $\text{Ag}(\text{phen})_2^+$, and that the equilibrium between them is governed exclusively by the ligand:metal ratio. Mechanistic probe experiments suggest that both aziridination and C-H amination are concerted processes, though we cannot rule out the possibility that one or both processes involve radical formation and rapid recombination. Moreover, the two processes display similar steady-state kinetic behavior, indicating that the reactions do not differ in steps crucial to determining the overall reaction rate. However, we observed that while $\text{Ag}(\text{phen})\text{OTf}$ appears to be a suitable catalyst for C-H amination, $\text{Ag}(\text{phen})_2^+$ fails to perform aziridination with sterically congested substrates, suggesting that the observed chemoselectivity arises from differences in the steric environments provided by the two catalysts.

5.2. Solution-state behavior of silver complexes.

A very brief introduction to silver coordination chemistry provides some insight into the behavior of our system. Silver coordination compounds are known to exhibit different binding modes and stoichiometries with a single ligand, depending on such factors as counterion, ligand:metal ratio, solvent, temperature and pH.¹ For example, with a 1:1 Ag:ligand ratio, the 5,5'-di-Me-bipyridyl (bipy) ligand can act as a bidentate ligand bridging two silver nuclei (**5.1**)^{1a}

or as a bidentate ligand bound to a single nucleus (**5.2**),^{1h} depending on choice of solvent and counterion (Figure 5.1). At a 2:3 Ag: 5,5'-di-Me-bipyridyl ratio, bridged dinuclear silver complexes can be formed (**5.3**).^{1a} Similarly, Ag:2,2'-bipyridyl combinations may form mononuclear 1:1 or 1:2 Ag:ligand complexes,¹ⁱ as well as oligomeric structures^{1a}, depending on solvent, counterion and stoichiometry. NMR and HRMS studies suggest that these oligomers do not persist in solution; rather, an equilibrium exists among these complexes due to rapid exchange on the NMR time scale.^{1a} Ag(phen)₂⁺ complexes typically exhibit pseudo-tetrahedral geometries in the solid state (**5.4**),^{1g,j} but often form pseudo-square planar networks in the presence of other metallic co-crystals (**5.5**).^{1k-m} Though limited analogy can be drawn between solid-state and solution behavior, these examples attest to the diversity of potential binding modes and nuclearities of silver species in solution.

Figure 5.1. Binding modes and coordination geometries of bidentate nitrogenated ligands with Ag.



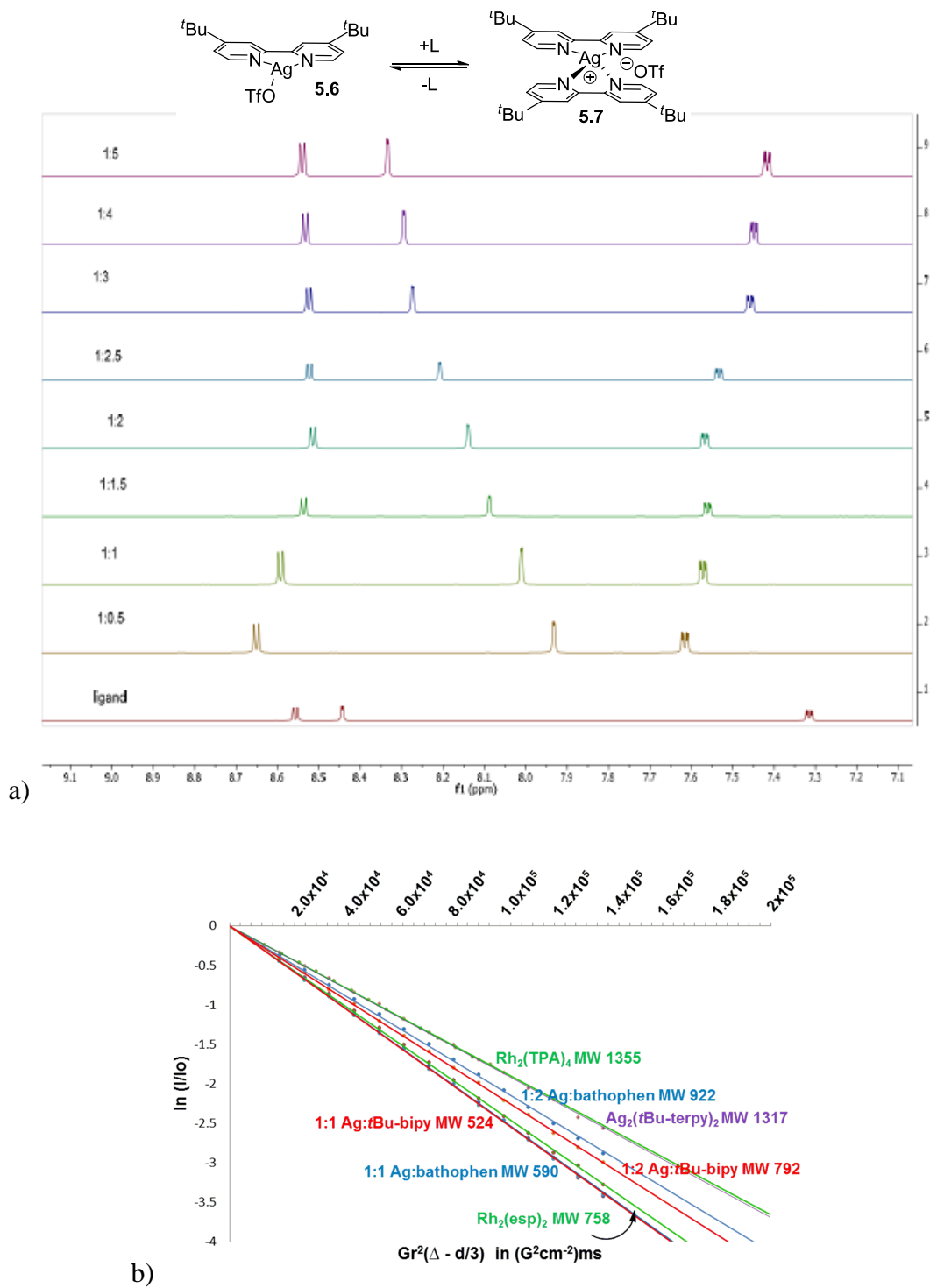
We first conducted NMR titration studies in an attempt to observe individual silver species in solution. To improve the solubility of the silver complexes, the phenanthroline ligand was replaced with 4,4'-di-*t*Bubipyridine, which provided chemoselectivities similar to the phenanthroline. When varied ratios of ligand:AgOTf were examined by $^1\text{H-NMR}$, variation in the proton chemical shifts was noted, but individual species could not be observed even at temperatures as low as -85°C , indicating that ligand exchange between nuclei is very rapid and that average chemical shifts are observed.

In their seminal publication on Ag-catalyzed aziridination, He and co-workers obtained crystals of a disilver(I) complex by evaporation of a catalyst solution and posited this as the active catalyst for the reaction.² We utilized DOSY (Diffusion Ordered Spectroscopy) NMR to determine the nuclearity of our own silver complexes in solution.³ These experiments indicated that the primary species at low ligand loading is $\text{Ag}(4,4'\text{-di-}t\text{Bubipy})\text{OTf}$, while higher ligand loadings result in the formation of $[\text{Ag}(4,4'\text{-di-}t\text{Bubipy})_2]\text{OTf}$ (similar to Figure 5.1, **5.4**). Examination of He's $[\text{Ag}_2(\text{terpy})_2(\text{NO}_3)]\text{NO}_3$ catalyst affirmed that it remains a dinuclear species in solution. The dynamic behavior of these silver complexes suggests that while metal:ligand stoichiometry may allow one species to dominate, both $\text{Ag}(4,4'\text{-di-}t\text{Bubipy})\text{OTf}$ and $[\text{Ag}(4,4'\text{-di-}t\text{Bubipy})_2]\text{OTf}$ may be present at low concentrations with all ligand loadings.

5.3. Experiments to assess the nature of the aziridination and C-H amination steps.

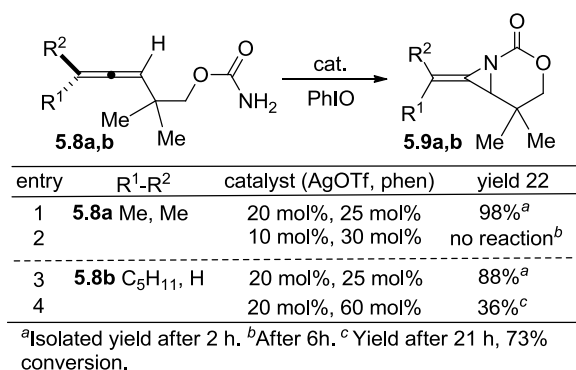
We considered the hypothesis that differences in the electronic structure of the nitrenes supported by each catalyst might account for the differences in chemoselectivity, perhaps through the promotion of different mechanistic pathways. A series of experiments was performed to assess the mechanisms of the aziridination and C-H amination steps. Throughout this section, the two catalysts will be described nominally as AgLOTf and AgL_2^+ , the two species present in solution under non-reactive conditions, but though it is possible that another species is in fact the active catalyst.

Figure 5.2. Spectroscopic study of Ag complexes in solution. a) NMR titration using 4,4'-di-*tert*-butylbipyridine. b) DOSY NMR experiments to assess the nuclearity of Ag complexes.



Steric effects. To determine the role that the coordination number of silver might play in chemoselectivity, we examined substrates with only one reactive site (Scheme 5.1). We were curious to know if the more sterically hindered AgL_2^+ catalyst would also be capable of promoting aziridination, and if the AgLOTf species would be able to promote C-H amination in the absence of an alkene. Standard amination conditions were applied to trisubstituted homoallenic carbamate **5.8a**, in which the allenic amination sites were blocked by methyl groups, but the substrate failed to react. Disubstituted homoallenic carbamate **5.8b** did undergo aziridination, albeit in 36% yield, with 73% conversion over 21 hours. This suggests that although the AgL_2OTf is capable of enabling aziridination, the greater steric bulk of the catalyst could be diverting the nitrene transfer through a different mechanistic pathway as compared to AgLOTf .

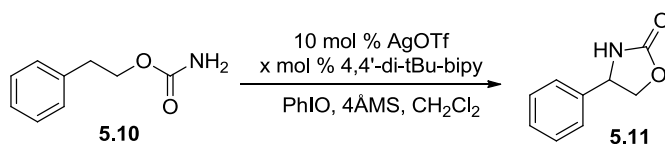
Scheme 5.1. Performance of AgL and AgL_2 systems in aziridination.



In contrast, homobenzylic carbamate **5.10** provided moderate yields of C-H amination products using both 1:1.25 and 1:3 ligand:metal ratios (Scheme 5.2). While it is possible that this reaction was catalyzed by low concentrations of the AgL_2 species, which is in rapid equilibrium with the dominate AgLOTf complex, the reactions showed similar overall reaction times and yields. This suggests that either the AgLOTf catalyst can mediate both aziridination or C-H

amination pathways, or that the small amounts of AgL_2 present catalyze the transformation (*vide infra*).

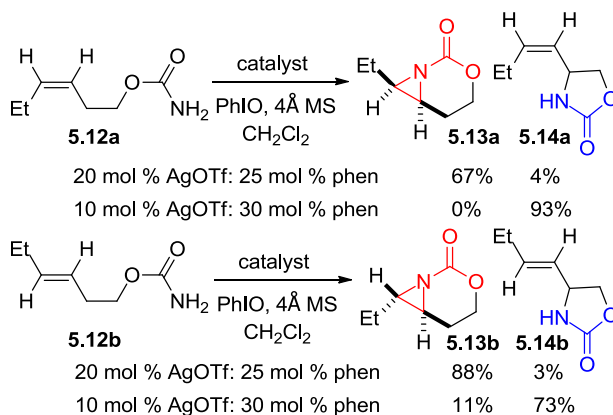
Scheme 5.2. Benzylic amination with AgLOTf and AgL_2^+ .



entry	4,4'-di- <i>t</i> Bu-bipy	yield
1	12.5 mol %	44%
2	30 mol %	54%

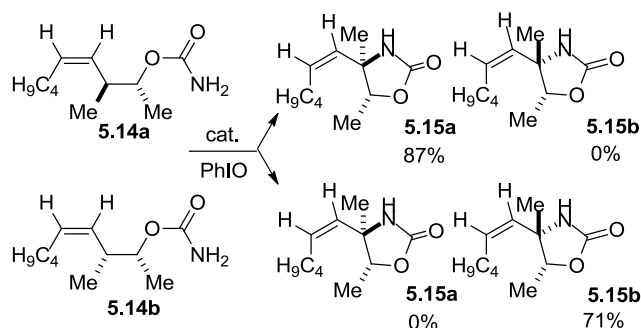
Stereochemical probe substrates. *Cis* and *trans* alkenes **5.12a** and **5.12b** were subjected to standard conditions for both aziridination and C-H amination, and single diastereomers of the product were obtained in each case (Scheme 5.3). As discussed in chapter 4, stereoisomerization in any of these reactions would support a stepwise mechanism, but retention of stereochemistry does not rule out a rapid radical rebound pathway.

Scheme 5.3. Isomerization probes for aziridination and C-H amination.



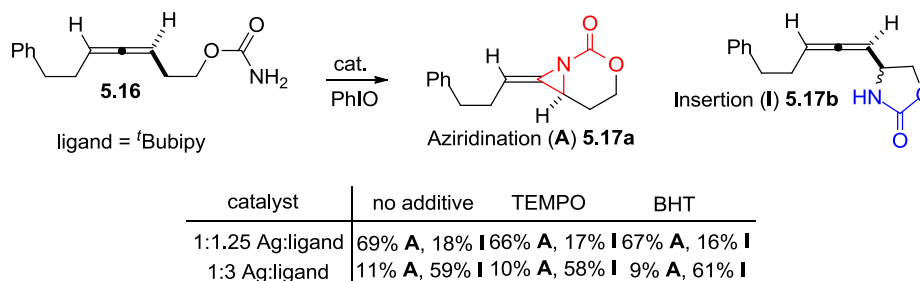
Diastereomeric stereochemical probe substrates **5.14a** and **5.14b** were subjected to C-H amination conditions. Both substrates gave a single diastereomer of product, offering further evidence against a stepwise mechanism (Scheme 5.4).

Scheme 5.4. Stereochemical probes for C-H insertion.



Radical inhibitors in C-H insertion and aziridination reactions. The C-H insertion and aziridination reactions were performed with homoallylic carbamate **5.16** in the presence of equimolar amounts of catalyst and a radical inhibitor, BHT (2,6-di-*t*Bu-hydroxytoluene) or TEMPO (2,2,6,6-tetramethylpiperidine-1-oxy radical). The differences between the yields obtained under each set of conditions were within the range of experimental error (Scheme 5.5). These results again indicate that either concerted amination pathways are operable, or that radical intermediates are formed but have lifetimes too short to be intercepted by these inhibitors.

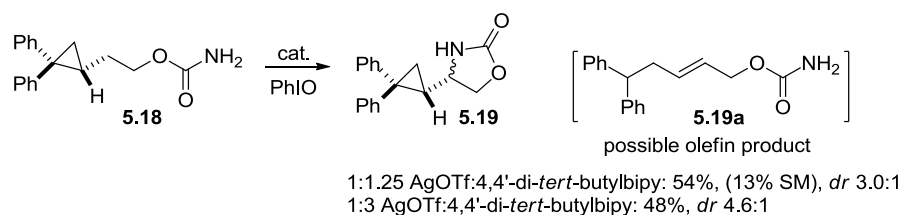
Scheme 5.5. Radical inhibition studies.



Radical trap experiments. A radical trap experiment was carried out to assess the presence of short-lived radical species. The rate constant for radical opening of **5.18** (Scheme 5.6) is approximately $4 \times 10^{11} \text{ s}^{-1}$; however, only insertion product **5.19** was observed and no olefins

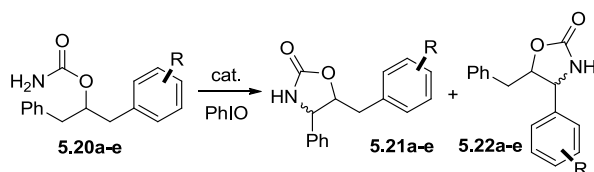
were detected.⁴ Additionally, this experiment was performed with a 1:1.25 Ag:ligand ratio, resulting in a 54% yield of the final product.

Scheme 5.6. Amination of a radical clock substrate.

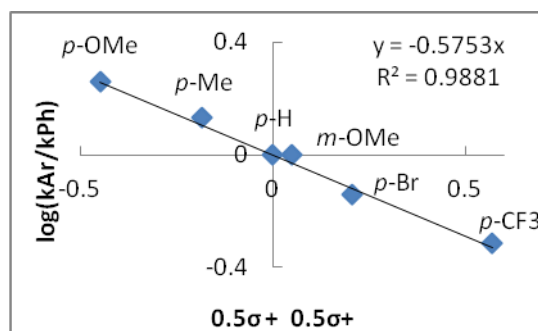


Hammett analysis. Intramolecular competition experiments were performed using bis-aryl carbamates **5.20a-e** (Scheme 5.7). Analysis of the resulting mixtures of benzylic amination products **5.21a-e** and **5.22a-e** allows straightforward computation of $\log(k_{Ar}/k_{Ph})$ for each substrate, where these rate constants correspond to a C-H functionalization step. Each reaction was performed in duplicate at a 20 mol% AgOTf loading to ensure full conversion. For the standard C-H amination catalyst system, the highest linearity was observed when $\log(k_{Ar}/k_{Ph})$ was plotted against an equally weighted average of σ and σ^+ parameters.⁵ Parameters that quantify radical involvement in benzylic C-H functionalization, such as spin delocalization constants,⁶ do not account for the strongly deactivating effect of the *p*-CF₃ group. A ρ value of -0.58 was calculated,⁷ indicating moderate positive charge buildup in the transition state of the amination step. Significantly, a ρ value of -0.57 was obtained when a 1:1.25 Ag: ligand ratio was used with the same collection of substrates (see Experimental Section). This result is similar to the ρ value of -0.55 obtained by Du Bois and co-workers in their examination of nitrene transfer reactions catalyzed by dinuclear Rh catalysts.⁸ While the value obtained is most consistent with a concerted asynchronous process, it might also arise from a stepwise C-H amination pathway featuring an early transition state with substantial positive charge buildup prior to C-H bond cleavage.

Scheme 5.7. Hammett studies of Ag-catalyzed C-H amination.

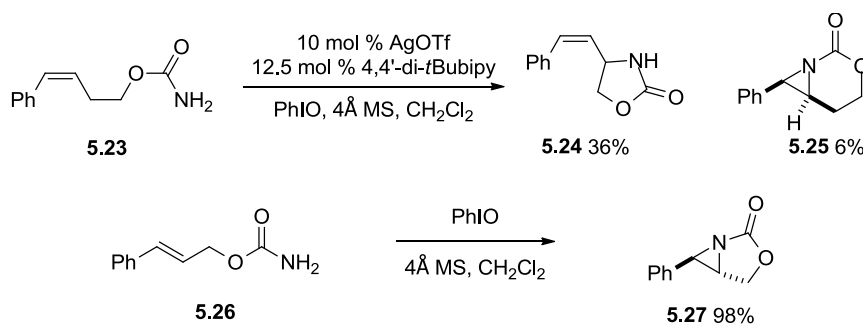


R	($0.5\sigma + 0.5\sigma^+$)	Ar/Ph	$\log(k_{Ar}/k_{Ph})$
<i>p</i> -OMe	-0.450	1.8:1.0	0.26
<i>p</i> -Me	-0.185	1.4:1.0	0.13
H	0.00	1.0:1.0	0
<i>m</i> -OMe	0.050	1.0:1.0	0
<i>p</i> -Br	0.205	1.0:1.4	-0.16
<i>p</i> -CF ₃	0.570	1.0:2.1	-0.31



While we considered conducting similar studies for Ag-catalyzed aziridination, we noted that intermolecular amination of styrenes **5.23** gave almost exclusively C-H amination when a two-carbon tether was present (Scheme 5.8). When a shorter tether is present, as in **5.26**, aziridination does not require a catalyst.⁹

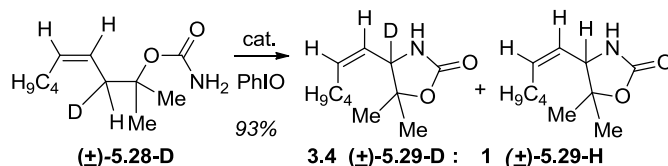
Scheme 5.8. Ag-catalyzed aziridination of styrenes.



Intrinsic Kinetic Isotope Effect. An intramolecular competition experiment with homoallylic carbamate **5.28-D** showed an intrinsic KIE of 3.4 (Scheme 5.9), somewhat lower than the KIEs

of 4-12 that often characterize stepwise C-H amination pathways,¹⁰ though higher than the intrinsic effect of 1.9 observed for Rh₂(OAc)₄.⁸

Scheme 5.9. Intrinsic KIE measurement.



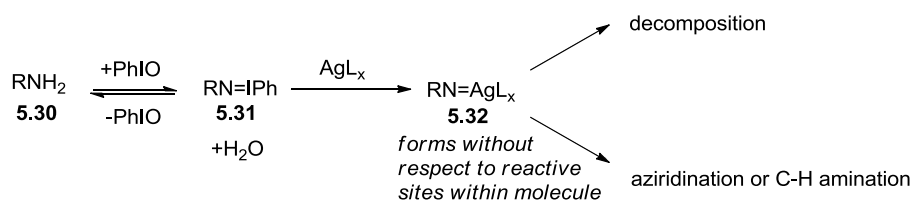
Together, these probes suggest that our system is mechanistically distinct among highly selective allylic C-H insertions.^{11a,b} In Du Bois's Ru system and in White's Fe system, the selectivity is attributed to the metal-nitrene's high propensity for H-atom abstraction. In both cases, mechanistic probes provided support for a stepwise pathway. In contrast, while our experiments on Ag-catalyzed C-H amination cannot entirely rule out a rapid radical rebound pathway, all results strongly suggest a concerted, asynchronous mechanism. On this basis, we may tentatively infer that the two metal-nitrenes possess a similar electronic structure, though Perez^{12a} and Zhao^{12b} have cast doubt on simple correlations between electronic structure and mechanism, as described in Chapter 4.

A significant question of interpretation arises with respect to the C-H amination experiments conducted with a 1:1.25 Ag:ligand ratio. We may on the one hand regard these results as evidence of the competence of the Ag(tBubipy)OTf catalyst in performing C-H amination. Alternatively, it is possible that small amounts of the Ag(tBubipy)₂⁺ species present under these conditions catalyze the C-H amination reaction. However, carbamate substrates should form metal-nitrene intermediates **5.32** in the presence of catalyst regardless of whether or not appropriate reactive sites are present in the molecule (Scheme 5.10). If these intermediates did follow a C-N bond-forming pathway, they would presumably follow non-productive

pathways, resulting in low mass balance. For example, subjecting *tert*-butylcarbamate to the 1:1.25 Ag:ligand conditions for 6 hours resulted in only 25% recovery of starting material.

Low mass balance was observed in the aziridination of **5.8b** with $\text{Ag}(\text{tBubipy})_2^+$. However, C-H insertions performed with AgLOTf as the primary catalytic species showed yields comparable to those obtained with AgL_2^+ as the dominant catalytic species. Based on the above results, we infer that both the $\text{Ag}(\text{tBubipy})\text{OTf}$ and $\text{Ag}(\text{tBubipy})_2^+$ species promote C-H amination. Hammett and radical clock studies imply that the catalysts followed similar C-H amination pathways and likely form electronically similar metal-nitrenes.

Scheme 5.10. Metal-nitrene formation and reaction in the presence of either catalyst.

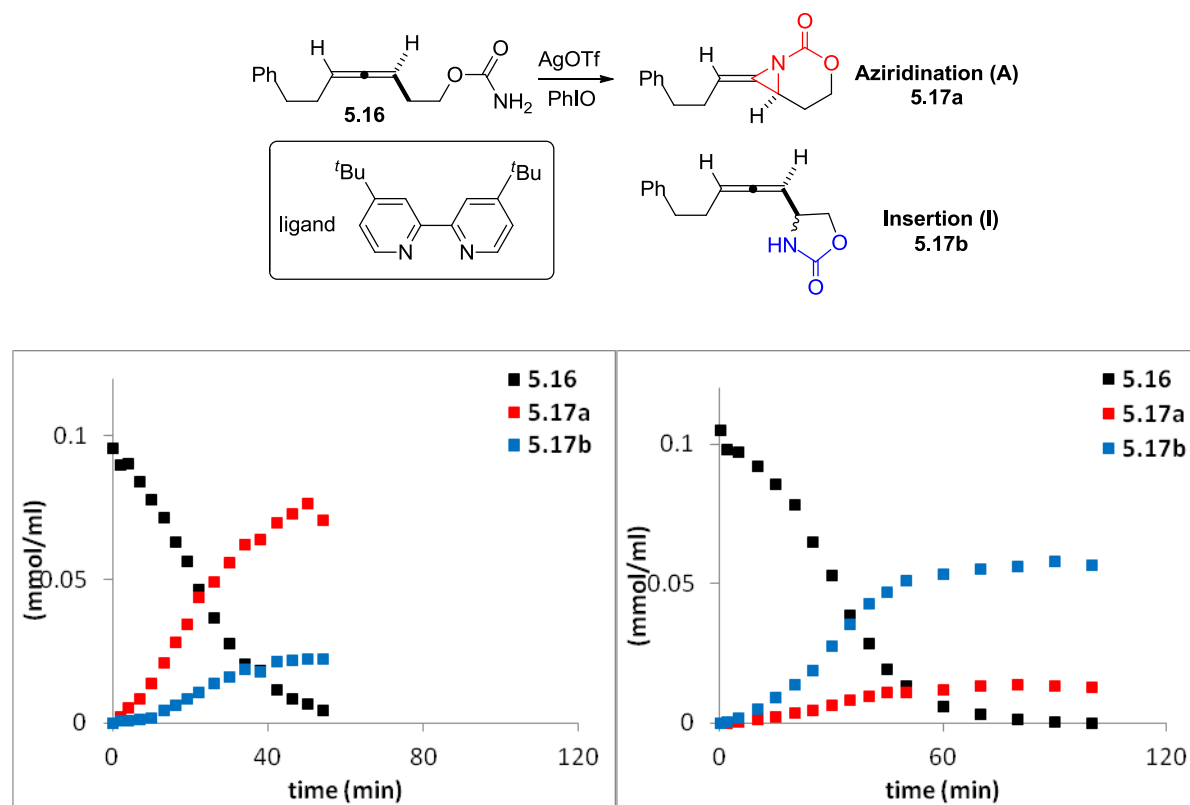


5.4. Kinetic analysis of dynamic silver catalysis.

As described in Chapter 4, kinetic analysis of nitrene transfer reactions is limited to a small number of examples, and such studies have been primarily concerned with initial rate behavior.^{8,13a-c} However, non-ideal behavior during the catalytic process due to catalyst activation, deactivation, substrate inhibition and by-product formation can render kinetic analysis by initial rate measurements untenable. Instead, methods utilizing the entire reaction profile for kinetic analysis, such as reaction progress kinetic analysis (RPKA)^{14a} or kinetic profiling^{14b} provide a means to readily assess non-ideal systems displaying complex kinetic behavior. To elucidate the origins of the observed ligand-dependent chemoselectivity and better understand the mechanistic underpinnings of the C-H amination and aziridination pathways, we have studied

the kinetic profile of our Ag catalyst systems using 4,4'-di-*tert*-butyl-2,2'-bipyridine (*t*Bubipy).. Reactions were monitored by removal of 16-18 aliquots at regular intervals over the reaction's full course and analyzed by HPLC. In early experiments, independent analysis of five aliquots by $^1\text{H-NMR}$ was used to cross-validate our HPLC method.

Figure 5.3. Kinetic profiles of a) aziridination and b) C-H amination under standard conditions.

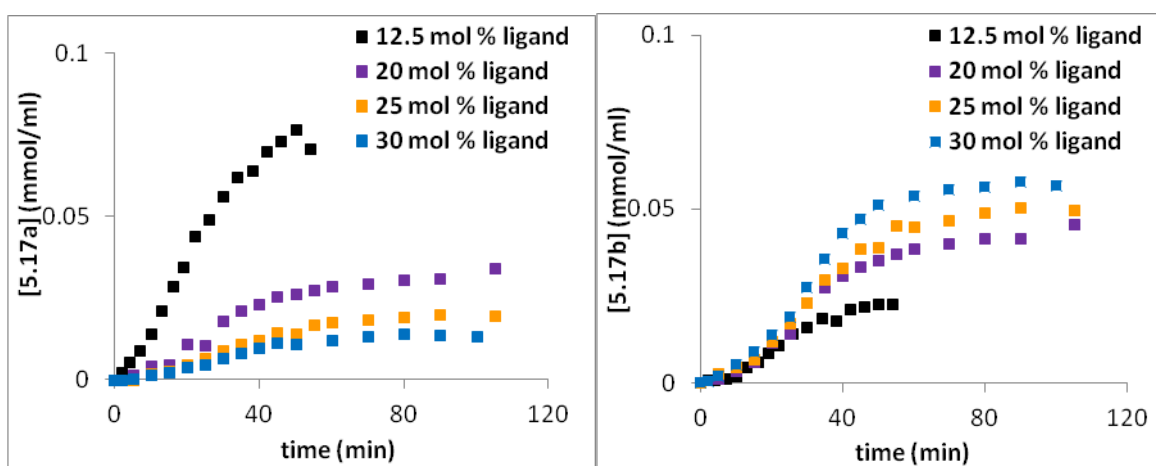


Rate of starting material **5.16** consumption between 20% and 80% conversion: a) $2.4 \times 10^{-3}\text{M/min}$, b) $2.5 \times 10^{-3}\text{M/min}$ between 20% and 80% conversion.

Reaction profiles were first obtained using 10 mol % AgOTf under standard aziridination (12.5 mol % ligand) and C-H amination conditions (30 mol % ligand), as illustrated in Figure 5.3. The C-H amination process displays an induction period of approximately 25 minutes before steady state is reached. Despite this difference in initial activity, both reactions showed

approximate linearity in substrate consumption and product formation between 20 and 80% conversion. Finally, the chemoselectivity given by **5.17a:5.17b** throughout the C-H amination reaction was consistently ~1:4, while erosion of selectivity was observed in the aziridination process, with **5.17a:5.17b** dropping from ~6:1 initially to ~3:1 after 30 min.

Figure 5.4. a) Aziridination at varied ligand loadings. b) C-H amination at varied ligand loadings.

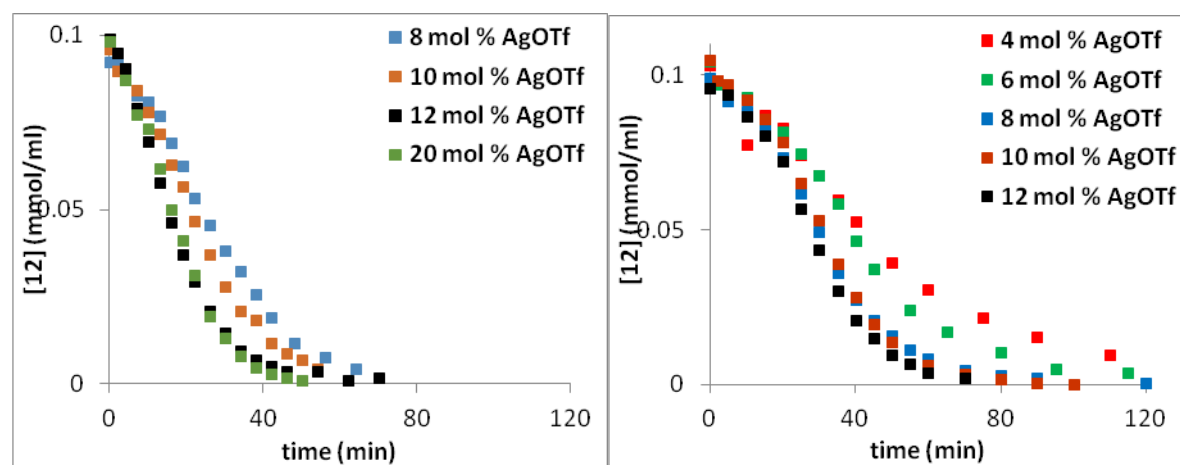


a) Rates of aziridine **5.17a** formation between 20-80% conversion: 12.5 mol %, 2.0×10^{-3} M/min; 20 mol %, 4.7×10^{-4} M/min; 25 mol %, 3.2×10^{-4} M/min; 30 mol %, 2.5×10^{-4} M/min. b) Rate of C-H amination **5.17b** formation between 20-80% conversion: 12.5 mol %, 5.2×10^{-4} M/min; 20 mol %, 7.1×10^{-4} M/min; 25 mol %, 7.2×10^{-4} M/min; 30 mol %: 7.5×10^{-4} M/min.

Further profiles were obtained at intermediate ligand loadings of 20 and 25 mol % (Figure 5.4). Comparison of product formation under the full range of loadings is instructive. While, the overall ratio of **5.17a:5.17b** decreased with ligand loading from 3.0:1 at 12.5 mol% to 1:4.3 at 30 mol %, this switch in chemoselectivity manifests due to different responses to product formation rates as a function of ligand concentration. The initial rate of aziridination is inversely correlated to ligand loading, dropping from 0.002 M/min to 0.0002 M/min. In contrast, the initial rate of C-H amination only increases slightly with increased ligand loading, from 0.0052 M/min at 12.5 mol % ligand to 0.0072 M/min at 30 mol %. This combined behavior suggests that the

amination process displays a pseudo-zero-order dependence on catalyst concentration during the induction period, as the concentration of C-H amination catalyst is expected to increase with the ligand-to-metal ratio.

Figure 5.5. Starting material consumption at varied AgOTf loadings at a) 1:1.25 Ag:ligand and b) 1:3 Ag:ligand.



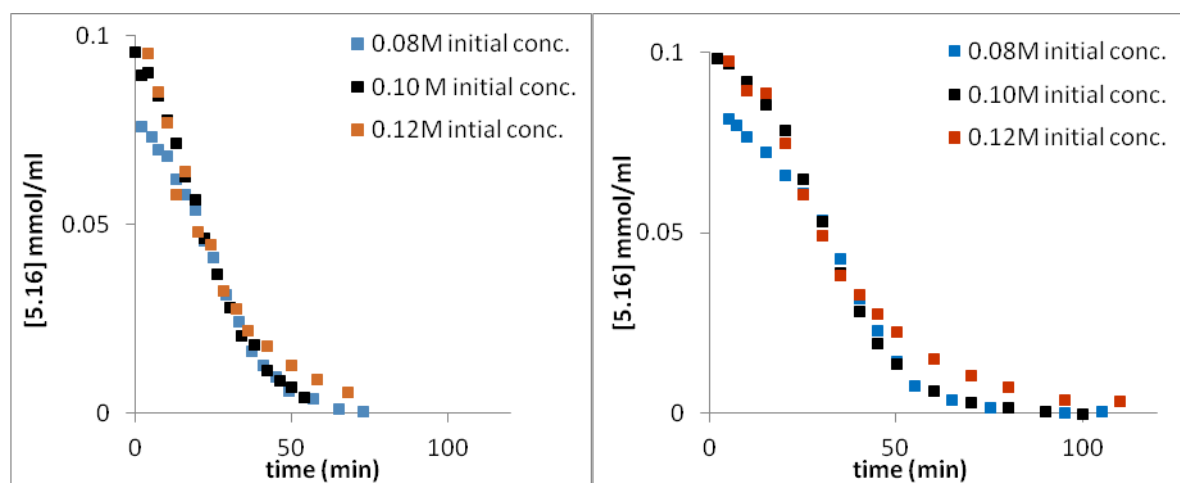
a) Rate of consumption of **5.16**: 8 mol % AgOTf, 1.99×10^{-3} M/min; 10 mol % AgOTf, 2.5×10^{-3} M/min; 12 mol % AgOTf, 3.2×10^{-3} M/min; 20 mol % AgOTf, 3.1×10^{-3} M/min. b) Rate of consumption of **5.16**: 4 mol %, 1.4×10^{-3} M/min; 6 mol %, 1.7×10^{-3} M/min; 8 mol %, 2.4×10^{-3} M/min; 10 mol %, 2.4×10^{-3} M/min; 12 mol %, 2.6×10^{-3} M/min.

Comparison of the reaction rates at constant Ag:ligand ratios and varied Ag loading indicates a small increase in reaction rate with increased catalyst loading, giving way to saturation for both catalyst systems (Figure 5.5). When using 1:3 Ag:ligand, the reaction rate increased from 1.4 to 2.4 mM/min as the loading of AgOTf increased from 4-8 mol %. No change in reaction rate was observed for further increases between 8-12 mol %. When a system with 1:1.25 Ag:ligand was employed, the rate increases from 2.0 – 3.2 mM/min when using between 8-12% AgOTf and shows no further increase when increased to 20 mol%. Interestingly, product ratios for the respective 1:1.25 and 1.3 Ag:ligand systems remains nearly constant across

catalyst loadings. This behavior is distinct from other catalytic systems, such as intramolecular C-H amination with $\text{Rh}_2(\text{O}_2\text{C}^t\text{Bu})_4$, which show no rate dependence on catalyst loading.

Kinetic profiles of the aziridination reaction were obtained at three initial concentrations of **5.16** (0.08 M-0.12 M), indicating a small positive order dependence on starting material, again leading to apparent saturation (Figure 5.6a). Time-adjusted plots obtained at initial concentrations of 0.08M and 0.10M **5.16** show good overlay after a brief induction period, indicating that catalyst death does not play a significant role in determining reaction rate under these conditions. However, the plot obtained at 0.12M initial concentration shows a reduced rate in the final 20% conversion, which may be attributed to either catalyst decomposition or to slight product inhibition (*vide infra*). Interestingly, variation in initial substrate concentration leads to variation in the final product ratio (**5.17a:5.17b**) from 5.3:1 at 0.08 M initial concentration to 2.5:1 at 0.12 M initial concentration.

Figure 5.6. Normalized starting material consumption at varied initial concentrations under a) aziridination conditions b) C-H amination conditions.



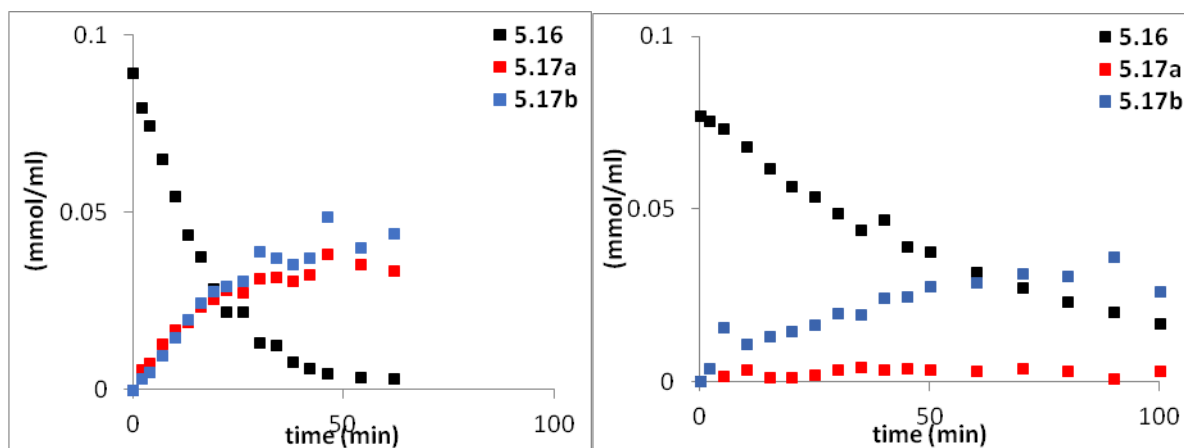
a) Times-adjusted consumption of **5.16** between 20-80% conversion: 0.08 M, 1.9×10^{-3} M; 0.10 M, 2.4×10^{-3} M; 0.12 M, 2.5×10^{-3} M. b) Consumption of **5.16** between 20-80% conversion: 0.08 M, 2.0×10^{-3} M; 0.10 M, 2.5×10^{-3} M; 0.12 M, 2.5×10^{-3} M.

Reactions under 1:3 Ag:ligand conditions (Figure 5.6b) showed a similar positive order dependence on initial substrate concentration, again leading to saturation at initial concentrations higher than 0.10 M. Good overlay was again observed at 0.10 M and 0.08 M initial substrate concentration, and again, after an initial substrate concentration of 0.12M, the final 25% conversion showed a reduced rate. A constant chemoselectivity of about 4:1 **5.17b**:**5.17a** was observed across all conditions.

Several experiments were conducted to assess effect of oxidant on the reaction. Varying the initial oxidant loading between 2.0 and 3.5 equivalents had no effect on the reaction profile for either catalyst system, though increasing the loading to 4.2 equivalents decreased the chemoselectivity of the aziridination system from 3.0:1 (70% **5.17a**:23% **5.17b**) to 2.0:1 (54% **5.17a**:27% **5.17b**). This change did not affect the C-H amination reaction. Evidence of oxidative degradation of the catalyst was obtained for both reactions. When the catalyst was stirred for two hours prior to the addition of substrate, both systems showed reduced rates, and the aziridination

system showed significantly reduced chemoselectivity (Figure 5.7a, 1:1 aziridination:C-H amination) in this reaction, while the C-H amination system showed almost no aziridine formation (Figure 5.7b).

Figure 5.7. Effect of the oxidant on the chemoselectivity. a) Aziridination with (^tBubipy)AgOTf. b) C-H amination with (^tBubipy)₂AgOTf.



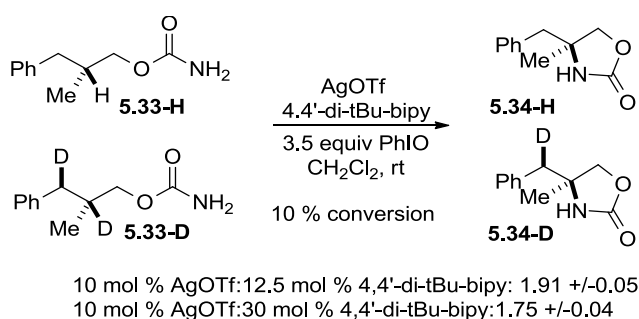
a) rate of **5.16** consumption between 20-80% conversion: 3.0×10^{-3} M/min. b) rate of **5.16** consumption between 20-80% conversion: 1.0×10^{-3} M/min.

NMR spectra of crude reaction mixtures indicated that the ligands are not oxidized in the course of the reaction, indicating that the silver nuclei themselves may be oxidized. This process would lead to a lower concentration of active catalyst, and a higher effective ligand to metal ratio, accounting for both the reduction in rate and the changes in chemoselectivity. Additionally, this process would account for the increased selectivity for the aziridine in reactions with lower initial concentrations of substrate. In these cases, less starting material translates to shorter reaction times, such that catalyst degradation is minimized.

Two sets of kinetic isotope effect measurements were used to assess the turnover-limiting step of the mechanism. In the first experiment, an intermolecular competition between labelled and unlabelled carbamates **5.33-H/D** was carried out under standard reaction conditions. The

reaction was analyzed at 10% overall conversion to assess the relative amounts of labelled and unlabelled substrate consumption. A KIE of 1.91 +/- 0.05 was observed when a 1:1.25 Ag:ligand ratio was used, while a KIE of 1.75 +/- 0.04 was observed with a 1::3 Ag:ligand ratio (Scheme 5.11). While this result implied that C-H bond cleavage might be the rate-limiting step of the reaction, such an effect could also be observed if the reaction's rate-limiting step did not involve substrate.

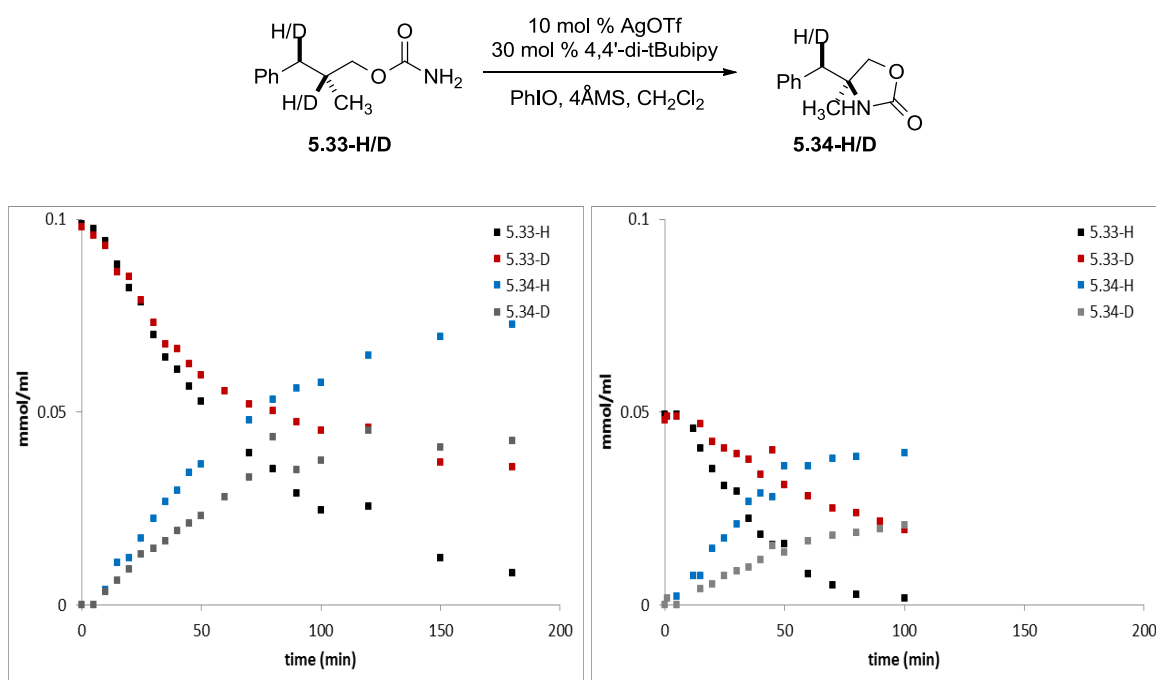
Scheme 5.11. Intermolecular competition to determine KIE.



Independent measurements of the rates of C-H amination with both **24-H** and **24-D** (Figure 5.8). A KIE based on initial starting material consumption of 1.20 was observed when the initial concentration of substrate was 0.1M, though the rate of consumption of **24-H** was faster than that of **24-D** beyond about 30% conversion. This result might indicate a true kinetic isotope effect observable at lower substrate concentrations, or it might be a result of enhanced catalyst degradation in transformation of the labelled substrate. To assess these possibilities, the measurements were carried out at an initial concentration of substrate of 0.05M. In this case, a KIE of 2.39 was observed. This result indicates that the C-H amination step is turnover-limiting, and has an increased effect on reaction rate at lower starting material concentrations. However, in the allene amination system, the similar rates observed for aziridination and C-H amination

indicate that the selectivity determining steps of the reaction do not contribute significantly to the overall rate, and hence are not turnover-limiting.

Figure 5.8. Independent rate measurement of labelled and unlabelled substrates.

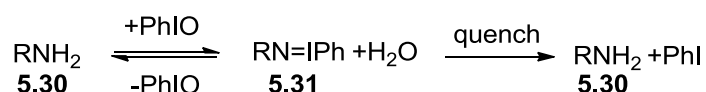


Two features of our kinetic analysis do not admit simple explanations: the sigmoidal shape of both starting material consumption and C-H amination production curves, and the saturation behavior of multiple reaction components: starting material, catalyst and oxidant. There are several common reasons why a reaction may display sigmoidal product curves: the active catalyst may form slowly,^{15a-b} an intermediate species involving substrate may attain an appreciable concentration prior to product formation,¹⁶ or a product or by-product may accelerate the reaction.^{5,21ea-c} Several experiments were conducted to investigate these possibilities. The sigmoidality of the aziridination reaction was not observed when PhIO was stirred with the catalyst for ten minutes prior to the addition of substrate, indicating that slow dissolution of the oxidant is responsible for the induction period in this reaction. However, this procedural change

did not affect the C-H amination reaction. Addition of 0.5 equivalents of either the C-H amination or methylene aziridine product to the catalyst systems did not obviate the induction period, and prompted a slight decrease in the rate of the C-H amination reaction (see experimental section). Addition of five equivalents of the byproduct PhI to either catalyst system gave an identical kinetic profile. These experiments ruled out autocatalysis or autoinduction as an explanation of the sigmoidality.

Initially, the parallel sigmoidalities of the starting material consumption and product formation curves seemed to rule out the possibility that intermediate buildup is responsible for the induction period. However, such an intermediate might be converted to starting material when prepared for the HPLC and NMR methods used in this study (Scheme 5.12).

Scheme 5.12. Possible decomposition of iminoiodinane intermediate.



To test this possibility, a solution of starting material was stirred with 4Å molecular sieves and iodosylbenzene for 30 minutes prior to the addition of a solution of the catalyst. Under these conditions, no induction period was observed for either starting material consumption or product formation. This suggests that pre-stirring the substrate and oxidant allows the presumed iminoiodinane intermediate to attain steady-state concentration prior to the introduction of catalyst (Figure 5.9). When these measurement were conducted, the maximum rate of starting material consumption was 1.8 mM/min under standard conditions, and 2.0 mM/min under the pre-stir conditions. When standard procedures are followed, the induction period then represents a pre-steady-state regime for iminoiodinane concentration. The consumption of iminoiodinane can be represented as follows.

Scheme 5.13. Iminoiodinane consumption.

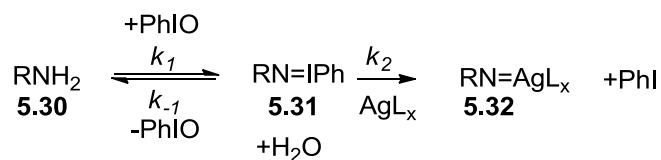
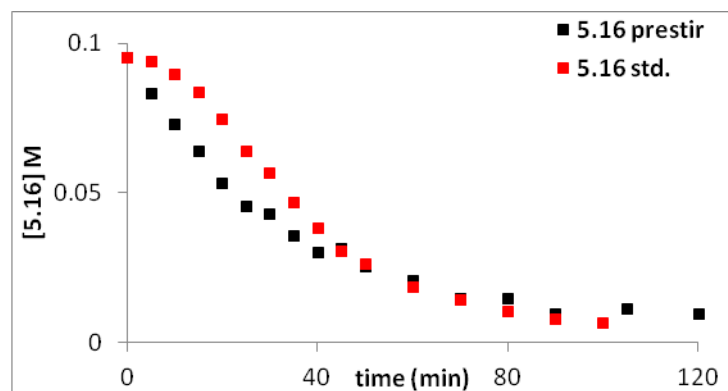


Figure 5.9 Pre-stir of oxidant and substrate obviates induction period.



This result has an important implication for metal-nitrene formation. Solving a steady-state expression for iminoiodinane concentration based on Scheme 5.10 gives the following expression:

$$[5.31] = \frac{k_1[\text{PhIO}][\text{RNH}_2]}{k_2[\text{cat.}] + k_{-1}}$$

Since attaining steady-state requires more time for the C-H amination catalyst, we may infer that the concentration of the iminoiodinane is higher in these reactions than in the aziridinations. Since all other terms are expected to be equivalent for the two systems, this implies that k_2 must be smaller for C-H amination than for aziridination, meaning that metal-nitrene formation is slower in this system.

With this understanding of the reaction's induction period, we must next consider the observed saturation dependence on multiple reaction components. The saturation behavior of the

catalyst may be explained by its irreversible reaction with the iminoiodinane to generate a metal-nitrene intermediate. In a simplified kinetic scenario, the rate of metal-nitrene formation may be treated as equal to that of product formation, and the overall rate of product formation is given by:

$$\frac{d[\text{pdt}]}{dt} = \frac{k_1 k_2 [\text{cat.}] [\text{PhIO}] [\text{RNH}_2]}{k_2 [\text{cat.}] + k_{-1}}$$

This scenario might be regarded as a more general version of that which Du Bois presents in his study of Rh-catalyzed C-H amination.⁸ In that study, zero order dependence on catalyst was observed through about 30% conversion, implying that $k_2[\text{cat.}] \gg k_{-1}$. First order dependence on both oxidant and substrate concentration was also observed. This provides precedent for saturation dependence on catalyst.

Saturation in substrate is a hallmark of Michaelis-Menten kinetics, in which a substrate-catalyst complex is formed reversibly, and this complex is the system's resting state. Such a scenario is clearly not consistent with that described above. One explanation for the saturation behavior of the substrate is that it binds to the catalyst as an inhibitor, but no evidence of binding between substrate and catalyst was observed by NMR. We instead suggest that the observed saturation dependence on substrate is instead a consequence of mass transfer limitations on reaction rate.¹⁸ Iodosylbenzene, a uniquely suitable oxidant for this chemistry, is highly reactive but poorly soluble in virtually all organic solvents, such that the rate of substrate oxidation may equal the rate of oxidant dissolution at high substrate concentrations. In support of this interpretation, we noted that "no stir" reactions failed to provide either any product over three hours for the two catalyst systems, and that loadings of iodosylbenzene below one equivalent gave irreproducible kinetic profiles. It is therefore posited that the observed kinetic data reflects a

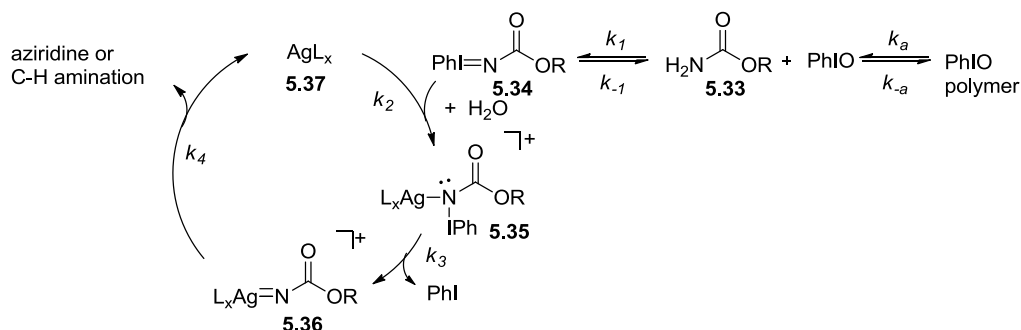
true saturation dependence on catalyst, but a first order dependence on substrate that is limited by the rate of mass transfer.

This kinetic analysis has significant implications for understanding the chemoselectivity of the aziridination and C-H amination reactions. The two reactions show similar dependences on substrate and catalyst concentration, and similar overall maximum rates maximum rates of starting material consumption of $2.5 \times 10^{-3}\text{M}/\text{min}$ for C-H amination and $3.1 \times 10^{-3}\text{M}/\text{min}$ for aziridination, at which point increasing either the starting material or catalyst concentration does not affect the rate. It is therefore unlikely that the reactions differ in early, kinetically significant mechanistic steps. Regardless of catalyst, the early steps of the reaction involve iminoiodinane formation, followed by metal-nitrene formation, and which point the reaction pathways diverge. Full kinetic profiling was essential to arriving at this conclusion, as studying only the initial rates of reaction would have lead to a dramatic misinterpretation of the kinetic data and erroneous mechanistic conclusions.

We therefore offer a fairly conventional mechanistic proposal for each reaction (Scheme 5.12) Iodosylbenzene oxidizes the carbamate substrate in solution to form an iminoiodinane species. Reversal of this process, by reaction with adventitious water or another reductive process, is competes with reaction with silver. The iminoiodinane then coordinates to the silver catalyst, and extrudes iodobenzene to form the active metal-nitrene species. This intermediate then performs concerted aziridination or C-H insertion, depending on catalyst choice, or may undergo non-productive reactions. Kinetic isotope effect studies suggest that this final step is turnover-limiting for C-H amination reactions. An absolute limit on reaction rate is presented by the low solubility of iodosylbenzene, which was a uniquely suitable oxidant for this system.

Enhancement of catalyst performance is hence likely to require the development of powerful, soluble oxidants.

Scheme 5.14. Mechanisms of Ag-catalyzed C-H amination and aziridination.



While this system did not prove amenable to numerical modeling, a rate law was derived in an effort to make sense of the available kinetic data. In this rate law, the mass transfer limitations are modelled by treating iodobenzene as maintaining a steady-state concentration throughout the reaction. Full derivation of the rate law is included at the end of the chapter. This law is not easy to verify quantitatively, but shows how limitations in oxidant concentration might lead to saturation in substrate. Moreover, it contains the isotopically sensitive constant k_4 , provides a greater contribution to the overall rate at lower substrate concentrations.

$$\frac{d[pdt]}{dt} = \frac{k_a k_1 k_2 k_3 k_4 [AgOTf]_o [RNH_2]}{k_3 k_4 (k_2 [AgOTf]_o + k_{-1}) (k_{-a} + k_1 [RNH_2]) + k_a k_1 k_2 (k_3 + k_4) [RNH_2]}$$

It is worth noting that in the case that $k_1 [RNH_2] \gg k_{-a}$, and $k_2 [AgOTf]_o \gg k_{-1}$ the rate law becomes:

$$\frac{d[pdt]}{dt} = \frac{k_a k_3 k_4 [AgOTf]_o}{k_3 k_4 [AgOTf]_o + k_a (k_3 + k_4)}$$

In the case that $k_3k_4[\text{AgOTf}_o] \gg k_a(k_3+k_4)$, then the overall rate of reaction is equal to k_a , illustrating that the maximum overall rate of reaction is governed by the rate of dissolution of iodosylbenzene.

5.5. Conclusions.

Given the dramatic differences in chemoselectivity for the two silver catalyst systems, it is surprising that the systems display similar behavior in virtually all the mechanistic experiments conducted. Both catalysts appear to promote concerted pathways, implying that they form metal-nitrenes with similar electronic structures. Moreover, they promote reactions with similar kinetic behavior, implicating similar mechanistic pathways through much of the reaction. However, a key difference between the reactivity of the two catalysts was noted in the aziridination of hindered homoallylic carbamates, suggesting that the origin of the differences in chemoselectivity is almost exclusively steric. The breadth of different ligands of diverse coordination geometries and steric constraints presents us with a unique opportunity to tune the selectivity of nitrene transfer solely through catalyst control, rather than the substrate control typically exhibited by other transition metal catalysts.

The examination of both catalytic pathways using kinetic profiling provided important insight into the reaction behavior that would have been missed with traditional initial rate studies. Simple examination of initial rates might have led us to conclude that the chemoselectivity originated in different mechanisms for the two catalysts. Additionally, we were able to determine that the solubility of iodosylbenzene presents an absolute limit on reaction rate and turnover frequency and underscores the need for the development of new oxidants or oxidant-free nitrene transfers capable of tunable chemoselectivity. It is our hope that these

studies will contribute to the understanding of metal-catalyzed nitrene transfer reactions in general, and will lead to improved design and application of dynamic catalyst systems.

5.6. Notes and References.

1. a) Hung-Low, F.; Renz, A.; Klausmeyer, K.K. *Polyhedron* **2009**, *28*, 407. b) Hung-Low, F.; Renz, A.; Klausmeyer, K.K. *J. Chem. Cryst.* **2011**, *41*, 1174. c) Du, J.; Hu, T.; Zhang, S.; Zeng, Y.; Bu, X. *CrystEngComm.* **2008**, *10*, 1866. d) Zhang, H.; Chen, L.; Song, H.; Zi, G. *Inorg. Chim. Acta* **2011**, *366*, 320. e) Hung-Low, F.; Renz, A.; Klausmeyer, K.K. *J. Chem. Cryst.* **2009**, *39*, 438. f) Levason, W.; Spicer, M.D. *Coord. Chem. Rev.* **1987**, *76*, 45. g) Leschke, M.; Rheinwald, G.; Lang, H. *Z. Anorg. Allg. Chem.* **2002**, *628*, 2470. h) Zhu, H.-L.; Chen, Q.; Peng, W.-l.; Qi, S.-J.; Xu, S.-J.; Xu, A.-L.; Chen, X.-M. *Chin. J. Chem.* **2001**, *19*, 263. i) Bowmaker, G. A.; Effendy; Marfua, S.; Skelton, B. W.; White, A. H. *Inorg. Chim. Acta* **2005**, *358*, 4371. j) Paramonov, S. E.; Kozmina, N. P.; Troganov, S. I. *Polyhedron* **2003**, *22* 837. k) Han, Z.; Wang, Y.; Wu, J.; Zhai, X. *Solid State Sci.* **2011**, *13*, 1560. l) Yuan, L.; Qin, C.; Wang, X.; Li, Y.; Wang, E. *Dalton Trans.* **2009**, 4169. m) Pang, H.-J.; Chen, J.; Peng, J.; Sha, J.-Q.; Shi, Z.-Y.; Tian, A.-X.; Zhang, P.-P. *Solid State Sci.* **2009**, *11*, 824.
2. Cui, Y.; He, C. *Angew. Chem. Int. Ed.* **2004**, *43*, 4210.
3. Price, W.S. *Concepts Magn. Reson.* **1997**, *9*, 299.
4. Newcomb, M.; Johnson, C. C.; Manek, M. B.; Varick, T. R. *J. Am. Chem. Soc.* **1992**, *114*, 10915.
5. Hansch, C.; Leo, A.; Taft, R. W. *Chem. Rev.*, **1991**, *91*, 165.
6. Jiang, X.-K.; Ji, G.-Z. *J. Org. Chem.* **1992**, *57*, 6051.
7. When only the σ^+ term was considered, as in Du Bois's study, a ρ value of -.41 was calculated.
8. Fiori, K.W.; Espino, C.G.; Brodsky, B.H.; Du Bois, J. *Tetrahedron* **2009**, *65*, 3042.
9. Deng, Q.-H.; Wang, J.-C.; Xu, J.-J.; Zhou, C.-Y.; Che, C.-M. *Synthesis* **2011**, *18*, 2959.
10. Liang, J.-L.; Yuan, S.-X.; Huang, J.-S.; Che, C.-M. *J. Org. Chem.* **2004**, *69*, 3610.
11. a) Harvey, M.E.; Musaev, D.G.; Du Bois, J. *J. Am. Chem. Soc.* **2011**, *133*, 17207. b) Paradine, S.M.; White, M.C. *J. Am. Chem. Soc.* **2012**, *134*, 2036.
12. Maestre, L.; Sameera, W.M.; Dia-Requejo, M.M.; Maseras, F.; Perez, P.J. *J. Am. Chem. Soc.* **2013**, *135*, 1338 b) Zhang, X.; Xu, H.; Zhao, C. *J. Org. Chem.* **2014**, *79*, 9799.
13. a) Aguila, M. J. B.; Badiei, Y. M.; Warren, T. H. *J. Am. Chem. Soc.* **2013**, *135*, 9399. b) Li, Z.; Quan, R. W.; Jacobsen, E. N. *J. Am. Chem. Soc.* **1995**, *117*, 5889. c) Han, H.; Park, S. B.; Kim, S. K.; Chang, S. *J. Org. Chem.* **2008**, 2862.
14. a) Blackmond, D. G. *Angew. Chem. Int. Ed.* **2005**, *44*, 4302. b) Hein, J. E.; Armstrong, A.; Blackmond, D. G. *Org Lett* **2011**, *13*, 4300–4303.
15. a) Shekhar, S.; Ryberg, P.; Hartwig, J.; Mathew, J. S.; Blackmond, D. G.; Strieter, E. R.; Buchwald, S. L. *J. Am. Chem. Soc.* **2006**, *126*, 3584. b) Rosner, T.; Pfaltz, A.; Blackmond, D. G. *J. Am. Chem. Soc.* **2001**, *123*, 4621.

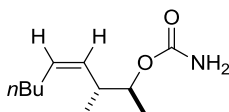
16. Benson, S. W. *J. Chem. Phys.* **1952**, *20*, 1605.
17. a) Mathew, S. P.; Klussman, M.; Iwamura, H.; Wells, D. H., Jr.; Armstrong, A.; Blackmond, D. G.; *Chem. Commun.* **2006**, 4291. b) Phua, P. H.; Mathew, S. P.; Wite, A. J. P.; de Vries, J. G.; Blackmond, D. G.; Hii, K. K. *Chem. Eur. J.* **2007**, *13*, 4602. c) Mower, M. P.; Blackmond, D. G. *J. Am. Chem. Soc.* **2015**, *137*, 2386.
18. a) For a discussion of mass-transfer-limitation effect in catalysis, see: Roberts, G. W. in *Catalysis in Organic Syntheses*: Rylander, P. N.; Greenfield, H., Eds.; Academic Press: New York, **1976**; pp 1-48. b) For a recent example of mass-transfer-limiting effects in homogeneous catalysis, see: Steinhoff, B. A.; Stahl, S. S. *J. Am. Chem. Soc.* **2006**, *128*, 4348.
19. Newcomb, M.; Daublain, P.; Horner, J. H. *J. Org. Chem.* **2002**, *67*, 8669.

5.7 Experimental Details and Characterization.

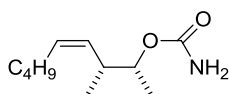
5.7.1. Synthesis of probe substrates.

General procedure for the synthesis of carbamates. The corresponding alcohol (between 0.5 g and 3.0 g, 1 equiv) was dissolved in dichloromethane (0.3 M) and placed in an ice bath at 0°C. Freshly distilled trichloroacetylisocyanate (1.2 equiv) was added dropwise over 30s – 1 min. The ice bath was removed and the reaction stirred until TLC indicated complete consumption of the starting material, 0.75-2 hours. The solvent was then removed and the crude reaction was dissolved in methanol (0.2 M). Potassium carbonate (0.2 equiv) was then added to the reaction and the mixture stirred at room temperature until TLC indicated complete consumption of the intermediate, 4-8 hours. Saturated aqueous NH₄Cl was added to the reaction and the mixture was extracted with three portions of dichloromethane. The combined organic phases were washed with sat. brine, dried with sodium sulfate, filtered with cotton and concentrated under reduced pressure. The crude products were purified by silica gel column chromatography. Depending on the purity of the trichloroacetylisocyanate used, traces of trichloroacetamide were often detected in the carbamate product by ¹³C-NMR, even after chromatographic purification. This impurity was found to significantly alter the rate and chemoselectivity of the reaction. To remove the

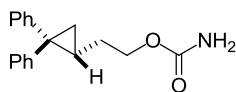
trichloroacetamide, the carbamate was dissolved in CH_2Cl_2 to form a 0.1 M solution. An equal volume of 1.0 M $\text{NaOH}_{(\text{aq})}$ was added, and the reaction was stirred vigorously for five minutes. The layers were separated and the aqueous layer extracted three times with an equal volume of CH_2Cl_2 . The organic layers were combined, dried with sodium sulfate, filtered with cotton and concentrated under reduced pressure.



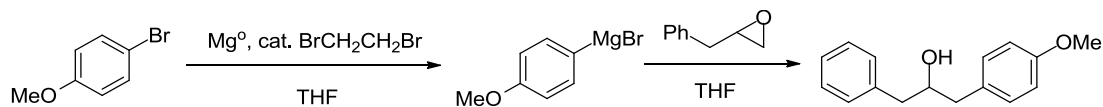
Compound 5.14a. The product was purified by column chromatography using a 0 \rightarrow 30% gradient of EtOAc in hexanes with 6% increments. The product was obtained in 91% yield as a white solid. ^1H NMR (500 MHz, CDCl_3) δ 5.43 (dt, $J = 10.0, 7.0$ Hz, 1H), 5.21 (t, $J = 10.0$ Hz, 1H), 4.72 (app p, $J = 5.2$ Hz, 1H), 4.56 (br s, 2H), 2.69-2.61 (m, 1H), 2.11-1.98 (m, 2H), 1.38-1.28 (m, 4H), 1.18 (d, $J = 6.4$ Hz, 3H), 0.97 (d, $J = 6.8$ Hz, 3H), 0.90 (t, $J = 6.8$ Hz, 3H); ^{13}C NMR (125.7 MHz, CDCl_3) δ 156.8, 131.1, 130.8, 74.8, 36.6, 32.0, 27.2, 22.4, 17.5, 16.9, 14.0.



Compound 5.14b. The product was purified by column chromatography using a 0 \rightarrow 30% gradient of EtOAc in hexanes with 6% increments. The product was obtained in 86% yield as a white solid. Traces (<10%) of the trans alkene were present. ^1H NMR: (500.0 MHz, CDCl_3) δ 5.41 (dt, $J = 11.2, 7.2$ Hz, 1H), 5.18 (t, $J = 11.2$ Hz, 1H), 4.87 (br s, 2H), 4.61 (p, $J = 6.7$ Hz, 1H), 2.65 (dp, $J = 9.8, 6.7$ Hz, 1H), 1.97-2.11 (m, 2H), 1.24-1.39 (m, 4H), 1.18 (d, $J = 6.7$ Hz, 3H), 0.97 (d, $J = 6.7$ Hz, 3H), 0.90 (t, $J = 7.0$ Hz, 3H); ^{13}C NMR: (125.7 MHz, CDCl_3) δ 158.43, 134.57, 128.18, 83.06, 61.53, 32.02, 28.48, 28.06, 22.37, 16.52, 13.96. HRMS (EI) m/z calculated for $\text{C}_{11}\text{H}_{21}\text{NO}_2$ [$\text{M}+\text{NH}_4^+$] 217.191, found 217.1909.

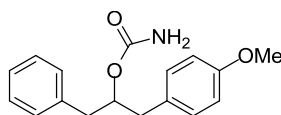


Compound 5.18. Synthesized according to the general procedure above. The product was obtained in 81% yield from 287 mg (1.20 mmol) of the corresponding alcohol.¹⁹ ¹H NMR (500 MHz, Chloroform-*d*) δ 7.38 – 7.25 (m, 4H), 7.25 – 7.15 (m, 5H), 7.15 – 7.07 (tt, $J = 7.0, 1.6$ Hz, 1H), 4.69 (s, 2H), 4.15 (dt, $J = 10.6, 6.6$ Hz, 1H), 4.10 (dt, $J = 10.6, 6.6$ Hz, 1H), 1.80 (dtd, $J = 13.9, 6.8, 5.3$ Hz, 1H), 1.73 – 1.64 (m, 1H), 1.33 – 1.18 (overlapping multiplets, 2H), 1.12 – 0.95 (ddt, $J = 14.1, 8.7, 6.5$ Hz, 1H). ¹³C NMR (126 MHz, CDCl₃) δ 157.24, 147.11, 141.58, 130.65, 128.51, 128.41, 127.97, 126.64, 125.99, 65.11, 35.25, 30.59, 22.80, 20.36. HRMS (ESI) m/z calculated for C₁₈H₁₉NO₂ [M+H⁺] 282.1489, found 282.1484.

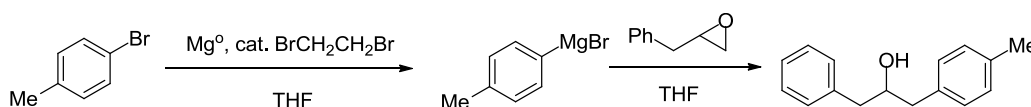


Compound S5.1. A 50 ml 3-necked flask was equipped with a stir bar and charged with Mg turnings (148 mg, 6.09 mmol, 4.2 equiv) and flame dried under vacuum. The flask was equipped with a stopper, rubber septum for additions, and a reflux condenser. The flask was then purged with N₂ and charged with THF (5.8 ml). The flask was cooled to 0°C with an ice bath, and charged with 1,2-dibromoethane (0.020 ml, 0.23 mmol, 0.16 equiv), then with *p*-bromoanisole (0.72 ml, 5.78 mmol, 4.0 equiv). The flask was then moved to a water bath at room temperature to absorb exotherms. Then solution turned a deep orange. After the exotherms ceased (approx. one hour), the solution was titrated to 0.62 M using phenanthroline and *n*PrOH. To a solution of allylbenzene oxide (194mg, 1.45 mmol, 1.0 equiv) in THF (4.8 ml), was added the Grignard reagent over 1 minute at 0°C. TLC indicated complete consumption of the epoxide after 50 min.

The reaction was quenched with sat. aq. NH_4Cl . The aqueous layer was extracted three times with EtOAc, and the combined organic extracts were washed with brine, dried over sodium sulfate, filtered and concentrated *in vacuo*. The product was purified by column chromatography using a 0 to 14% gradient of EtOAc in hexanes with 2% increments, and obtained as a colorless oil in 42% yield. ^1H NMR (500 MHz, Chloroform-*d*) δ 7.31 (dd, $J = 8.6, 6.5$ Hz, 2H), 7.23 (overlapping multiplets, 3H), 7.14 (d, $J = 8.6$ Hz, 2H), 6.85 (d, $J = 8.6$ Hz, 2H), 4.01 (tt, $J = 8.4, 4.6$ Hz, 1H), 3.79 (s, 3H), 2.87-2.66 (overlapping multiplets, 4H). ^{13}C NMR (126 MHz, CDCl_3) δ 158.48, 138.72, 130.56, 129.60, 128.73, 126.66, 114.17, 73.89, 55.45, 43.48, 42.64. MS (EI) m/z calculated for $\text{C}_{16}\text{H}_{18}\text{O}_2$ $[\text{M}]^+$ 242.31, found 242.1302.

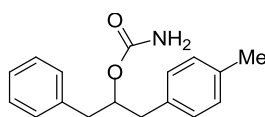


Compound 5.20a. Synthesized according to the general procedure above. The product was obtained in 84% yield from 127 mg (0.524 mmol) of the corresponding alcohol. ^1H NMR (500 MHz, Chloroform-*d*) δ 7.28 (dd, $J = 8.0, 6.6$ Hz, 2H), 7.23 – 7.18 (m, 3H), 7.11 (d, $J = 8.6$ Hz, 2H), 6.83 (d, $J = 8.6$ Hz, 2H), 5.15 (p, $J = 6.4$ Hz, 1H), 4.51 (br s, 2H), 3.79 (s, 3H), 2.85 (d, $J = 6.4, 2.9$ Hz, 2H), 2.80 (dd, $J = 6.4, 2.9$ Hz, 2H). ^{13}C NMR (126 MHz, CDCl_3) δ 158.42, 156.47, 137.78, 130.65, 129.68, 128.53, 126.63, 113.96, 76.27, 55.42, 40.00, 39.21. HRMS (ESI) m/z calculated for $\text{C}_{17}\text{H}_{19}\text{NO}_3$ $[\text{M}+\text{NH}_4^+]$ 303.1704, found 303.1707.



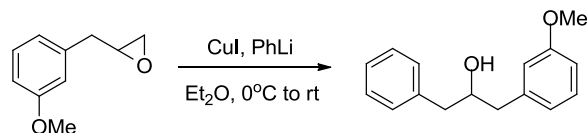
Compound S5.2. A 50 ml 3-necked flask was equipped with a stir bar and charged with Mg turnings (381 mg, 15.7 mmol, 4.2 equiv) and flame dried under vacuum. The flask was equipped with a stopper, rubber septum for additions, and a reflux condenser. The flask was then purged

with N₂ and charged with THF (15 ml). The flask was cooled to 0°C with an ice bath, and charged with 1,2-dibromoethane (0.051 ml, 0.597 mmol, 0.16 equiv), then with *p*-bromotoluene (1.83 ml, 14.9 mmol, 4.0 equiv). The flask was then moved to a water bath at room temperature to absorb exotherms. Then solution turned a deep orange. After the exotherms ceased (approx. one hour), the solution was titrated to 0.69 M. To a solution of allylbenzene oxide (500 mg, 3.73 mmol, 1.0 equiv) in THF (13 ml), was added the Grignard reagent over 1 minute at 0°C. TLC indicated complete consumption of the epoxide after 40 min. The reaction was quenched with sat. aq. NH₄Cl. The aqueous layer was extracted three times with EtOAc, and the combined organic extracts were washed with brine, dried over sodium sulfate, filtered and concentrated *in vacuo*. The product was purified by column chromatography using a 0 to 14% gradient of EtOAc in hexanes with 2% increments, and obtained as a colorless oil in 37% yield. ¹H NMR (500 MHz, Chloroform-*d*) δ 7.38 – 7.27 (m, 2H), 7.28 – 7.16 (m, 3H), 7.12 (apparent singlet, 4H), 4.04 (tt, *J* = 8.5, 4.7 Hz, 1H), 2.91-2.68 (overlapping multiplets, 4H), 2.33 (s, 3H). ¹³C NMR (126 MHz, CDCl₃) δ 138.72, 136.23, 135.45, 129.62, 129.49, 129.47, 128.74, 126.67, 73.84, 43.54, 43.13, 21.24. MS (EI) *m/z* calculated for C₁₆H₁₈O [M]⁺ 226.31, found 225.1353..

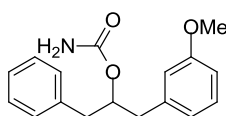


Compound 5.20b. Synthesized according to the general procedure above. The product was obtained in 94% yield from 159 mg (0.702 mmol) of the corresponding alcohol. ¹H NMR (500 MHz, Chloroform-*d*) δ 7.28 (dd, *J* = 8.0, 6.6 Hz, 2H), 7.24 – 7.17 (m, 3H), 7.08 (apparent s, 4H) 5.18 (p, *J* = 6.4 Hz, 1H), 4.49 (s, 2H), 2.88-2.79 (overlapping second order multiplets, 4H), 2.32 (s, 3H). ¹³C NMR (126 MHz, CDCl₃) δ 156.46, 137.79, 136.15, 134.54, 129.70, 129.57, 129.26,

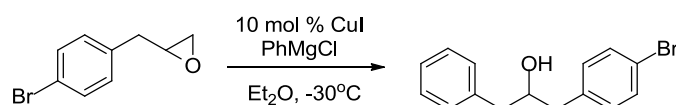
128.53, 126.63, 76.19, 40.03, 39.67, 21.27. HRMS (ESI) m/z calculated for $C_{17}H_{19}NO_2$ $[M+NH_4^+]$ 287.1755, found 287.1749.



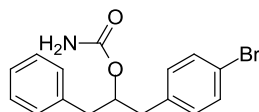
Compound S5.3. A 25 ml round bottom flask was charged with freshly purified CuI (200 mg, 1.05 mmol, 1.3 equiv), and Et_2O (0.54 ml) under nitrogen. The flask was cooled to $0^\circ C$ with an ice bath, and $PhLi$ (1.14 M in Bu_2O , 1.85 ml, 2.11 mmol, 2.6 equiv), was added over 30 seconds. A green slurry developed. After 20 minutes, a solution of the epoxide (133 mg, 0.810 mmol, 1.0 equiv) in 0.81ml Et_2O was added and the flask was moved to room temperature. The reaction was monitored by TLC and showed completion after 80 minutes. The reaction was quenched with sat. aq. NH_4Cl and filtered through Celite. The Celite was washed three times with $EtOAc$, and the combined organic extracts were dried over sodium sulfate, filtered and concentrated *in vacuo*. The product was purified by column chromatography using a 0 to 15% gradient of $EtOAc$ in hexanes with 3% increments, and obtained as a colorless oil in 65% yield. 1H NMR (500 MHz, Chloroform-*d*) δ 7.35 – 7.29 (m, 2H), 7.25 – 7.20 (m, 4H), 6.82 (dt, $J = 7.4, 1.2$, 1H), 6.80 – 6.77 (m 2H), 4.07 (ttd, $J = 8.1, 4.7, 2.9$ Hz, 1H), 3.80 (s, 3H), 2.87 (dd, $J = 13.6, 4.7$, 1H), 2.85 (dd, $J = 13.2, 4.7$, 1H) 2.77 (dd, $J = 13.6, 8.1$ Hz, 2H), 2.74 (dd, $J = 13.2, 8.1$ Hz, 1H). ^{13}C NMR (126 MHz, $CDCl_3$) δ 159.97, 140.23, 138.63, 129.64, 128.77, 126.73, 121.94, 115.31, 112.09, 73.72, 55.39, 43.65, 43.60. HRMS (ESI) m/z calculated for $C_{16}H_{18}O_2$ $[M+H^+]$ 260.1646, found 260.1645.



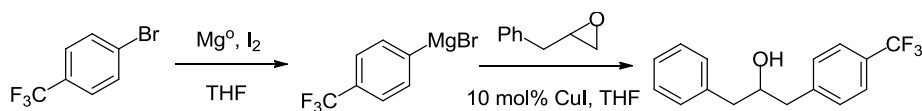
Compound 5.20c. Synthesized according to the general procedure above. The product was obtained in 92% yield from 190 mg (0.797 mmol) of the corresponding alcohol. ^1H NMR (500 MHz, Chloroform-*d*) δ 7.31 – 7.26 (m, 2H), 7.24 – 7.17 (m, 4H), 6.81 – 6.72 (m, 3H), 5.19 (p, J = 6.5 Hz, 1H), 4.57 (s, 2H), 3.78 (s, 3H), 2.91 – 2.79 (overlapping m, 4H). ^{13}C NMR (126 MHz, CDCl_3) δ 159.74, 156.49, 139.25, 137.68, 129.69, 129.50, 128.54, 126.66, 122.07, 115.40, 112.01, 55.36, 40.11. HRMS (ESI) m/z calculated for $\text{C}_{17}\text{H}_{19}\text{NO}_3$ $[\text{M}+\text{H}^+]$ 286.1438, found 286.1444.



Compound S5.4. A 25 ml round bottom flask was charged with freshly purified CuI (40.8 mg, 0.214 mmol, 0.10 equiv), and flushed with nitrogen. Et₂O (3.6 ml) was added, then PhMgCl solution (1.29 M in THF, 2.49 ml, 3.21 mmol, 1.5 equiv). The reaction was stirred for 20 minutes, then a solution of the epoxide (456 mg, 2.14 mmol, 1.0 equiv) in Et₂O (3.6 ml) was added via cannula over 2 minutes. The reaction was monitored by TLC and showed completion after 20 minutes. The reaction was quenched with sat. aq. NH_4Cl and filtered through Celite. The Celite was washed three times with EtOAc, and the combined organic extracts were dried over sodium sulfate, filtered and concentrated *in vacuo*. The product was purified by column chromatography twice using a 0 to 21% gradient of EtOAc in hexanes with 3% increments, and obtained as a colorless oil in 71% yield. ^1H NMR (500 MHz, Chloroform-*d*) δ 7.43 (d, J = 8.4 Hz, 2H), 7.32 (dd, J = 8.1, 6.9 Hz, 2H), 7.26 – 7.18 (m, 3H), 7.11 (d, J = 8.4 Hz, 2H), 4.03 (tt, J = 8.0, 4.5 Hz, 1H), 2.85 (dd, J = 13.4, 4.5, 1H), 2.82 (dd, J = 13.6, 4.5 Hz, 1H), 2.73 (dd, J = 13.4, 8.0, 1H), 2.71 (dd, J = 13.6, 8.0 Hz, 1H). ^{13}C NMR (126 MHz, CDCl_3) δ 138.32, 137.71, 131.76, 131.37, 129.60, 128.85, 126.85, 120.57, 73.55, 43.67, 42.86. MS (EI) m/z calculated for $\text{C}_{15}\text{H}_{15}\text{BrO}$ $[\text{M}]^+$ 291.18, found 290.00.

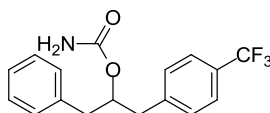


Compound 5.20d. Synthesized according to the general procedure above. The product was obtained in 87% yield from 434 mg (1.49 mmol) of the corresponding alcohol. ^1H NMR (500 MHz, Chloroform-*d*) δ 7.39 (d, $J = 8.3$ Hz, 2H), 7.28 (dd, $J = 8.1, 6.6$ Hz, 2H), 7.25 – 7.21 (m, 1H), 7.20 – 7.15 (m, 2H), 7.05 (d, $J = 8.3$ Hz, 2H), 5.14 (p, $J = 6.4$ Hz, 1H), 4.69 (s, 2H), 2.81 (dd, $J = 14.0, 6.4$, 1H), 2.74 (dd $J = 14.0, 6.4$) 2.71 – 2.69 (overlapping multiplets, 2H). ^{13}C NMR (126 MHz, CDCl_3) δ 156.52, 137.38, 136.68, 131.59, 131.37, 129.62, 128.59, 126.75, 120.56, 75.69, 40.15, 39.43. HRMS (ESI) m/z calculated for $\text{C}_{16}\text{H}_{16}\text{BrNO}_2$ [$\text{M}+\text{NH}_4^+$] 351.0698, found 351.0703.

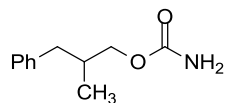


Compound S5.5. A 50 ml 3-necked flask was equipped with a stir bar and charged with Mg turnings (74 mg, 3.03 mmol, 1.57 equiv) and flame dried under vacuum. The flask was equipped with a stopper, rubber septum for additions, and a reflux condenser. The flask was then purged with N_2 and charged with THF (3.2 ml) and an I_2 chip. The flask was cooled to 0°C and charged with *p*-trifluoromethylbromotoluene (0.40 ml, 2.90 mmol, 1.50 equiv). The flask was then moved to a water bath at room temperature to absorb exotherms. Then solution turned a deep orange. After the exotherms ceased (approx. one hour), CuI (55 mg, 0.290 mmol, 0.15 equiv) was added, then a solution of allylbenzene oxide (250 mg, 1.93 mmol, 1.0 equiv) in THF (3.2 ml), was added to the Grignard solution over 1 minute at 0°C . TLC indicated complete consumption of the epoxide after 50 min. The reaction was quenched with sat. aq. NH_4Cl and filtered through Celite. The Celite was washed three times with EtOAc, and the combined

organic extracts were dried over sodium sulfate, filtered and concentrated *in vacuo*. The product was purified by column chromatography twice using a 0 to 14% gradient of EtOAc in hexanes with 2% increments, and obtained as a colorless oil in 43% yield. ^1H NMR (500 MHz, Chloroform-*d*) δ 7.57 (d, $J = 8.0$ Hz, 2H), 7.36 (d, $J = 8.0$ Hz, 2H), 7.32 (d, $J = 7.6$ Hz, 2H), 7.27 – 7.24 (m, 2H), 7.24 – 7.20 (m, 2H), 4.09 (tt, $J = 8.5, 4.4$ Hz, 1H), 2.92 (dd, $J = 13.8, 4.4$ Hz, 1H), 2.88 (dd, $J = 13.7, 4.4$ Hz, 1H), 2.83 (dd, $J = 13.8, 8.5$ Hz, 1H), 2.76 (dd, $J = 13.8, 8.5$ Hz, 1H). ^{13}C NMR (126 MHz, CDCl_3) δ 142.99, 138.14, 129.96, 129.60, 129.15, 128.92, 126.95, 125.53, 123.41, 73.47, 43.84, 43.24. MS (EI) m/z calculated for $\text{C}_{16}\text{H}_{15}\text{F}_3\text{O}$ $[\text{M}]^+$ 280.28, found 280.10.

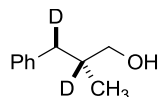


Compound 5.20e. Synthesized according to the general procedure above. The product was obtained in 94% yield from 229 mg (0.797 mmol) of the corresponding alcohol. ^1H NMR (500 MHz, Chloroform-*d*) δ 7.53 (d, $J = 8.0$ Hz, 2H), 7.32 – 7.27 (m, 4H), 7.25 – 7.21 (m, 1H), 7.21 – 7.17 (d, $J = 8.0$ Hz, 2H), 5.20 (p, $J = 6.5$ Hz, 1H), 4.66 (s, 2H), 2.96 – 2.87 (overlapping multiplets, 3H), 2.84 (dd, $J = 13.9, 6.5$ Hz, 1H). ^{13}C NMR (126 MHz, CDCl_3) δ 159.74, 156.49, 139.25, 137.68, 129.69, 129.50, 128.54, 126.66, 122.07, 115.40, 112.01, 55.36, 40.11. HRMS (ESI) m/z calculated for $\text{C}_{17}\text{H}_{16}\text{F}_3\text{NO}_2$ $[\text{M}+\text{NH}_4^+]$ 341.1472, found 341.1474.

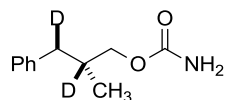


Compound 5.30-H. Synthesized according to the general procedure above. The product was obtained in 86% yield from 452 mg (3.01 mmol) of the corresponding alcohol. ^1H NMR (500 MHz, Chloroform-*d*) δ 7.28 (dd, $J = 8.1, 6.7$ Hz, 2H), 7.20 (tt, $J = 8.1, 1.3$ Hz, 1H), 7.17 – 7.13

(m, 2H), 4.62 (br s, 2H), 3.96 (dd, $J = 10.6, 6.8$ Hz, 1H), 3.92 (dd, $J = 10.6, 6.8$ Hz, 1H) 2.75 (dd, $J = 13.5, 8.2$ Hz, 1H), 2.43 (dd, $J = 13.5, 8.2$ Hz, 1H), 2.10 (dhex, $J = 8.2, 6.8$ Hz) 1H), 0.92 (d, $J = 6.8$ Hz, 3H). ^{13}C NMR (126 MHz, CDCl_3) δ 157.21, 140.27, 129.36, 128.50, 126.21, 69.68, 39.95, 35.03, 16.71. HRMS (ESI) m/z calculated for $\text{C}_{10}\text{H}_{17}\text{NO}_2$ $[\text{M}+\text{NH}_4^+]$ 211.1442, found 211.1437.



Compound S5.6-D. A 50 ml round bottomed flask was charged with (*E*)-2-methyl-3-phenylpropen-1-ol (741 mg, 0.72 ml, 5.00 mmol) and THF 16.5 ml). Pd on carbon (5% w/w, 74 mg) was then added and the flask was flushed with nitrogen. The flask was then fitted with a balloon filled with deuterium gas and flushed for 30 seconds with a vent needle. The needle was then removed and the reaction allowed to stir under deuterium gas. Due to co-elution of starting material and product by silica chromatography, the reaction was monitored by removal of aliquots via syringe, concentration, and NMR analysis. The reaction showed completion after 3 hours, and was filtered through Celite, which was then washed with several 30 ml portions of EtOAc. The product was purified by column chromatography using a 0 to 20% gradient of EtOAc in hexanes with 5% increments. The resulting colorless oil was obtained in 78% yield with 88% deuterium incorporation at the methinyl position. ^1H NMR (500 MHz, Chloroform-*d*) δ 7.28 (dd, $J = 8.0, 6.8$ Hz, 2H), 7.22 – 7.15 (m, 3H), 3.53 (d, $J = 10.6$ Hz, 1H), 3.48 (d, $J = 10.6$ Hz, 1H), 2.41 (s, 1H), 0.91 (s, 3H). ^{13}C NMR (126 MHz, CDCl_3) δ 140.63, 129.15, 128.28, 125.90, 67.62, 39.26, 37.39, 16.35. MS (EI) m/z found for $\text{C}_{10}\text{H}_{12}\text{D}_2\text{O}$ $[\text{M}]^+$, calculated 152.23, found 152.1165.



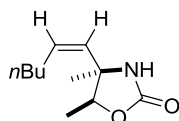
Compound 5.30-D. Synthesized according to the general procedure above. The product was obtained in 89% yield from 496 mg (3.26 mmol) of the corresponding alcohol. ^1H NMR (500 MHz, Chloroform-*d*) δ 7.28 (dd, $J = 8.1, 6.8$, 2H), 7.23 – 7.17 (m, 1H), 7.17 – 7.13 (m, 2H), 4.66 (s, 2H), 3.95 (d, $J = 10.6$ Hz, 1H), 3.92 (d, $J = 10.6$ Hz, 1H), 2.41 (s, 1H), 0.91 (s, 3H). ^{13}C NMR (126 MHz, CDCl_3) δ 157.24, 140.23, 129.34, 128.64, 126.19, 69.64, 39.94, 34.64, 16.68. HRMS (ESI) m/z calculated for $\text{C}_{11}\text{H}_{13}\text{D}_2\text{NO}_2$ [$\text{M}+\text{NH}_4^+$] 213.1567, found 213.1561.

5.7.2. Characterization of amination products.

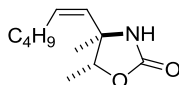
General amination procedure. A pre-dried reaction flask was charged with silver triflate (0.10 equiv), ligand (0.125 or 0.3 equiv) and powdered 4A molecular sieves (4 times substrate mass). Dichloromethane (0.02 M in AgOTf) was added and the mixture was stirred vigorously for 15 min. A solution of the carbamate (1 equiv) in dichloromethane (0.2 M in substrate) was added to the reaction flask. After two minutes iodosobenzene (3.5 equiv) was added in one portion and the reaction mixture was allowed to stir at room temperature until TLC indicated complete consumption of the starting material (2-14h). The reaction mixture was filtered through a glass frit and the filtrate was concentrated under reduced pressure. The crude products were purified by silica gel column chromatography using a hexane/EtOAc gradient.

In the cases of radical inhibition experiments, 10 mol % of a radical inhibitor was added at the outset of the reaction.

Compounds **5.21ea** and **5.17b** were synthesized as described in a prior report using 4,4'-di-*tert*-butyl bipyridine as the ligand.

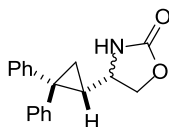


Compound 5.15a. The procedure for Ag-catalyzed C-H insertion was used with **5.14a** as the substrate. The product was purified by column chromatography using a 0 \rightarrow 40% gradient of EtOAc in hexanes with 8% increments. The product was obtained in 86% yield as a clear oil. ^1H NMR (500.0 MHz, CDCl_3) δ 6.20 (br s, 1H), 5.48 (dt, $J = 11.9, 7.5$ Hz, 1H), 5.28 (dt, $J = 11.9, 1.4$ Hz, 1H), 4.51 (q, $J = 6.8$ Hz, 1H), 2.30-2.16 (m, 2H), 1.41-1.29 (overlapping m, 11H), 0.91 (t, $J = 7.1$ Hz, 3H); ^{13}C NMR (125.7 MHz, CDCl_3) δ 158.9, 134.8, 130.4, 82.0, 61.0, 31.9, 27.8, 22.7, 22.3, 14.1, 14.0.



Compound 5.15b. The procedure for Ag-catalyzed C-H insertion was used, with compound **5.14b** as the substrate. The product was purified by column chromatography using a 0 \rightarrow 40% gradient of EtOAc in hexanes with 8% increments. The product was obtained in 73% yield as a clear oil when BHT was added to the reaction mixture. Traces (<10%) of the *trans*-alkene were present in both starting material and product, but no trace of compound **5.15a** was detected. ^1H NMR: (500.0 MHz, CDCl_3) δ 5.84 (br s, 1H), 5.54 (dt, $J = 12.2, 4.3$ Hz, 1H), 5.21 (d, $J = 12.2$ Hz, 1H), 4.42 (q, $J = 6.6$ Hz, 1H), 2.15 (qd, $J = 7.3, 1.5$ Hz, 2H), 1.46 (s, 3H), 1.31-1.41 (m, 4H), 1.28 (d, $J = 7.3$ Hz, 3H), 0.91 (t, $J = 7.0$ Hz, 3H); ^{13}C NMR: (125.7 MHz, CDCl_3) δ 158.30,

134.43, 128.05, 82.93, 61.40, 31.89, 28.35, 27.93, 22.24, 16.38, 13.83; HRMS (EI) m/z calculated for $C_{11}H_{19}NO_2$ $[M+H^+]$ 198.1489, found 198.1491.



Compounds 5.19. Synthesized according to the general procedure above. When 0.30 equiv 4,4'-di-*t*Bubipyridine was used as the ligand with 56 mg (0.20 mmol) of the corresponding carbamate, the product was obtained as a 3:1 ratio of diastereomers in 48% yield after 6.5 hours. The relative stereochemistry of the products was not determined.

Major diastereomer: 1H NMR (500 MHz, Chloroform-*d*) δ 7.36 – 7.22 (m, 9H), 7.22 – 7.17 (m, 1H), 5.14 (s, 1H), 4.44 (t, $J = 8.5$ Hz, 1H), 4.27 (dd, $J = 8.5, 6.4$ Hz, 1H), 3.01 (dddd, $J = 9.7, 8.5, 6.4, 1.2$ Hz, 1H), 1.97 (ddd, $J = 9.7, 8.8, 5.4$ Hz, 1H), 1.44 (t, $J = 5.4$ Hz, 1H), 1.31 – 1.19 (m, 1H). ^{13}C NMR (126 MHz, $CDCl_3$) δ 159.08, 144.75, 140.43, 129.30, 129.16, 128.58, 128.30, 127.27, 126.66, 70.05, 54.20, 35.60, 29.35, 16.20. HRMS (ESI) m/z calculated for $C_{18}H_{17}NO_2$ $[M+NH_4^+]$ 297.1598, found 297.1591.

Minor diastereomer: 1H NMR (500 MHz, Chloroform-*d*) δ 7.35 – 7.31 (m, 2H), 7.30 – 7.23 (m, 5H), 7.22 – 7.11 (m, 3H), 4.53 (s, 1H), 4.42 (t, $J = 8.4$ Hz, 1H), 4.36 (dd, $J = 8.4, 6.2$ Hz, 1H), 3.31 (td, $J = 8.4, 6.2$ Hz, 1H), 1.92 (td, $J = 8.4, 5.7$ Hz, 1H), 1.35 (dd, $J = 8.6, 5.7$ Hz, 1H), 1.28-1.25 (m, 1H). ^{13}C NMR (126 MHz, $CDCl_3$) δ 158.76, 145.18, 140.59, 129.97, 129.29, 128.77, 127.78, 127.55, 126.72, 70.58, 54.11, 35.37, 31.16, 17.81. HRMS (ESI) m/z calculated for $C_{18}H_{17}NO_2$ $[M+NH_4^+]$ 297.1598, found 297.1593.

Procedural modifications for substrates used to generate Hammett plots.

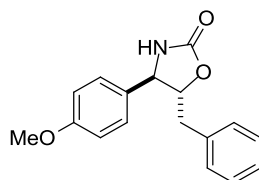
The general amination procedure was followed, using 20 mol % AgOTf with 25 or 60 mol % 2,2'-bipyridine as the ligand. Low conversion was observed at lower catalyst loadings. All reactions were performed initially with 100-200 mg substrate in order to allow for isolation of individual product isomers when possible. Reaction mixtures were purified by silica gel chromatography using 100g silica/g crude mixture and an EtOAc/hexane gradient with 5% increments, 0 to 35% EtOAc. Because isomers were not easily distinguished by TLC, fractions containing product were concentrated systematically (every four fractions), and analyzed by NMR. Fractions containing a significant excess of one isomer were combined with the two surrounding fractions and subjected to up to three iterations of chromatographic purification.

Products were characterized by ^1H , ^{13}C and gCOSY NMR. In cases in which inseparable product mixtures were obtained, careful analysis of gCOSY spectra allowed assignment of key peaks to a particular regioisomer of the compound. Quantitative ^{13}C -NMR using an inverse gated pulse sequence allowed the assignment of select carbon peaks to individual regioisomers. After characterization of benzylic amination products, reactions were performed in duplicate on a smaller scale (25-50 mg). The crude mixtures were then injected with 10 μl 1,1,1,2-tetrachloroethane as a standard and analyzed by both ^1H -NMR and quantitative ^{13}C -NMR using an inverse gated pulse sequence with a five second receiver delay.

The reaction of carbamate **5.20a** gave mixtures of the following products under the above conditions. Products ratios are tabulated below.

Trial	Mol % ligand	Yield	<i>Regiomer ratio</i>	<i>Dias. ratio</i>
1	25	44%	2.03:1	5.3:1
2	25	56%	1.83:1	3.7:1
AVG		50%	1.93:1	4.5:1
1	60	69%	1.76:1	3.1:1

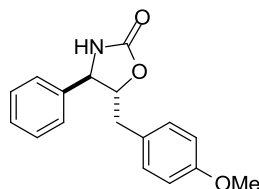
2	60	74%	1.86:1	2.7:1
AVG		72.5%	1.81:1	2.9:1



Compound 5.22aa:

Major regioisomer, major diastereomer.

^1H NMR (500 MHz, Chloroform-*d*) δ 7.34 – 7.29 (m, 2H), 7.26 (s, 3H), 7.09 (d, J = 8.7 Hz, 2H), 6.86 (d, J = 8.7 Hz, 2H), 5.04 (s, 1H), 4.58 (td, J = 6.6, 5.6 Hz, 1H), 4.52 (dd, J = 6.6, 1.0 Hz, 1H), 3.80 (s, 3H), 3.13 (dd, J = 14.3, 5.6 Hz, 1H), 3.05 (dd, J = 14.3, 5.6 Hz, 1H). ^{13}C NMR (126 MHz, CDCl_3) δ 158.45, 135.37, 131.14, 129.89, 128.93, 127.73, 127.40, 114.70, 85.57, 60.47, 55.58, 39.78. HRMS (ESI) m/z calculated for $\text{C}_{17}\text{H}_{17}\text{NO}_3$ [$\text{M}+\text{NH}_4^+$] 301.1547, found 301.1555.

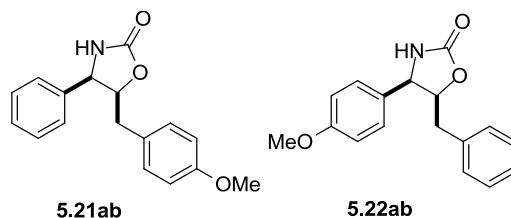


Compound 5.21aa:

Minor regioisomer, major diastereomer.

^1H NMR (500 MHz, Chloroform-*d*) δ 7.40 – 7.31 (m, 3H), 7.21 – 7.17 (m, 2H), 7.16 (d, J = 8.6 Hz, 2H), 6.85 (d, J = 8.6 Hz, 2H), 5.04 (s, 1H), 4.63 – 4.50 (m, 2H), 3.80 (s, 3H), 3.08 (dd, J = 14.3, 5.3 Hz, 1H), 3.02 (dd, 14.3, 5.1 Hz, 1H). ^{13}C NMR (126 MHz, CDCl_3) δ 130.97, 129.38, 129.03, 127.17, 126.41, 114.35, 85.54, 60.47, 55.52, 38.93. Due to the low quantities of pure material available for analysis, the carbonyl and several two aromatic peaks could not be

identified in the ^{13}C NMR spectrum. HRMS (ESI) m/z calculated for $\text{C}_{17}\text{H}_{17}\text{NO}_3$ $[\text{M}+\text{NH}_4^+]$ 301.1547, found 301.1557.



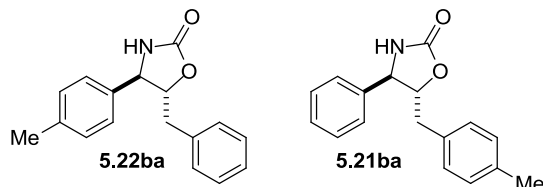
Compounds 5.21ab and 5.22ab.

Minor diastereomers.

^1H NMR (500 MHz, Chloroform-*d*) δ 7.43 – 7.39 (m, 2H **5.21ab**), 7.25 – 7.18 (m, 3H **5.22ab**, 3H **5.21ab**), 7.17 (d, $J = 8.6$ Hz, 2H **5.22ab**), 7.05 – 7.00 (m, 2H **5.22ab**), 6.93 (d, $J = 8.6$, 2H **5.22ab**), 6.92 (d, 8.9 Hz, 2H, **5.21ab**), 6.76 (d, $J = 8.7$ Hz, 2H **5.21ab**), 5.28 (br s, 1H **5.21ab**), 5.25 (br s 1H **5.22ab**), 5.11 – 5.01 (m, 1H **5.22ab**, 1H **5.21ab**), 4.90 (d, $J = 7.9$ Hz, 1H **5.21ab**), 4.86 (d, $J = 7.8$ Hz, 2H **5.22ab**), 3.84 (s, 3H **5.22ab**), 3.77 (s, 3H **5.21ab**), 2.65 (dd, $J = 14.8, 9.0$ Hz, 1H **5.22ab**), 2.58 (dd, $J = 14.8, 9.1$ Hz, 1H **5.21ab**), 2.39 (dd, $J = 14.8, 4.8$ Hz, 1H **5.22ab**), 2.33 (dd, $J = 14.8, 4.8$ Hz, 1H **5.21ab**). ^{13}C NMR (126 MHz, CDCl_3) δ 160.33, 159.26, 158.64, 136.81, 136.60, 130.27, 129.88, 129.27, 129.13, 128.92, 128.78, 128.69, 128.64, 128.46, 127.72, 127.59, 126.96, 114.69, 114.48, 114.05, 81.86, 81.84, 59.87 (**5.22ab**), 59.44 (**5.21ab**), 55.60, 55.45, 37.49 (**5.22ab**), 36.63 (**5.21ab**), 29.92. HRMS (ESI) m/z calculated for $\text{C}_{17}\text{H}_{17}\text{NO}_3$ $[\text{M}+\text{NH}_4^+]$ 301.1547, found 301.1550.

The reaction of carbamate **5.20b** gave mixtures of the following products under the above conditions. Products ratios are tabulated below.

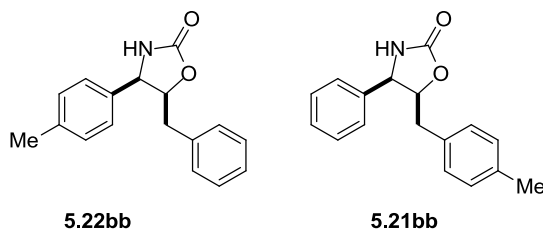
Trial	Mol % ligand	Yield	Regiomer ratio	Dias. ratio
1	25	57%	1.45:1	3.4:1
2	25	59%	1.28:1	3.5:1
AVG		58%	1.36:1	3.45:1
1	60	54%	1.32:1	3.5:1
2	60	63%	1.36:1	2.9:1
AVG		58.5%	1.34:1	3.2:1



Compounds **5.21ba** and **5.22ba**.

Mixture of major diastereomers.

^1H NMR (500 MHz, Benzene- d_6) δ 7.07-6.97 (m, 3H **5.22ba**, 3H **5.21ba**), 6.93-6.87 (overlapping m, 2H **5.22ba**, 2H **5.21ba**), 6.86- 6.80 (m, 3H **5.22ba**, 3H **5.21ba**), 6.77-6.74 (m, 1H **5.22ba**, 1H **5.21ba**), 4.97 (s, 1H **5.22ba**), 4.91 (s, 1H **5.21ba**), 4.56 – 4.37 (m, 1H **5.22ba**, 1H **5.21ba**), 3.90 (dd, $J = 12.0, 7.7$ Hz, 1H **5.22ba**, 1H **5.21ba**), 2.48-2.38 (overlapping m, 2H **5.22ba**, 2H **5.21ba**), 2.09 (s, 3H **5.21ba**), 2.07 (s, 3H **5.22ba**). ^{13}C NMR (126 MHz, C_6D_6) δ 159.44, 140.73, 138.40, 137.68, 136.84, 136.39, 133.18, 130.24, 130.21, 130.06, 129.83, 129.50, 129.36, 129.10, 128.97, 128.90, 128.68, 128.49, 128.30, 127.86, 127.43, 126.75, 126.72, 85.40 (**5.22ba**), 85.33 (**5.21ba**), 61.01, 40.34 (**5.22ba**), 39.95 (**5.21ba**), 21.36, 21.32. HRMS (ESI) m/z calculated for $\text{C}_{17}\text{H}_{17}\text{NO}_2$ [$\text{M}+\text{NH}_4^+$] 285.1598, found 285.1560.



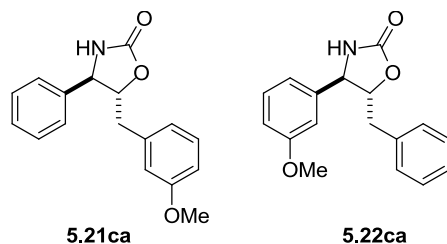
Compounds 5.21bb and 5.22bb.

Minor diastereomers

¹H NMR (500 MHz, Benzene-*d*₆) δ 7.08-6.98 (m, 3H **5.22bb**, 3H **5.21bb**), 6.88 (dd, *J* = 7.8, 5.8 Hz, 2H **5.22bb**, 2H **5.21bb**), 6.85- 6.80 (m, 2H **5.22ba**, 2H **5.21ba**), 6.76 (dd, *J* = 10.0, 7.8 Hz, 2H **5.22ba**, 2H **5.21ba**), 4.97 (s, 1H **5.22ba**), 4.91 (s, 1H **5.21ba**), 4.56 – 4.37 (m, 1H **5.22ba**, 1H **5.21ba**), 3.90 (dd, *J* = 12.0, 7.7 Hz, 1H **5.22ba**, 1H **5.21ba**), 2.48-2.38 (overlapping m, 2H **5.22ba**, 2H **5.21ba**), 2.09 (s, 3H **5.21ba**), 2.07 (s, 3H **5.22ba**). ¹³C NMR (126 MHz, C₆D₆) δ 159.26, 159.22, 138.62, 137.92, 137.59, 134.93, 134.42, 129.79, 129.72, 129.64, 129.04, 128.91, 127.91, 127.85, 127.15, 81.19, 81.11, 59.80 (**5.21bb**), 59.64 (**5.22bb**), 38.02 (**5.22bb**), 37.59 (**5.21bb**), 21.39, 21.35. HRMS (ESI) *m/z* calculated for C₁₇H₁₇NO₂ [M+NH₄⁺] 285.1598, found 285.1594.

The reaction of carbamate **5.20c** gave mixtures of the following products under the above conditions. Products ratios are tabulated below. Because regioisomer were obtained in equal ratios and were unseparable under all attempted chromatographic conditions, individual peaks were not assigned.

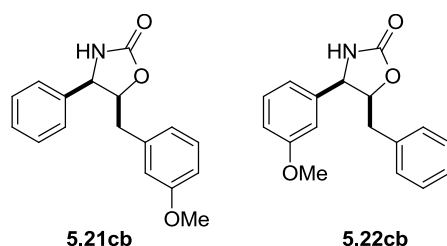
Trial	Mol % ligand	Yield	<i>Regiomer ratio</i>	<i>Dias. ratio</i>
1	25	65%	1.0:1	2.6:1
2	25	56%	1.0:1	2.7:1
AVG		60.5%	1.0:1	2.65:1
1	60	56%	1.0:1	3.3:1
2	60	65%	1.0:1	3.1:1
AVG		60.5%	1.0:1	3.2:1



Compound 5.21ca and 5.22ca.

Major diastereomers

^1H NMR (500 MHz, Benzene- d_6) δ 7.07 – 6.92 (m, 8H, unassigned), 6.89 – 6.83 (m, 2H, unassigned), 6.78 (dd, $J = 6.7, 2.9$ Hz, 2H, unassigned), 6.71 – 6.61 (m, 3H, unassigned), 6.54 (dt, $J = 7.6, 1.2$ Hz, 1H, unassigned), 6.49 – 6.46 (m, 1H **5.21ca**, 1H **5.22ca**), 5.48 (s, 1H unassigned), 5.28 (s, 1H unassigned), 4.22 (q, $J = 6.4$ Hz, 1H, unassigned), 4.20 (q, $J = 6.1$ Hz, 1H, unassigned), 3.92 (d, $J = 3.4$ Hz, 1H), 3.91 (d, $J = 3.6$ Hz, 1H), 3.29 (s, 3H unassigned), 3.24 (s, 3H unassigned), 2.67 (dd, $J = 14.2, 6.7$ Hz, 1H, unassigned), 2.64 (dd, $J = 14.5, 6.6$ Hz, 1H), 2.55 (dd, $J = 14.2, 6.1$ Hz, 1H, unassigned), 2.53 (dd, $J = 14.2, 6.2$ Hz, 1H). ^{13}C NMR (126 MHz, C_6D_6) δ 159.35, 159.20, 157.46, 157.35, 140.77, 139.09, 136.16, 134.68, 129.01, 128.76, 128.61, 127.80, 127.59, 127.21, 125.93, 125.21, 120.98, 117.14, 114.34, 113.00, 111.76, 110.54, 83.51, 83.40, 59.36, 53.58, 38.88, 38.73. HRMS (ESI) m/z calculated for $\text{C}_{17}\text{H}_{17}\text{NO}_3$ [$\text{M}+\text{NH}_4^+$] 301.1547, found 301.1547



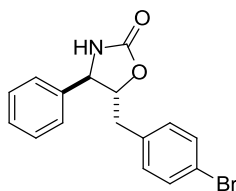
Compounds 5.21cb and 5.22cb.

Minor diastereomers.

^1H NMR (500 MHz, Benzene- d_6) δ 7.07 – 6.93 (m, 4H **5.21cb**, 4H **5.22cb**), 6.84 – 6.73 (m, 1H **5.21cb**, 1H **5.22cb**), 6.78 – 6.73 (m, 1H **5.21cb**, 1H **5.22cb**), 6.66 (dtd, $J = 7.84, 2.55, 0.8$ Hz, 1H **5.21cb**, 1H **5.22cb**) 6.54 – 6.43 (m, 2H **5.21cb**, 2H **5.22cb**), 4.47 (ddd, $J = 8.7, 7.4, 4.4$, 1H, unassigned), 4.43 (ddd, $J = 9.3, 7.7, 4.4$ Hz, 1H, unassigned), 4.22 (s, 1H, un assigned), 4.15 (s, 1H, unassigned), 3.79 (d, $J = 4.8$ Hz, 1H), 3.77 (d, $J = 4.8$, 1H, unassigned) 3.28 (s, 3H, not assigned), 3.27 (s, 3H, unassigned), 2.47 (dd, $J = 14.6, 8.9$ Hz, 1H, unassigned), 2.43 (dd, $J = 14.6, 9.4$ Hz, 1H, unassigned), 2.11 (dd, $J = 14.6, 4.2$, 1H, unassigned), 2.06 (dd, $J = 14.3, 4.7$ Hz, 1H). ^{13}C NMR (126 MHz, C_6D_6) δ 129.05, 121.22, 114.73, 113.78, 112.26, 80.16, 59.01. HRMS (ESI) m/z calculated for $\text{C}_{17}\text{H}_{17}\text{NO}_3$ [$\text{M}+\text{NH}_4^+$] 301.1547, found 301.1547. Due to the small amount of diastereomerically pure sample available for characterization, not all expected carbon signals were observed.

The reaction of carbamate **5.20d** gave mixtures of the following products under the above conditions. Products ratios are tabulated below.

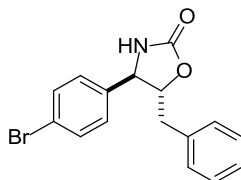
Trial	Mol % ligand	Yield	Regiomer ratio	Dias. ratio
1	25	46%	1:1.39	2.9:1
2	25	48%	1:1.43	3.0:1
AVG		47%	1:1.41	2.95:1
1	60	49%	1:1.43	3.1:1
2	60	46%	1:1.35	2.9:1
AVG		47.5%	1:1.39	3.0:1



Compound 5.21da.

Major regioisomer, major diastereomer.

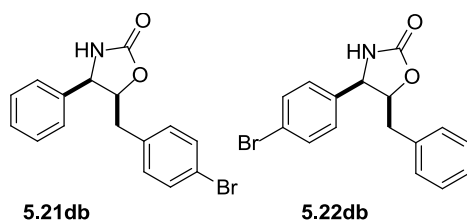
^1H NMR (500 MHz, Chloroform-*d*) δ 7.44 (d, $J = 8.2$ Hz, 2H), 7.40 – 7.27 (m, 3H), 7.12 (d, $J = 8.4$ Hz, 2H), 5.22 (s, 1H), 4.61 – 4.48 (m, 2H), 3.11 – 2.99 (m, 2H). ^{13}C NMR (126 MHz, CDCl_3) δ 158.35, 138.96, 134.33, 132.03, 131.57, 129.49, 129.24, 126.45, 121.48, 85.00, 61.08, 39.19. Peak data were obtained by comparison of spectra of pure **5.22da** with spectra obtained from a mixture of **5.21da** and **5.22da**. HRMS was obtained for pure **5.22da**.



Compound 5.22da.

Minor regioisomer, major diastereomer.

^1H NMR (500 MHz, Chloroform-*d*) δ 7.45 (d, $J = 8.4$ Hz, 2H), 7.36 – 7.27 (m, 3H), 7.24 – 7.20 (m, 3H), 6.99 (d, $J = 8.4$ Hz, 2H), 5.16 (s, 1H), 4.58 – 4.50 (m, 2H), 3.21-3.14 (m, 1H), 3.08 – 2.99 (m, 1H). ^{13}C NMR (126 MHz, CDCl_3) δ 158.31, 138.46, 134.89, 132.51, 129.89, 129.37, 129.06, 128.01, 127.60, 123.00, 85.17, 77.48, 77.43, 77.23, 76.98, 60.18, 39.99. HRMS (ESI) m/z calculated for $\text{C}_{16}\text{H}_{14}\text{BrNO}_2$ [$\text{M}+\text{NH}_4^+$] 350.0550, found 350.0547.



Compounds 5.21db and 5.22db

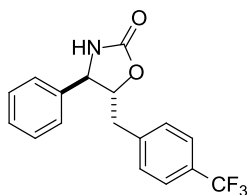
Mix of minor diastereomers.

^1H NMR (500 MHz, Chloroform-*d*) δ 7.56 (d, $J = 8.4$ Hz, 2H **5.22db**), 7.45 – 7.38 (m, 1H **5.21db**, 1H **5.22db**), 7.35 (d, $J = 8.4$ Hz, 2H **5.21db**), 7.25 – 7.16 (m, 3H **5.21db**, 3H **5.22db**),

7.12 (d, $J = 8.4$ Hz, 2H, **5.22db**), 7.03 – 6.96 (m, 1H **5.21db**, 1H **5.22db**), 6.90 (d, $J = 8.2$ Hz, 2H **5.21db**), 5.18 (s, 1H **5.21db**, 1H **5.22db**), 5.11 (ddd, $J = 9.0, 7.9, 5.1$ Hz, 1H **5.22db**), 5.05 (td, $J = 9.1, 7.8, 4.5$ Hz, 1H **5.21db**), 4.93 (d, $J = 7.9$ Hz, 1H **5.21db**), 4.88 (d, $J = 7.9$ Hz, 1H **5.22db**), 2.66 (dd, $J = 14.8, 9.1$ Hz, 1H **5.22db**), 2.56 (dd, $J = 14.8, 9.0$ Hz, 1H, **5.21db**), 2.38 (dd, $J = 14.8, 5.0$ Hz, 1H **5.22db**), 2.35 – 2.31 (m, 1H **5.21db**). ^{13}C NMR (126 MHz, CDCl_3) δ 159.09, 135.88, 135.57, 132.13, 131.53, 130.80, 129.05, 128.98, 128.53, 127.28, 126.92, 81.05, 59.11, 37.24, 29.71. HRMS (ESI) m/z calculated for $\text{C}_{16}\text{H}_{14}\text{BrNO}_2$ $[\text{M}+\text{NH}_4^+]$ 350.0550, found 350.0539. The carbon spectrum did not allow assignment of individual diastereomers. ^1H NMR peaks were sufficiently separated for quantitative analysis. Though **5.22db** is the major product in the analytical sample, **5.21db** was the major product in the crude reaction mixture.

The reaction of carbamate **5.20e** gave mixtures of the following products under the above conditions. Products ratios are tabulated below.

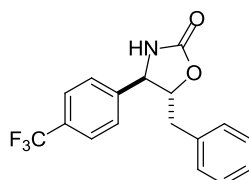
Trial	Mol % ligand	Yield	Regiomeric ratio	Dias. ratio
1	20	60%	1:1.96	3.7:1
2	20	55%	1:2.14	3.8:1
AVG		57.5%	1:2.05	3.75:1
1	60	66%	1:1.96	3.8:1
2	60	62%	1:2.06	3.4:1
AVG		64%	1:2.01	3.6:1



Compound 5.21ea

Major regioisomer, major diastereomer.

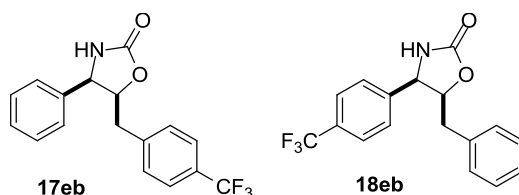
^1H NMR (500 MHz, Chloroform-*d*) δ 7.58 (d, $J = 8.0$ Hz, 2H), 7.37 – 7.28 (m, 1H), 7.25 – 7.18 (m, 4H), 5.28 (s, 1H), 4.66 – 4.62 (m, 1H), 4.58 (q, $J = 6.3$ Hz, 1H), 3.22 (dd, $J = 14.2, 6.1$ Hz, 1H), 3.06 (dd, $J = 14.2, 6.5$ Hz, 1H). ^{13}C NMR (126 MHz, CDCl_3) δ 158.30, 134.70, 129.91, 129.12, 127.70, 126.70, 126.37, 126.35, 85.04, 60.16, 40.10. HRMS (ESI) m/z calculated for $\text{C}_{17}\text{H}_{14}\text{F}_3\text{NO}_2$ [$\text{M}+\text{NH}_4^+$] 339.1315, found 339.1313.



Compound 18ea

Minor regioisomer, major diastereomer.

^1H NMR (500 MHz, Chloroform-*d*) δ 7.57 (d, $J = 8.0$ Hz, 2H), 7.37 (ddt, $J = 4.9, 3.1, 1.8, 1.8$ Hz, 5H), 7.25 – 7.17 (m, 2H), 5.52 (s, 1H), 4.60 (td, $J = 7.0, 6.9, 4.9$ Hz, 1H), 4.56 (dd, $J = 6.8, 0.8$ Hz, 1H), 3.19 (dd, $J = 14.5, 7.0$ Hz, 1H), 3.14 (dd, $J = 14.5, 4.9$ Hz, 1H). ^{13}C NMR (126 MHz, CDCl_3) δ 158.46, 139.54, 138.76, 130.18, 129.49, 129.29, 126.46, 125.87, 125.80, 84.89, 61.39, 39.60. HRMS (ESI) m/z calculated for $\text{C}_{17}\text{H}_{14}\text{F}_3\text{NO}_2$ [$\text{M}+\text{NH}_4^+$] 339.1315, found 339.1313.



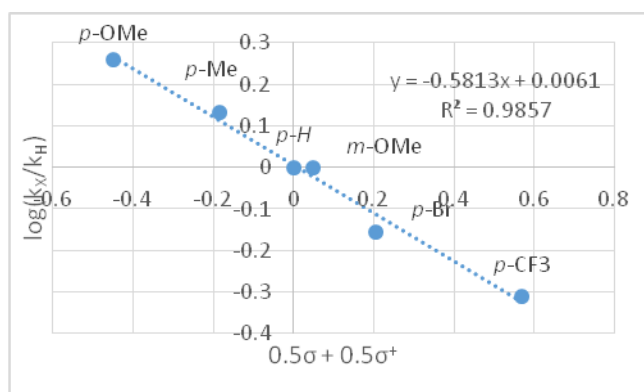
Compounds 5.21eb and 5.22eb.

Mix of minor diastereomers.

^1H NMR (500 MHz, Chloroform-*d*) δ 7.67 (d, $J = 8.0$ Hz, 2H **5.22eb**), 7.49 (d, $J = 8.0$ Hz, 2H **5.21eb**), 7.46-7.41 (m, 2H **5.21eb**), 7.38 (d, $J = 8.0$ Hz, 2H **5.22eb**), 7.30 – 7.18 (m, 6H), 7.16 (d, $J = 8.0$ Hz, 2H **5.21eb**), 7.01 – 6.95 (m, 2H **5.22eb**), 5.37 (s, 1H), 5.30 (s, 1H), 5.17 (ddd, $J = 8.9, 7.9, 5.1$ Hz, 1H **5.22eb**), 5.09 (ddd, $J = 9.5, 8.0, 4.1$ Hz, 1H **5.21eb**), 5.00 (d, $J = 7.9$ Hz, 2H **5.22eb**), 4.97 (d, $J = 8.0$ Hz, 1H **5.21eb**), 2.69 – 2.60 (m, 1H **5.22eb**, 1H **5.21eb**), 2.45 (dd, $J = 14.8, 4.1$ Hz, 1H **5.21eb**), 2.37 (dd, $J = 14.7, 5.1$ Hz, 1H **5.22eb**). ^{13}C NMR (126 MHz, CDCl_3) δ 159.09, 135.88, 135.57, 132.13, 131.53, 130.80, 129.05, 128.98, 128.53, 127.28, 126.92, 81.05 (**5.22eb**), 80.91 (**5.21eb**), 59.11, 37.33 (**5.21eb**), 37.24 (**5.22eb**), 29.71. HRMS (ESI) m/z calculated for $\text{C}_{17}\text{H}_{14}\text{F}_3\text{NO}_2$ [$\text{M}+\text{NH}_4^+$] 339.1311, found 339.1315. Though **5.21eb** was the major of the two regioisomers in the reaction, it was the minor component of the analytical sample.

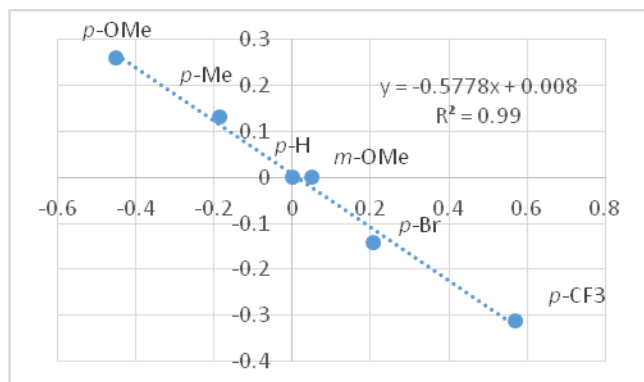
Plots were generated using values given by Hantsch and co-workers. Coefficients for σ and σ^+ totaling 1.0 were examined at intervals of 0.1 units and the highest correlation was found to occur at 0.5 σ and 0.5 σ^+ . The most linear plots are shown below:

Hammett plot using AgL catalyst system.

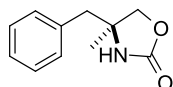


The extracted ρ value is -0.58 for the AgL catalyst system (20 mol % AgOTf, 25 mol % 2,2'-bipyridyl).

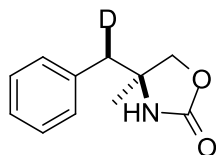
Hammett plot using AgL₂ catalyst system.



The extracted ρ value is -0.58 for the AgL₂ catalyst system (20 mol % AgOTf, 60 mol % 2,2'-bipyridyl).



Compound 5.31-H. Synthesized according to the general procedure above. The product was obtained in 57% yield from 39 mg (0.202 mmol) of the corresponding alcohol using 0.3 equiv 2,2'-bipyridine as the ligand. ¹H NMR (500 MHz, Chloroform-*d*) δ 7.36 – 7.27 (m, 3H), 7.21 – 7.16 (m, 2H), 5.46 (s, 1H), 4.28 (d, J = 8.4 Hz, 1H), 4.08 (d, J = 8.4 Hz, 1H), 2.90 (d, J = 13.4 Hz, 1H), 2.83 (d, J = 13.4 Hz, 1H), 1.32 (s, 3H). ¹³C NMR (126 MHz, CDCl₃) δ 158.57, 135.30, 130.15, 128.87, 127.07, 75.48, 58.05, 46.23, 25.29. HRMS (ESI) m/z calculated for C₁₁H₁₃NO₂ [M+H⁺] 192.1020, found 192.1013.

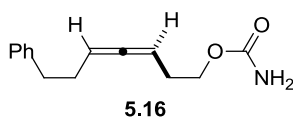


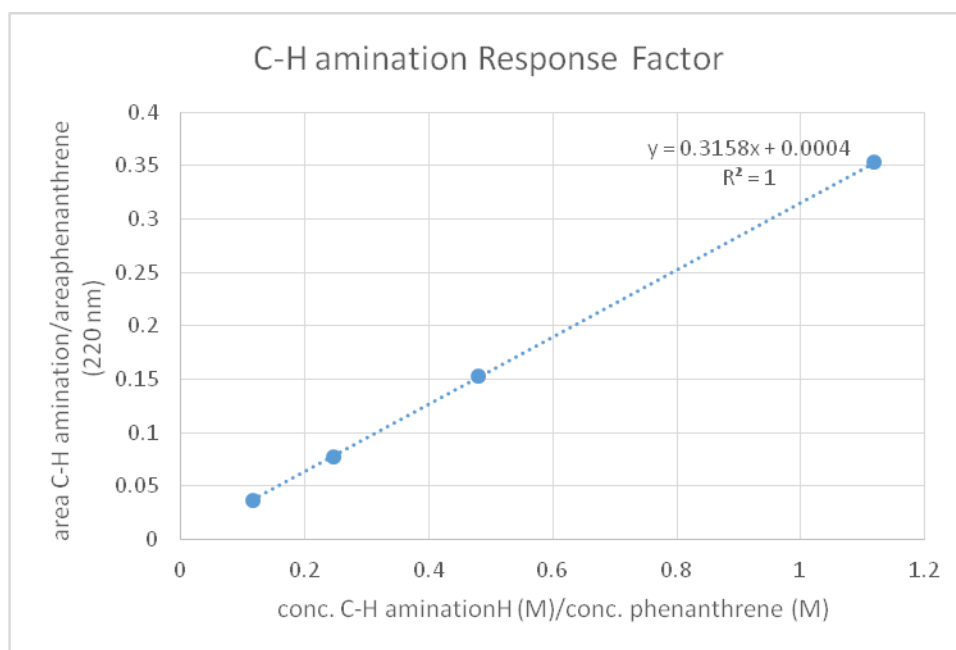
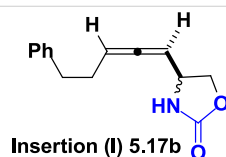
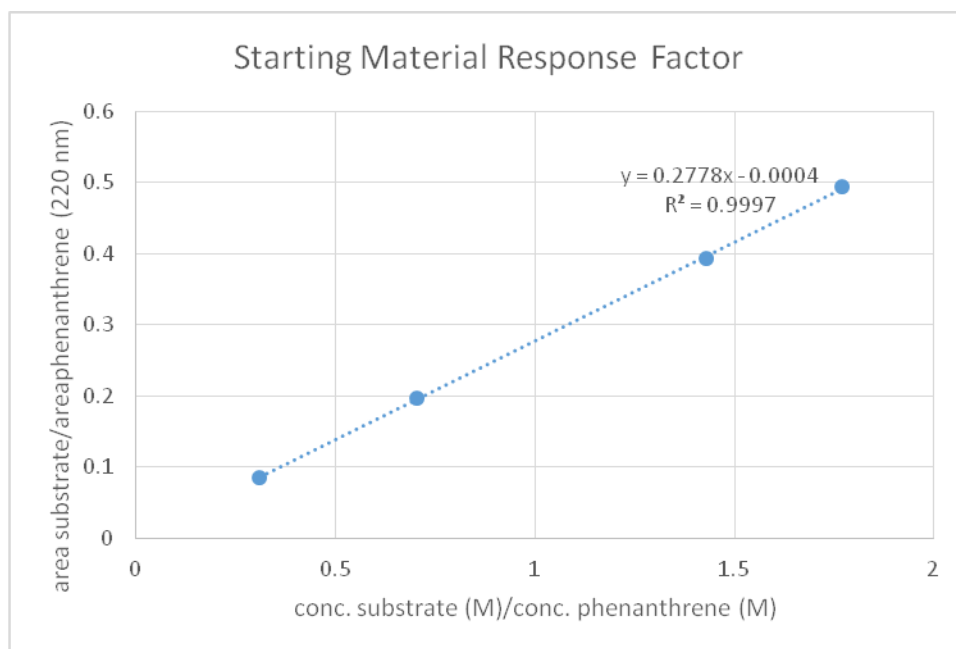
Compound 5.31-D. Synthesized according to the general procedure above. The product was obtained in 60% yield from 39 mg (0.202 mmol) of the corresponding alcohol using 0.3 equiv

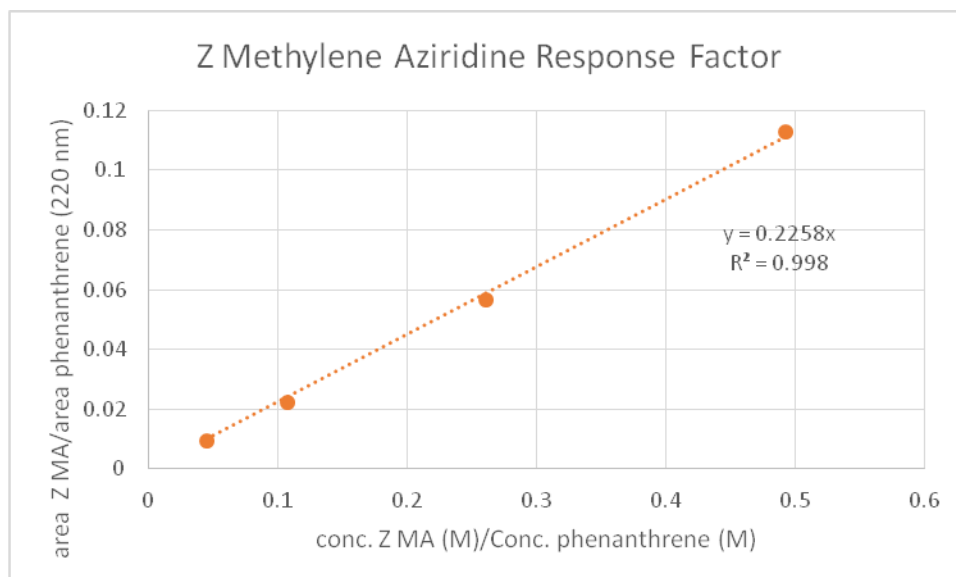
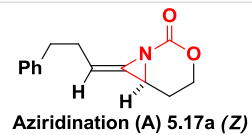
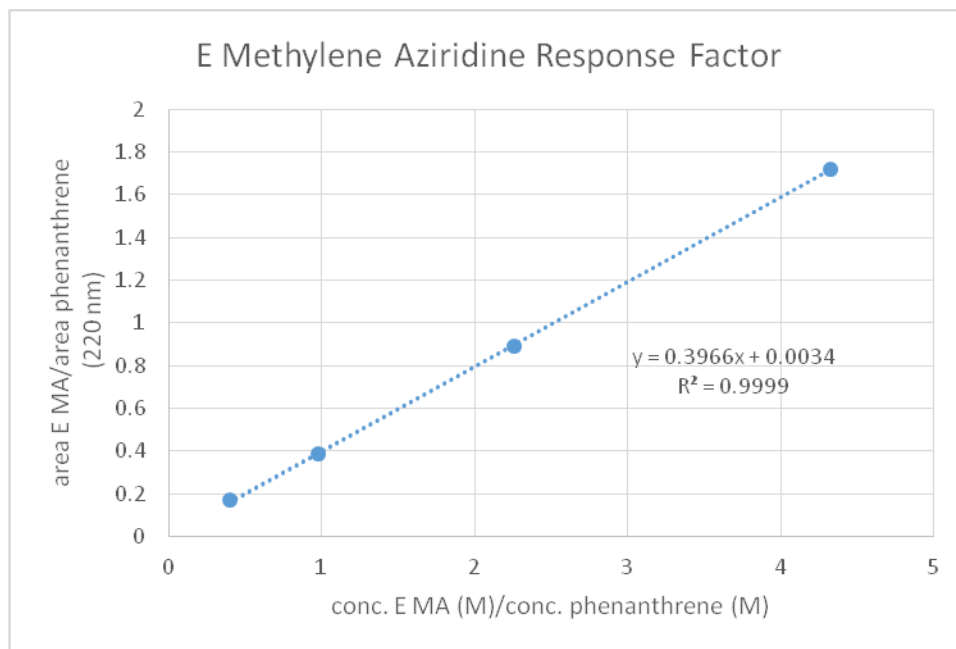
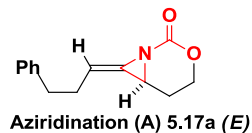
4,4'-di-*tert*-butylbipyridyl as the ligand. ^1H NMR (500 MHz, Chloroform-*d*) δ 7.32 (dd, $J = 8.1$, 6.4 Hz, 2H), 7.30 – 7.25 (m, 1H), 7.21 – 7.15 (m, 2H), 6.25 (s, 1H), 4.28 (d, $J = 8.5$ Hz, 1H), 4.03 (d, $J = 8.5$ Hz, 1H), 2.83 (s, 1H), 1.33 (s, 3H). ^{13}C NMR (126 MHz, CDCl_3) δ 159.23, 135.51, 130.31, 128.75, 127.37, 77.48, 77.46, 77.23, 76.98, 75.22, 58.26, 46.02, 45.87, 45.71, 25.72, 25.69. HRMS (ESI) m/z calculated for $\text{C}_{11}\text{H}_{12}\text{DNO}_2$ $[\text{M}+\text{NH}_4^+]$ 210.1353, found 210.1348.

5.7.3. Kinetic Analysis of Amination Reactions.

Calibration curves for reaction components. Response factor curves were created for the starting material, C-H amination product and combined diastereomers of the methylene aziridine using phenanthrene as the internal standard. The measured reaction components were synthesized according to standard procedures and purified by flash chromatography as described in previous publications^{cite}. Relative UV absorptivities at 220 nm were analyzed by 5 μl injections via HPLC at varied concentration ratios, generating the following calibration curves.



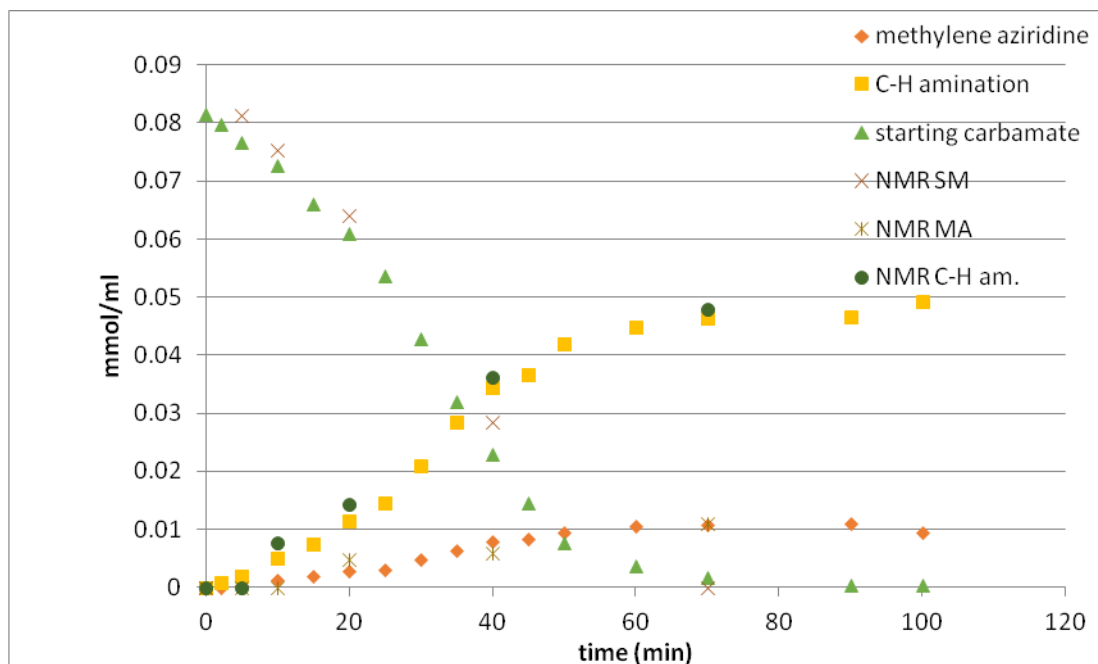




General procedure for acquisition of kinetic data.

A pre-dried reaction 10 ml round-bottomed flask was charged with silver triflate (0.04-0.20 equiv), ligand (1.25 or 3 equiv relative to silver triflate), phenanthrene (approx. 0.06M in CH₂Cl₂) and powdered 4A molecular sieves (1g/mmol substrate). Dichloromethane was added and the mixture was stirred vigorously for 15 min. A solution of the carbamate (1 equiv) in dichloromethane (0.025-0.4 M in substrate) was added to the reaction flask. After two minutes, iodosobenzene was added in one portion, marking $t = 0$, and the reaction mixture was allowed to stir at room temperature. Aliquots (20 μ l) were removed at regular intervals by autopipette and injected into 1.5 ml mixtures of HPLC grade 10:90 iPrOH/hexanes. The mixtures were filtered and analyzed by HPLC. Concentrations of major reaction components were determined according to the calibration curves displayed above.

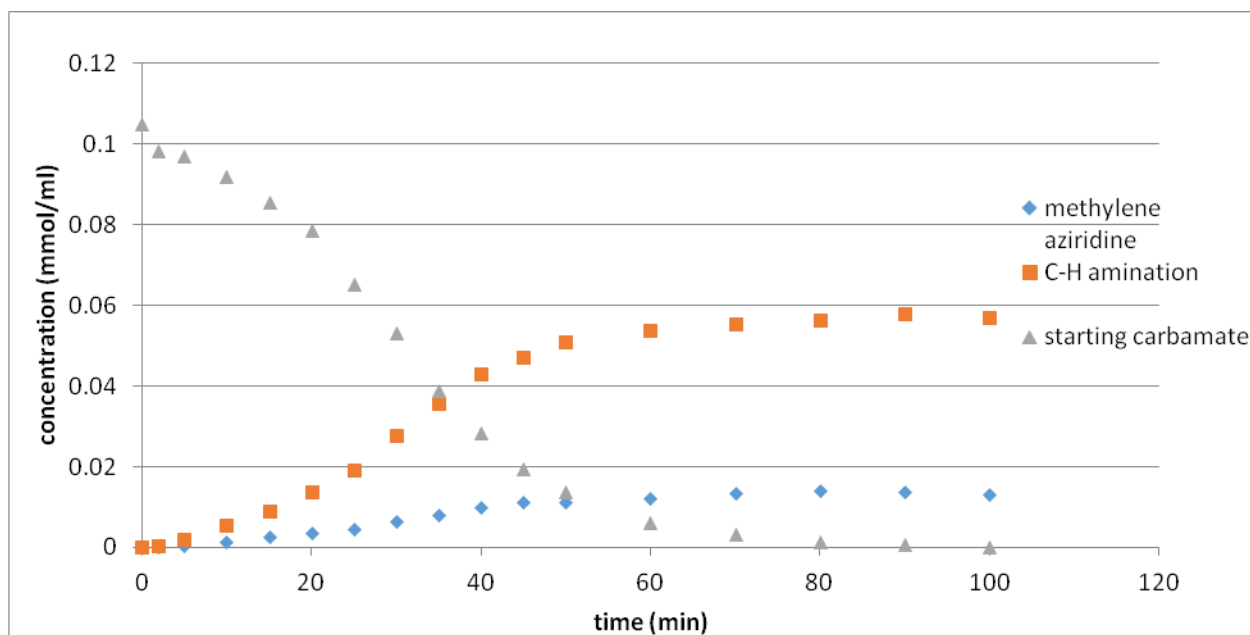
Validation of HPLC-UV-Vis as a method for reaction analysis. Validation of HPLC-UV-Vis as a method of analysis was performed by concentration of HPLC samples attained using the above method. The samples were concentrated, dissolved in approximately 1 ml CDCl₃ and analyzed by ¹H-NMR with a ten second receiver delay. Reasonable agreement between these two methods of analysis confirms HPLC-UV-Vis as a valid method for monitoring these reactions.



Ag-catalyzed amination under standard C-H amination conditions.

Initial conditions: 0.10M carbamate, 0.010M AgOTf, 0.030M 4,4'-di-*t*Bubipyridyl

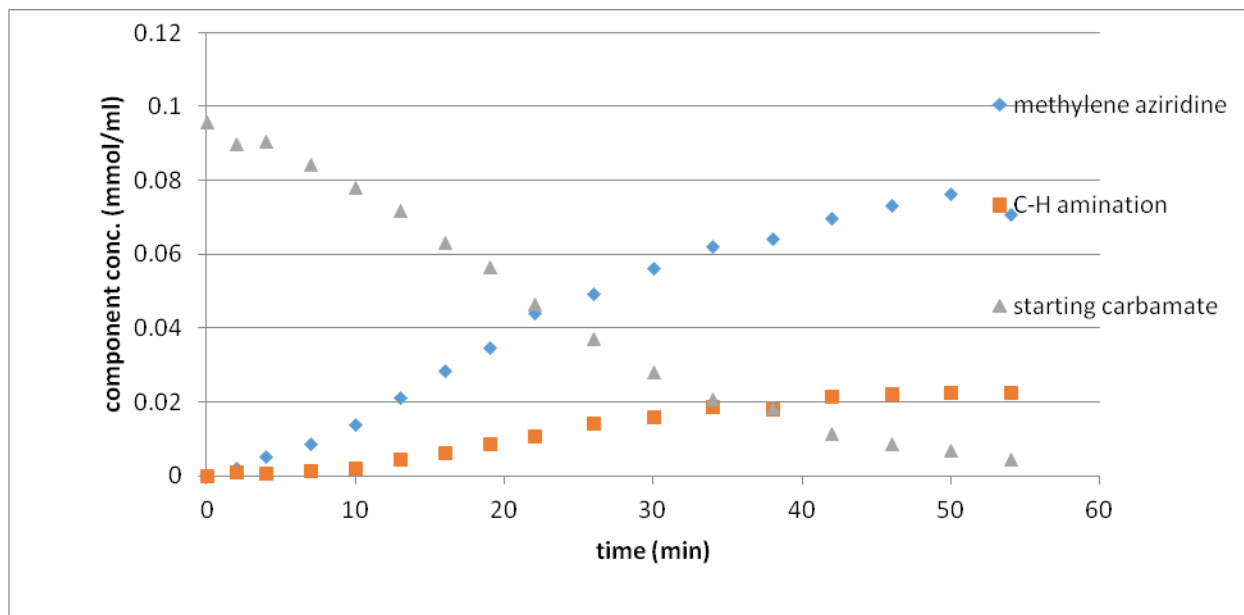
Rate of starting material consumption (calculated from linear regression of starting material curve from 20-80% conversion): 2.4×10^{-3} M/min



Ag-catalyzed amination under standard aziridination conditions.

Initial conditions: 0.10M carbamate, 0.010M AgOTf, 0.0125M 4,4'-di-*t*Bubipyridyl

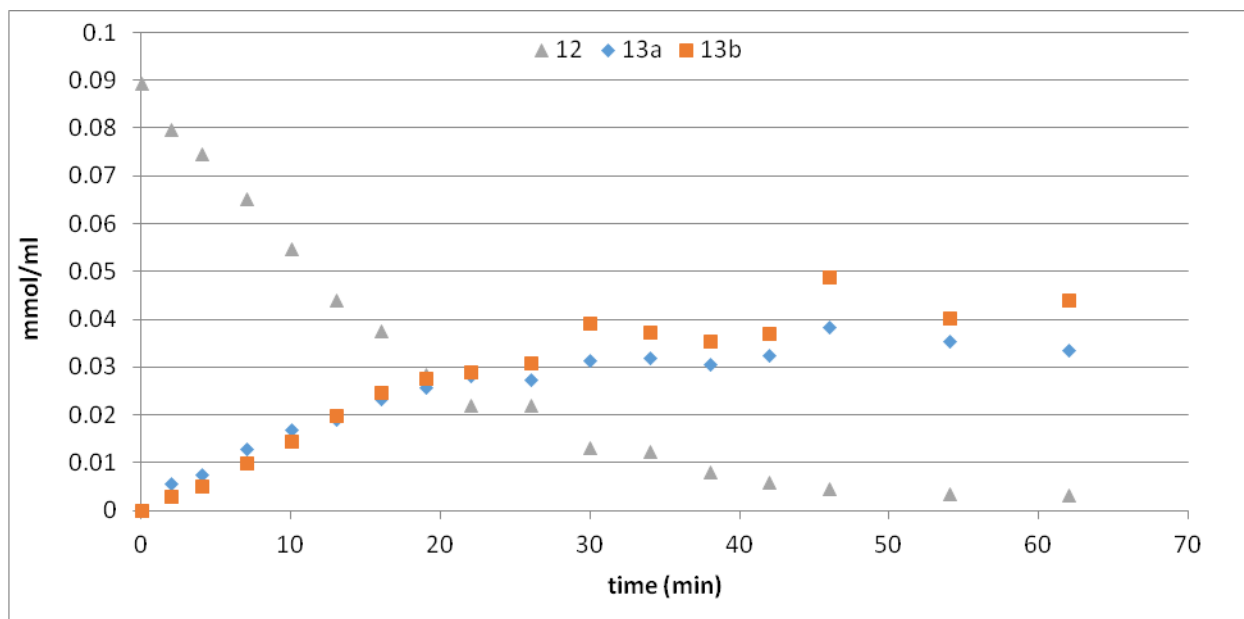
Rate of starting material consumption (20-80% conversion): 2.5×10^{-3} M/min



Portionwise addition of oxidant to C-H amination reaction

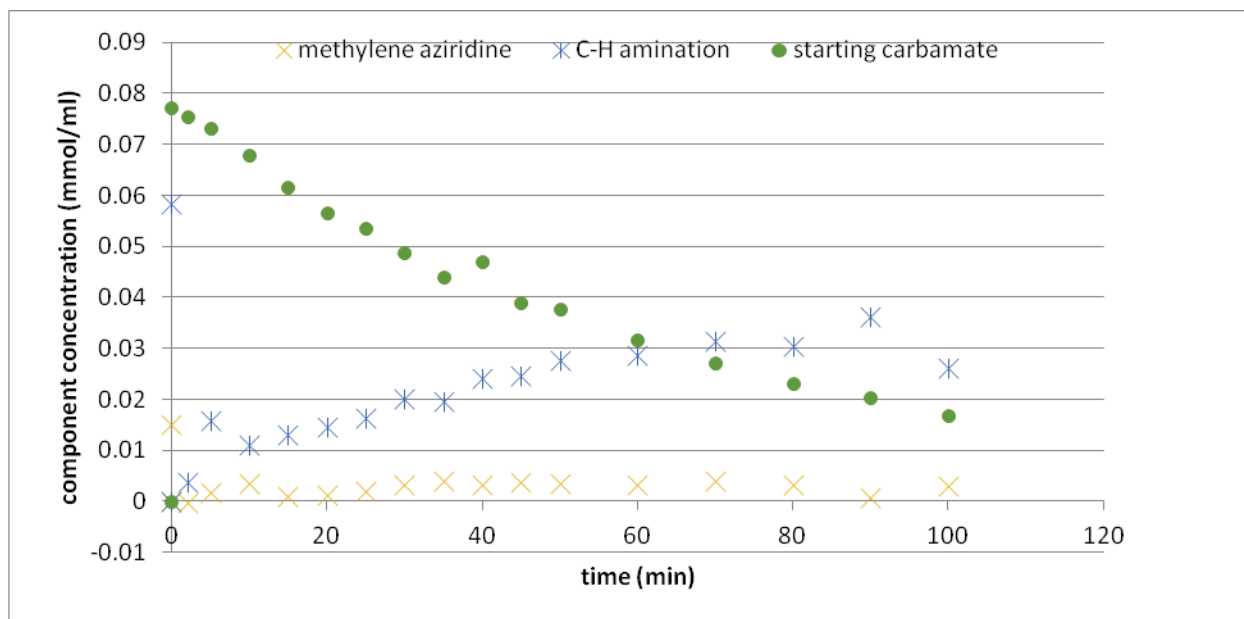
A pre-dried reaction 10 ml round-bottomed flask was charged with silver triflate (0.1 equiv), ligand (1.25 equiv relative to silver triflate), phenanthrene (approx. 0.06M in CH₂Cl₂) and powdered 4A molecular sieves (1g/mmol substrate). Dichloromethane was added and the mixture was stirred vigorously for 15 min. A solution of the carbamate (1 equiv) in dichloromethane (overall 0.1M in substrate) was added to the reaction flask. After two minutes, 3.5 equivalents PhIO were added to the flask. The reaction was stirred for two hours, after which a second charge of 1.0 equivalents carbamate were added, along with 3.5 equivalents PhIO after 30 seconds. The reaction was sampled at regular intervals as described above. The timecourse below shows product quantities formed after this second charge of substrate and oxidant.

Initial rate: 3.1×10^{-3} M/min



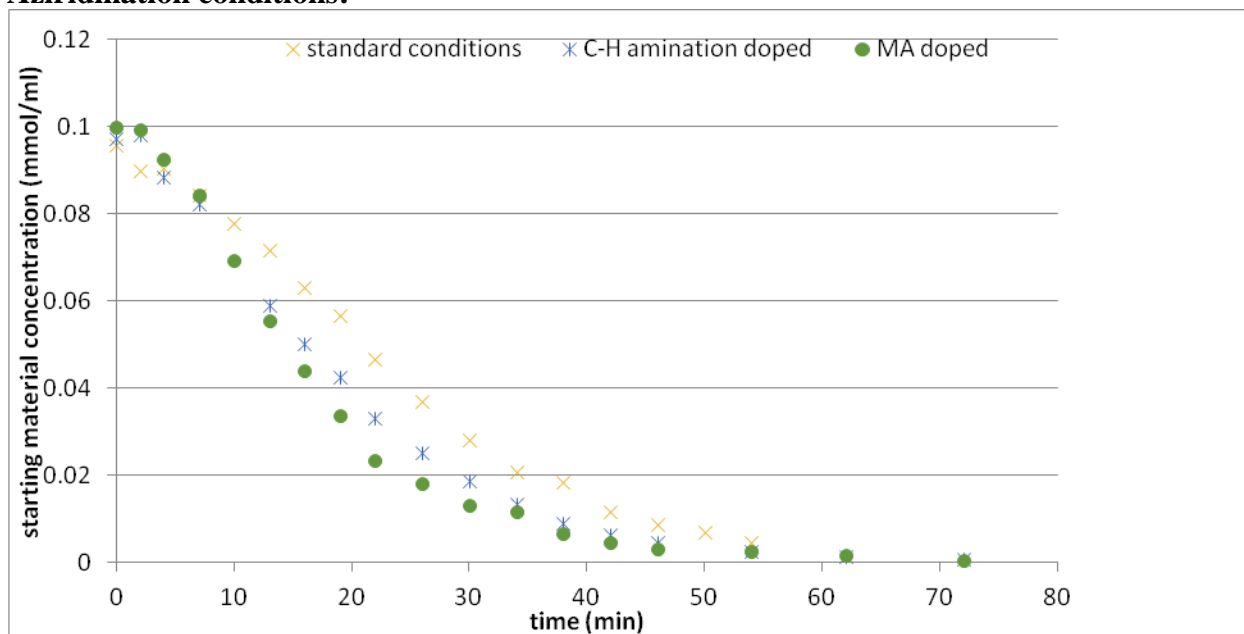
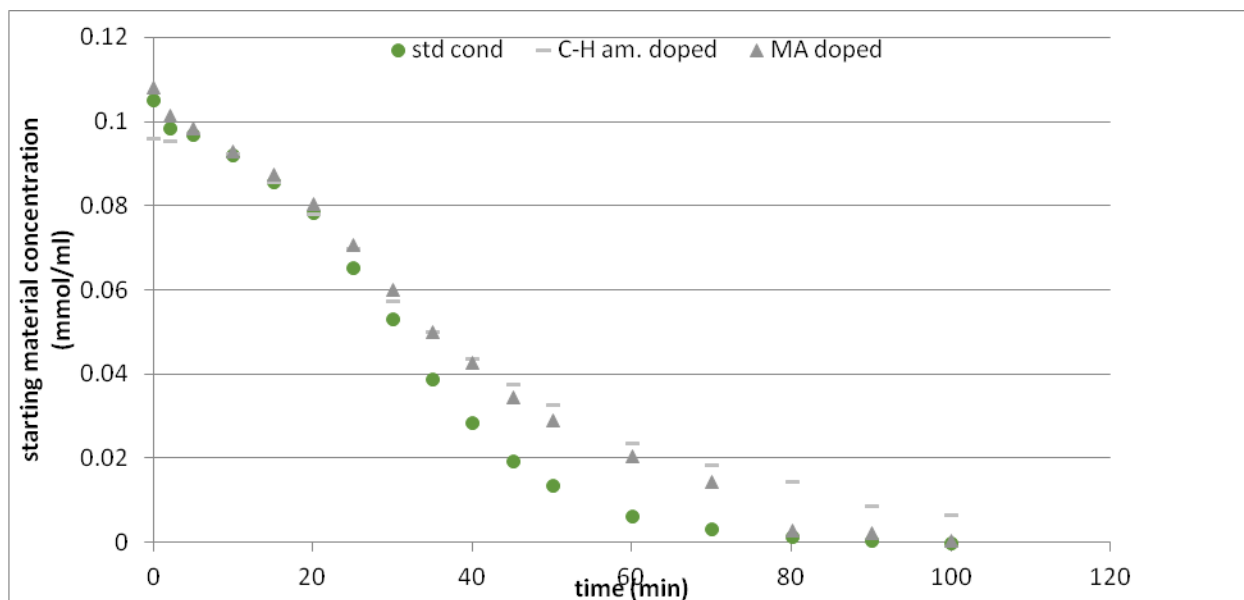
A pre-dried reaction 10 ml round-bottomed flask was charged with silver triflate (0.1 equiv), ligand (3.0 equiv relative to silver triflate), phenanthrene (approx. 0.06M in CH₂Cl₂) and powdered 4A molecular sieves (1g/mmol substrate). Dichloromethane was added and the mixture was stirred vigorously for 15 min. A solution of the carbamate (1 equiv) in dichloromethane (overall 0.1M in substrate) was added to the reaction flask. After two minutes, 3.5 equivalents PhIO were added to the flask. The reaction was stirred for two hours, after which a second charge of 1.0 equivalents carbamate were added, along with 3.5 equivalents PhIO after 30 seconds. The reaction was sampled at regular intervals as described above. The timecourse below shows product quantities formed after this second charge of substrate and oxidant.

Initial Rate: $1.0 \times 10^{-3} \text{M/min}$



Product inhibition studies.

The general procedures for aziridination and C-H amination were followed, but a sufficient amount of methylene aziridine or C-H amination product was added to the reaction to attain a 0.05M concentration. Slight rate acceleration was observed under aziridination conditions, and slight inhibition was observed under the C-H amination conditions. Induction periods were observed in each case, indicating that autocatalysis is not a factor in this reaction.

Aziridination conditions:**C-H amination conditions:****Study of catalysts under oxidative conditions.****Aziridination catalyst system.**

The catalyst was studied under reaction stoichiometrics. A flame-dried 10 ml round bottomed flask was charged with AgOTf (6.4 mg, 0.0250 mmol, 1.0 equiv) and 4,4'-di-*t*Bu-bipyridyl (8.4

mg, 0.0313 mmol, 1.25 equiv), and 2.5 ml CD₂Cl₂, and stirred for 15 minutes. PhIO was added (192 mg, 0.875 mmol, 35 equiv) and the reaction was stirred 2 hours. The solution was filtered *via* microporous frit. ¹H-NMR and ¹³C-NMR spectra were obtained.

The shifts of the 4,4'-di-*t*Bu-bipyridyl peaks compared to a standard catalyst solution indicated a possible decrease in the relative Ag(I):ligand ratio.^{cite our previous paper} This provides evidence of oxidative catalyst degradation.

C-H amination catalyst system.

The catalyst was studied under reaction stoichiometrics. A flame-dried 10 ml round bottomed flask was charged with AgOTf (6.4 mg, 0.0250 mmol, 1.0 equiv) and 4,4'-di-*t*Bu-bipyridyl (20.1 mg, 0.0750 mmol, 3.0 equiv), and 2.5 ml CD₂Cl₂, and stirred for 15 minutes. PhIO was added (192 mg, 0.875 mmol, 35 equiv) and the reaction was stirred 2 hours. The solution was filtered *via* microporous frit. ¹H-NMR and ¹³C-NMR spectra were obtained.

The shifts of 4,4'-di-*t*Bu-bipyridyl were not significantly different from those obtained from a standard catalyst solution.

5.7.4. Rate law for aziridination reaction.

The proposed mechanism for the aziridination reaction follows the scheme:

$$\frac{d[Int2]}{dt} \approx 0 = k_2[Int1][AgLOTf] - k_3[Int2]$$

$$\frac{d[Int1]}{dt} \approx 0 = k_1[RNH_2][PhIO] - k_2[Int1][AgLOTf] - k_{-1}[Int1]$$

$$\frac{d[PhIO]}{dt} \approx 0 = k_a - k_{-a}[PhIO] - k_1[PhIO][RNH_2]$$

Rate of overall product formation:

$$\frac{d[pdt]}{dt} = k_4[Int3] = k_3[Int2] = k_2[Int1][AgLOTf]$$

Substituting into the mass balance equation, we have two options, leading eventually to distinct solutions:

Solution 1:

$$[AgOTf]_o = [AgLOTf] \left(\frac{k_3k_4 + (k_2k_4 + k_2k_3)[Int1]}{k_3k_4} \right)$$

$$[AgLOTf] = \frac{k_3k_4[AgOTf]_o}{k_3k_4 + (k_2k_4 + k_2k_3)[Int1]}$$

Then, the overall rate is given by:

$$\frac{d[pdt]}{dt} = \frac{k_2k_3k_4[AgOTf]_o[Int1]}{k_3k_4 + (k_2k_4 + k_2k_3)[Int1]}$$

Solving the above steady-state equations gives:

$$[Int1] = \frac{k_1[RNH_2][PhIO]}{k_{-1} + k_2[AgLOTf]}$$

$$[PhIO] = \frac{k_a}{k_{-a} + k_1[RNH_2]}$$

Substituting [PhIO] into the expression for [Int1]:

$$[Int1] = \frac{k_a k_1 [RNH_2]}{(k_{-1} + k_2 [AgLOTf]) (k_{-a} + k_1 [RNH_2])}$$

Let:

$$a = k_3k_4[AgOTf]_o$$

$$b = k_3k_4 + (k_2k_4 + k_2k_3)[Int1]$$

So,

$$[AgLOTF] = \frac{a}{b}$$

Then:

$$[Int1] = \frac{k_a k_1 [RNH_2]}{(k_{-1} + k_2 \frac{a}{b})(k_{-a} + k_1 [RNH_2])} = \frac{k_a k_1 [RNH_2] b}{(k_{-1} b + k_2 a)(k_{-a} + k_1 [RNH_2])}$$

$$(k_{-a} + k_1 [RNH_2])(k_{-1} b + k_2 a)[Int1] = k_a k_1 [RNH_2] b$$

Expanding terms containing [Int1]:

$$(k_{-a} + k_1 [RNH_2])(k_{-1}(k_3 k_4 + (k_2 k_4 + k_2 k_3)[Int1])[Int1] + k_2 k_3 k_4 [AgOTf]_o [Int1]) = k_a k_1 [RNH_2] b$$

Assuming $[Int1]^2 \approx 0$,

$$(k_{-a} + k_1 [RNH_2])(k_{-1} k_3 k_4 + k_2 k_3 k_4 [AgOTf]_o)[Int1] = k_a k_1 [RNH_2] (k_3 k_4 + (k_2 k_4 + k_2 k_3)[Int1])$$

$$[Int1] = \frac{k_a k_1 k_3 k_4 [RNH_2]}{(k_{-a} + k_1 [RNH_2])(k_{-1} k_3 k_4 + k_2 k_3 k_4 [AgOTf]_o) - k_a k_1 (k_2 k_4 + k_2 k_3)[RNH_2]}$$

Let:

$$c = k_a k_1 k_3 k_4 [RNH_2]$$

$$d = (k_{-a} + k_1 [RNH_2])(k_{-1} k_3 k_4 + k_2 k_3 k_4 [AgOTf]_o) - k_a k_1 (k_2 k_4 + k_2 k_3)[RNH_2]$$

Then:

$$\begin{aligned} \frac{d[pdt]}{dt} &= \frac{k_2 k_3 k_4 [AgOTf]_o \frac{c}{d}}{k_3 k_4 + (k_2 k_4 + k_2 k_3) \frac{c}{d}} = \frac{k_2 k_3 k_4 [AgOTf]_o c}{k_3 k_4 d + (k_2 k_4 + k_2 k_3) c} = \\ &= \frac{k_2 k_3 k_4 [AgOTf]_o c}{k_3 k_4 d + (k_2 k_4 + k_2 k_3) k_a k_1 k_3 k_4 [RNH_2]} = \frac{k_2 [AgOTf]_o c}{d + (k_2 k_4 + k_2 k_3) k_a k_1 [RNH_2]} = \\ &= \frac{k_a k_1 k_2 k_3 k_4 [AgOTf]_o [RNH_2]}{(k_{-a} + k_1 [RNH_2])(k_{-1} k_3 k_4 + k_2 k_3 k_4 [AgOTf]_o)} = \frac{k_a k_1 k_2 [AgOTf]_o [RNH_2]}{(k_{-a} + k_1 [RNH_2])(k_{-1} + k_2 [AgOTf]_o)} \end{aligned}$$

From the low observed dependence on substrate concentration, we may infer that $k_1 [RNH_2] \gg k_{-a}$, except at low substrate concentration.

Solution 2.

Alternatively, we can defer solving the mass balance equation in terms of $[AgLOTF]$ and $[AgOTf]_o$.

Then, use the following for further substitution:

$$[AgLOTf] = [AgOTf]_o - [Int2] - [Int3] = [AgOTf]_o - [Int2]\left(1 + \frac{k_3}{k_4}\right)$$

Substituting into the steady-state equation for $[Int2]$ gives:

$$\frac{d[Int2]}{dt} \approx 0 = -k_3[Int2] + k_2[Int1][AgOTf]_o - k_2\left(1 + \frac{k_3}{k_4}\right)[Int1][Int2]$$

$$[Int2] = \frac{k_2[Int1][AgOTf]_o}{k_3 + k_2\left(1 + \frac{k_3}{k_4}\right)[Int1]}$$

Now, substituting the expression for $[AgLOTf]$ into the steady state equation for $[Int1]$:

$$\begin{aligned} \frac{d[Int1]}{dt} \approx 0 &= k_1[RNH_2][PhIO] - k_2[Int1][AgLOTf] - k_{-1}[Int1] \\ &= k_1[RNH_2][PhIO] - k_{-1}[Int1] - k_2[AgOTf]_o[Int1] + k_2\left(1 + \frac{k_3}{k_4}\right)[Int1][Int2] \end{aligned}$$

Solving for $[Int1]$:

$$[Int1] = \frac{k_1[RNH_2][PhIO]}{k_2[AgOTf]_o + k_{-1} - k_2\left(1 + \frac{k_3}{k_4}\right)[Int2]}$$

$$\text{Let } a = k_1[RNH_2][PhIO], \quad b = k_2[AgOTf]_o + k_{-1} - k_2\left(1 + \frac{k_3}{k_4}\right)[Int2],$$

So,

$$[Int1] = \frac{a}{b}$$

We now have expressions for $[Int1]$ and $[Int2]$ that can be solved in terms of one another.

$$\begin{aligned} [Int2] &= \frac{k_2[Int1][AgOTf]_o}{k_3 + k_2\left(1 + \frac{k_3}{k_4}\right)[Int1]} = \frac{k_2 \frac{a}{b} [AgOTf]_o}{k_3 + k_2\left(1 + \frac{k_3}{k_4}\right) \frac{a}{b}} = \frac{k_2[AgOTf]_o a}{k_3 b + k_2\left(1 + \frac{k_3}{k_4}\right) a} \\ &= \frac{k_1 k_2 [AgOTf]_o [RNH_2][PhIO]}{k_3(k_2[AgOTf]_o + k_{-1}) + k_1 k_2\left(1 + \frac{k_3}{k_4}\right)[RNH_2][PhIO]} \end{aligned}$$

Now, assuming that $[Int2]^2 \sim 0$, we have:

$$[Int2] = \frac{k_1 k_2 [AgOTf]_o [RNH_2][PhIO]}{k_3(k_2[AgOTf]_o + k_{-1}) + k_1 k_2\left(1 + \frac{k_3}{k_4}\right)[RNH_2][PhIO]}$$

As above, we have:

$$[PhIO] = \frac{k_a}{k_{-a} + k_1[RNH_2]}$$

Let $c = k_{-a} + k_1[RNH_2]$

Then,

$$\begin{aligned} [Int2] &= \frac{k_1 k_2 [AgOTf]_o [RNH_2] (\frac{k_a}{c})}{k_3 (k_2 [AgOTf]_o + k_{-1}) + k_1 k_2 (1 + \frac{k_3}{k_4}) [RNH_2] \frac{k_a}{c}} \\ &= \frac{k_a k_1 k_2 [AgOTf]_o [RNH_2]}{k_3 (k_2 [AgOTf]_o + k_{-1}) (k_{-a} + k_1 [RNH_2]) + k_a k_1 k_2 (1 + \frac{k_3}{k_4}) [RNH_2]} \\ &= \frac{k_a k_1 k_2 k_4 [AgOTf]_o [RNH_2]}{k_3 k_4 (k_2 [AgOTf]_o + k_{-1}) (k_{-a} + k_1 [RNH_2]) + k_a k_1 k_2 (k_3 + k_4) [RNH_2]} \end{aligned}$$

Substituting into the rate equation gives us:

$$\frac{d[pdt]}{dt} = \frac{k_a k_1 k_2 k_3 k_4 [AgOTf]_o [RNH_2]}{k_3 k_4 (k_2 [AgOTf]_o + k_{-1}) (k_{-a} + k_1 [RNH_2]) + k_a k_1 k_2 (k_3 + k_4) [RNH_2]}$$

The two solutions differ in the choice of approximation. Either $[Int1]^2 \sim 0$ or $[Int2]^2 \sim 0$. The preferred solution is solution two, as demonstrated by the inclusion of an isotopically sensitive term, and by the demonstration that **Int1** must obtain significant concentration before steady-state is attained.

The derived rate law for C-H amination is the same.

Chapter 6. Development of Enantioselective Silver (I)-Catalyzed Intramolecular Aziridinations.

6.1. Introduction.

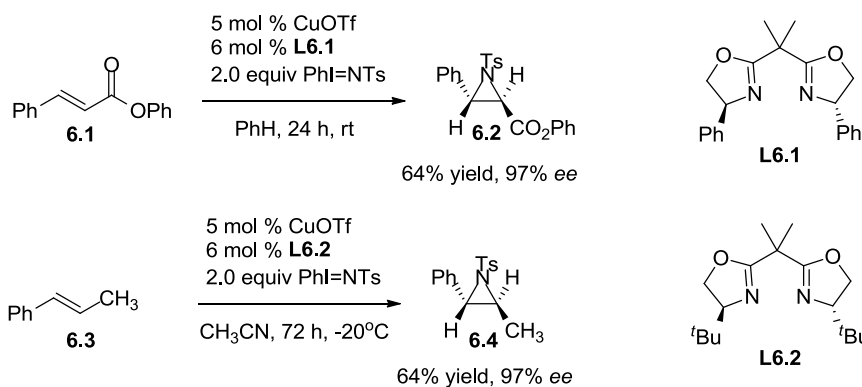
Asymmetric epoxidation is a highly developed, studied, and utilized tool for the construction of stereodefined carbon-heteroatom bonds. The nitrogen analog, asymmetric aziridination, is comparatively underdeveloped. The many reports of asymmetric aziridination are limited by one or more of the following problems: narrow substrate scope, modest enantioselectivity, or synthetically imposing catalysts. However, reliable, general methods of asymmetric aziridination would greatly reduce the difficulty of synthesizing versatile building blocks containing stereodefined carbon-nitrogen bonds. This chapter describes early and ongoing efforts to develop methods of enantioselective silver(I)-catalyzed intramolecular aziridination. The best results to date feature excellent yield and good enantioselectivities for both *cis*- and *trans*-disubstituted alkenes. This method features synthetically accessible, tunable bisoxazoline ligands, making it particularly attractive for general use. Further improvements will focus on the synthesis of new bisoxazoline ligands with increased steric bulk.

6.2. Highly enantioselective methods of alkene aziridination *via* nitrene transfer.

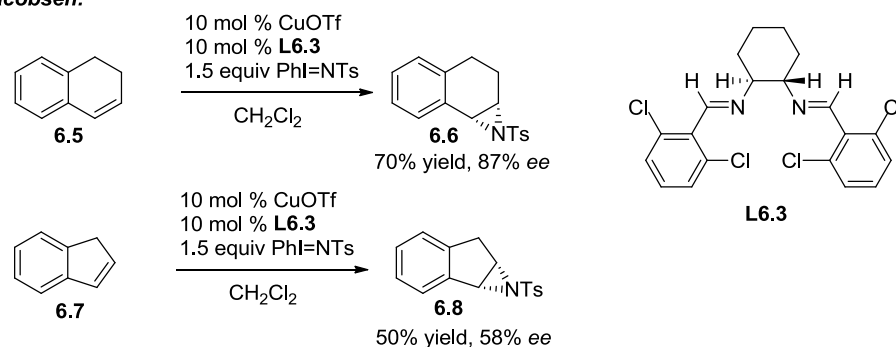
Numerous methods of catalytic enantioselective aziridination have been reported, but few, if any, have achieved widespread use. As two recent reviews describe the field in comprehensive detail, this chapter will present only a few illustrative examples.^{1,2} In the early 1990s, Evans³ and Jacobsen⁴ simultaneously reported enantioselective intermolecular aziridinations using Cu catalysts and PhI=NTs as the nitrogen source. Evans's method in particular serves to illustrate the promise and problems associated with enantioselective aziridination (Scheme 6.1). With *trans*-cinnamyl ester **6.1**, 97% *ee* was obtained; however, *trans*- β -methyl styrene **6.3** afforded only 70% *ee*, and required a different ligand to obtain optimal enantioselectivity. Jacobsen's method suffered from similar limitations in substrate scope.

Scheme 6.1. Intermolecular aziridination with chiral copper catalysts.

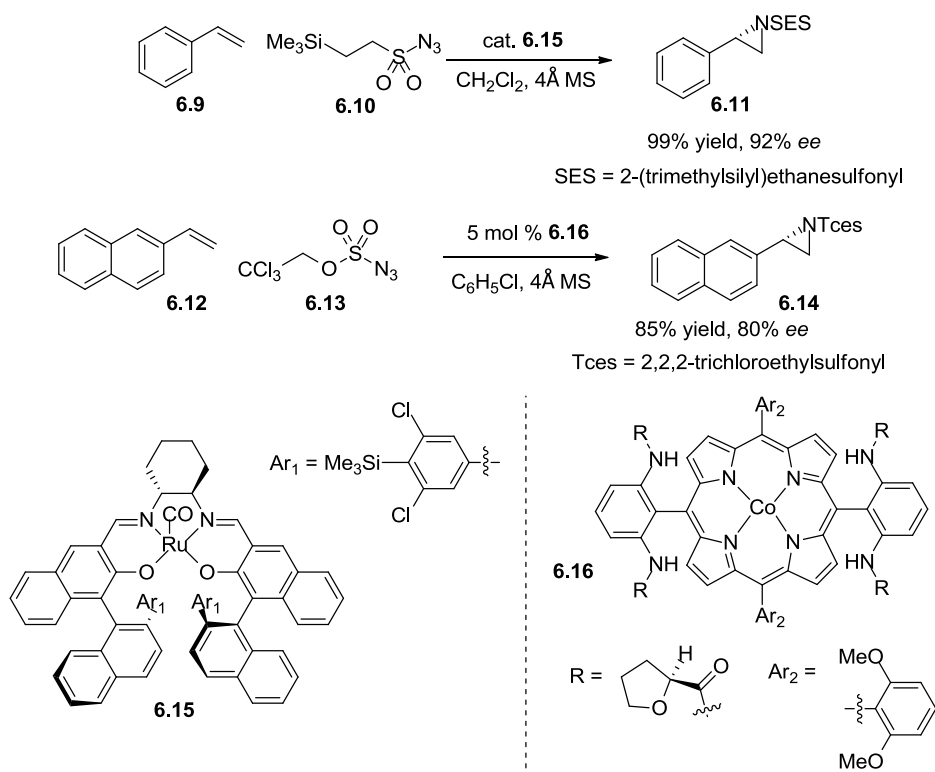
Evans:



Jacobsen:

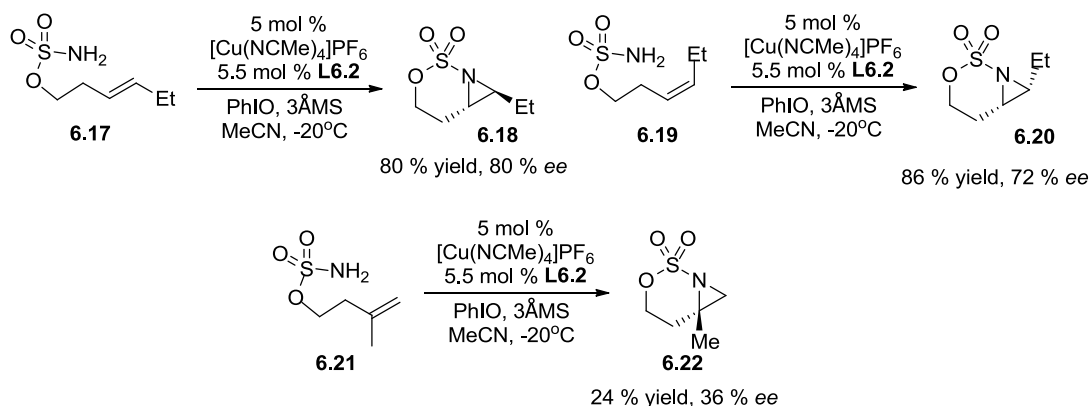


To date, the highest selectivities in intermolecular aziridination have been obtained using azides as the nitrogen sources. Katsuki and co-workers have developed complex Ru-salen catalysts for the aziridination of terminal olefins with azides.^{5a-f} The development of 2-(trimethylsilyl)ethanesulfonyl azide (SESN₃) as the nitrogen source has provide *ee* that is regularly > 95%, as well as high yields and broad substrate scope (Scheme 6.2). The method, is however, limited to terminal olefins and vinyl ketones,^{5e} and the high molecular weight and synthetic challenges associated with the catalyst limit its overall appeal. Zhang and co-workers have also developed Co-porphyrin complexes that provide high enantioselectivities for azides, but these methods have similar limitations in scope and accessibility and often feature low product yields.⁶

Scheme 6.2. Intermolecular aziridinations using azides as nitrogen sources.

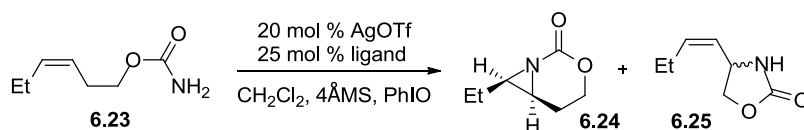
Asymmetric intramolecular aziridination is perhaps even more difficult to achieve. Dauban and co-workers have reported the most successful version to date, attaining moderate enantioselectivities in Cu-catalyzed aziridinations with sulfamates (Scheme 6.3).⁷ For *trans*-alkene **6.17**, 80% *ee* was attained, 72% *ee* for the *cis*-analog **6.19**, but only 36% *ee* for the 1,1'-disubstituted alkene **6.21**. The utility of the products of intramolecular alkene aziridination is well established, such that the development of reliable methods for enantioselective aziridination would significantly improve chemists' ability to access stereochemically-complex nitrogen-containing molecules.

Scheme 6.3. Copper-catalyzed enantioselective intramolecular aziridinations.

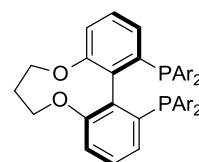
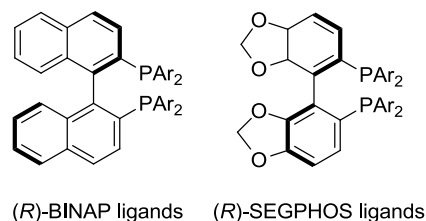


6.3. Development of silver(I)-catalyzed asymmetric aziridination.

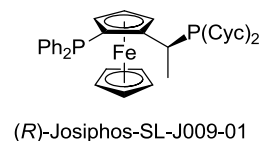
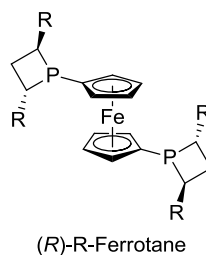
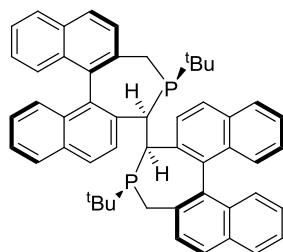
As part of our efforts toward this goal, we have sought to develop a general method of enantioselective silver(I)-catalyzed intramolecular aziridination. While many asymmetric transformations have been developed using silver-based chiral Lewis acids,⁸ to the best of our knowledge, no asymmetric group transfer reactions catalyzed by silver have been reported. Initially, we examined commercially-available chiral ligands with AgOTf as catalysts for the transformation (Table 6.1). Chiral bisphosphine ligands gave promising *ee* for aziridination of *cis*-alkene **6.23**. (*R*)-H₈ BINAP, (*R*)-TUNEPHOS, (*R*)-BINAPINE each gave *ee* over 40% (entries 4, 6, and 7). However, ³¹P-NMR of the product mixtures indicated that the ligands were completely oxidized to the corresponding phosphine oxides over the course of the reaction. The catalytic activities of the phosphine oxides were not determined.

Table 6.1. Bisphosphine ligands as potential catalysts for Ag(I)-catalyzed aziridination.

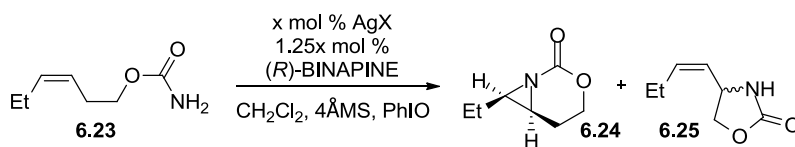
entry ^a	ligand	yield 6.24	yield 6.25	%ee 6.24
1	none	31	8	NA
2	(<i>R</i>)-T BINAP	69	7	37
3	(<i>R</i>)-DM BINAP	51	3	27
4	(<i>R</i>)-H ₈ BINAP	39	0	42
5	(<i>R</i>)-SEGPHOS	73	5	15
6	(<i>R</i>)-BINAPINE	46 ^b	0	57
7	(<i>R</i>)-TUNEPHOS	46	0	47
8	(<i>R</i>)-DTBM SEGPHOS	57	0	-7
9	(<i>R</i>)-Et-Ferrotane	0	0	NA
10	(<i>R</i>)-iPr-Ferrocene	19	0	NA
11	(<i>R</i>)-Josiphos-SL-J009-01	51	32	17



^aExperiments run with 0.1M 6.23, 2.0 equiv PhIO, 1g 4ÅMS/mmol 6.23, 24 hrs. ^b88% conversion after 40 hours.



Nevertheless, the complex bisphosphine (*R*)-BINAPINE⁹ showed promising enantioselectivity and was selected for further optimization efforts (Table 6.2). To our delight, replacing the OTf ion with ClO₄⁻ improved the *ee* from 57 to 68%, and provided full conversion of the starting material with 68% yield (entry 3). Completely noncoordinating ions such as BF₄⁻ and SbF₆⁻ provided low conversion and yields (entries 2 and 4). Decreasing the catalyst loading decreased both yield and enantioselectivity. Lowering the temperature to 0°C lowered conversion and did not significantly improve the enantioselectivity (entry 7). Given the lack of tunability of this ligand, we turned our attention to other classes.

Table 6.2. Optimization of aziridination conditions using (*R*)-BINAPINE.

entry ^a	Ag salt	yield 6.24	yield 6.25	%ee 6.24
1	20 mol % AgOTf	46	0	57
2	20 mol % AgBF ₄	12	0	NA
3	20 mol % AgClO ₄	68	0	68
4	20 mol % AgSbF ₆	26	0	NA
5	15 mol % AgClO ₄	56 ^b	4	60
6	10 mol % AgClO ₄	0 ^c	0	NA
7 ^d	20 mol % AgClO ₄	33	0	72

^aExperiments run with 0.1M **6.23**, 2.0 equiv PhIO, 1g 4ÅMS/mmol **6.23**, 24 hrs. ^b82% conversion after 41 hours. ^c29% conversion after 41 hours. ^dRun at 0°C for 48 hours.

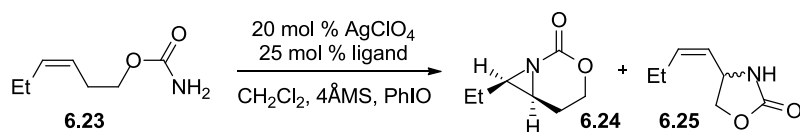
Among chiral bidentate nitrogenated ligands, (*R*)-BINAM did not provide any conversion (entry 1), while chiral diimines provided low conversion and minimal enantioselectivity (entry 2). However, *i*Pr-bisoxazoline ligand **L6.5** gave good yield of the aziridine product, and some enantioselectivity (entry 3). Replacing the isopropyl group with phenyl, benzyl, and then *tert*-butyl groups afforded improvements in the enantioselectivity (entries 4-6).

Table 6.3. Examination of chiral bidentate nitrogen-containing ligands.

entry ^a	Ag salt	yield 6.24	yield 6.25	%ee 6.24
1	(<i>R</i>)-BINAM	30	14	NA
2	L6.4	42	11	6
3	<i>i</i> Pr-bisoxazoline L6.5	81	11	23
4	Ph-bisoxazoline L6.1	46	7	16
5	Bn-bisoxazoline L6.6	77	6	45
6	<i>t</i> Bu-bisoxazoline L6.2	78	11	48

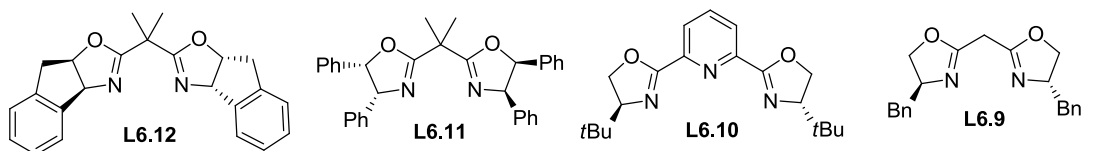
^aExperiments run with 0.1M **6.23**, 2.0 equiv PhIO, 1g 4ÅMS/mmol **6.23**, 24 hrs. ^b82% conversion after 41 hours. ^c29% conversion after 41 hours. ^dRun at 0°C for 48 hours.

We then examined modifications to the ligand scaffold. Removing the bridge decreased both enantio- and chemo-selectivity (entry 1), while removing the *gem*-demethyl groups decreased conversion and enantioselectivity (entry 2). Using pybox ligand **L6.10** provided no conversion to product, while the quinoline-oxazoline ligand **L6.7** provided little enantioselectivity. Ligands with additional chiral centers decreased both conversion and enantioselectivity (entries 6 and 7). Use of an sulfamate substrate gave full conversion of starting material, but essentially no yield of identifiable product with **L6.6**, presumably due to the enhanced susceptibility of the product to ring-opening reactions.

Table 6.4. Bisoxazoline scaffold modifications.

entry ^a	ligand	% conversion	% 6.24	% 6.25	% <i>ee</i> 6.24
1	L6.6	100	77	6	45
2	L6.7	74	28	12	1
3	L6.8	77	23	31	26
4	L6.9	100	81	10	20
5	L6.10	0	0	0	NA
6	L6.11	64	24	0	-28
7	L6.12	88	71	6	32

^aExperiments run with 0.1M **6.23**, 2.0 equiv PhIO, 1g 4ÅMS/mmol **6.23**, 24 hrs. ^b82% conversion after 41 hours. ^c29% conversion after 41 hours. ^dRun at 0°C for 48 hours.



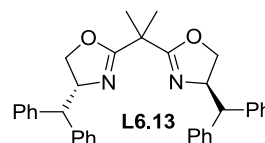
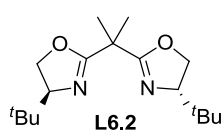
Given the superior performance of the standard bisoxazoline scaffold, we sought to optimize other aspects of the transformation for a single ligand, then examine ligands with more sterically demanding substituents (Table 6.5). The reaction performed well at reduced catalyst loading, though the improved selectivity was likely a function of higher batch substrate in this trial (entry 1).¹⁰ Examining several counterions for the transformation showed that OTf provided the highest enantioselectivity (entries 2-4). Finally, the dibenzyl-substituted ligand **L6.13** was synthesized and tested with OTf as the counterion, and provided -81% *ee* in the transformation.

Table 6.5. Further optimization of enantioselective intramolecular aziridination.

entry	Ag salt	ligand	% 6.24	% 6.25	% ee 6.24	entry	Ag salt	ligand	% 6.27	% C-H	% ee 6.27
1	AgClO ₄	L6.2	78 ^a	11	58	1	AgClO ₄	L6.2	43	4	75
2	AgOTf	L6.2	63	10	67	2	AgOTf	L6.2	14 ^a	3	NA
3	AgSbF ₆	L6.2	83	8	40	3	AgSbF ₆	L6.2	83	8	80
4	AgOAc	L6.2	29 ^b	16	6	4	AgClO ₄	L6.2	45 ^b	4	76
5	AgOTf	L6.13	86	6	-81	5	AgClO ₄	L6.13	88	10	-83

^aYields determined by NMR using a mesitylene standard. ^b45% conversion after 20 hours.

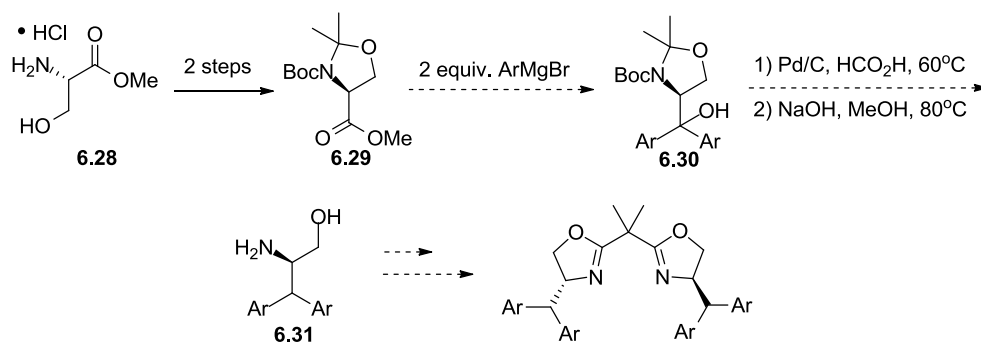
^a58% conversion after 20 hours.
^bIsolated yield.



To our delight, simultaneous optimization of *trans* alkene **6.26** afforded even higher enantioselectivities, as summarized in table 6.5. Surprisingly, AgOTf afforded poor results for this substrate, while decreased yield was observed for AgClO₄ with the *tert*-butyl substituted ligand. However, using the dibenyl ligand **L6.12** provided high 83% *ee*. The higher yield obtained with this ligand is somewhat unexpected, but was reproduced in subsequent trials.

Investigations of this system are ongoing, and will include both the synthesis of new ligands, and the further optimization of counterion and temperature. The method for the synthesis of the amino alcohol required to obtain the dibenyl ligand should be adaptable to other aryl substituents, including naphthyl and *o*-tolyl groups (Scheme 6.4).¹¹ These ligands will likely enhance *ee* to the threshold of 90% that marks high synthetic utility.

Scheme 6.4. Synthesis of novel amino alcohols.



6.4. Conclusions.

The above investigations have led to the development of a promising catalyst system for intramolecular aziridination. The preferred ligand scaffold is readily accessible and is relatively easy to modify to include bulkier substituents. The high enantioselectivity observed with both *cis*- and *trans*-substituted alkenes indicates that the method may be quite general. Additionally, the ease of substrate preparation makes this a particularly attractive method for broad use. Further investigations will focus on reaction optimization and the demonstration of substrate scope. One significant question that arose in the course of these studies was the applicability of “dynamic catalysis” to asymmetric transformations. Unfortunately, the addition of further equivalents of ligand to the catalyst systems shut down all reactivity. However, application of this system to asymmetric C-H aminations has not yet been attempted. In all, this is a promising system that may represent both the first highly enantioselective asymmetric intramolecular aziridination, and the first instance of an asymmetric group transfer reaction catalyzed by silver.

6.5. Notes and References.

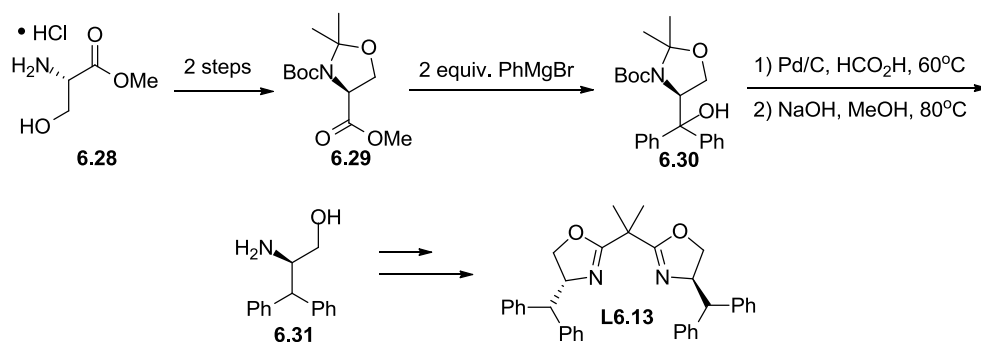
1. Degennaro, L.; Trinchera, P; Luisi, R. *Chem. Rev.* **2014**, *114*, 7881.
2. Pellissier, H. *Tetrahedron*, **2010**, *66*, 1509.

3. Evans, D. A.; Faul, M. M.; Bilodeau, M. T.; Anderson, B. A.; Barnes, D. M. *J. Am. Chem. Soc.* **1993**, *115*, 5328.
4. Li, Z.; Conser, K. R.; Jacobsen, E. N. *J. Am. Chem. Soc.* **1993**, *115*, 5326.
5. a) Omura, K.; Murakami, M.; Uchida, T.; Irie, R.; Katsuki, T. *Chem. Lett.* **2003**, *32*, 354.
b) Omura, K.; Uchida, T.; Irie, R.; Katsuki, T. *Chem. Commun.* **2004**, 2060. c) Kawabata, H.; Omura, K.; Katsuki, T. *Tetrahedron Lett.* **2006**, *47*, 1571. d) Kawabata, H.; Omura, K.; Uchida, T.; Katsuki, T. *Chem. Asian. J.* **2007**, *2*, 248. e) Fukunaga, Y.; Uchida, T.; Ito, Y.; Matsumoto, K.; Katsuki, T. *Org. Lett.* **2012**, *14*, 4658. f) Kim, C.; Uchida, T.; Katsuki, T. *Chem. Commun.* **2012**, 48, 7188.
6. a) Jones, J. E.; Ruppel, J. V.; Gao, G.-Y.; Moore, T. M.; Zhang, X. P. *J. Org. Chem.* **2008**, *73*, 7260. b) Subbarayan, V.; Ruppel, J. V.; Zhu, S.; Perman, J. A.; Zhang, X. P. *Chem. Commun.* **2009**, 4266. c) Jin, L.-M.; Lu, H.; Cui, X.; Wojtas, L.; Zhang, X. P. *Angew. Chem. Int. Ed.* **2013**, *52*, 5309.
7. Esteoule, A.; Duran, F.; Retailleau, P.; Dodd, R. H.; Dauban, P. *Synthesis* **2007**, 1251.
8. Naodovis, M.; Yamamoto, H. *Chem. Rev.* **2008**, *108*, 3132.
9. Tang, W.; Wang, W.; Chi, Y.; Zhang, X. *Angew. Chem. Int. Ed.* **2003**, *42*, 3509.
10. The presence of as little as 3 mol % trichloroacetamide, a common impurity arising from the synthesis of the carbamate substrate, prevented the reaction from occurring. Since this discovery, a standard protocol for removal of this impurity has been adopted for carbamate synthesis.
11. Nunez, M. G.; Farley, A. J. M.; Dixon, D. *J. Am. Chem. Soc.* **2013**, *135*, 16348.
12. Dalko, P. I.; Moisan, L.; Cossy, J. *Angew. Chem. Int. Ed.* **2002**, *41*, 625.

13. Evans, D. A.; Peterson, G. S.; Johnson, J. S.; Barnes, D. M.; Campos, K. R.; Woerpel, K. *A. J. Org. Chem.* **1998**, *63*, 4541.
14. Zhang, Y.; Sigman, M. S. *J. Am. Chem. Soc.* **2007**, *129*, 3076.
15. Denmark, S. E.; O'Connor, S. P. *J. Org. Chem.* **1997**, *62*, 3375.
16. Bandini, M.; Bernardi, F.; Bottoni, A.; Cozzi, P. G.; Miscione, G. P.; Umani-Ronchi, A. *Eur. J. Org. Chem.* **2003**, *15*, 2972.
17. Schaus, S. E.; Jacobsen, E. N. *Org. Lett.* **2000**, *7*, 1001.
18. Bovino, M. T.; Chemler, S. R. *Angew. Chem. Int. Ed.* **2012**, *51*, 3923.
19. Kanemasa, S.; Adachi, K.; Yamamoto, H.; Wada, E. *Bull. Chem. Soc. Jap.* **2000**, *73*, 681.

6.6. Experimental Details and Characterization.

Carbamates **6.24** and **6.26** were synthesized according to procedures described in chapter 3. All bisphosphine ligands were purchased from Sigma-Aldrich or Alfa Aesar and used without further purification. Ligand **L6.4** was synthesized according to the procedure of Cossy and co-workers.¹² Ligands **L6.1**, **L6.2**, **L6.5**, and **L6.6** were synthesized according to the general procedure of Evans and co-workers.¹³ **L6.7** was synthesized according to the procedure of Sigman and Zhang.¹⁴ **L6.8** was synthesized according to the procedure of Denmark and O'Connor.¹⁵ **L6.9** was synthesized according to the procedure of Umani-Ronchi and co-workers.¹⁶ **L6.10** was synthesized according to the procedure of Schaus and Jacobsen.¹⁷ **L6.11** and **L6.12** were synthesized according to the method of Bovino and Chemler.¹⁸



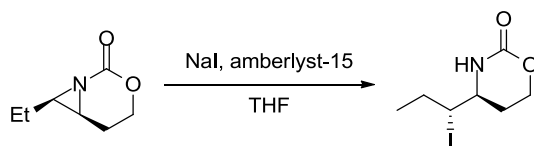
Procedure for synthesis of ligand L6.13: The method of Dixon and co-workers¹¹ was used to obtain alcohol **6.30**. From here, their procedure was adapted as follows. A 250 ml Schlenk flask was charged with formic acid (81 ml), Pd(OH)₂ (50% wet, 600 mg, 40% of substrate mass), and alcohol **6.30** (1.50 g, 3.90 mmol, 1.0 equiv). A vacuum was attached to the arm of the Schlenk flask with the stopcock closed. The mixture was stirred and a balloon of hydrogen was attached using a scintered gas adapter with stopcock. The balloon was opened to the flask for 30 seconds, and the stopcock was then closed. The valve was opened to vacuum and evacuated for 30 seconds, then closed and the flask was re-filled with hydrogen. This cycle was repeated three times. The stopcock to the hydrogen source was closed, and the balloon was removed. The flask was placed in an oil bath and heated to 60°C for 18 hours. The reaction was monitored by cooling to room temperature and removal of aliquots from the sidearm of the Schlenk flask. Aliquots were concentrated and analyzed by NMR.

After completion, the reaction was cooled to room temperature, diluted with 81 ml H₂O, and extracted three times with CH₂Cl₂. The organic layer was washed repeatedly with aq. NaHCO₃ until neutral, then dried over Na₂SO₄ and concentrated *in vacuo*. To the product was added 50 ml H₂O, 50 ml MeOH, and 1.50 g NaOH. A reflux condenser was attached, and the reaction refluxed at 80°C under air for 12 hours. The reaction was then cooled to room temperature and the MeOH was removed *in vacuo*. The aqueous layer was extracted three times

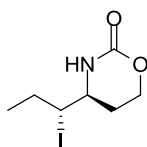
with a 3:1 mixture of CHCl_3 :*i*PrOH. The organic layers were dried over MgSO_4 , then filtered and concentrated *in vacuo*. The approximate purity of the resulting amino alcohol was determined by NMR analysis of a small sample of known mass with mesitylene as internal standard. The crude mixture was immediately used according to the procedures described by Wada and co-workers.¹⁹

General procedure for asymmetric aziridination: Reactions were typically performed using 0.200 mmol carbamate substrate. A 10 ml, flame-dried round bottomed flask was charged with 0.2 equiv of a silver salt, 0.25 equivalents of the appropriate ligand, and sufficient volume of dichloromethane to attain a solution 0.1 M in substrate. The solution was stirred for 15 minutes, after which 4Å molecular sieves were added (1 g MS/mmol substrate). After another five minutes, 1.0 equiv carbamate were added. After another two minutes, 2.0 equivalent iodobenzene was added. The mixture was stirred at room temperature and monitored by TLC. Upon completion, the crude mixture was filtered through a glass frit, which was washed with several portions dichloromethane, and the solution was concentrated *in vacuo*. Crude reaction mixtures were analyzed by NMR using mesitylene as the internal standard. The crude mixture could be purified using flash chromatography on silica with a 0 to 40% EtOAc/hexanes gradient. For screening reactions, the crude mixture was directly subjected to the ring-opening described below.

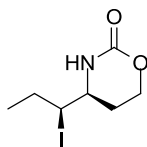
Aziridines **6.24** and **6.27** were synthesized according to this procedure. Analytical data was found to be in agreement with that reported in chapter 3.



General procedure for ring-opening of aziridine products: A 10 ml round-bottomed flask, was charged with the aziridine and THF (0.1 M in substrate), followed by NaI (2.0 equiv) and amberlyst-15 (1.5 mg/mg substrate). The reaction was stirred at room temperature for 4 hours, and monitored by TLC. Upon completion, the reaction was diluted with an equal volume of EtOAc and quenched with aqueous NH₄Cl. Layers were separated and the aqueous layer was extracted three times with EtOAc. The combined organic layers were dried over Na₂SO₄, filtered and concentrated *in vacuo*. The mixture could be analyzed directly by HPLC (*vide infra*), or purified *via* flash chromatography on silica gel using a 0 to 90% EtOAc/hexane gradient with 15% increments.



Compound S6.1. Obtained in 90% yield from **6.24** according to the general procedure above. ¹H NMR (500 MHz, CDCl₃) δ 5.36 (br s, 1H), 4.34 (dt, *J* = 11.4, 3.8 Hz, 1H), 4.21 (td, *J* = 11.4, 2.4 Hz, 1H), 3.95 (ddd, *J* = 8.9, 7.0, 4.0 Hz, 1H), 3.55 (ddd, *J* = 10.3, 7.0, 5.1 Hz, 1H), 2.18-2.12 (m, 1H), 1.92-1.75 (overlapping multiplets, 3H), 1.12 (t, *J* = 7.2 Hz). ¹³C NMR (126 MHz, CDCl₃) δ 153.78, 65.24, 56.55, 44.29, 29.07, 14.33. HRMS (ESI) *m/z* calculated for [C₇H₁₂INO₂+H⁺] 269.9986, found 269.9987.



Compound S6.2. Obtained in 90% yield from **6.27** according to the general procedure above. ¹H NMR (500 MHz, Chloroform-*d*) δ 6.48 (br s, 1H), 4.41(dt, *J* = 11.3, 4.1 Hz, 1H), 4.24 (dt, *J* = 11.3, 6.6 Hz, 1H), 4.08 (dt, *J* = 9.3, 4.6 Hz, 1H), 3.34 (q, *J* = 6.6 Hz, 1H), 2.06 (td, *J* = 6.6, 4.1

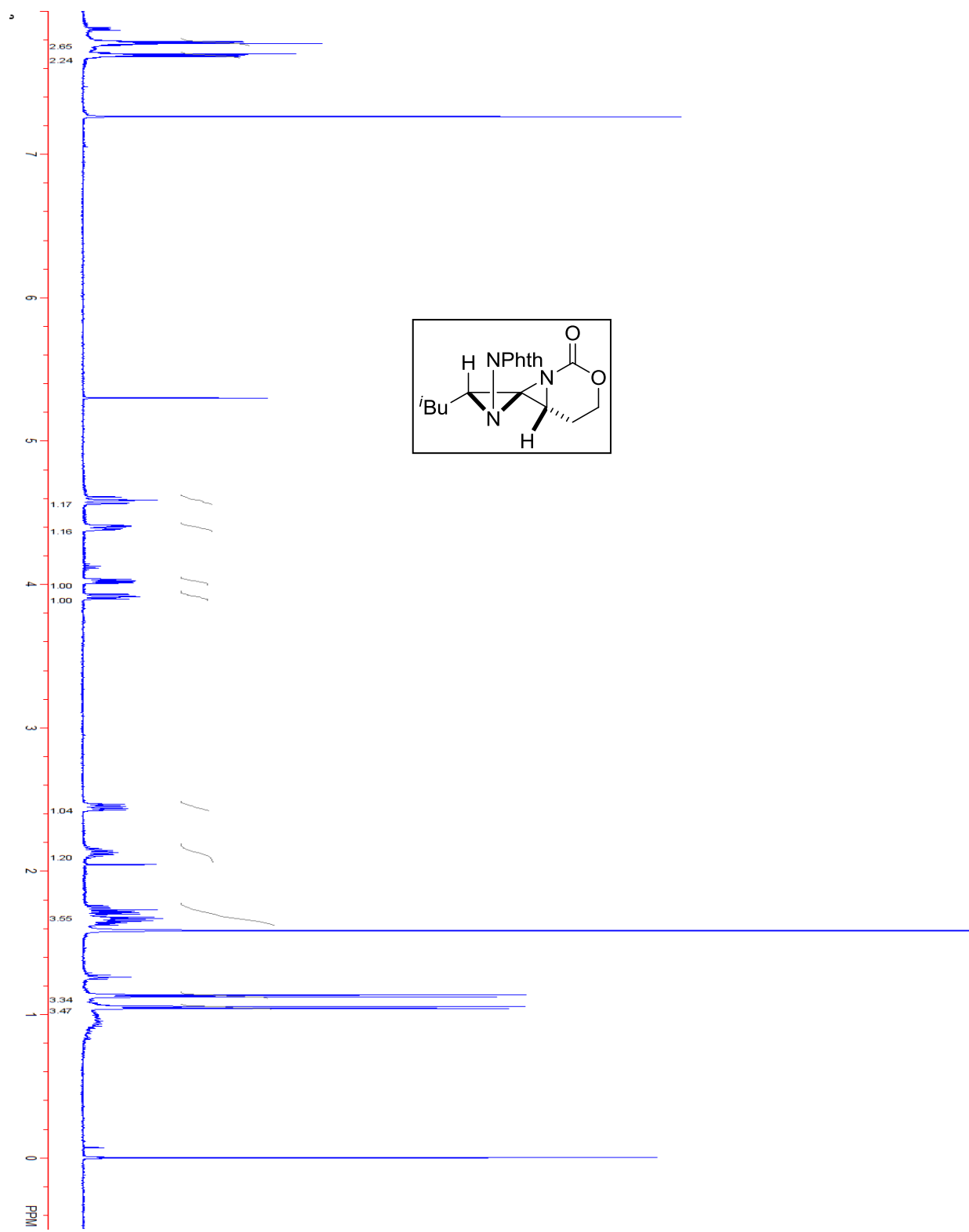
Hz, 2H), 1.89 – 1.73 (m, 2H), 1.09 (t, $J = 7.2$ Hz, 3H). ^{13}C NMR (126 MHz, CDCl_3) δ 154.58, 64.98, 55.54, 44.32, 31.14, 28.86, 26.89, 14.58.

Analysis of enantioinduction.

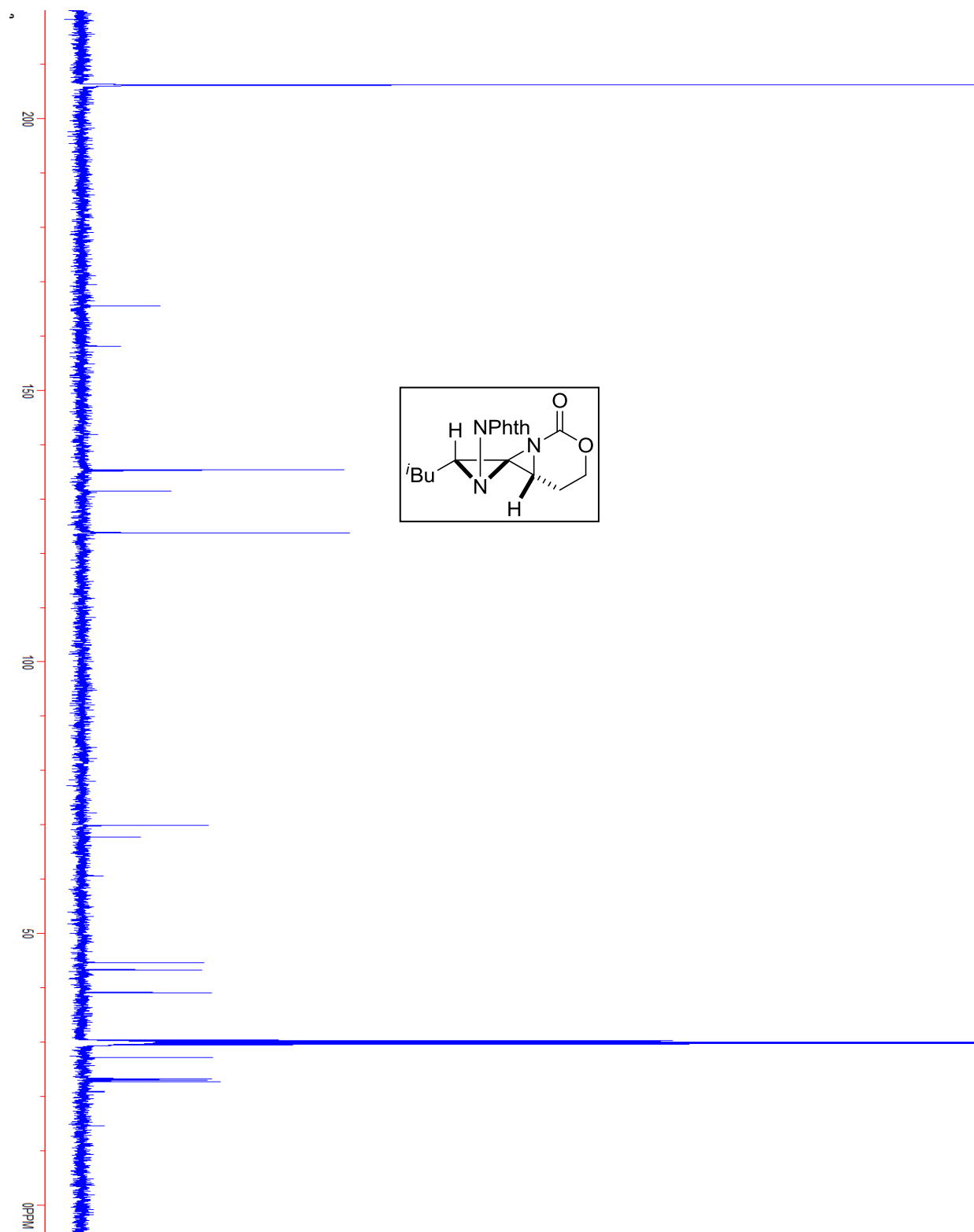
High-pressure liquid chromatography analyses were performed at 255 and 260 nm using Shimadzu HPLc, Model LC-20AB. An AD-H column (4.6 μm diameter x 258 mm) was employed, maintained at a temperature of 40°C, with a flow rate of 1.0 ml/min and a gradient beginning at 5:95 *i*PrOH:hexane and increasing to 30:70 *i*PrOH:hexane over 10 minutes. The eluent composition was held at this composition for another 4 minutes to complete the analysis. This method of analysis was used for both substrates.

Appendix A. ^1H -NMR and ^{13}C -NMR spectra of new compounds.

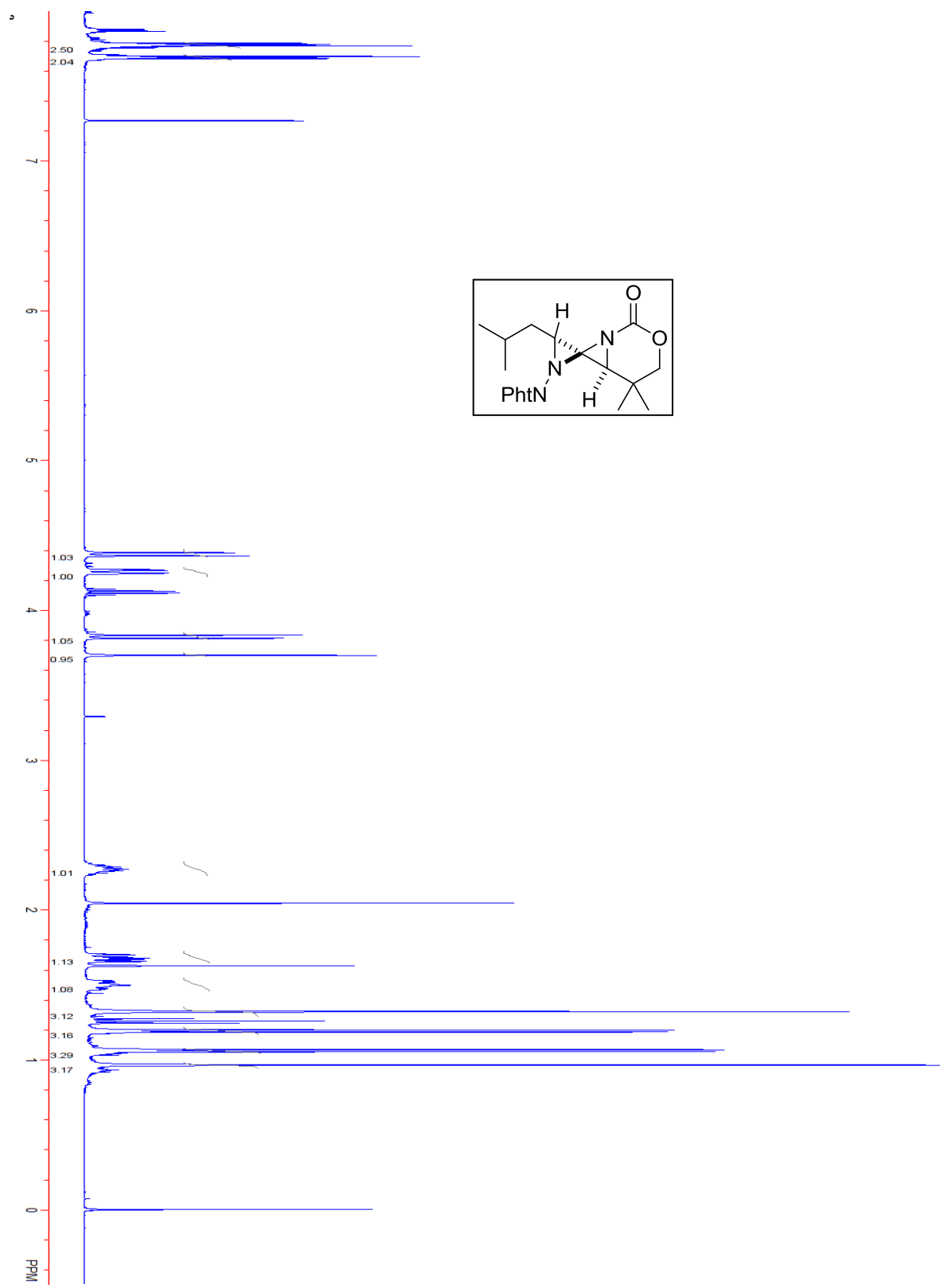
Compound 1.30a.



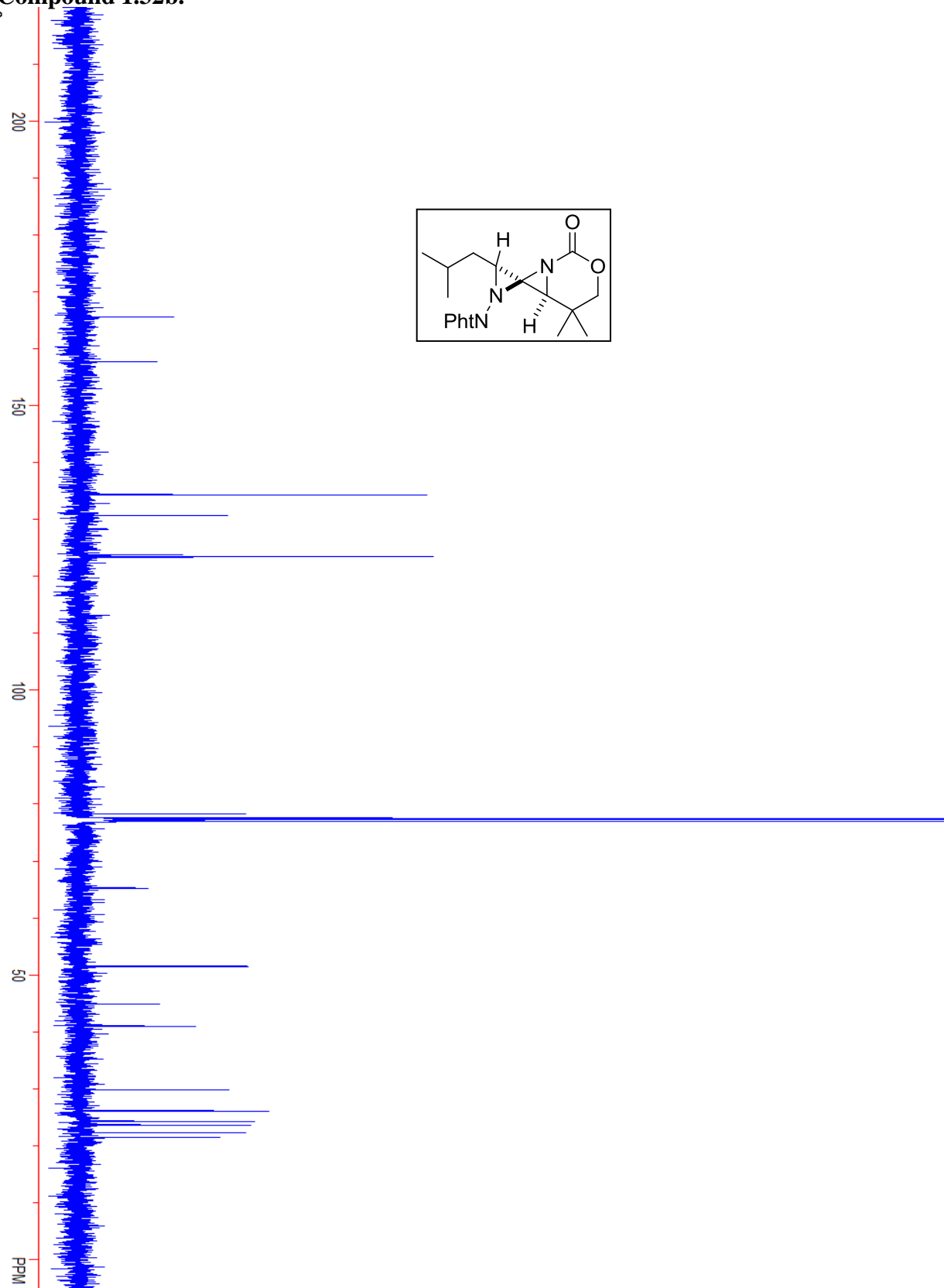
Compound 1.30a.

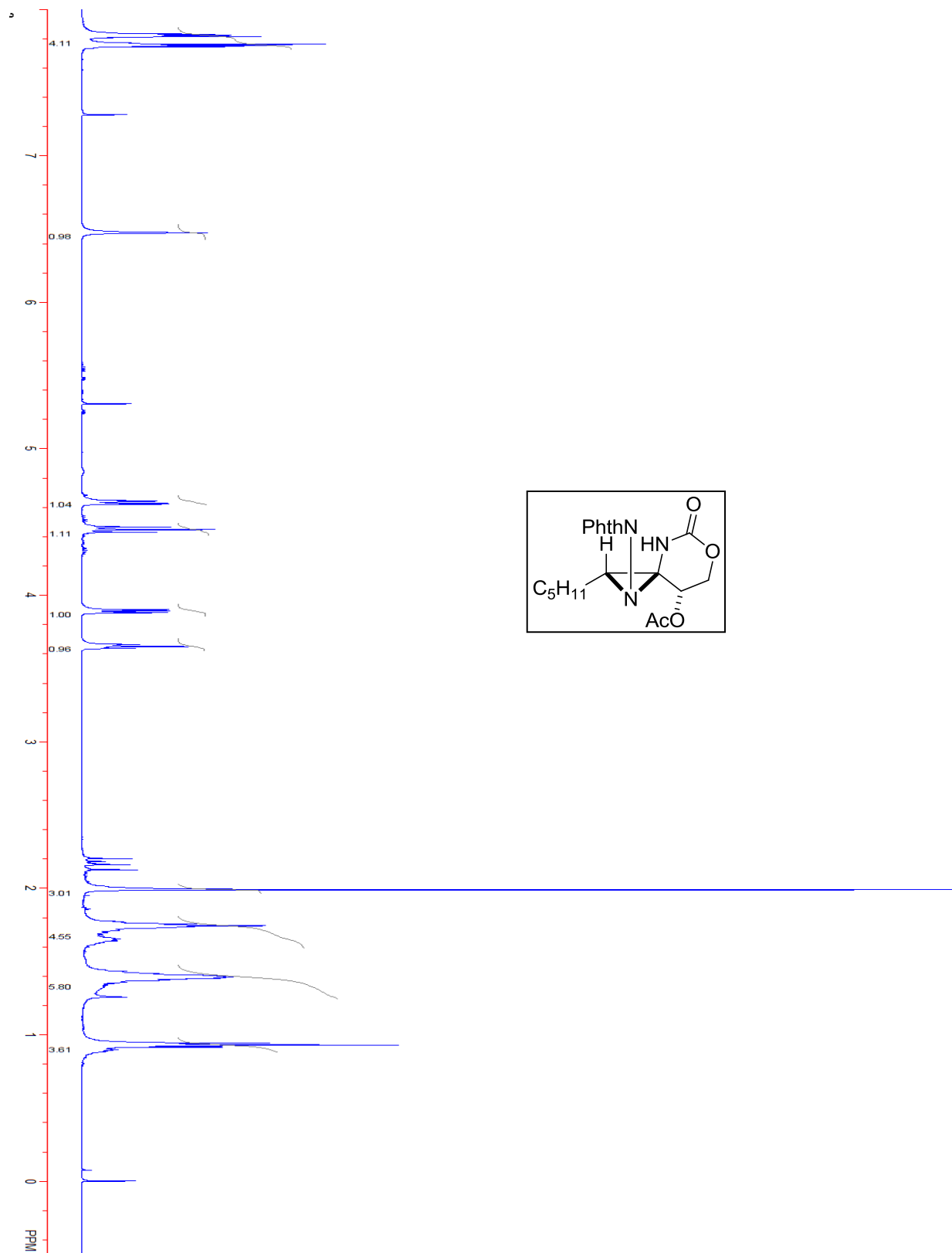


Compound 1.32a.

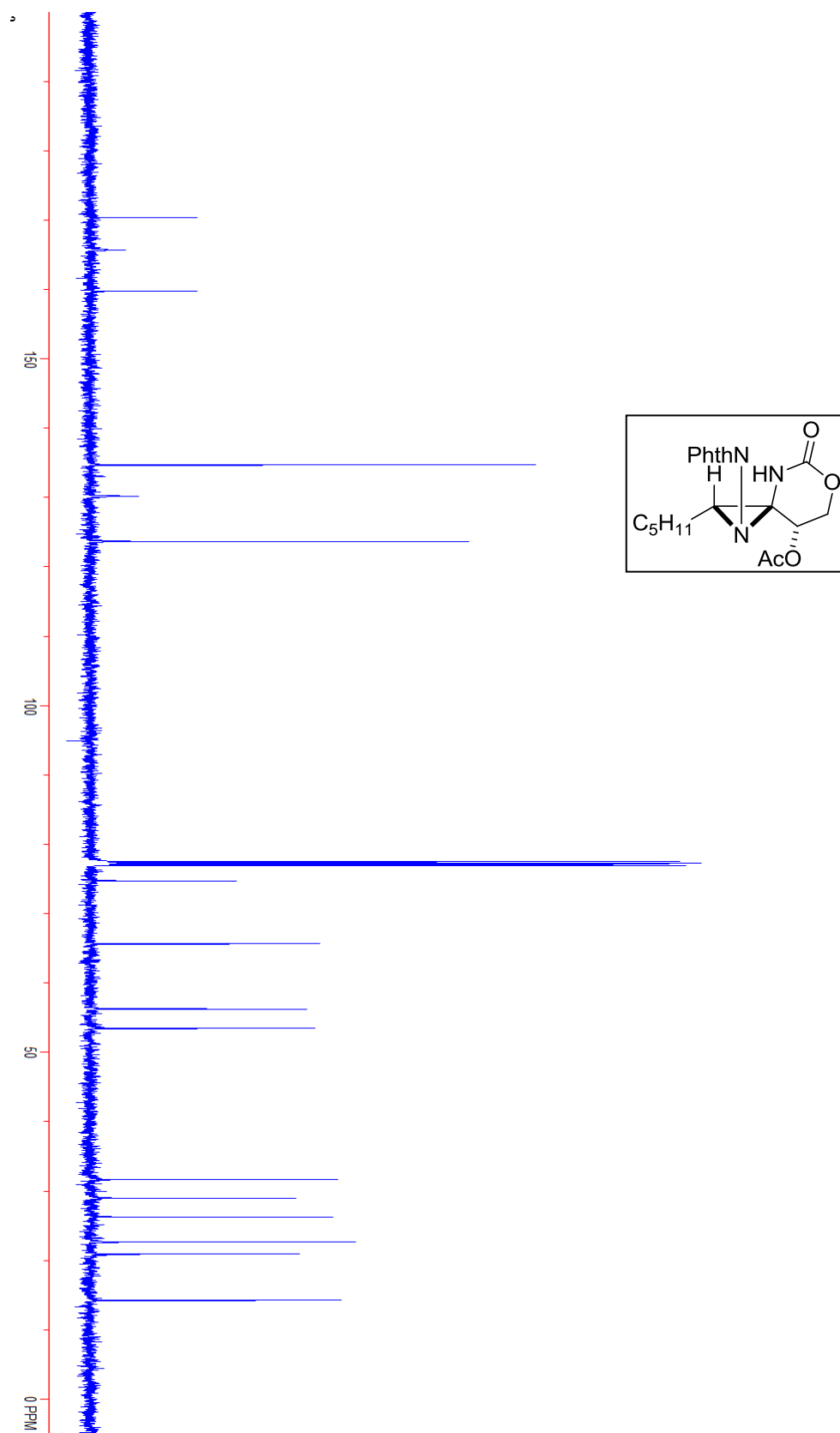


Compound 1.32b.

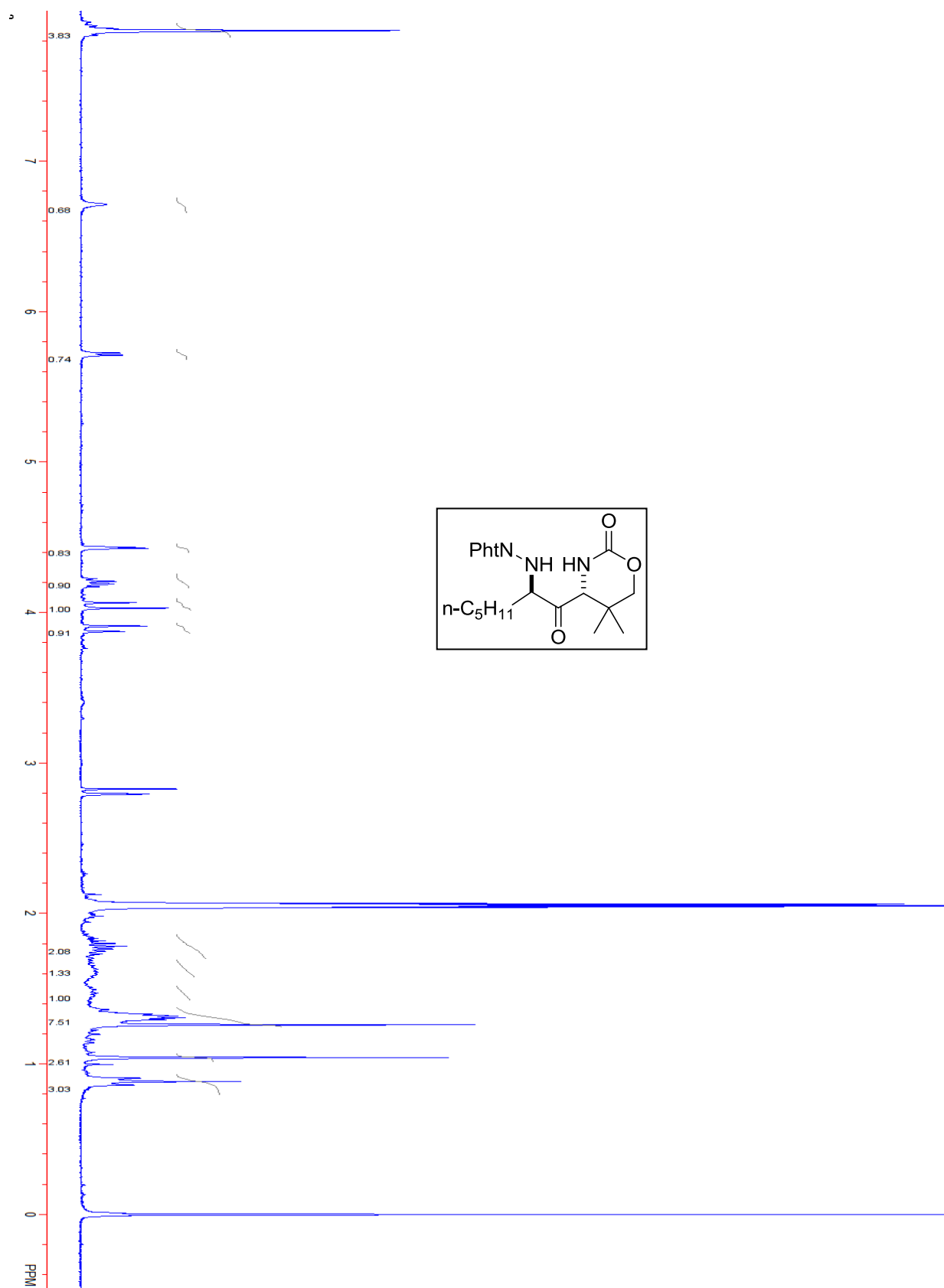


Compound S1.1.

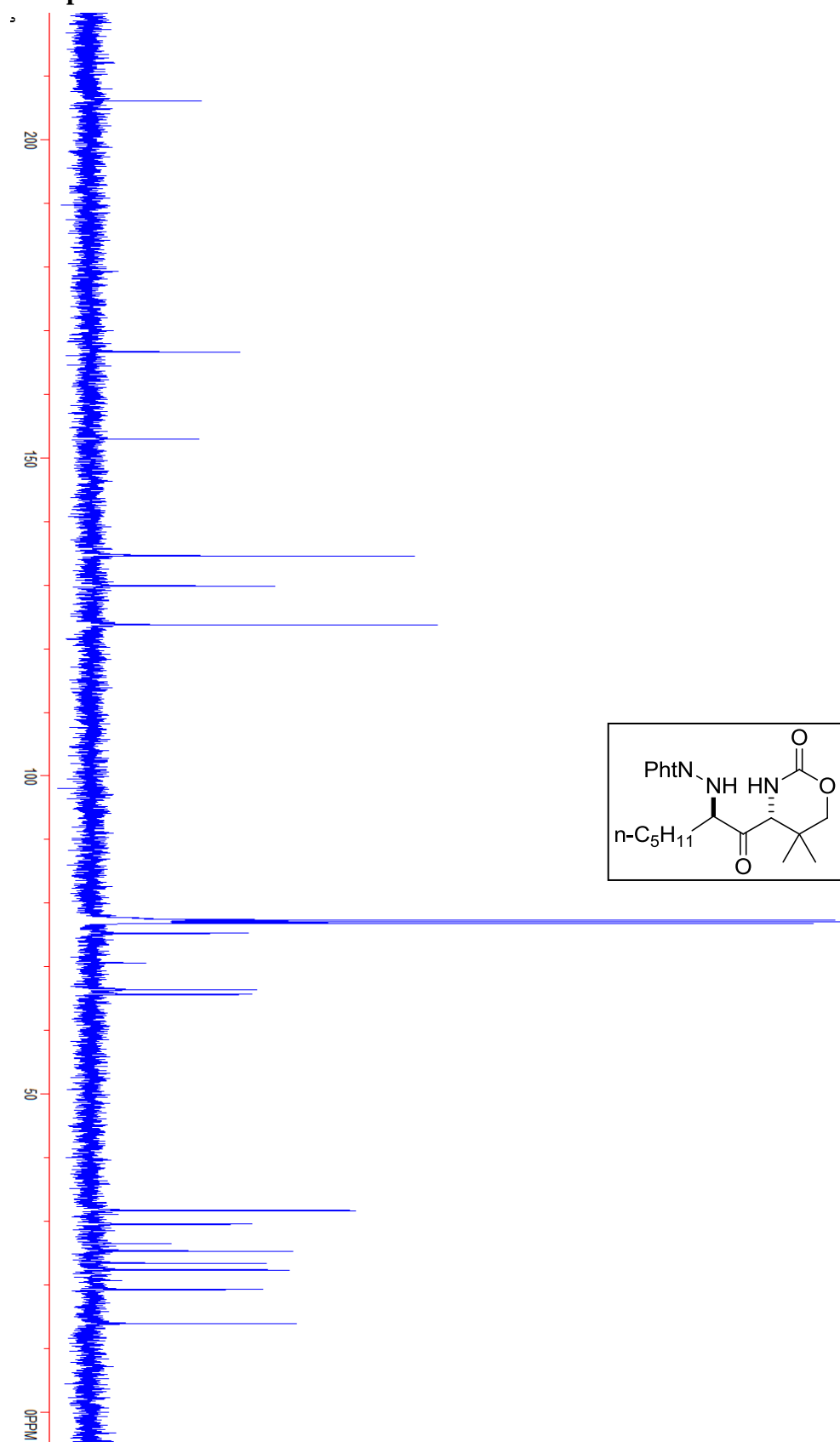
Compound S1.1.



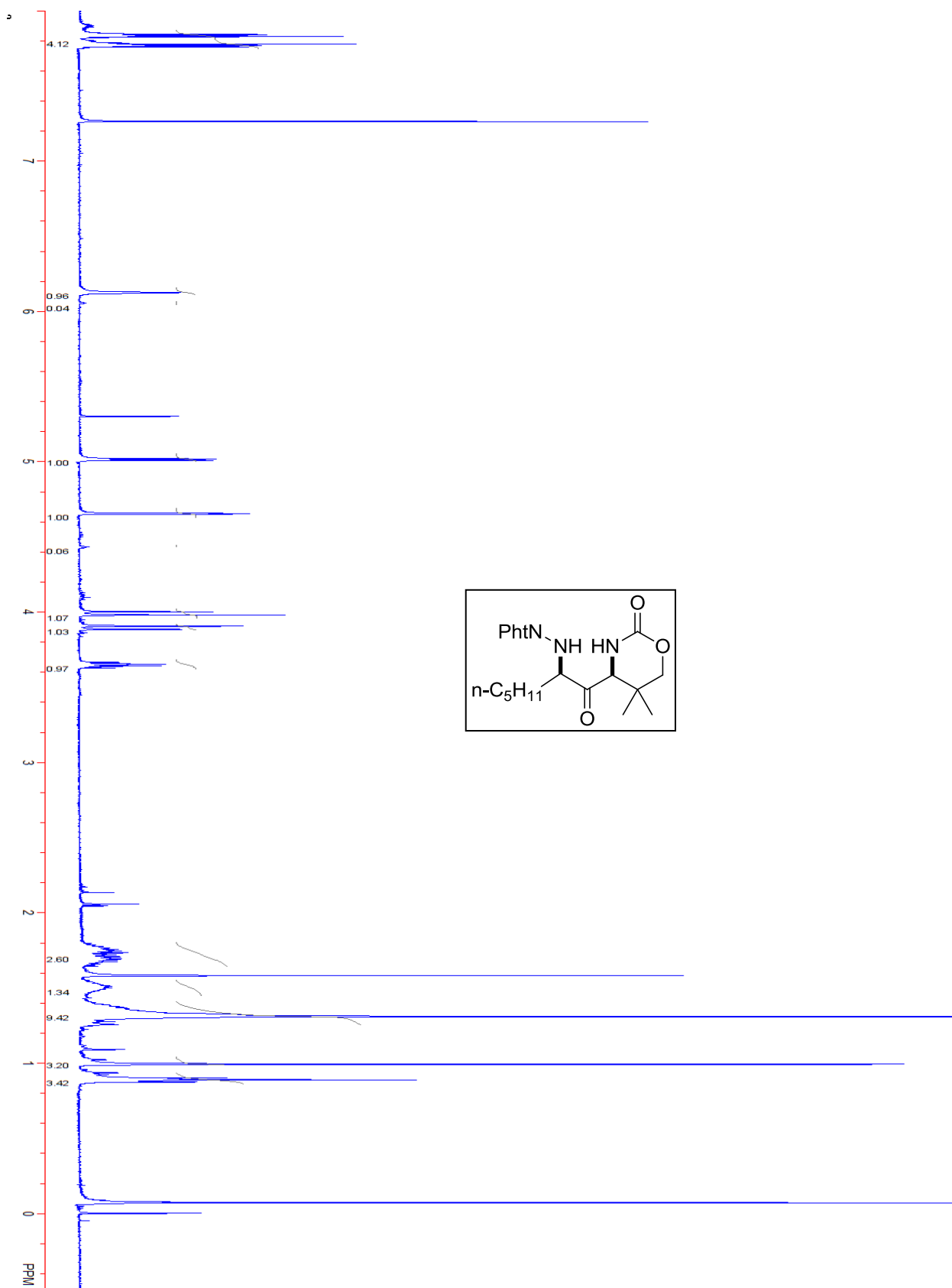
Compound 1.25.



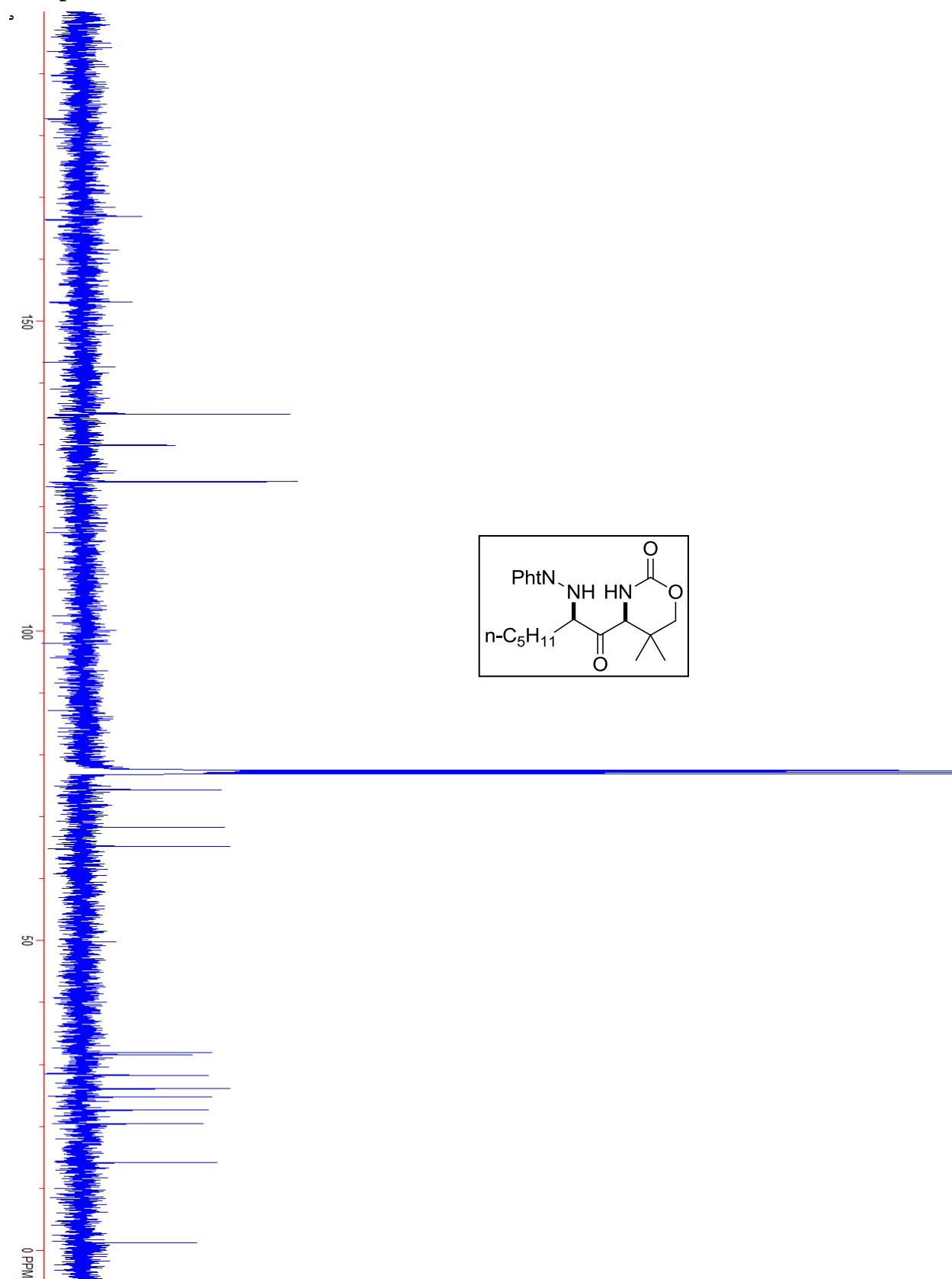
Compound 1.25.



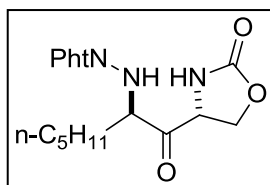
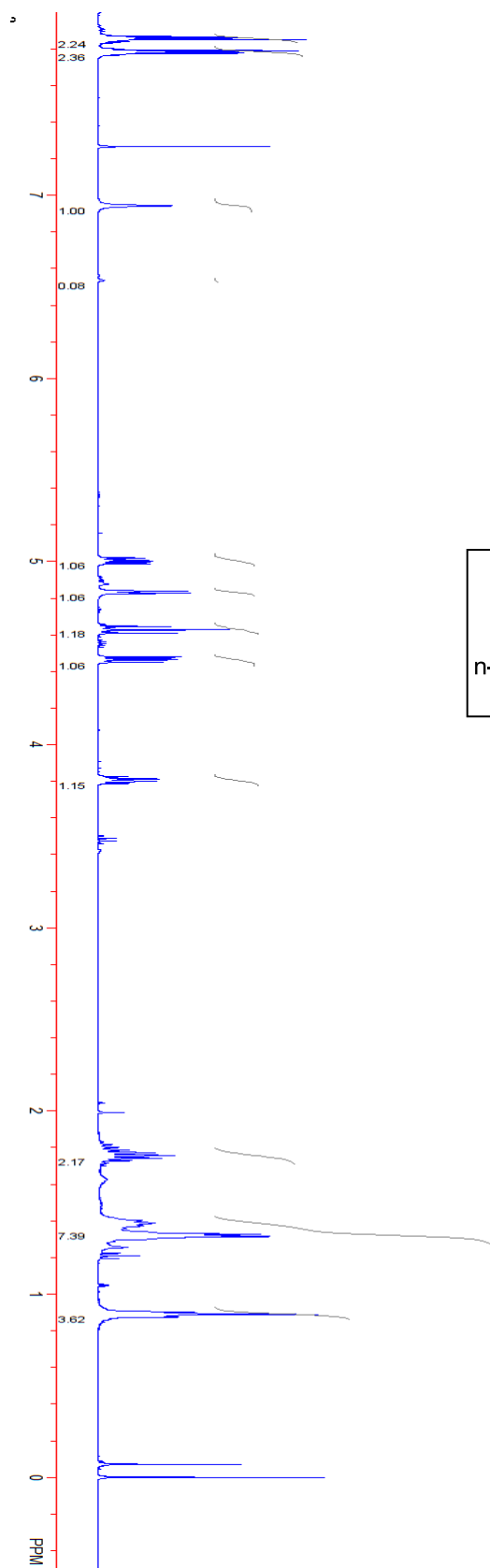
Compound 1.27b.



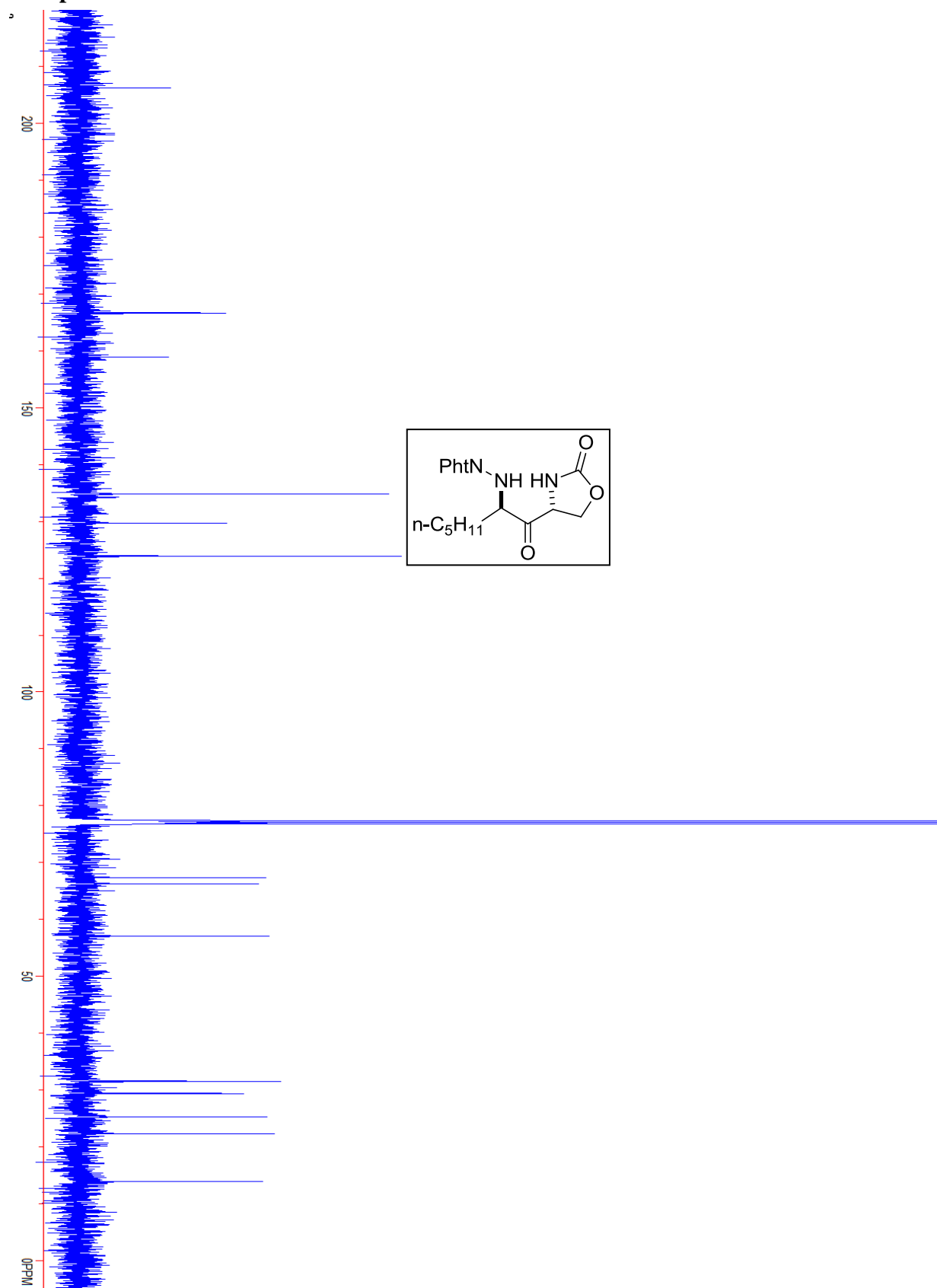
Compound 1.27b.



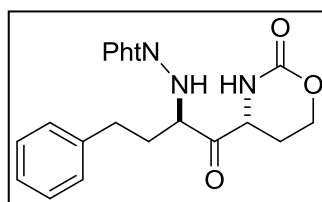
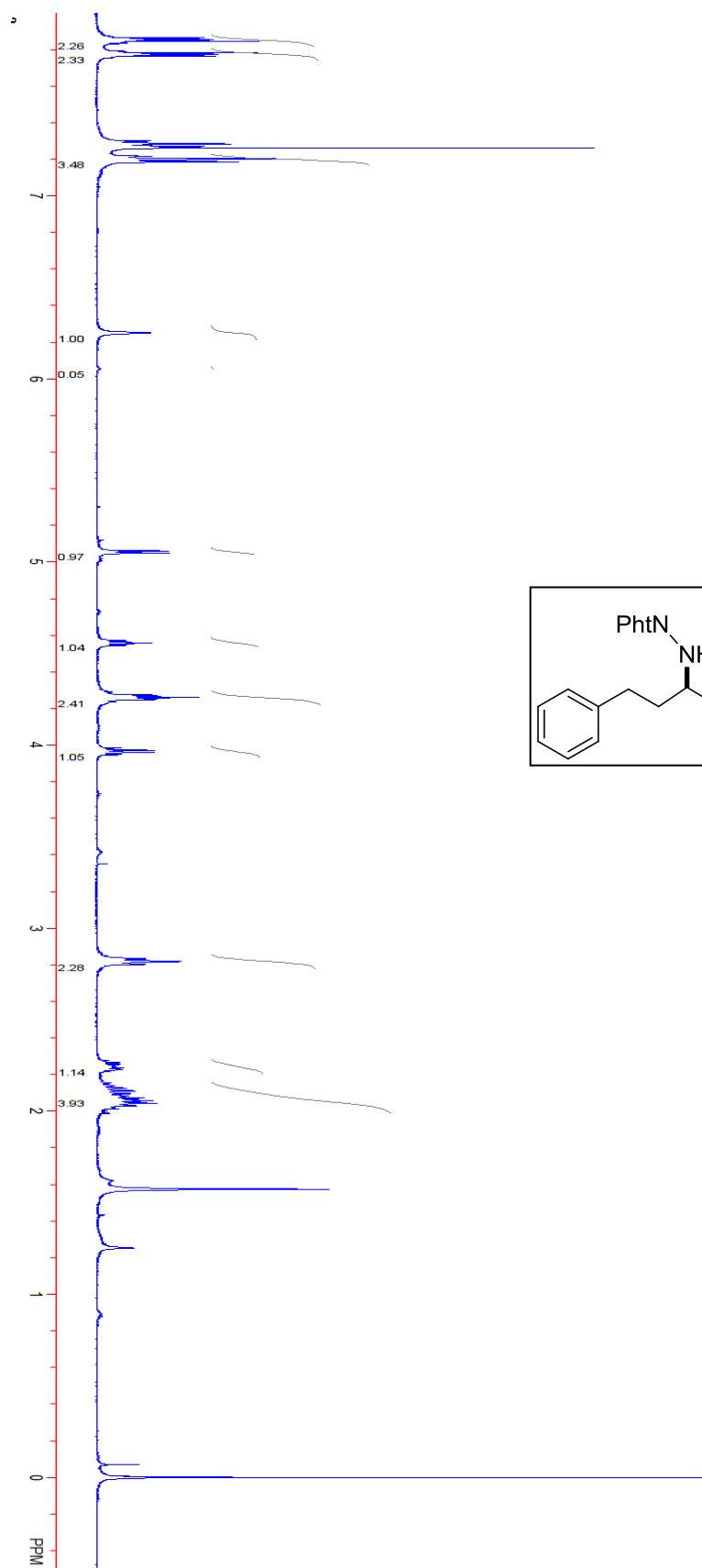
Compound 1.28b.



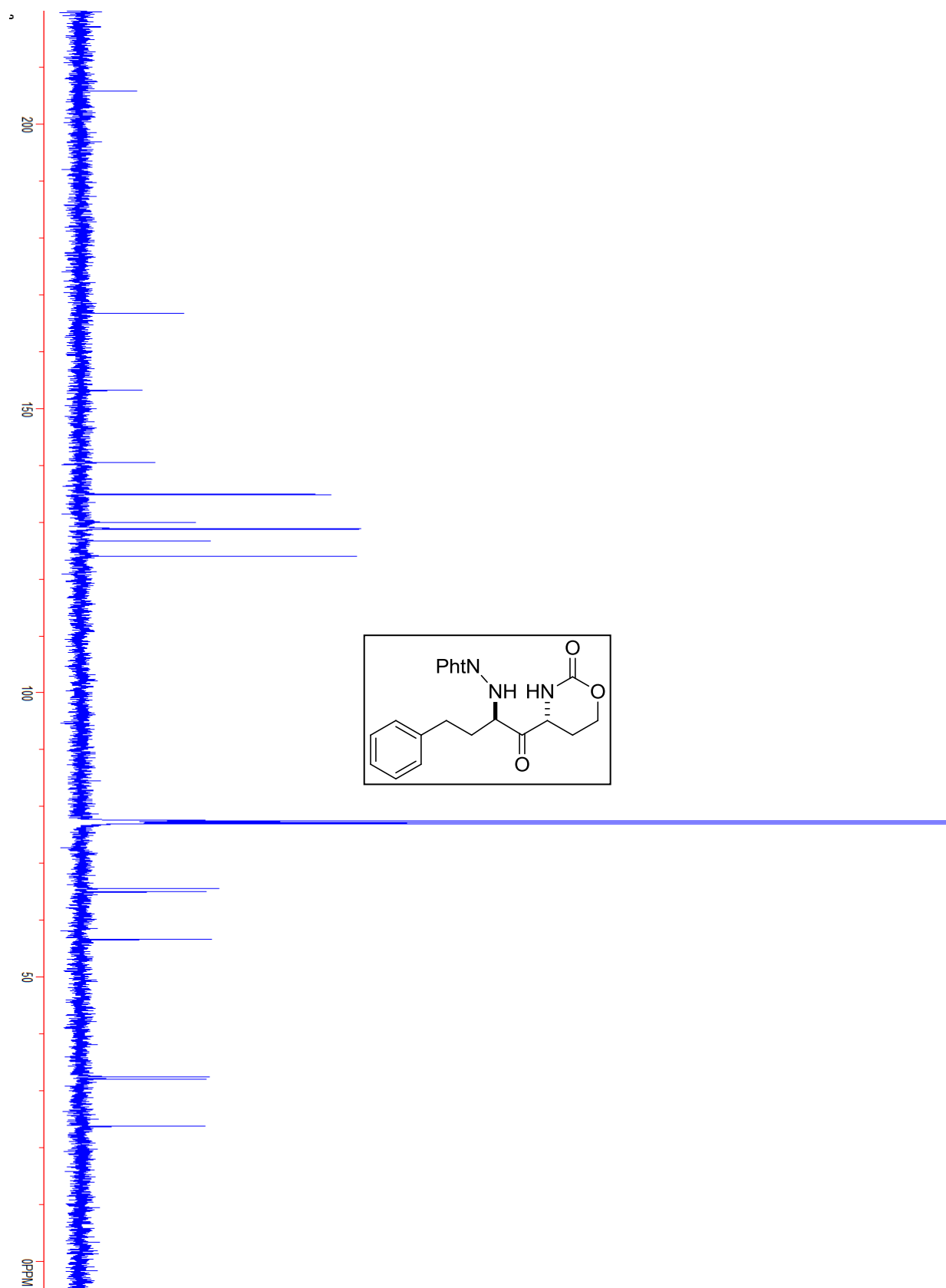
Compound 1.28b.



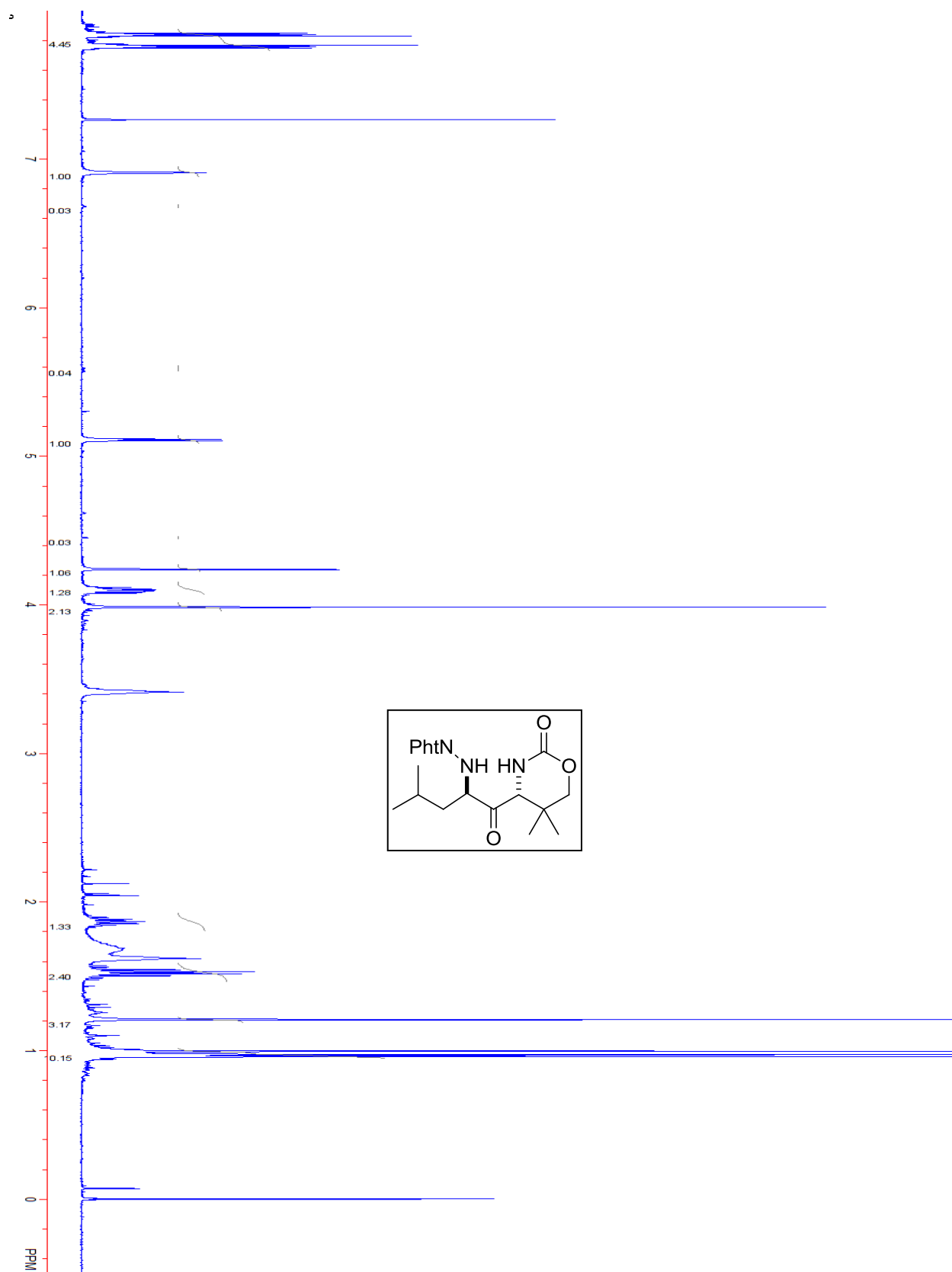
Compound 1.29b.

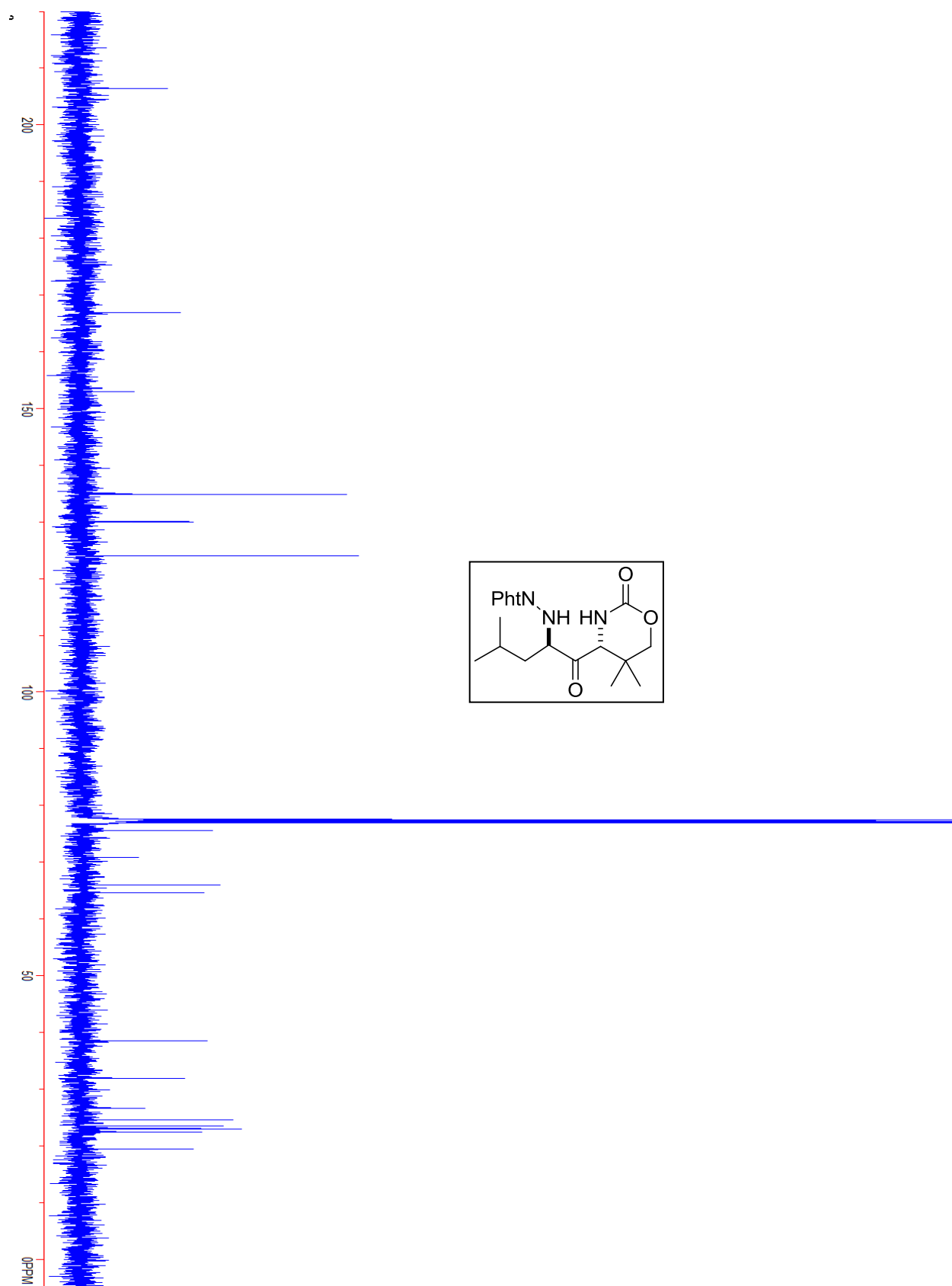


Compound 1.29b.

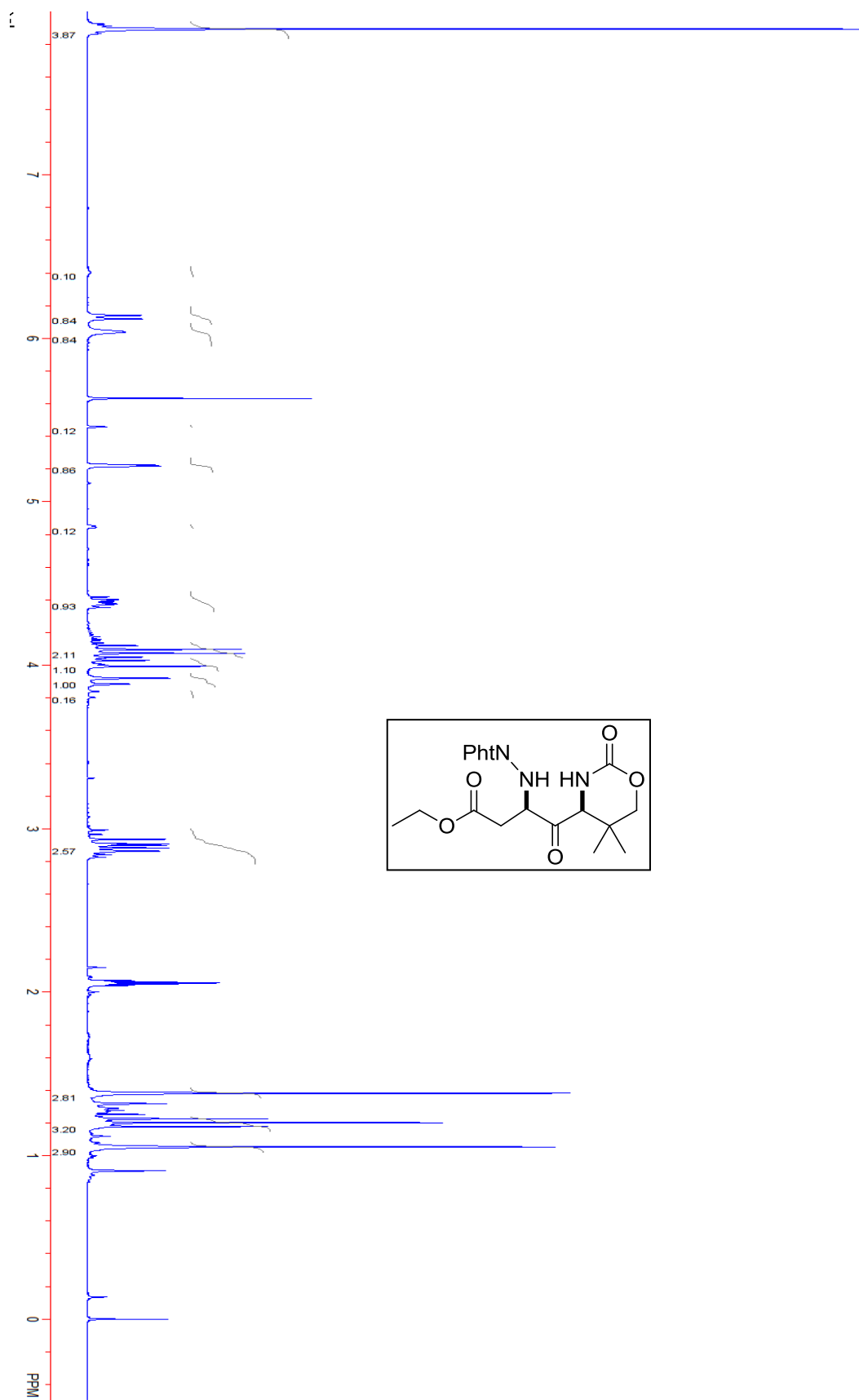


Compound 1.30b.

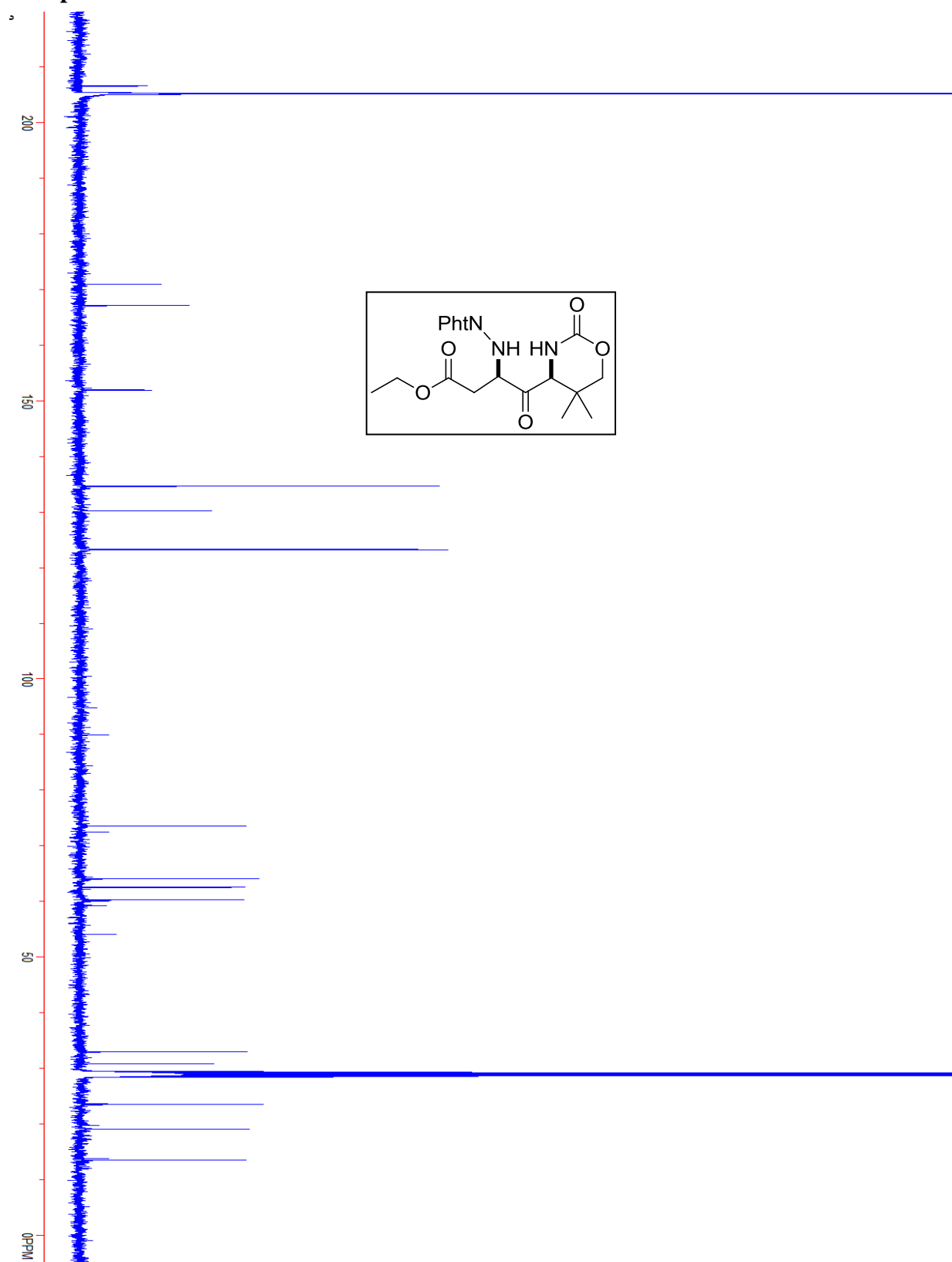


Compound 1.30b.

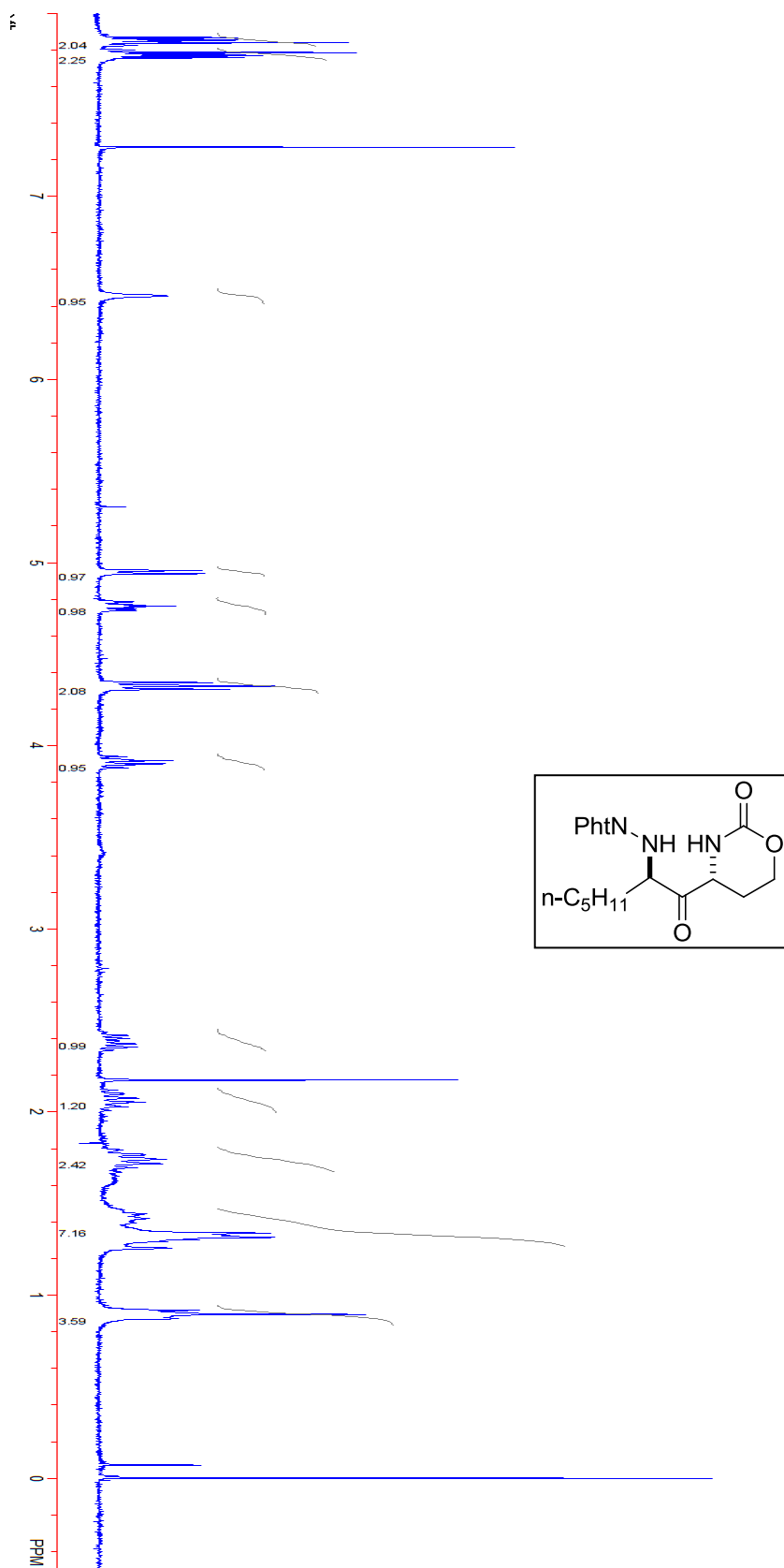
Compound 1.31b.



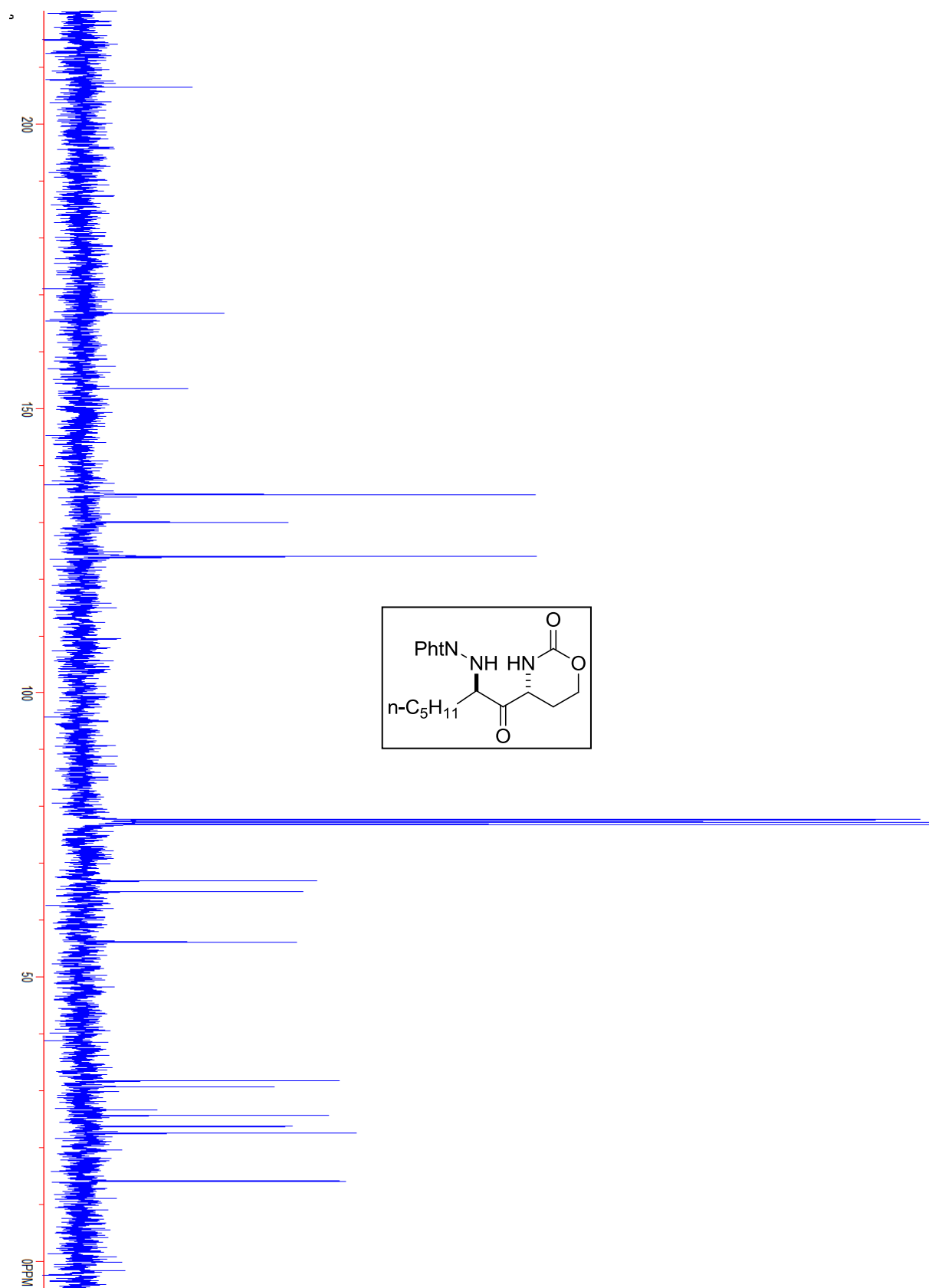
Compound 1.31b.



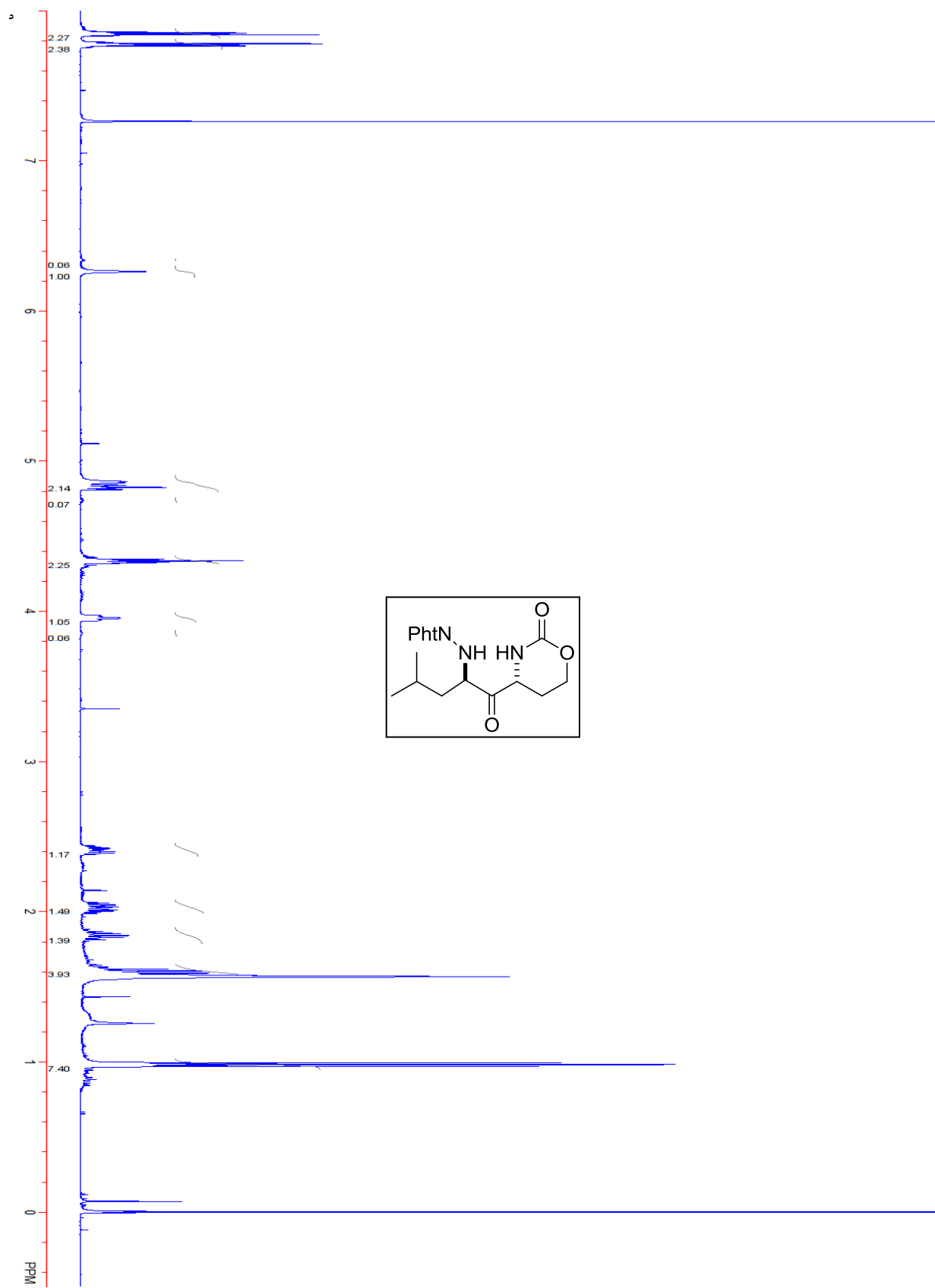
Compound 1.32b.



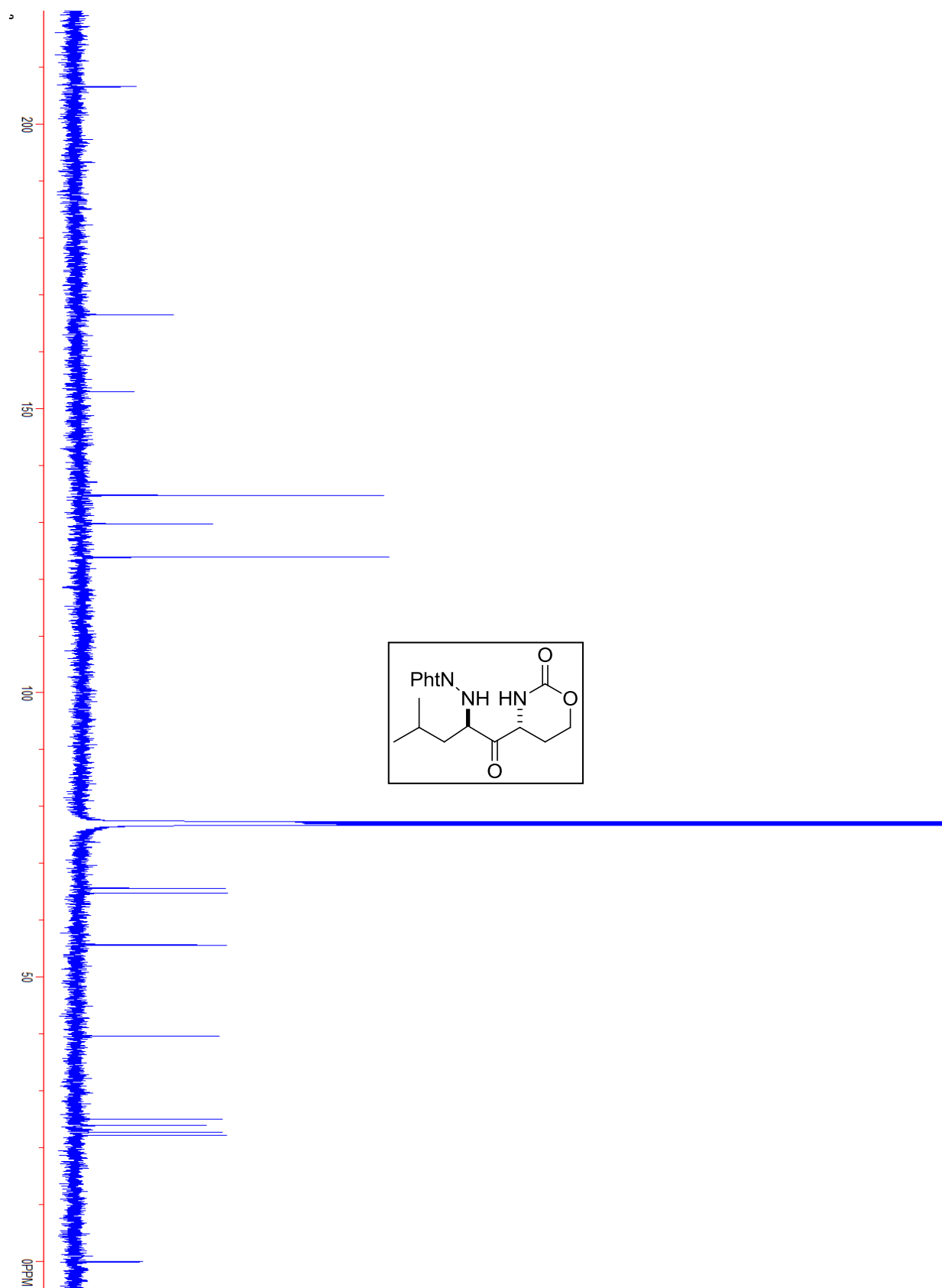
Compound 1.32b.



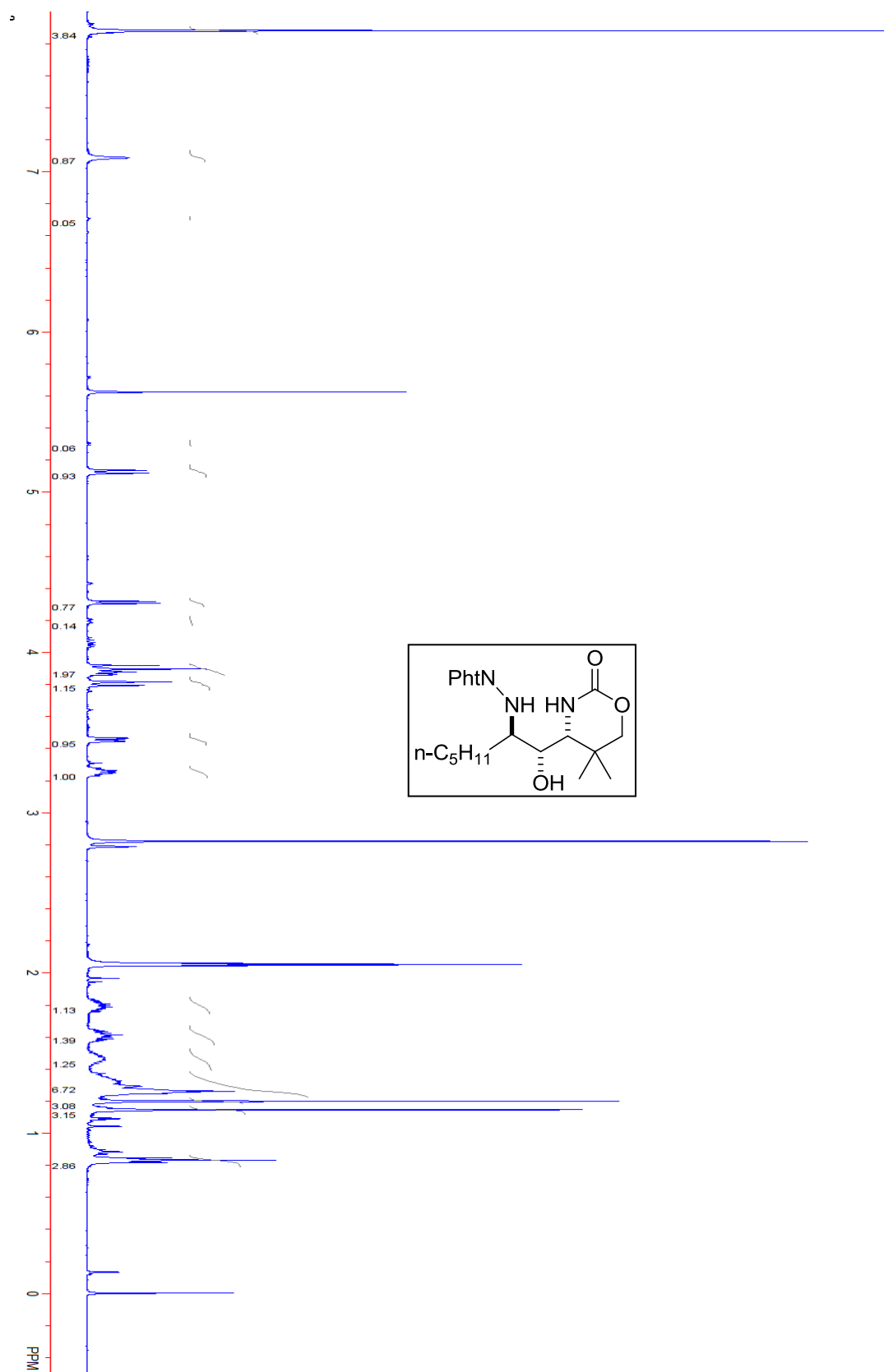
Compound 1.33b.



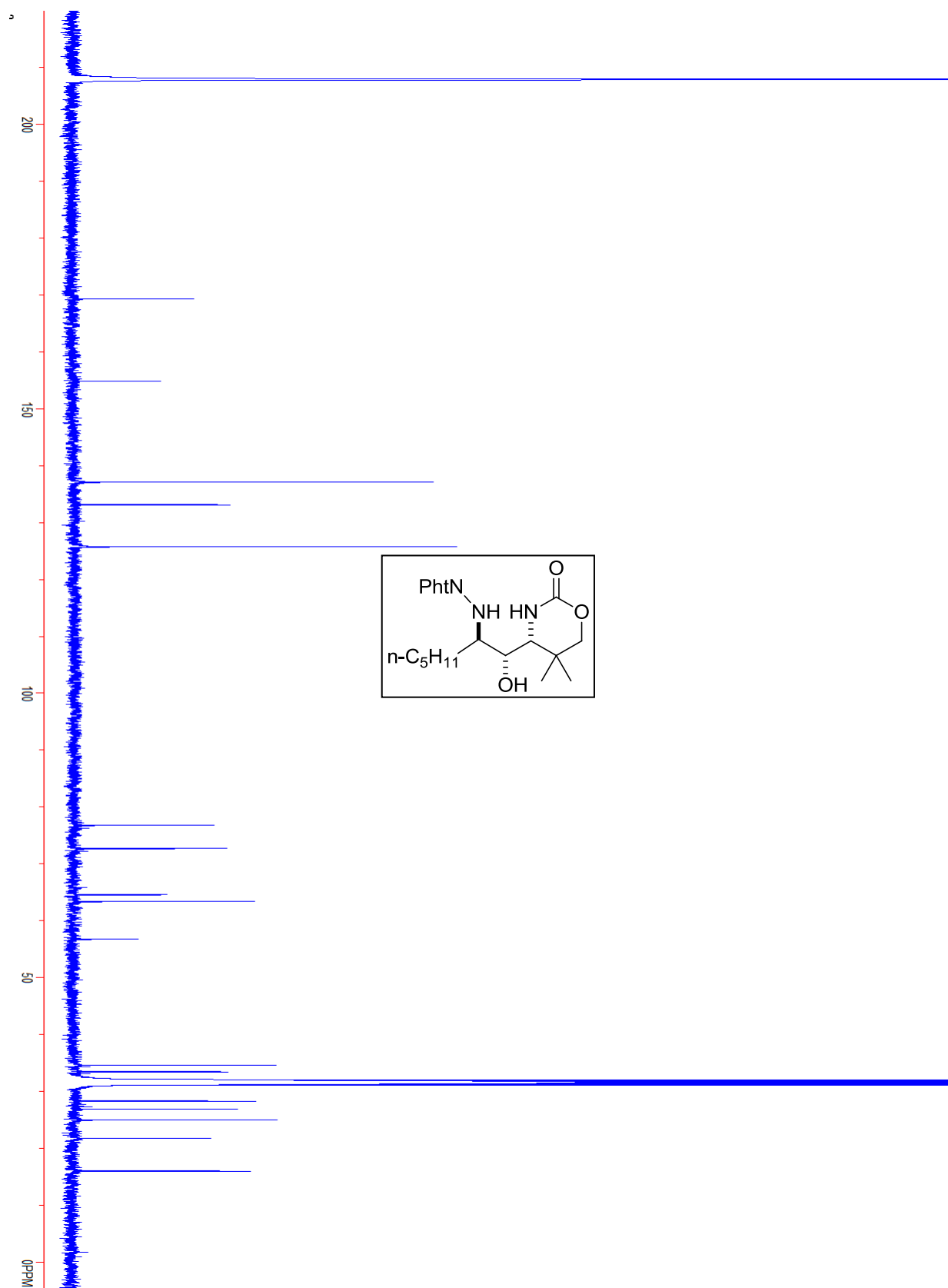
Compound 1.33b.



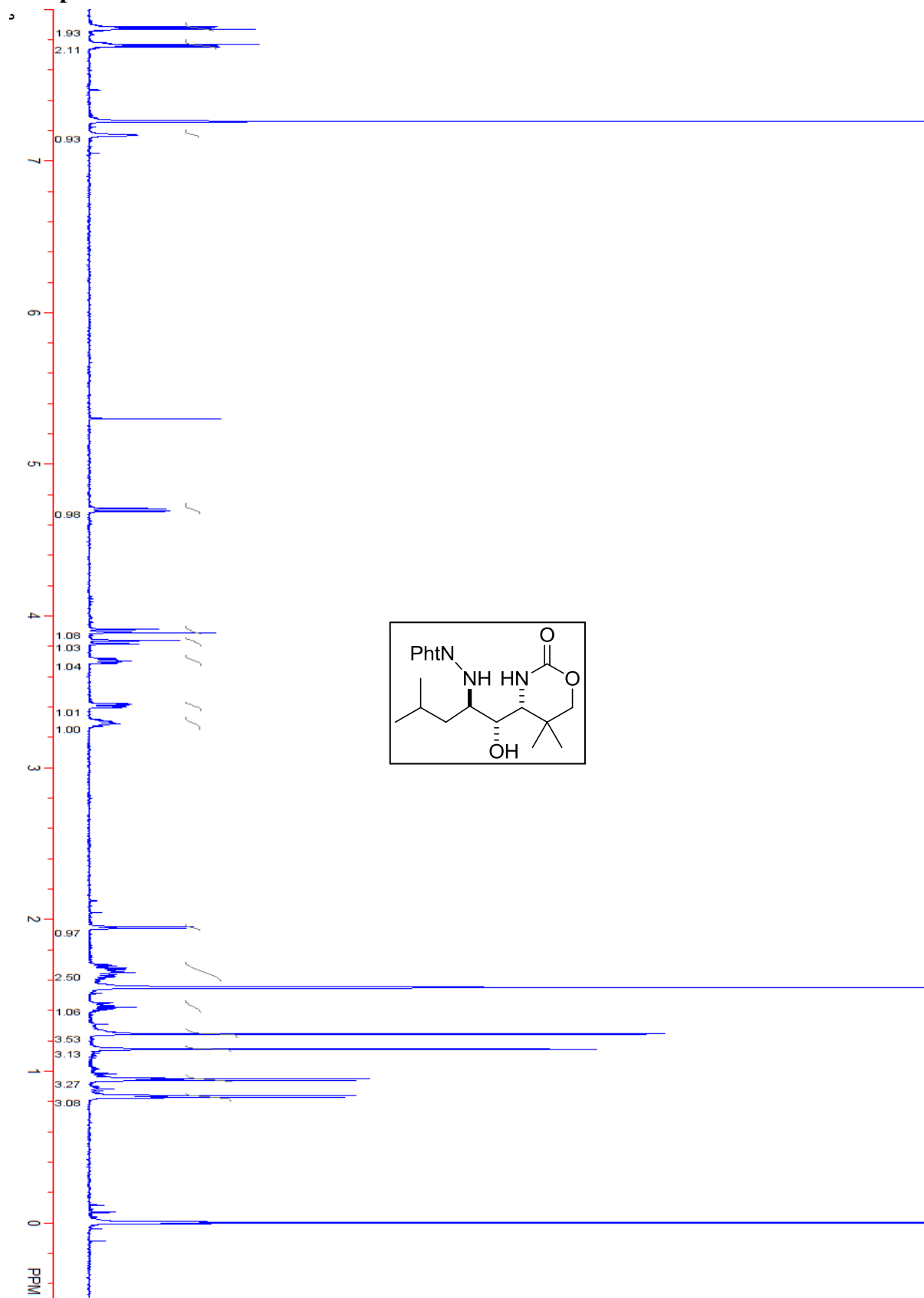
Compound 1.38.

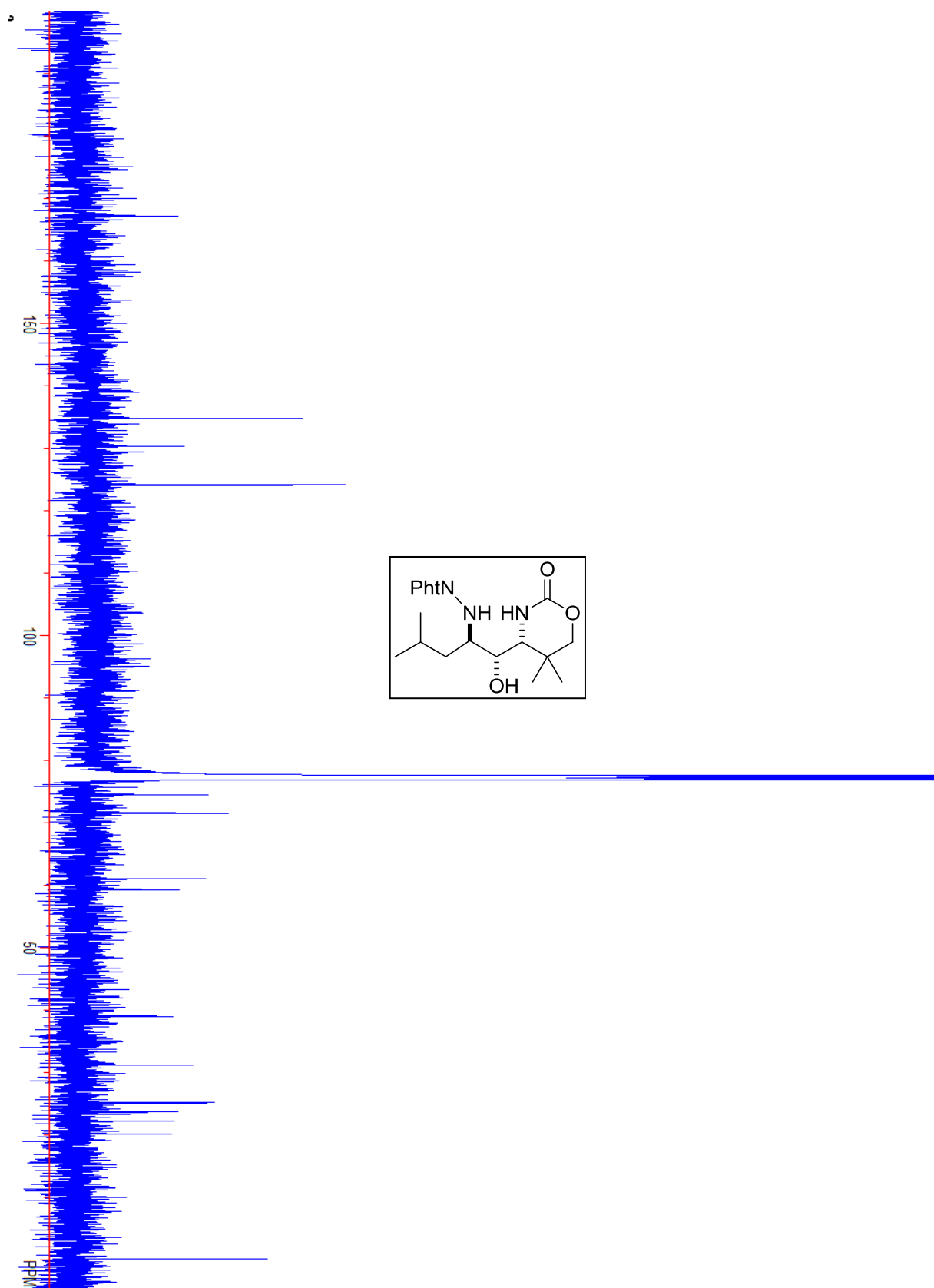


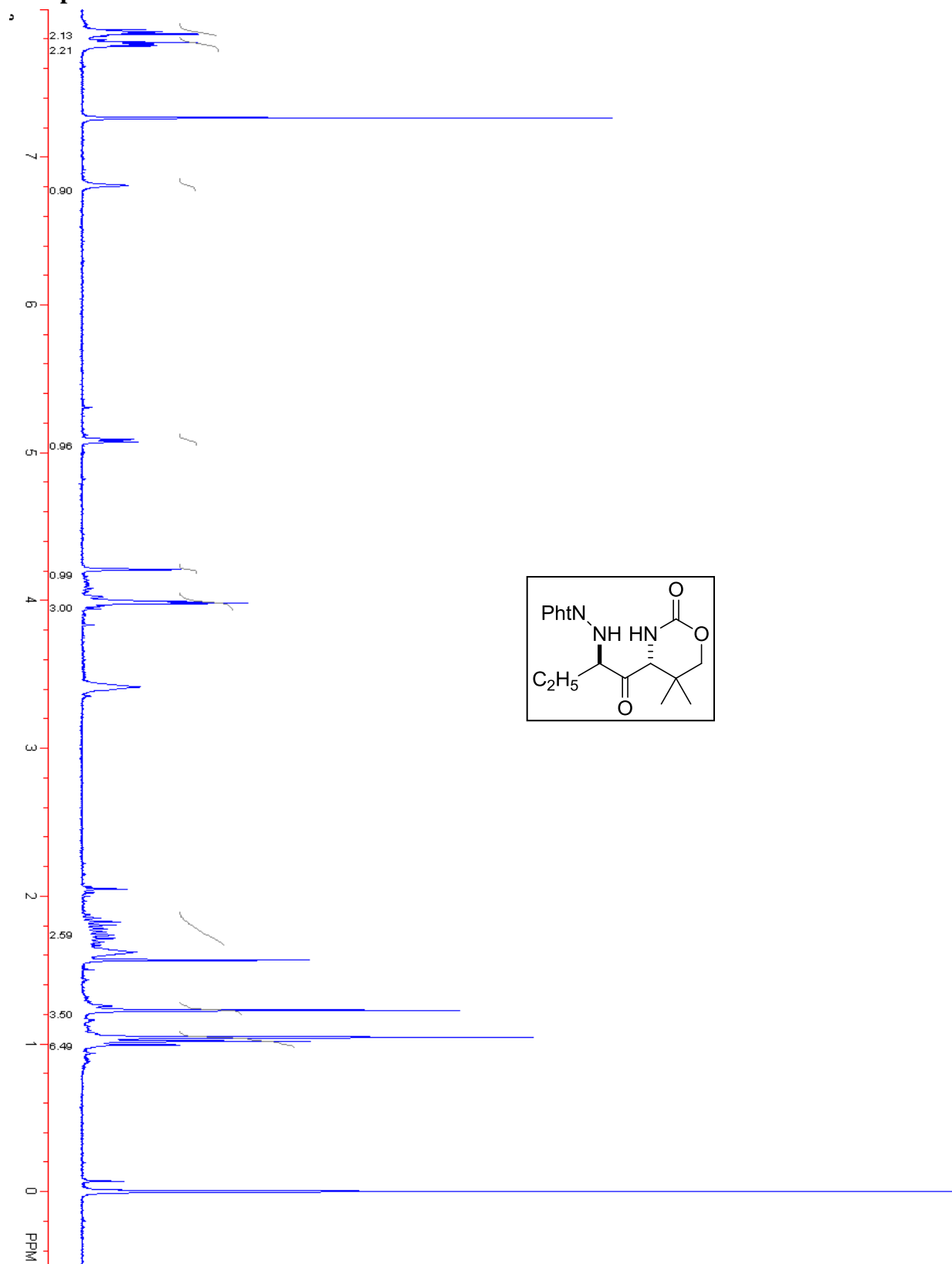
Compound 1.38.



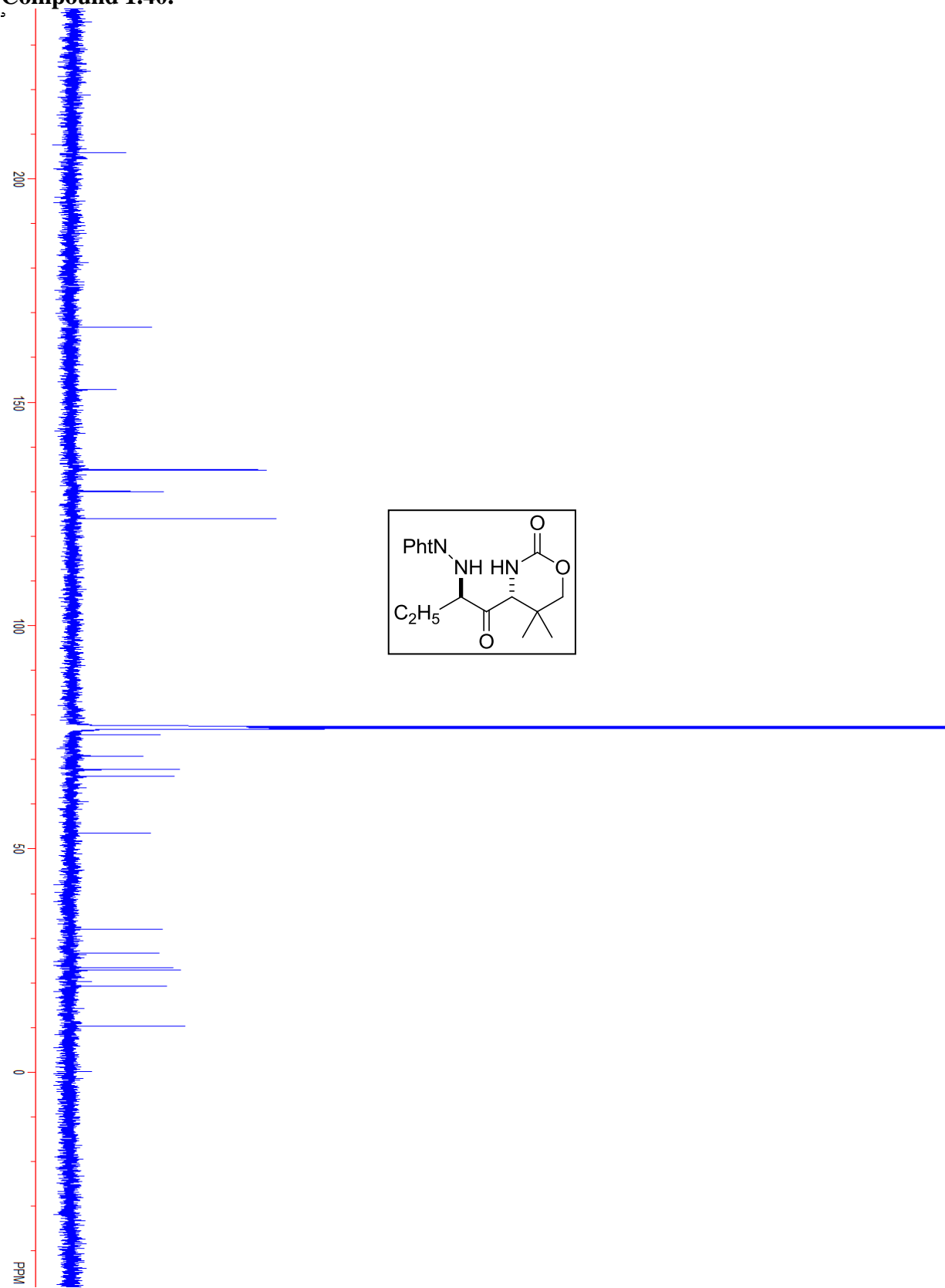
Compound 1.40.

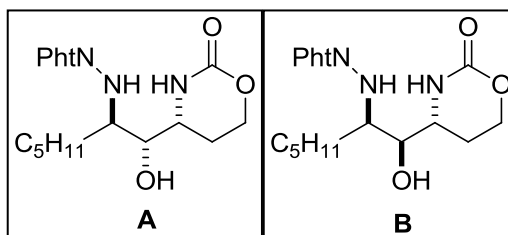
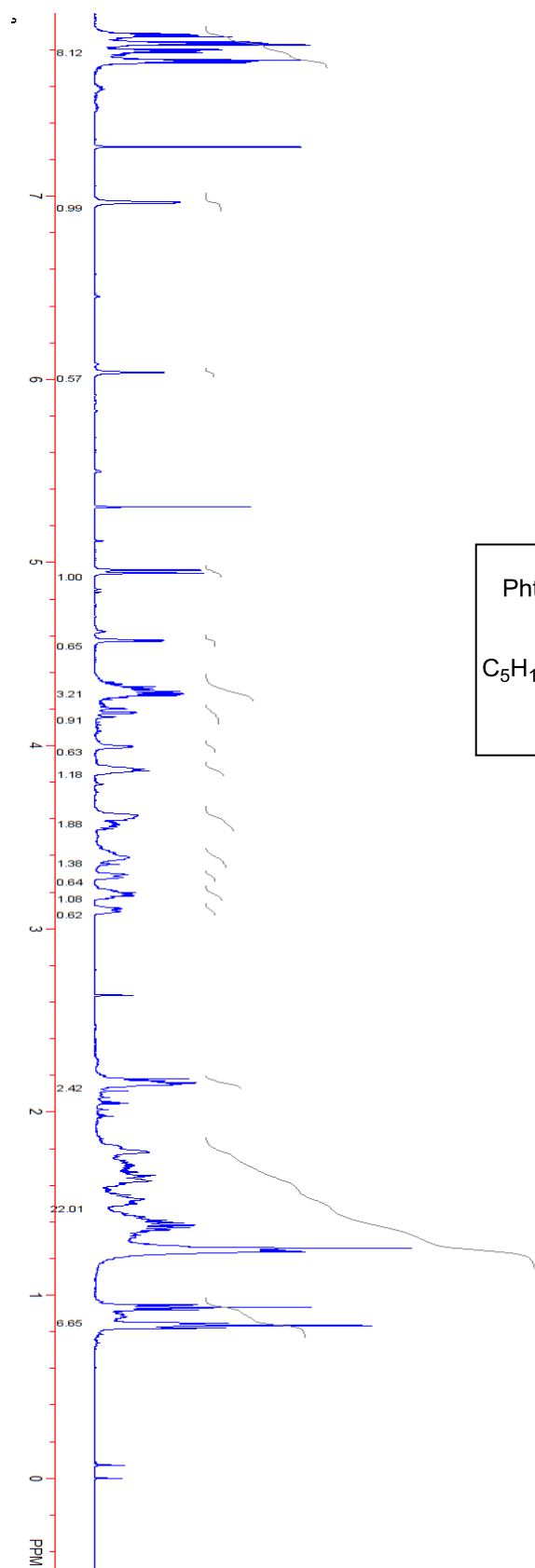


Compound 1.39.

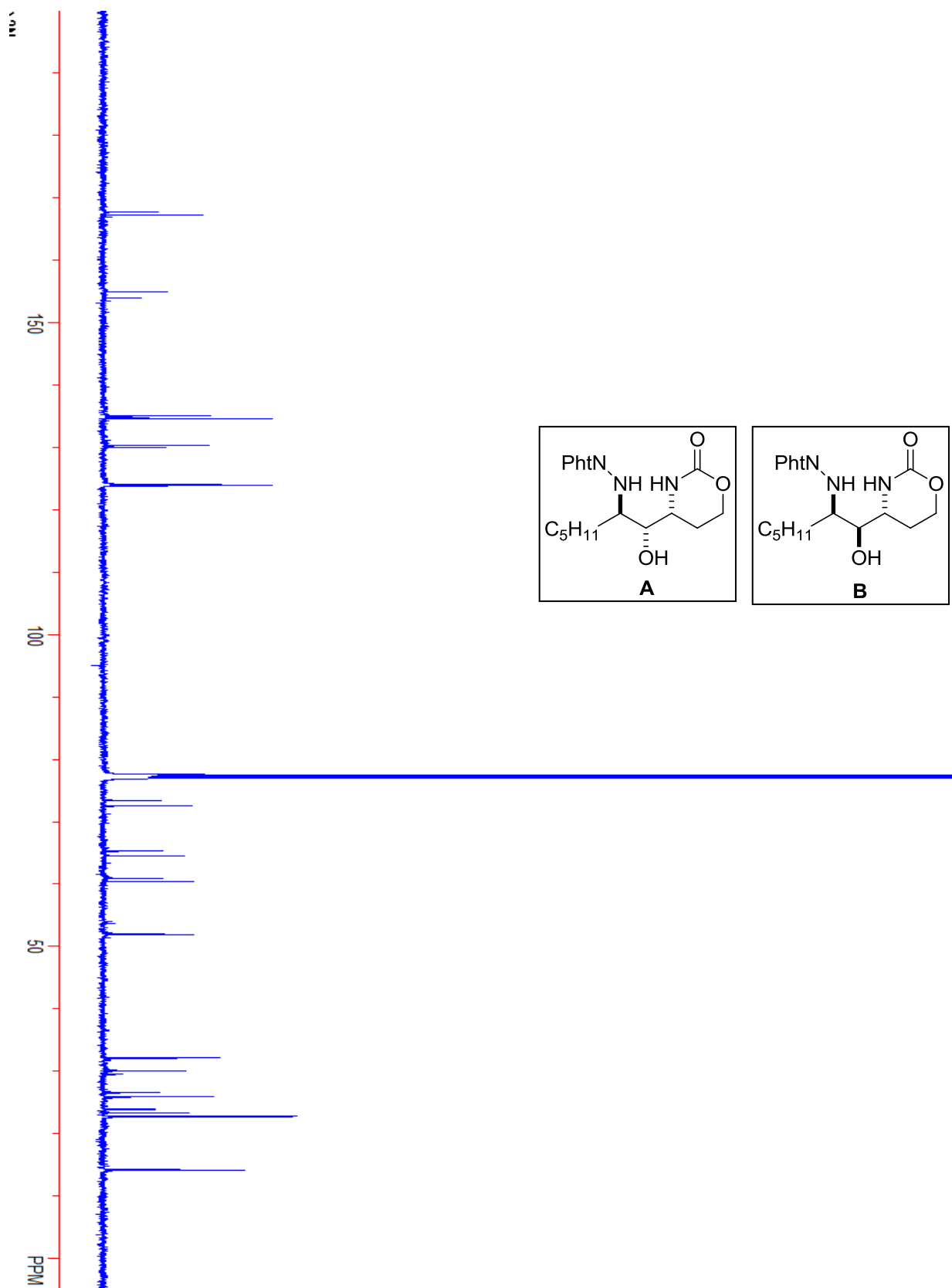
Compound 1.40.

Compound 1.40.

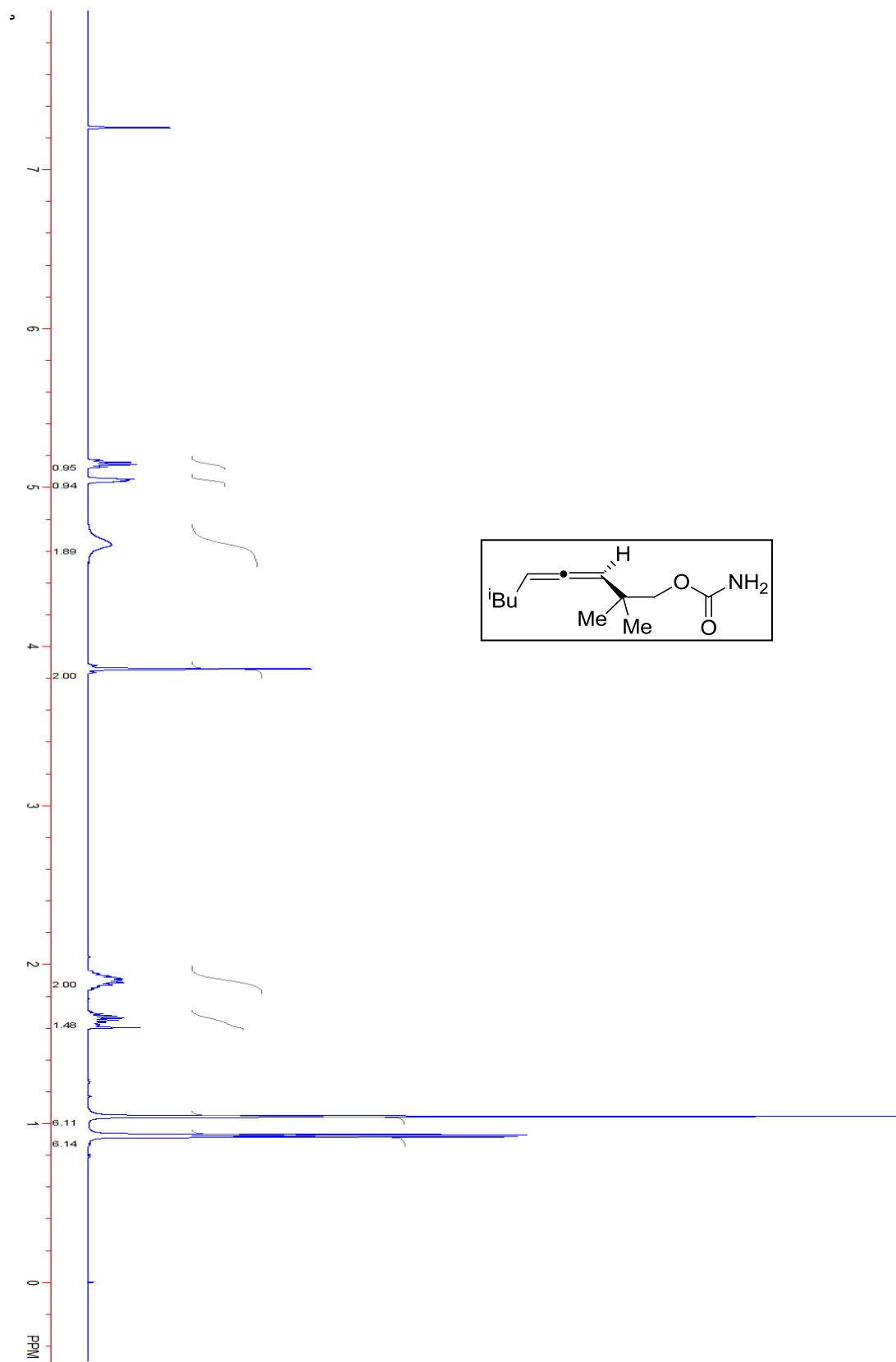


Compound 1.41.

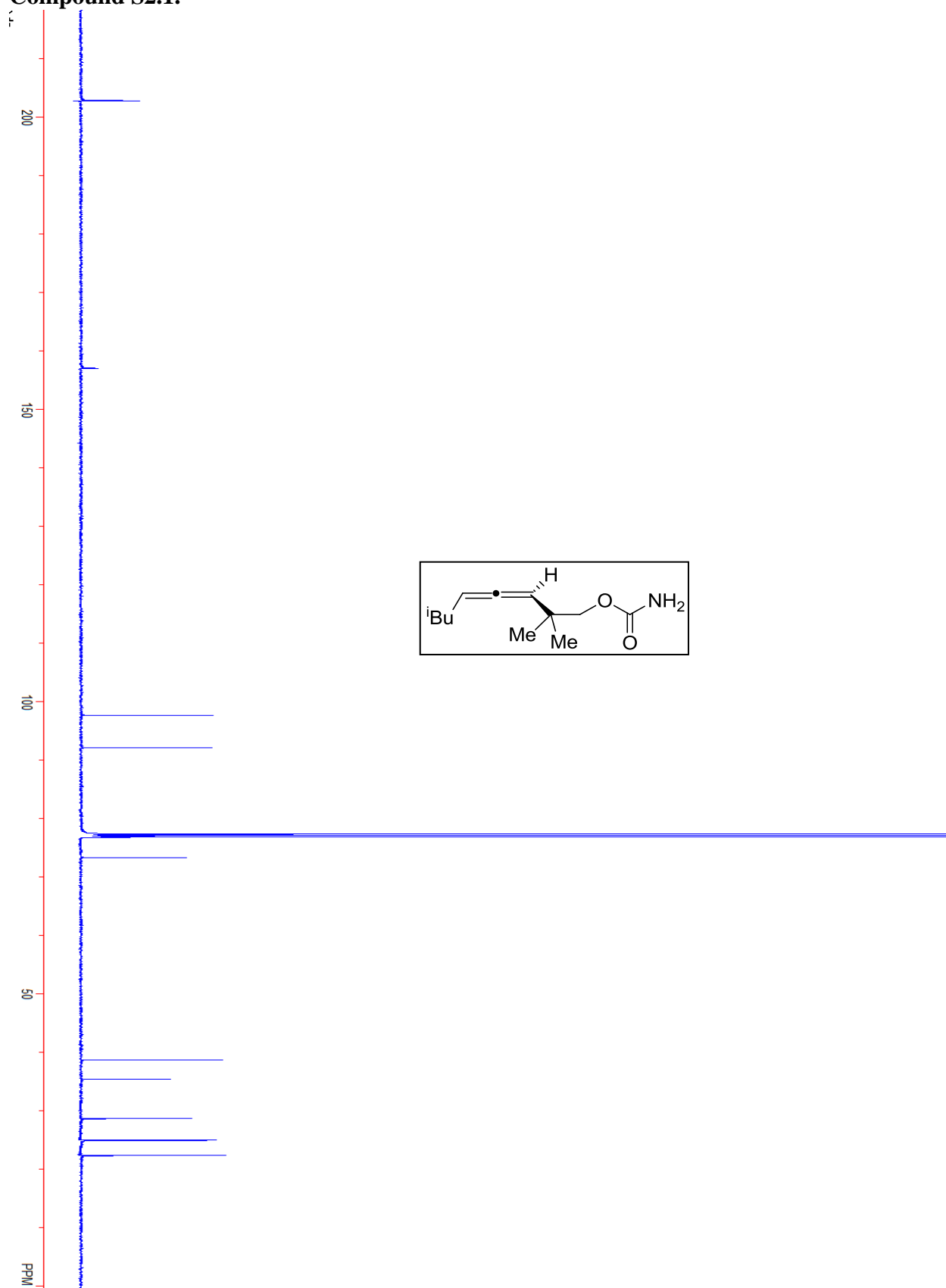
Compound 1.41.



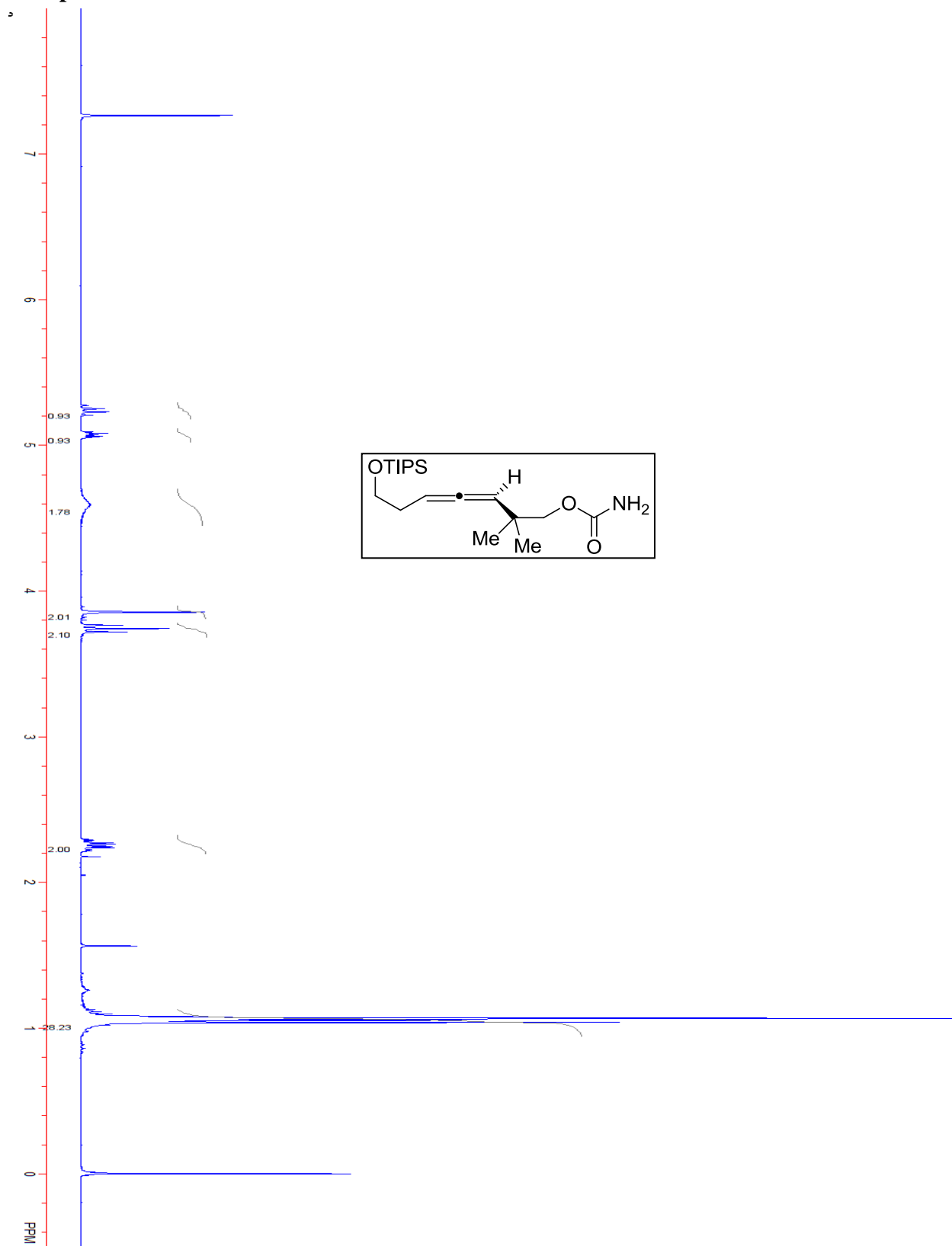
Compound S2.1.



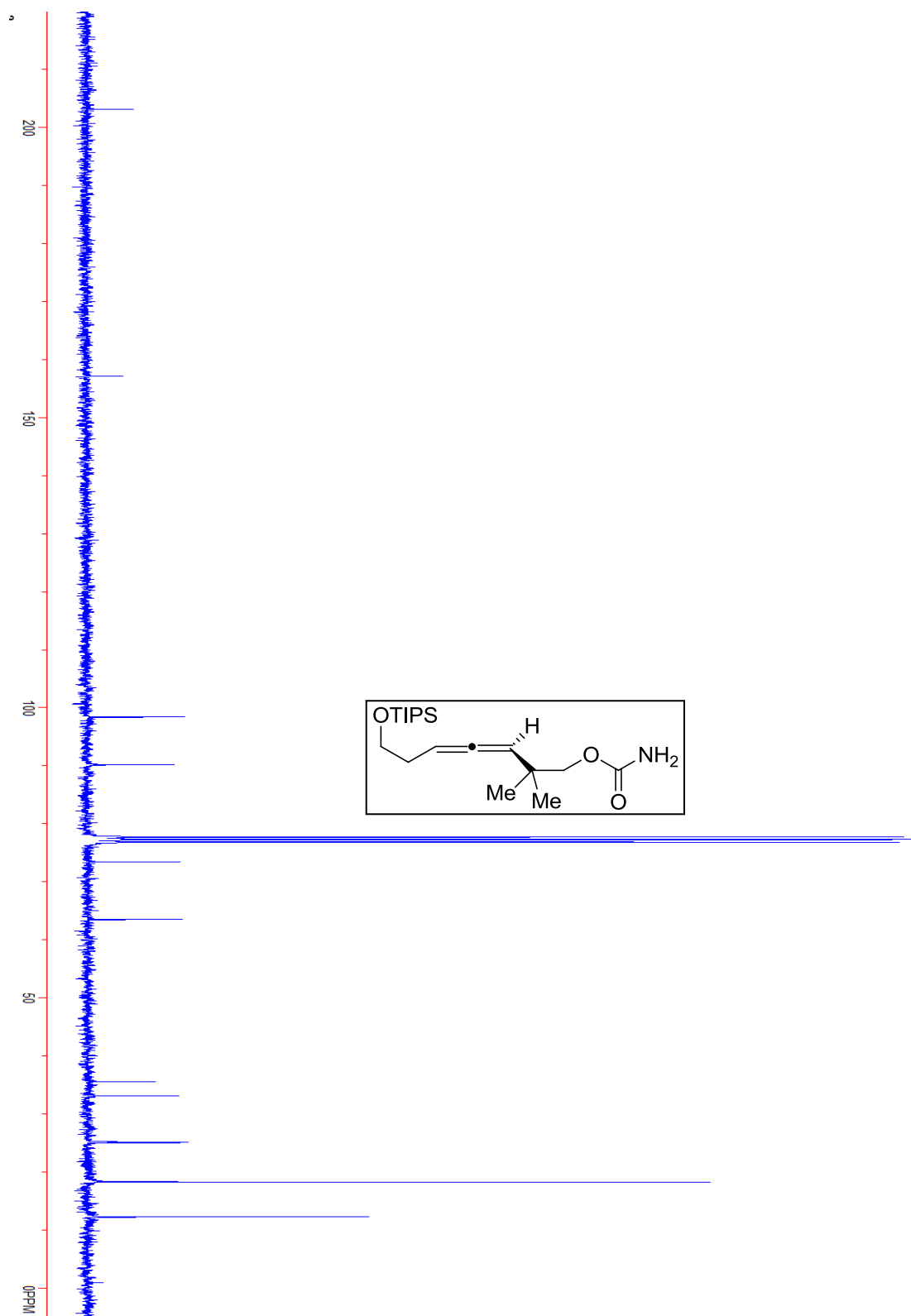
Compound S2.1.



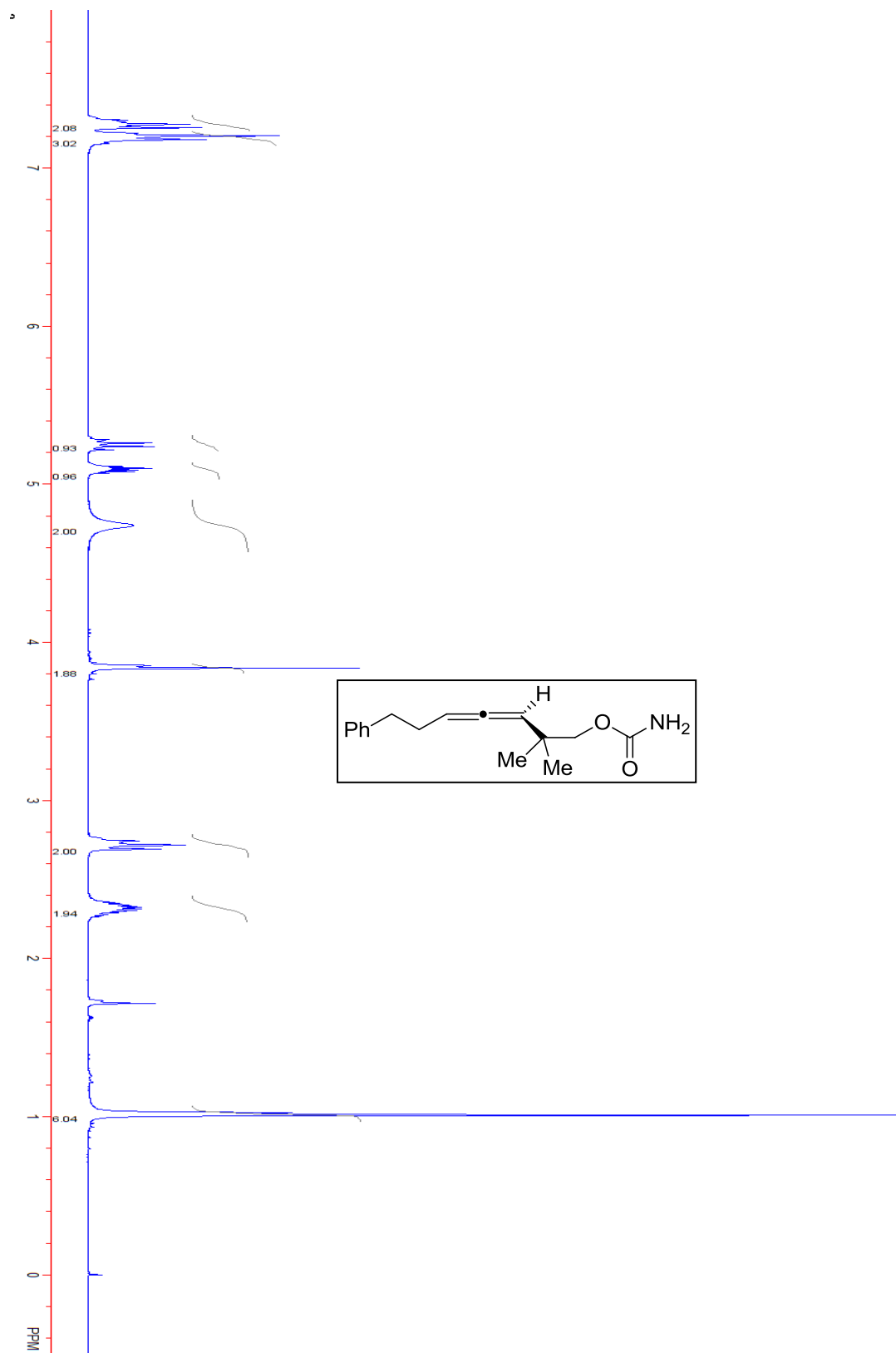
Compound S2.2.



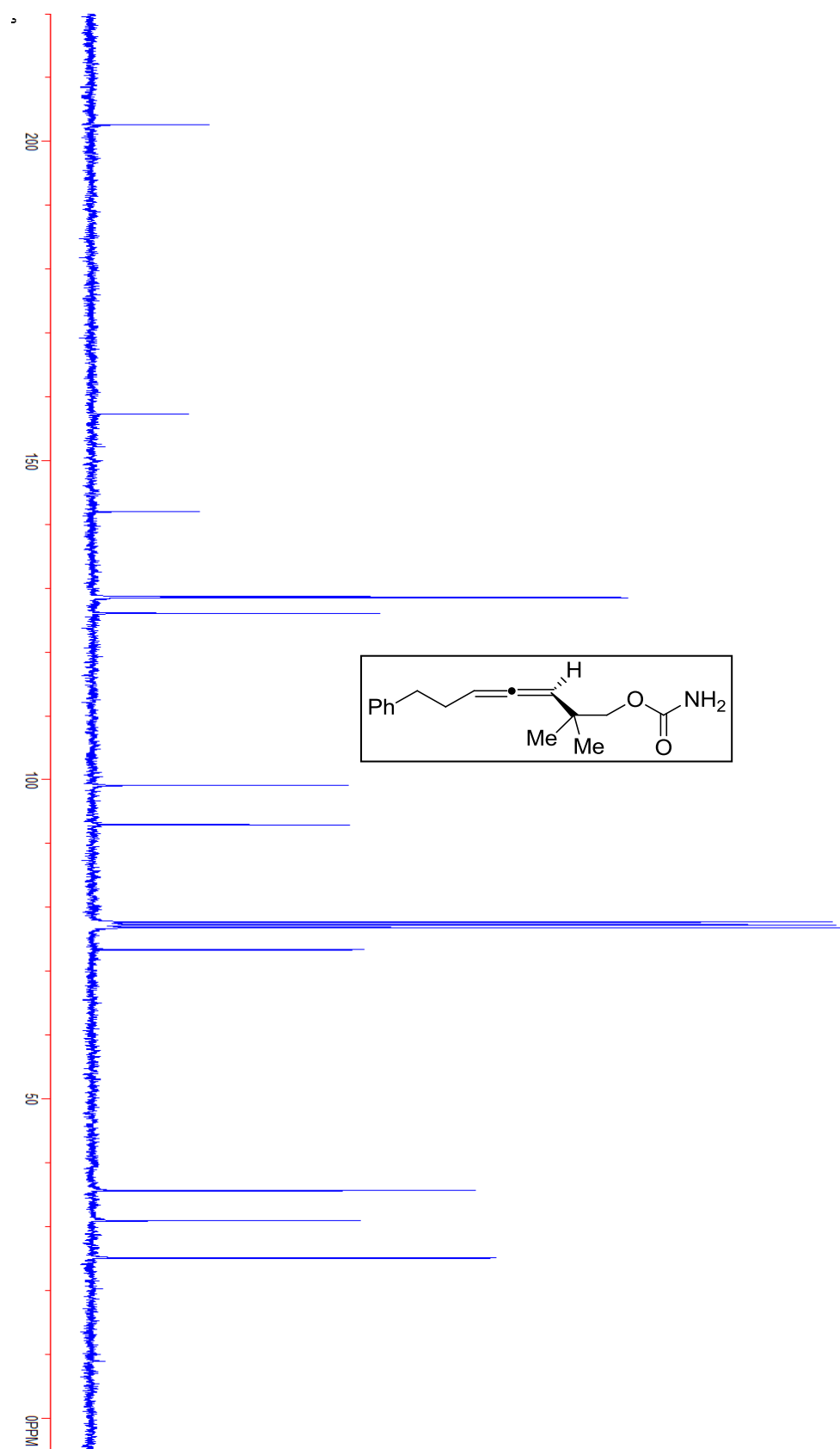
Compound S2.2.



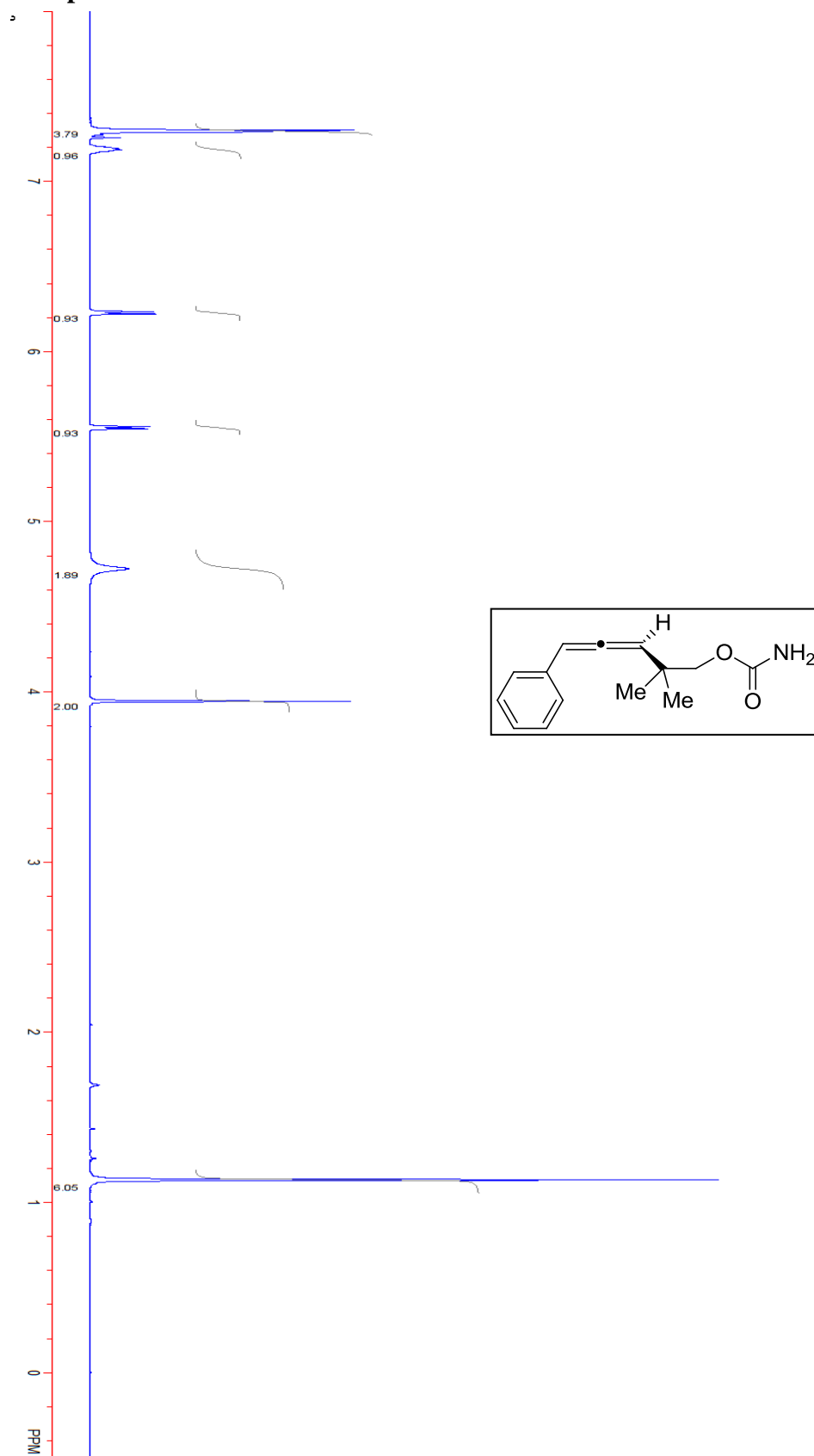
Compound S2.3.



Compound S2.3.



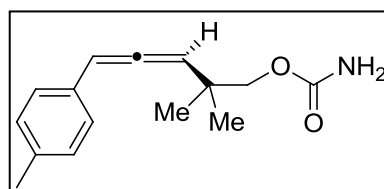
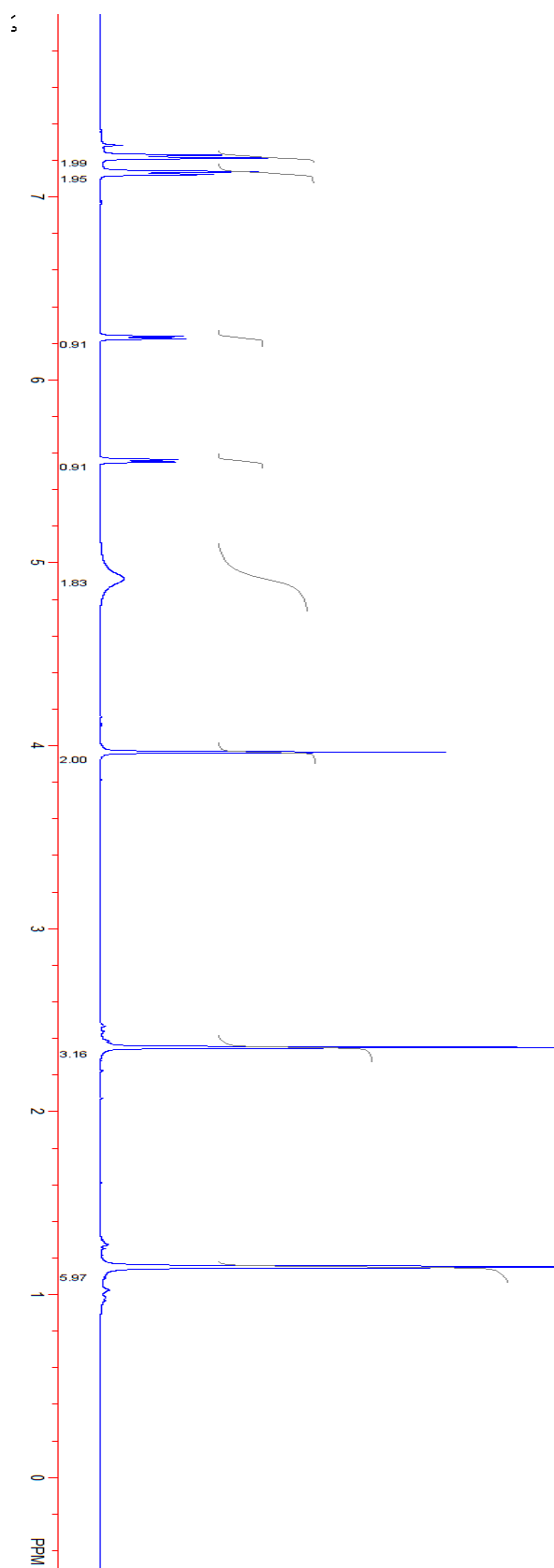
Compound S2.4.



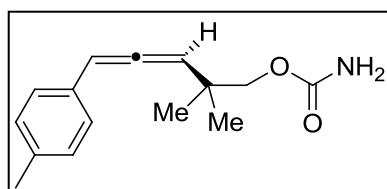
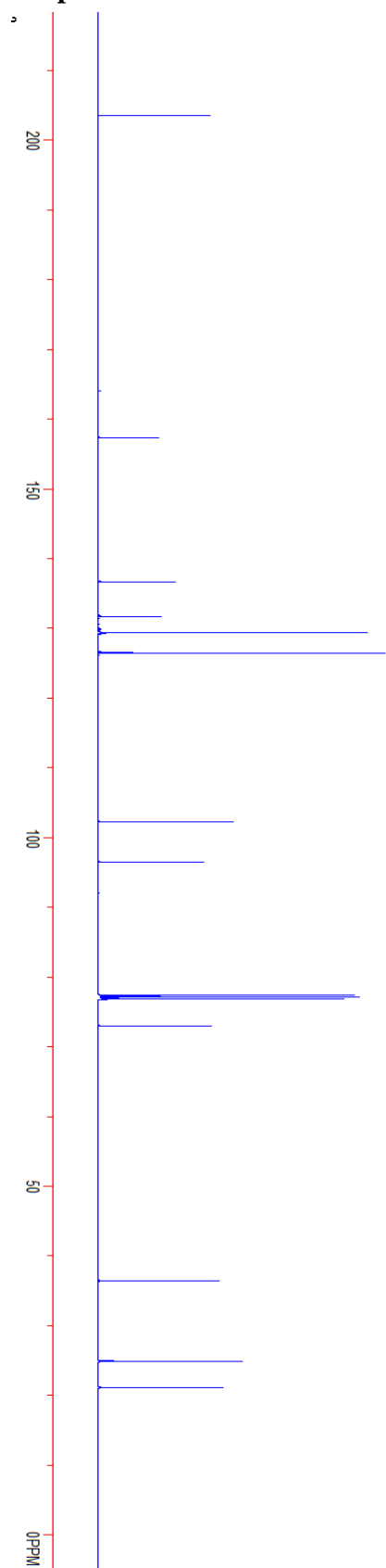
Compound S2.4.



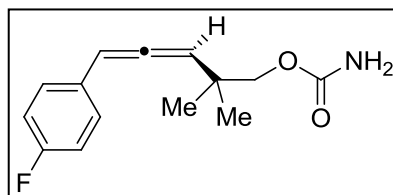
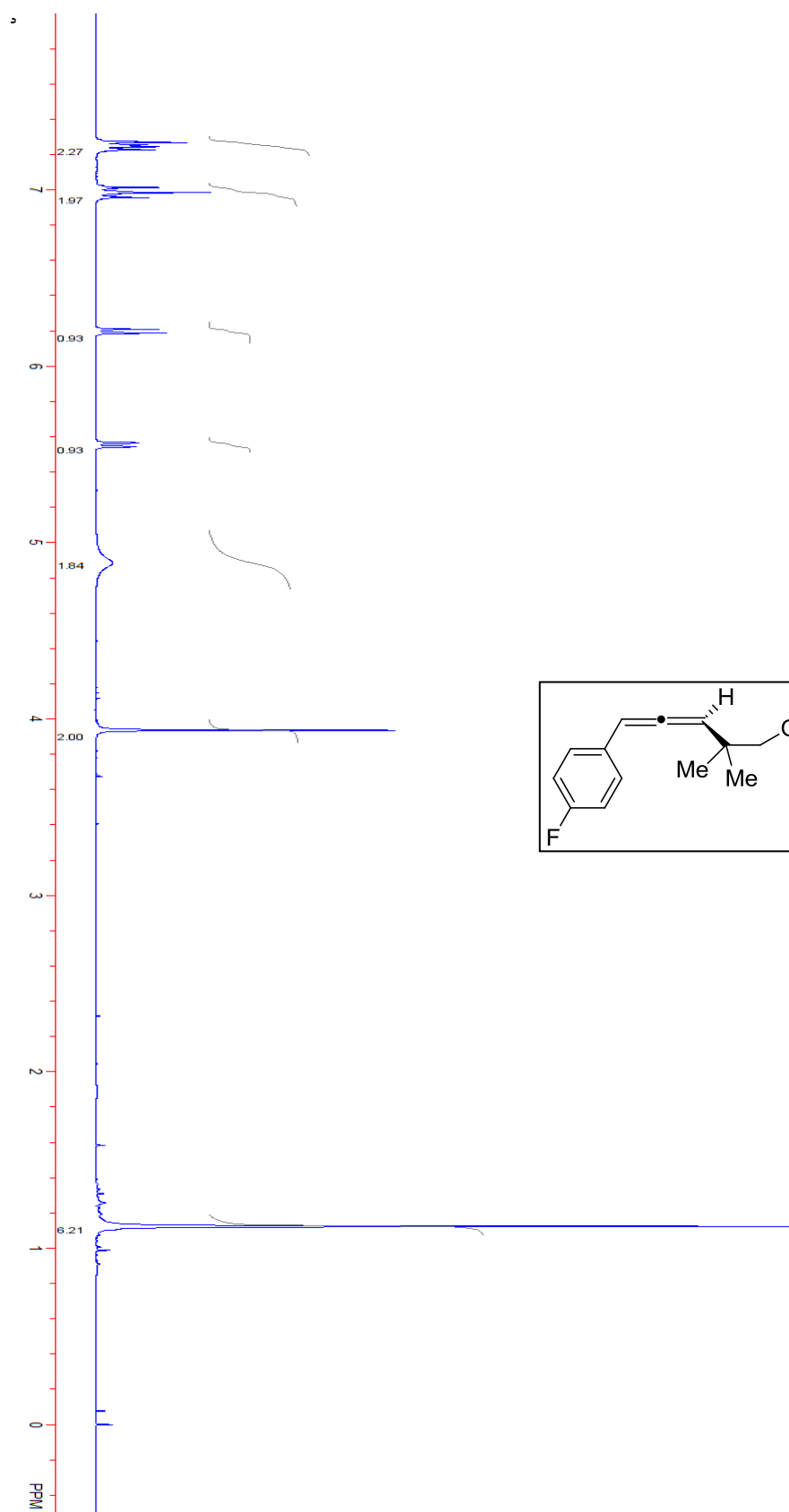
Compound S2.5.



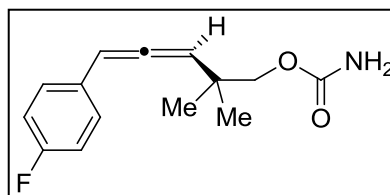
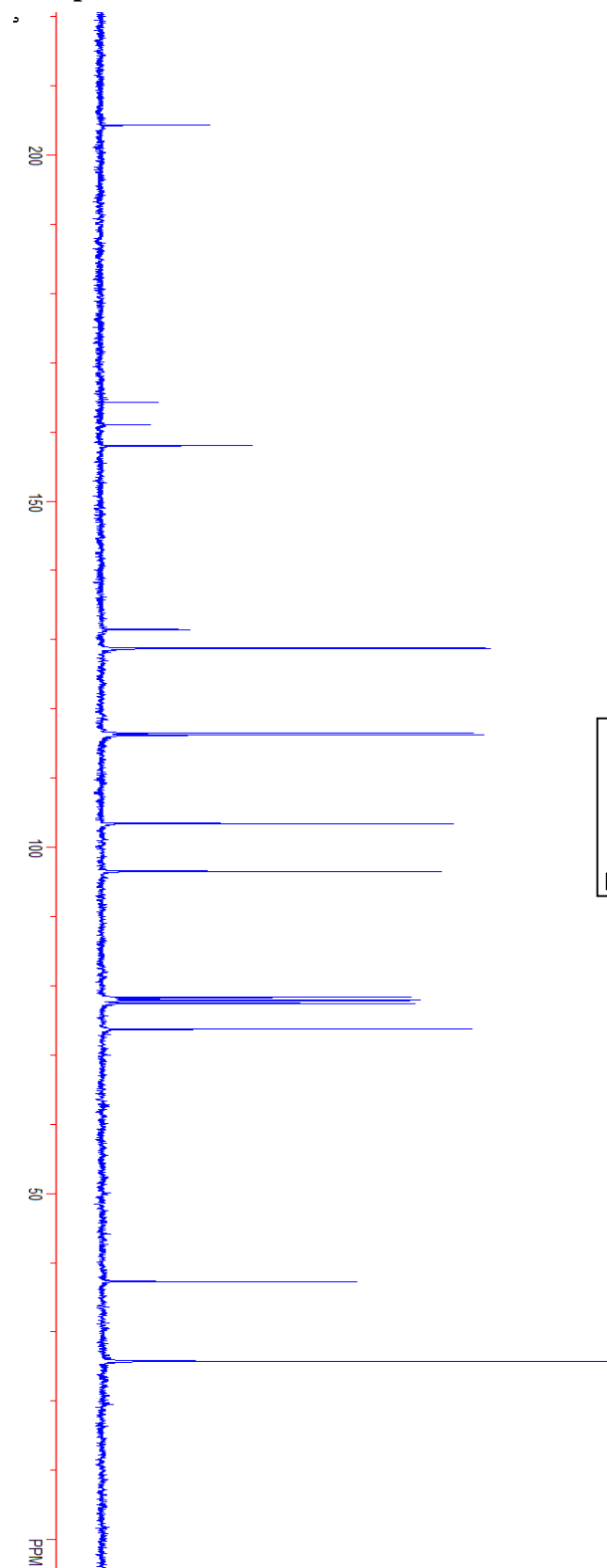
Compound S2.5.



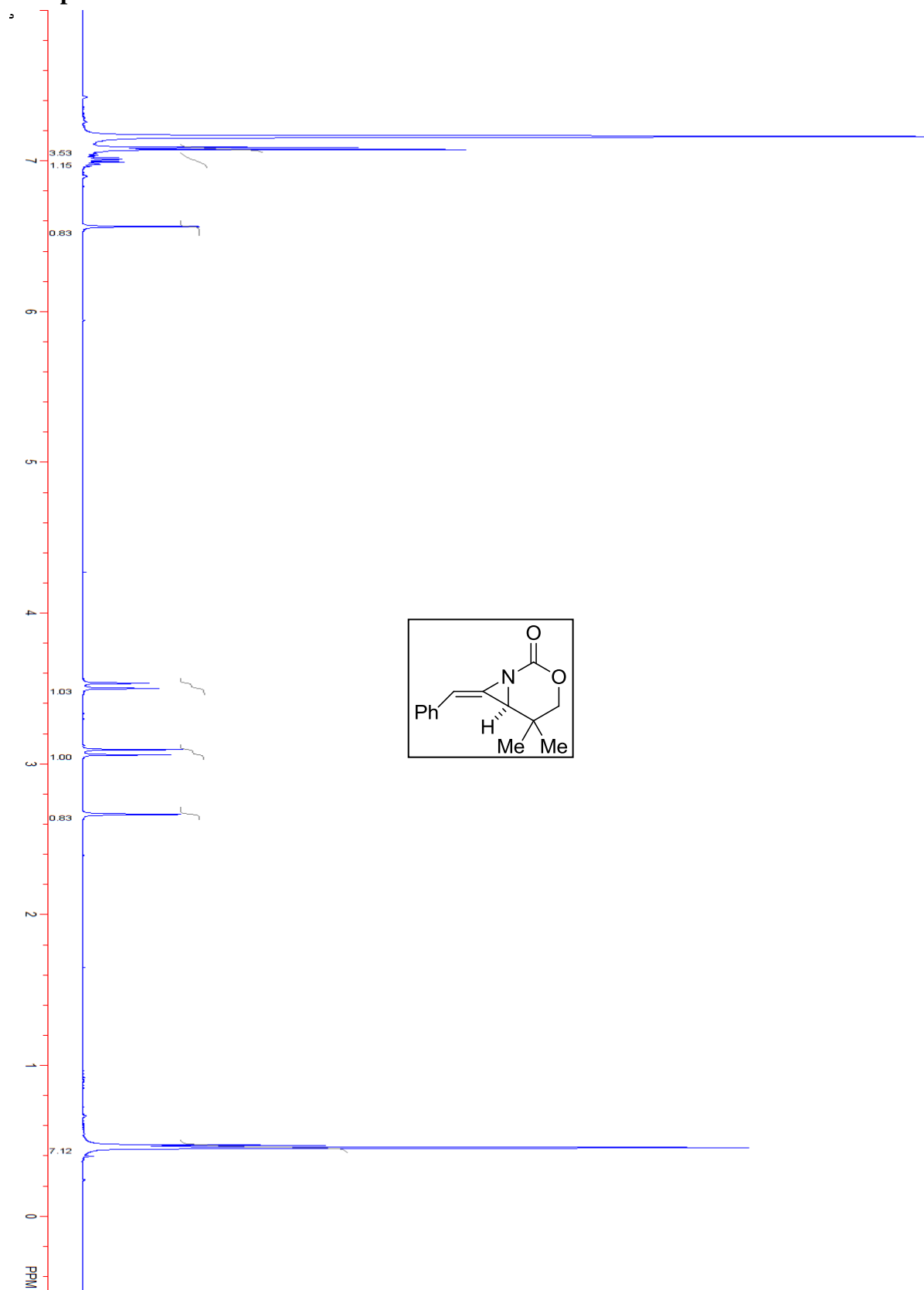
Compound S2.6.



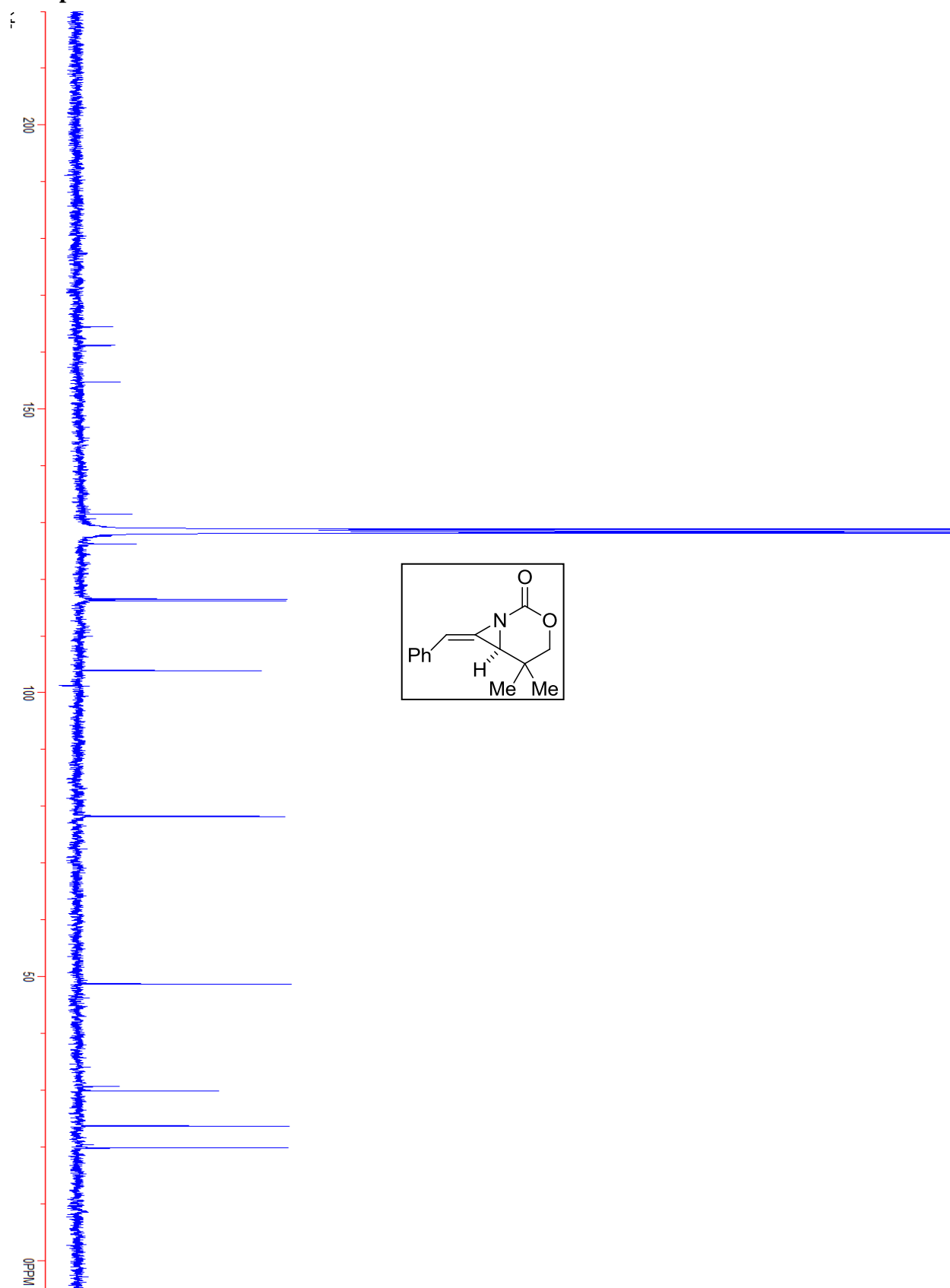
Compound S2.6.



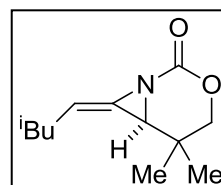
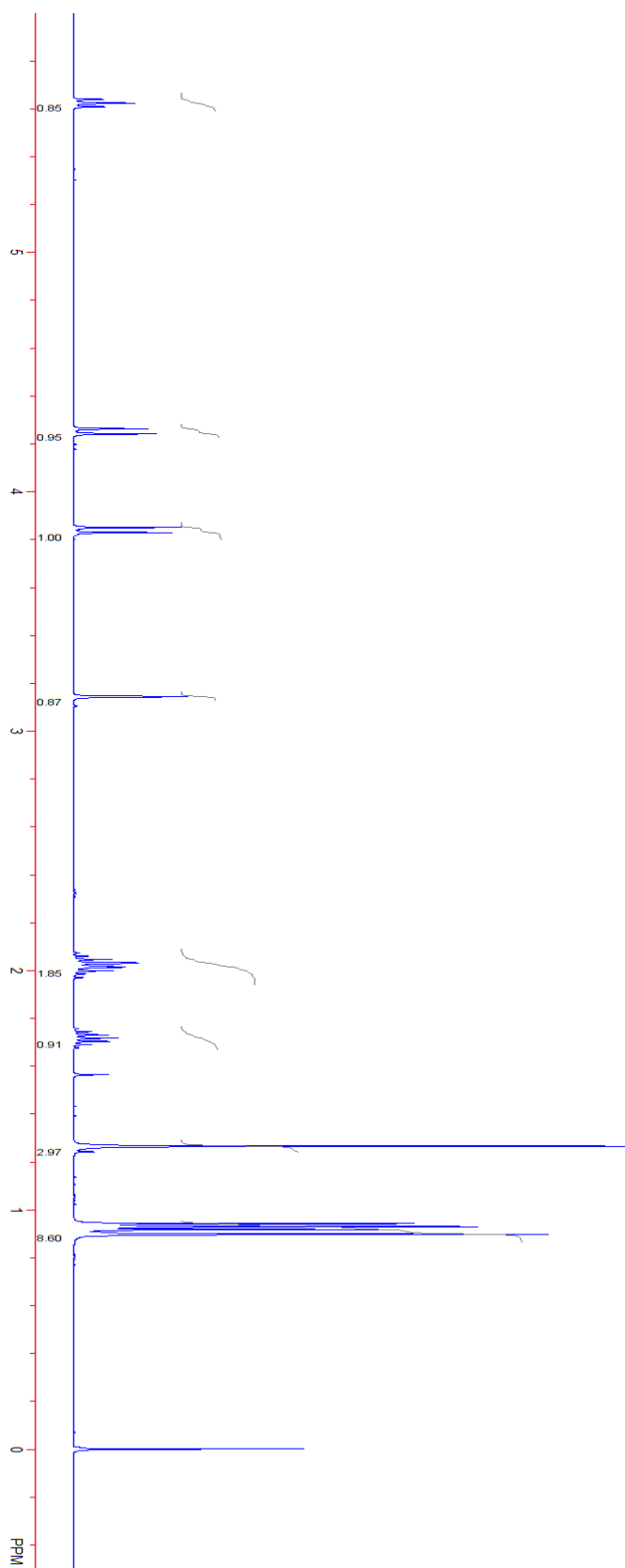
Compound 2.17.



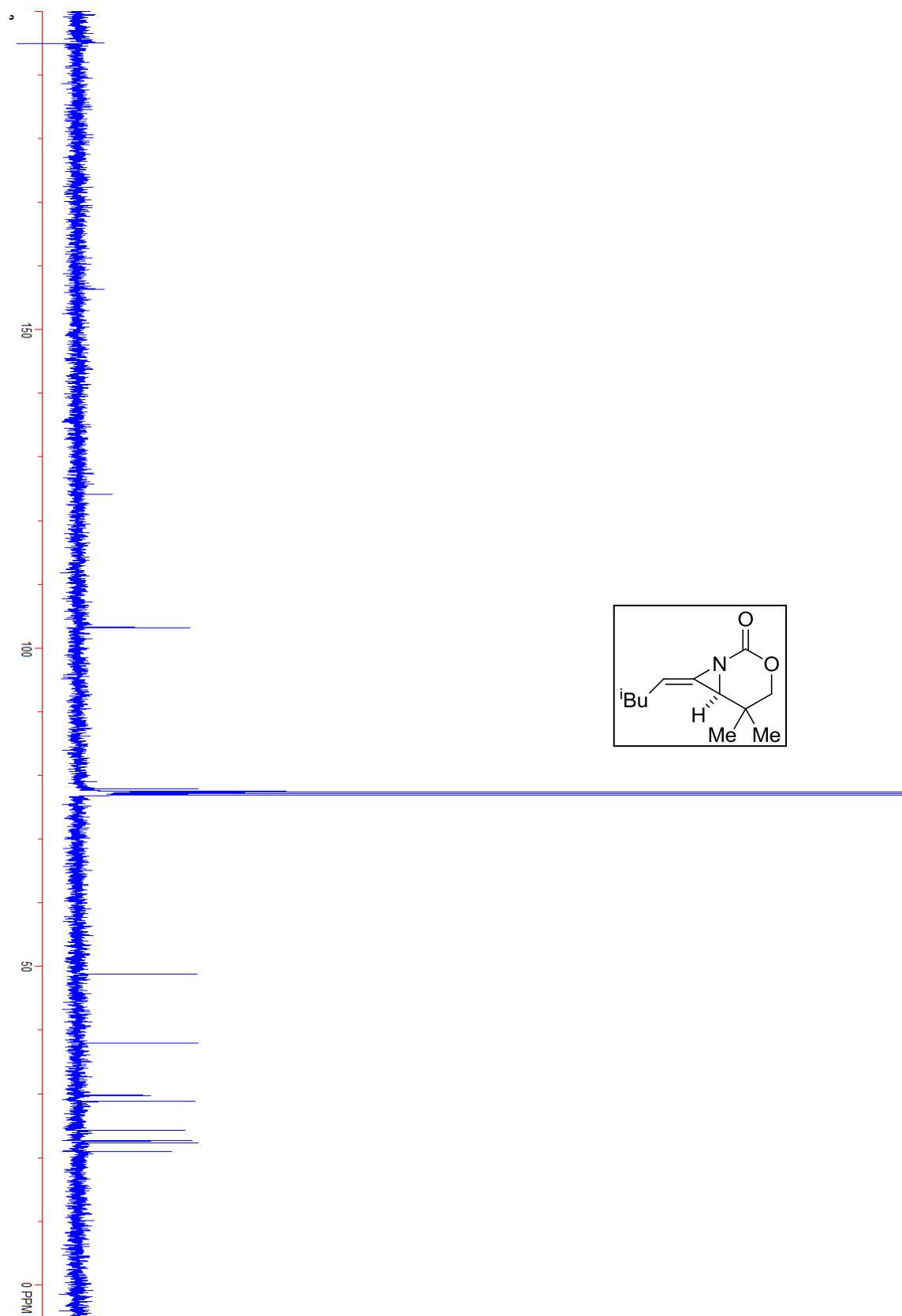
Compound 2.17.

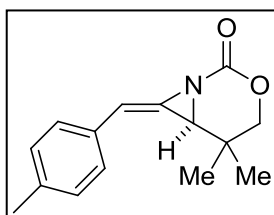
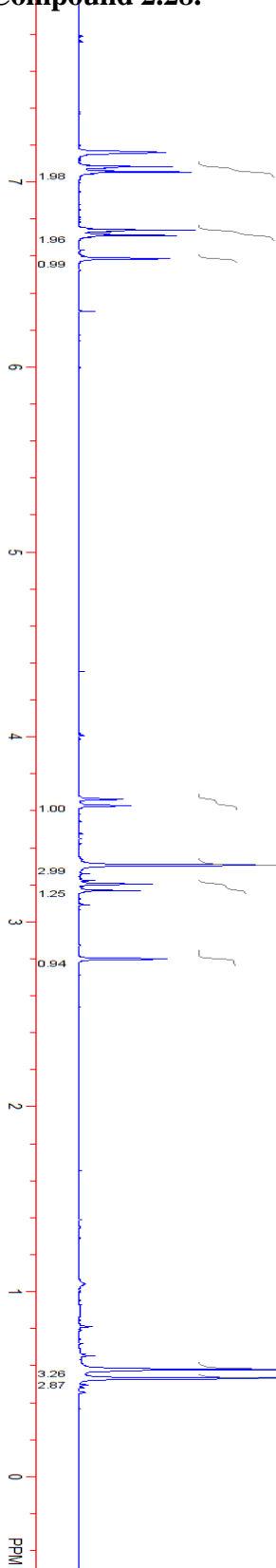


Compound 2.24.

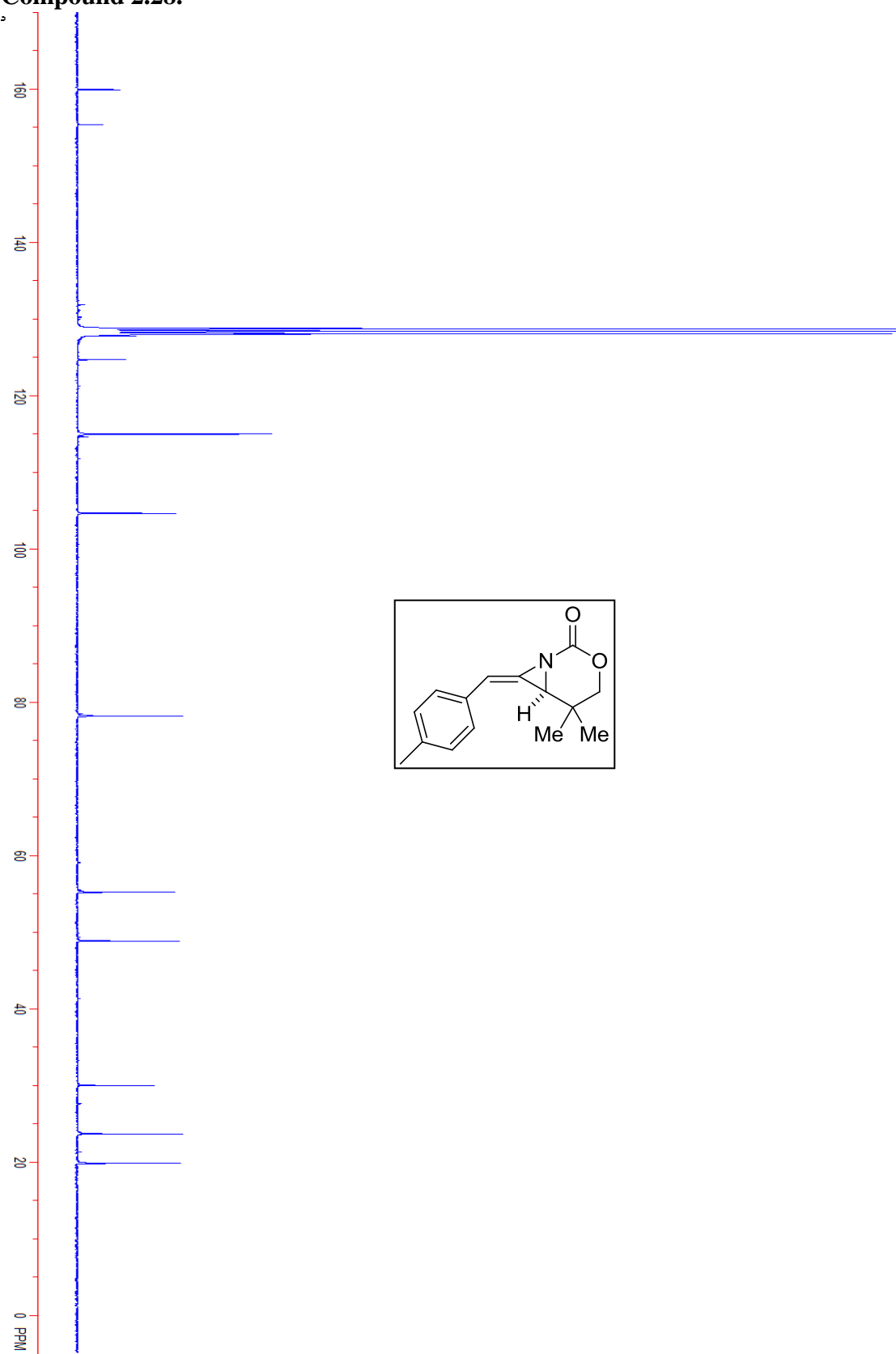


Compound 2.24.

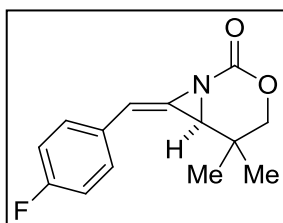
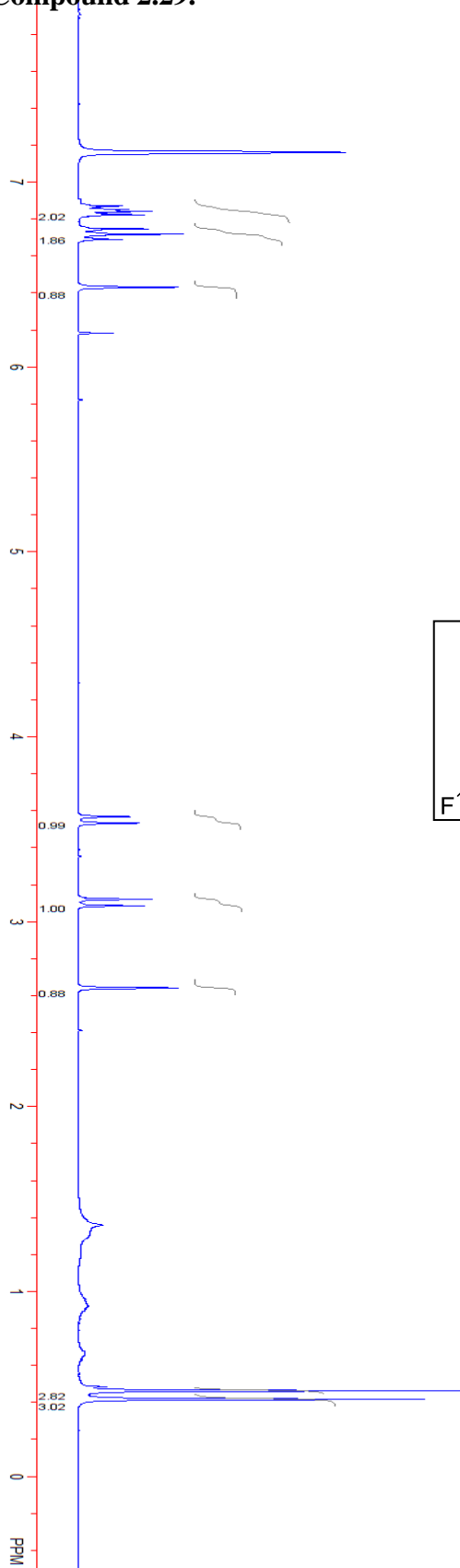


Compound 2.28.

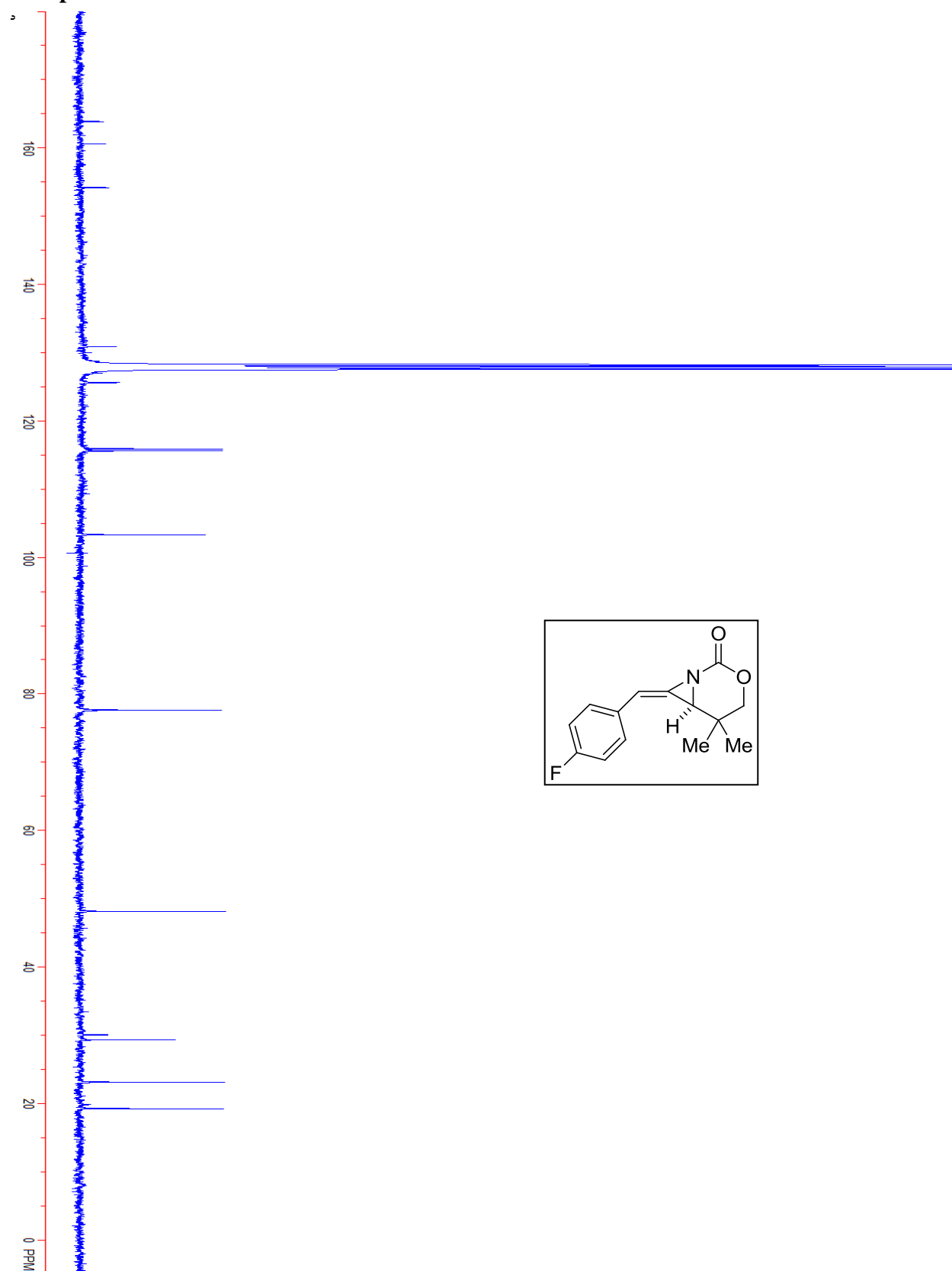
Compound 2.28.

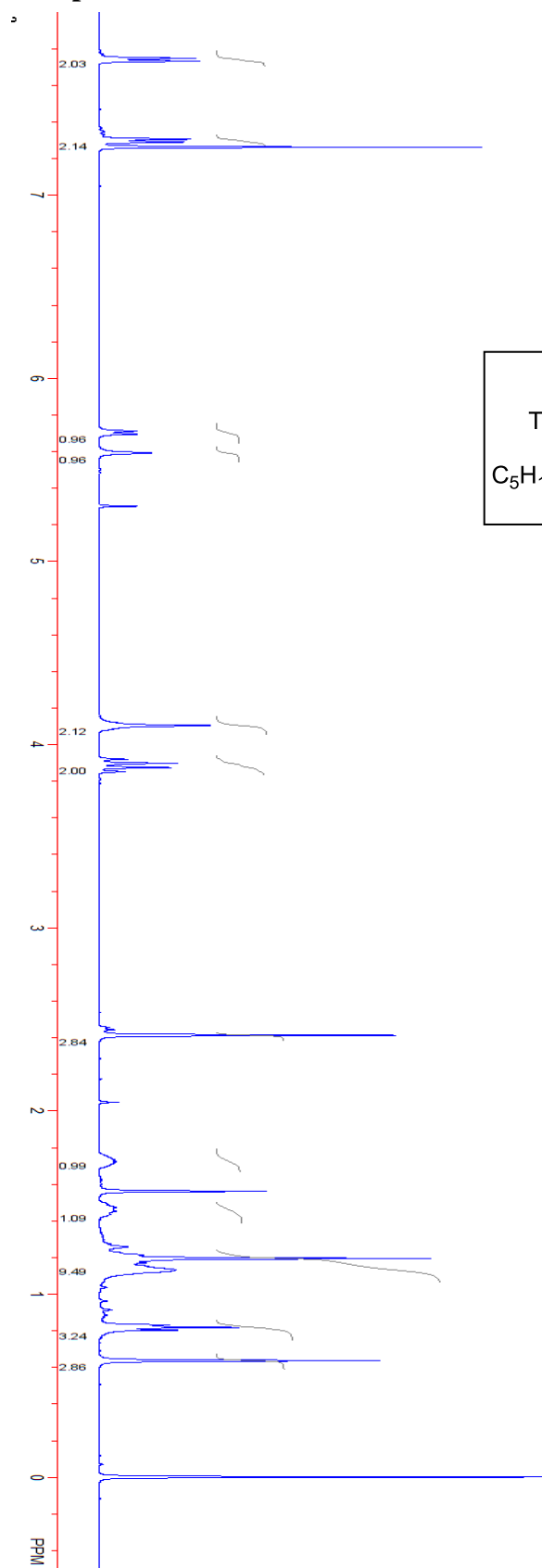


Compound 2.29.

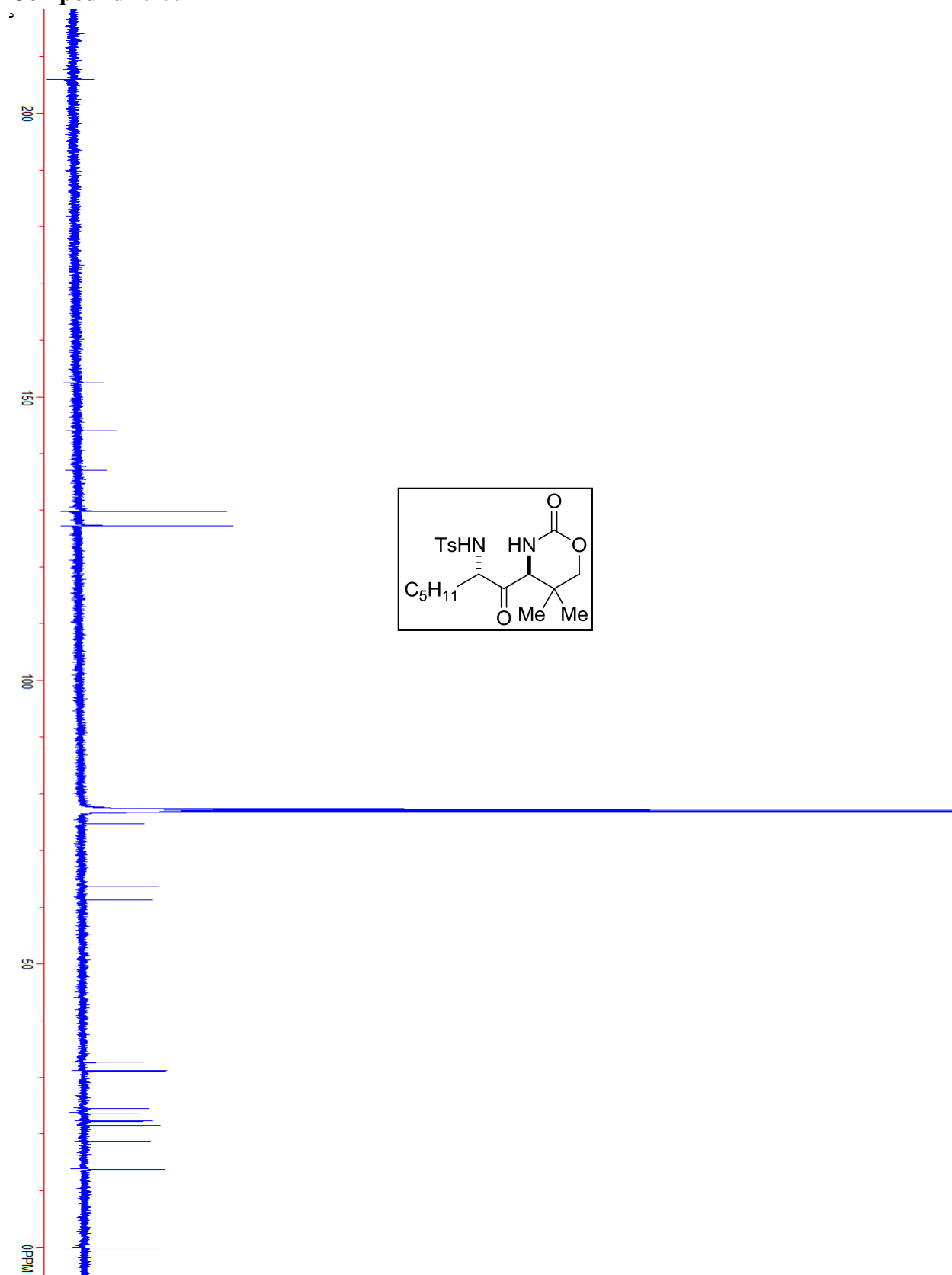


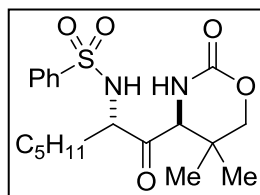
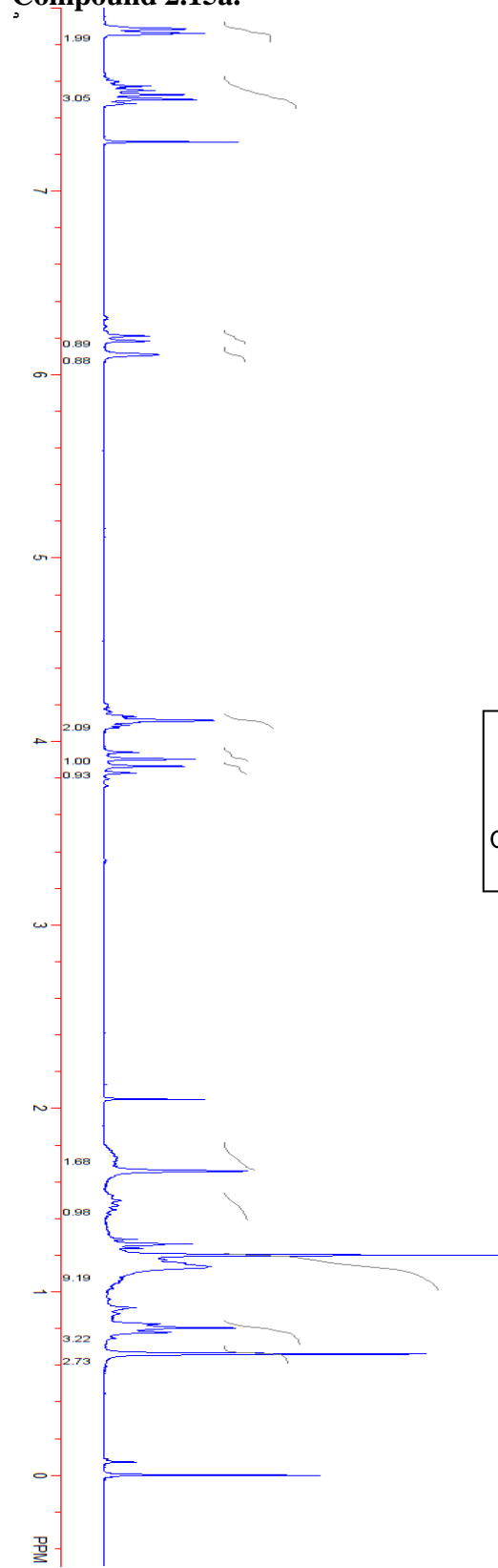
Compound 2.29.



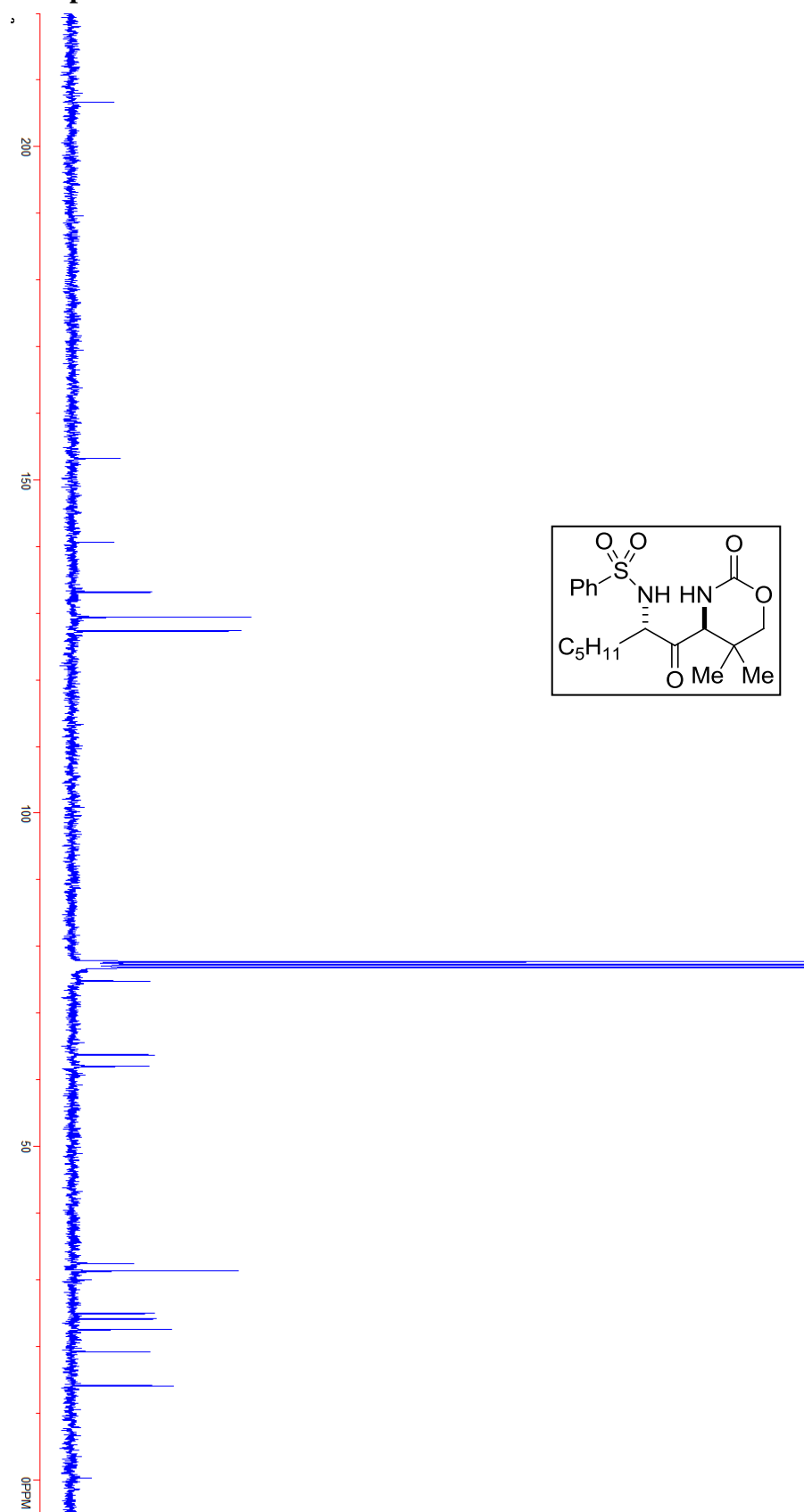
Compound 2.15.

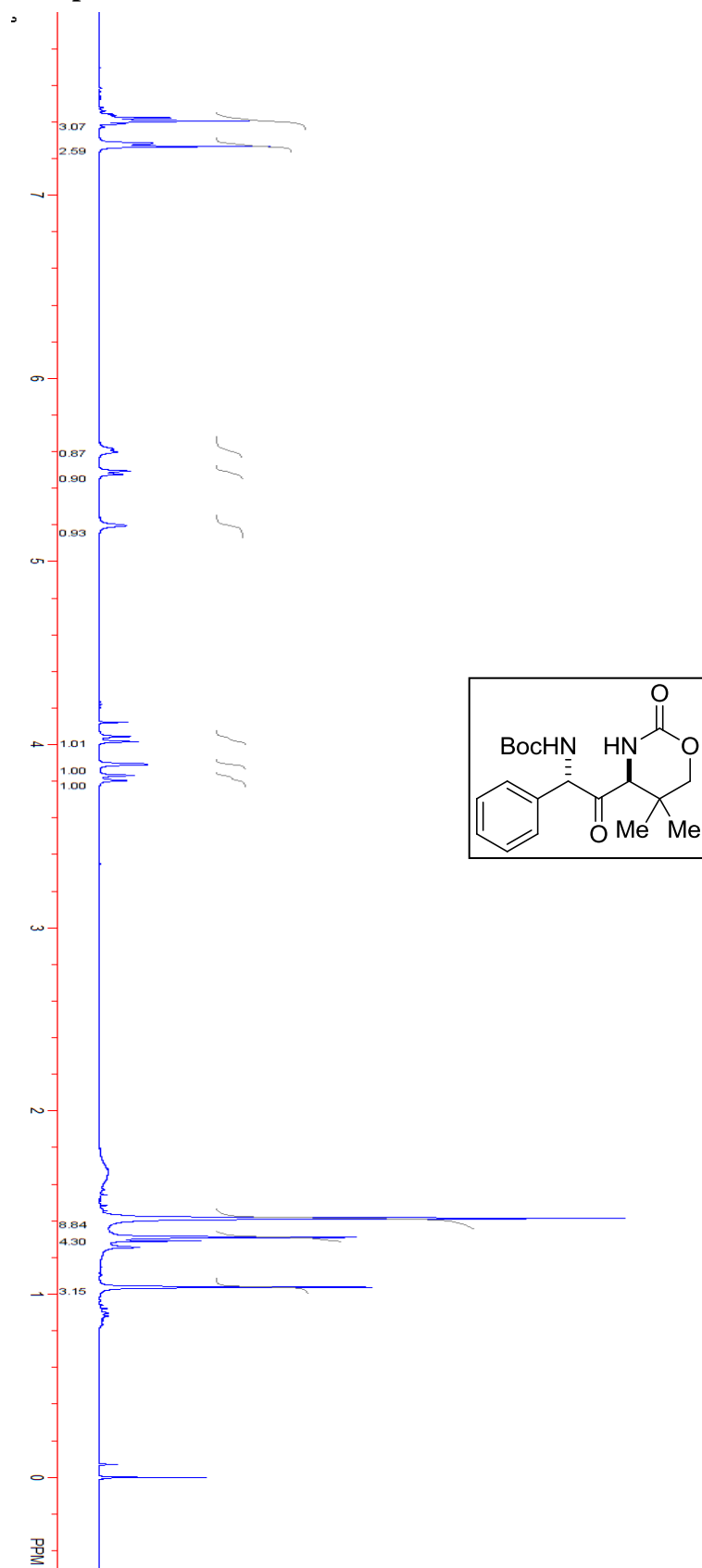
Compound 2.15.



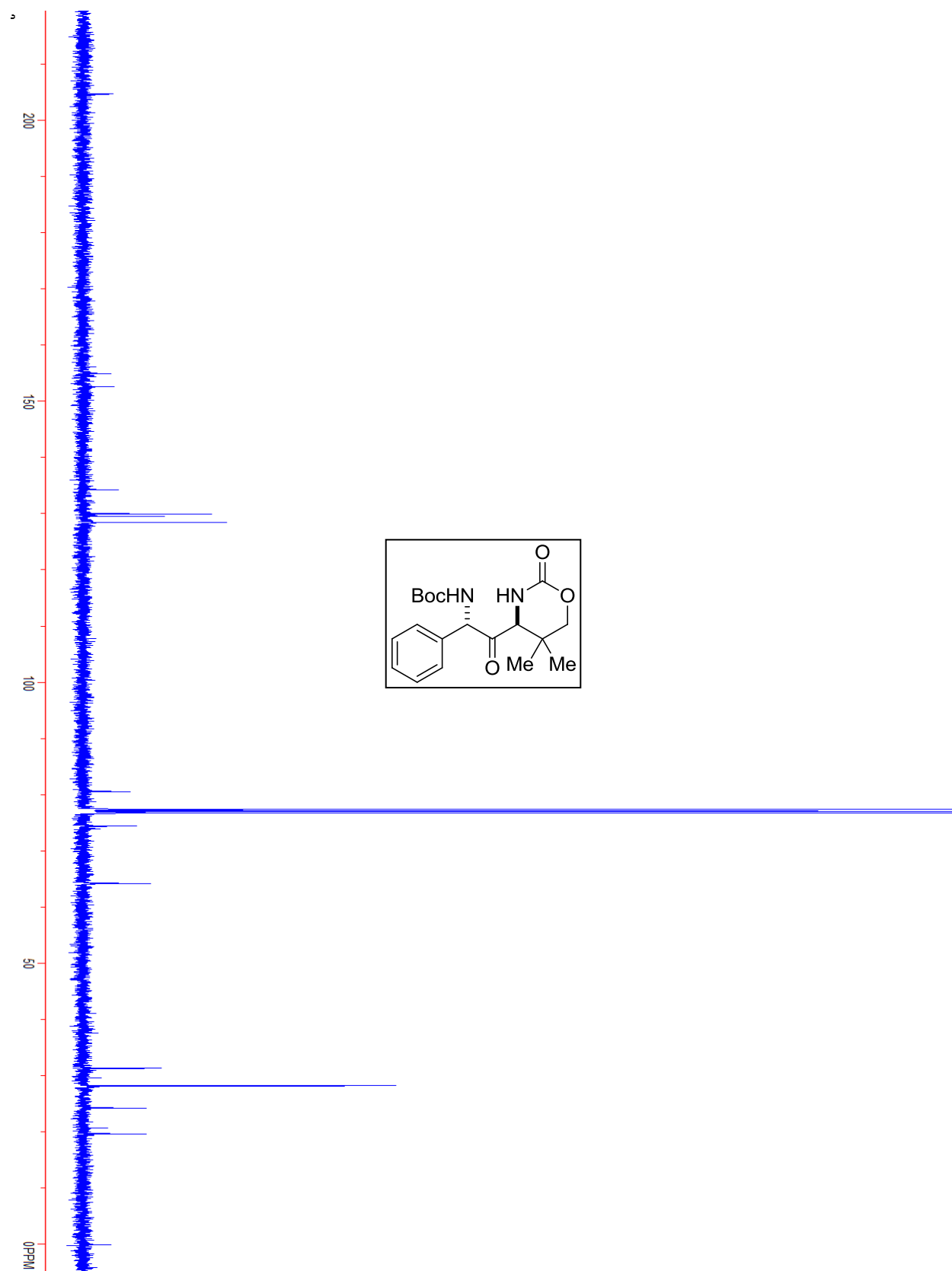
Compound 2.15a.

Compound 2.15a.

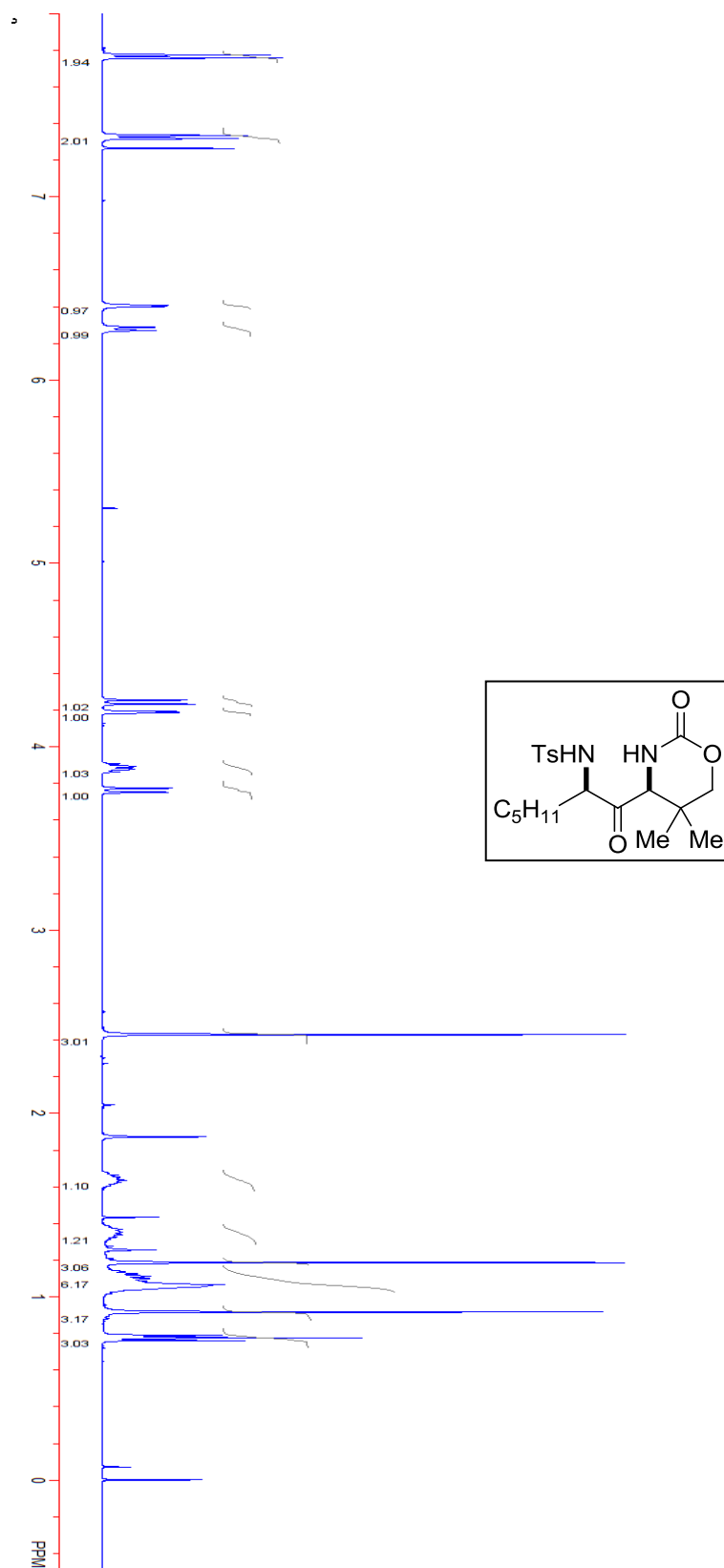


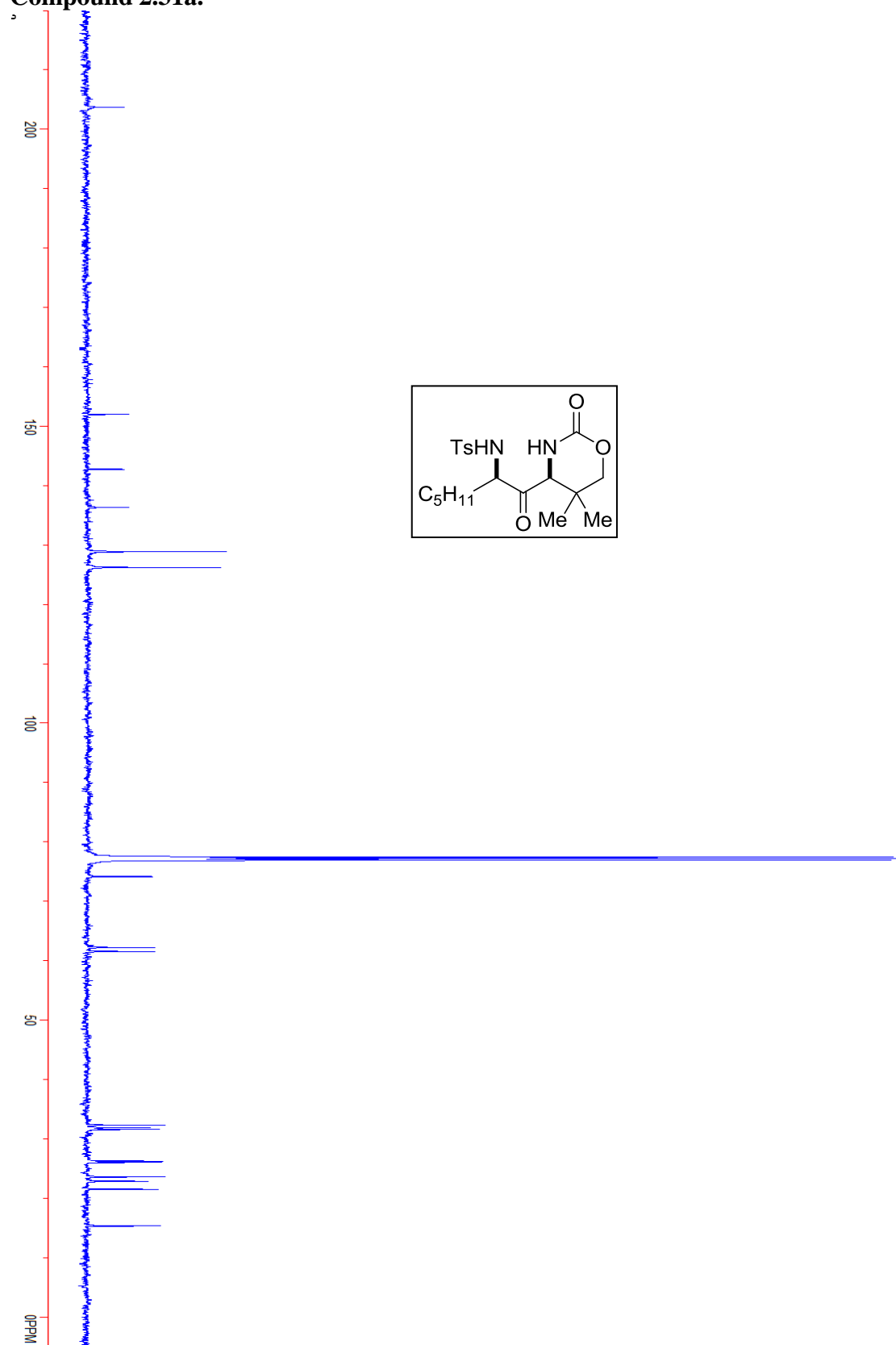
Compound 2.18.

Compound 2.18.

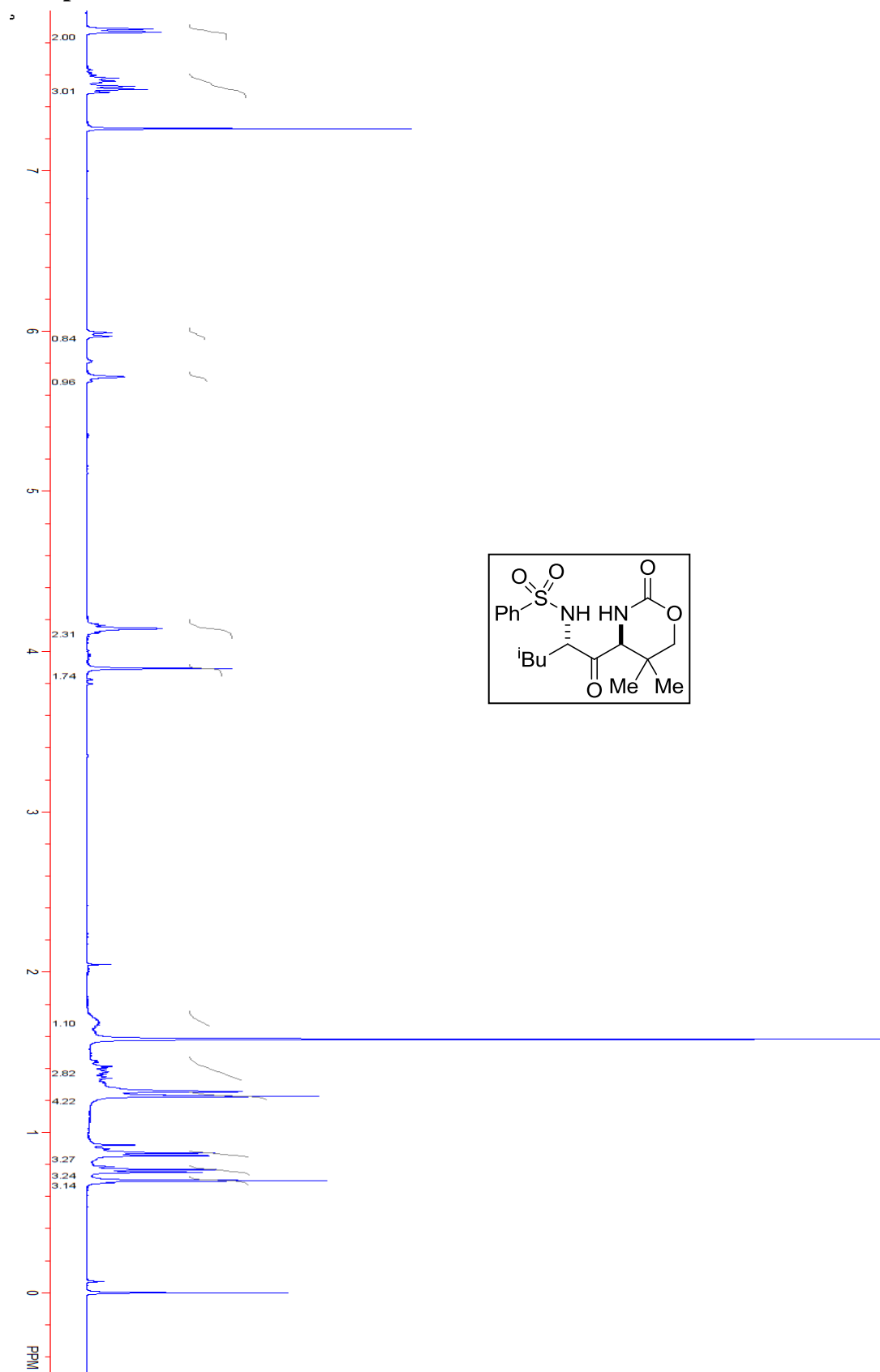


Compound 2.31a.

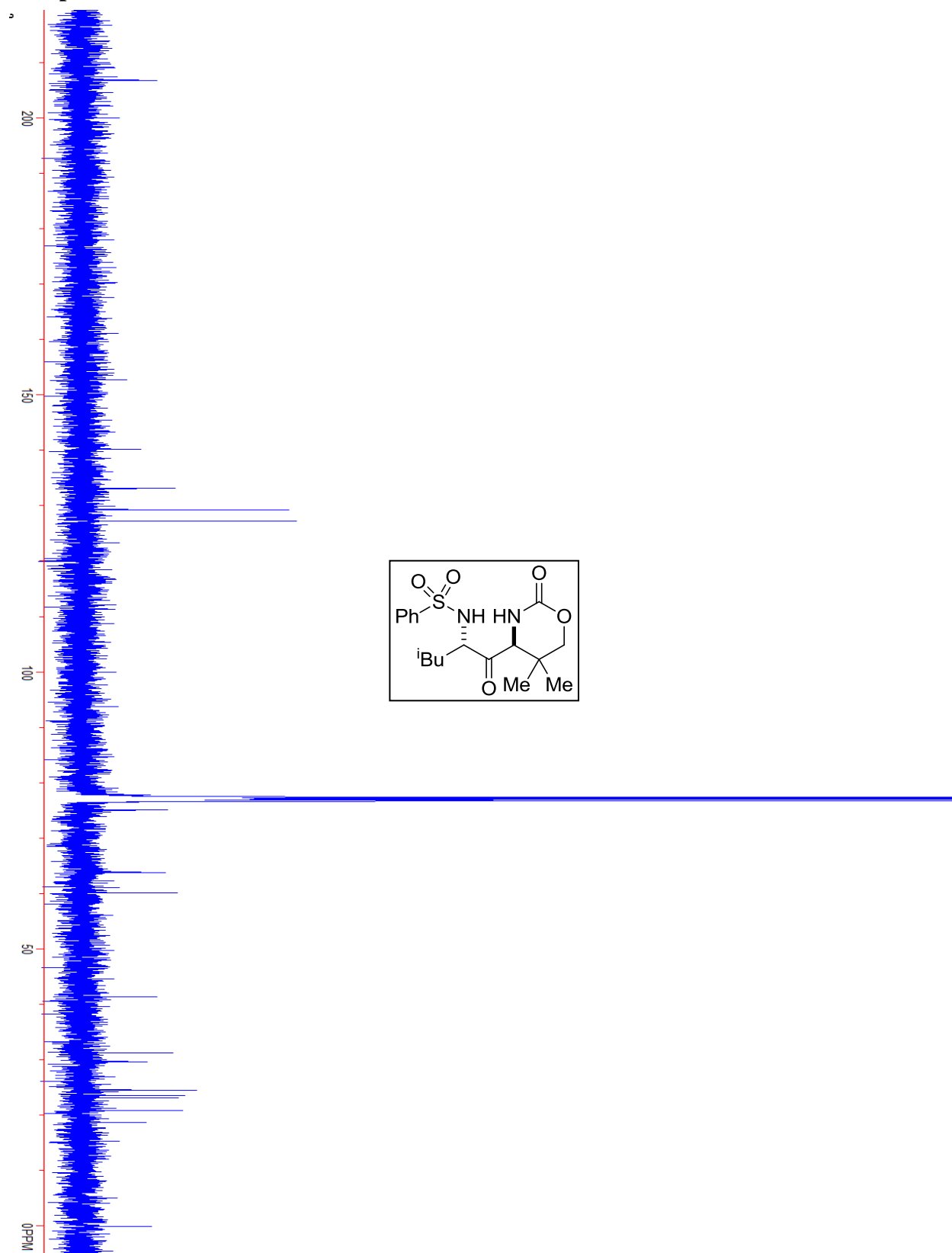


Compound 2.31a.

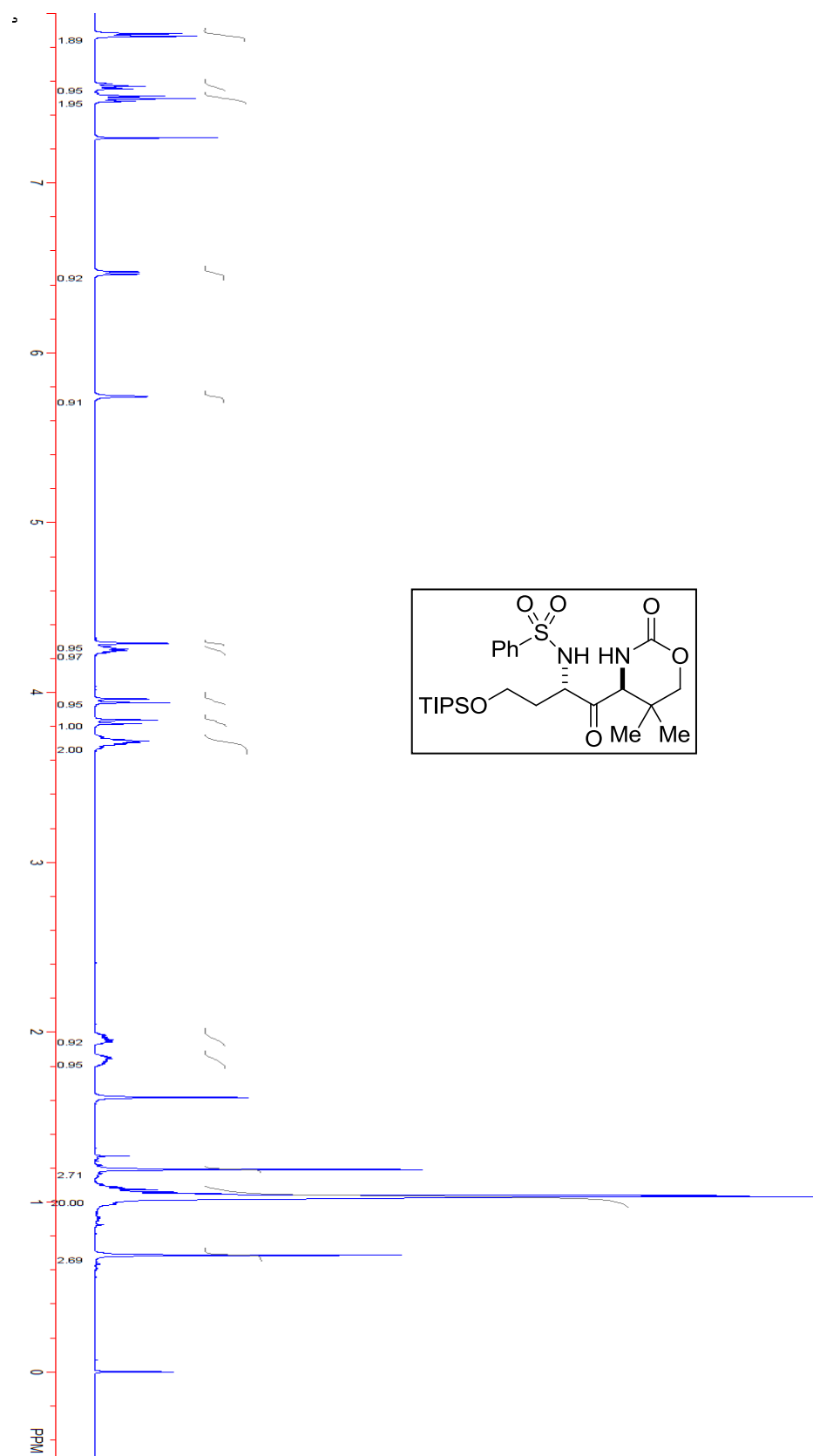
Compound 2.32a.



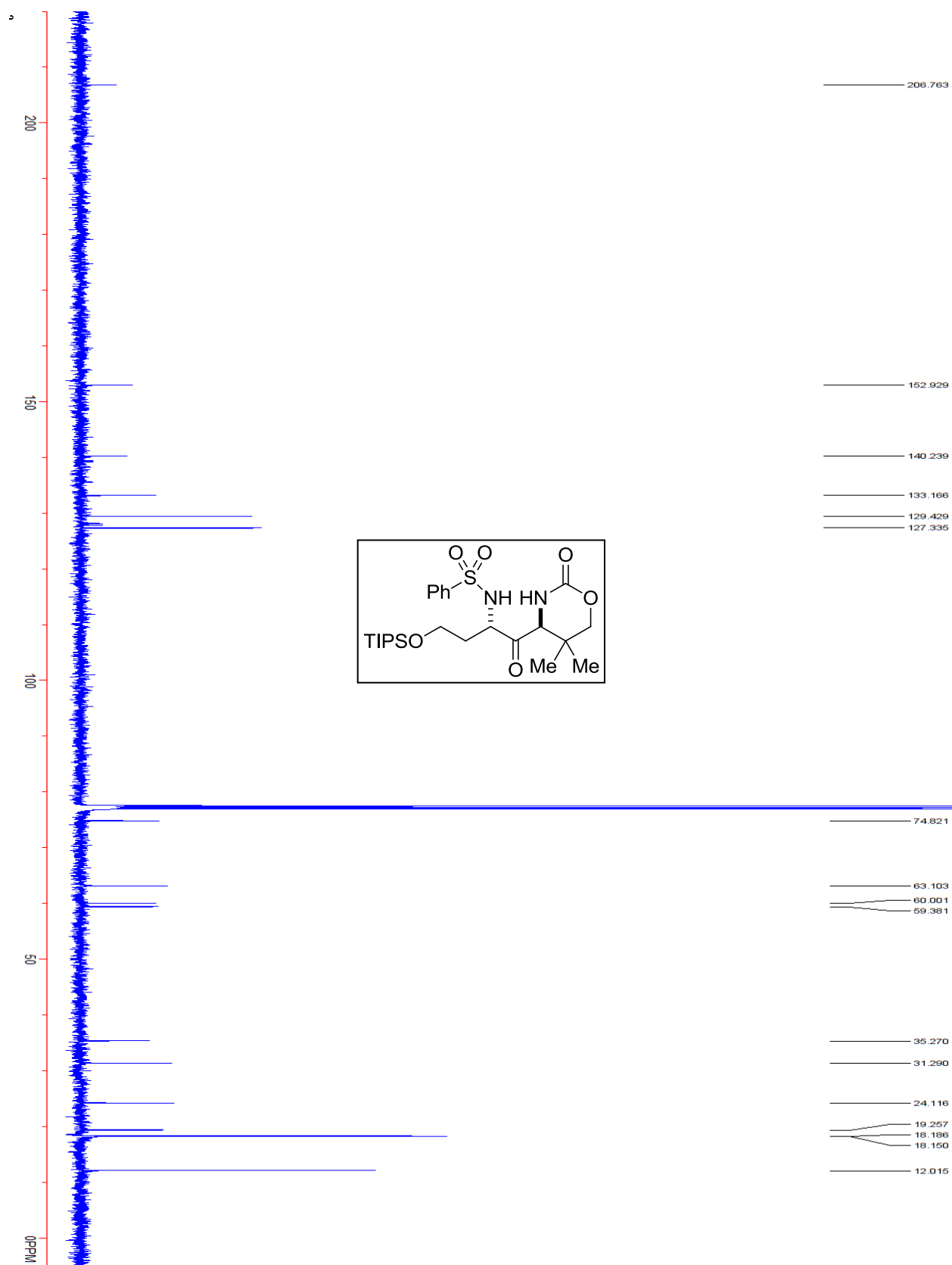
Compound 2.32a.



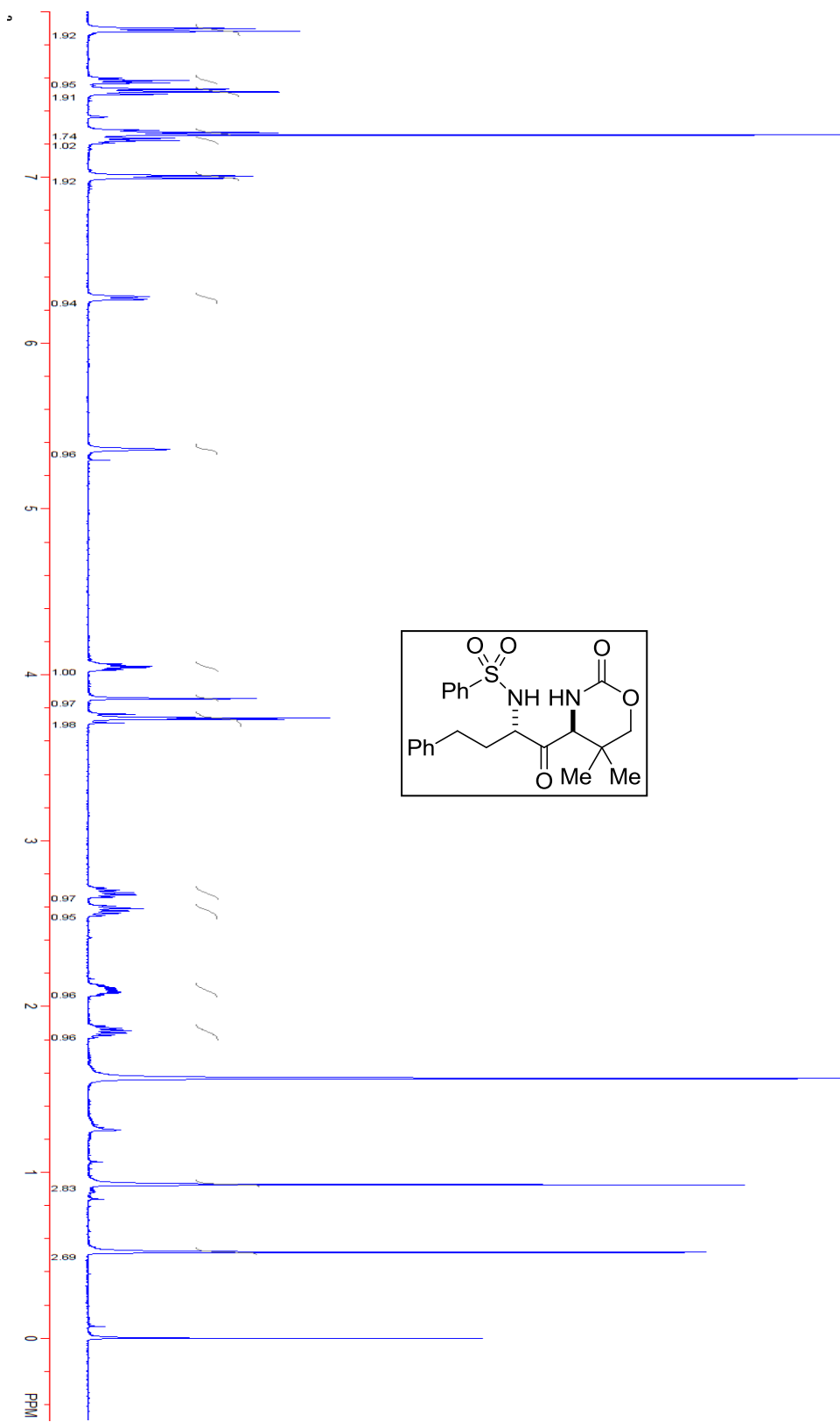
Compound 2.33a.



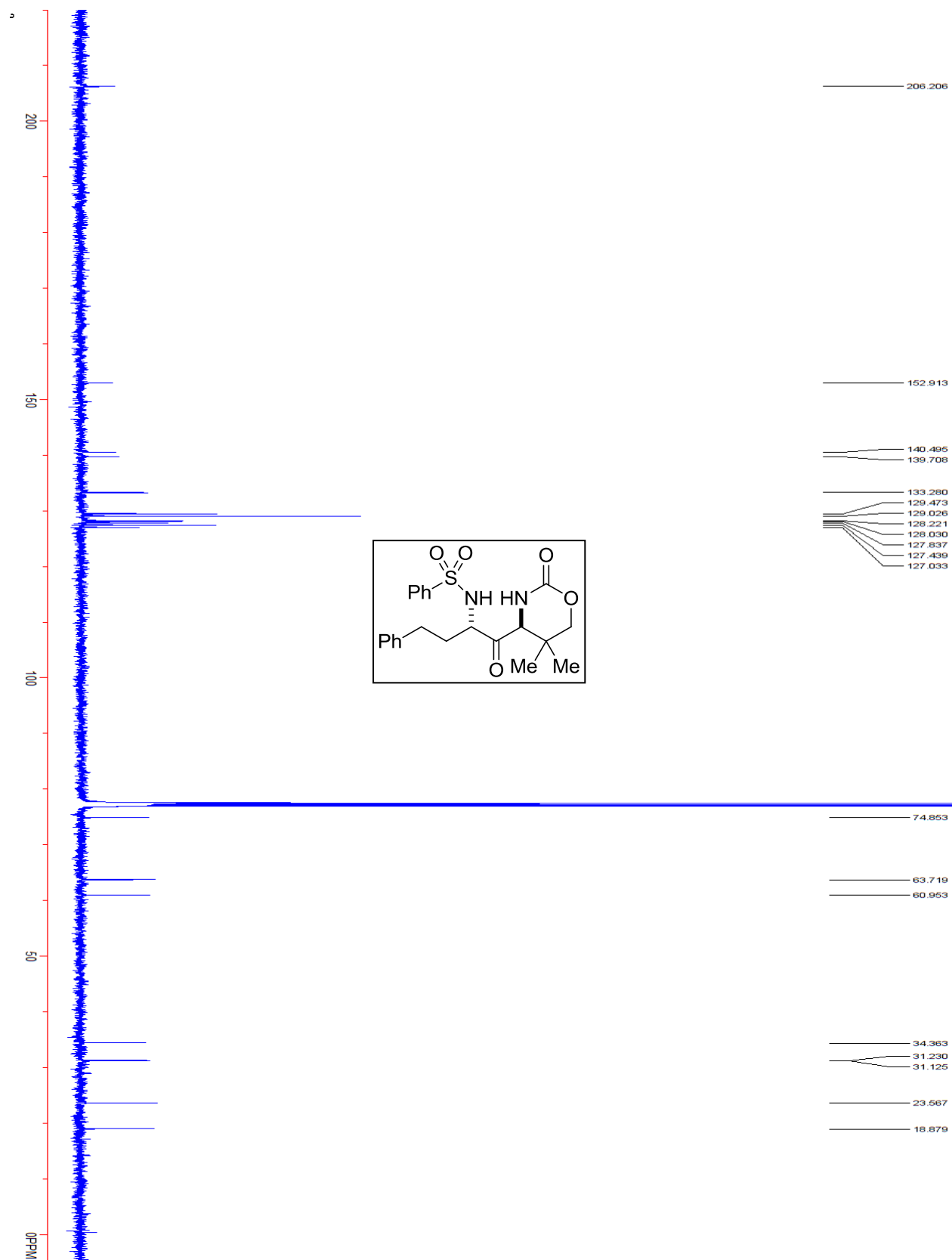
Compound 2.33a.



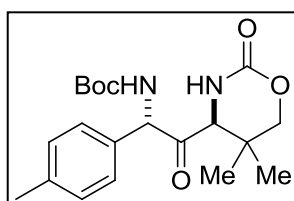
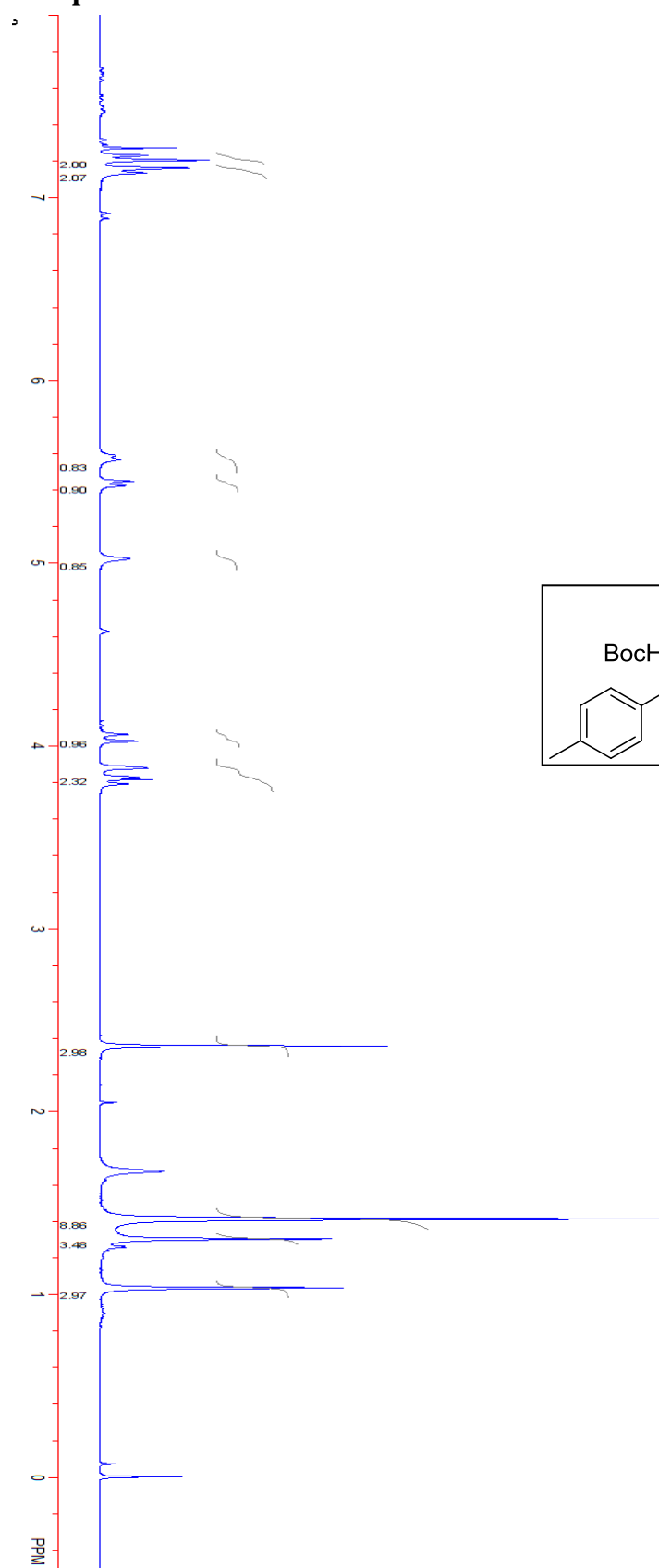
Compound 2.34a.



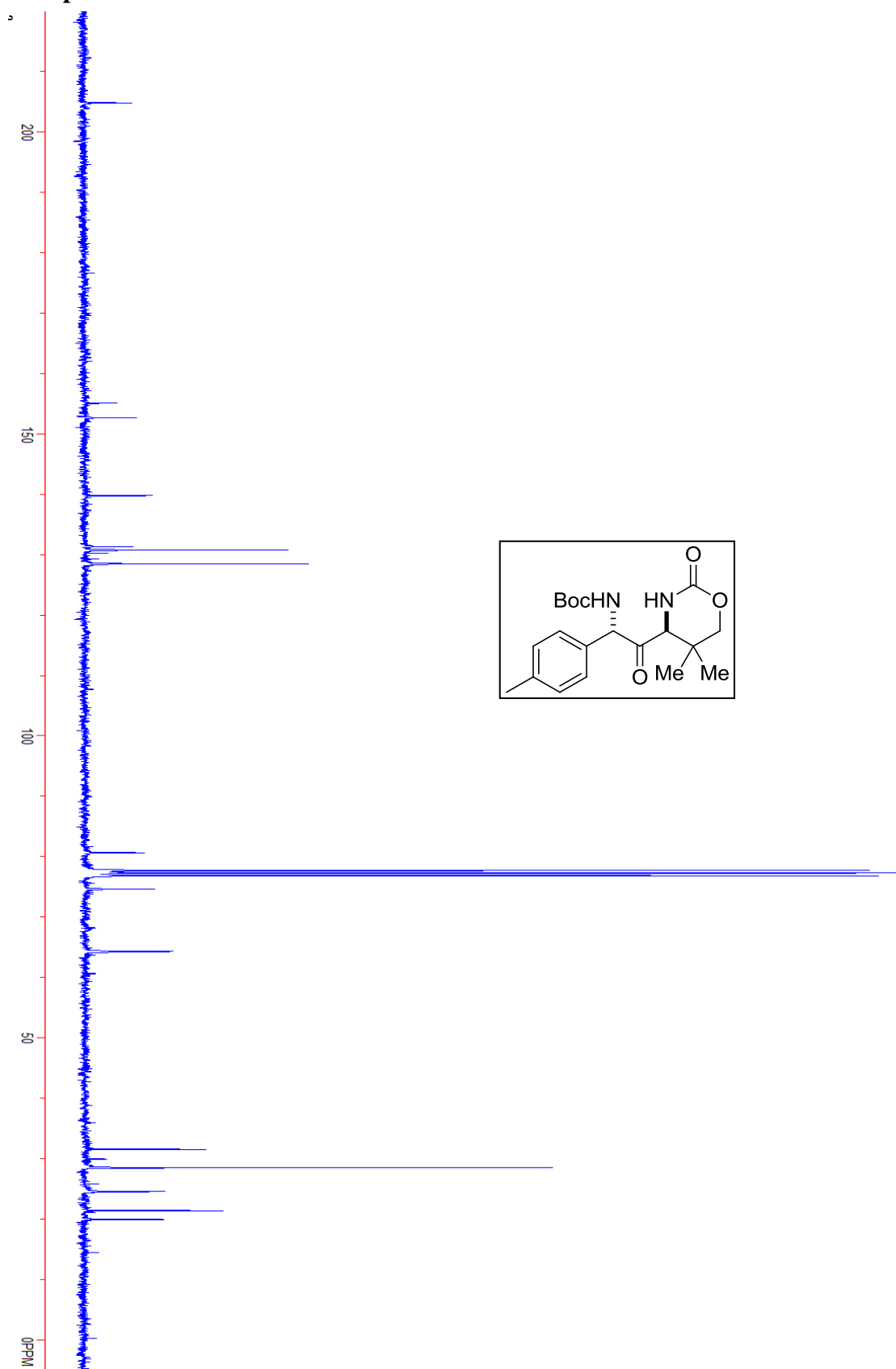
Compound 2.34a.



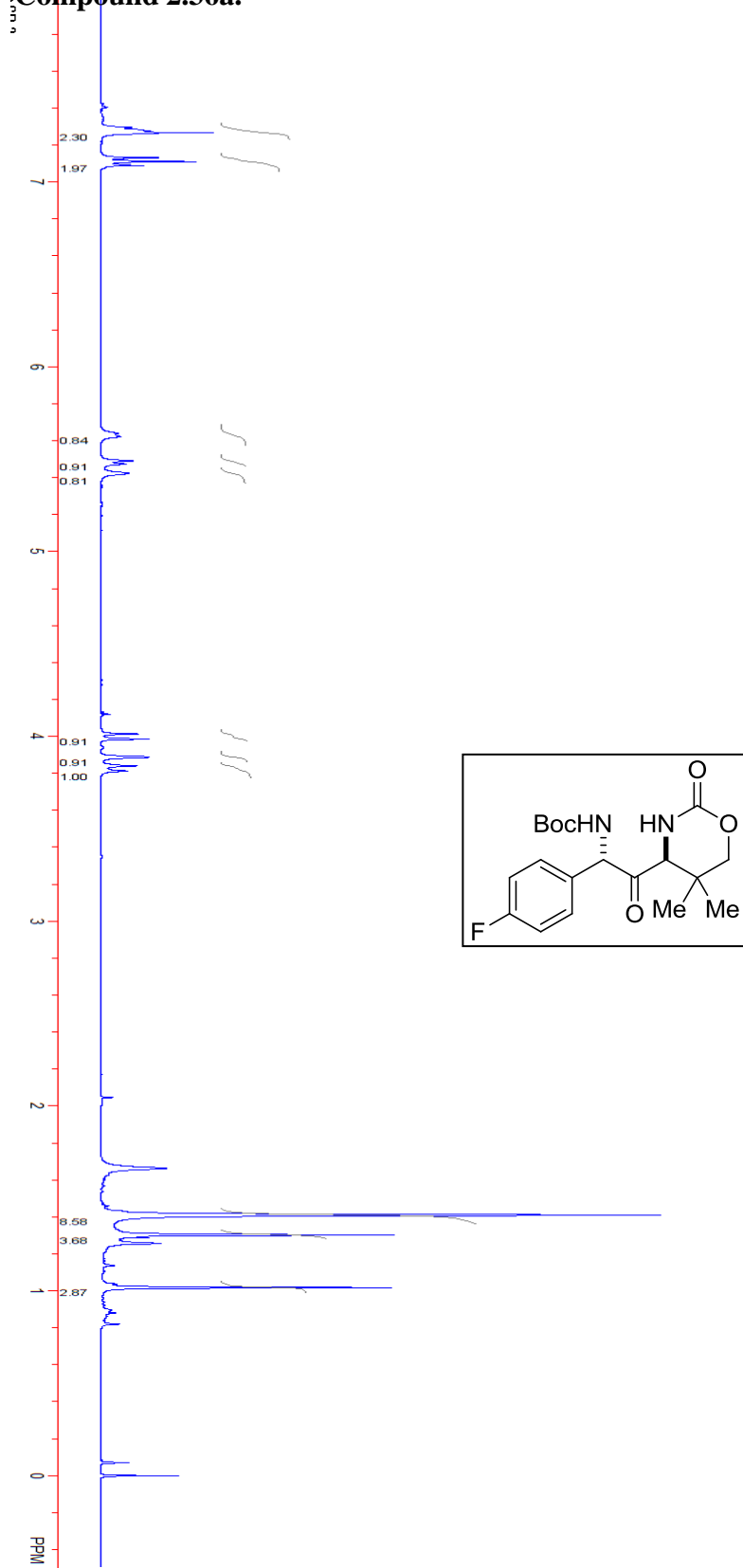
Compound 2.35a.



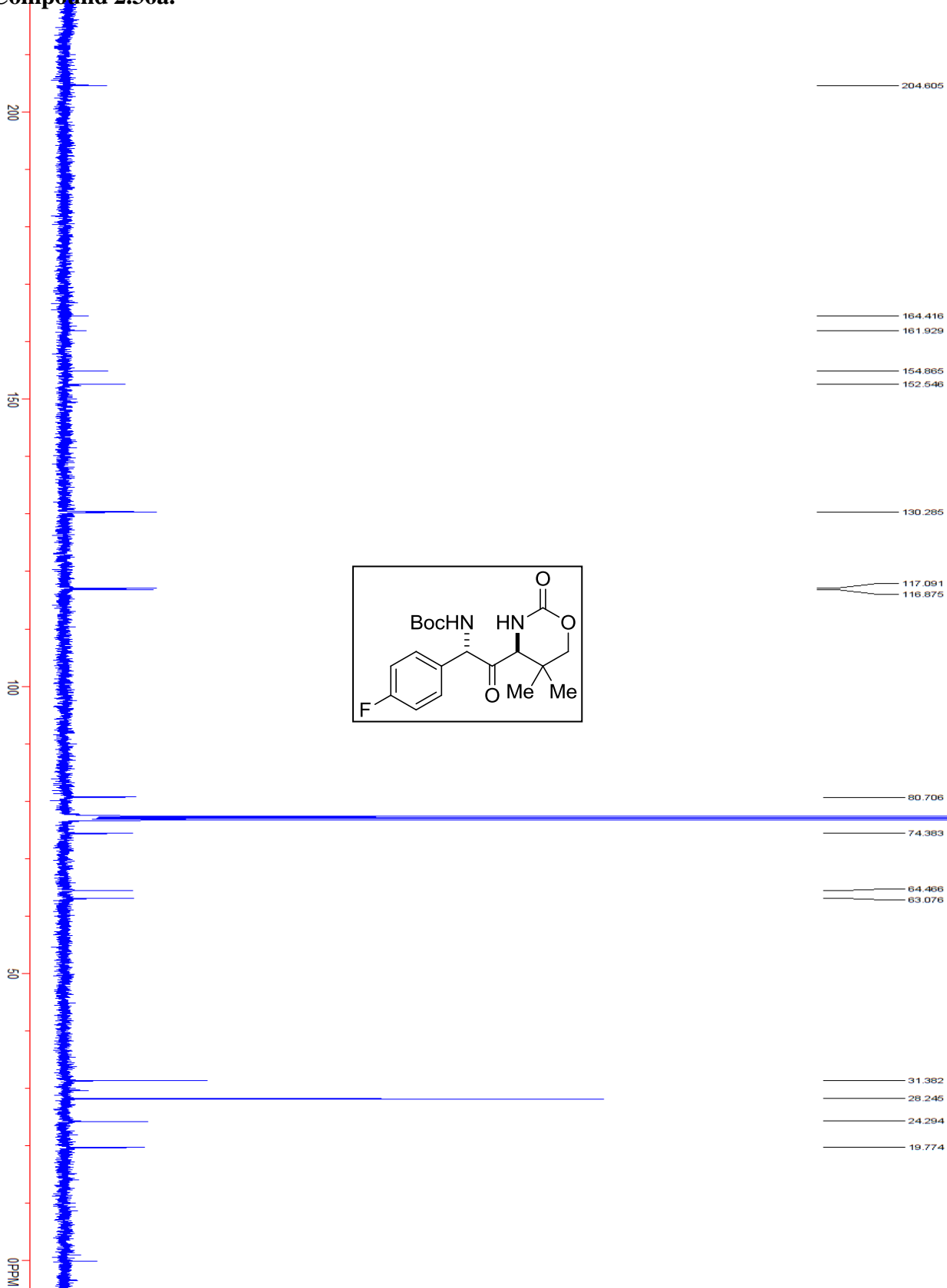
Compound 2.35a.

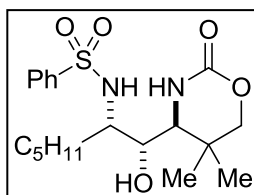
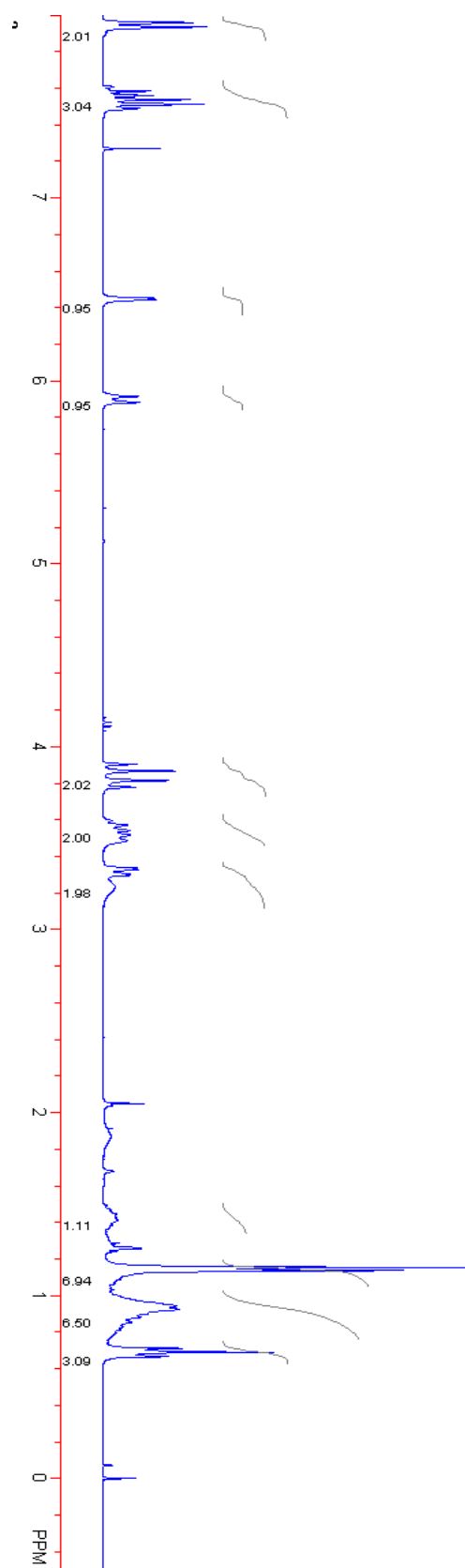


Compound 2.36a.

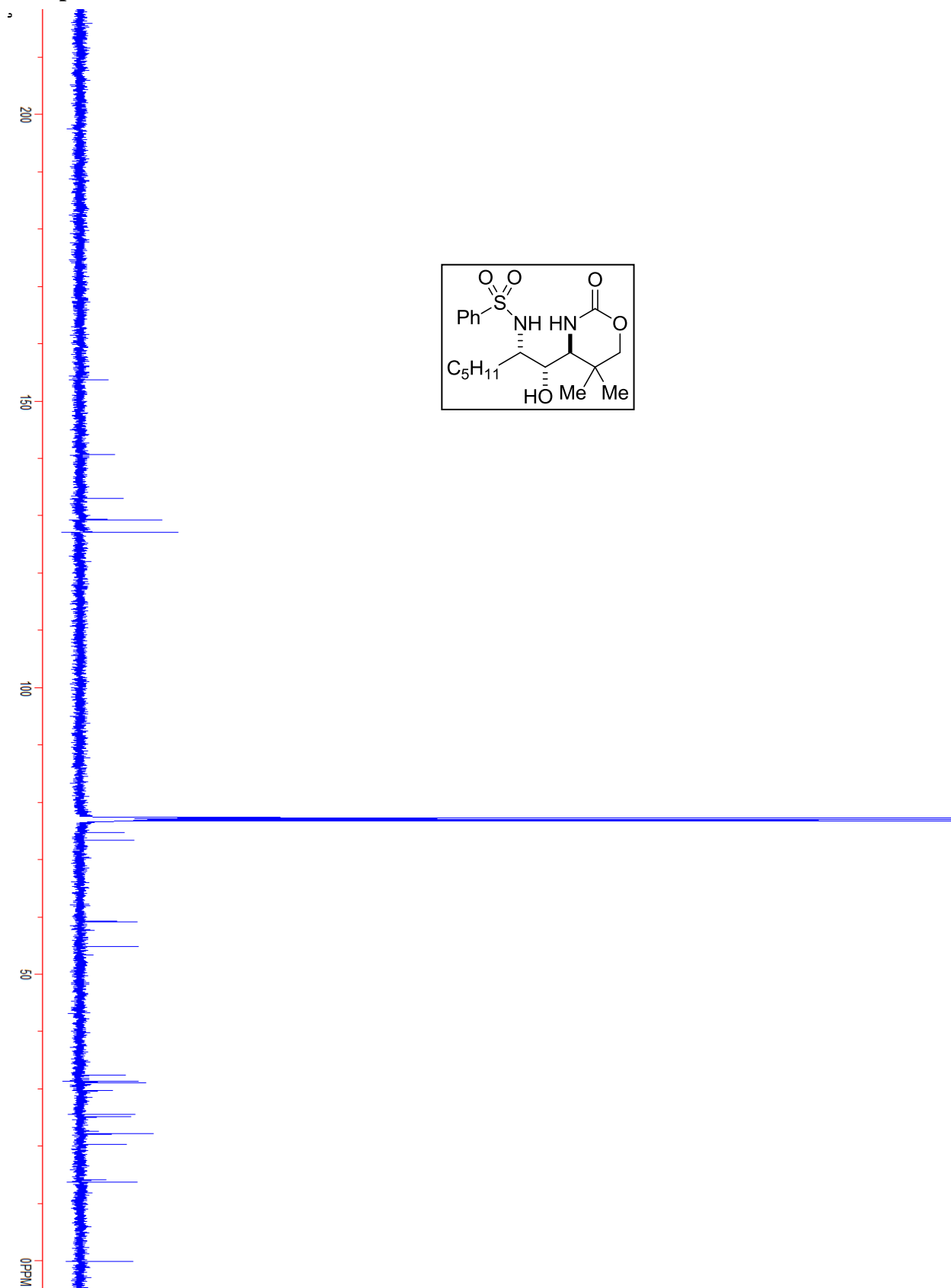


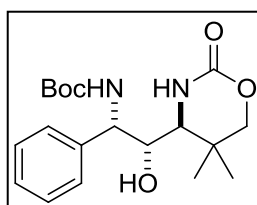
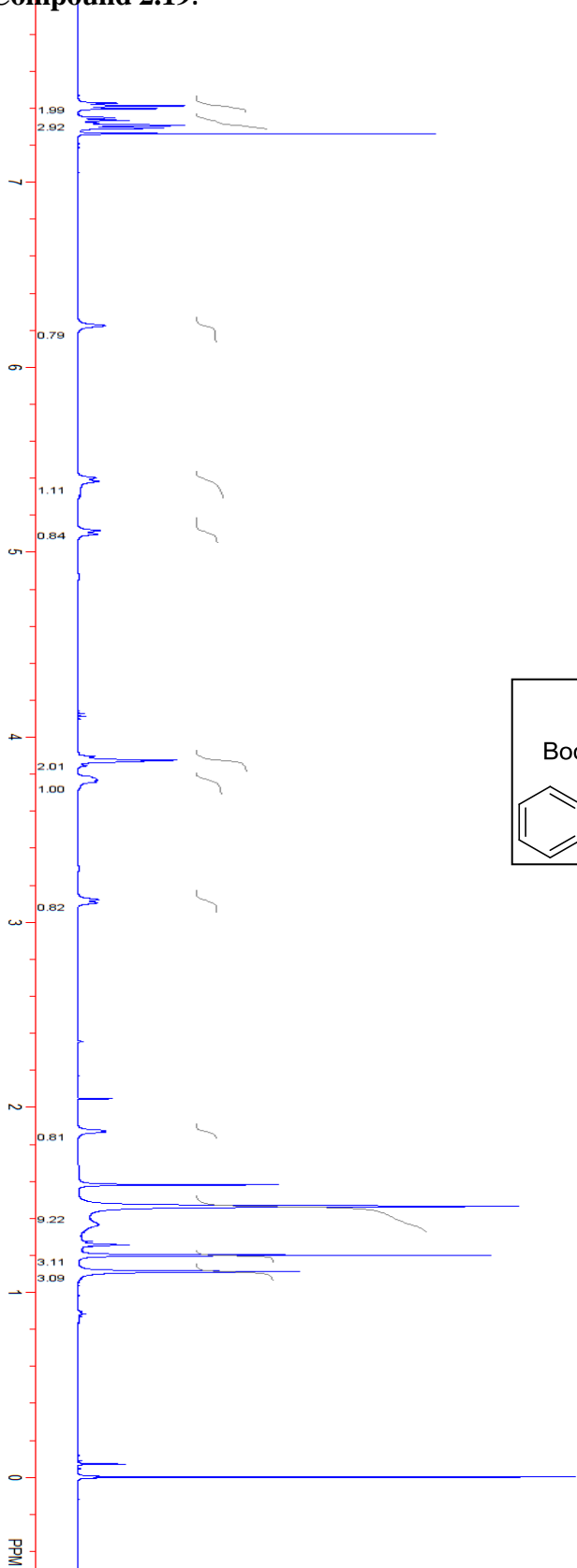
Compound 2.36a.



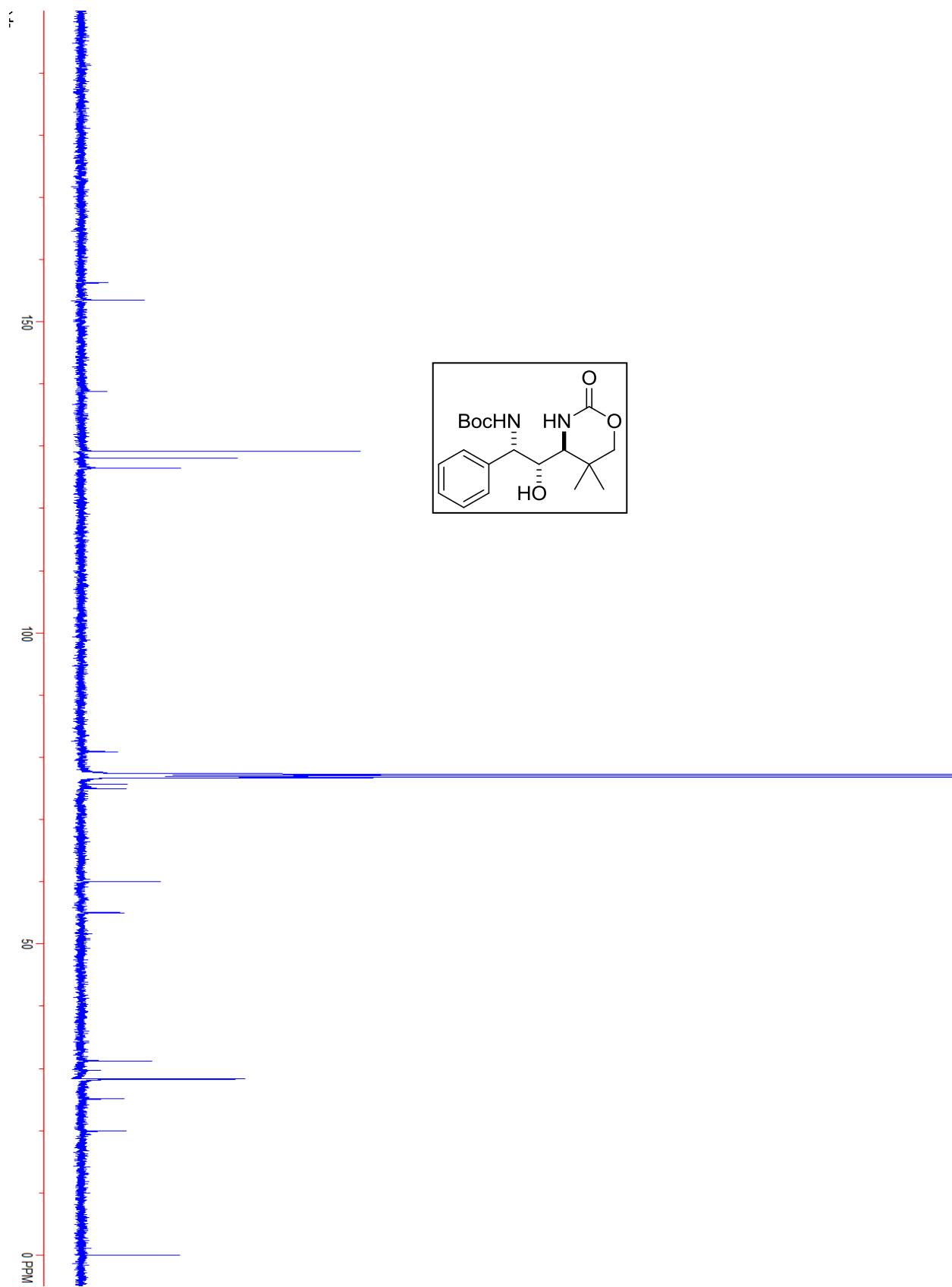
Compound 2.16.

Compound 2.16.

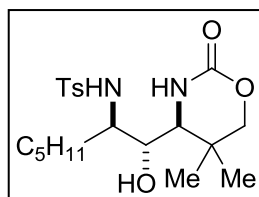
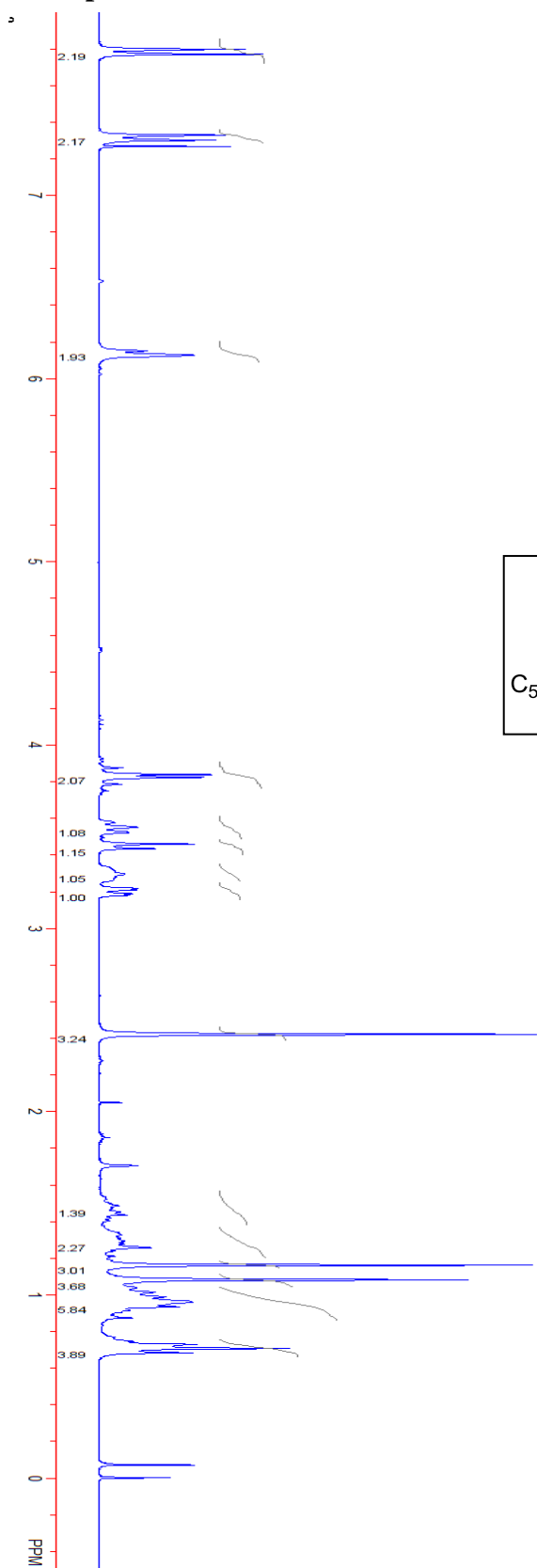


Compound 2.19.

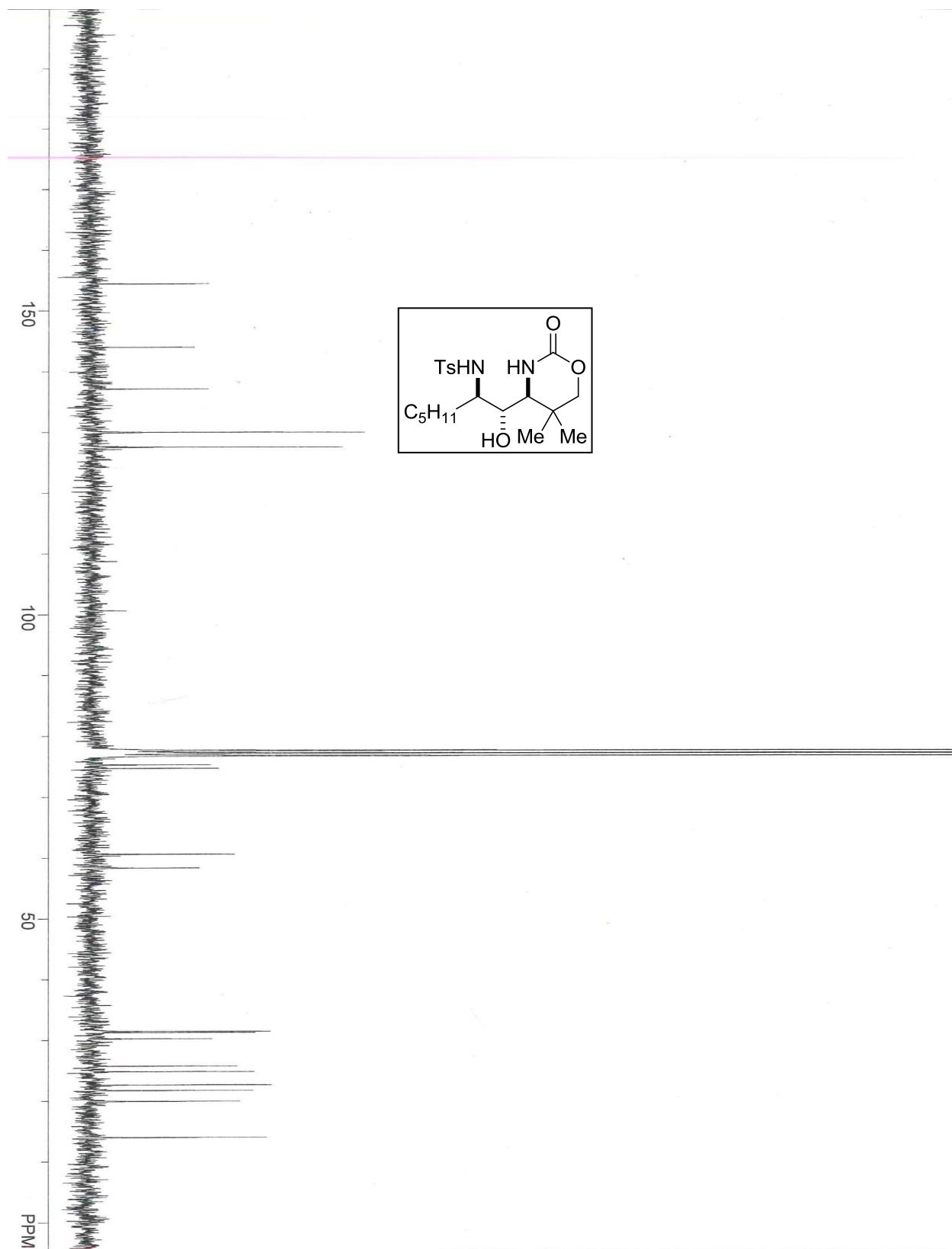
Compound 2.19.



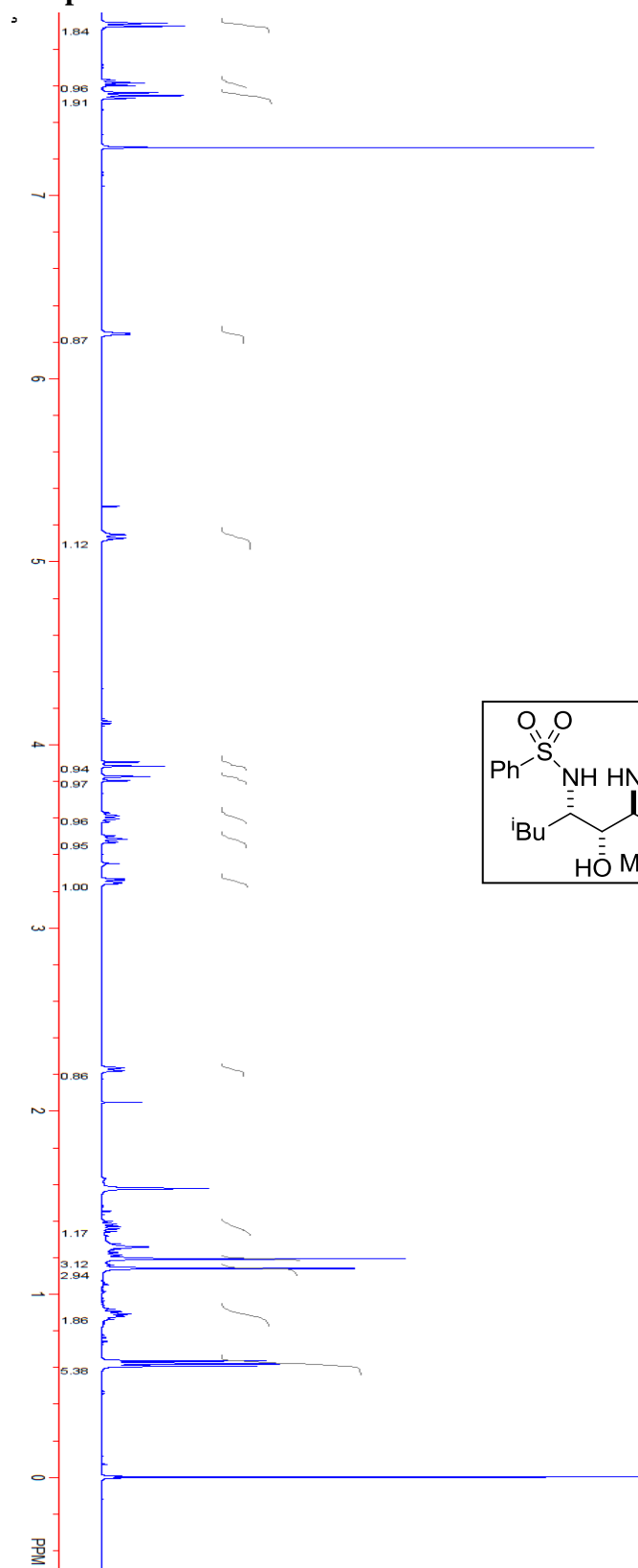
Compound 2.31b.



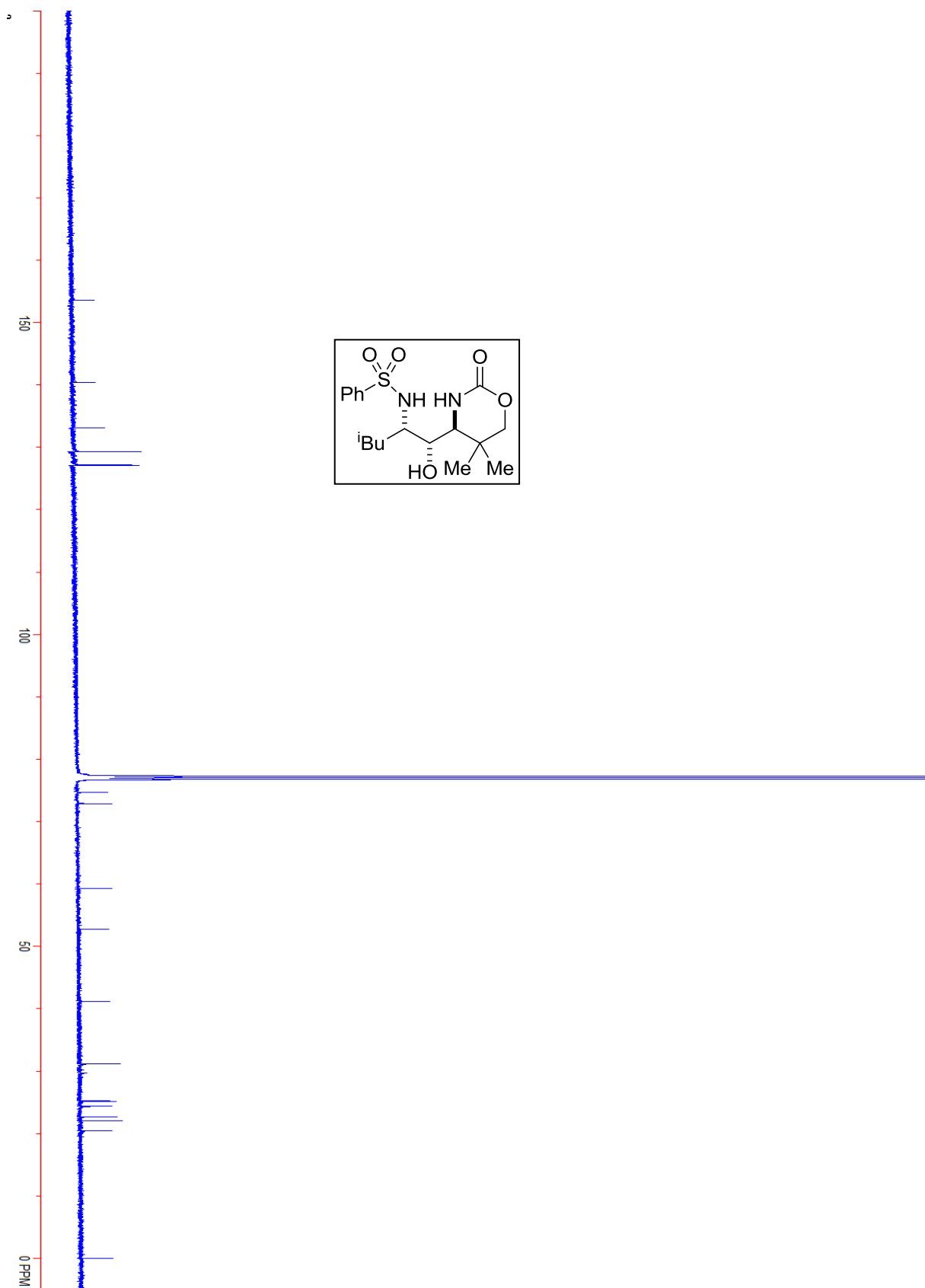
Compound 2.31b.



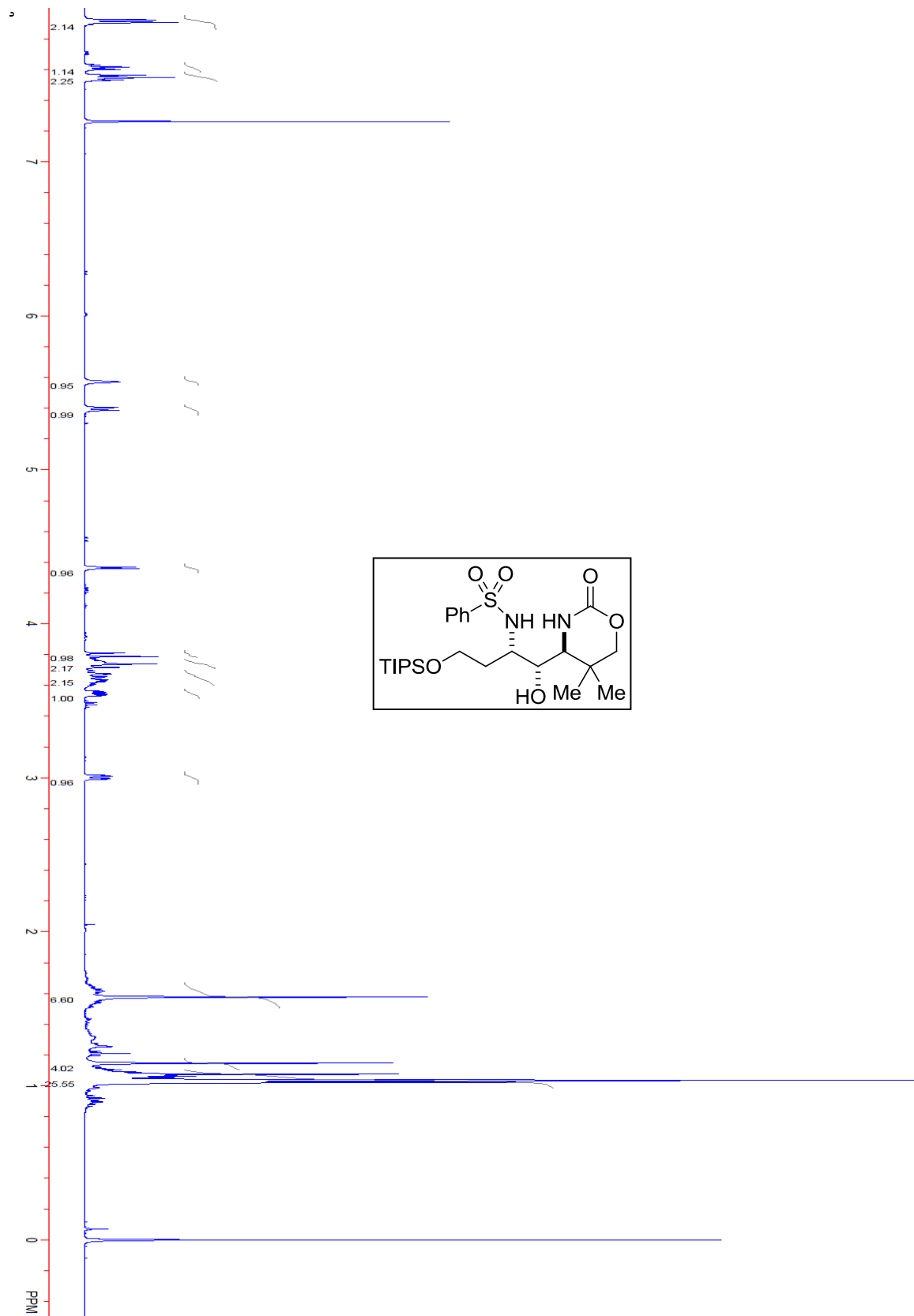
Compound 2.32b.



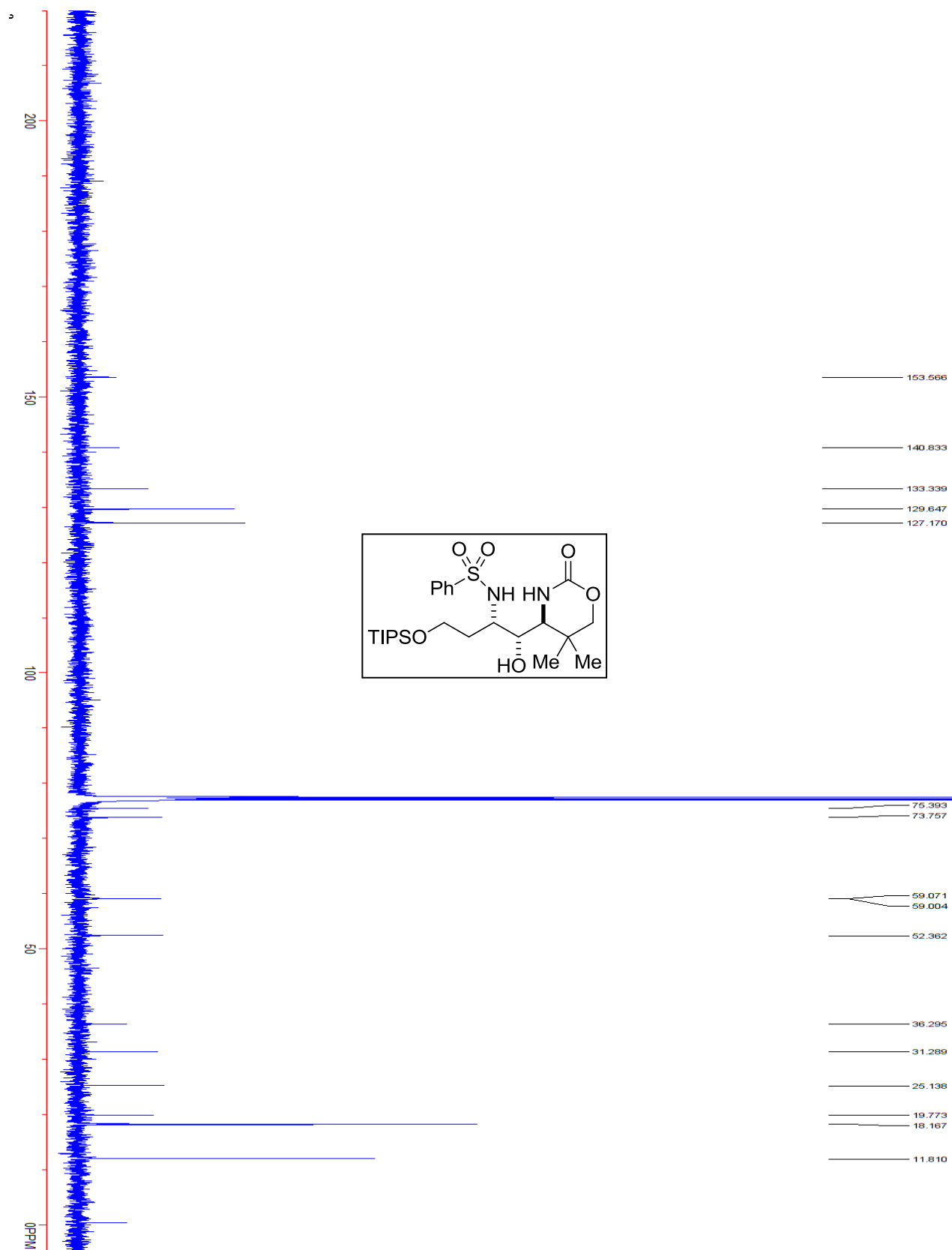
Compound 2.32b.



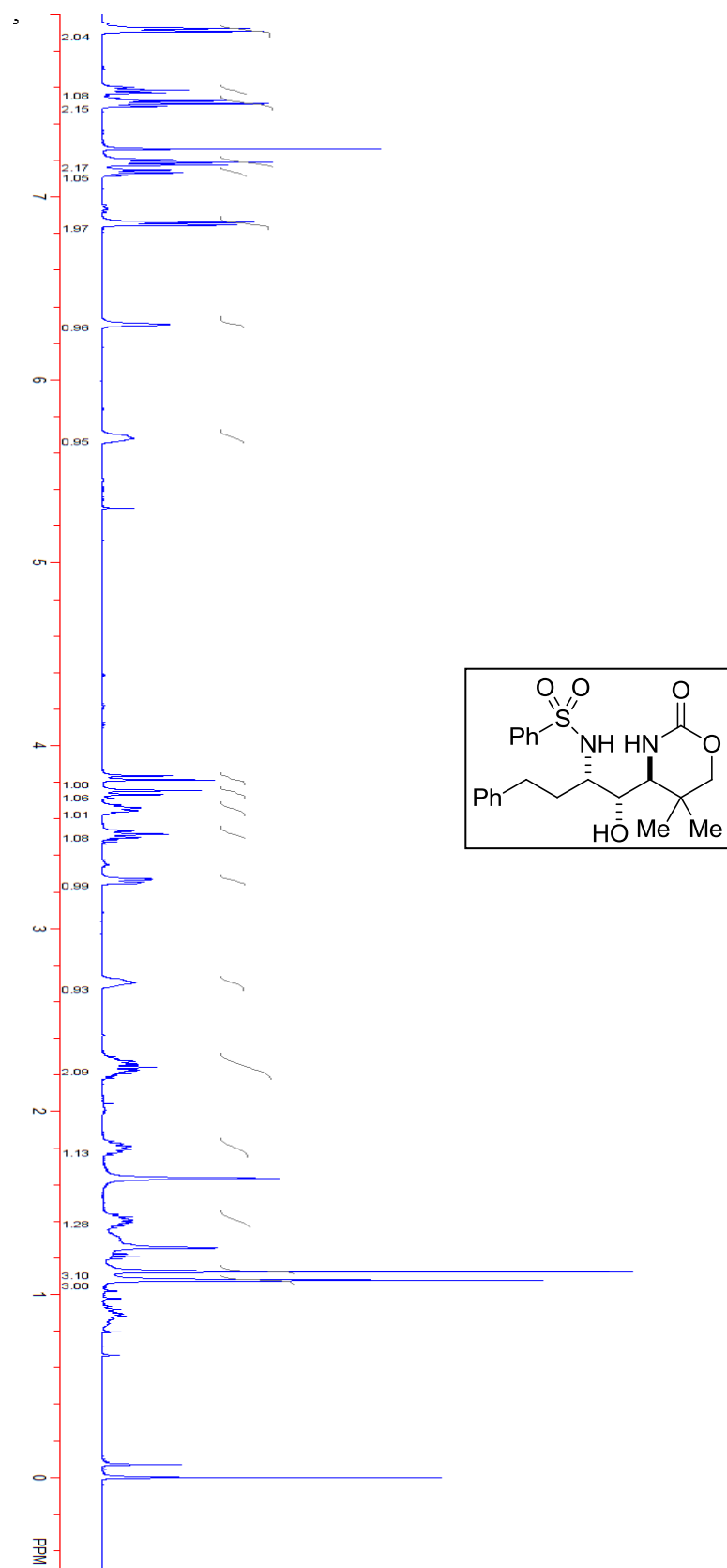
Compound 2.33b.



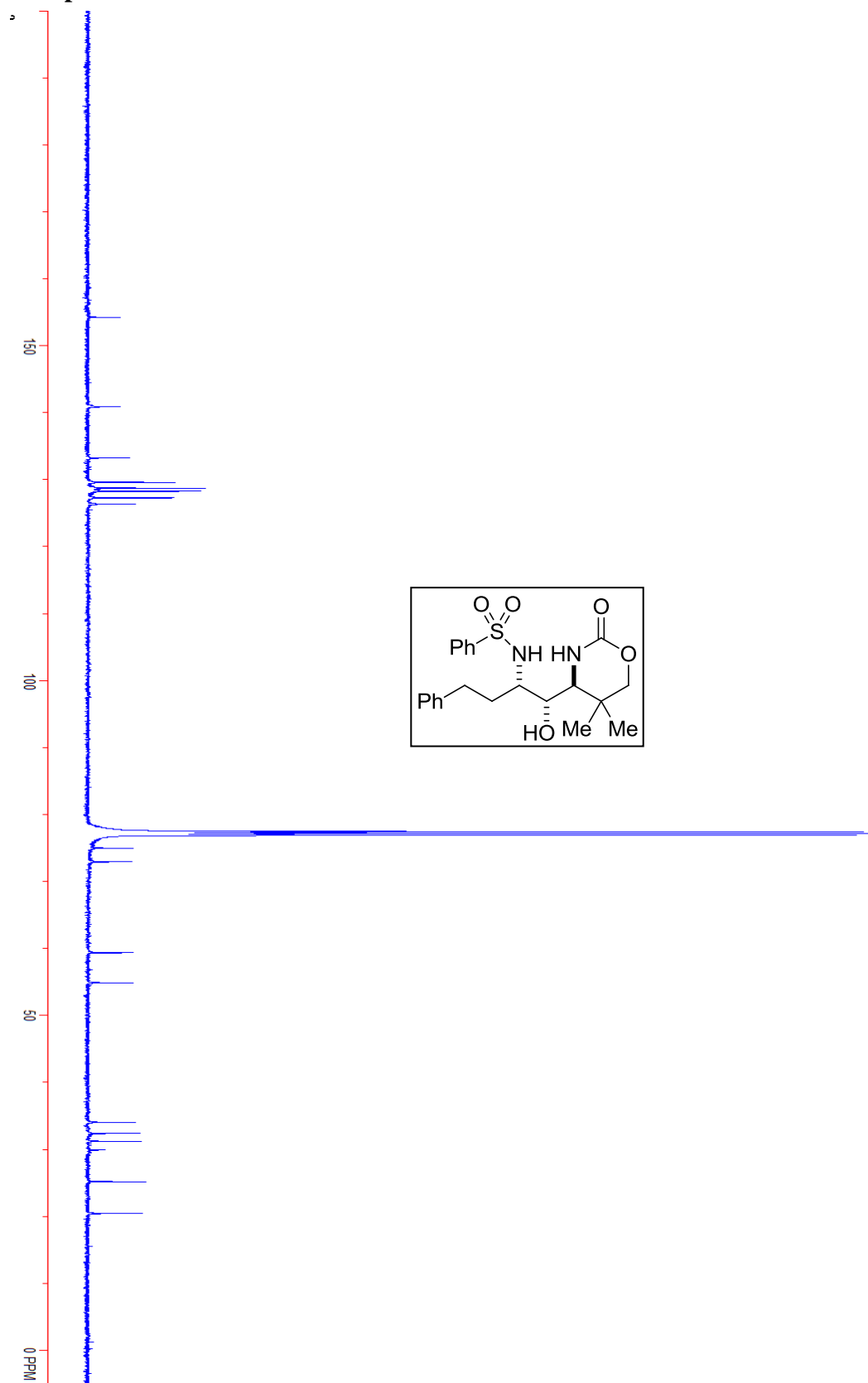
Compound 2.33b.

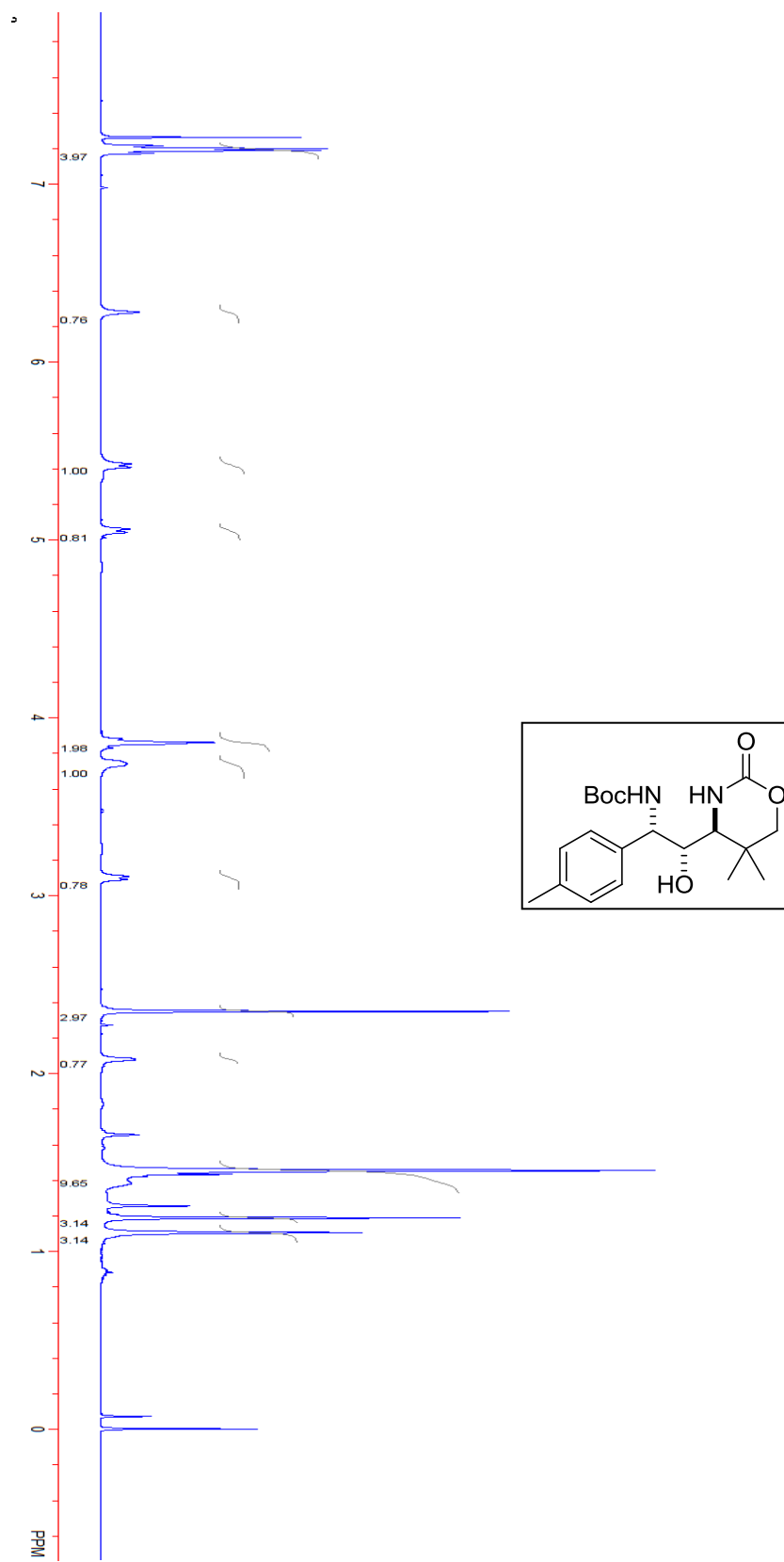


Compound 2.34b.

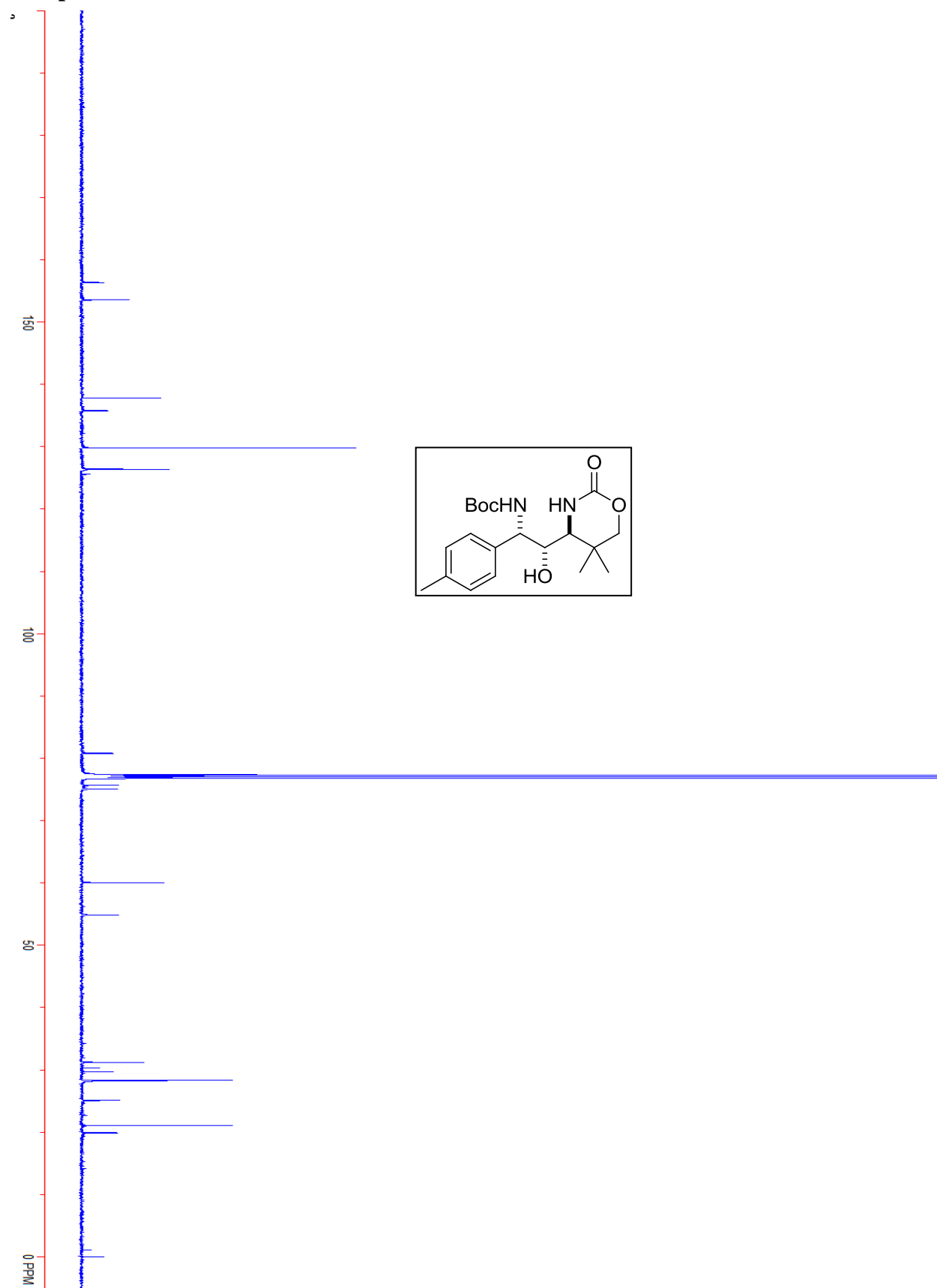


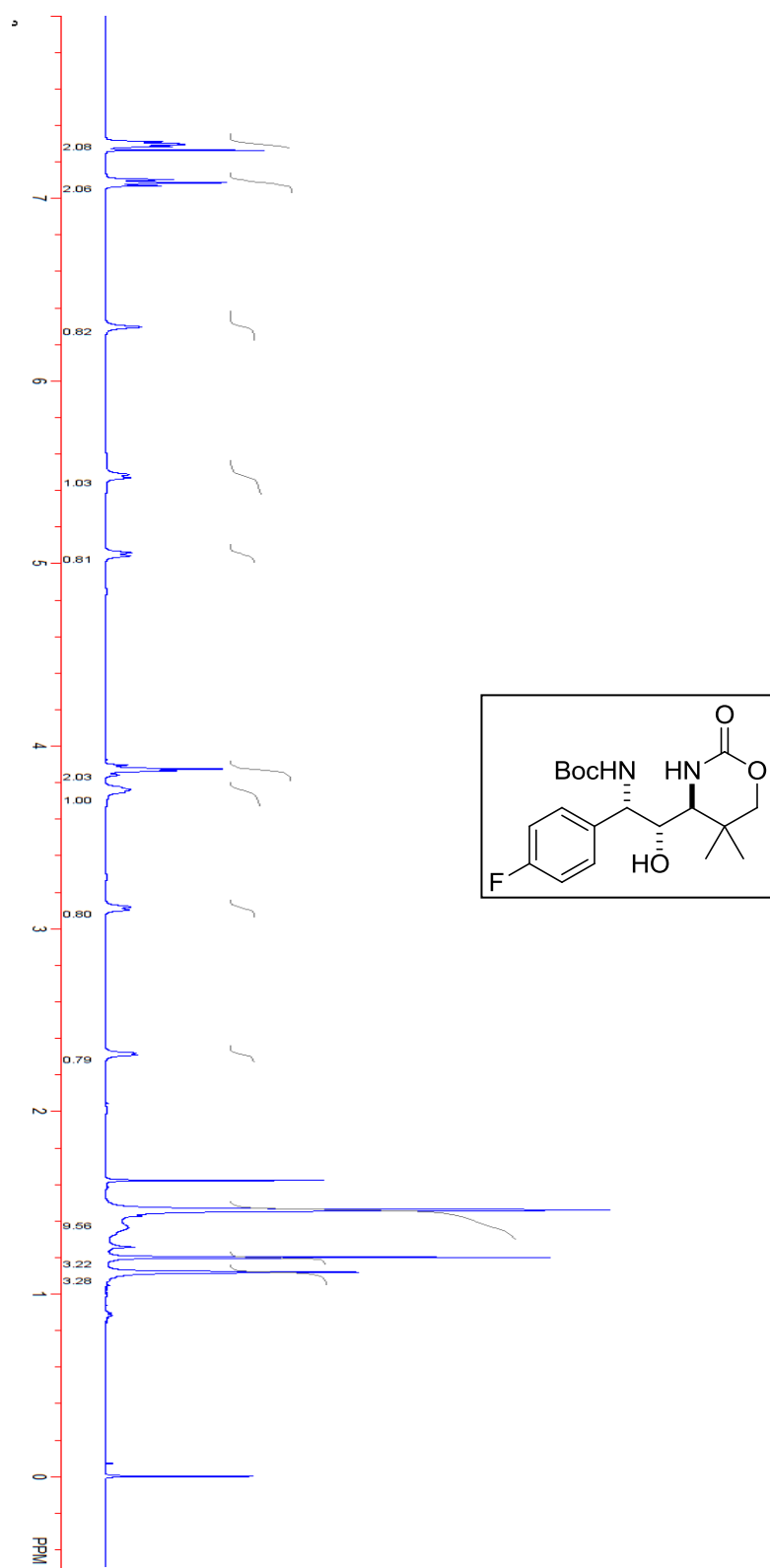
Compound 2.34b.



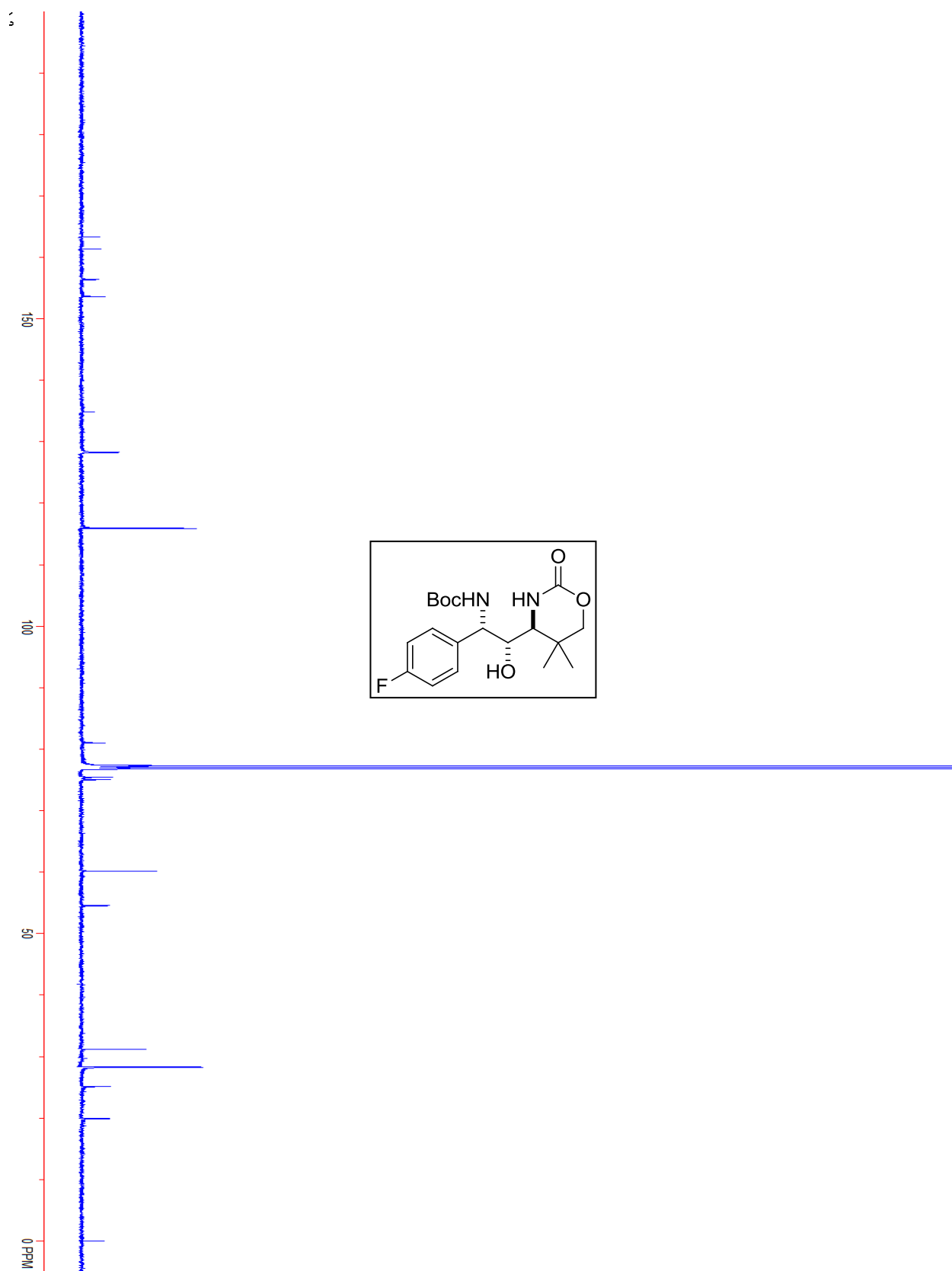
Compound 2.35b.

Compound 2.35b.

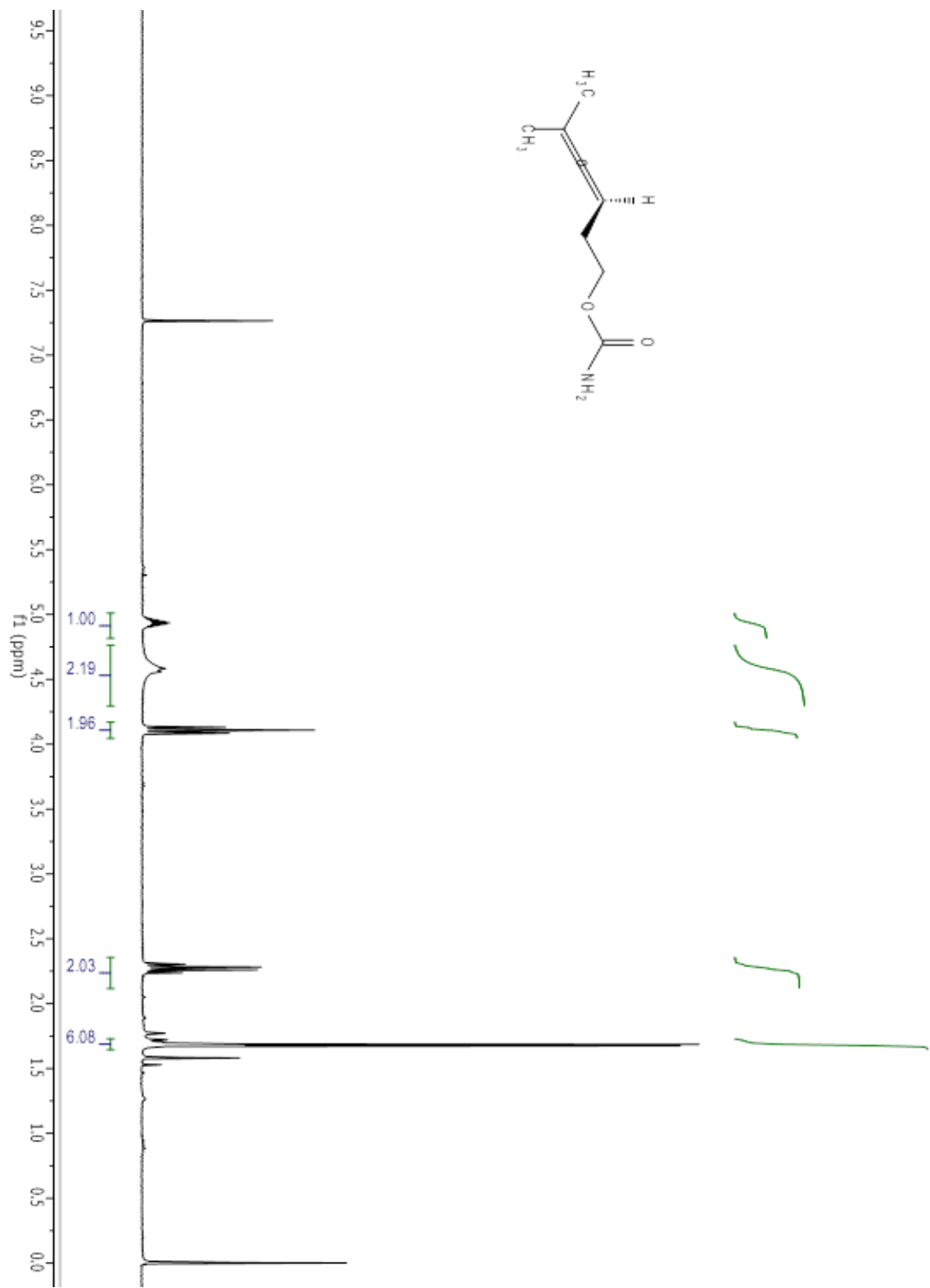


Compound 2.36b.

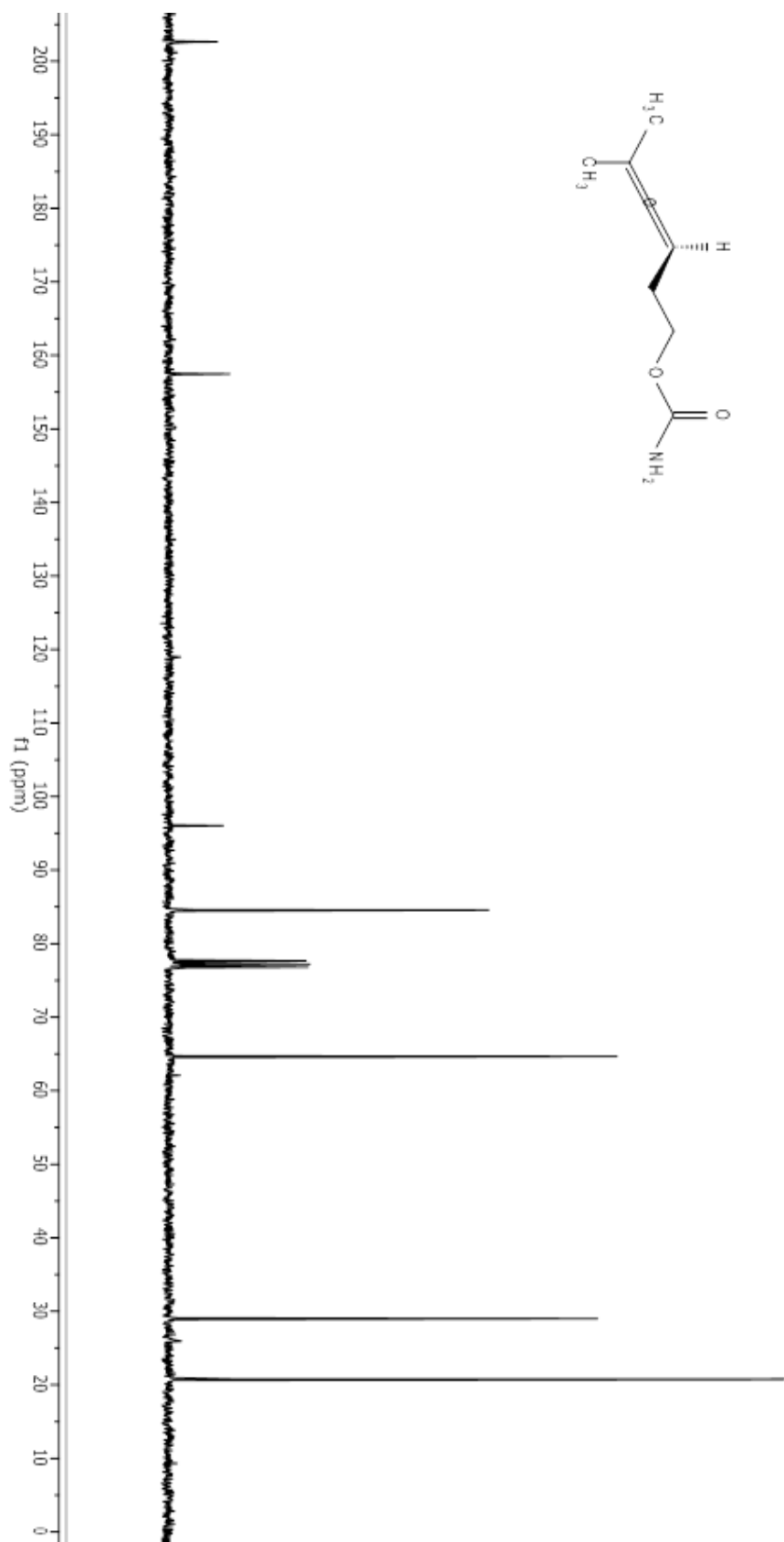
Compound 2.36b.

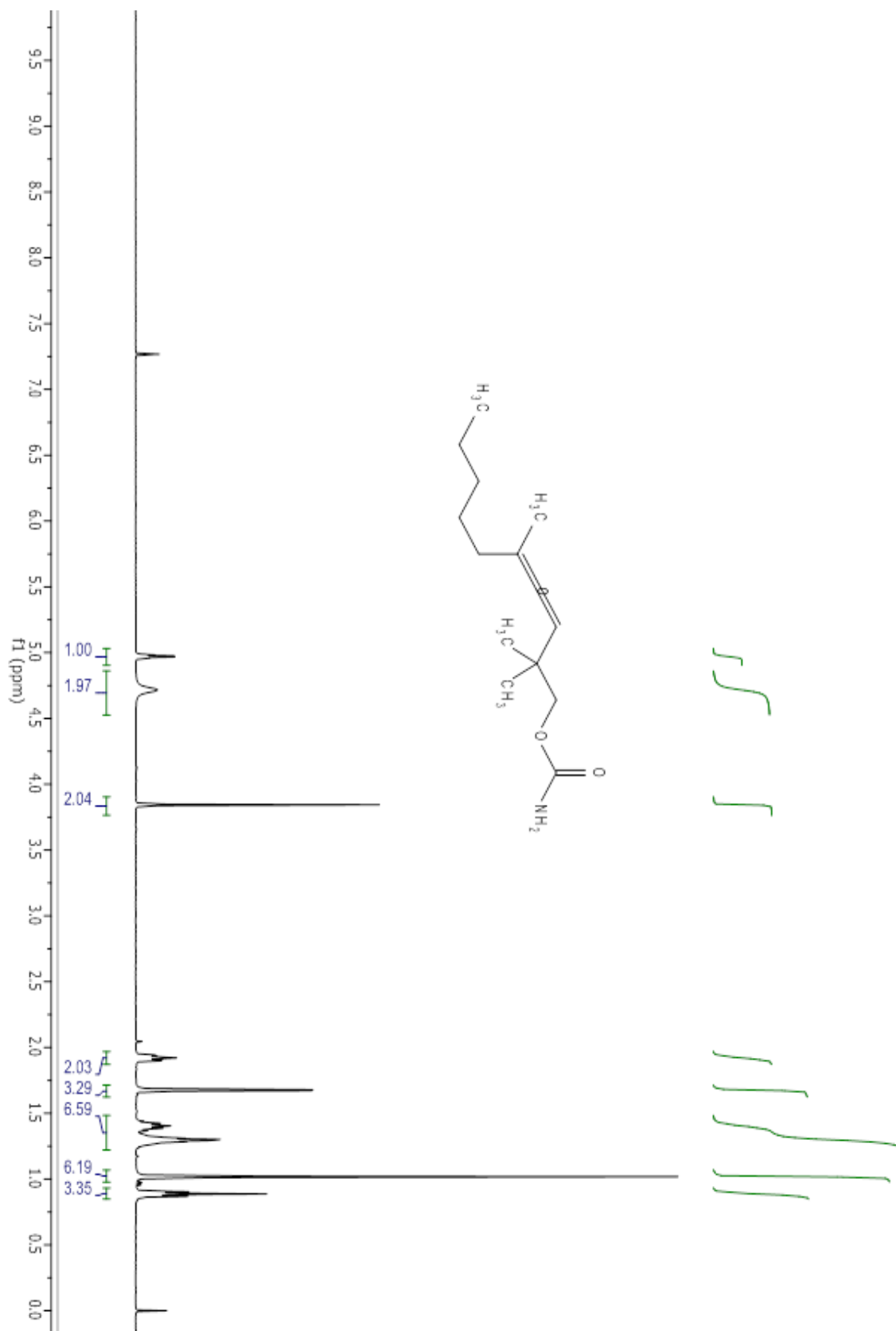


Compound 3.6a.

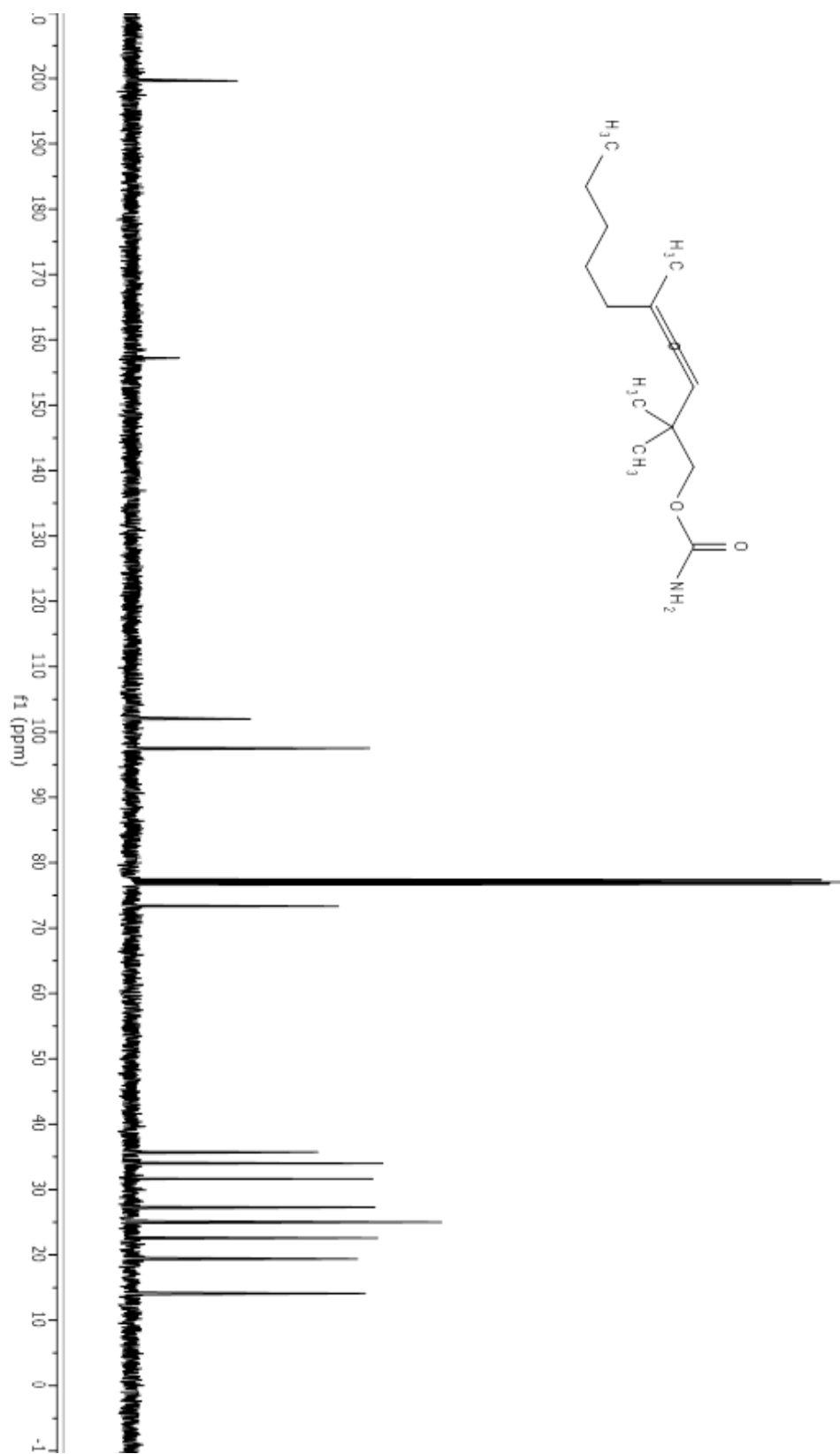


Compound 3.6a.

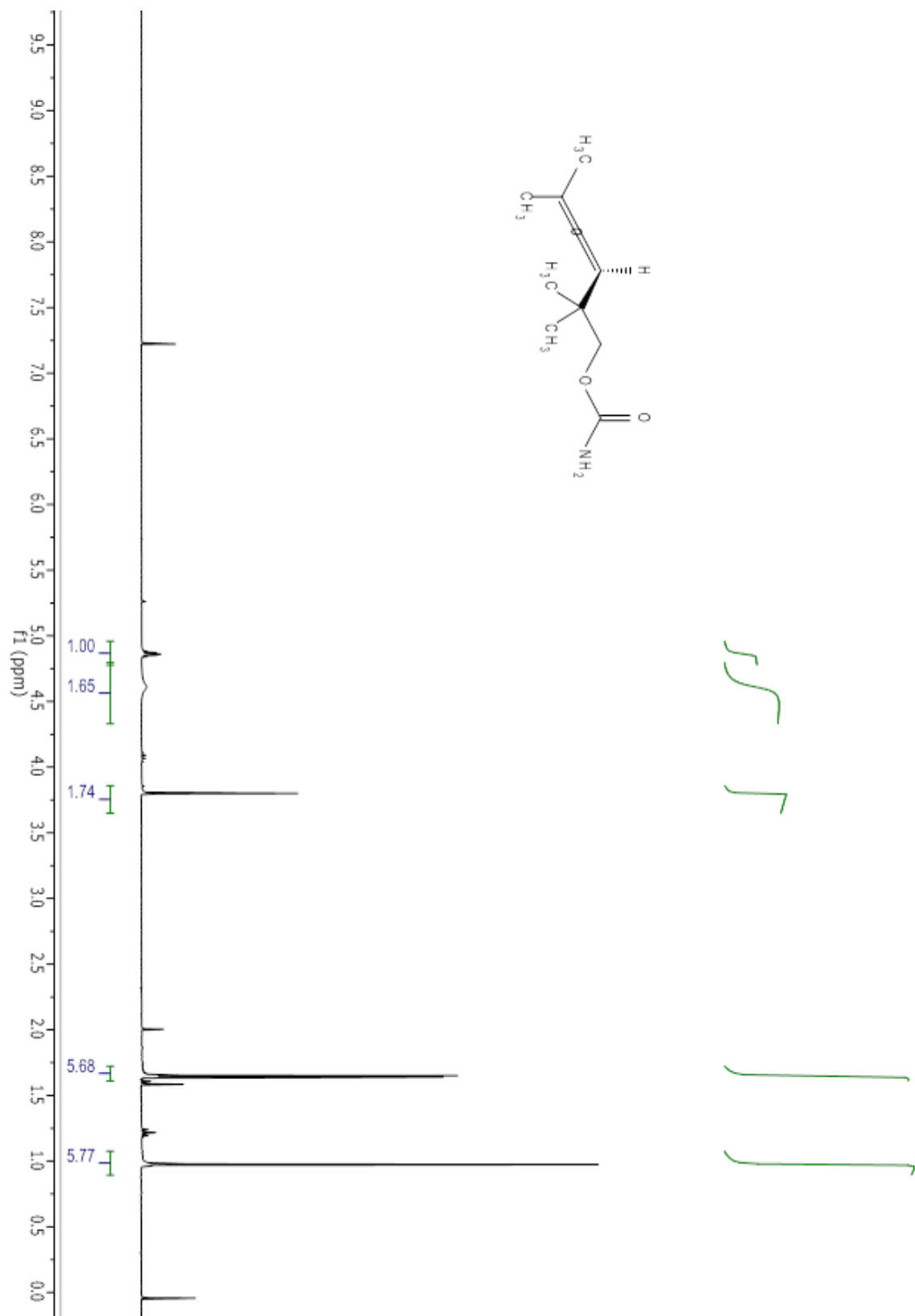


Compound 3.9b.

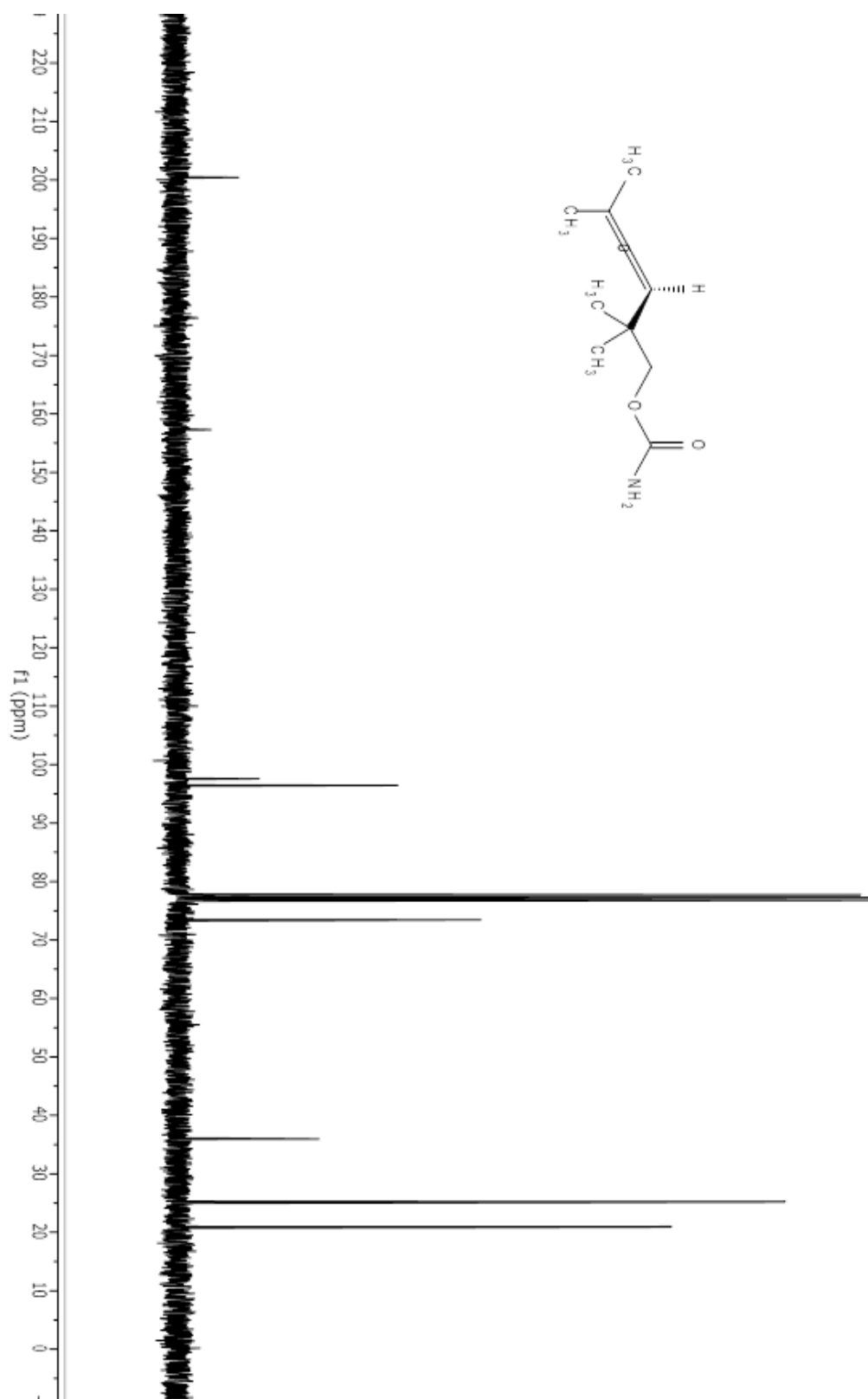
Compound 3.9b.



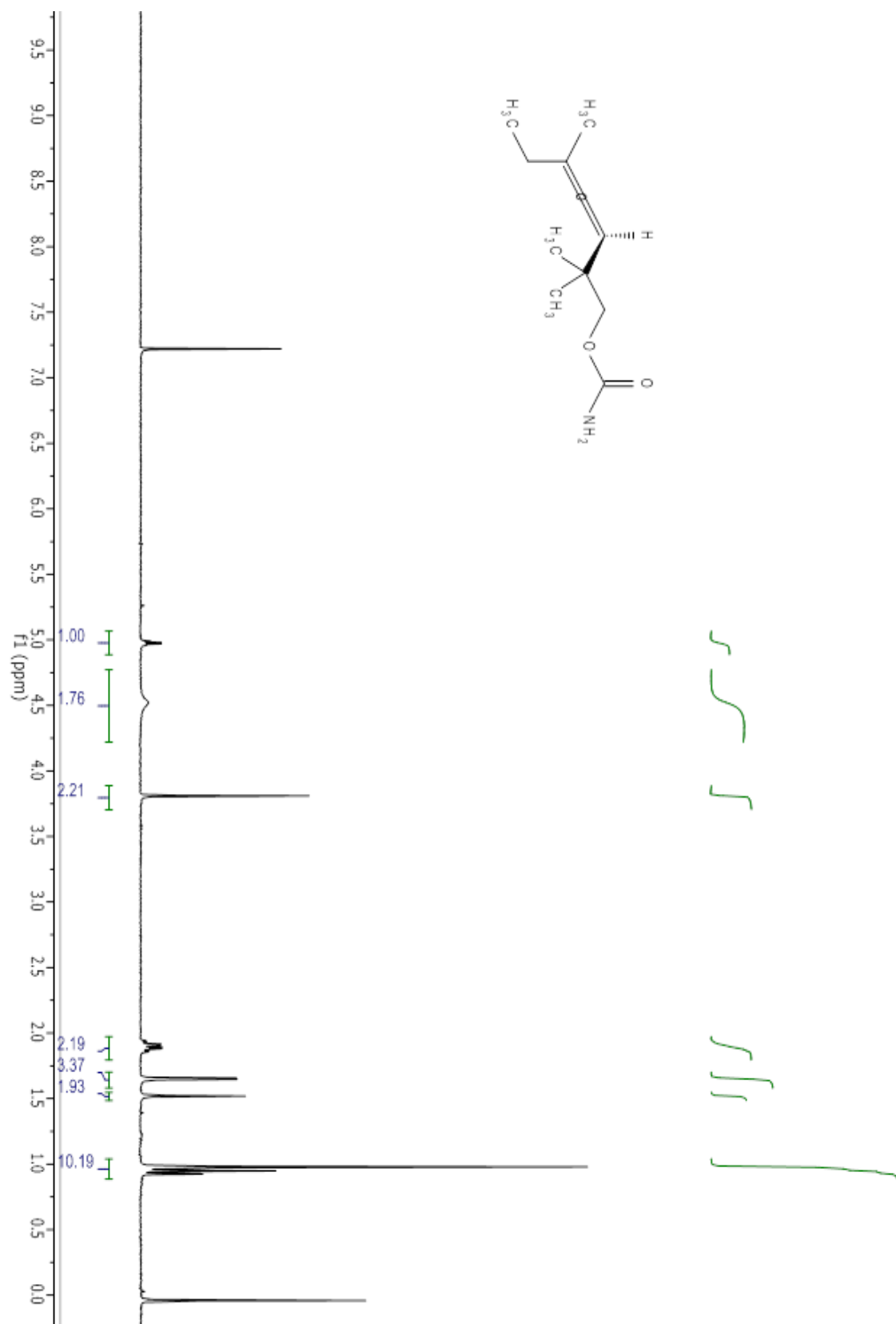
Compound 3.9e.



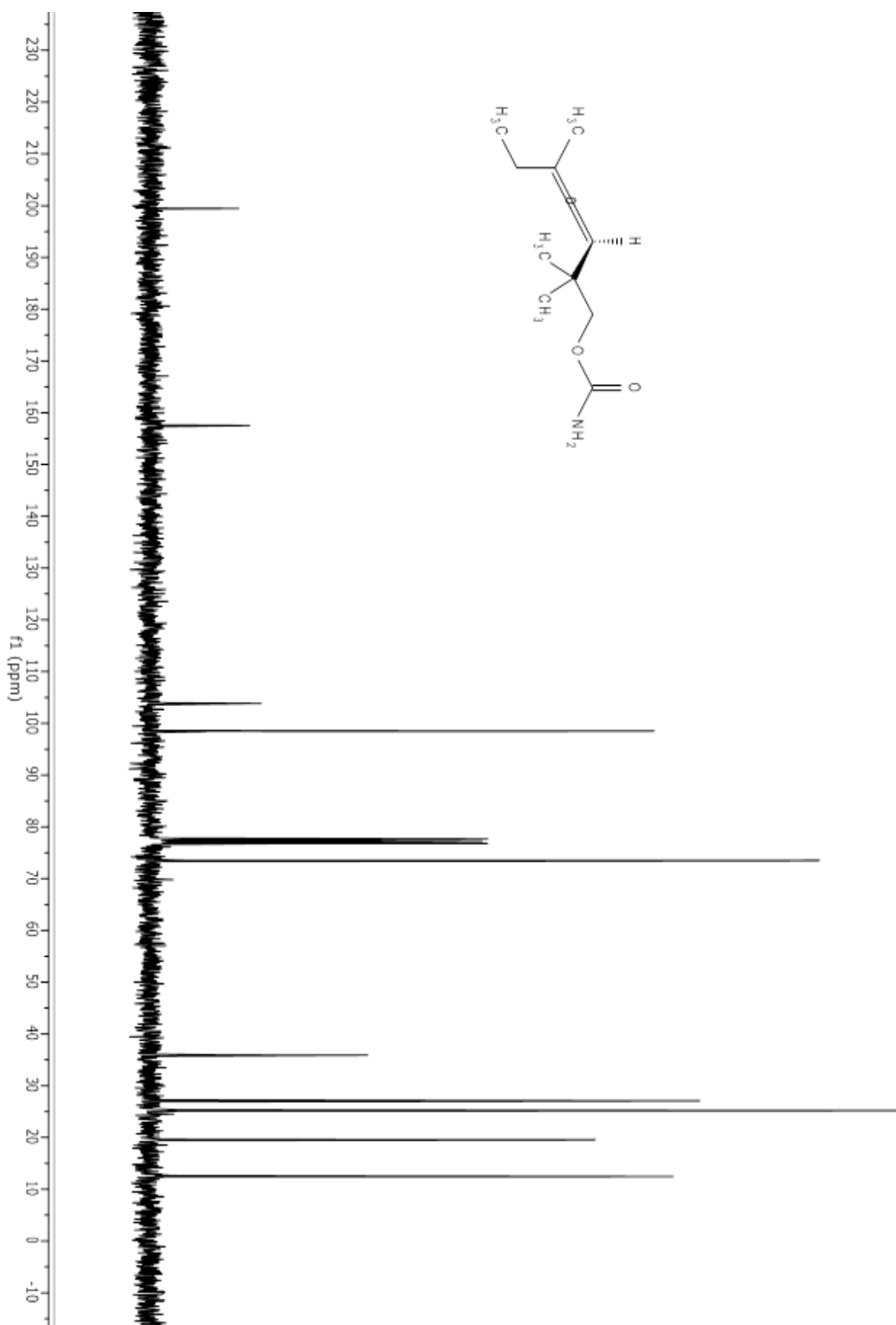
Compound 3.9e.



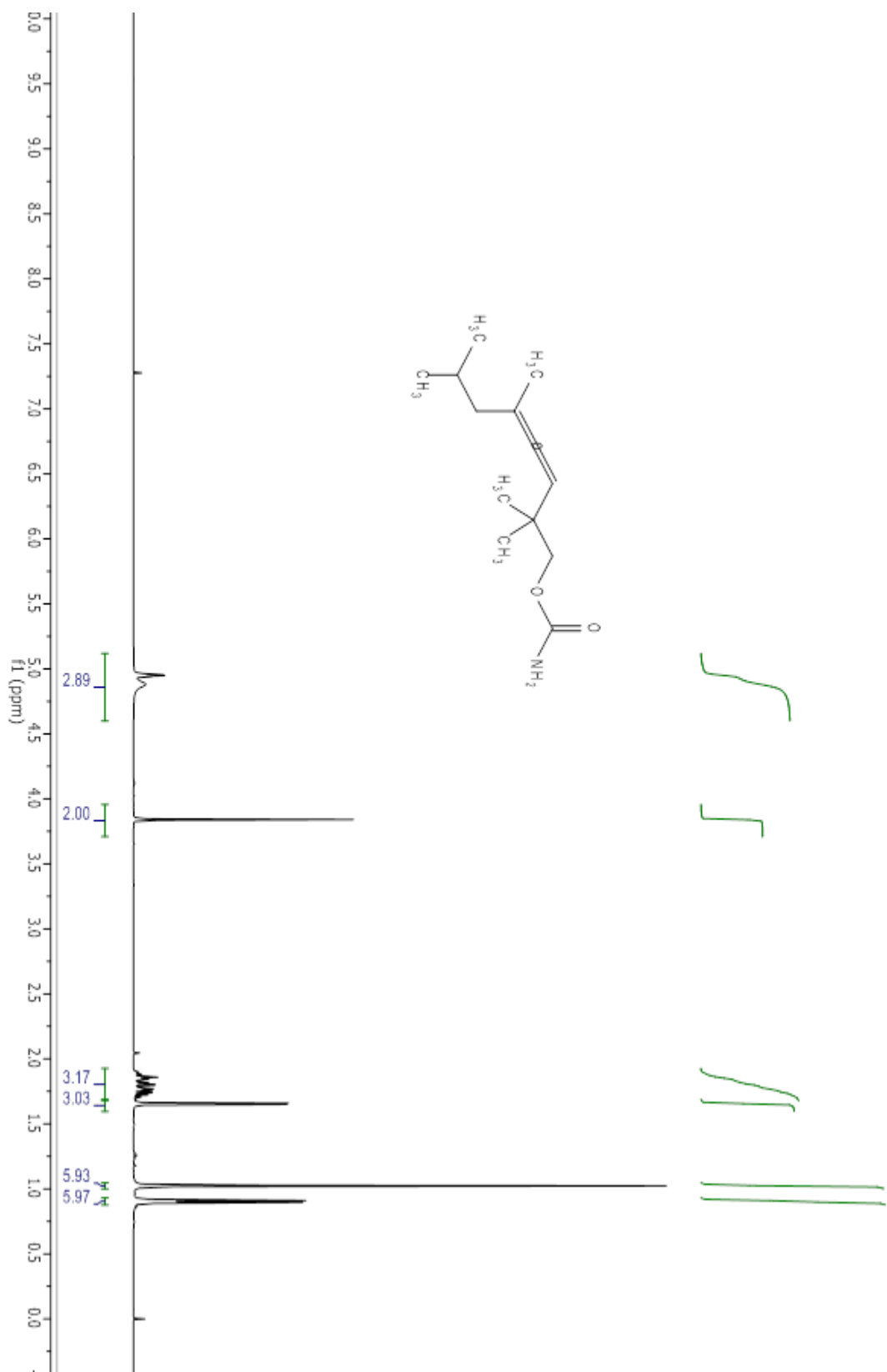
Compound 3.9f.



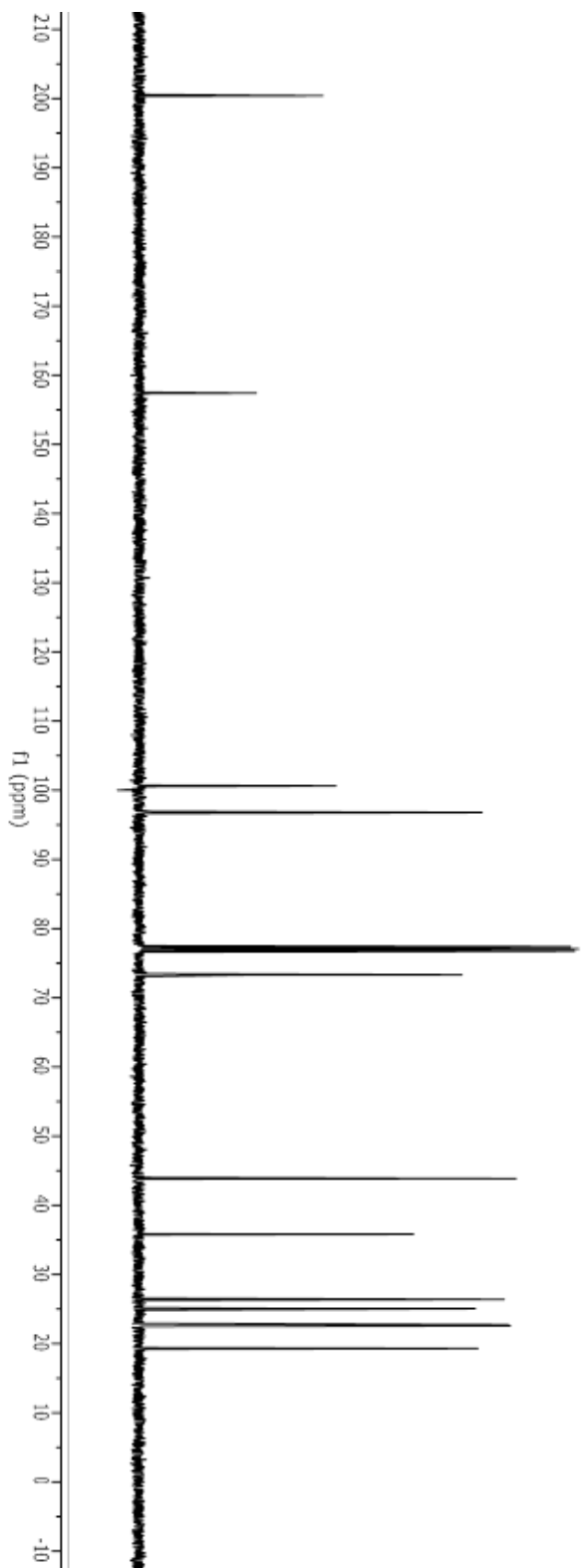
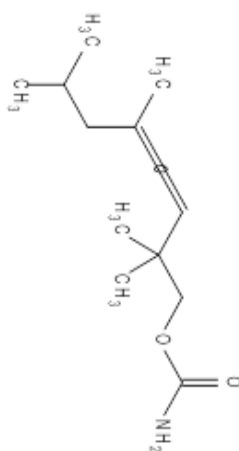
Compound 3.9f.



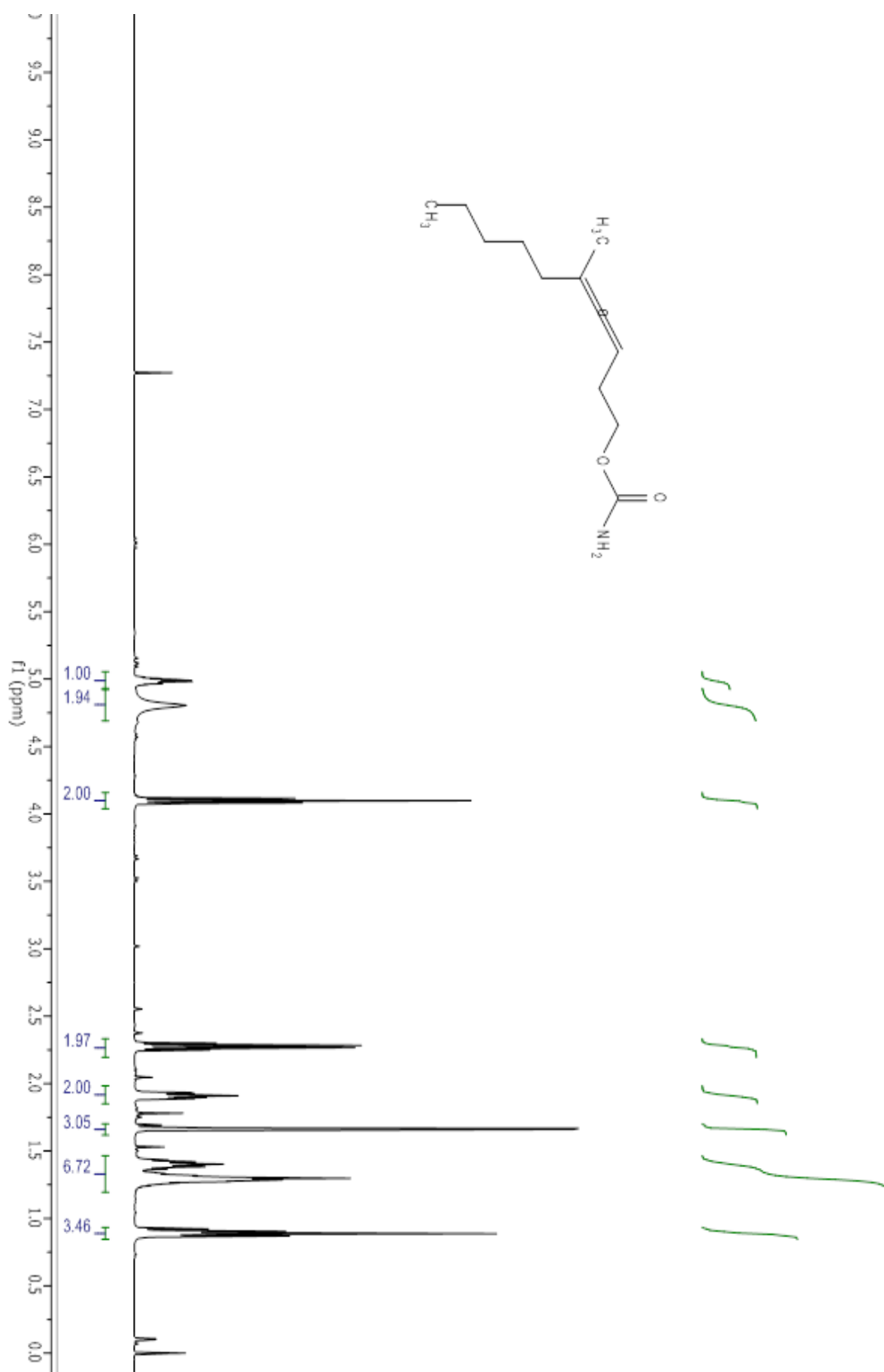
Compound 3.9g.



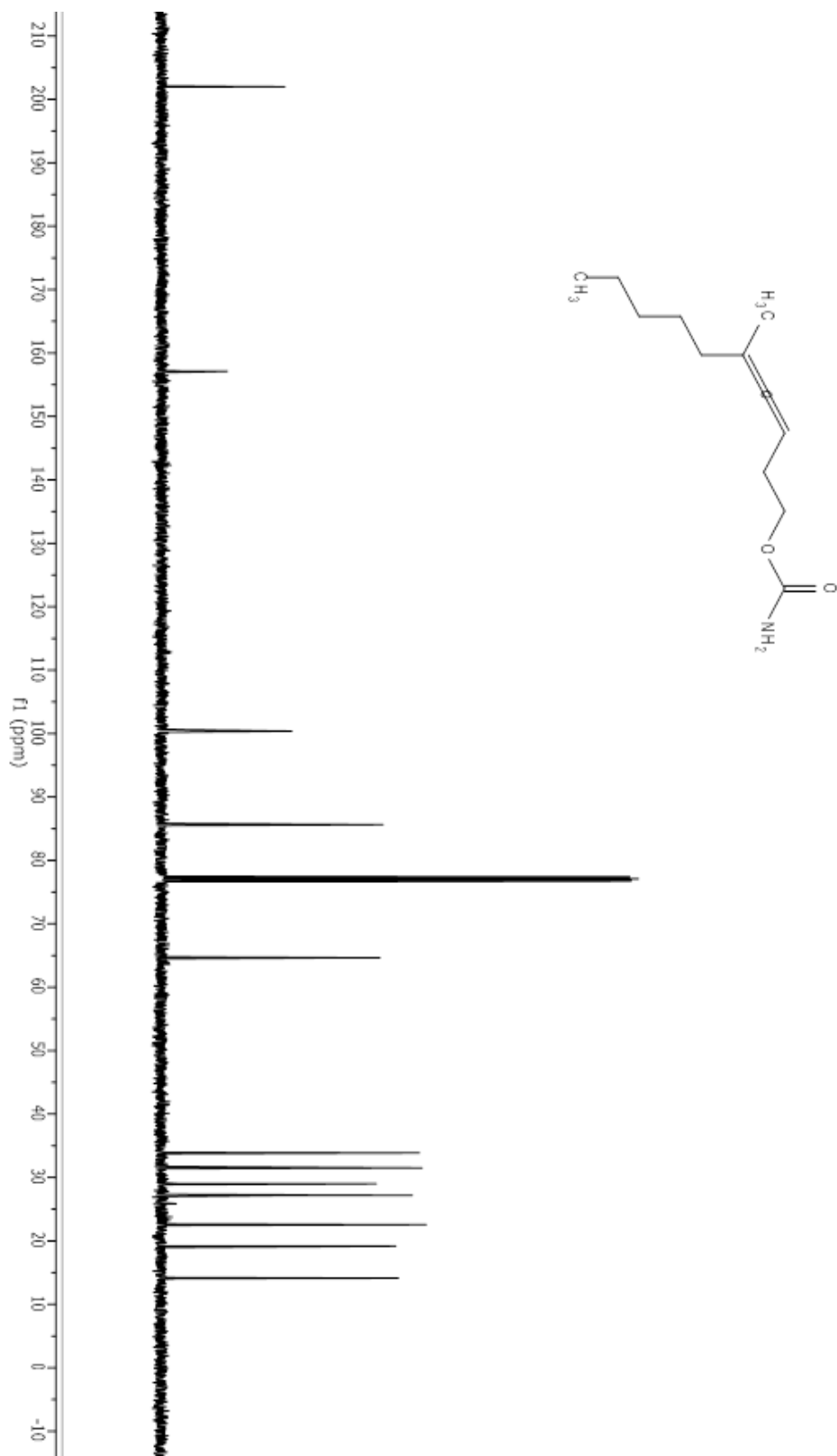
Compound 3.9g.



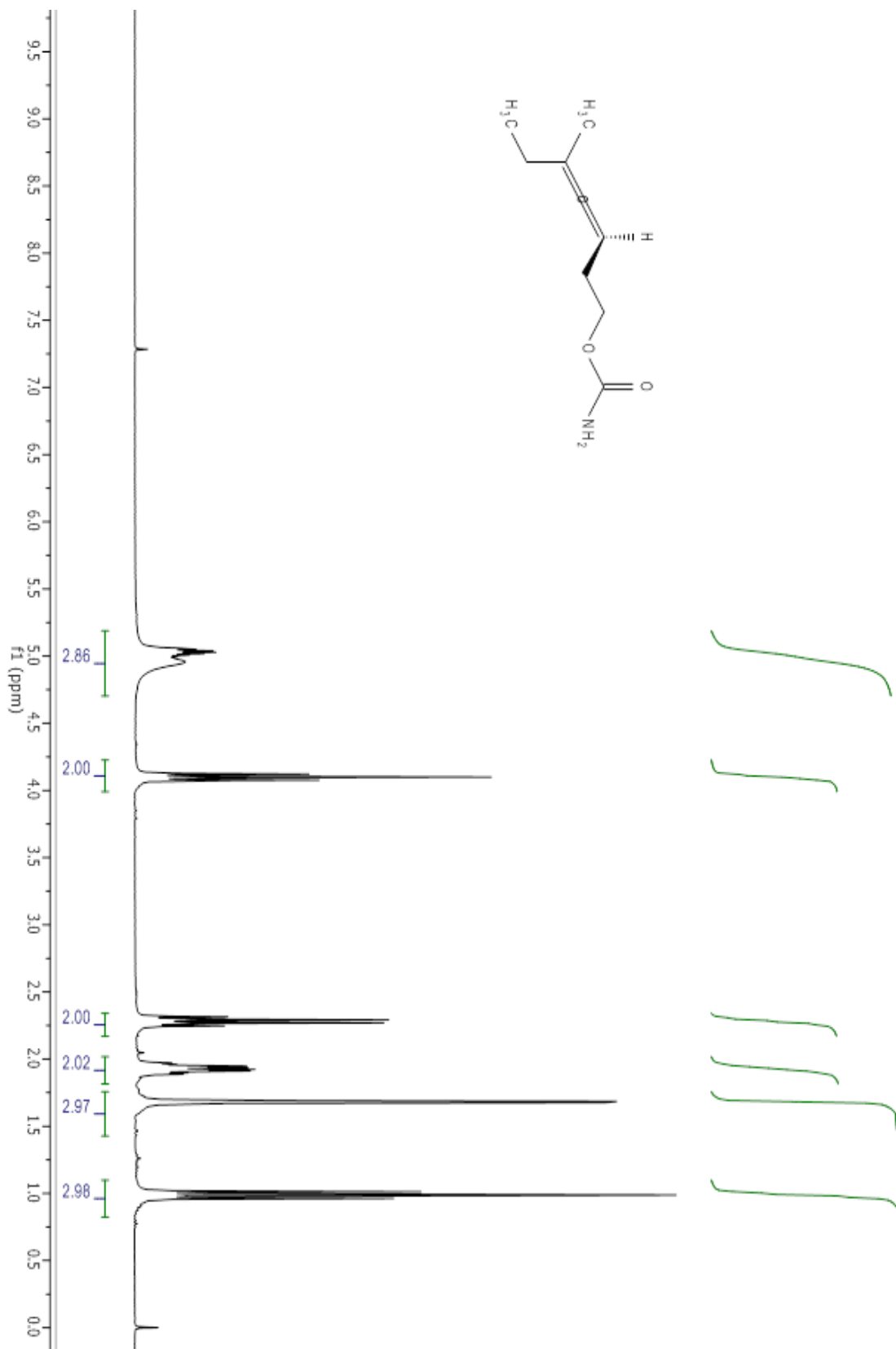
Compound 3.11c.



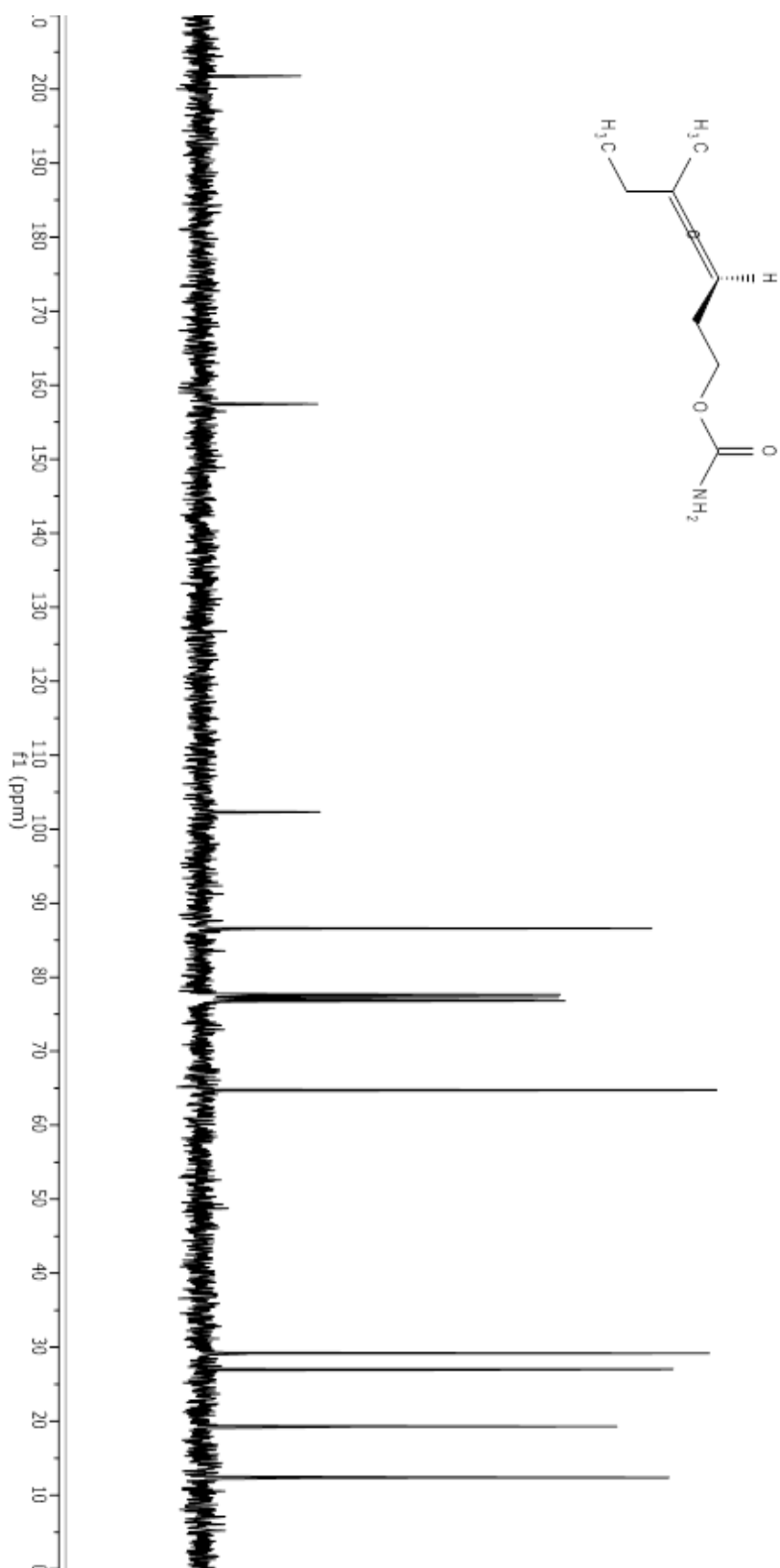
Compound 3.11c.



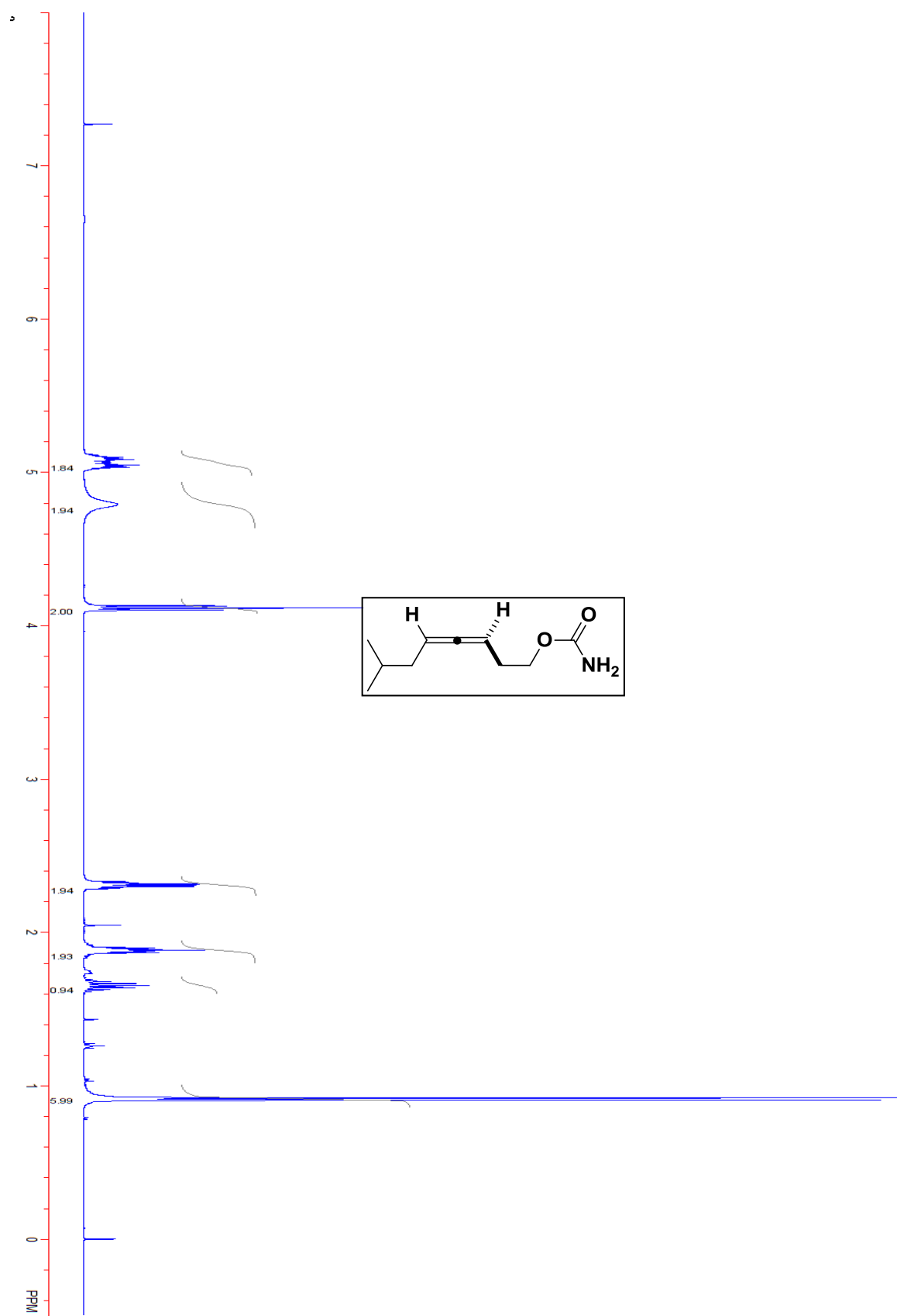
Compound 3.11d.

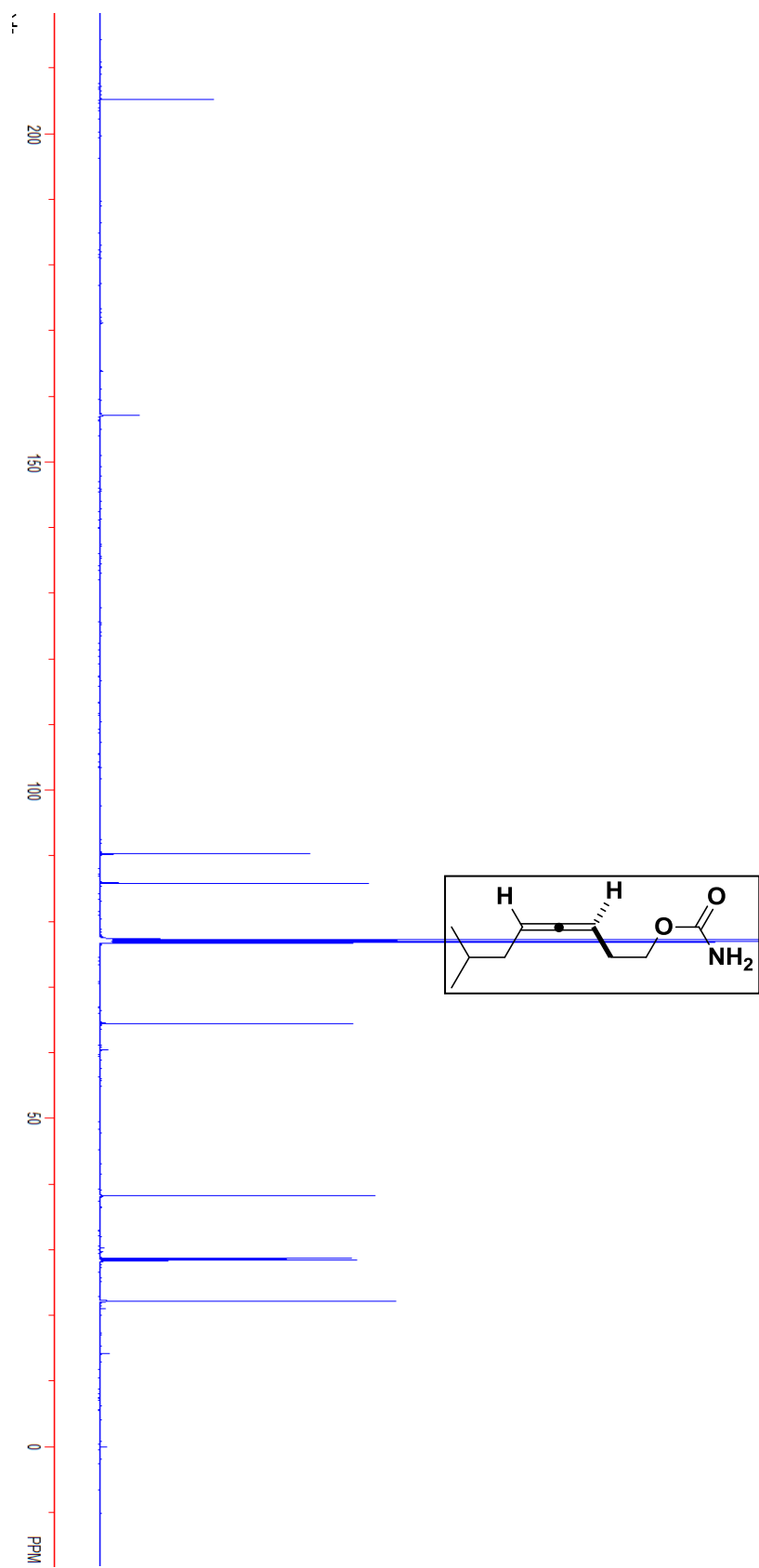


Compound 3.11d.

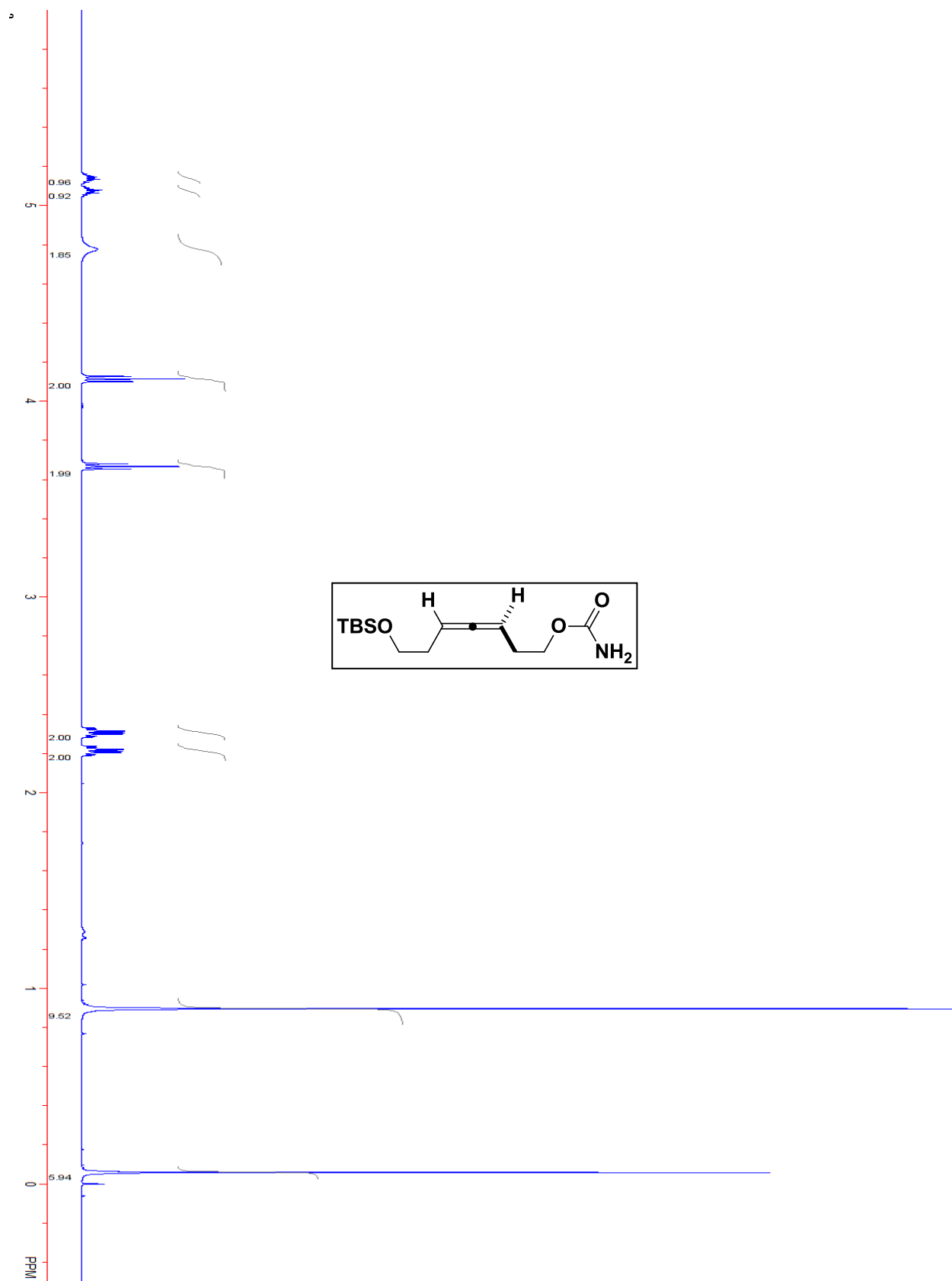


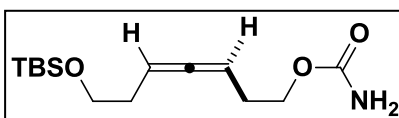
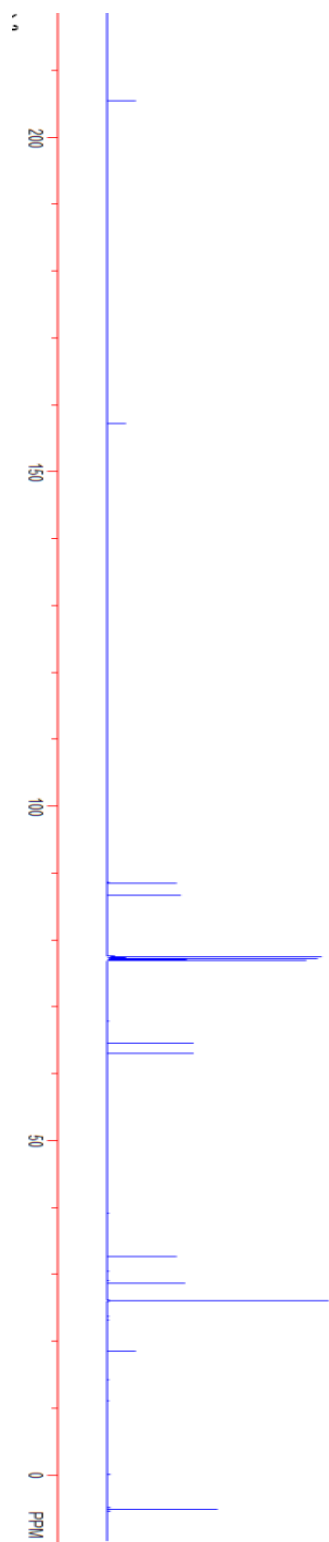
Compound 3.14a.



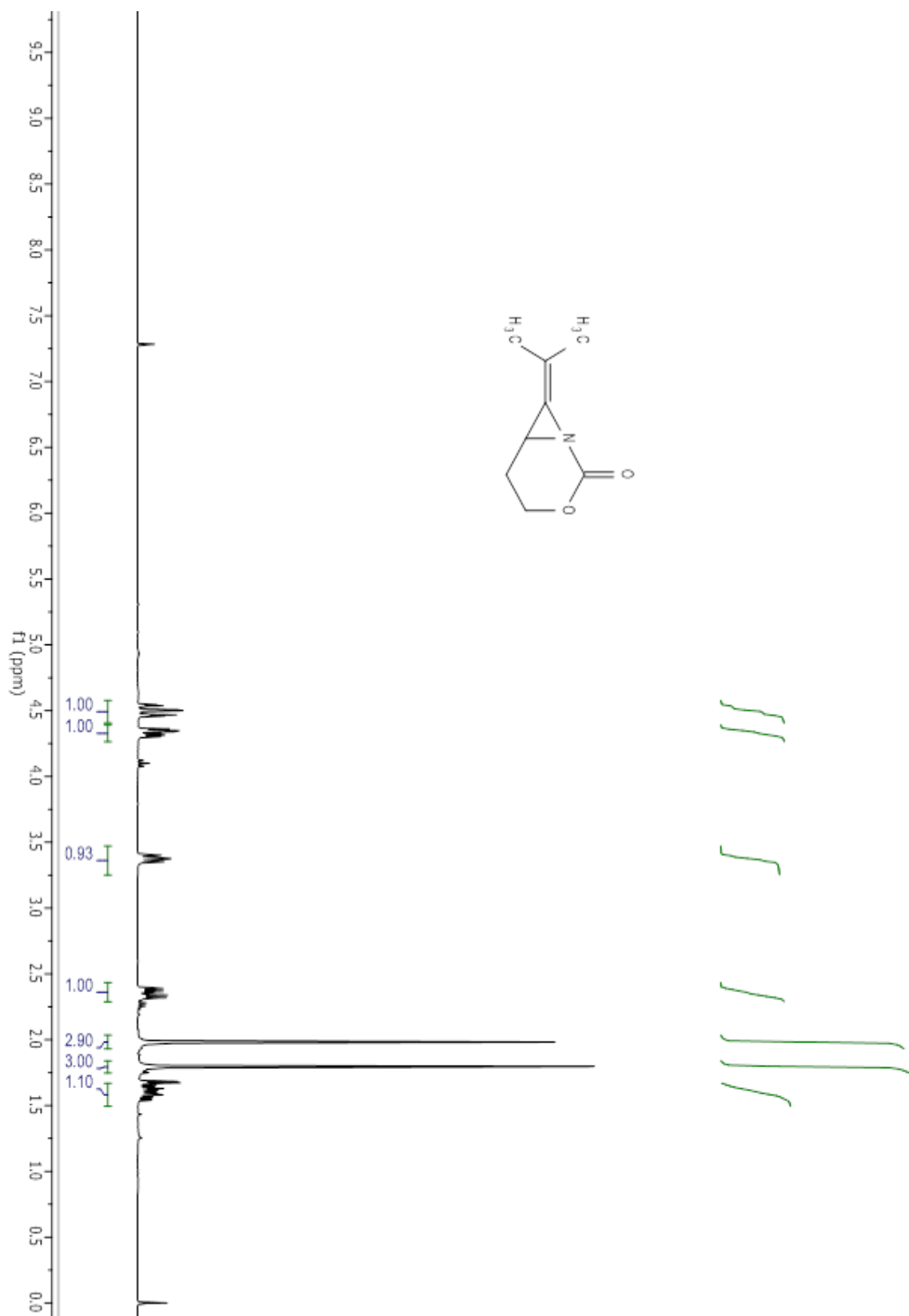
Compound 3.14a.

Compound 3.14c.

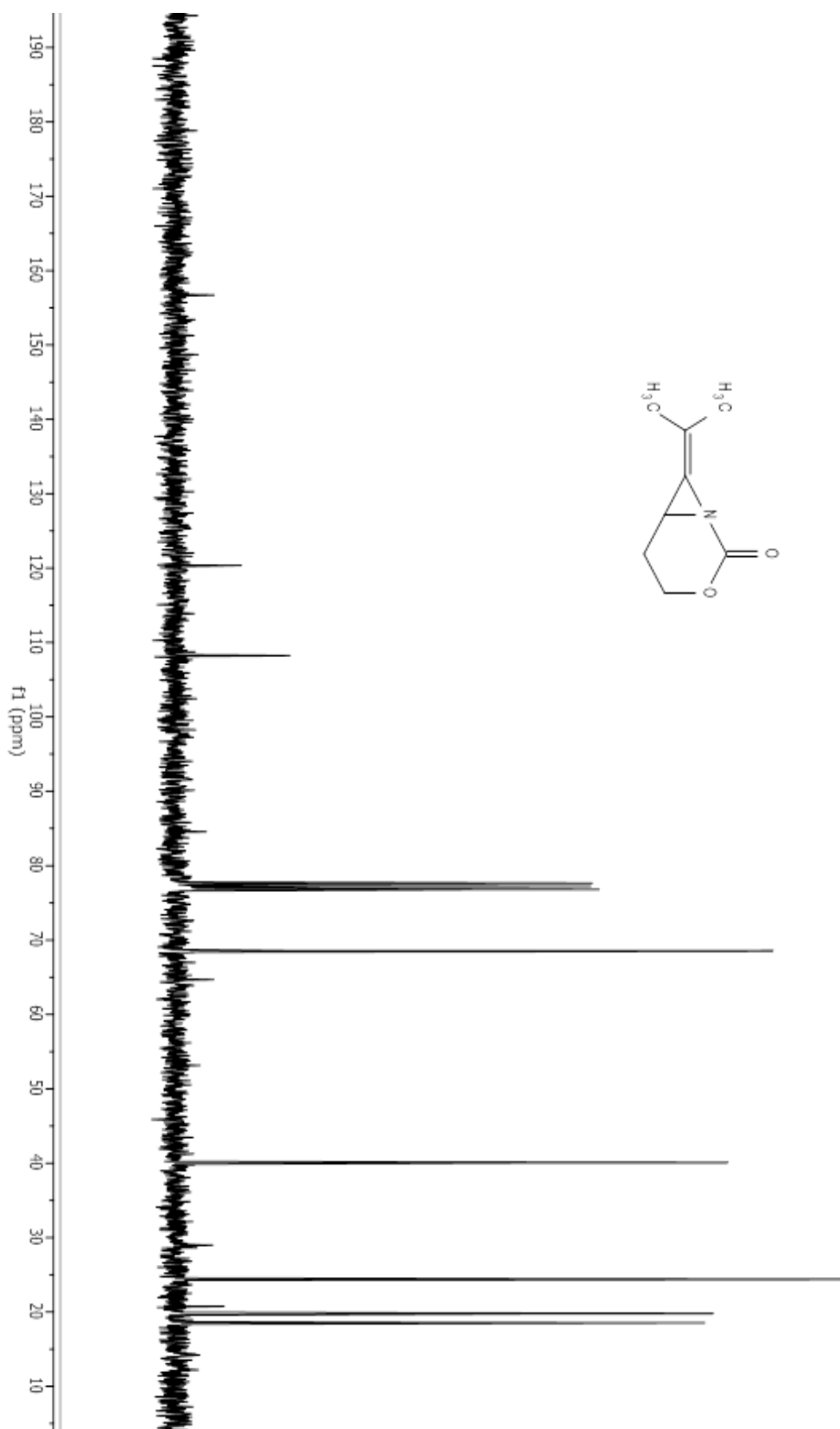


Compound 3.14c.

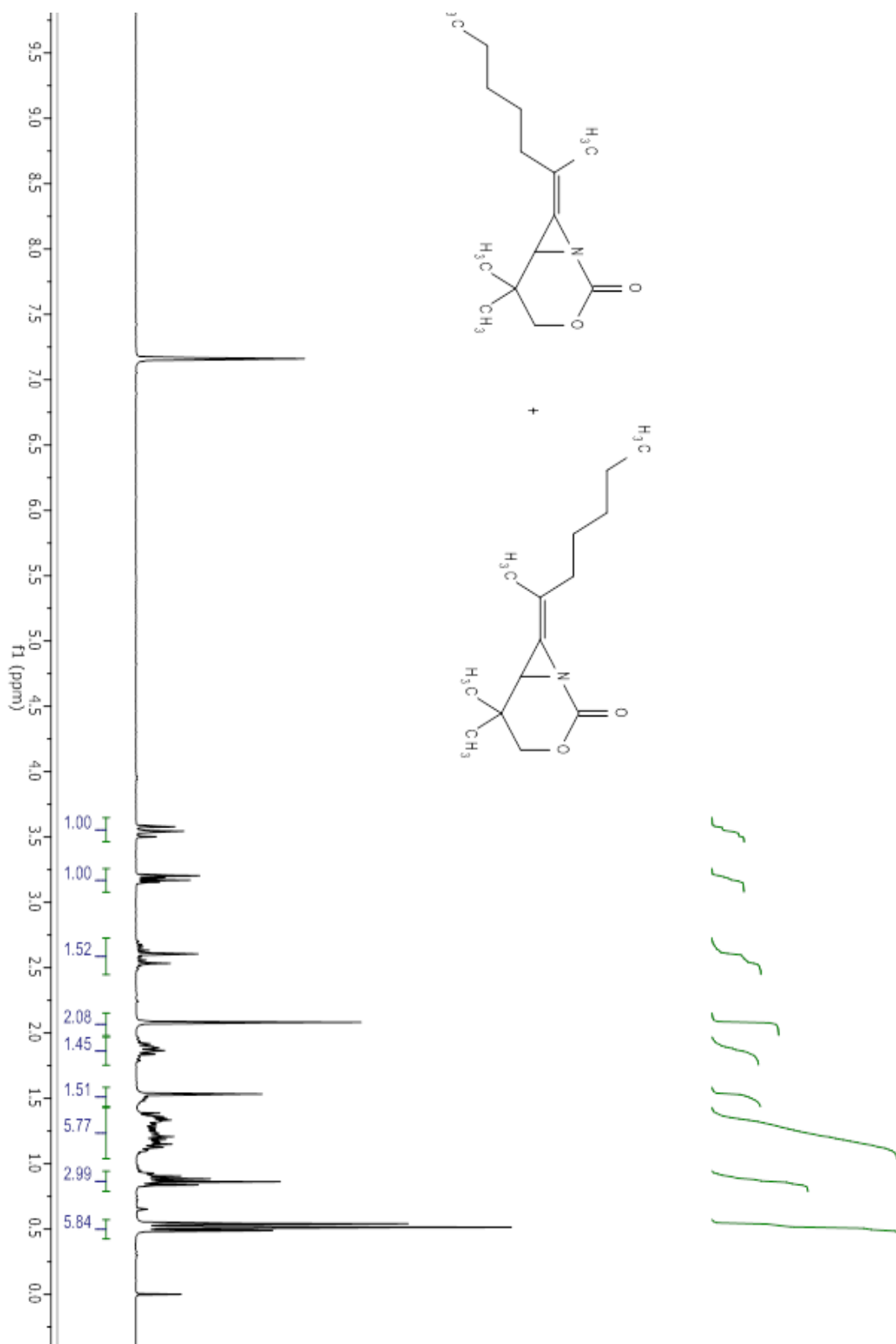
Compound 3.7a.



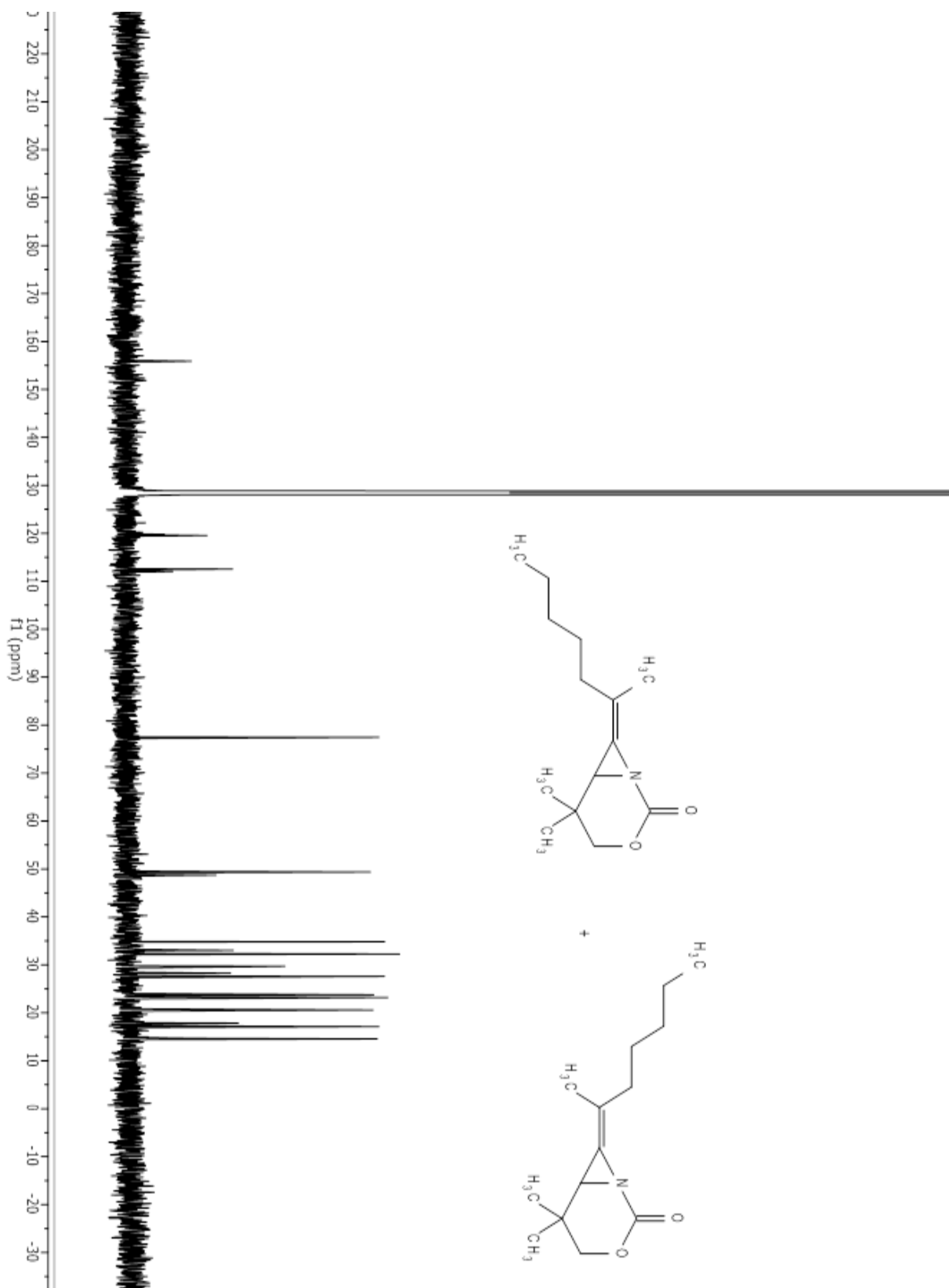
Compound 3.7a.

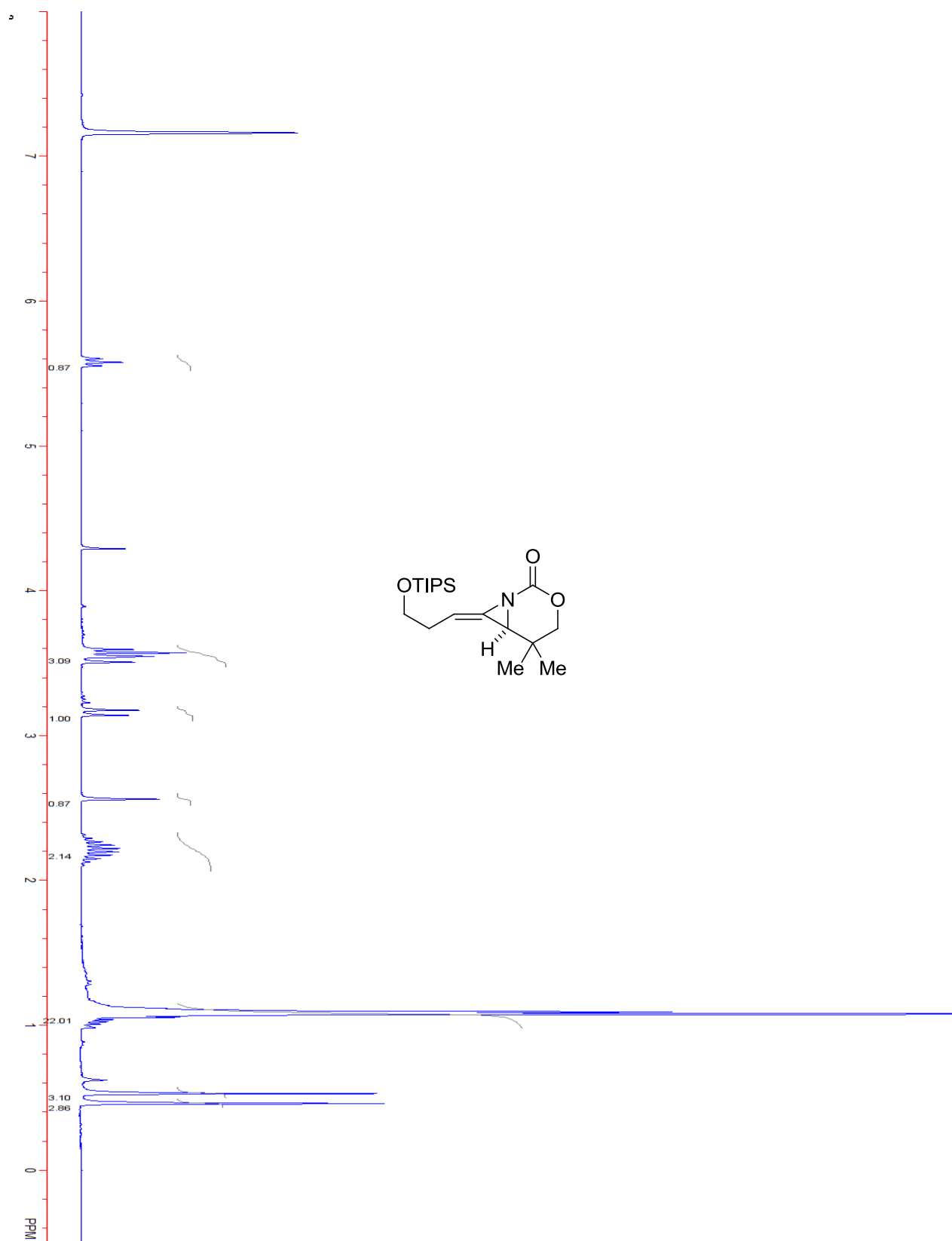


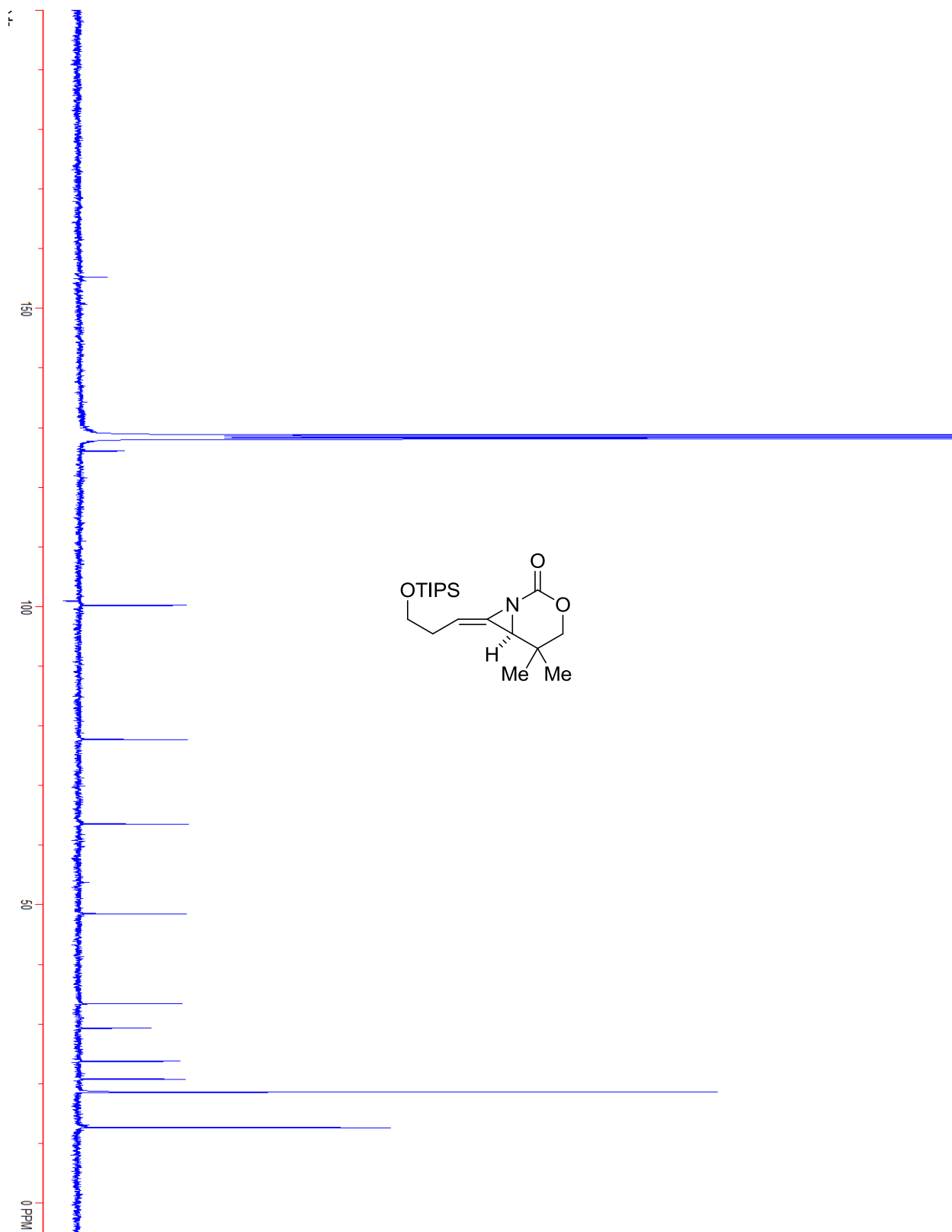
Compound 3.10b.



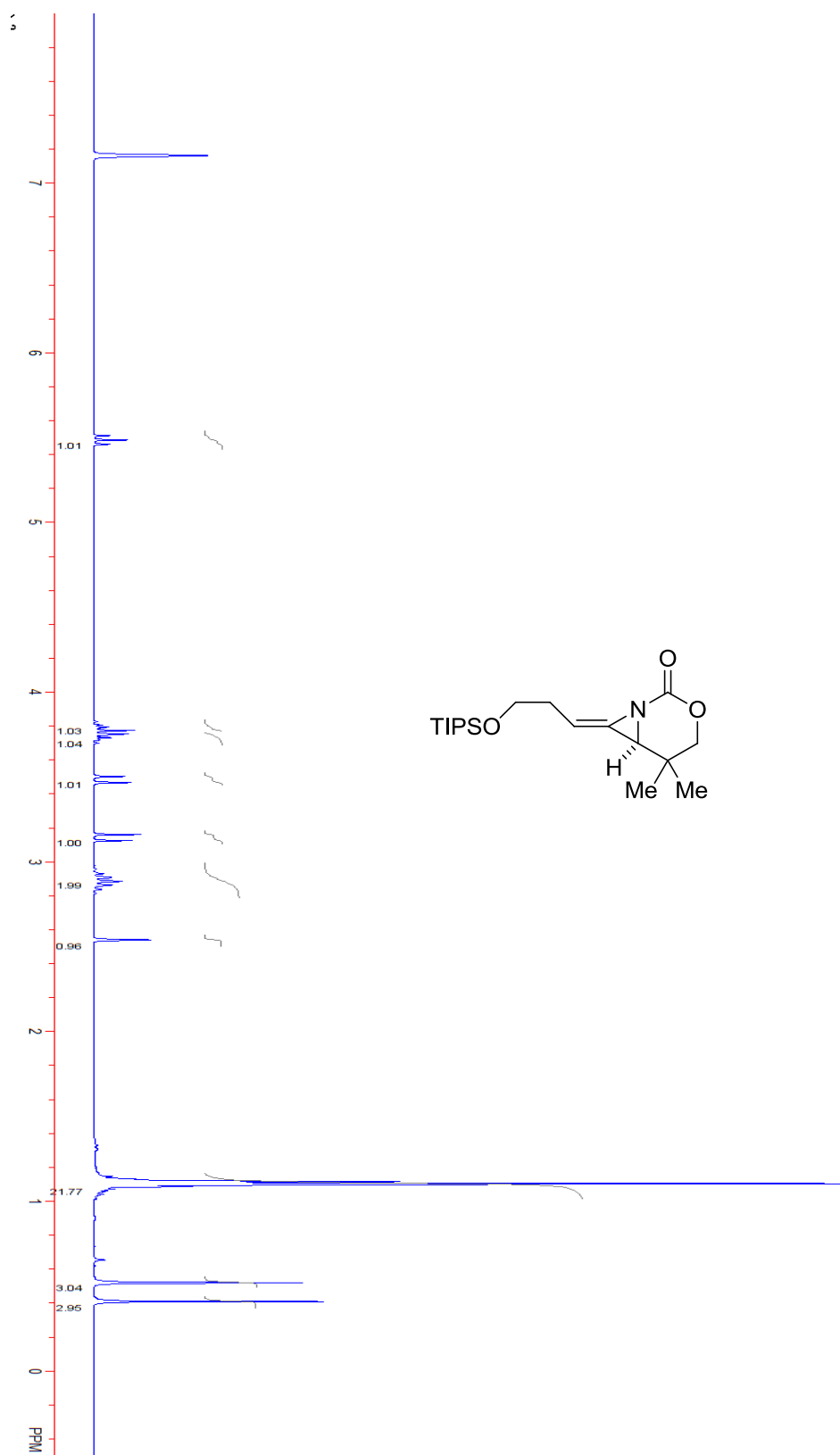
Compound 3.10b.



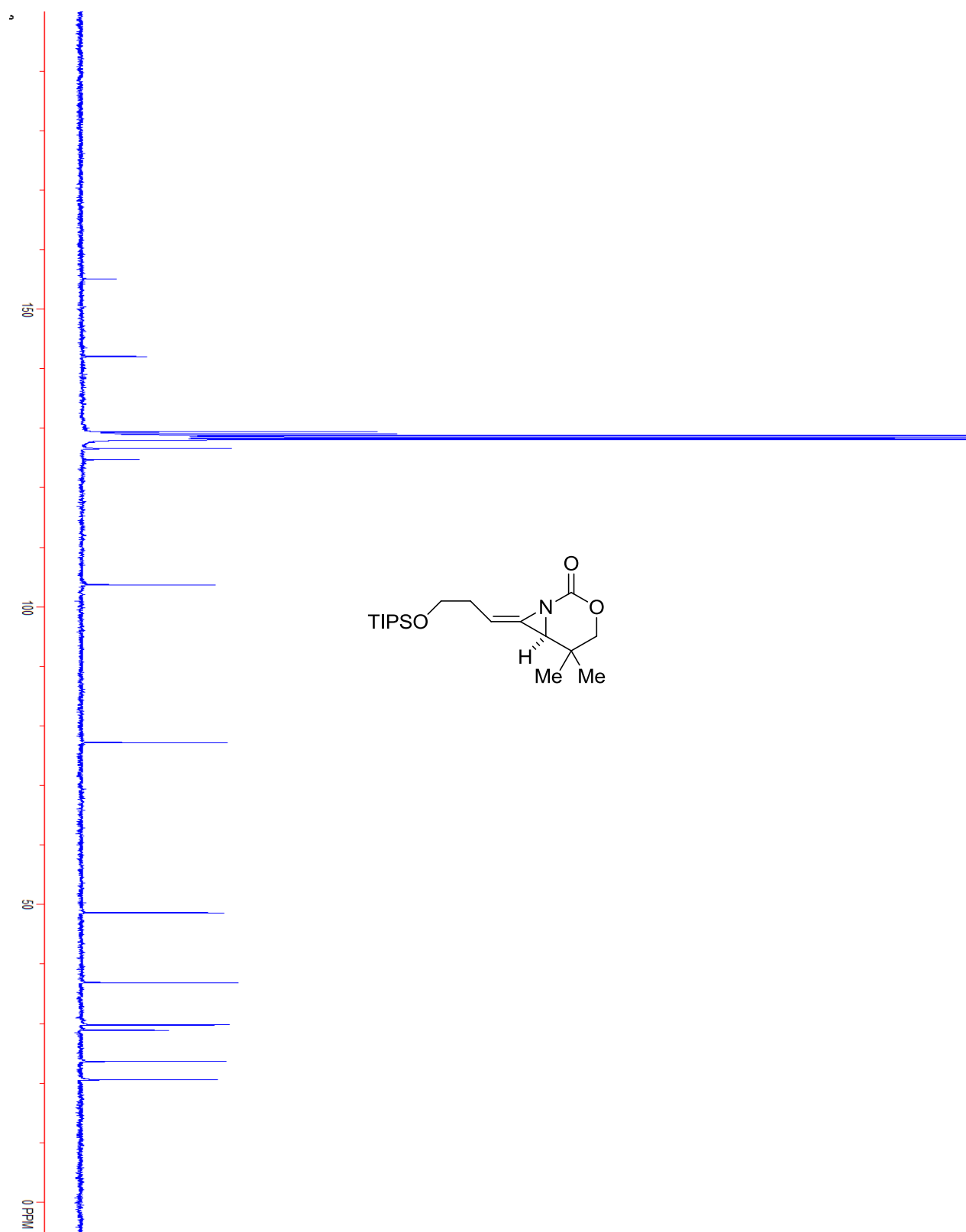
Compound 3.10c. *E* isomer.

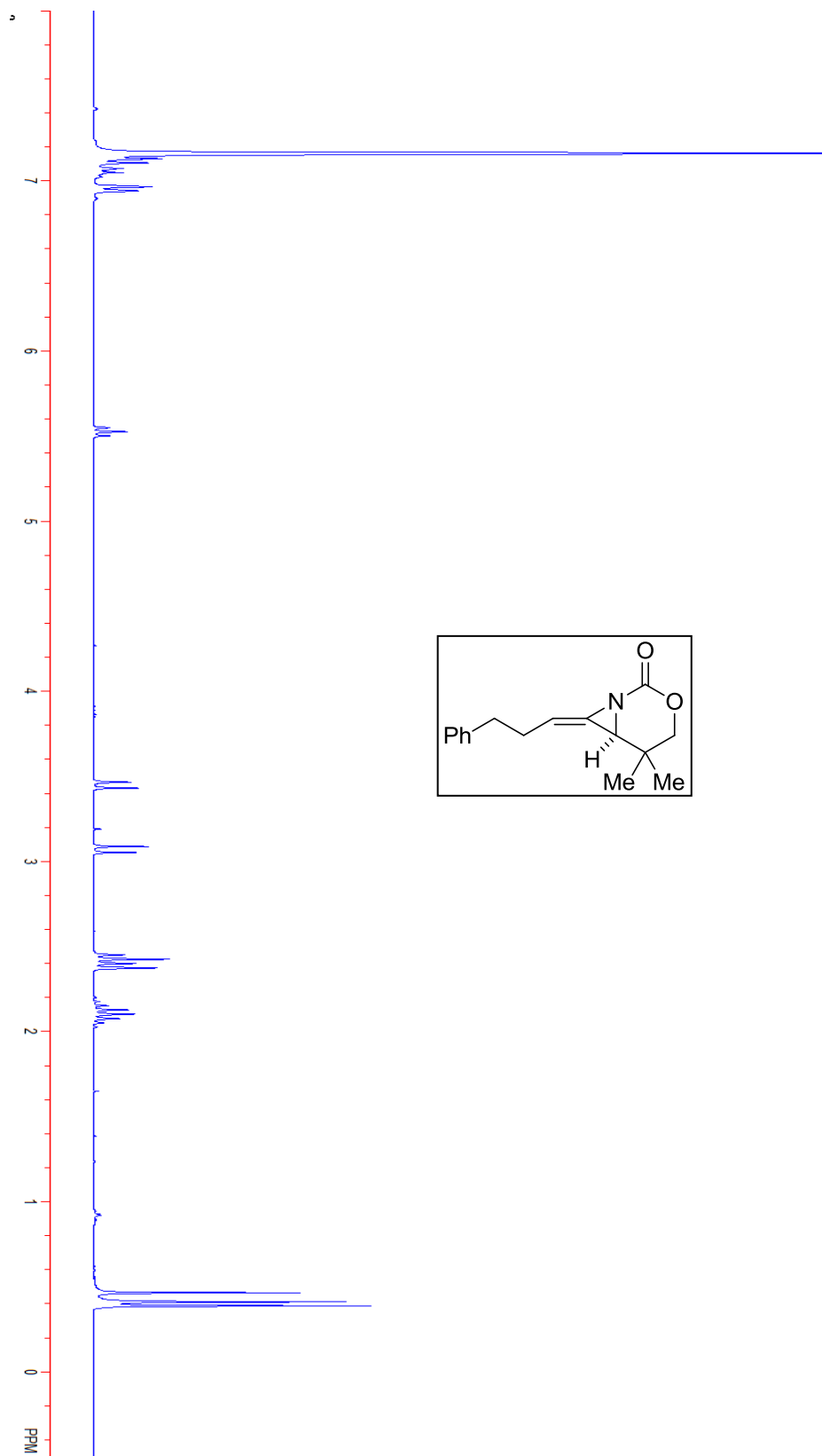
Compound 3.10c. *E* isomer.

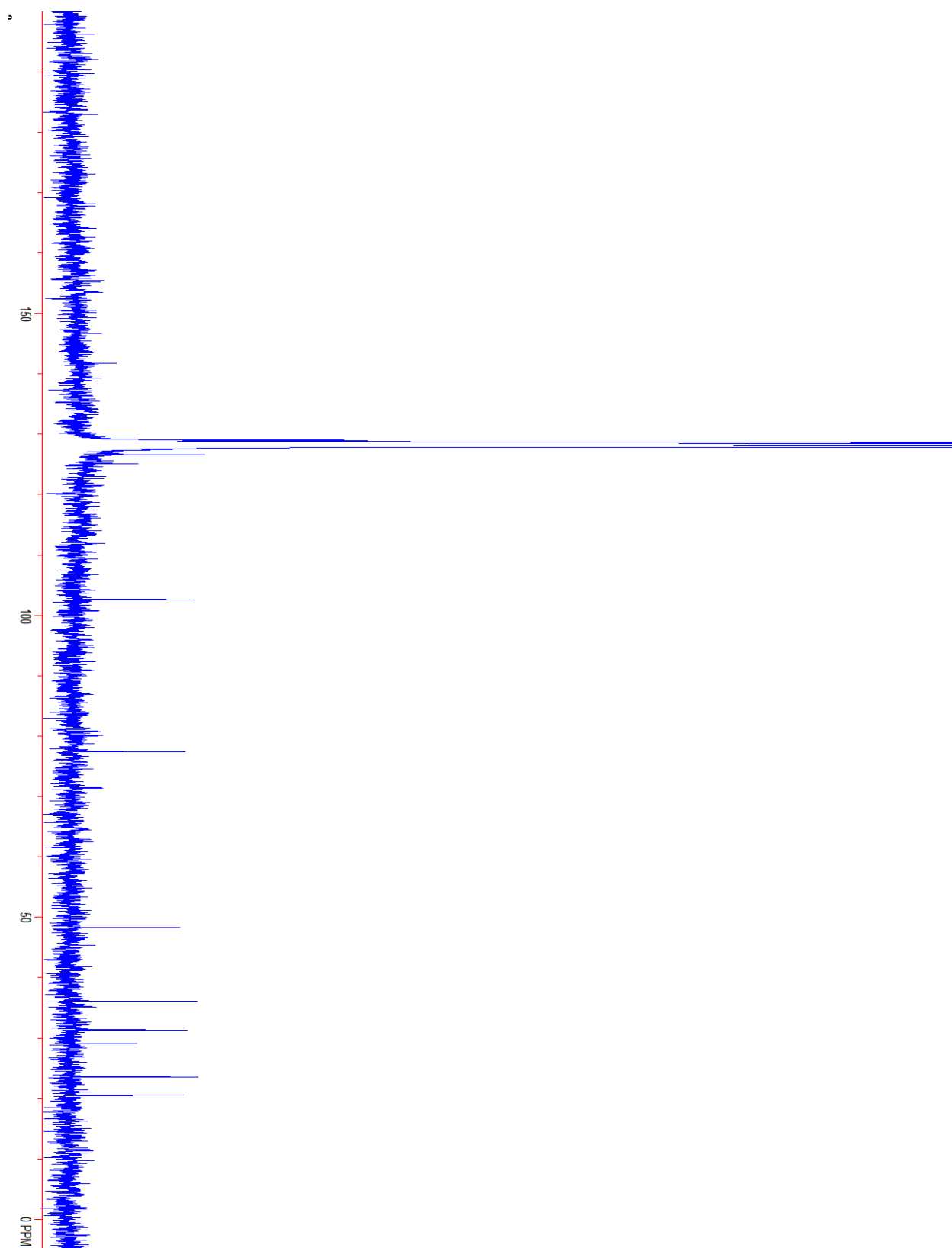
Compound 3.10c. Z isomer.

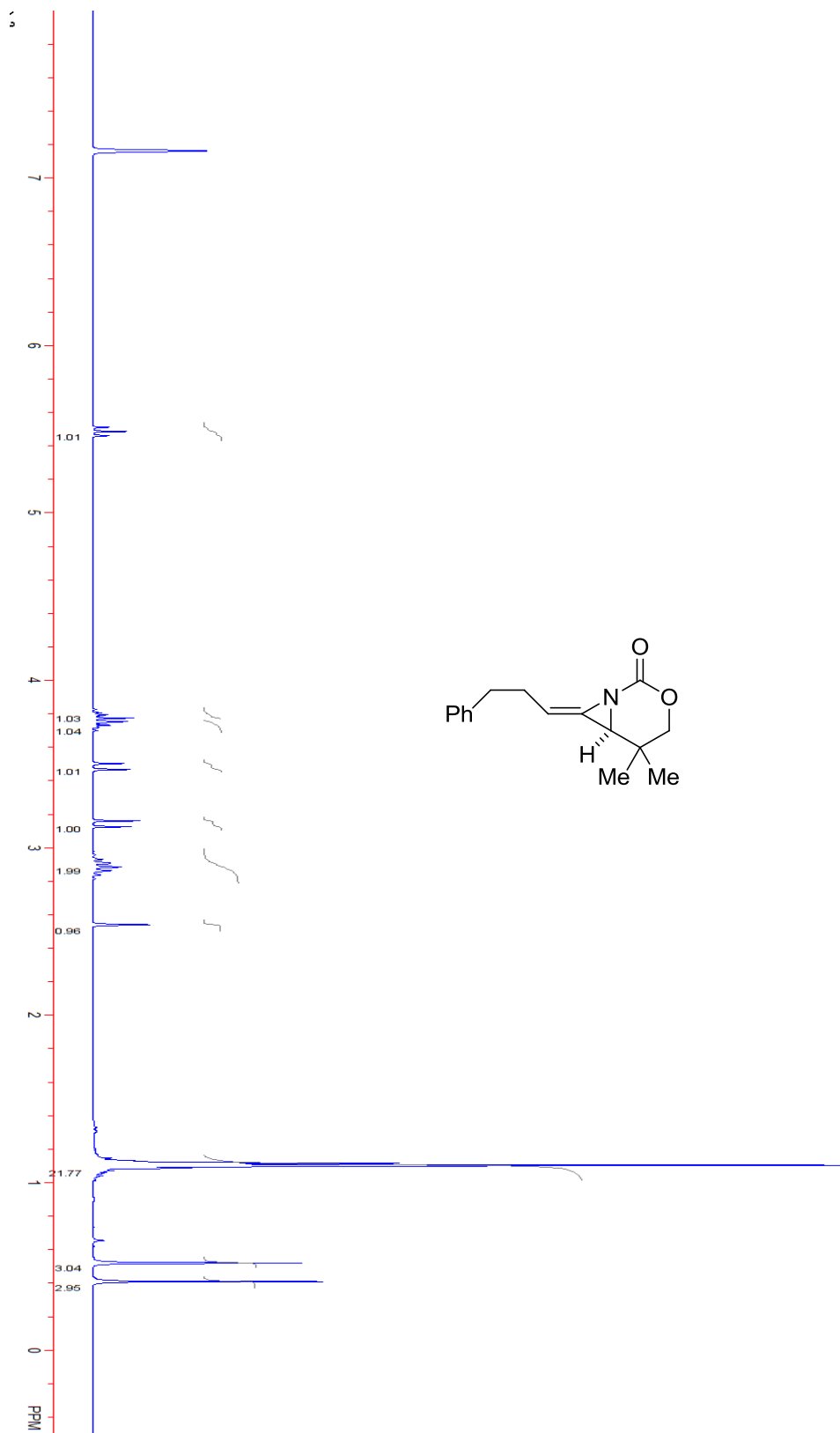


Compound 3.10c. Z isomer.

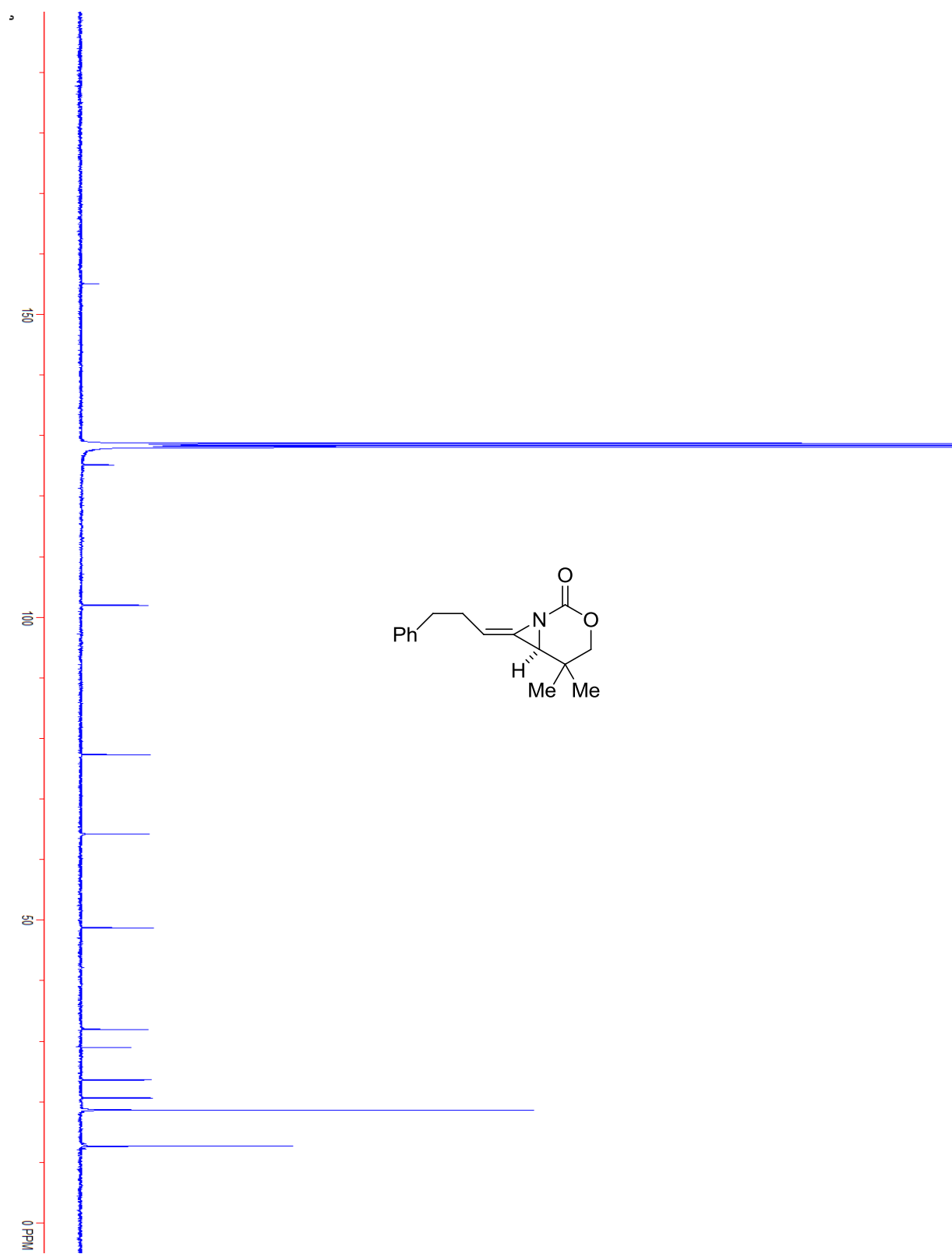


Compound 3.10d. *E* isomer.

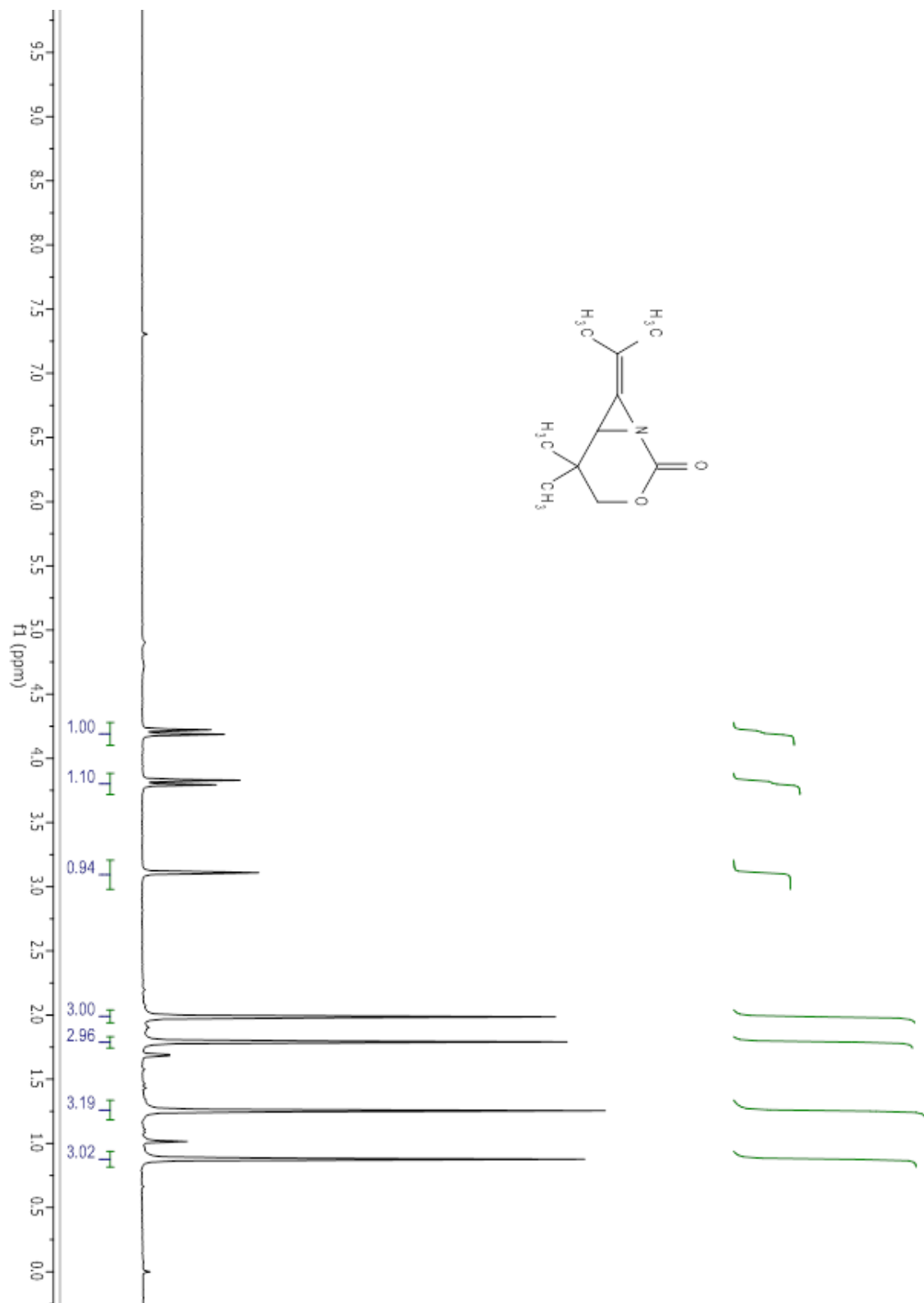
Compound 3.10d. *E* isomer.

Compound 3.10d. Z isomer.

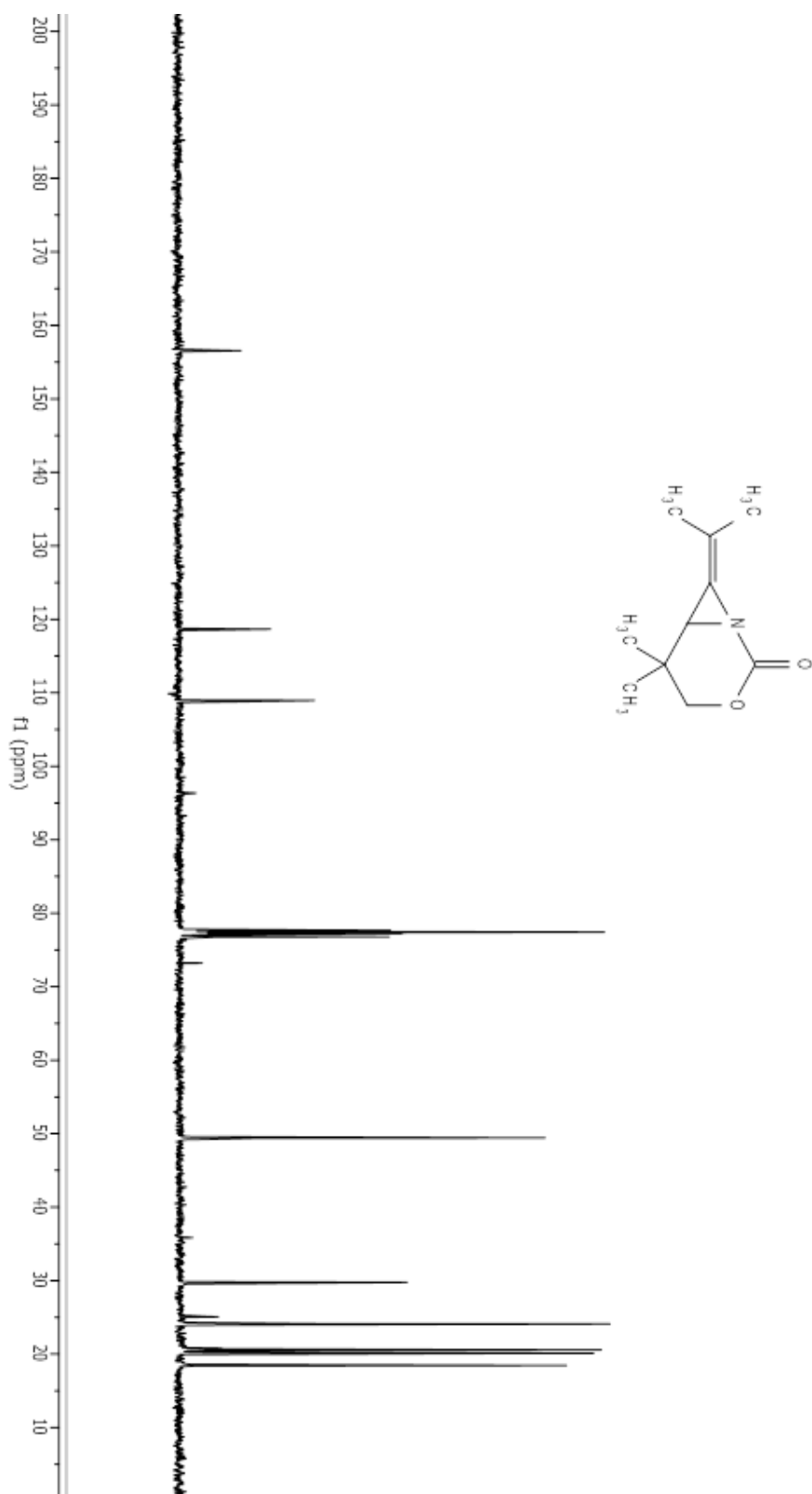
Compound 3.10d. Z isomer.



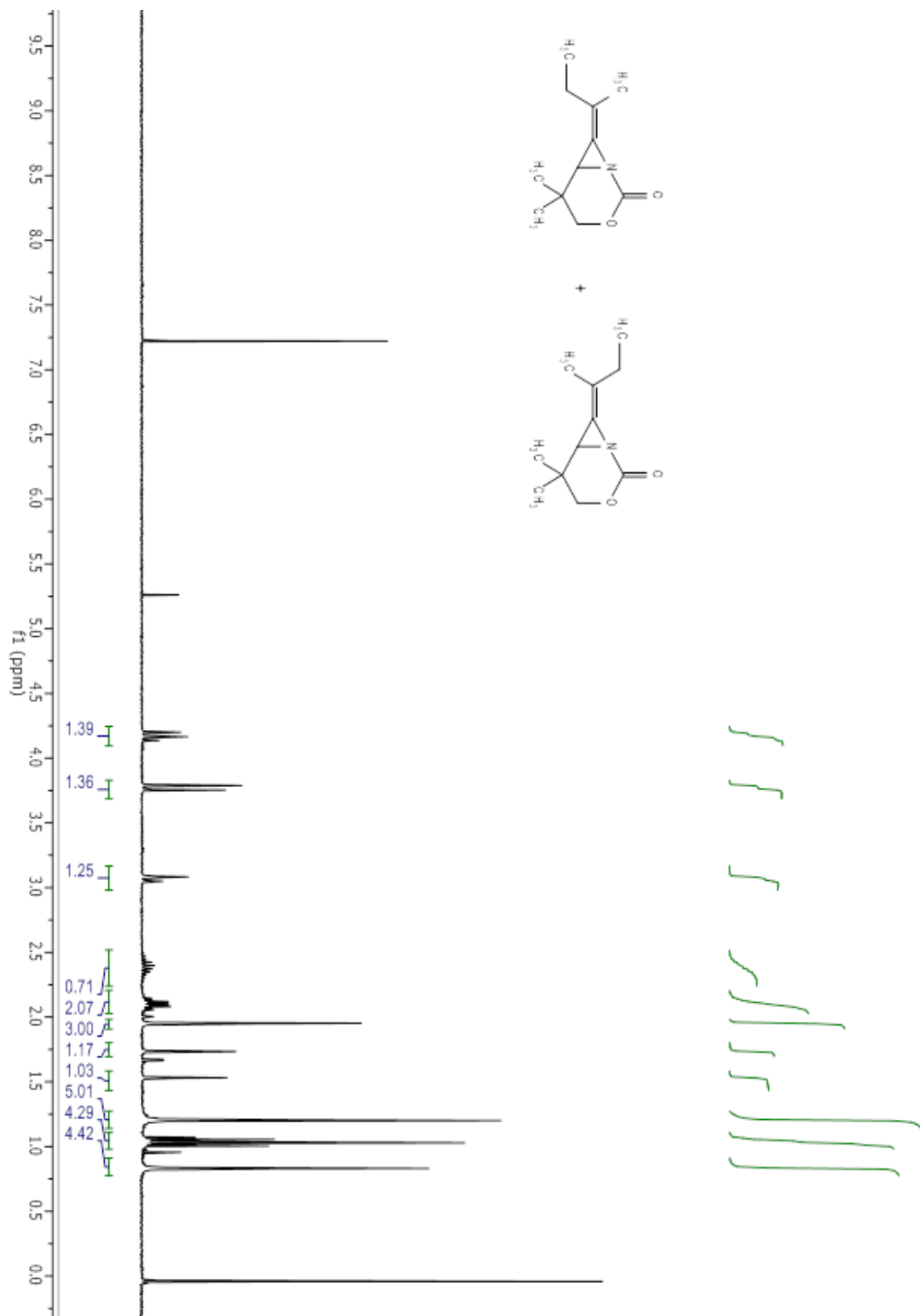
Compound 3.10e.



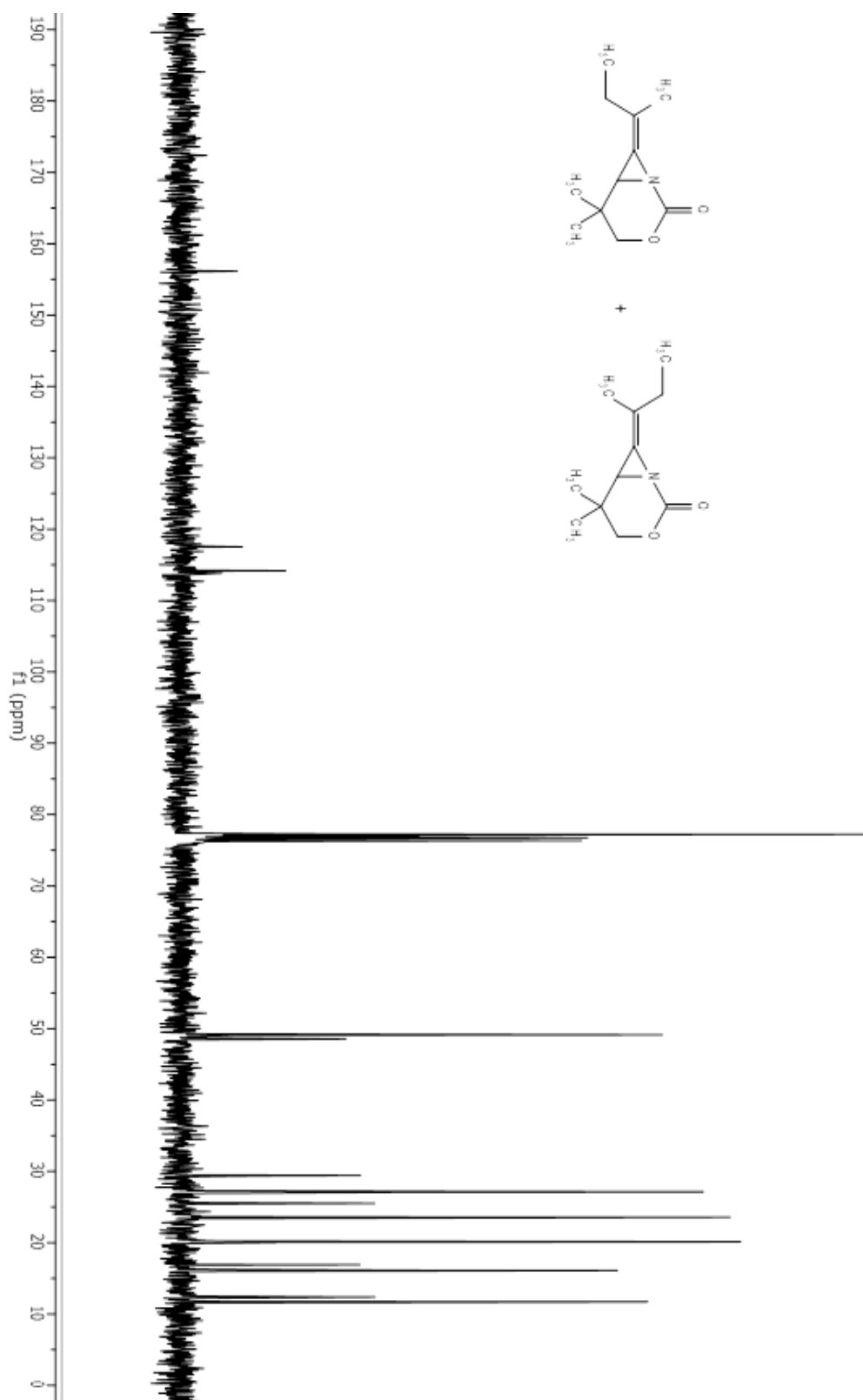
Compound 3.10e.



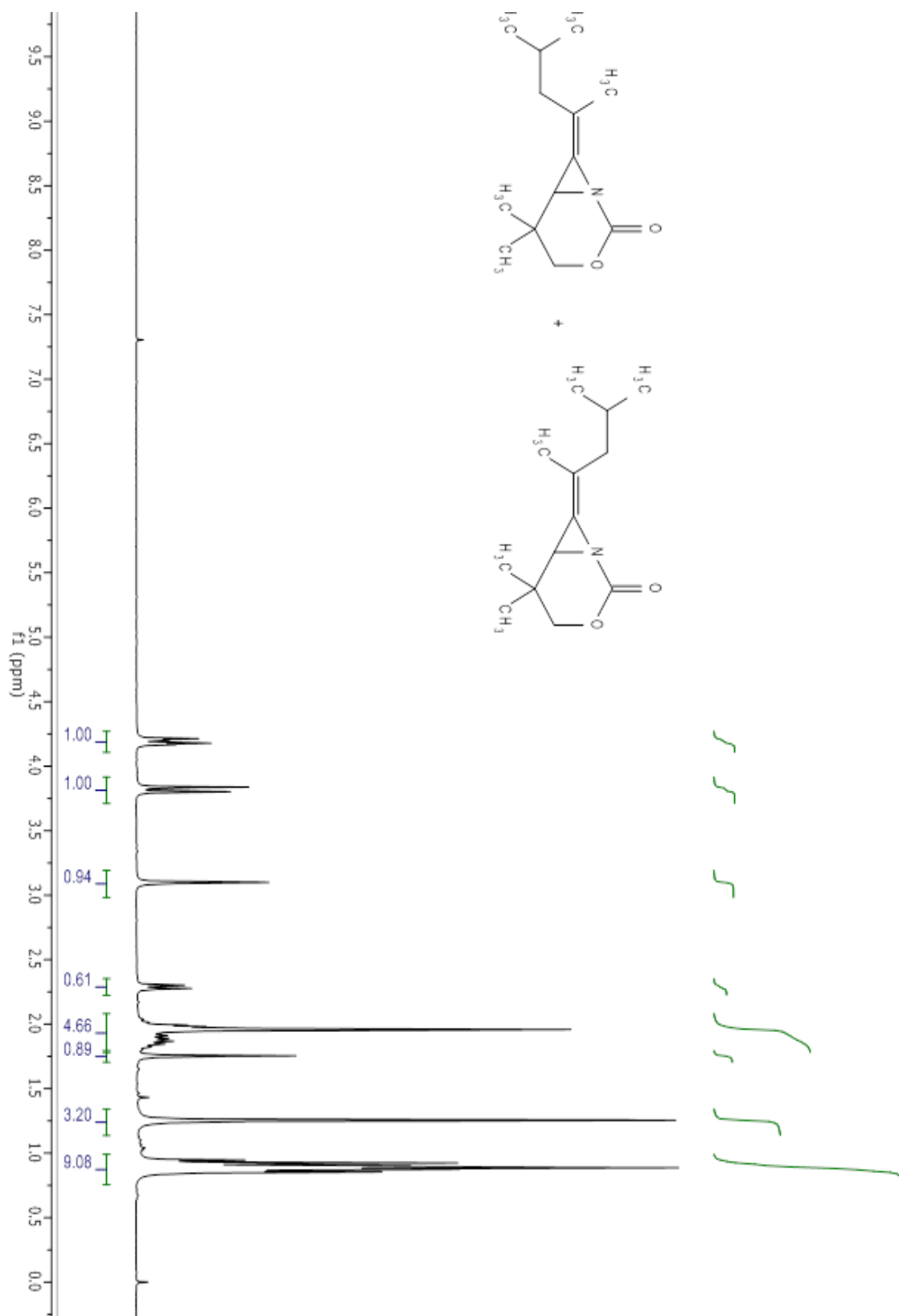
Compound 3.10f.



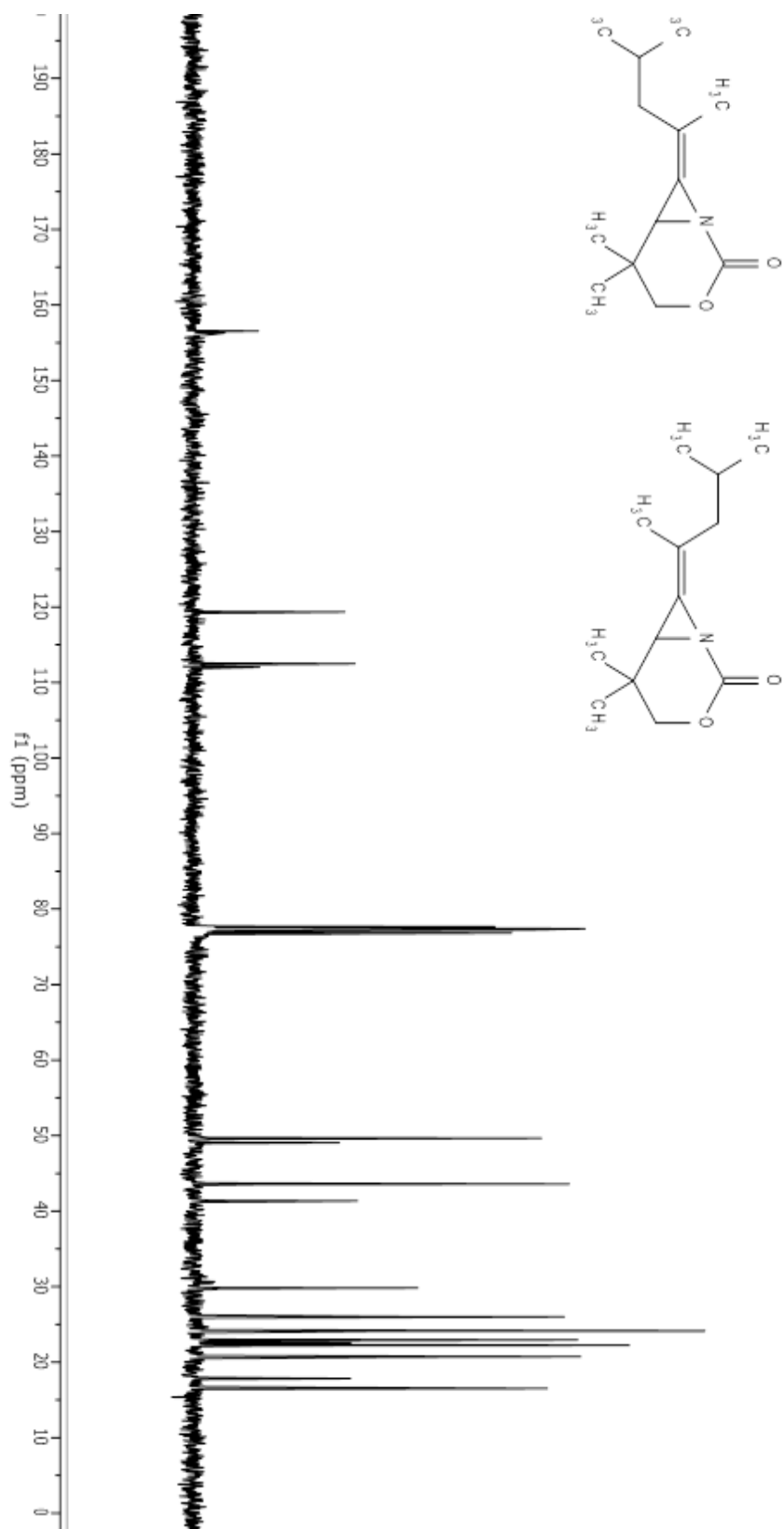
Compound 3.10f.

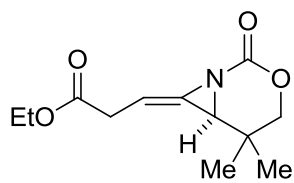
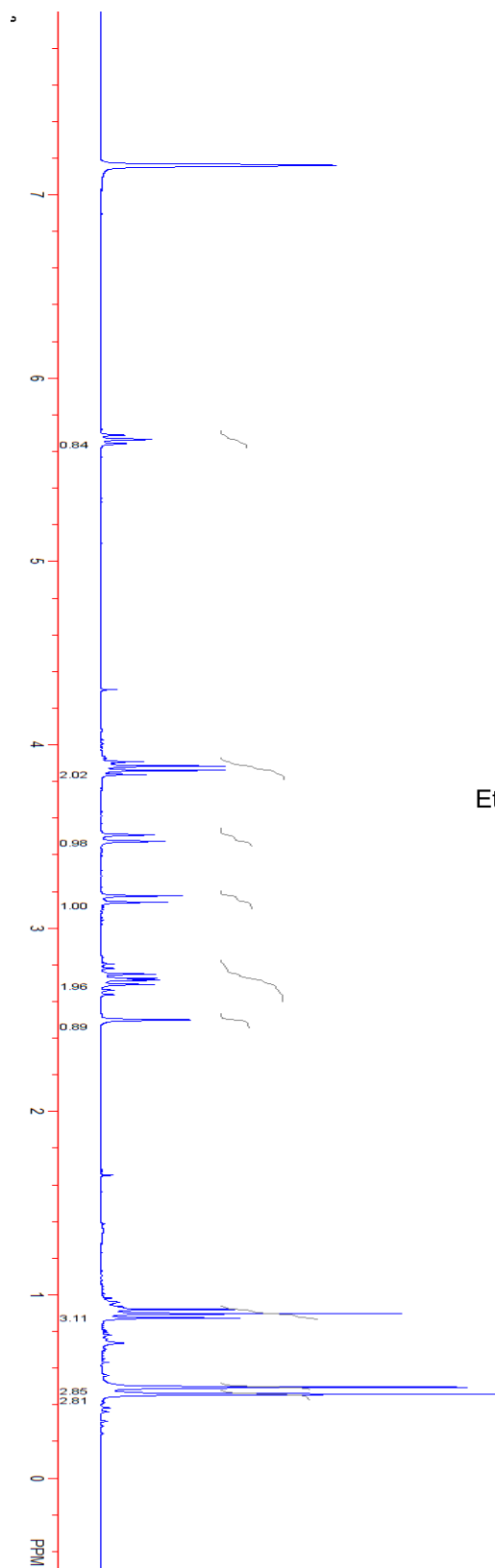


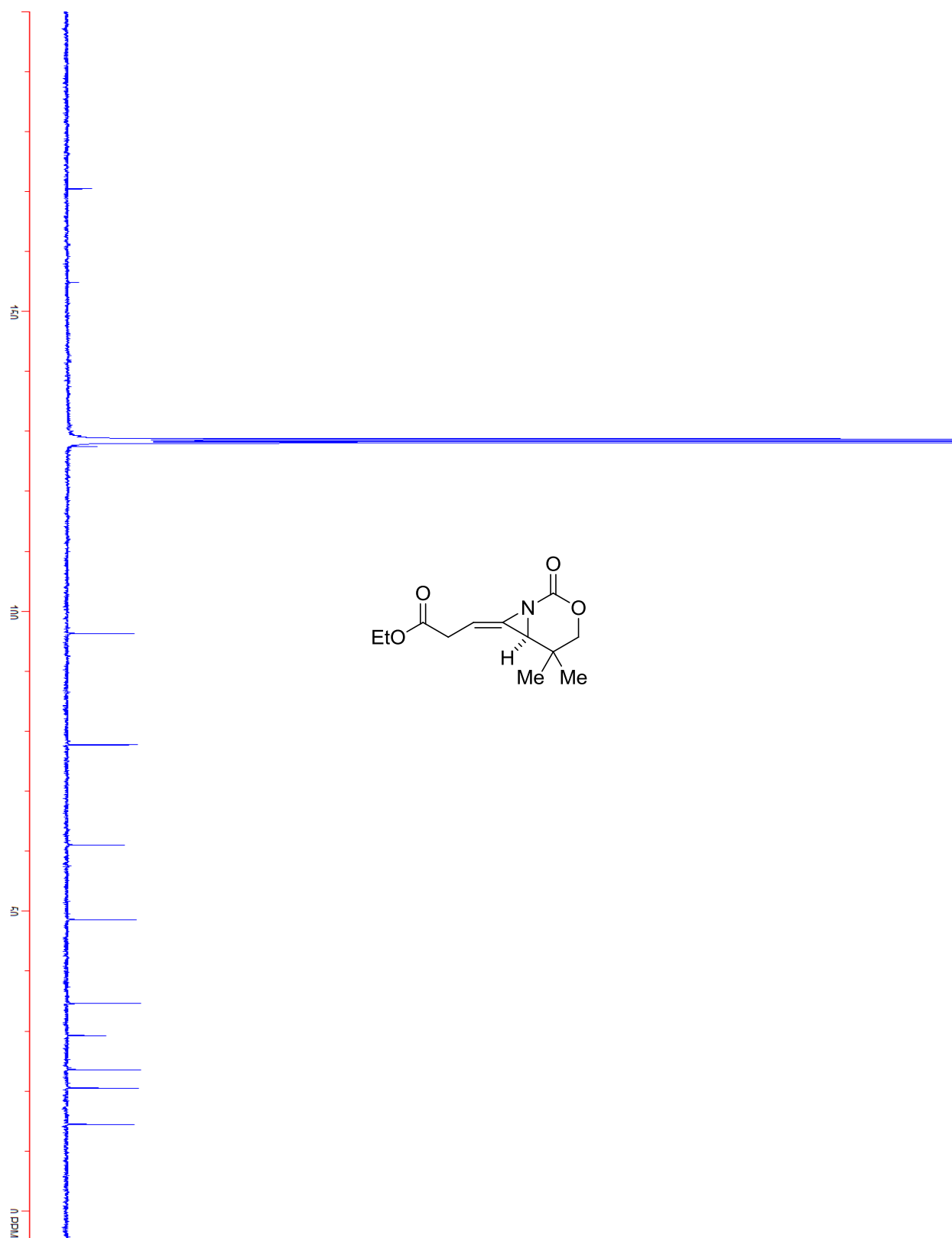
Compound 3.10g.



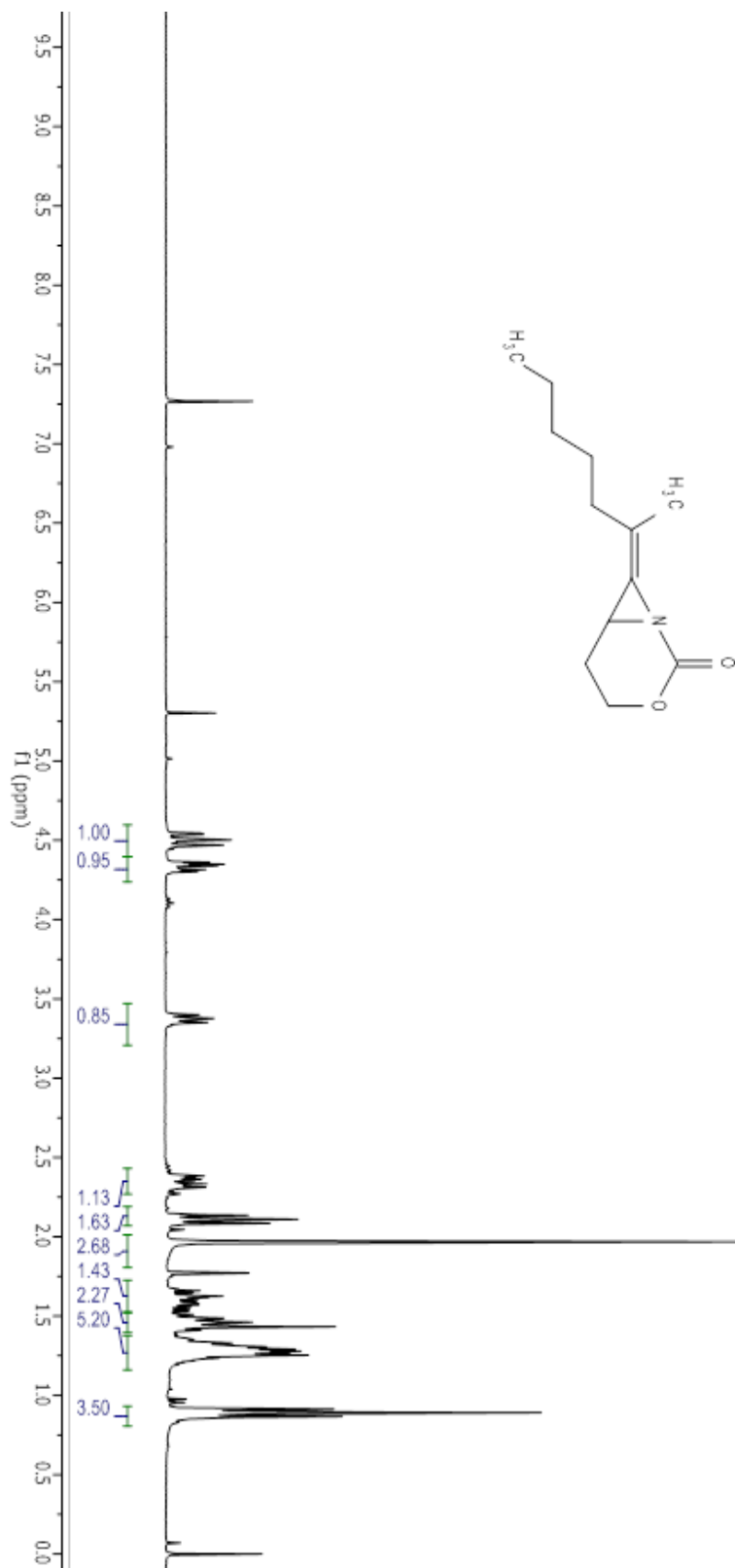
Compound 3.10g.



Compound 3.10h. *E* isomer.

Compound 3.10h. *E* isomer.

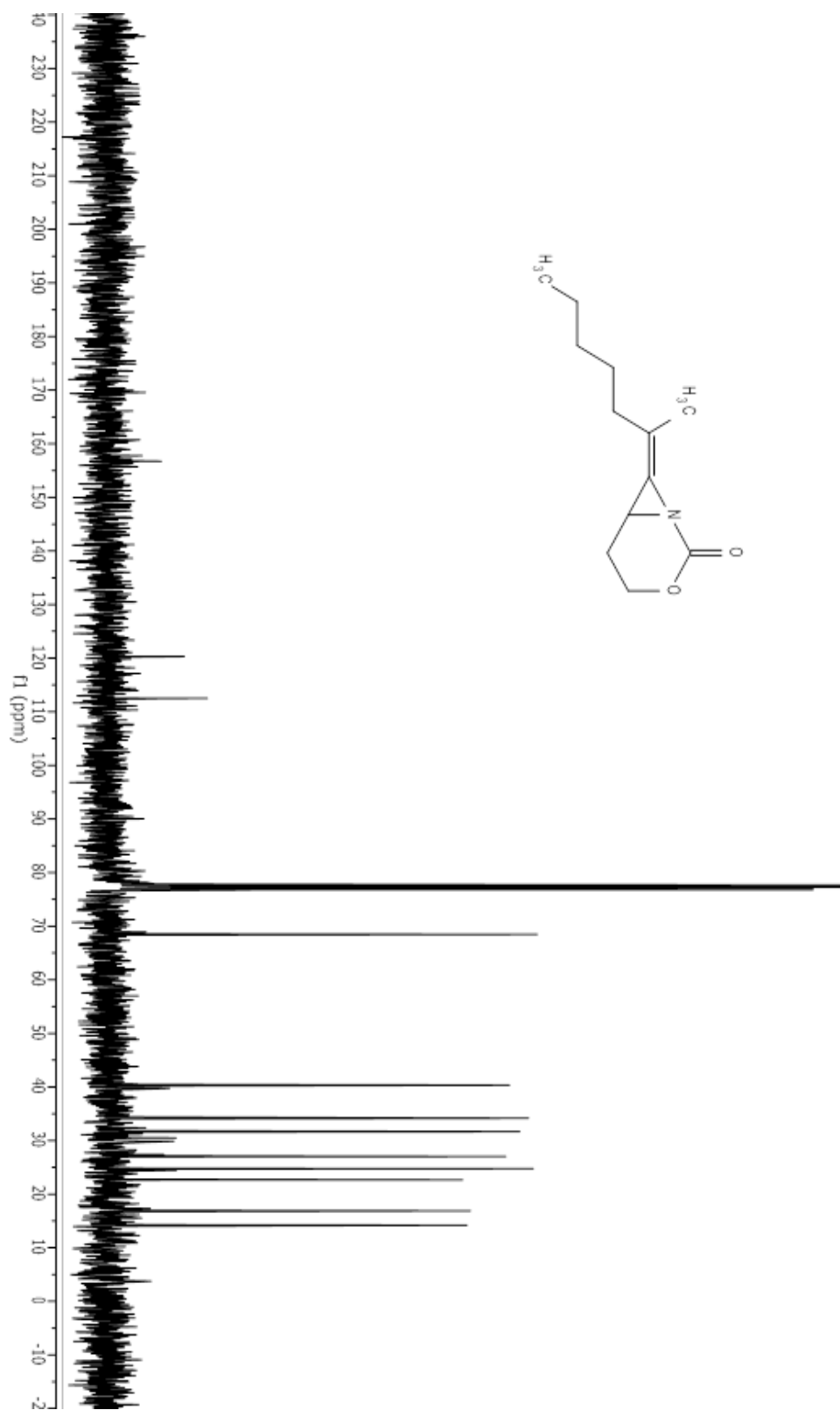
Compound 3.12c.



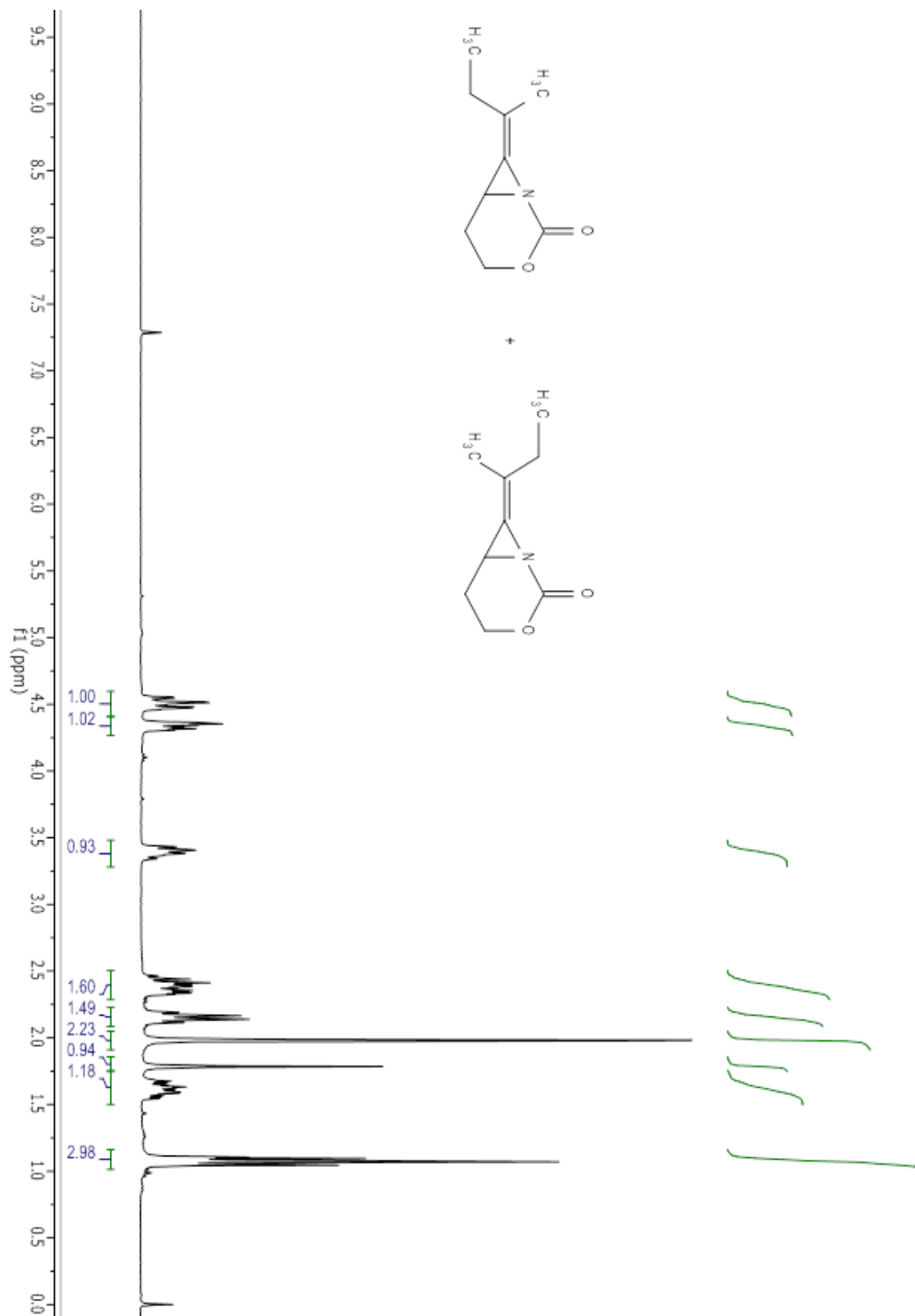
Handwritten notes in green ink:

|||
r

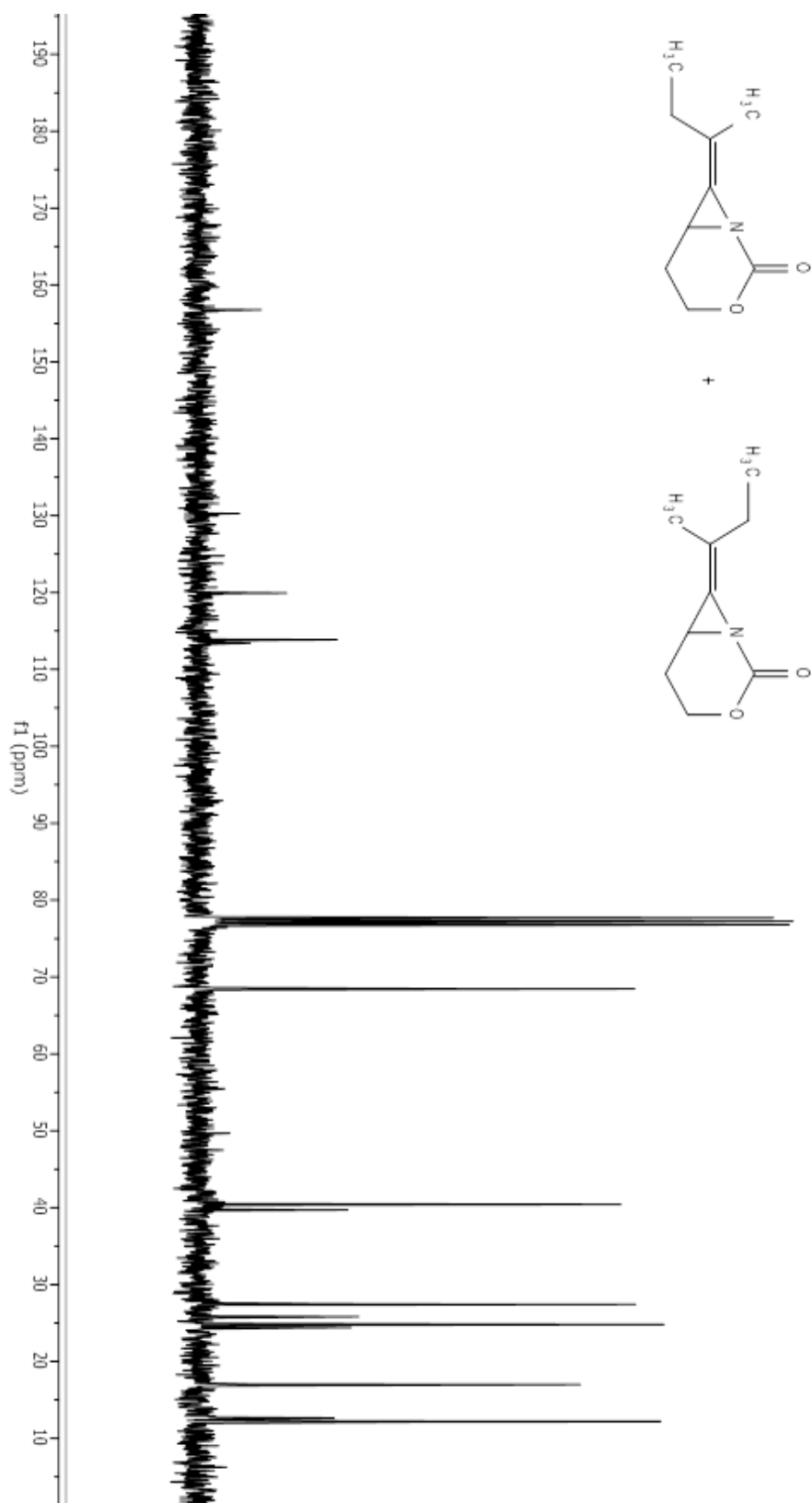
Compound 3.12c.



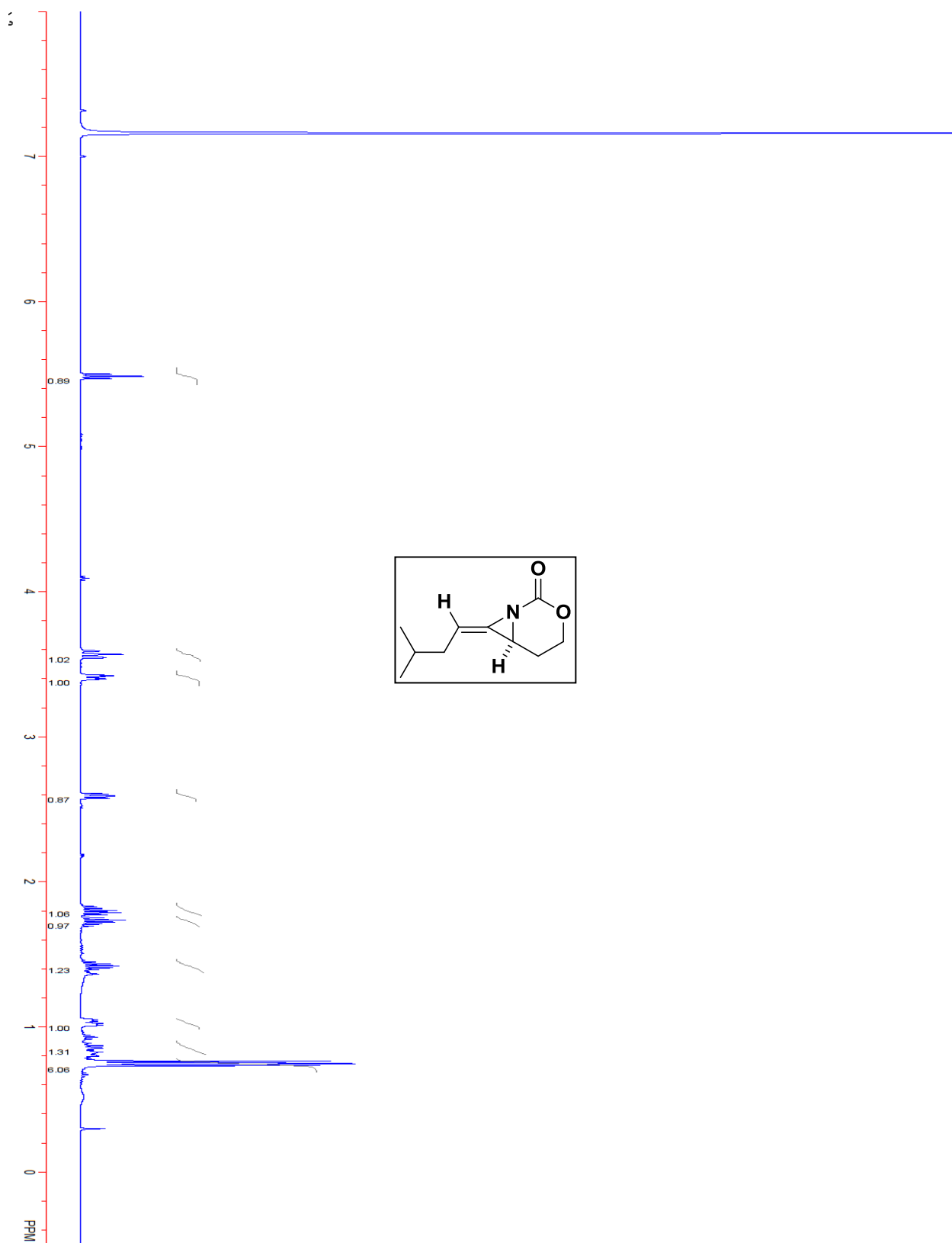
Compound 3.12d.



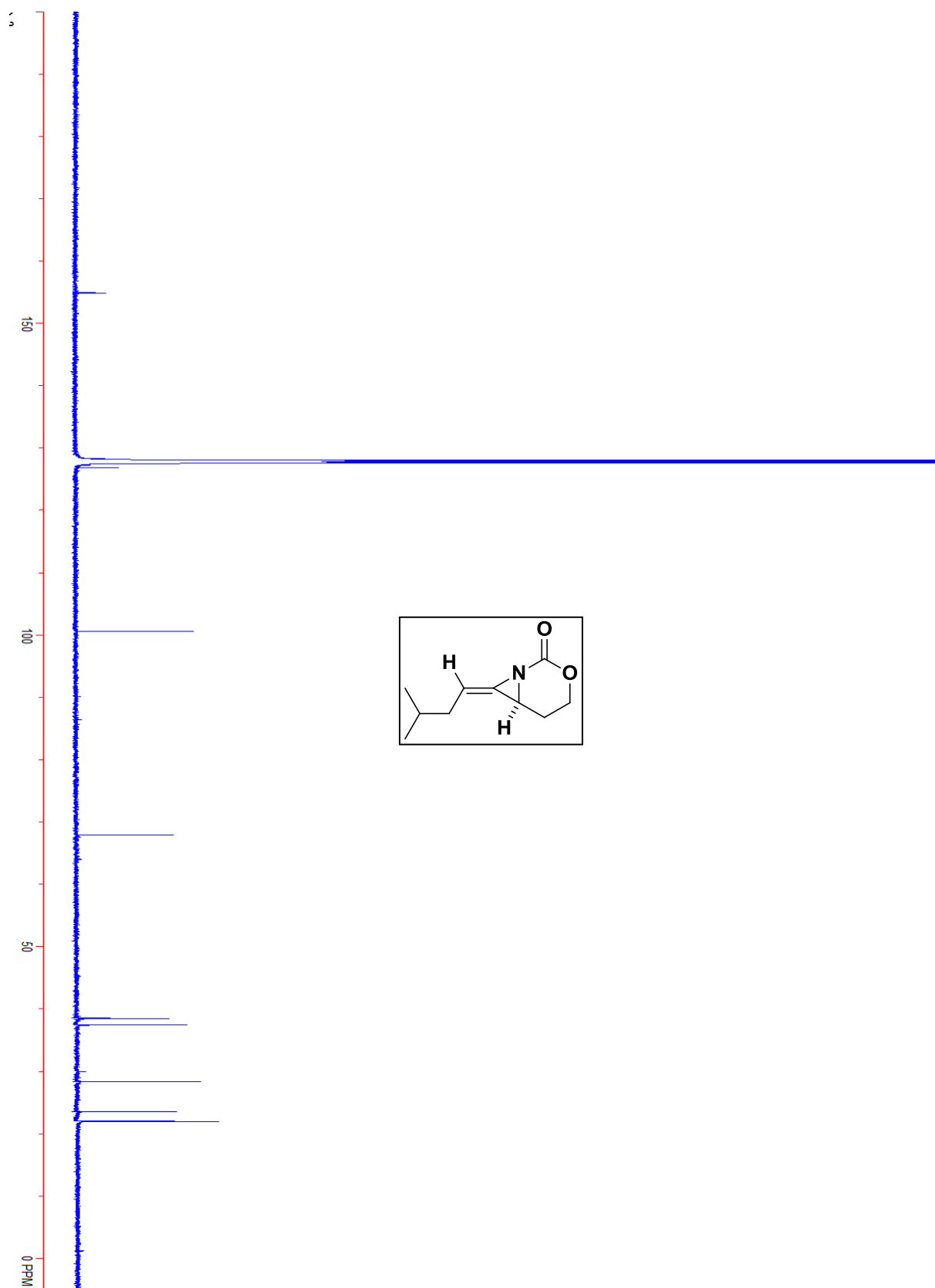
Compound 3.12d.



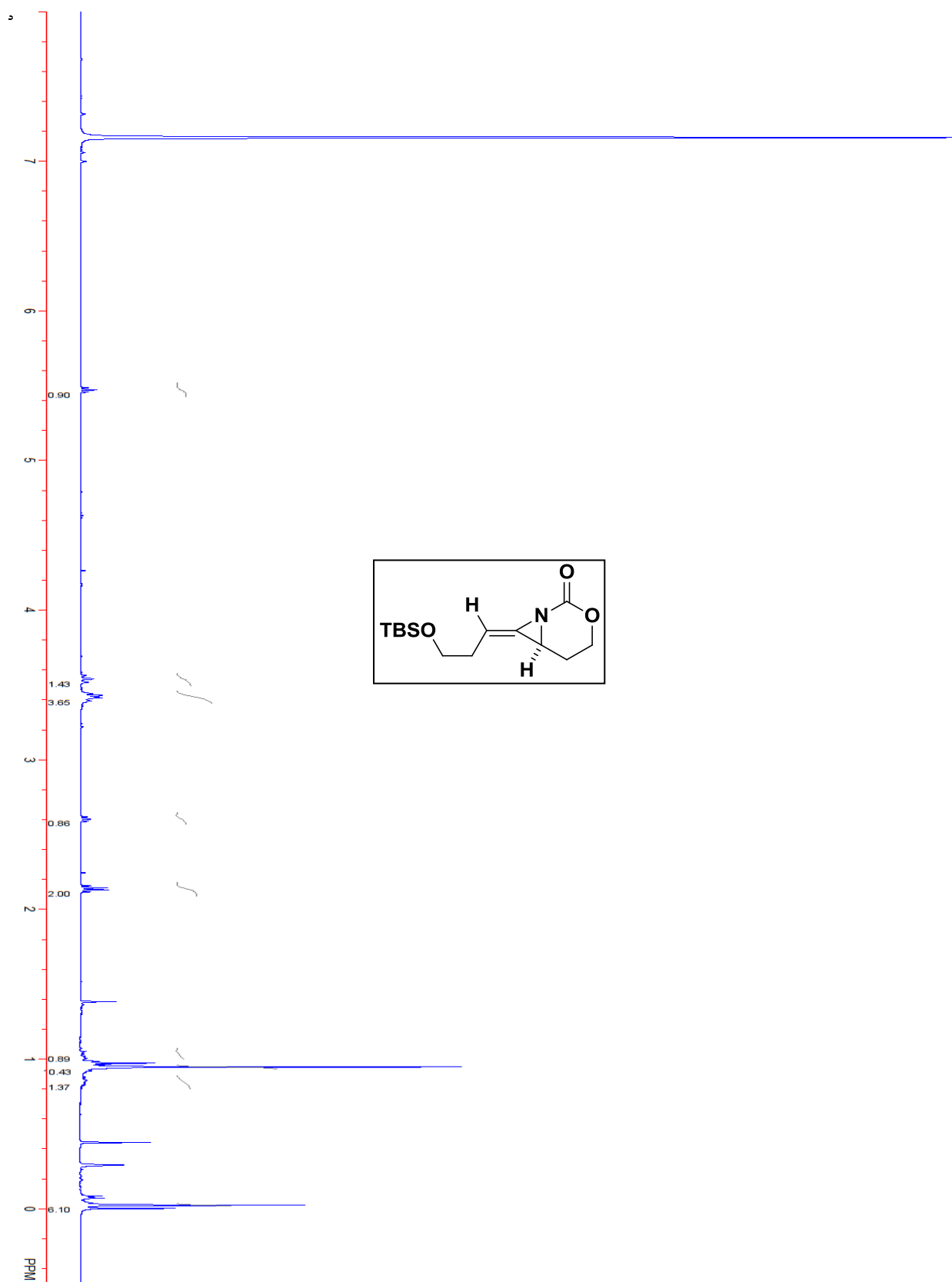
Compound 3.14aA.



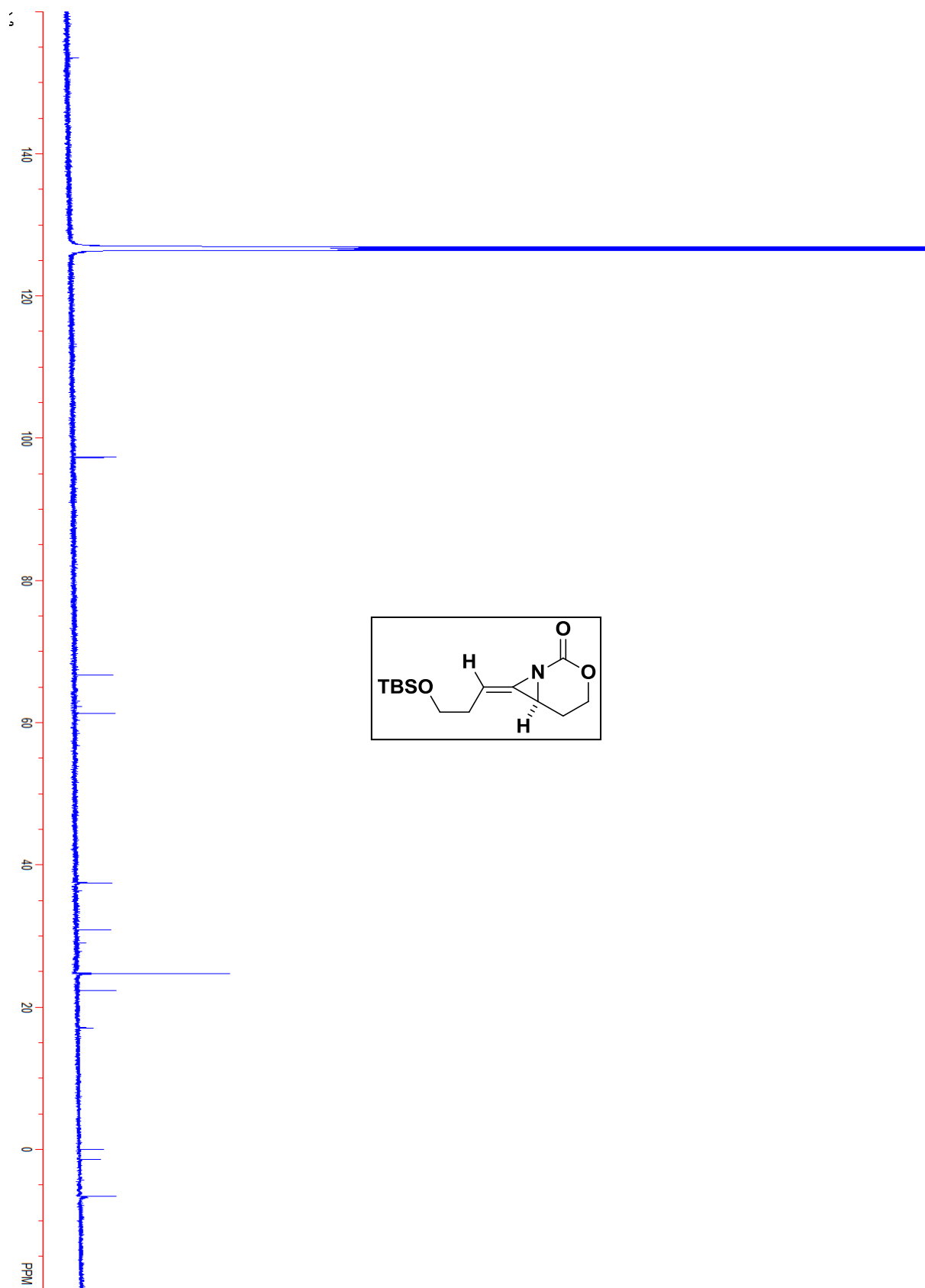
Compound 3.14aA.



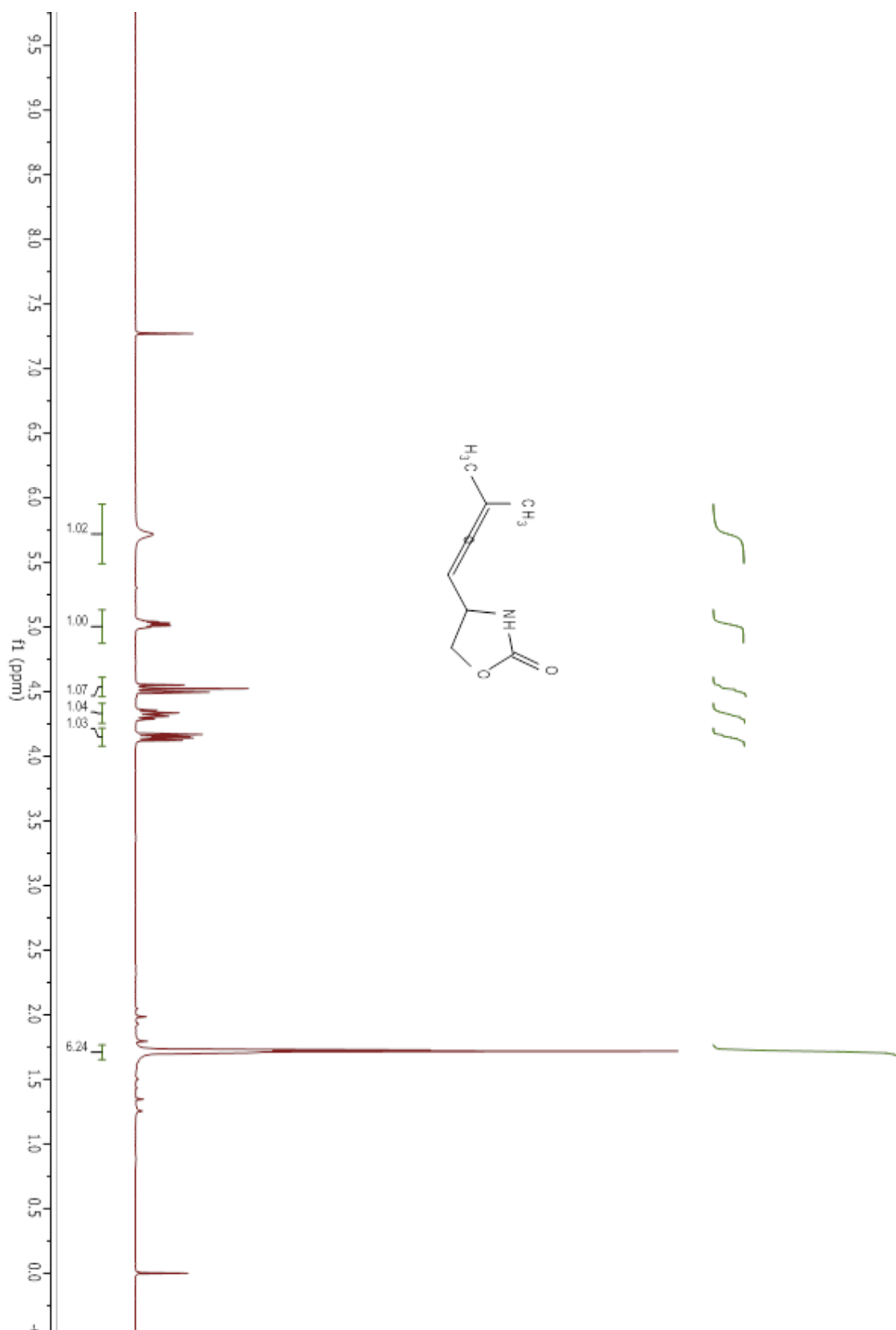
Compound 3.14bA.

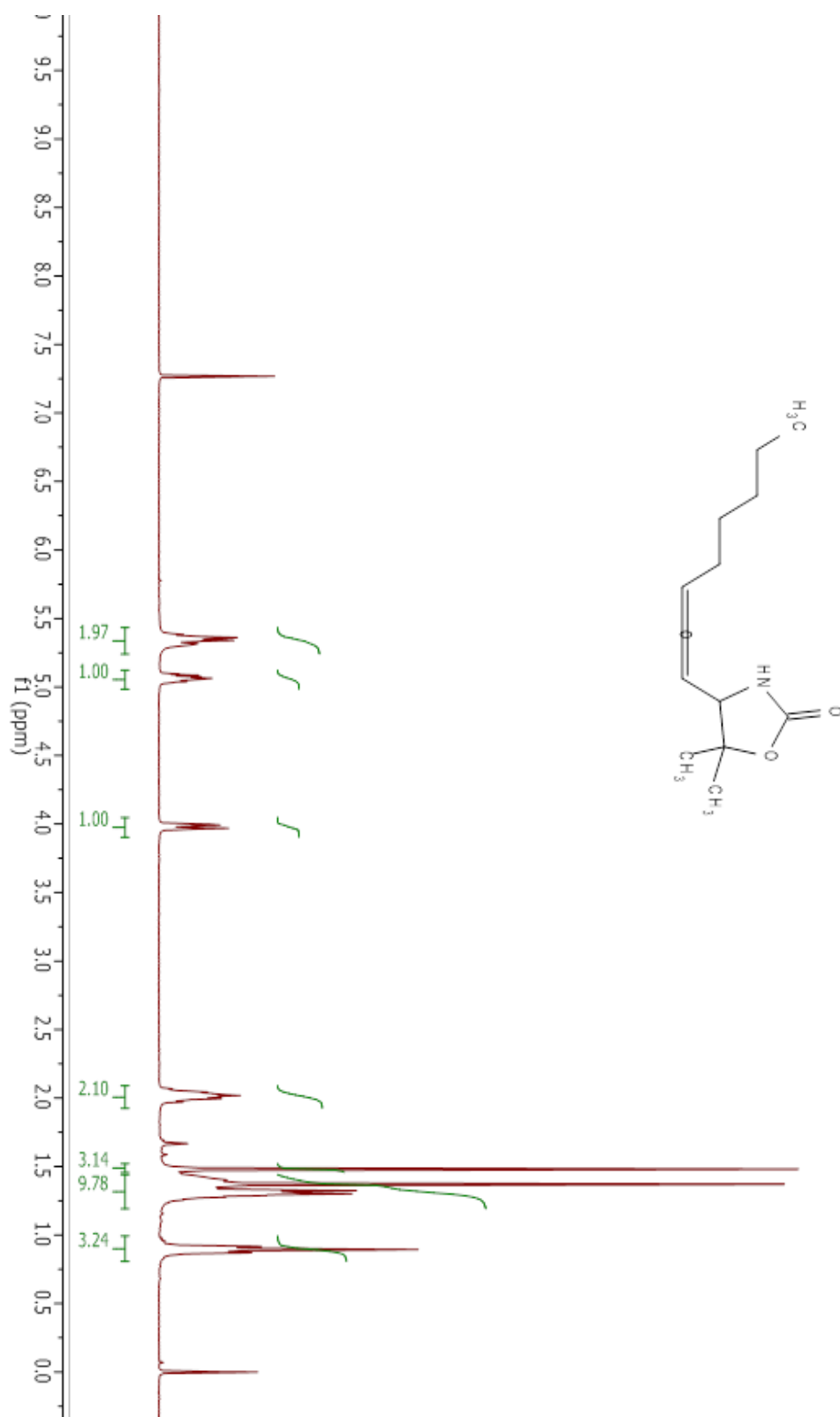


Compound 3.14bA.

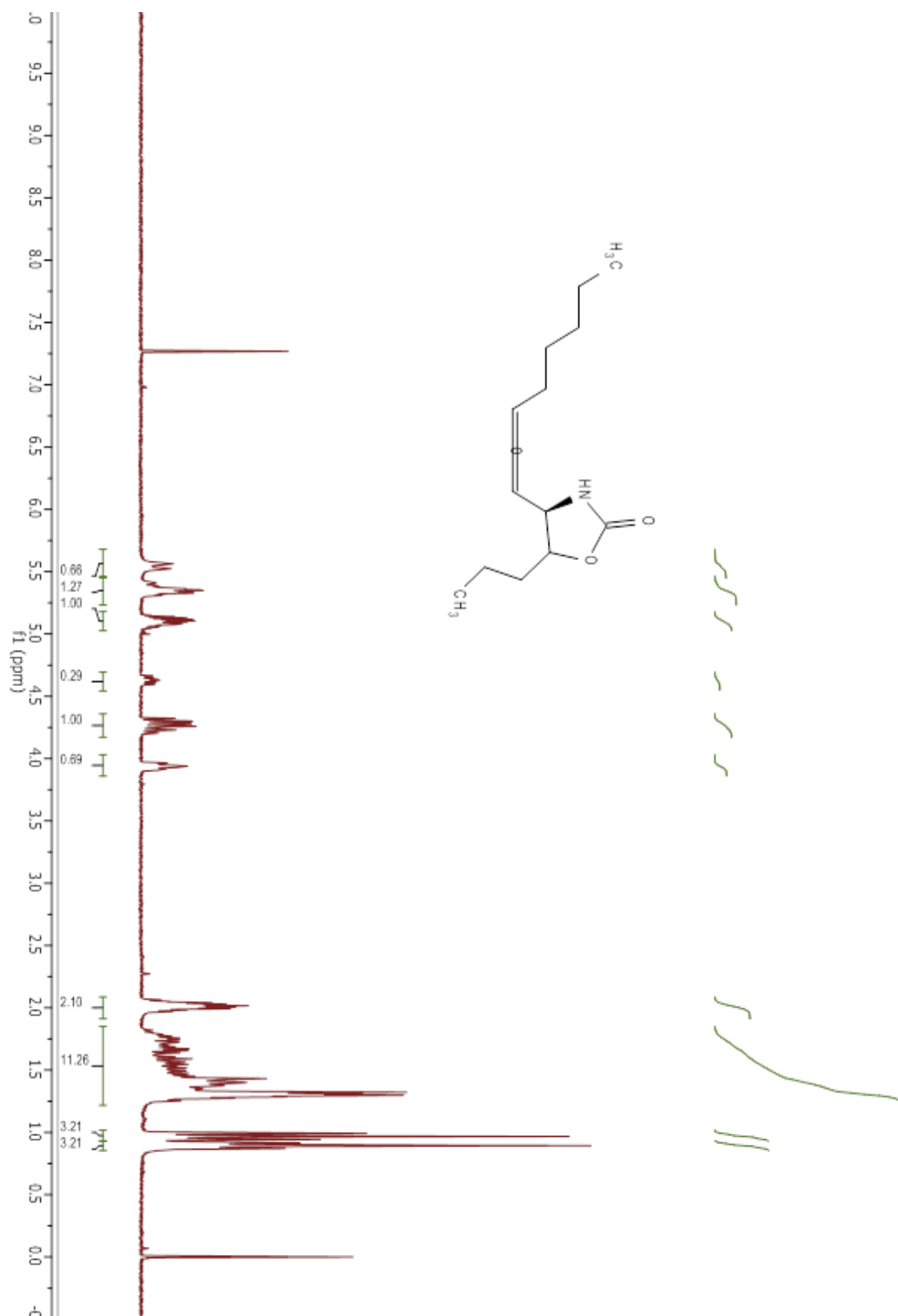


Compound 3.8a.

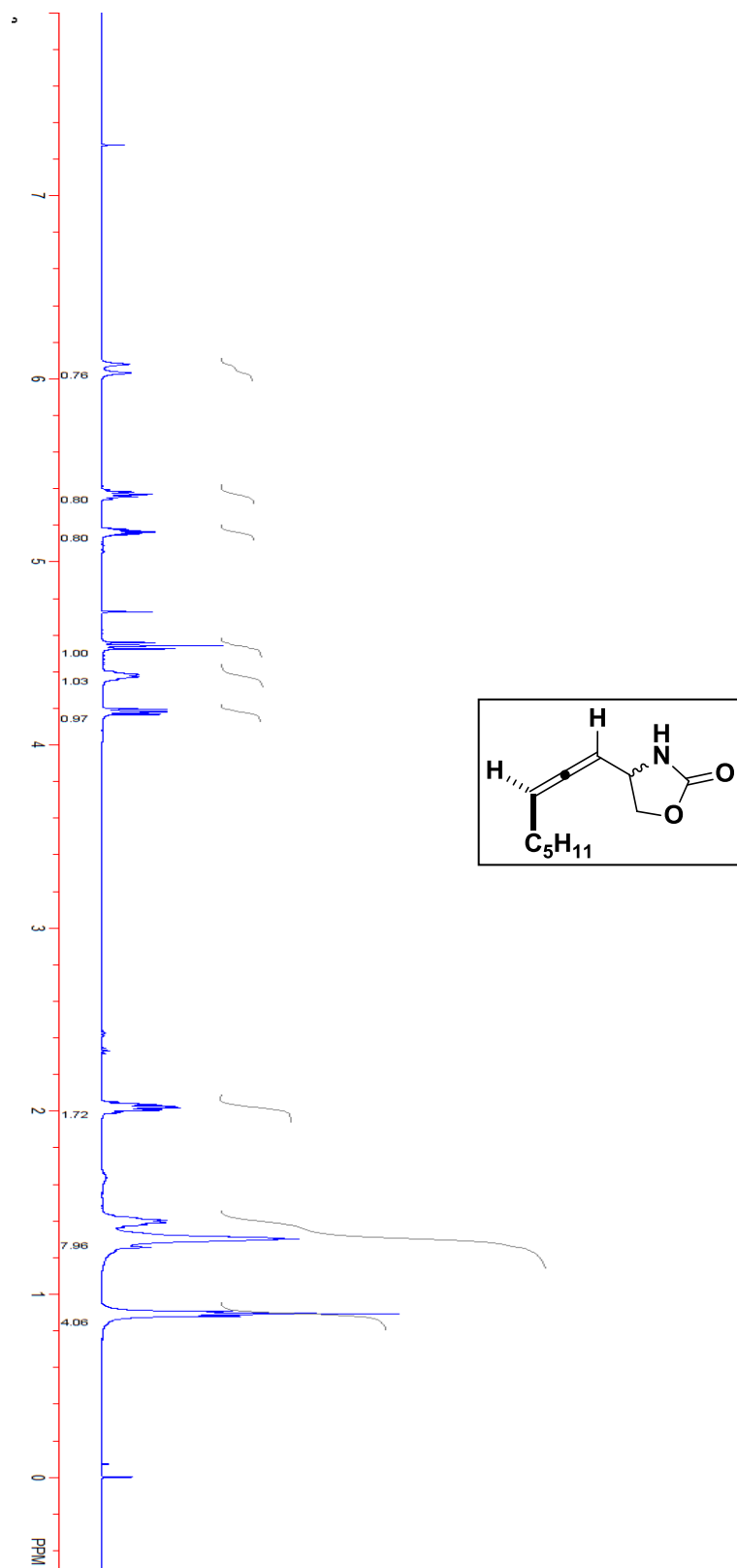


Compound 3.8b.

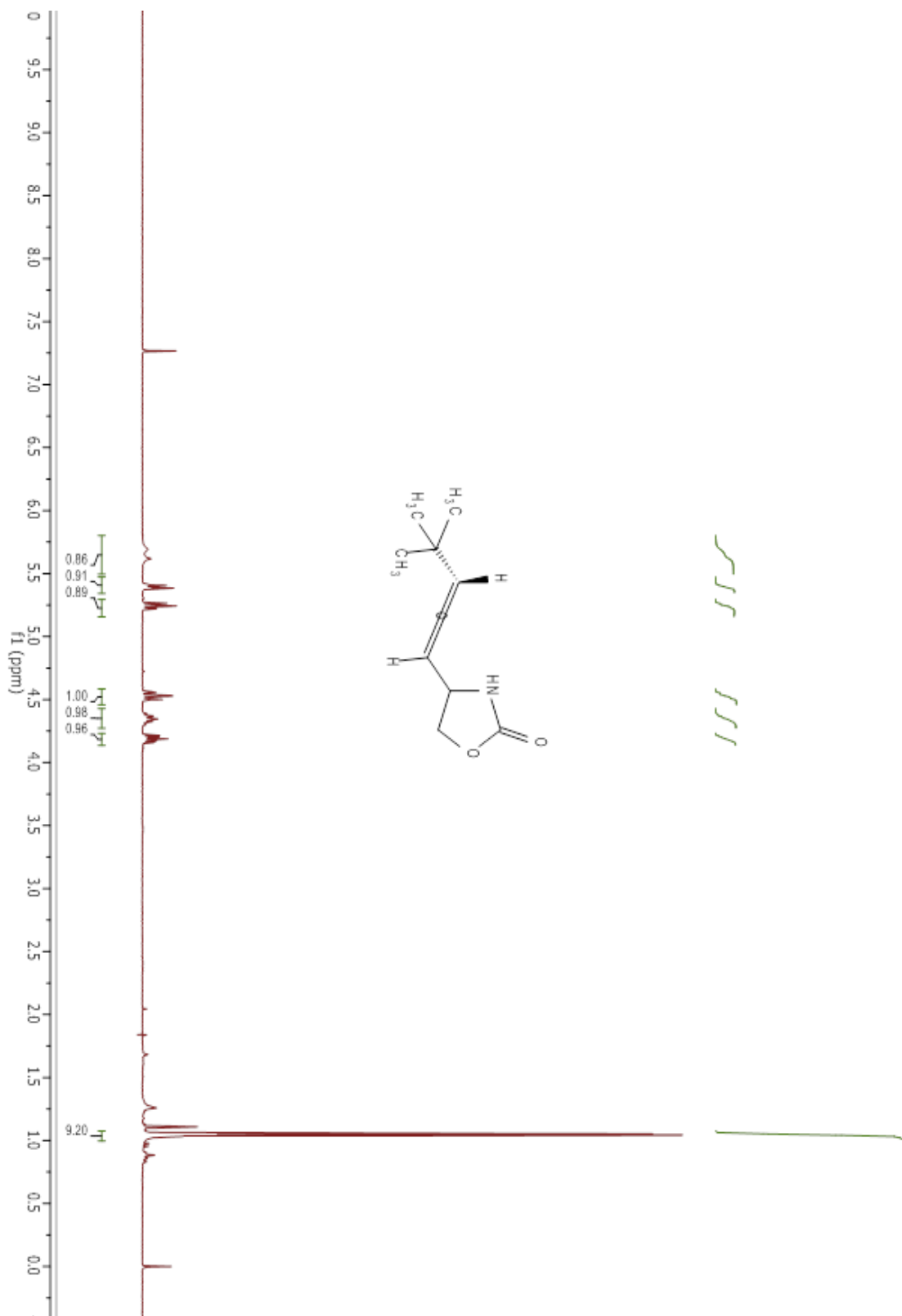
Compound 3.13b.



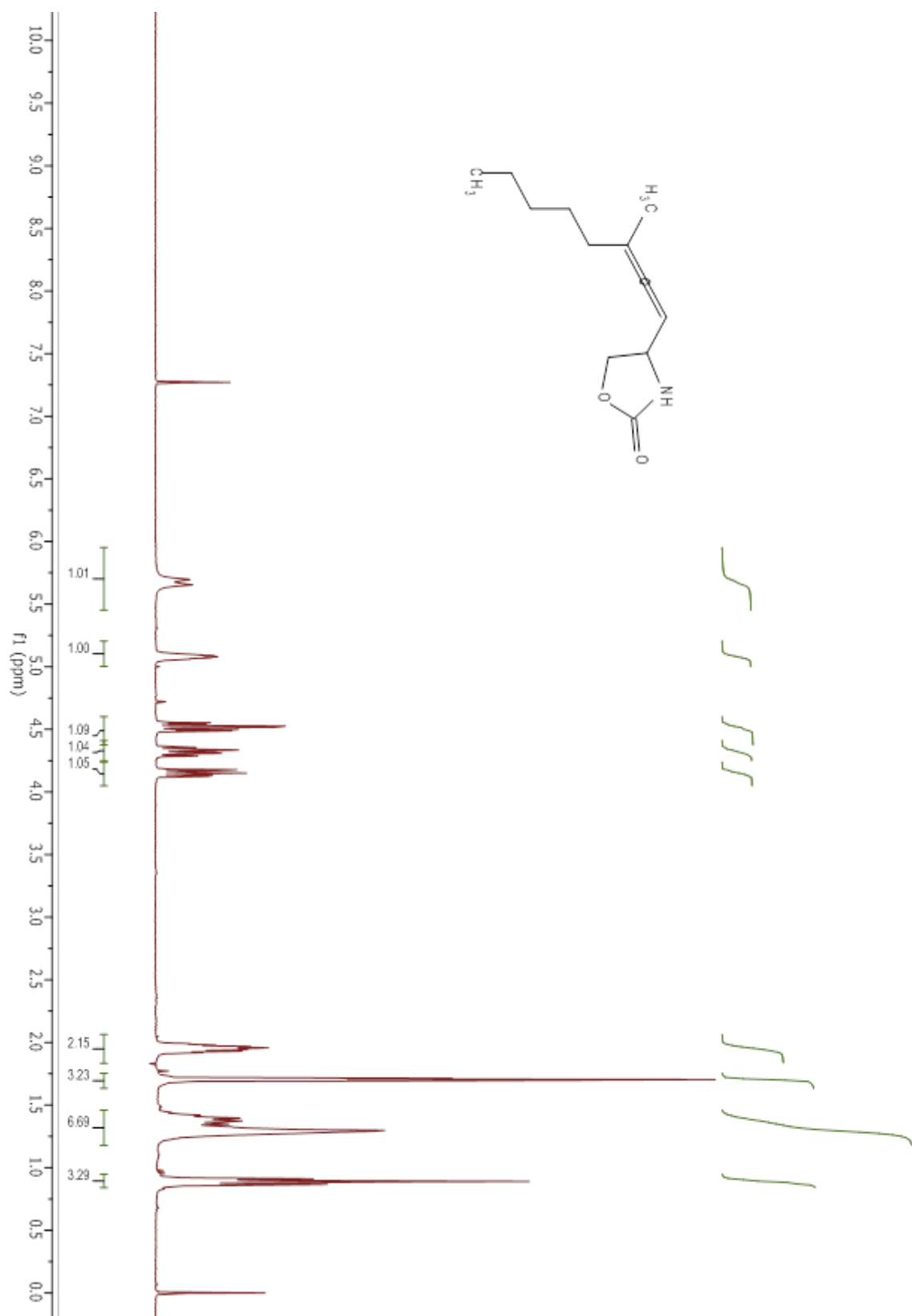
Compound 3.5.



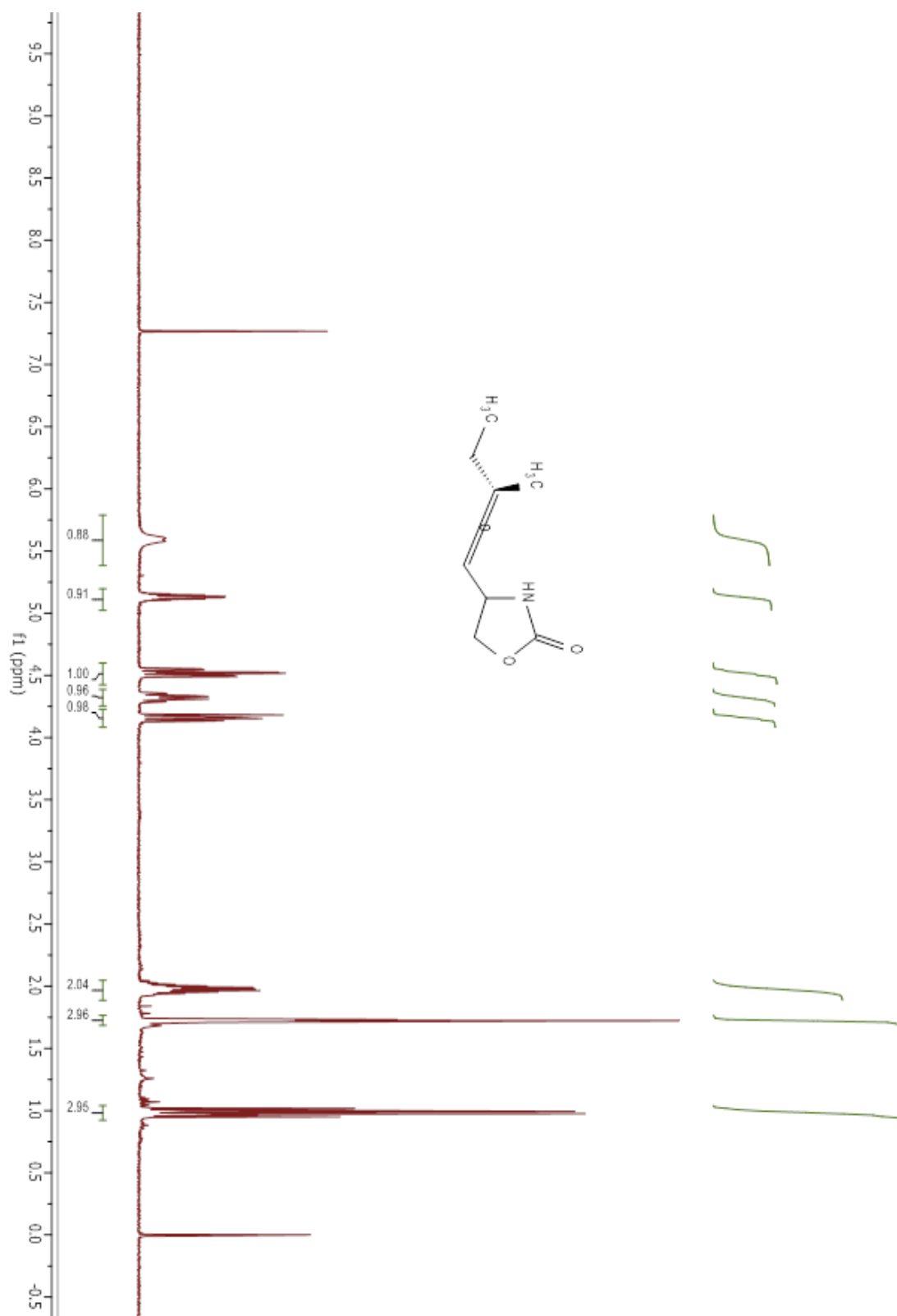
Compound 3.13a.



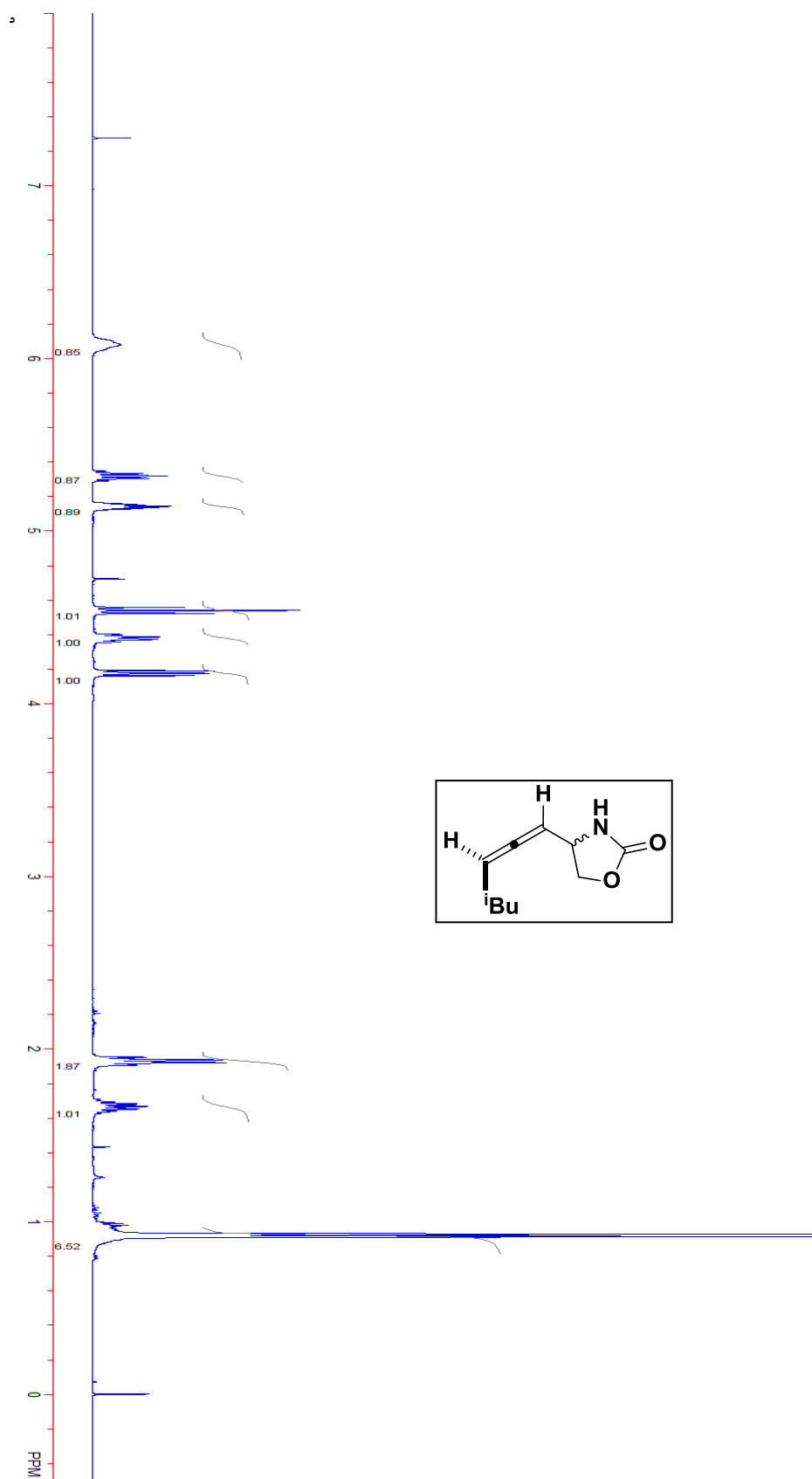
Compound 3.13c.

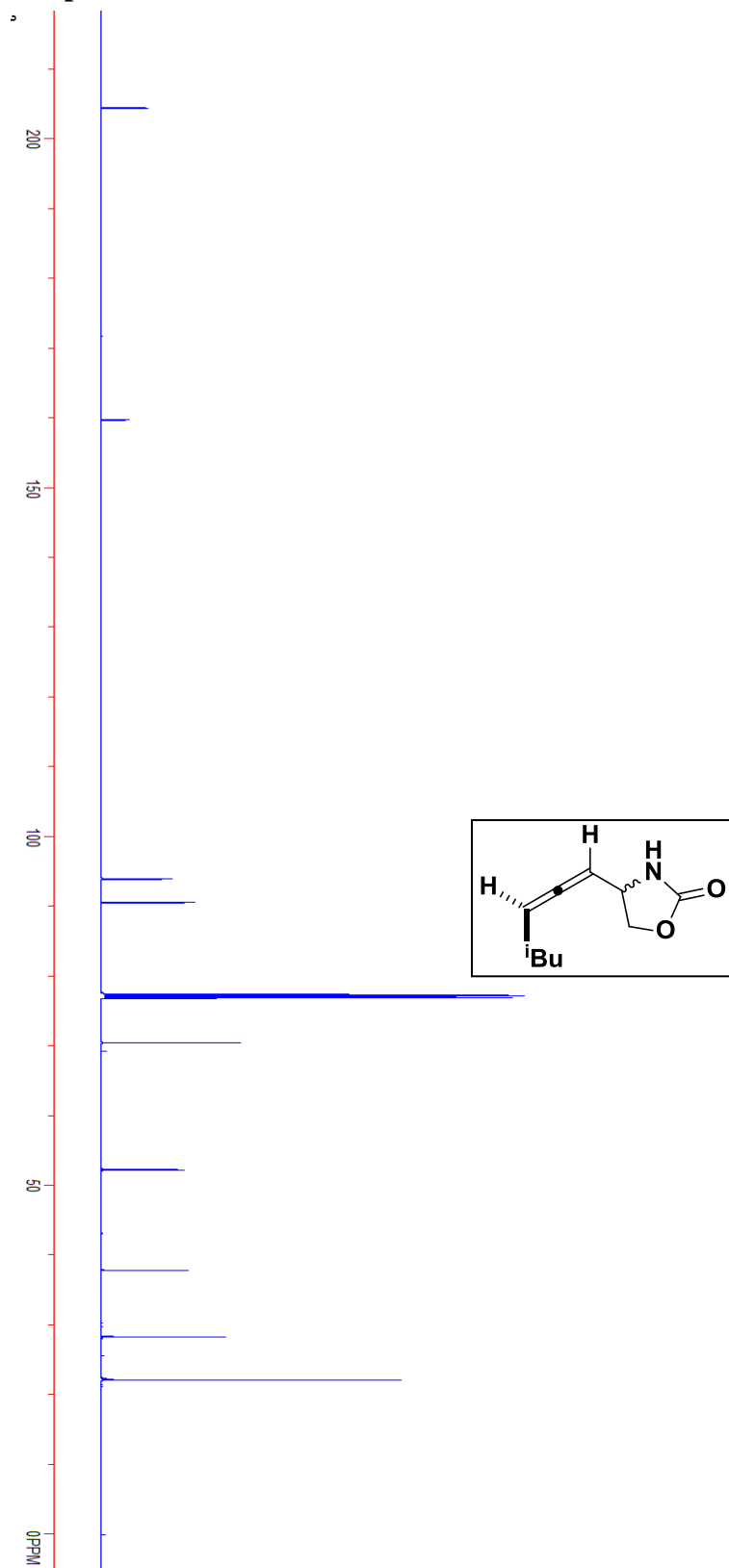


Compound 3.13d.

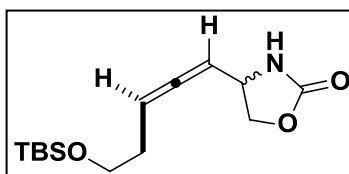
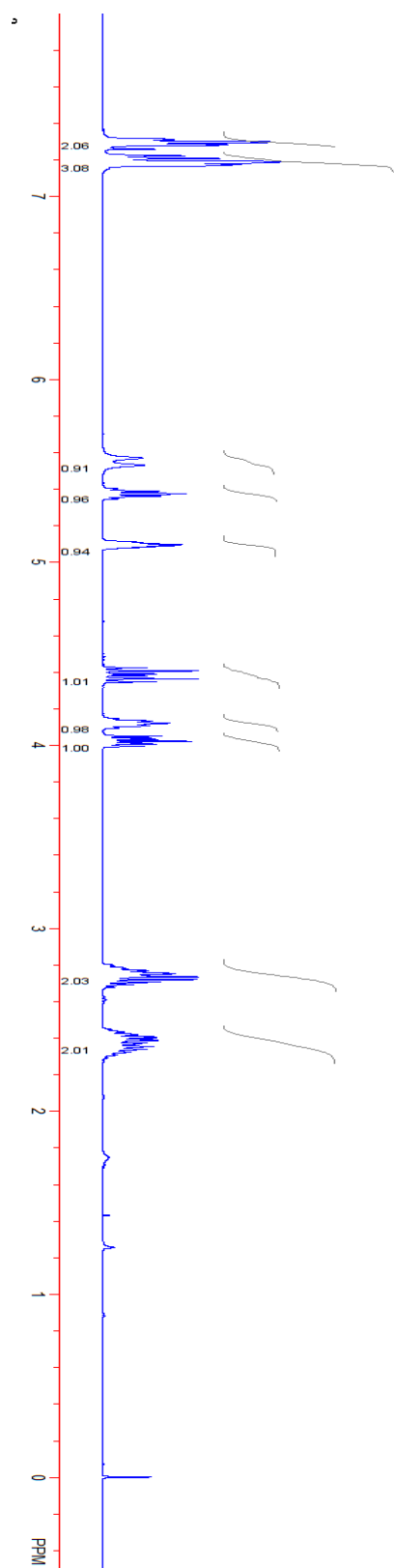


Compound 3.14aI.

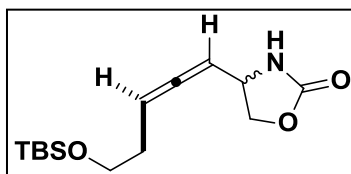
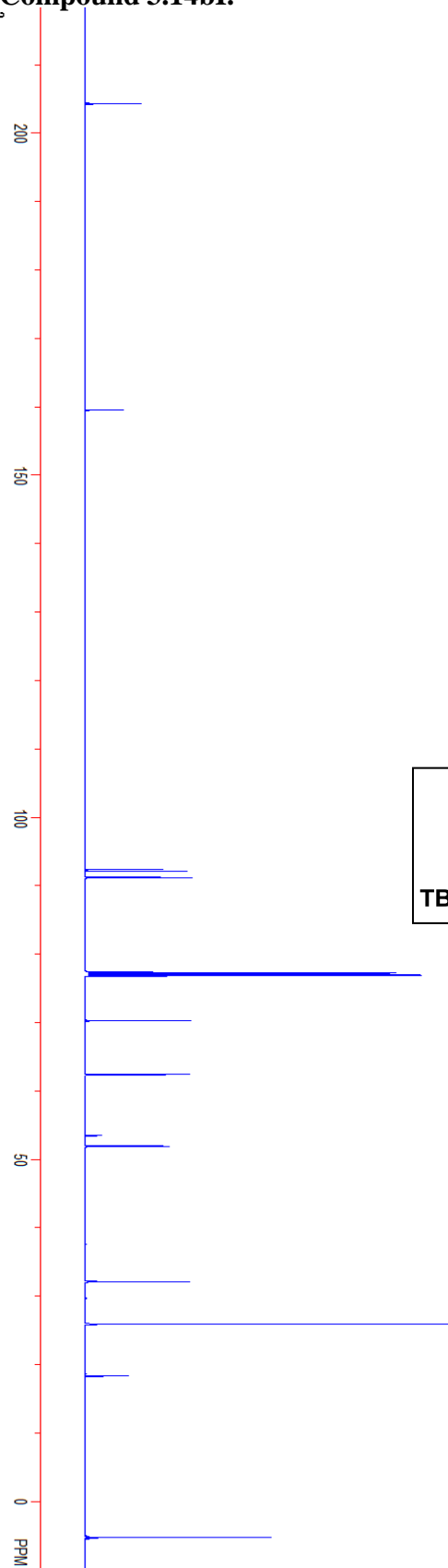


Compound 3.14aI.

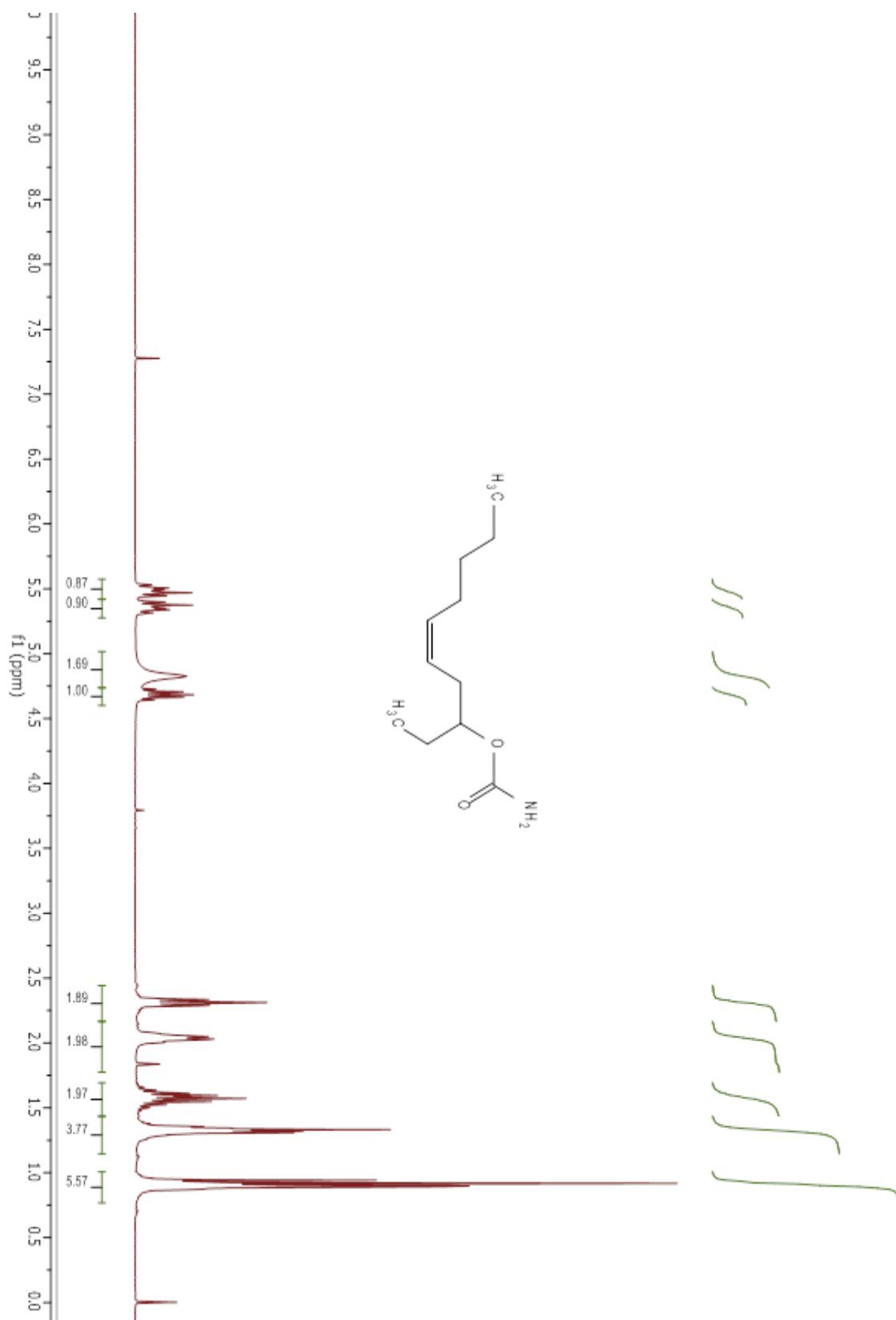
Compound 3.14bI.



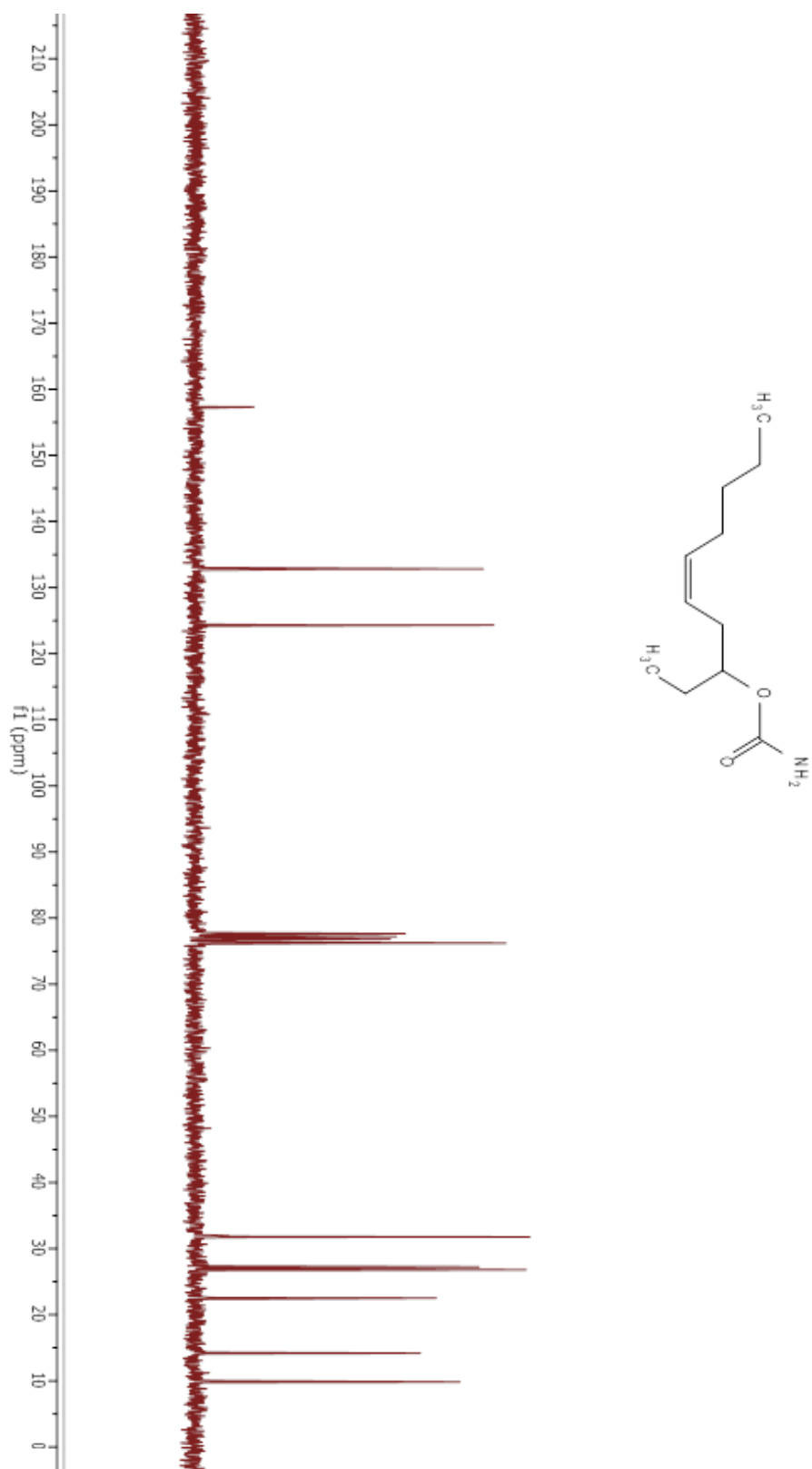
Compound 3.14bI.



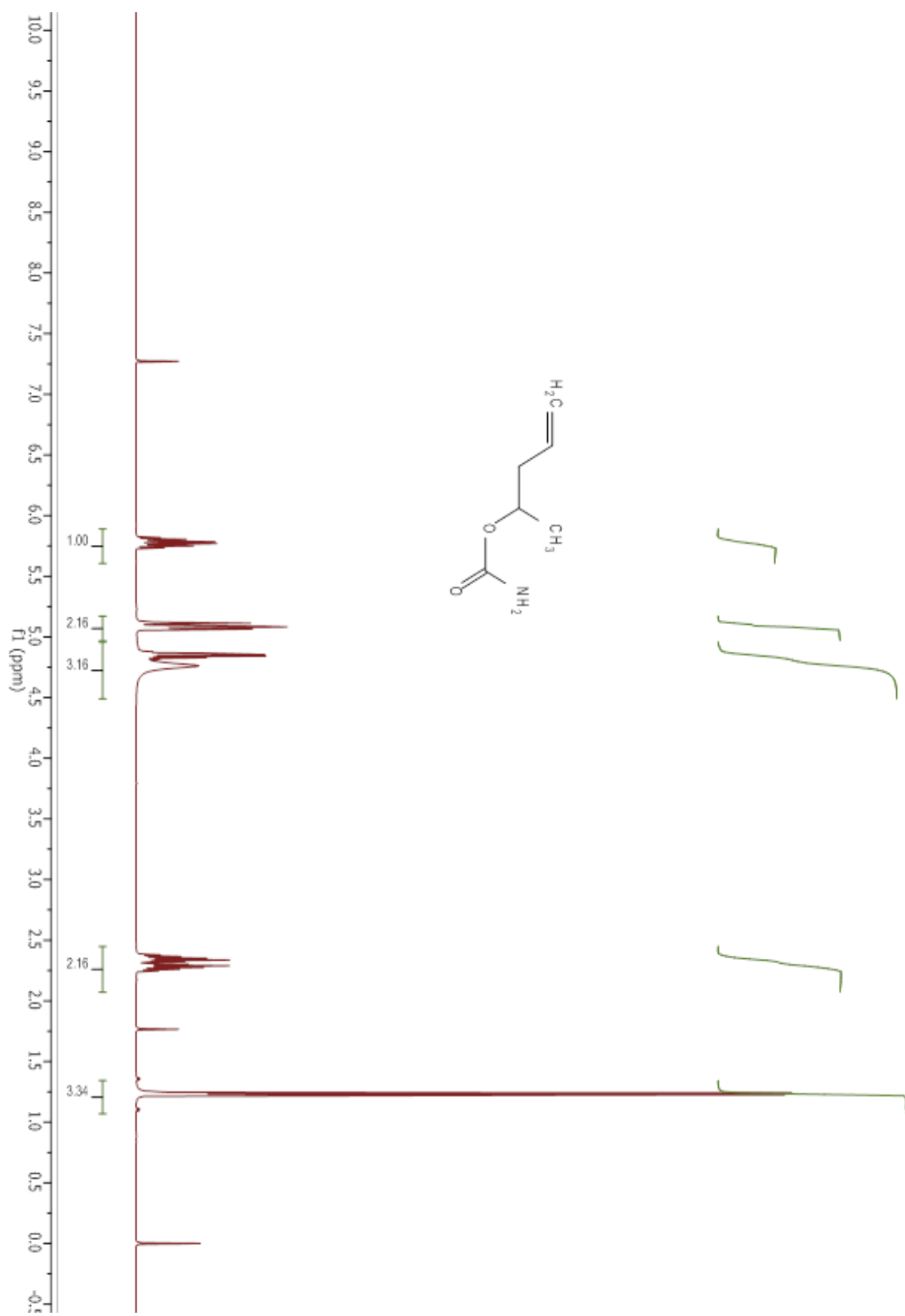
Compound 3.15b.



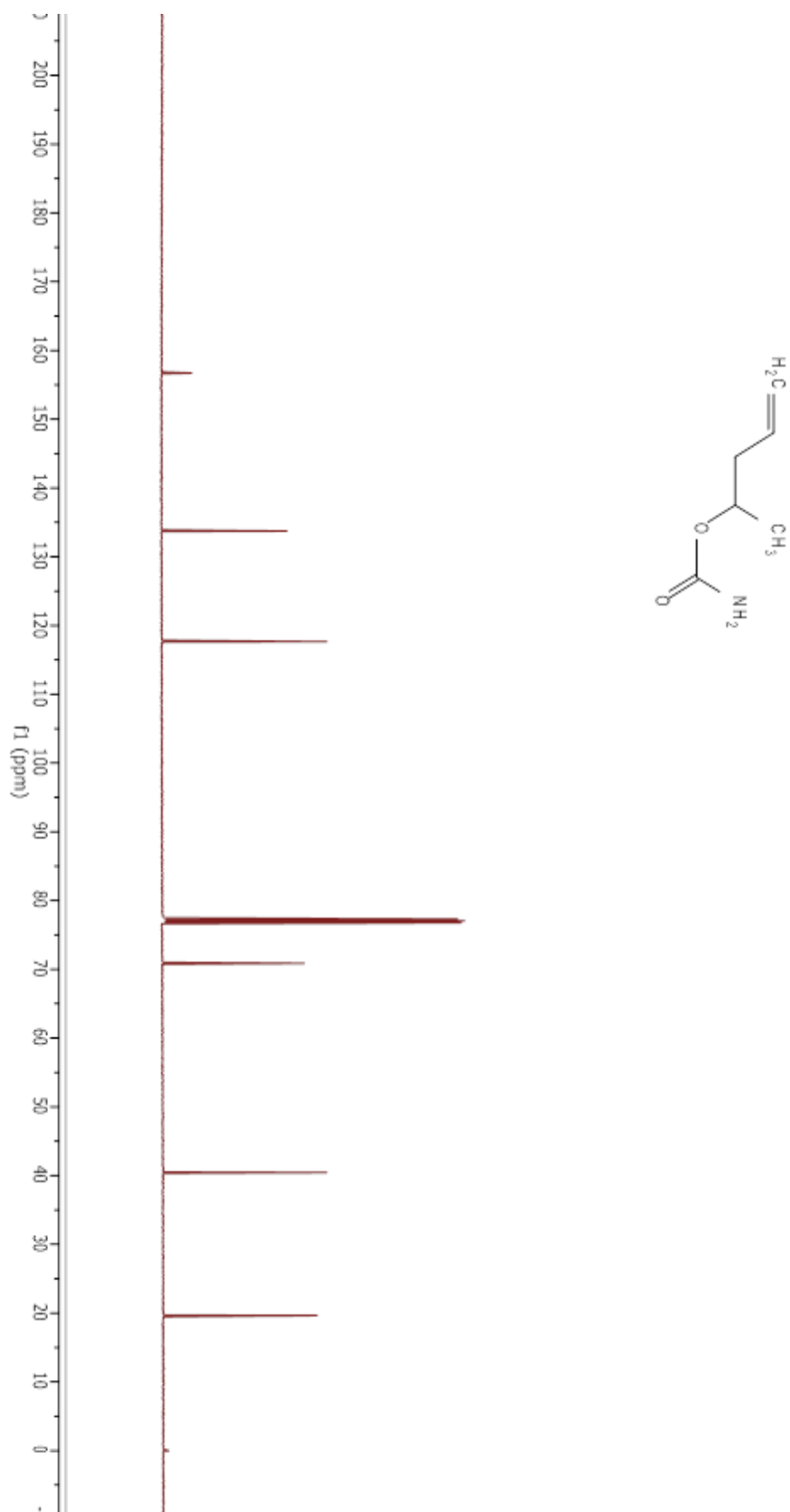
Compound 3.15b.



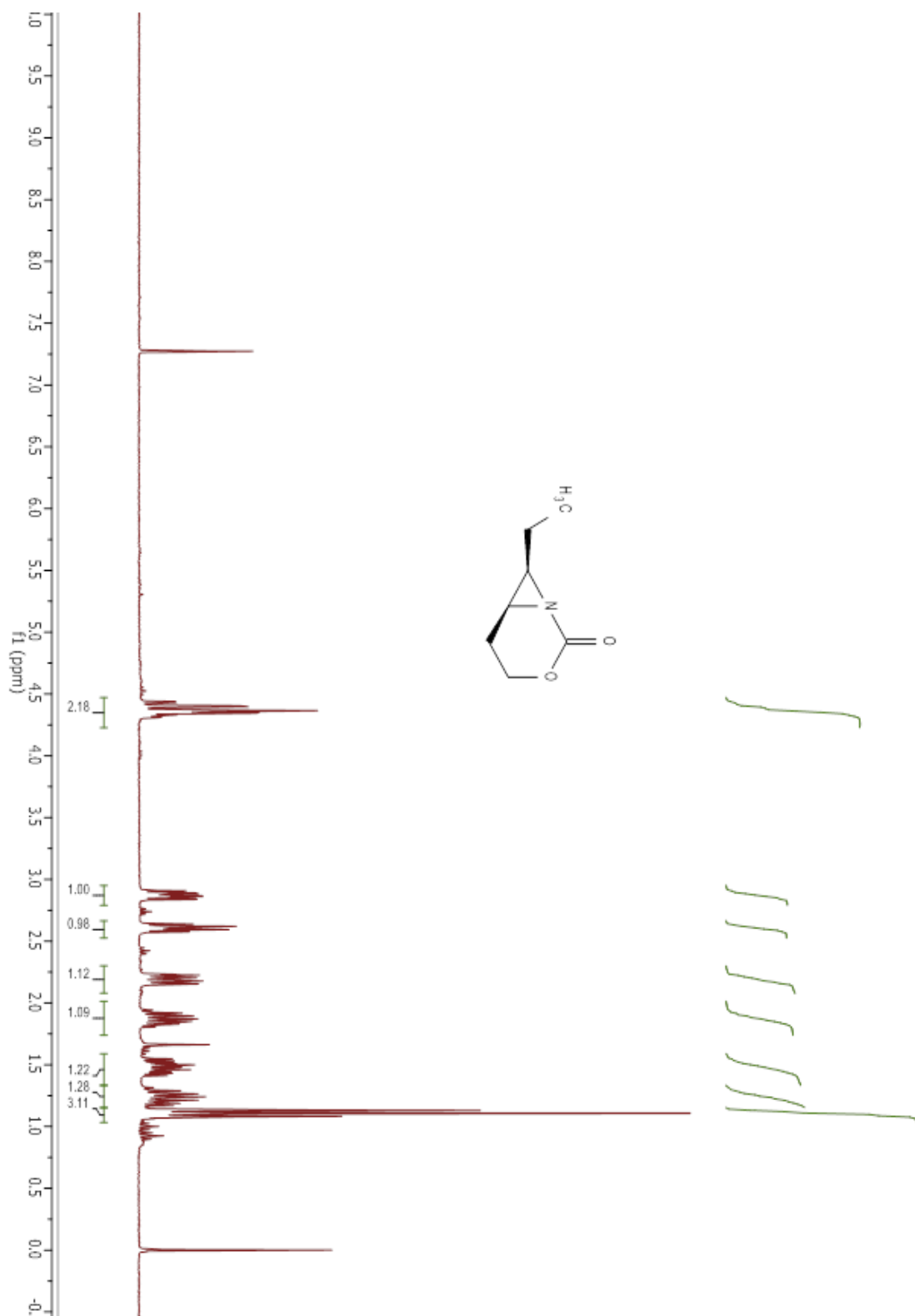
Compound 3.15e.



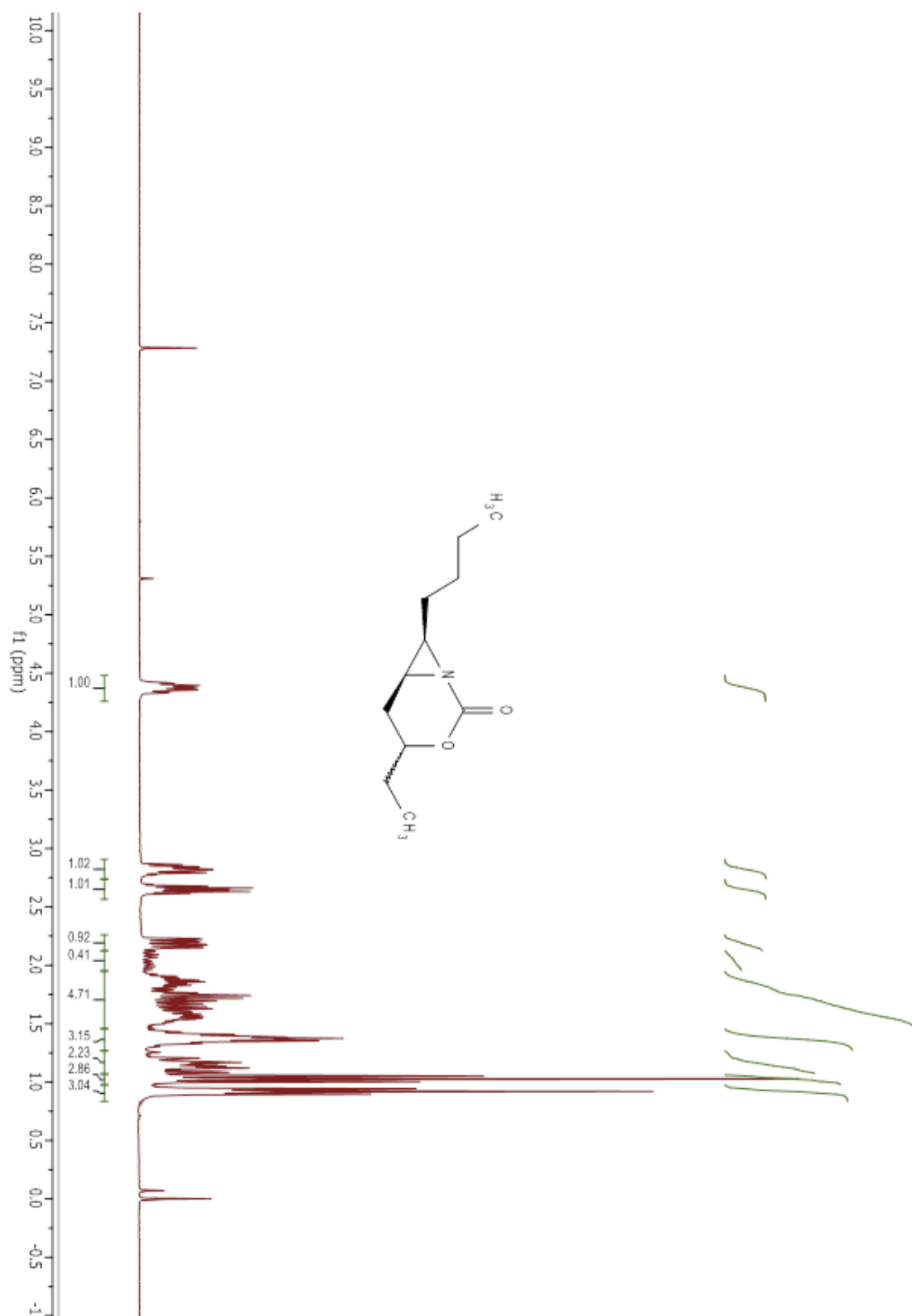
Compound 3.15e.



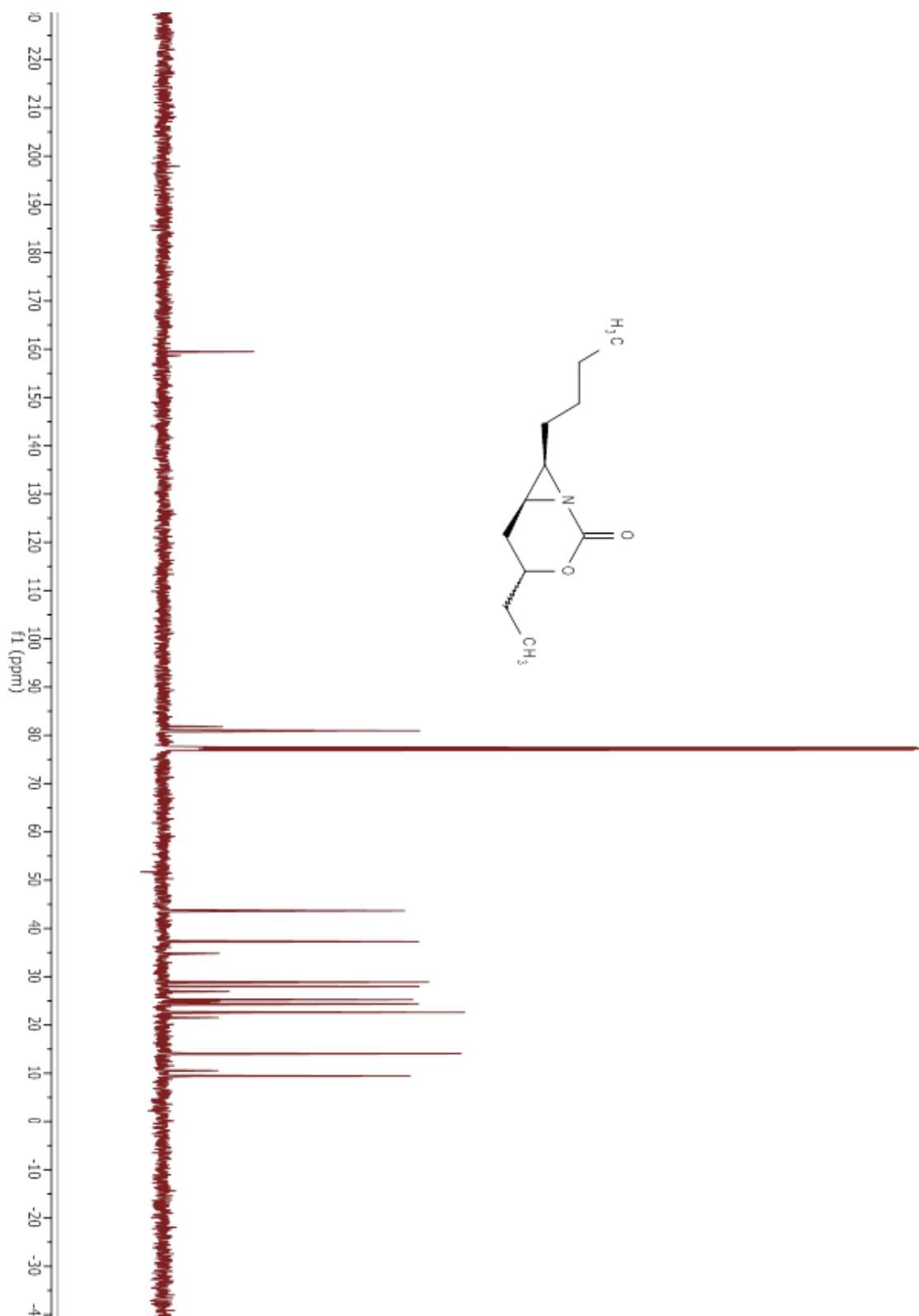
Compound 3.16a.



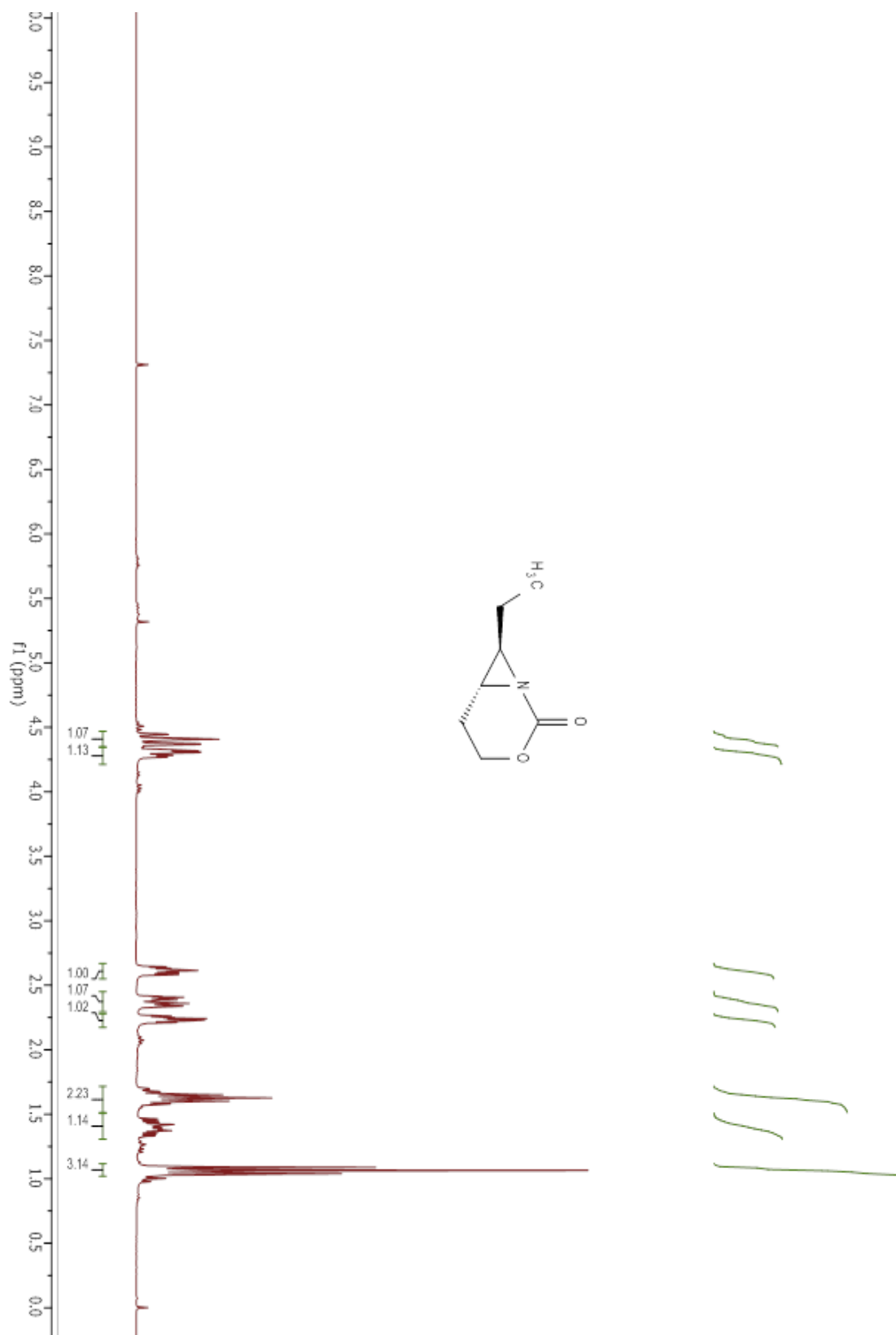
Compound 3.16b.



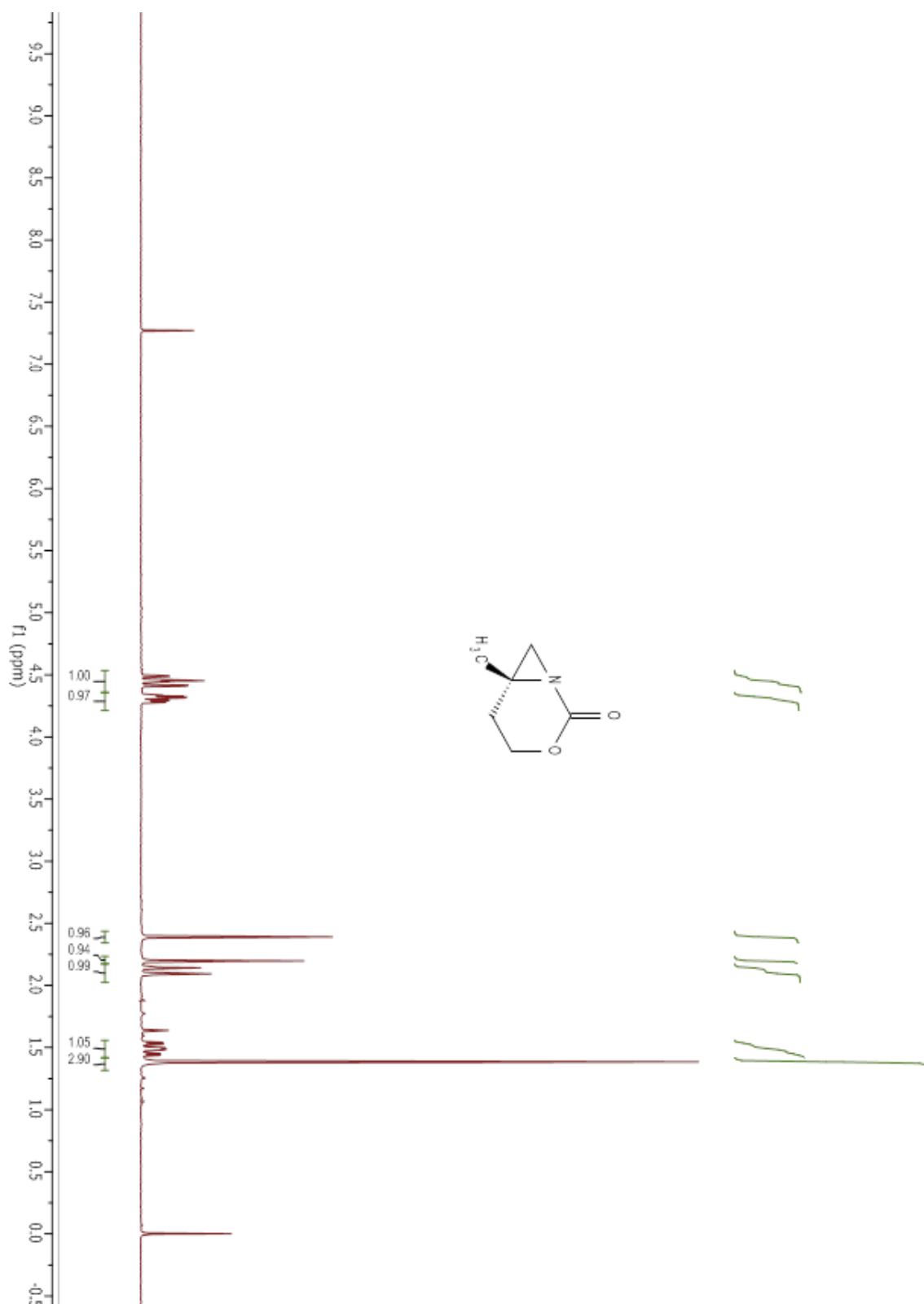
Compound 3.16b.



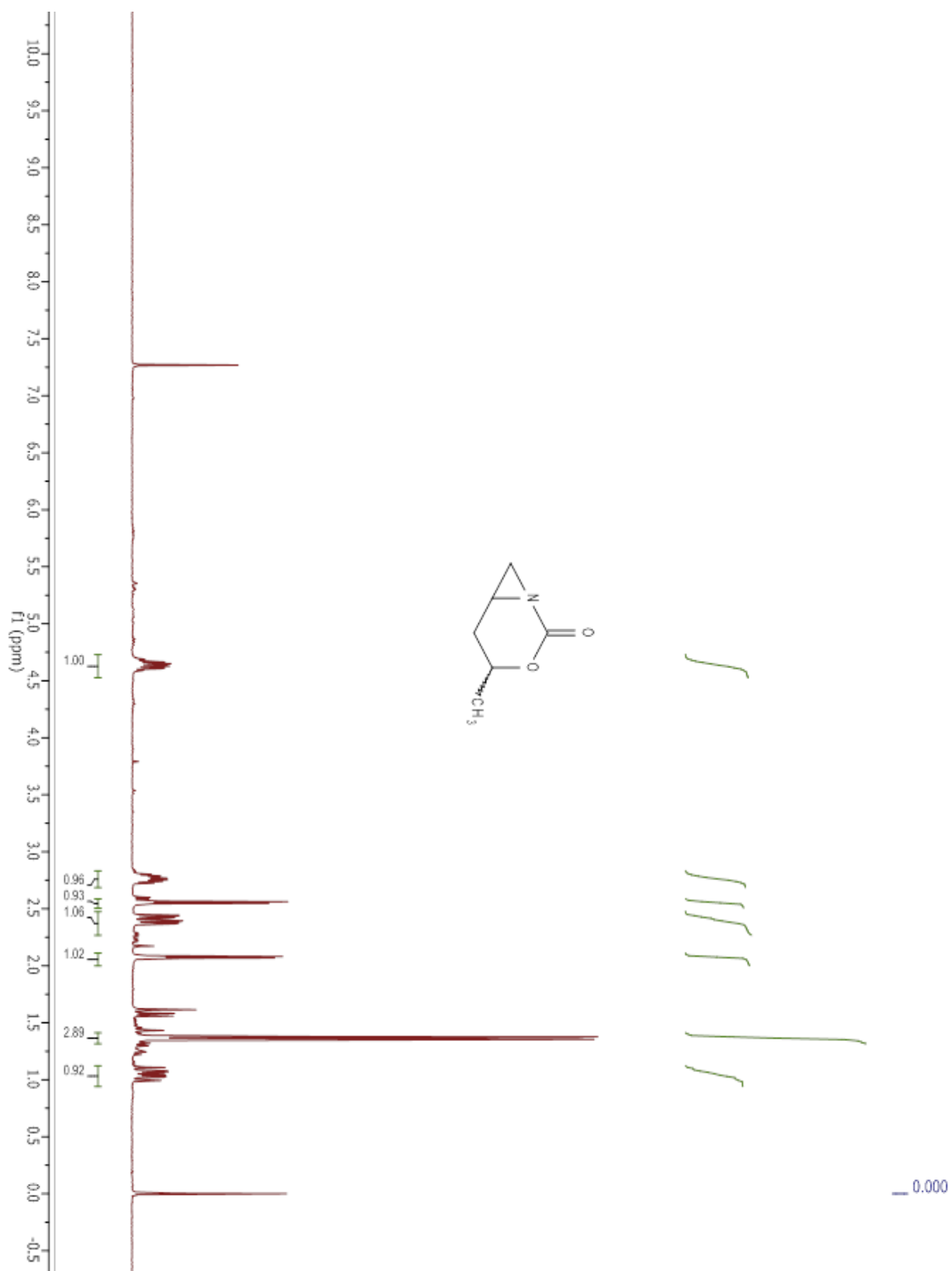
Compound 3.16c.



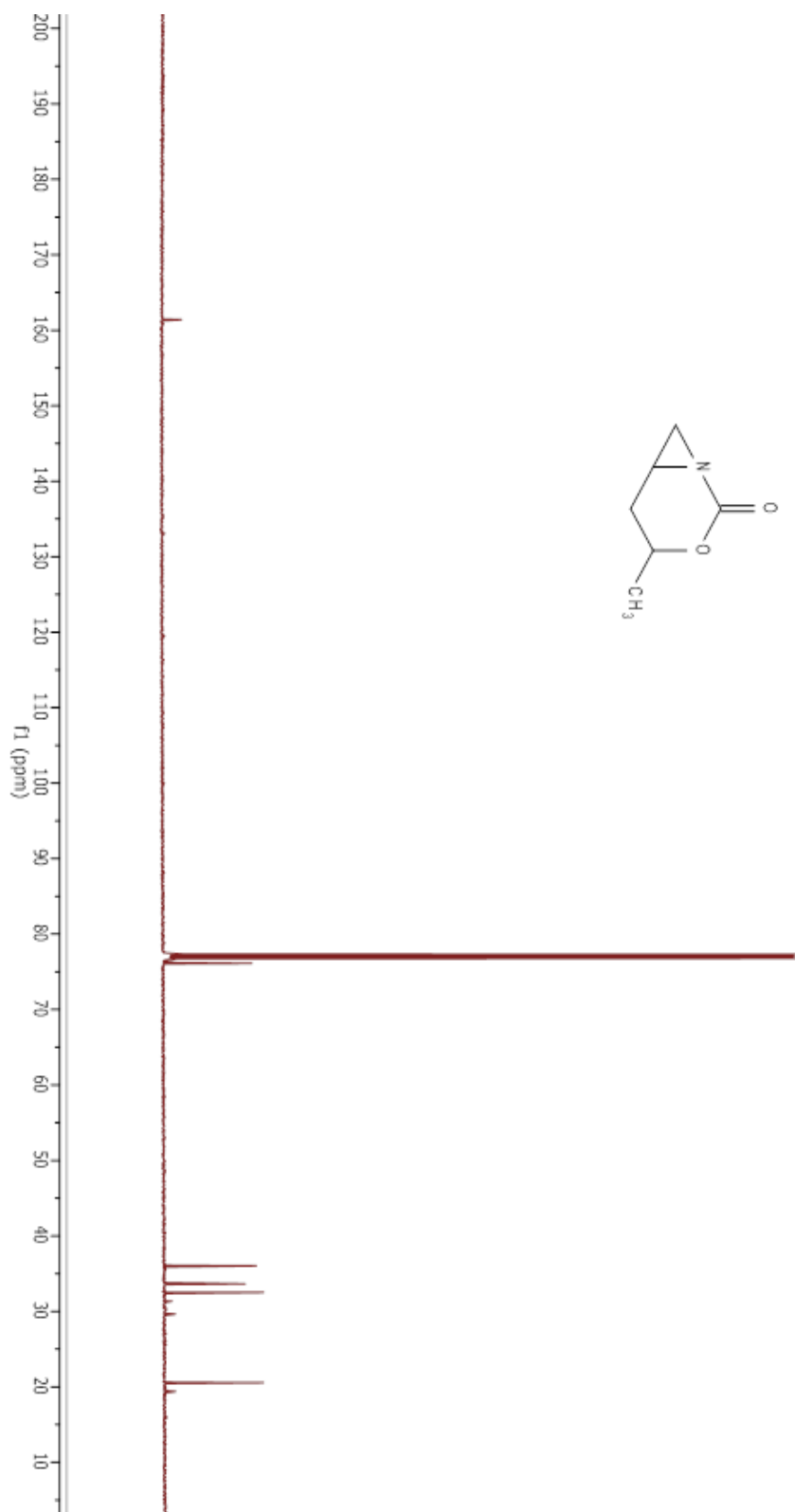
Compound 3.16d.



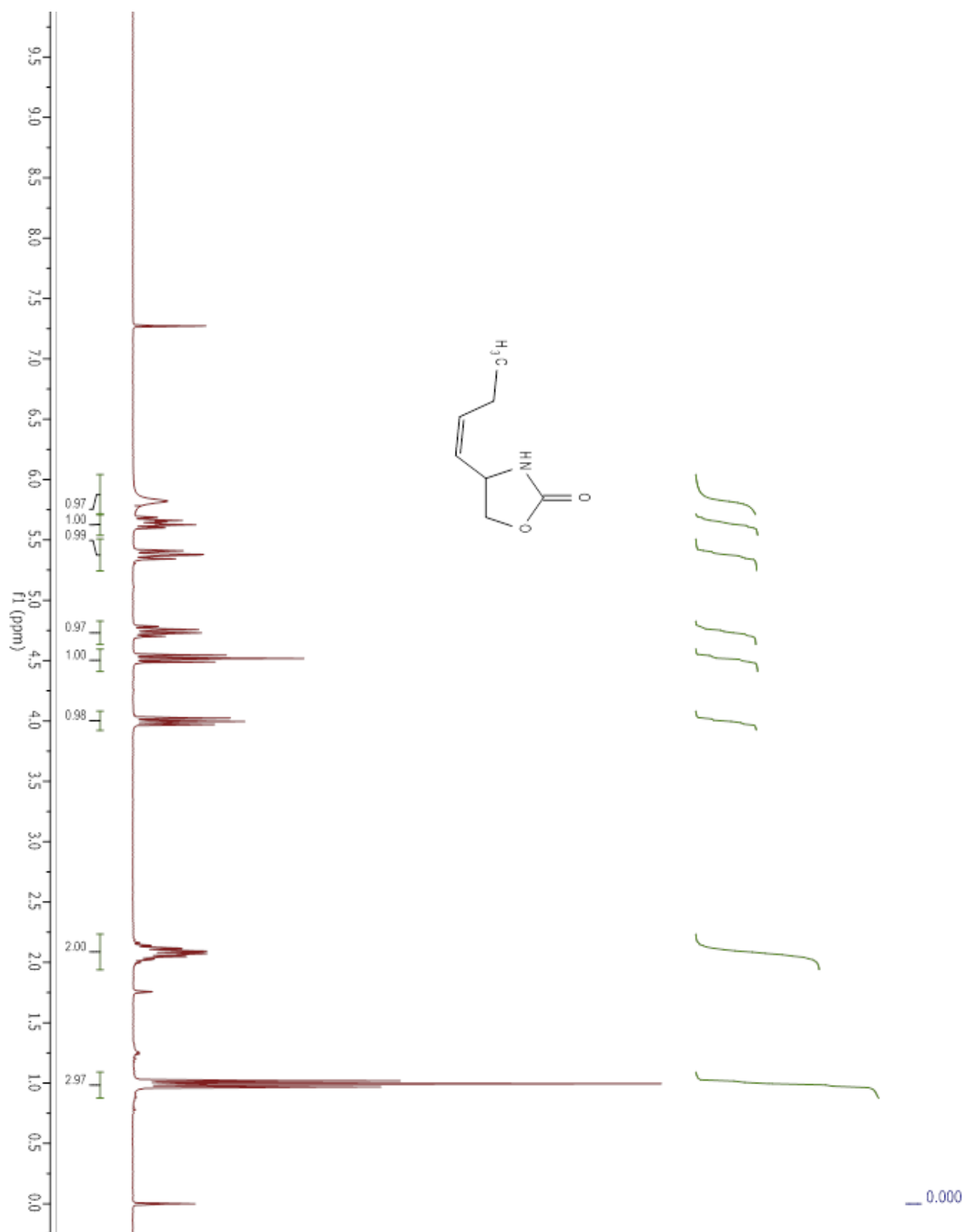
Compound 3.16e.



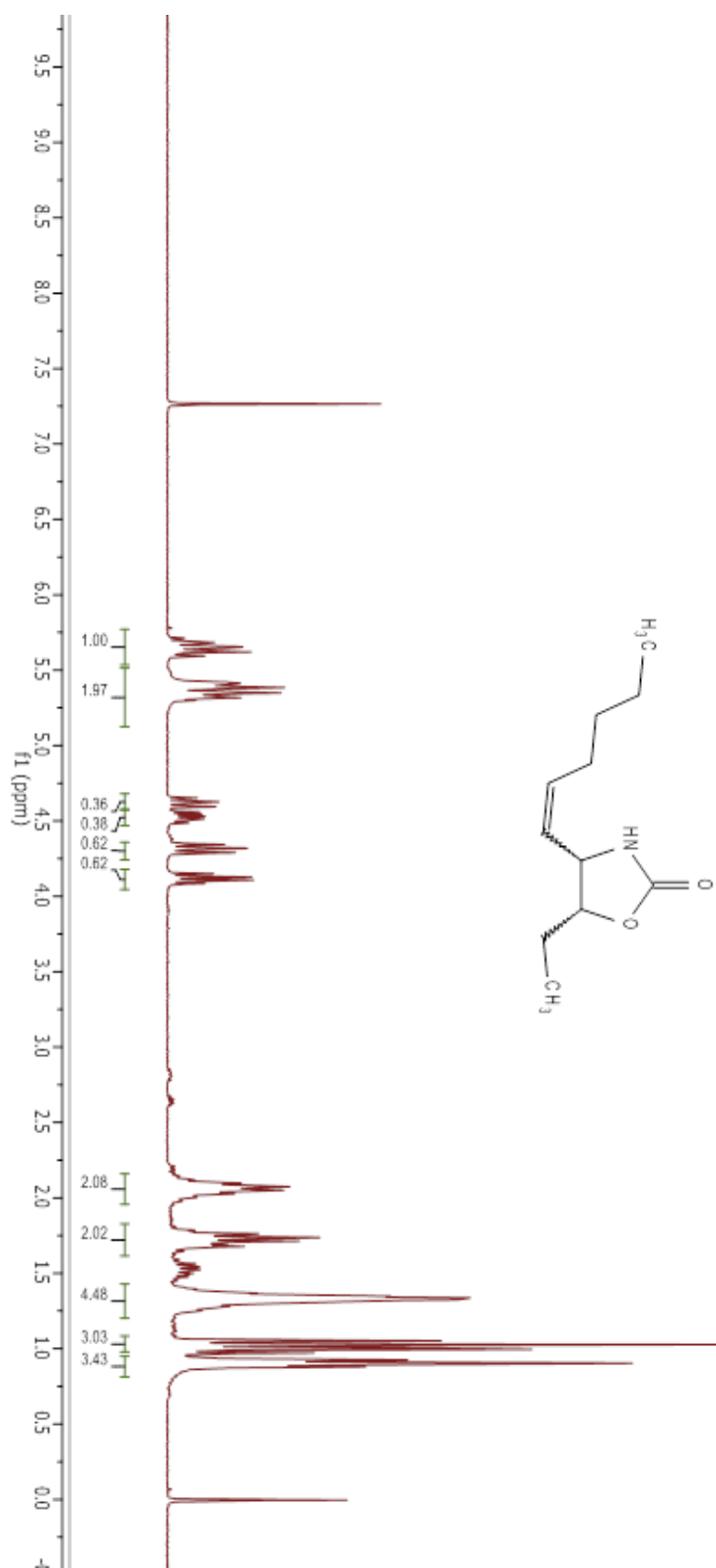
Compound 3.16e.



Compound 3.17a.

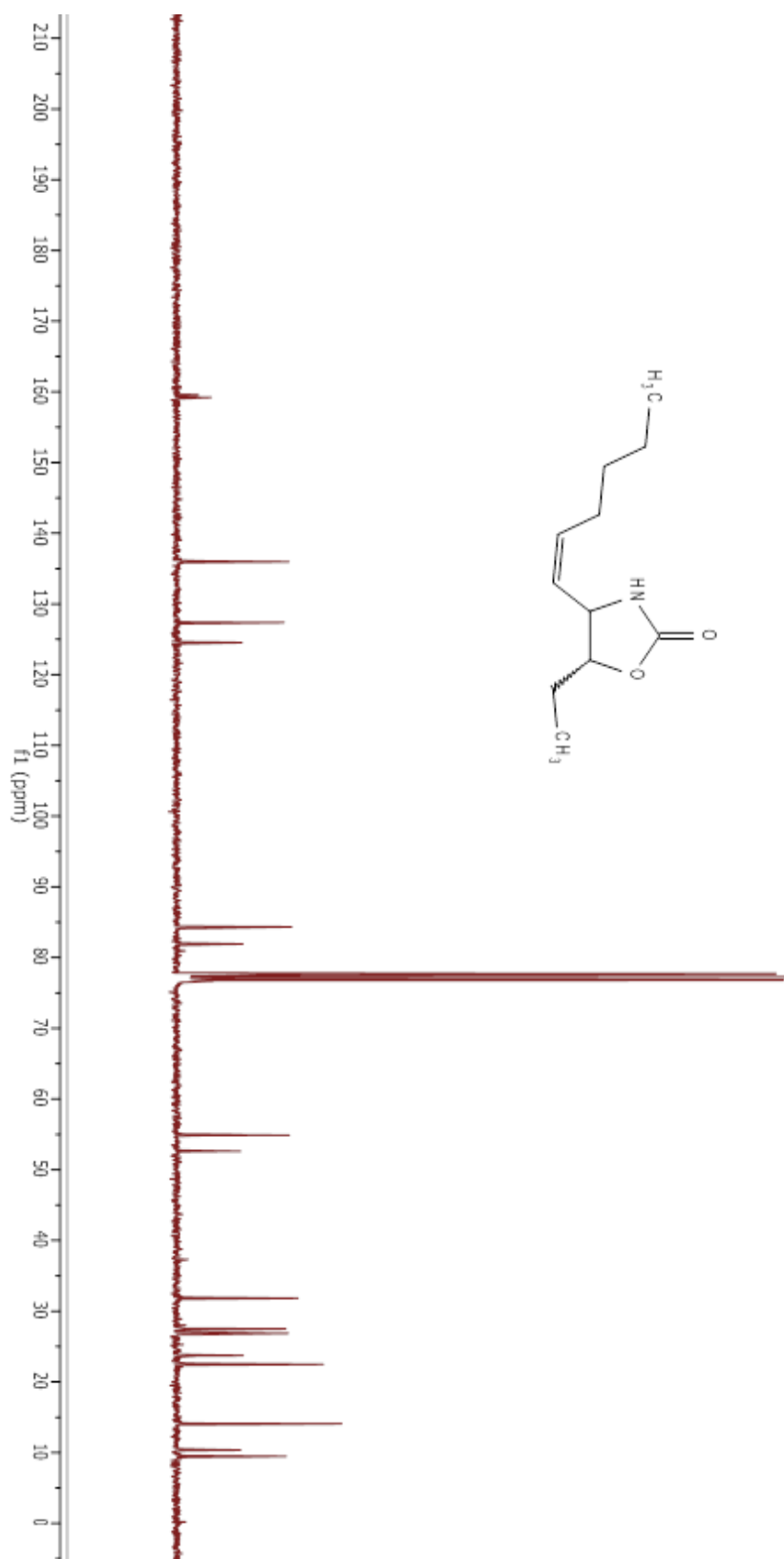


Compound 3.17b.

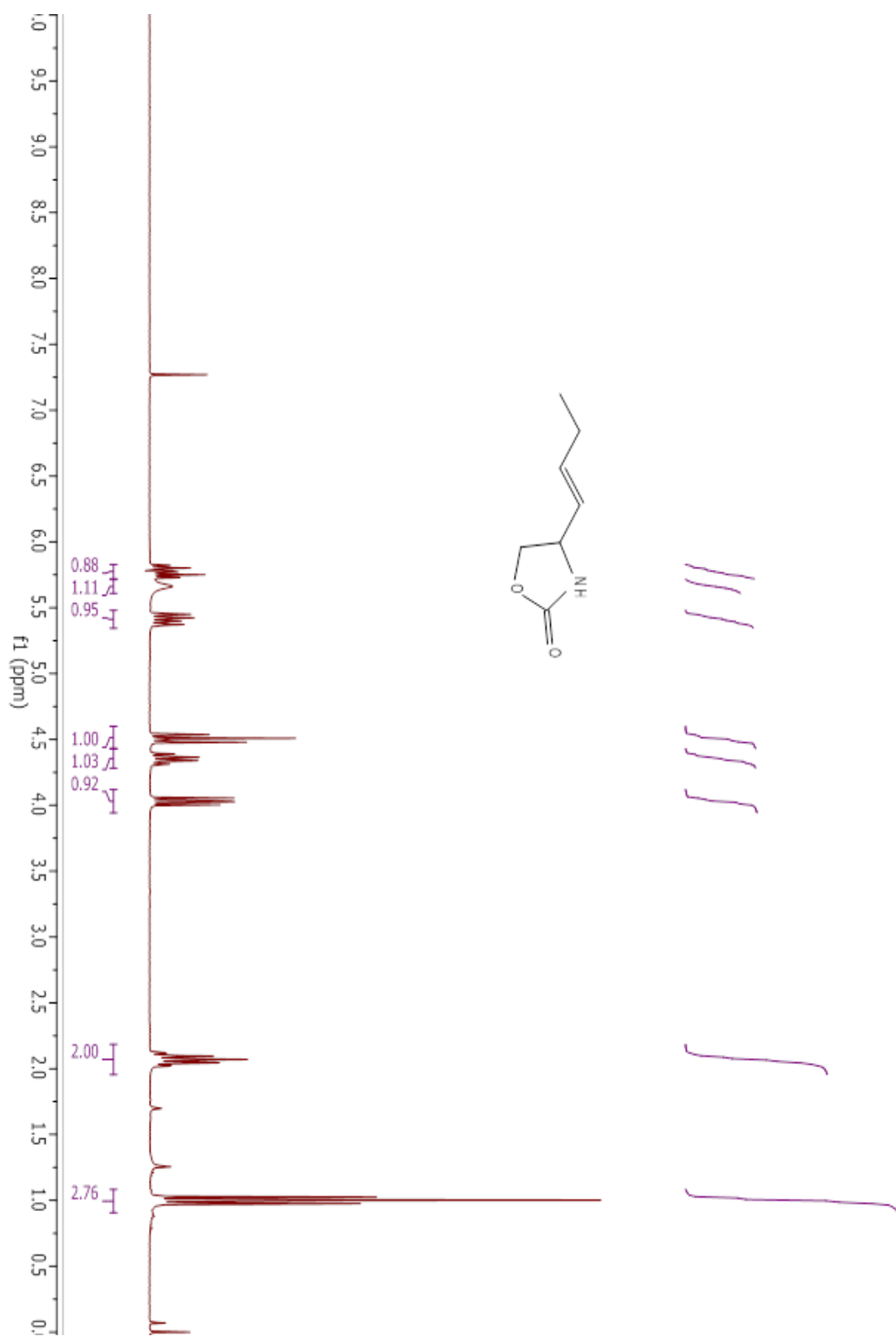


Handwritten notes in green ink, consisting of several vertical lines and brackets, likely indicating peak assignments or integration regions.

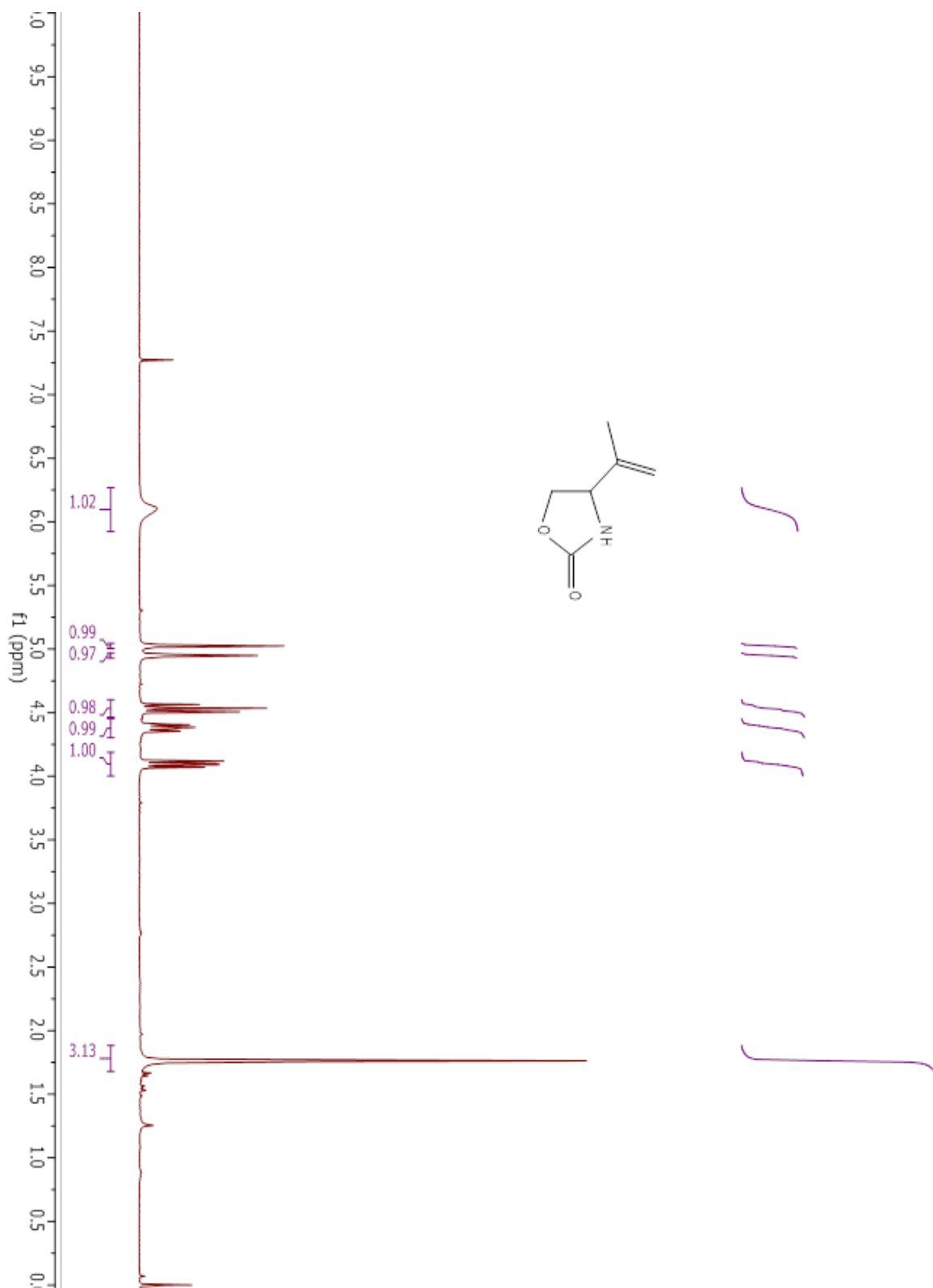
Compound 3.17b.



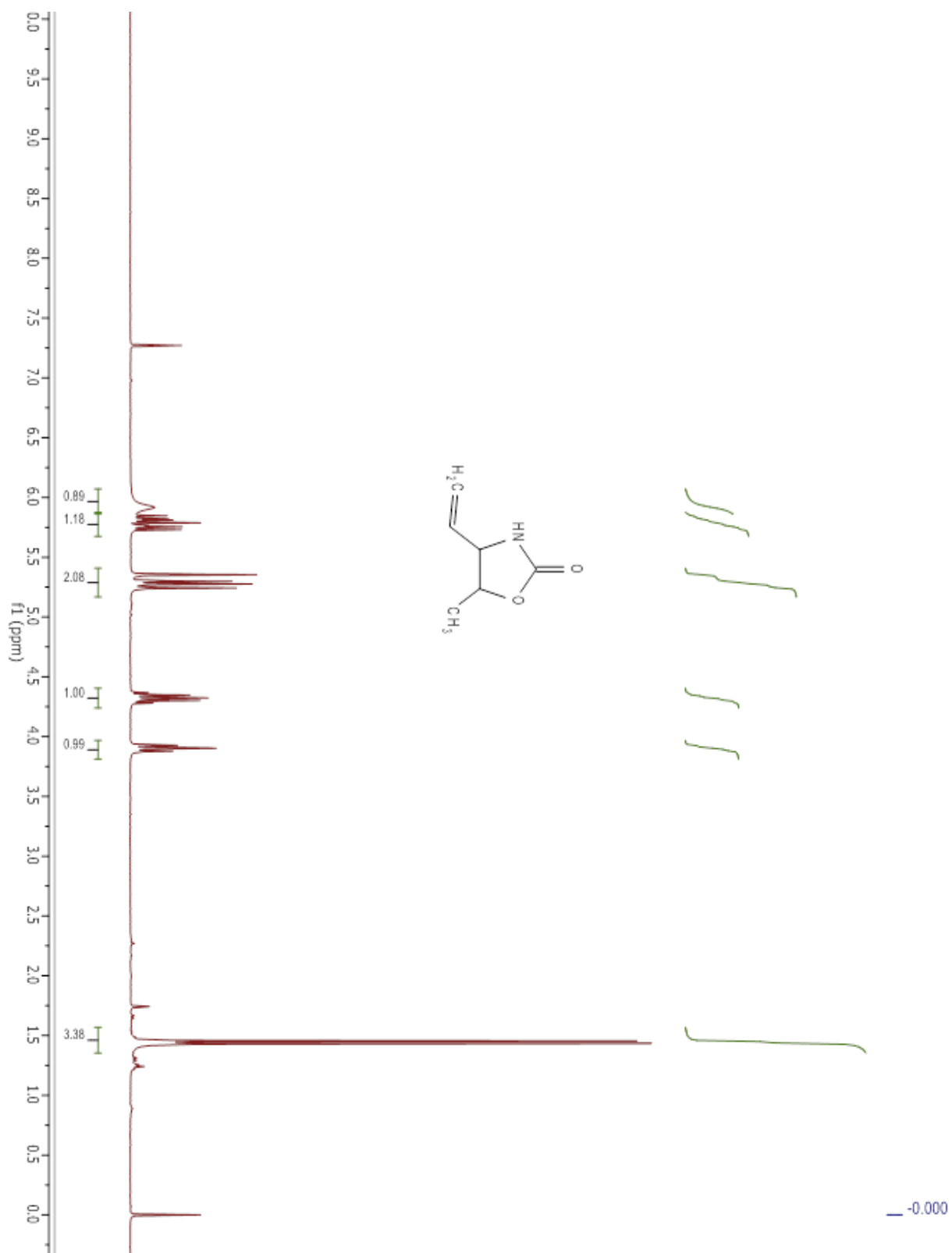
Compound 3.17c.

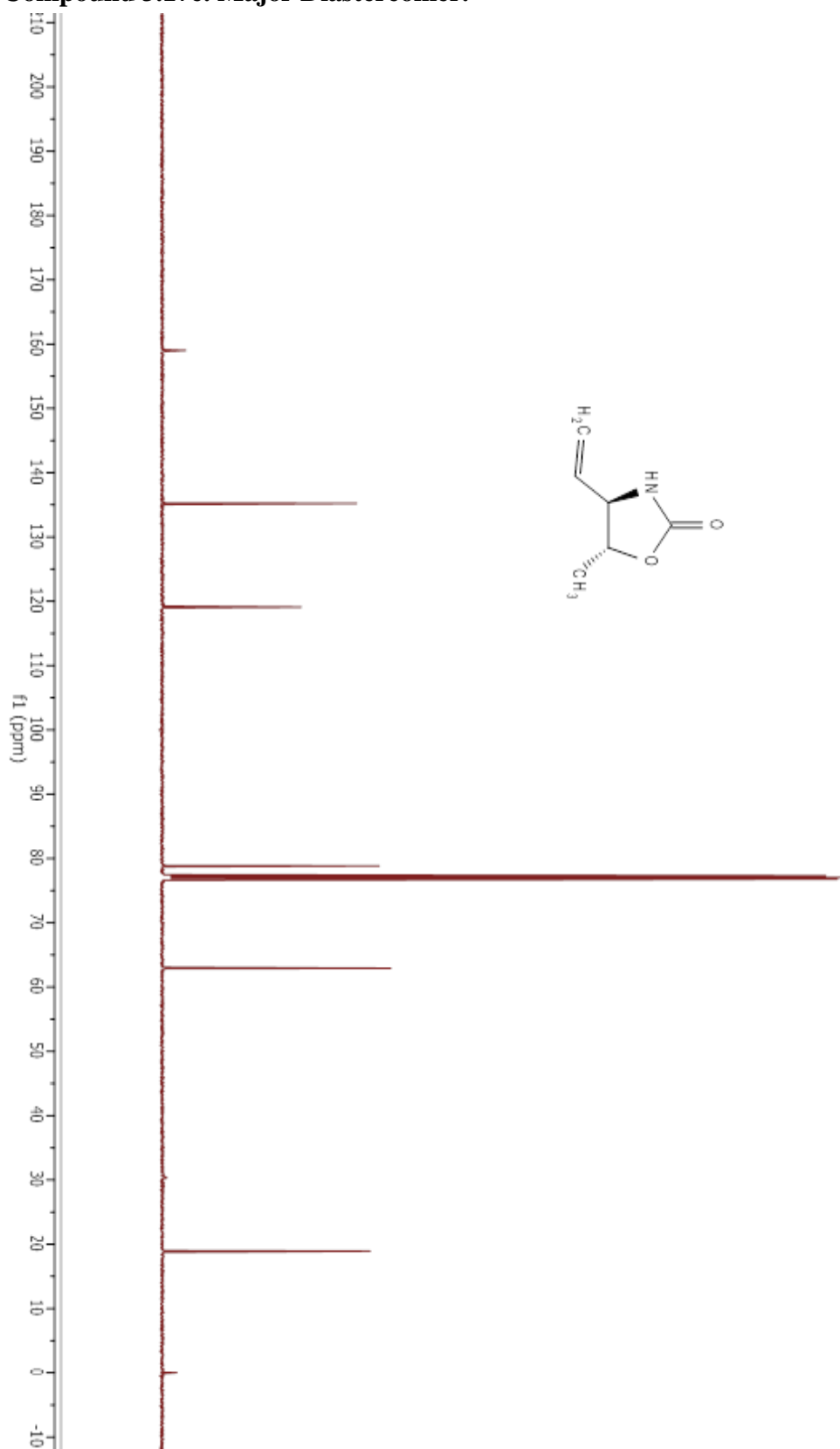


Compound 3.17d.

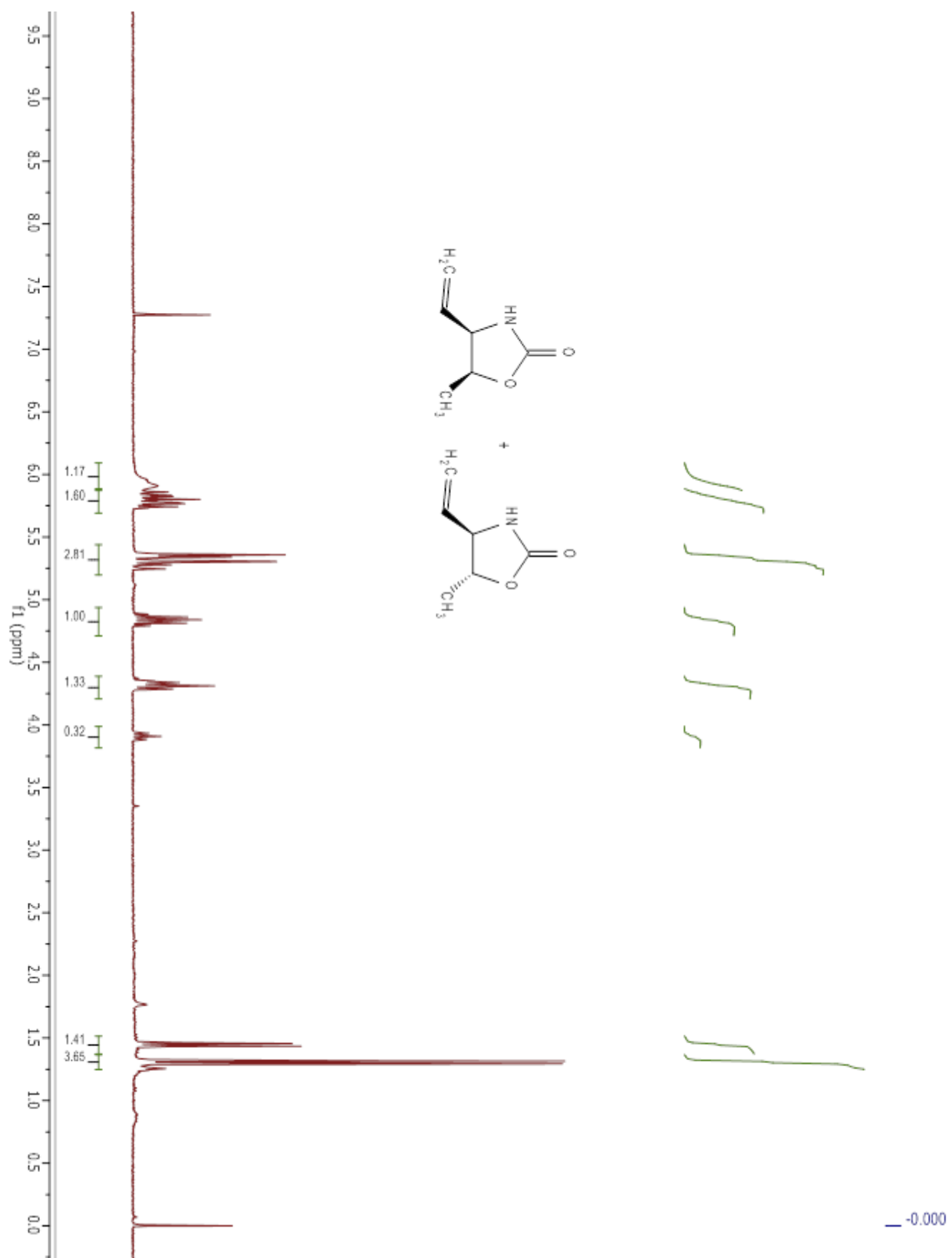


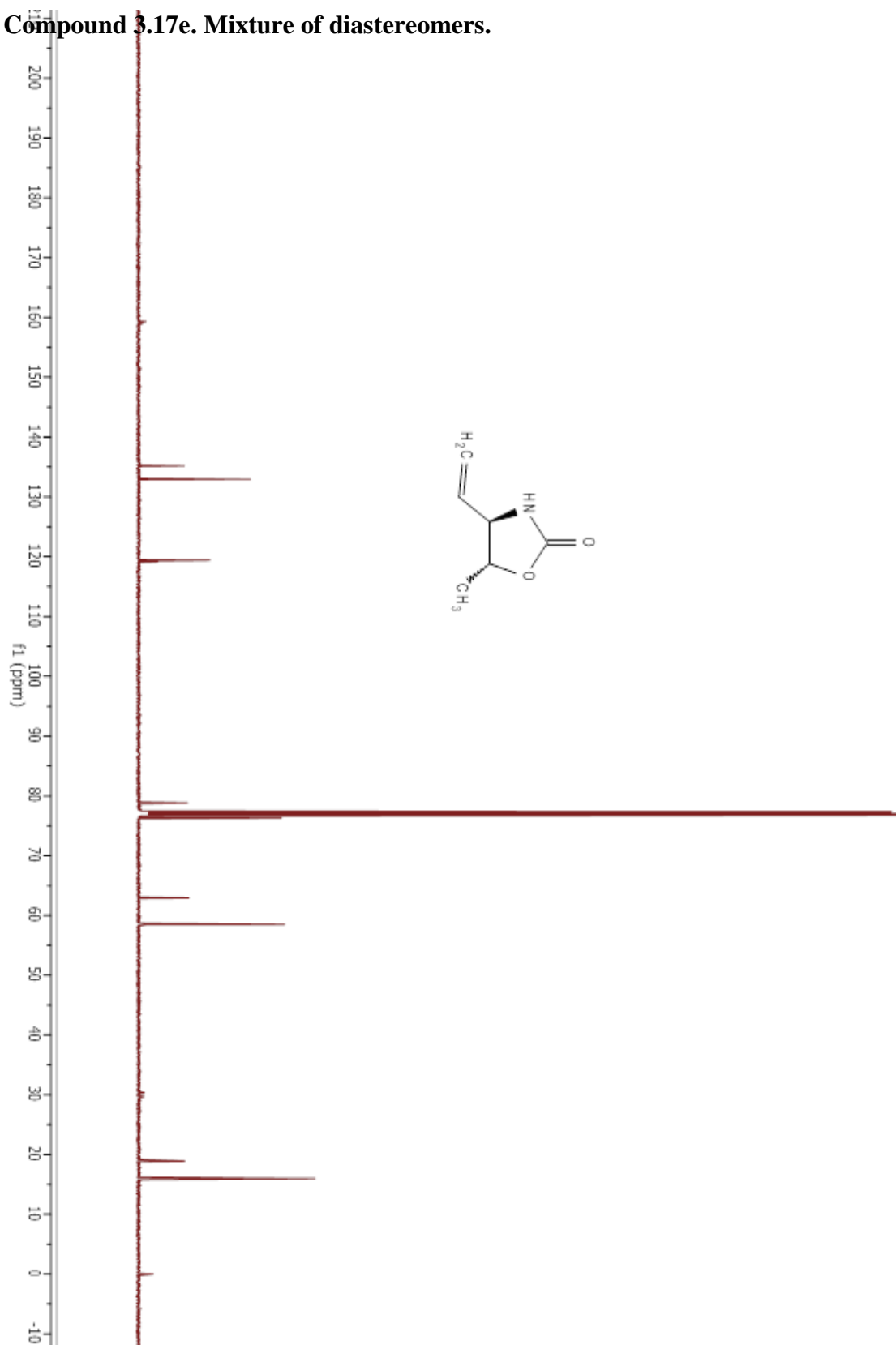
Compound 3.17e. Major diastereomer.



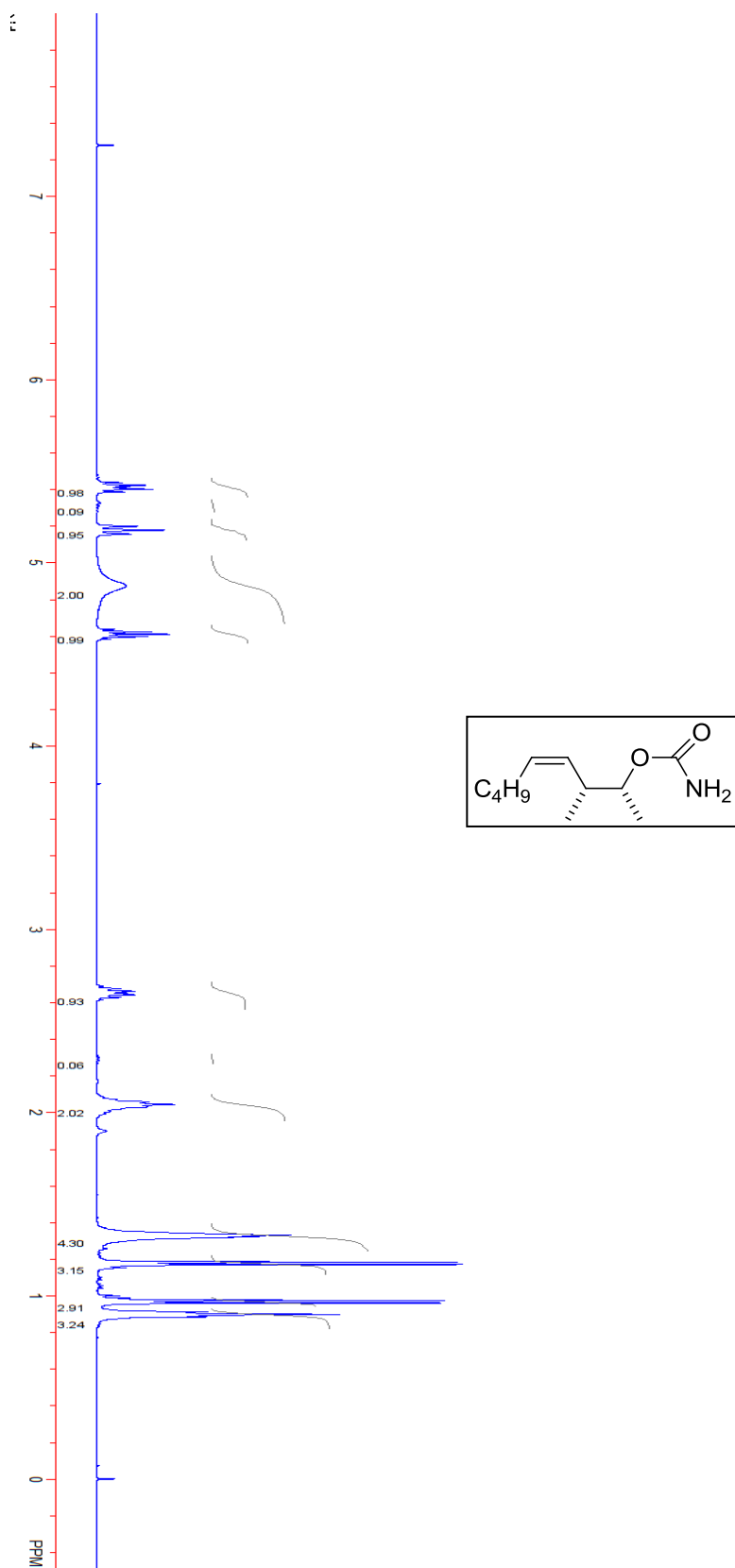
Compound 3.17e. Major Diastereomer.

Compound 3.17e. Mixtures of diastereomers.

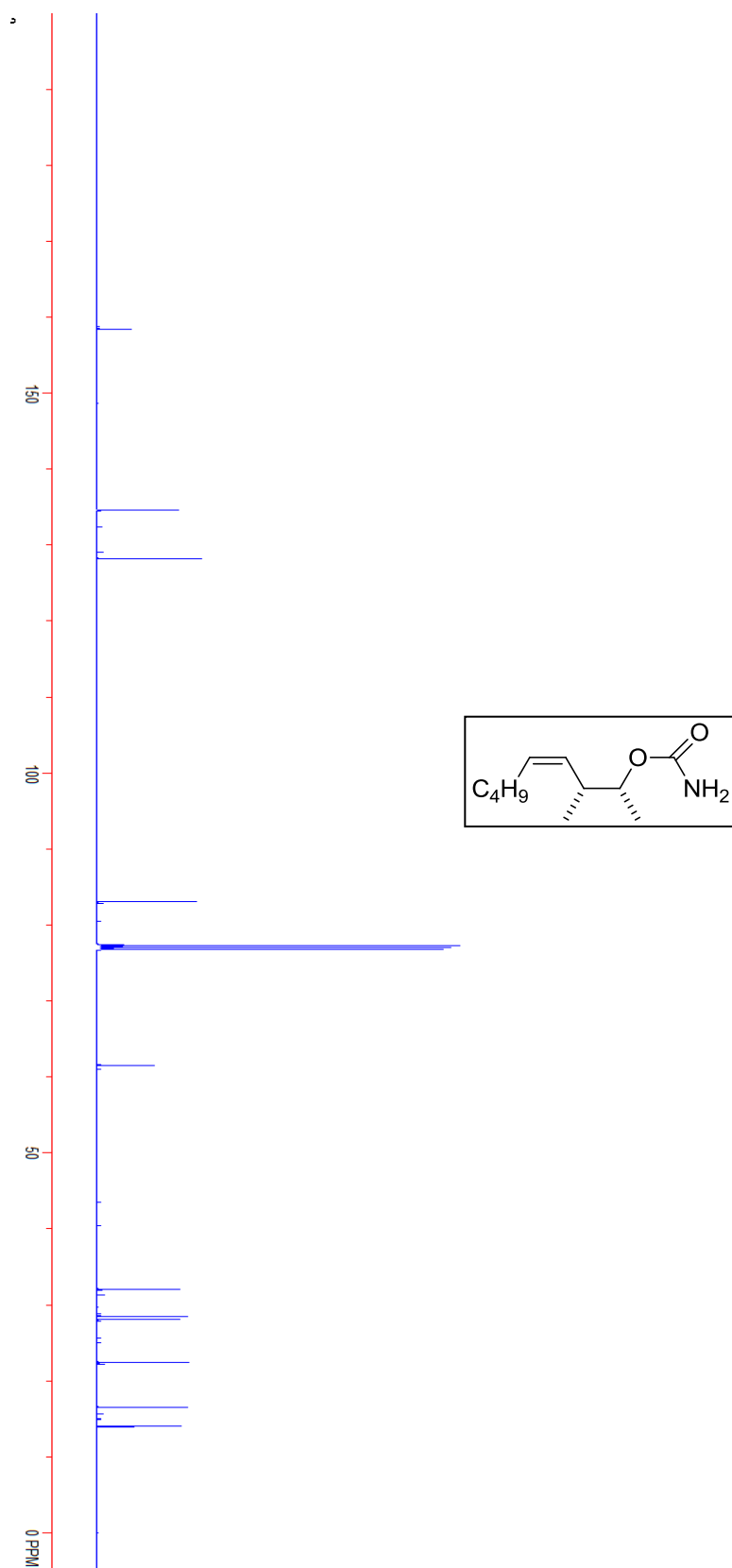


Compound 3.17e. Mixture of diastereomers.

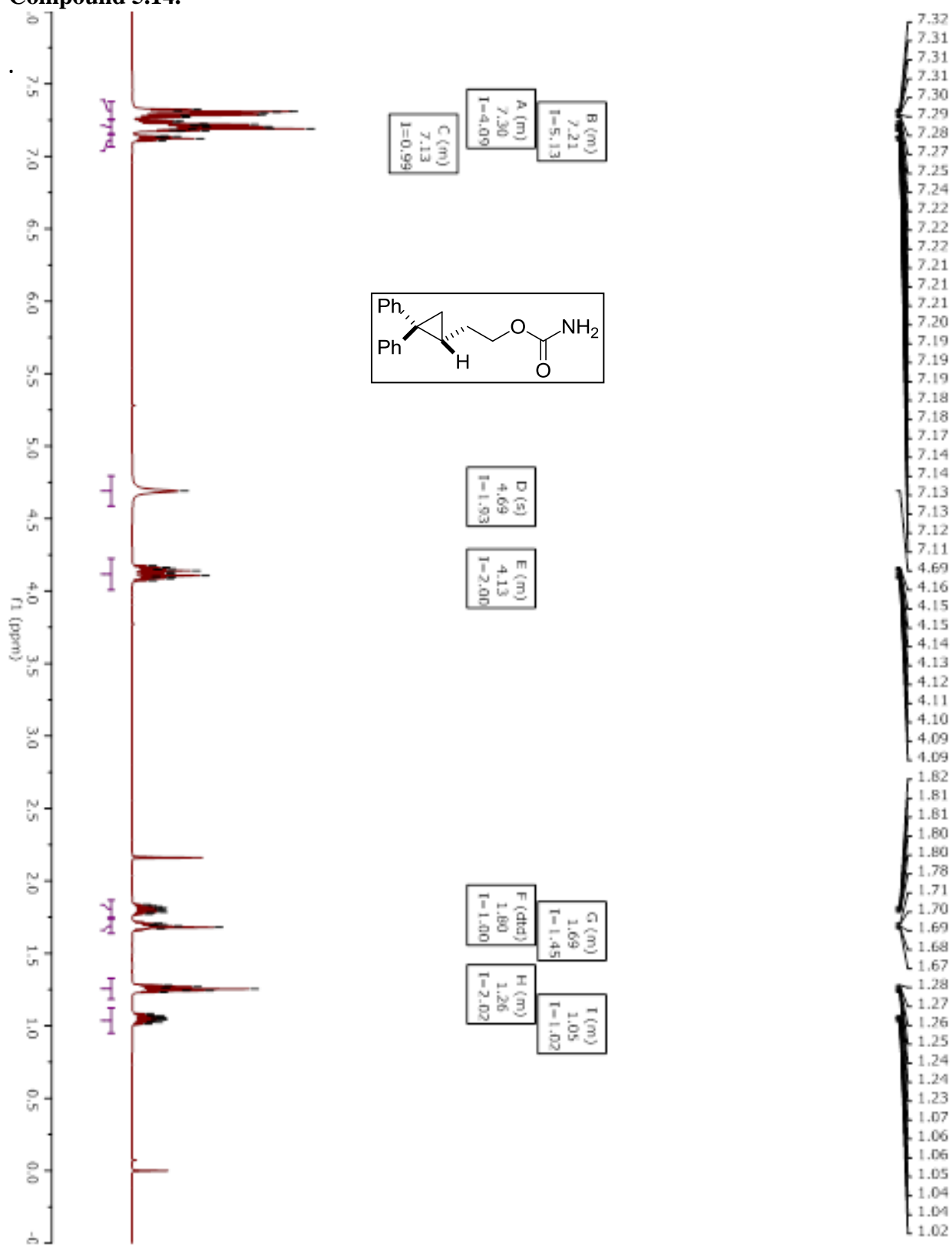
Compound 5.14b.



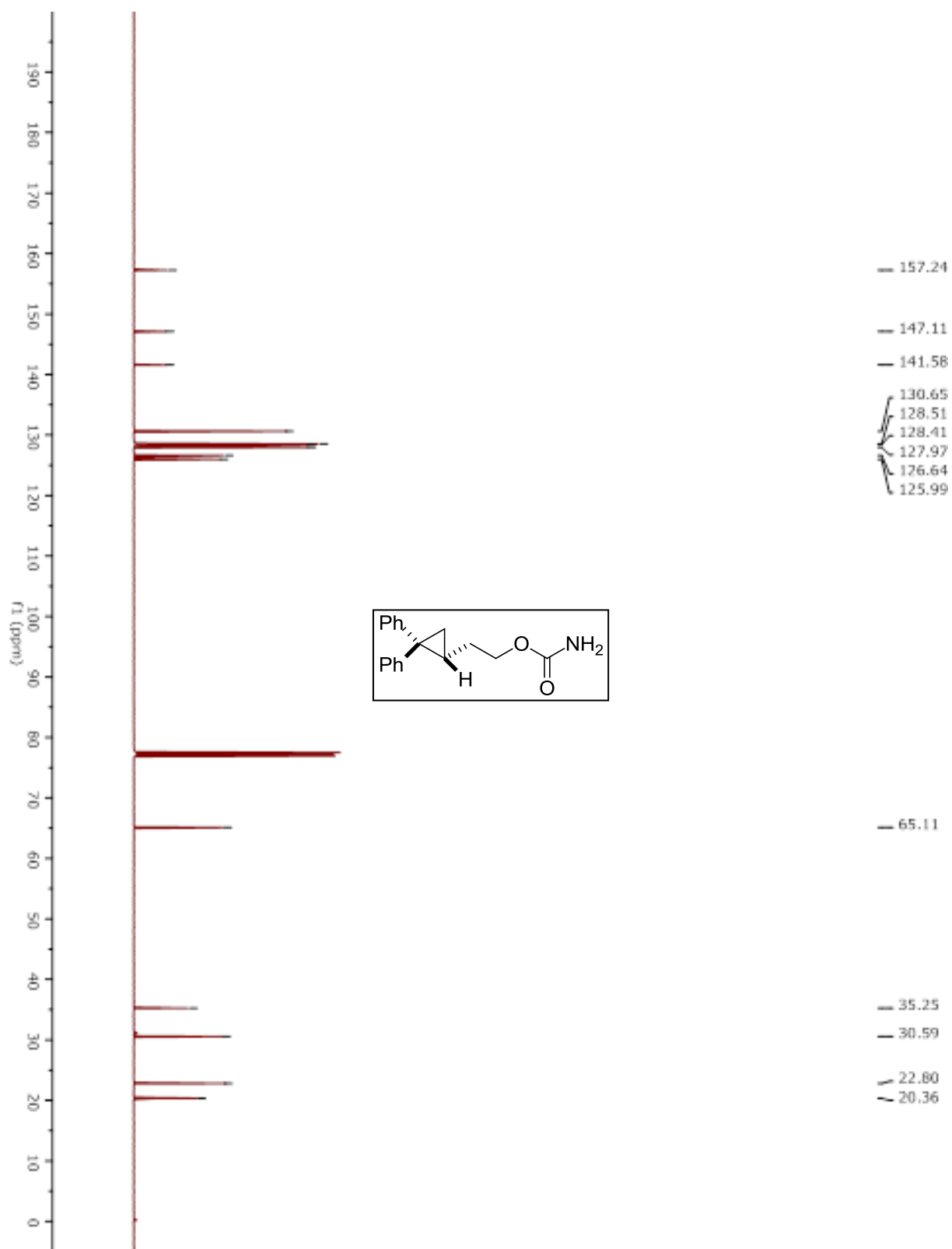
Compound 5.14b.



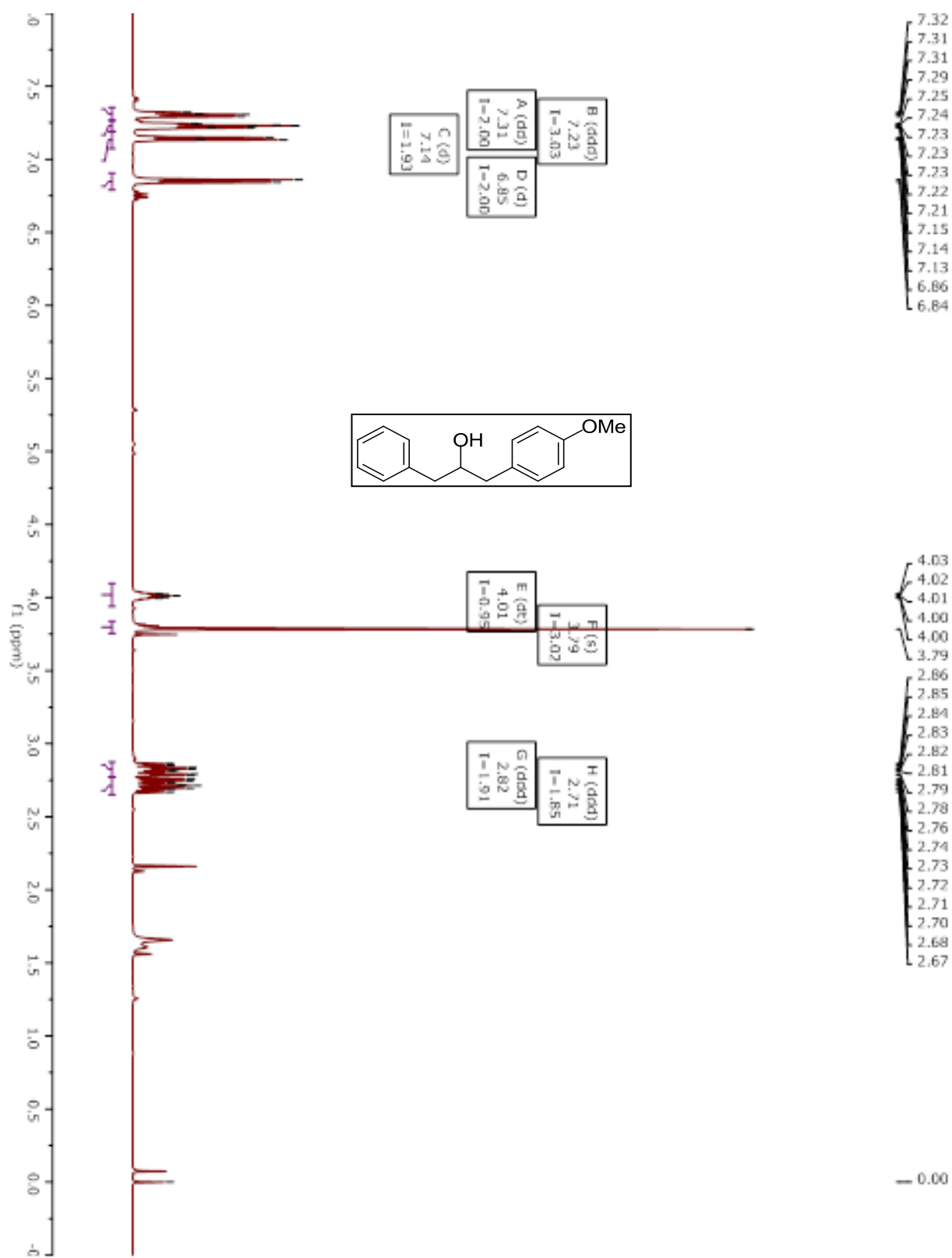
Compound 5.14.



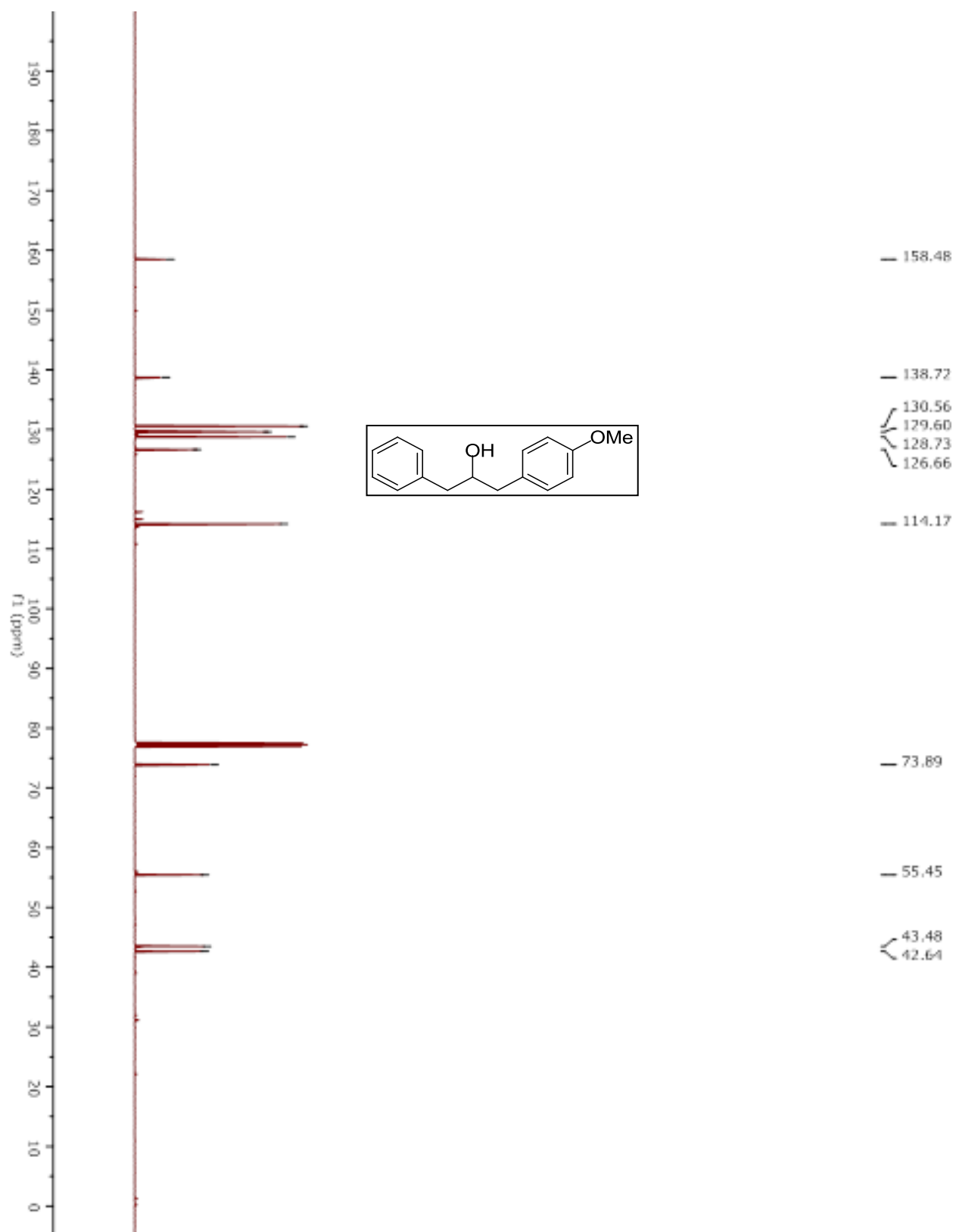
Compound 5.14.



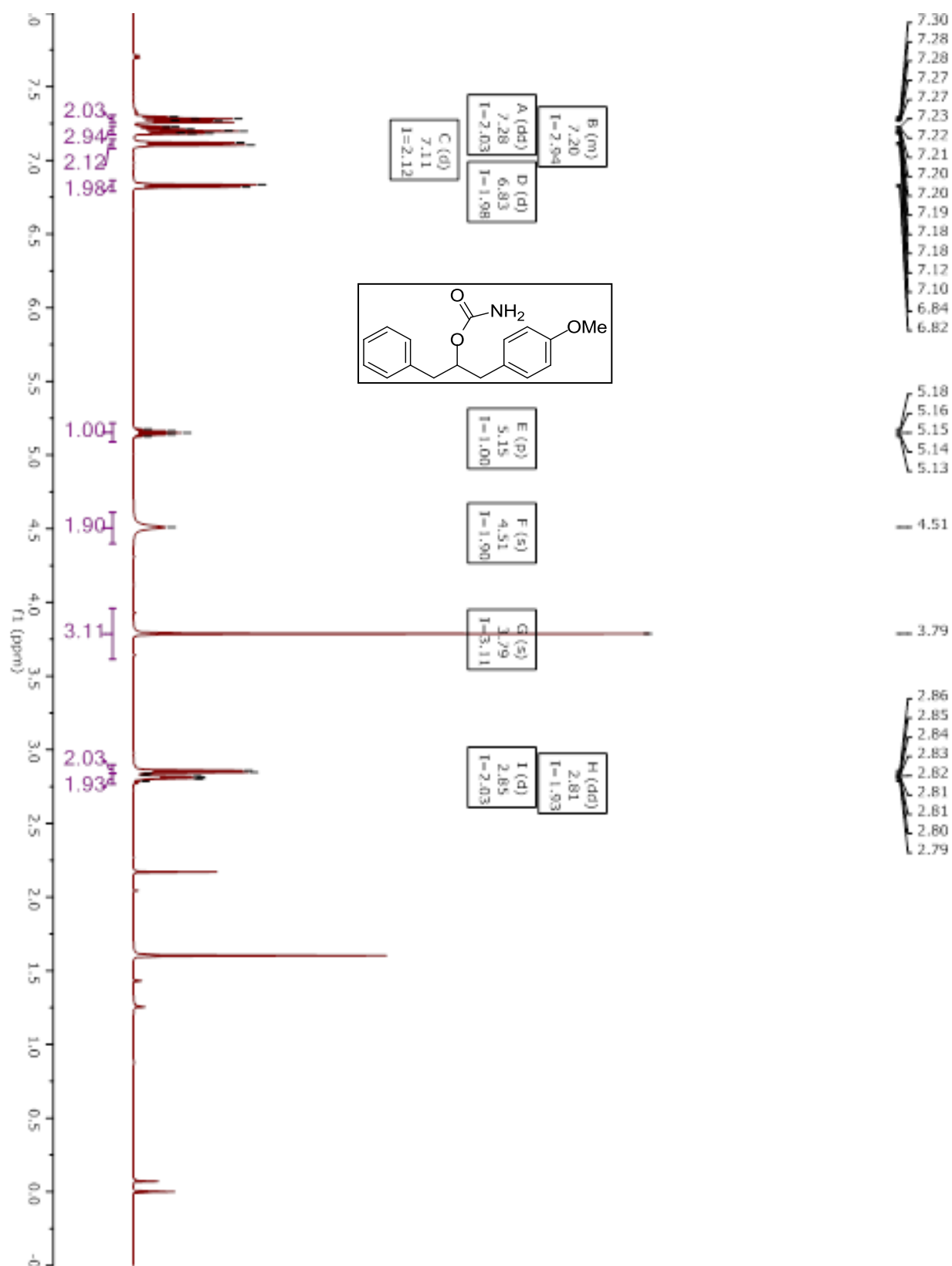
Compound S5.1.



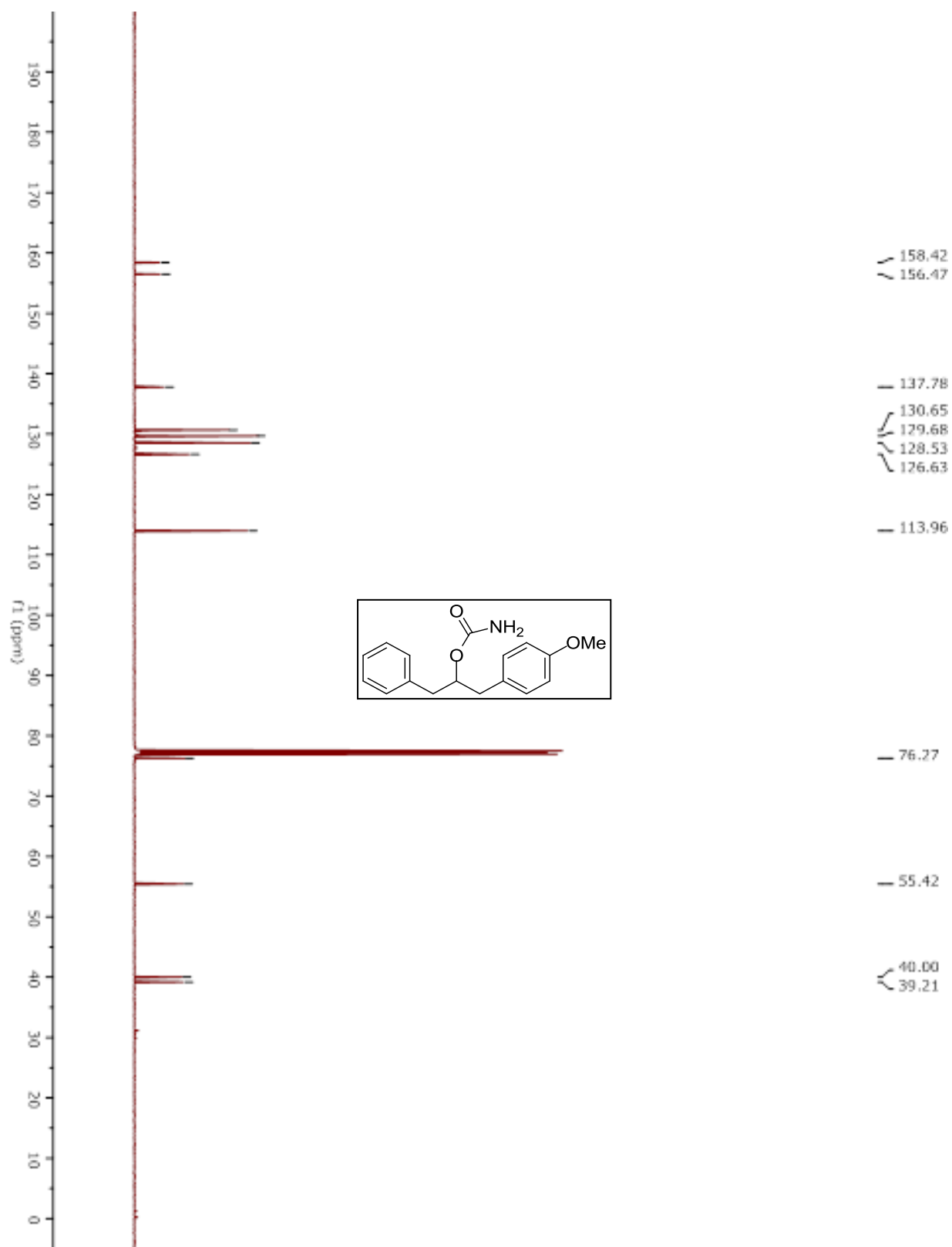
Compound S6.1.



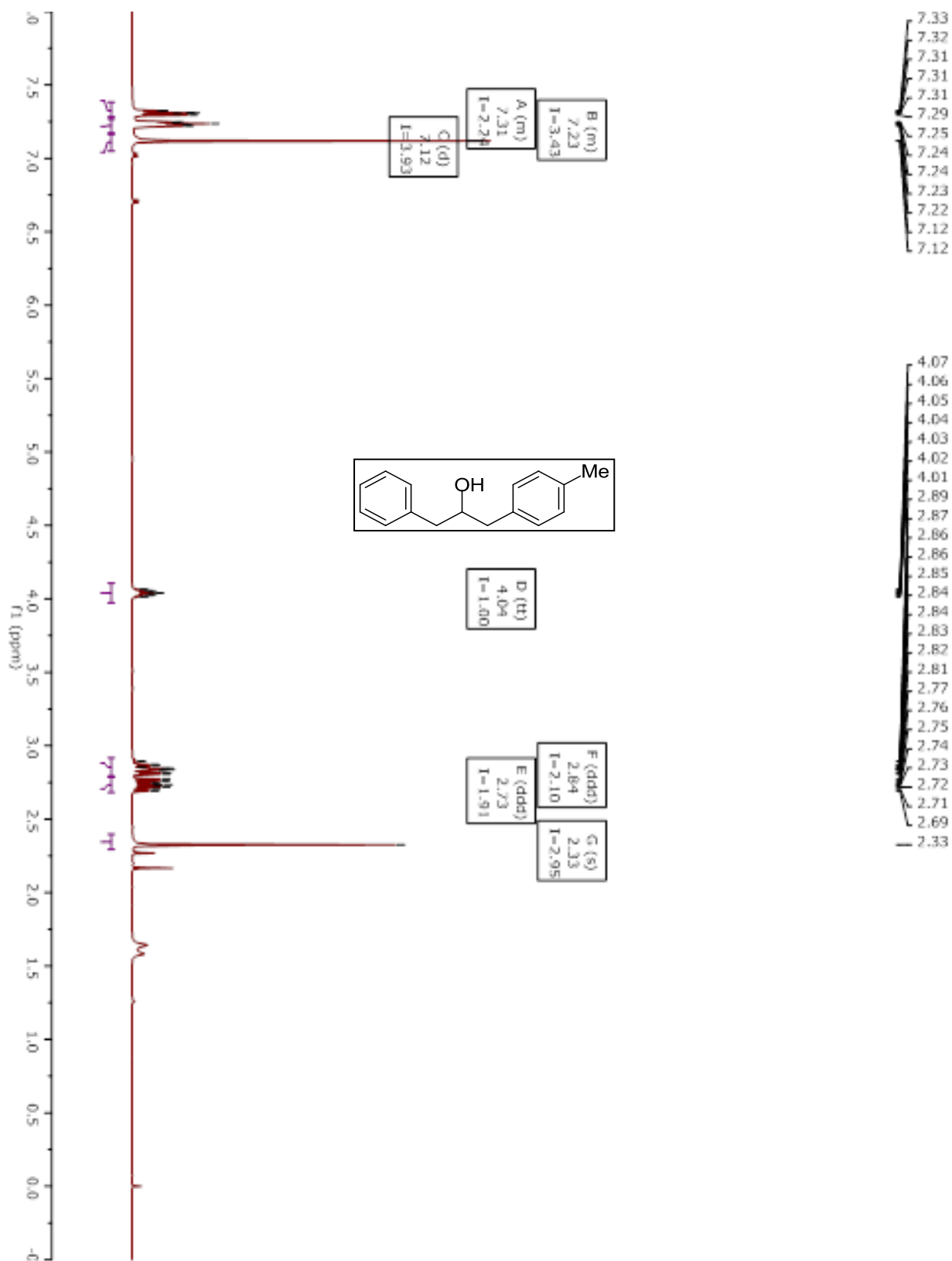
Compound 5.20a.



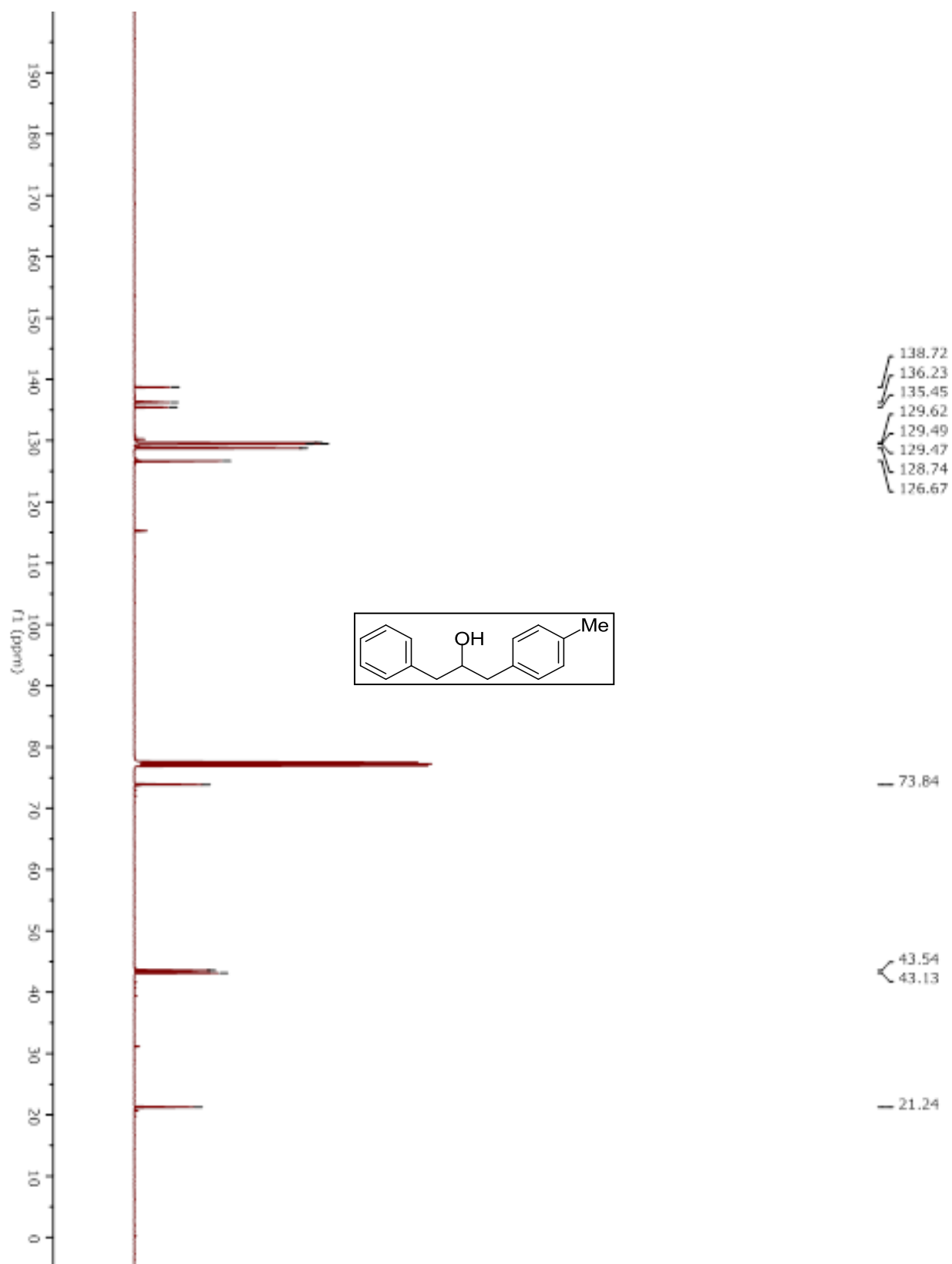
Compound 5.20a.



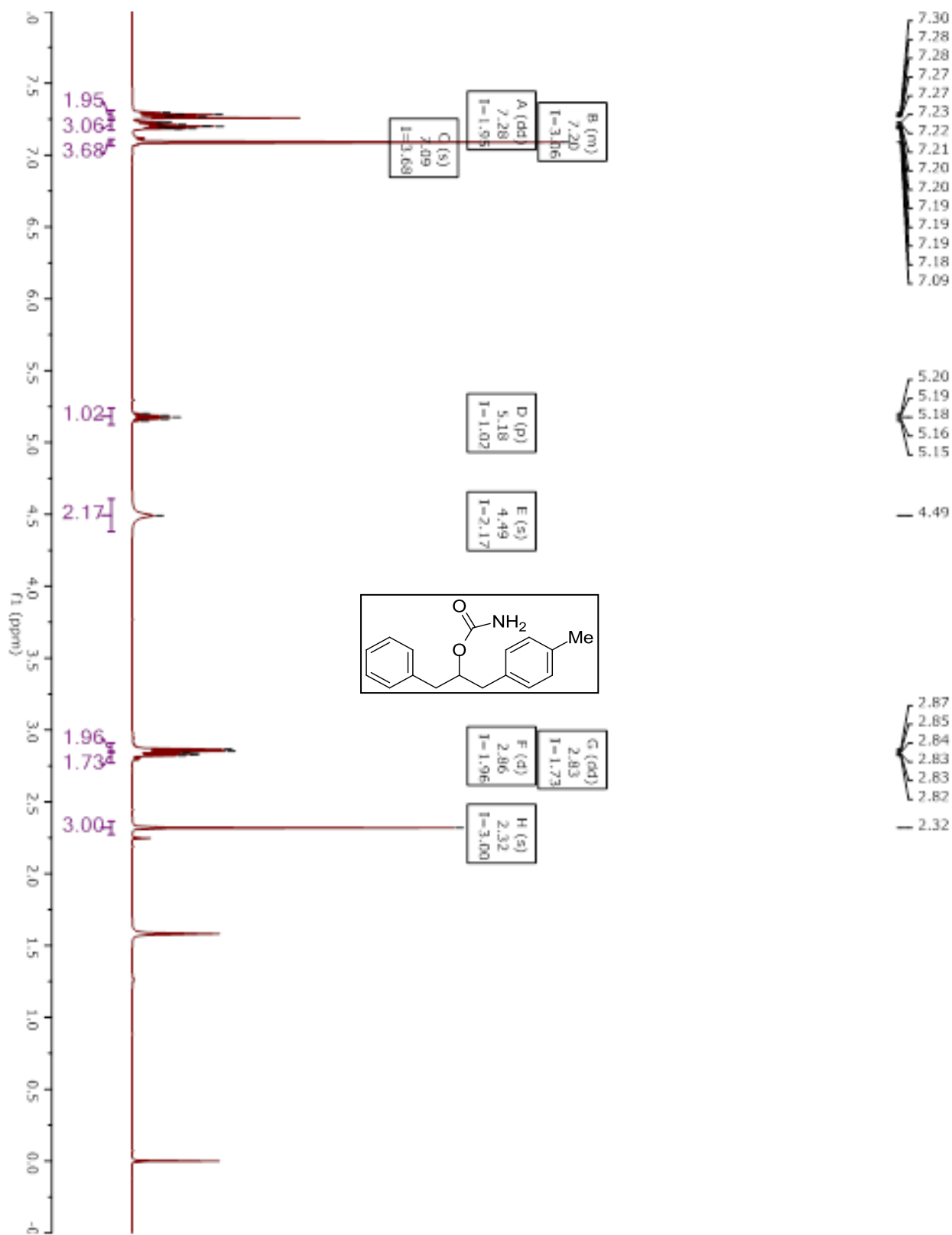
Compound S6.2.



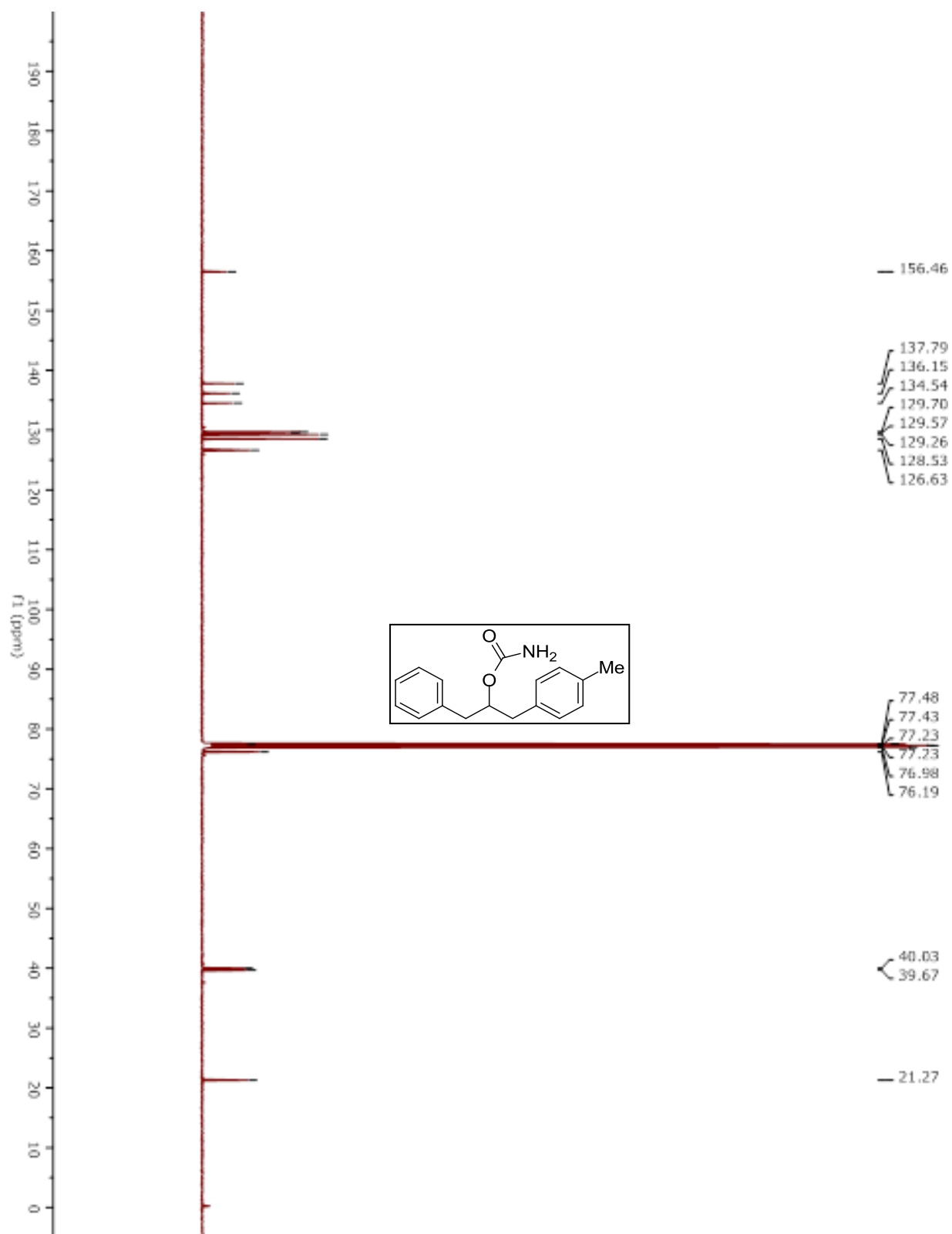
Compound S6.2.



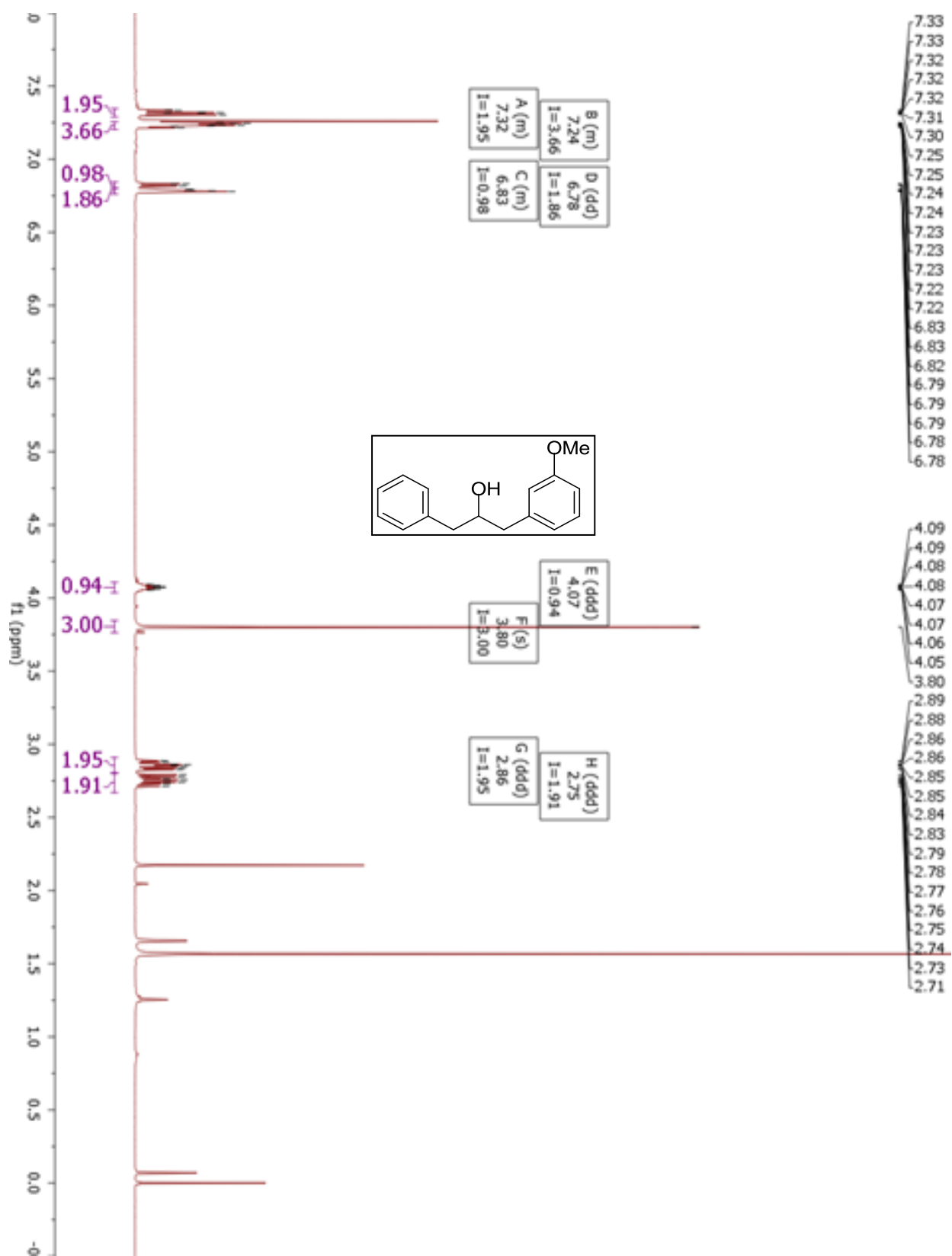
Compound 5.20b.



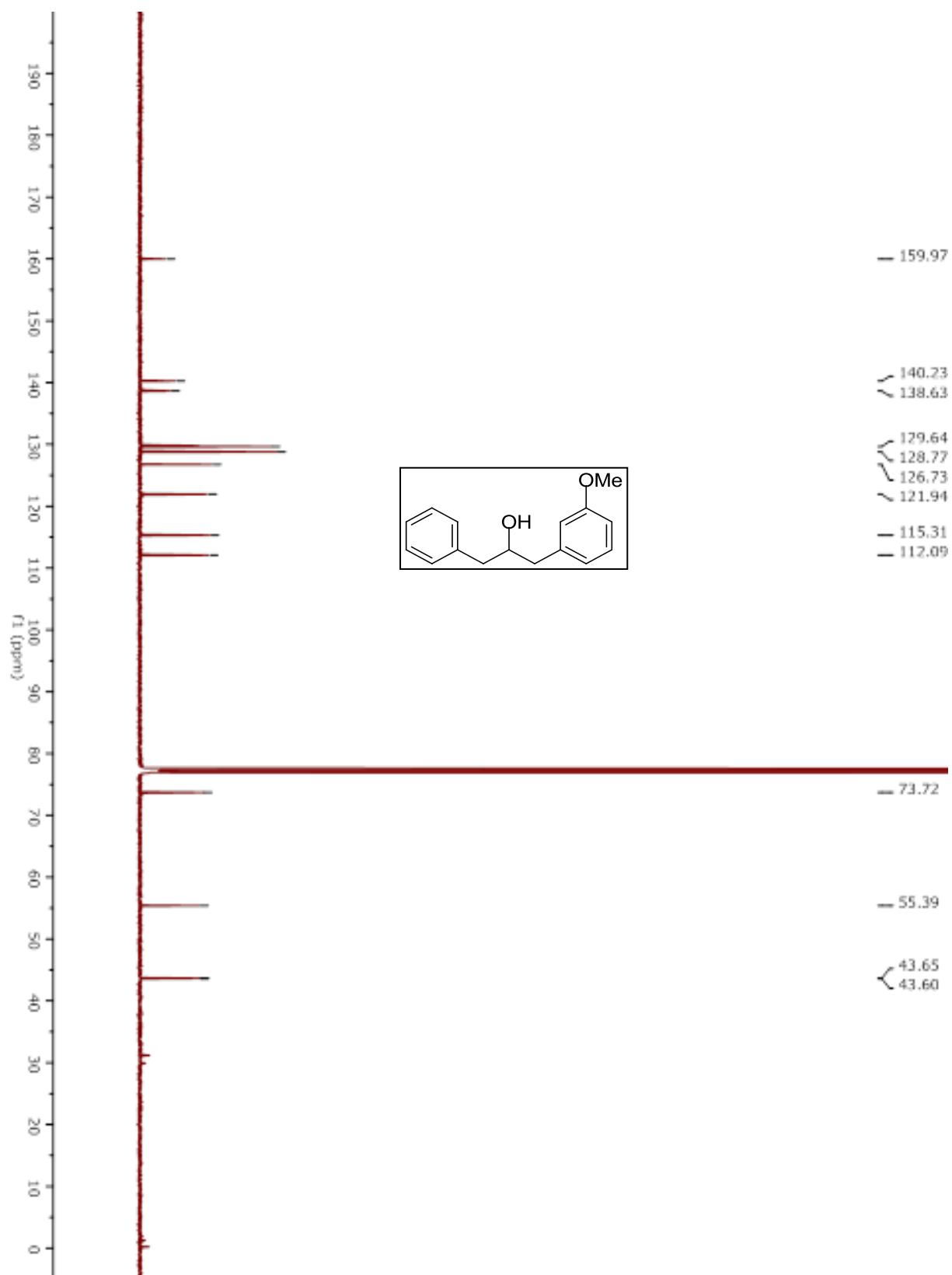
Compound 5.20b.



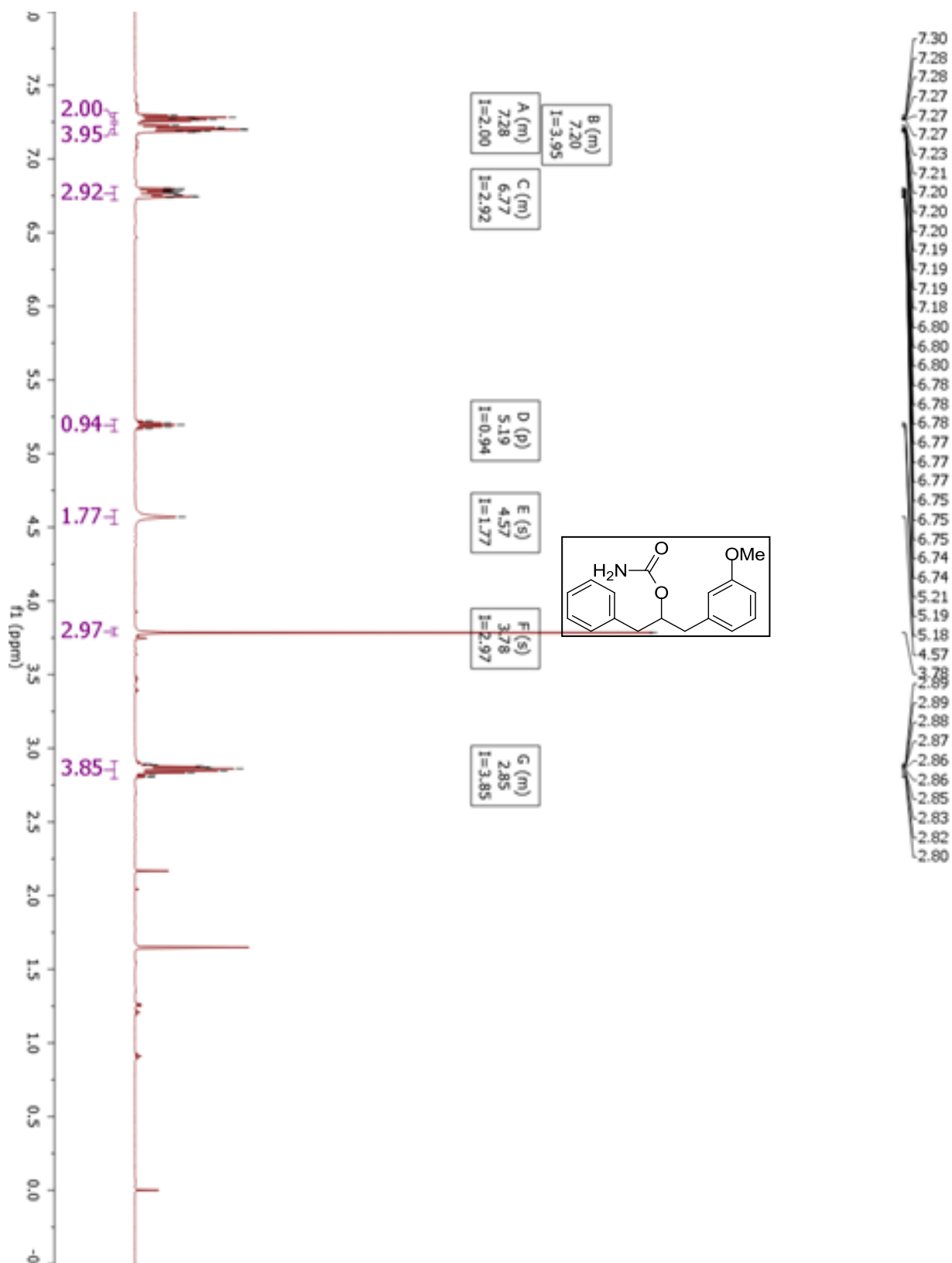
Compound S6.3.



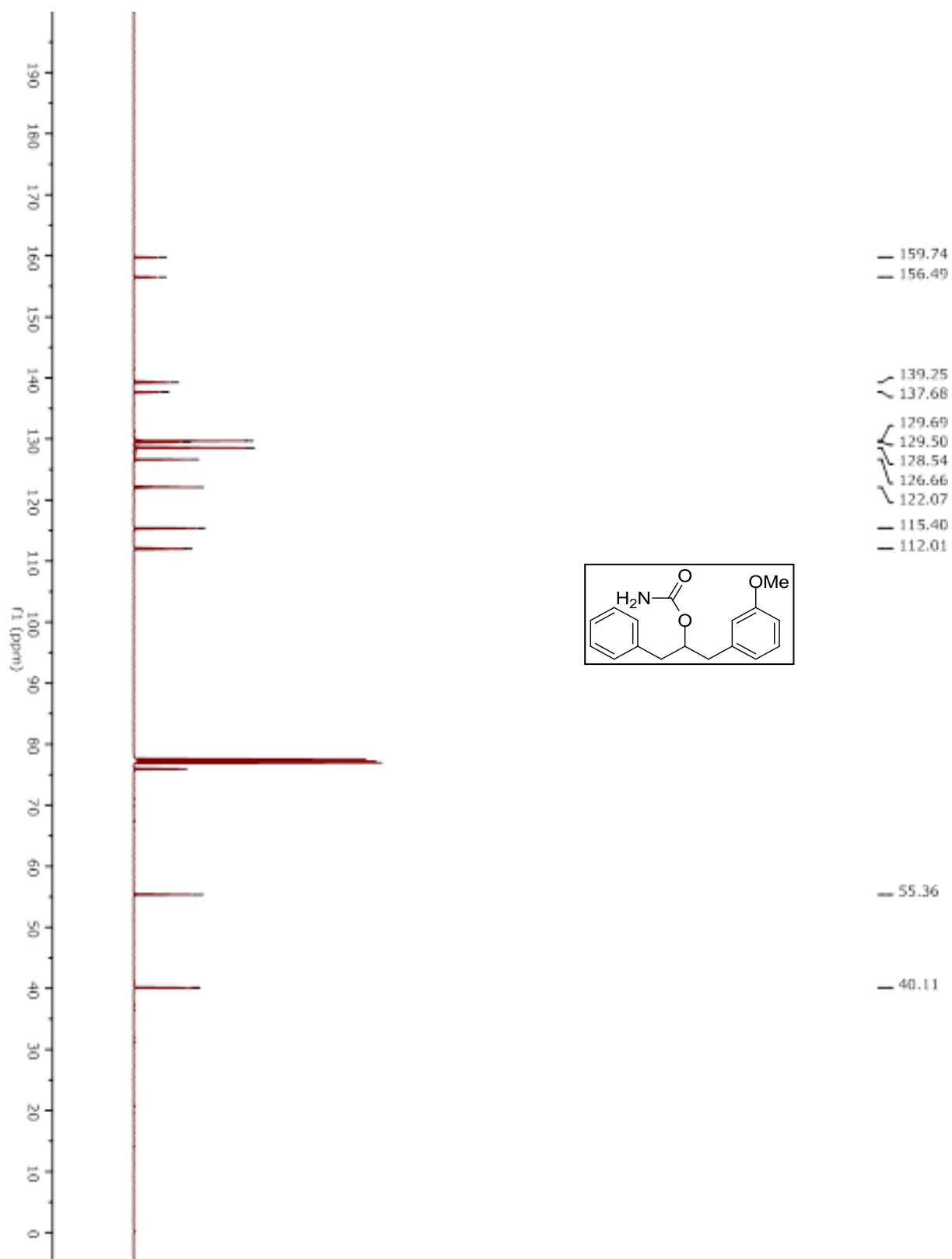
Compound S6.3.



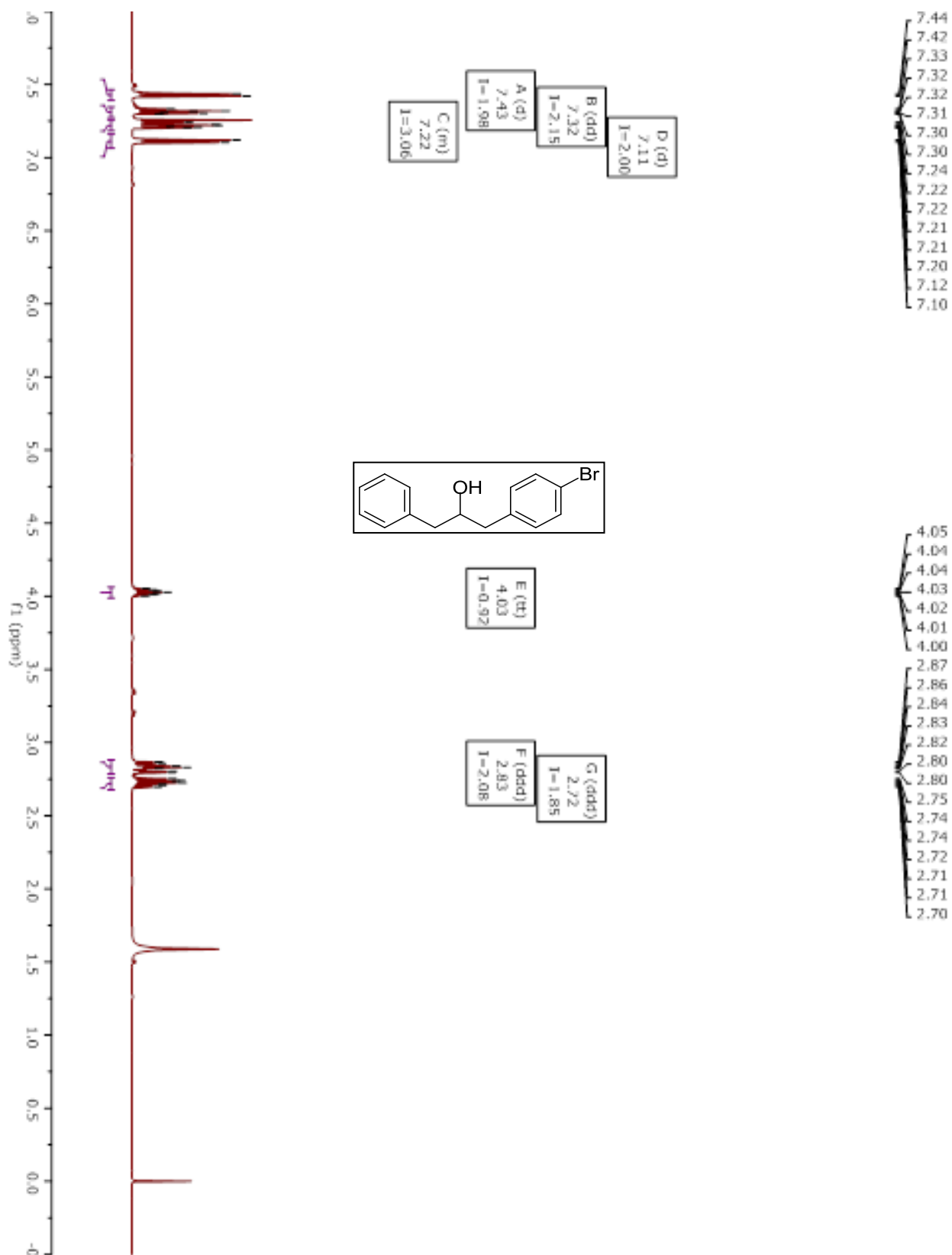
Compound 5.20c.



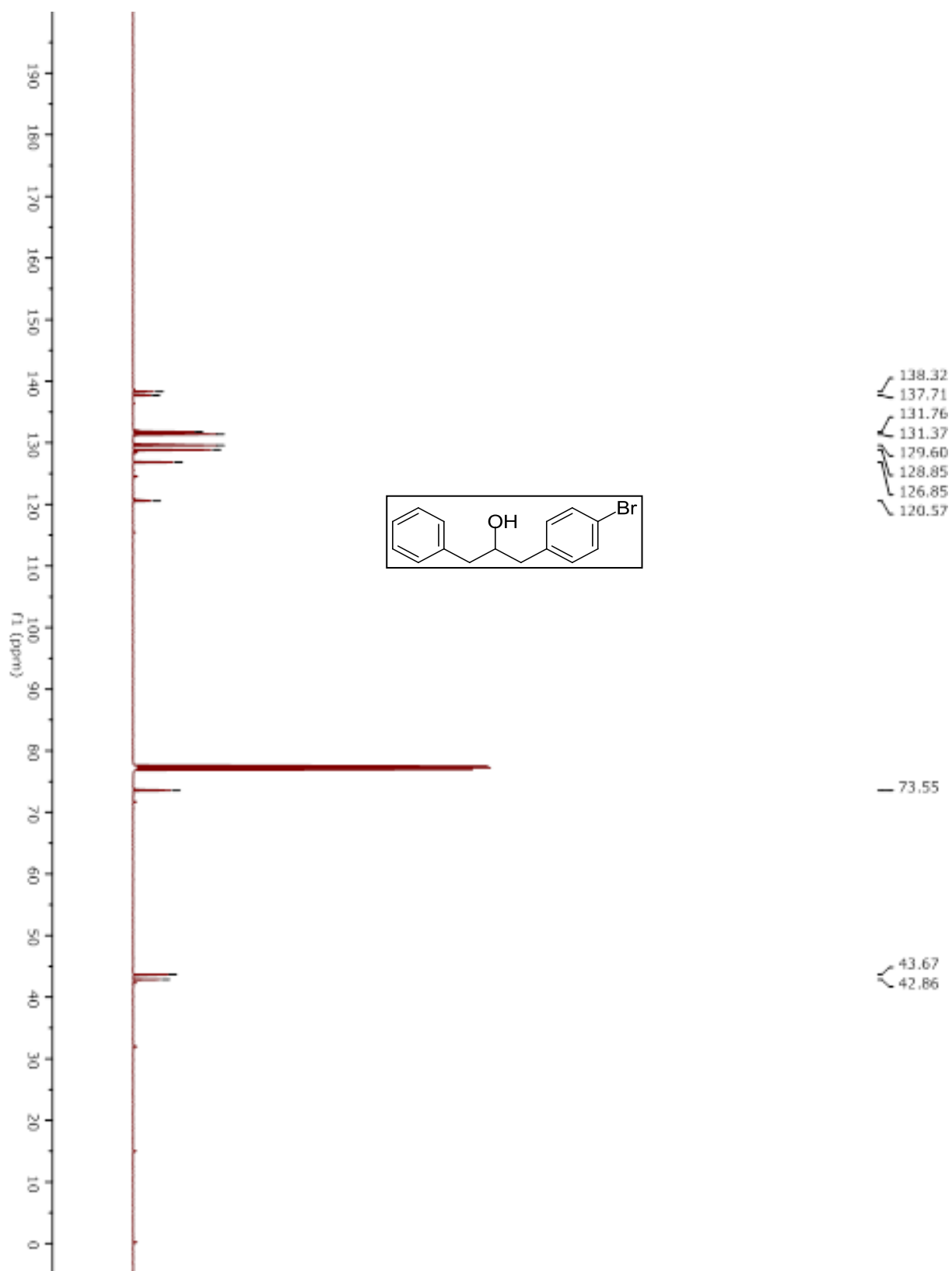
Compound 5.20c.



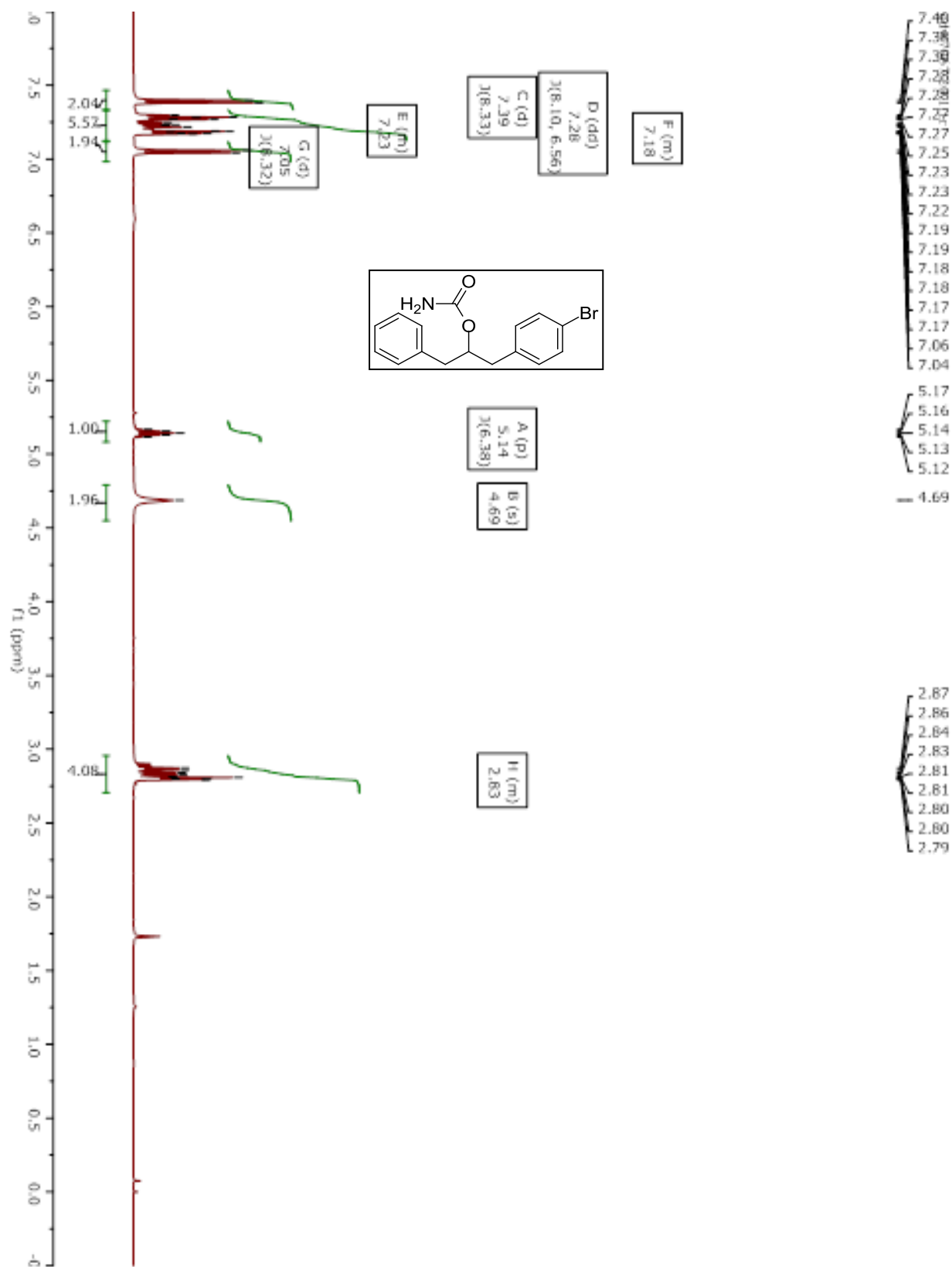
Compound S6.4.



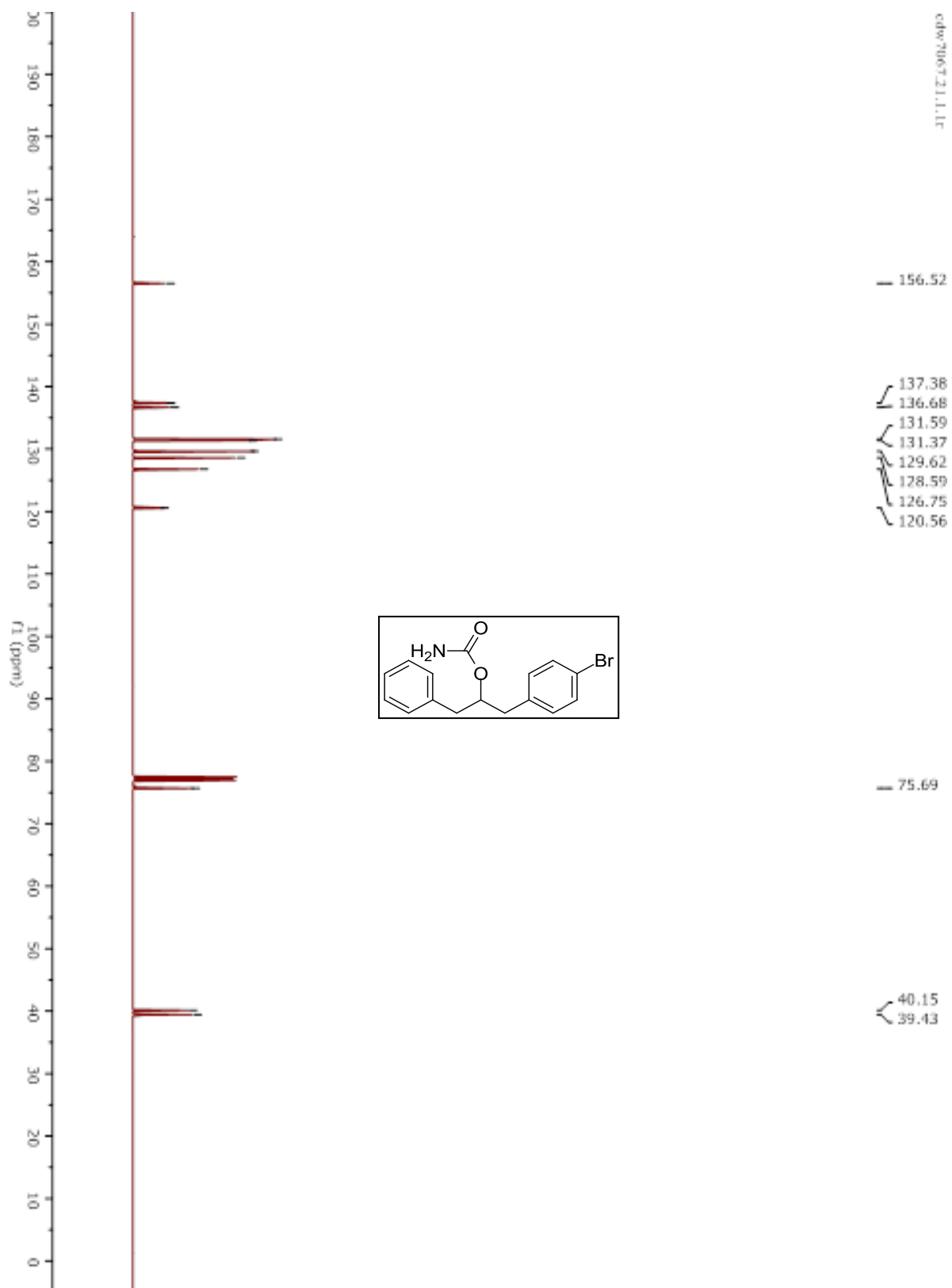
Compound S6.4.



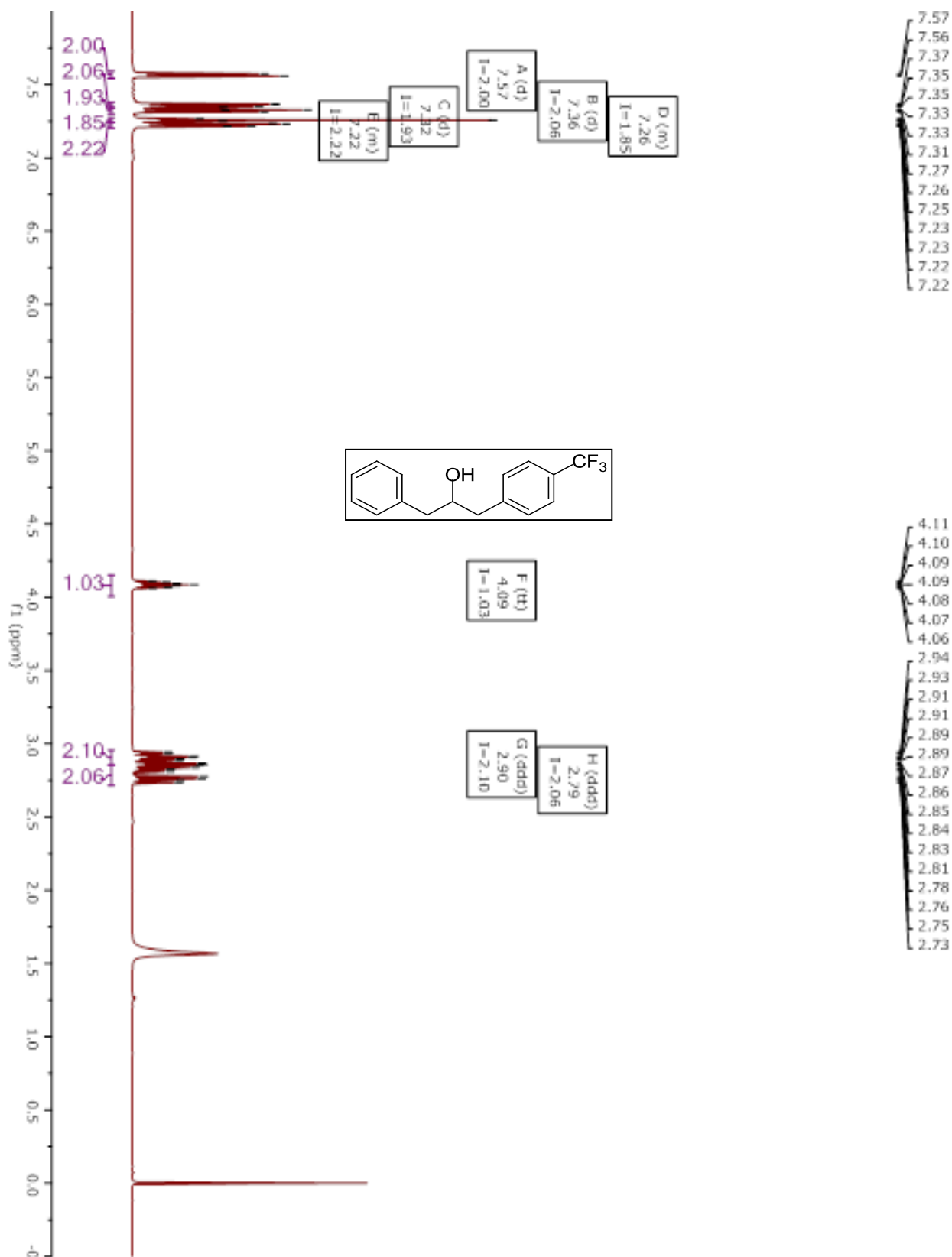
Compound 5.20d.



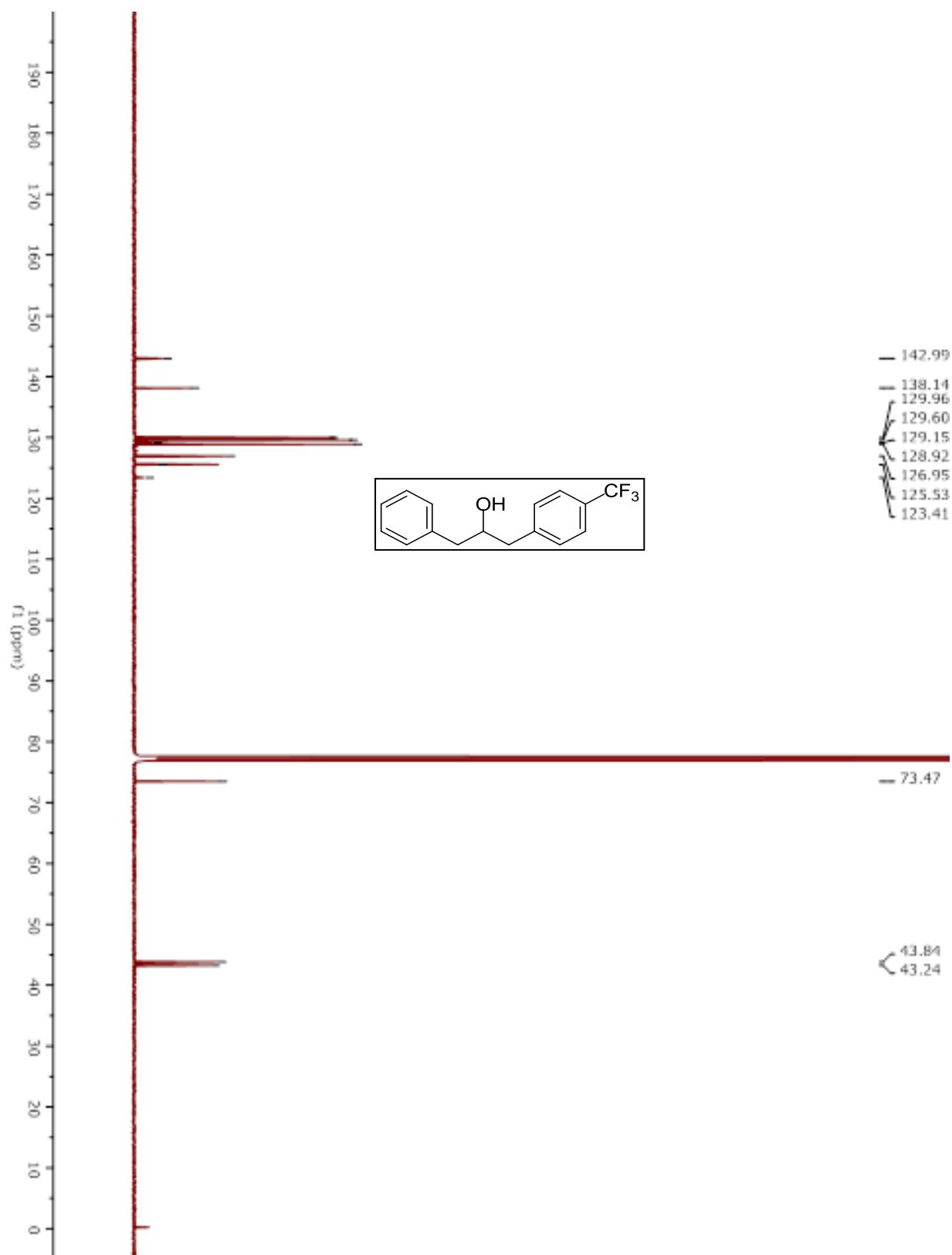
Compound 5.20d.



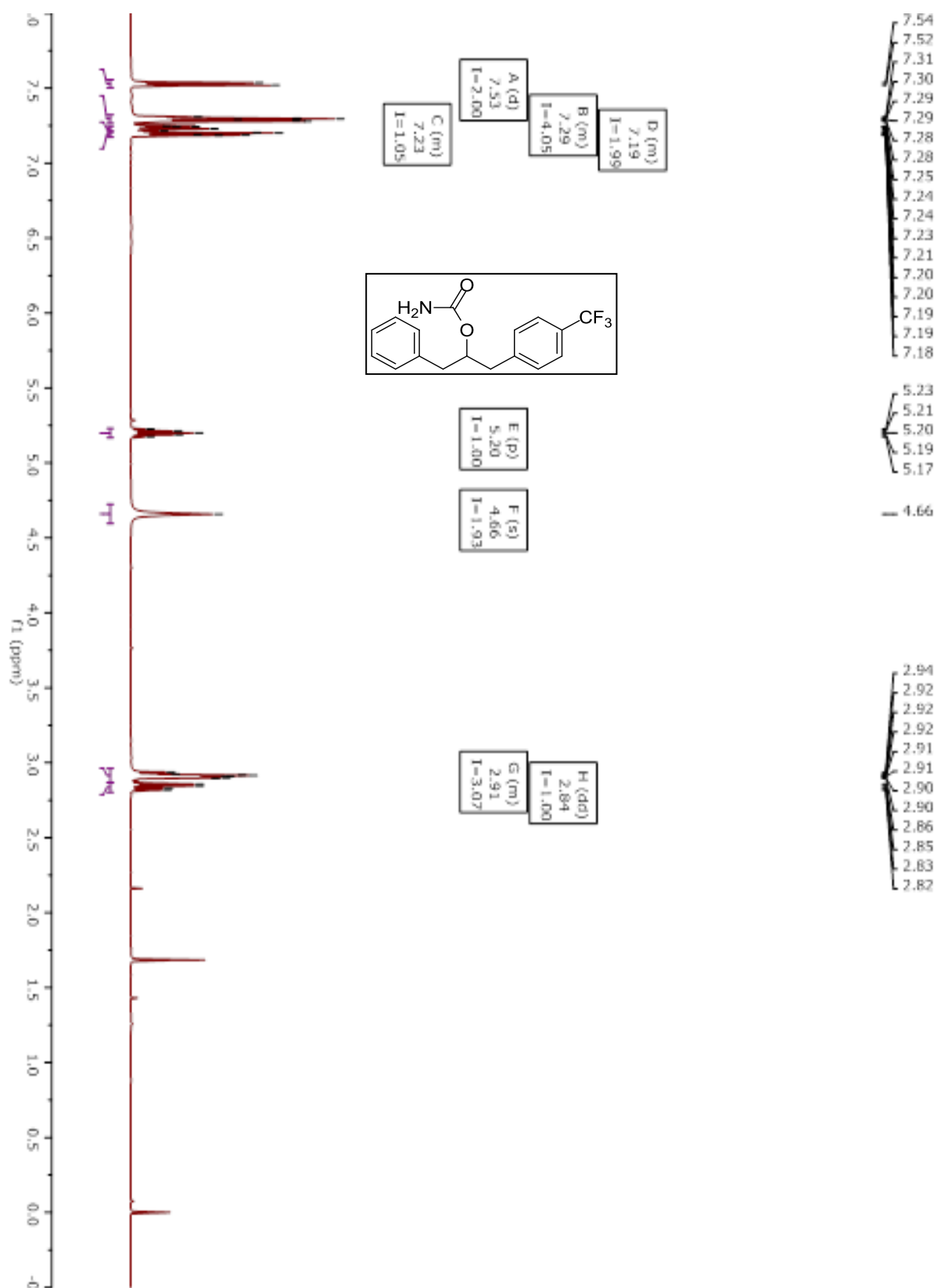
Compound S6.5.



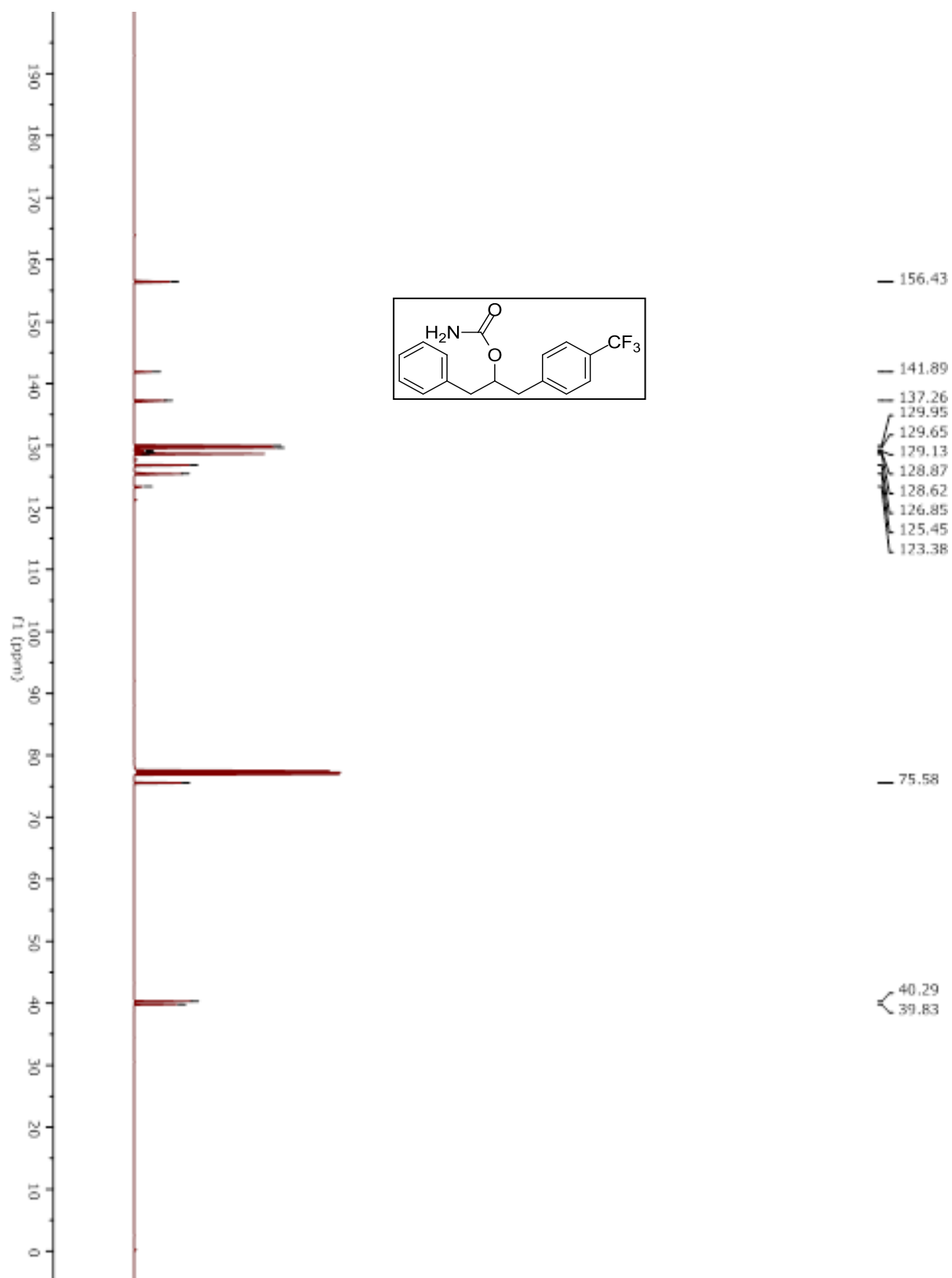
Compound S6.5.



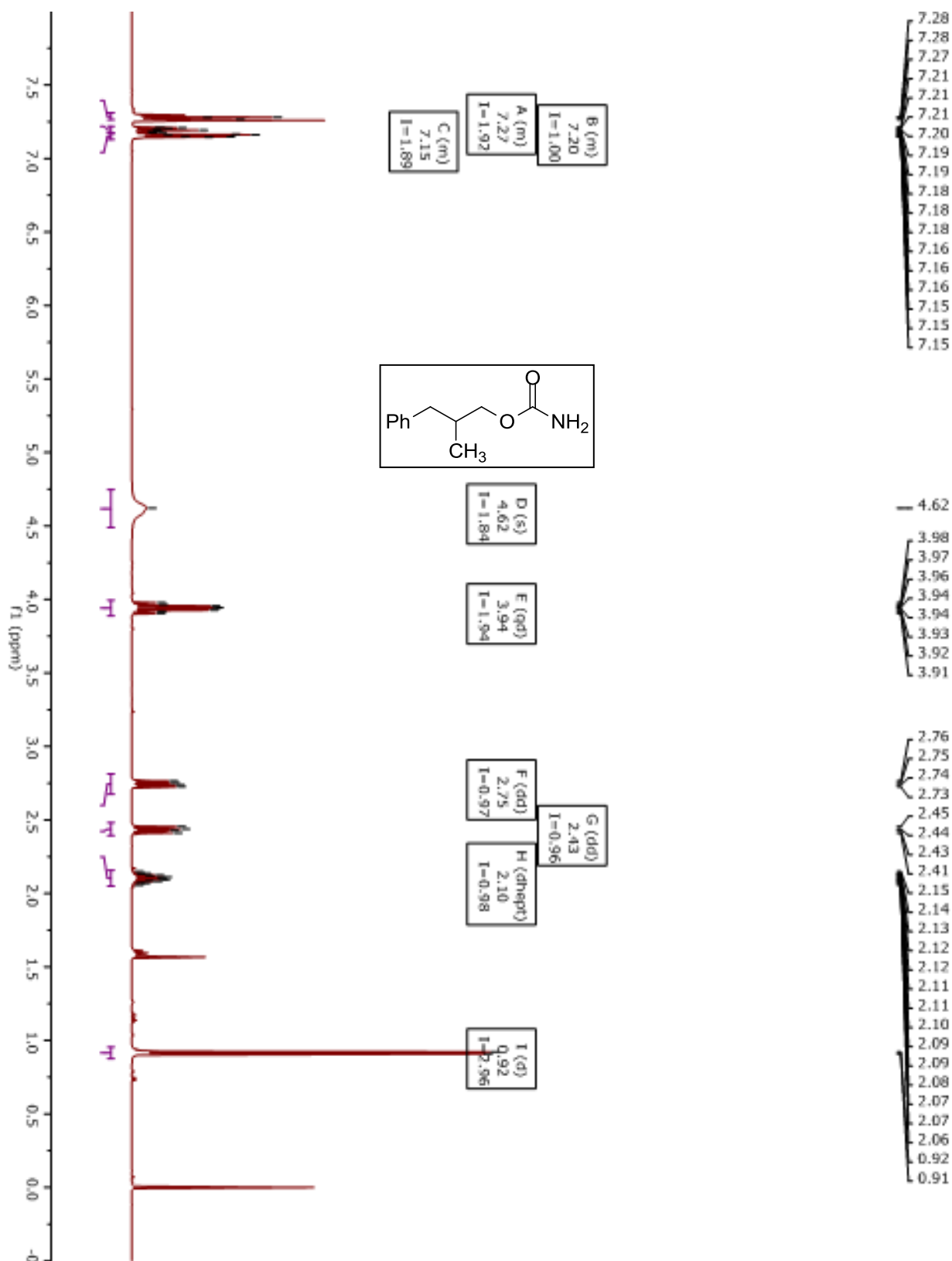
Compound 5.20e.



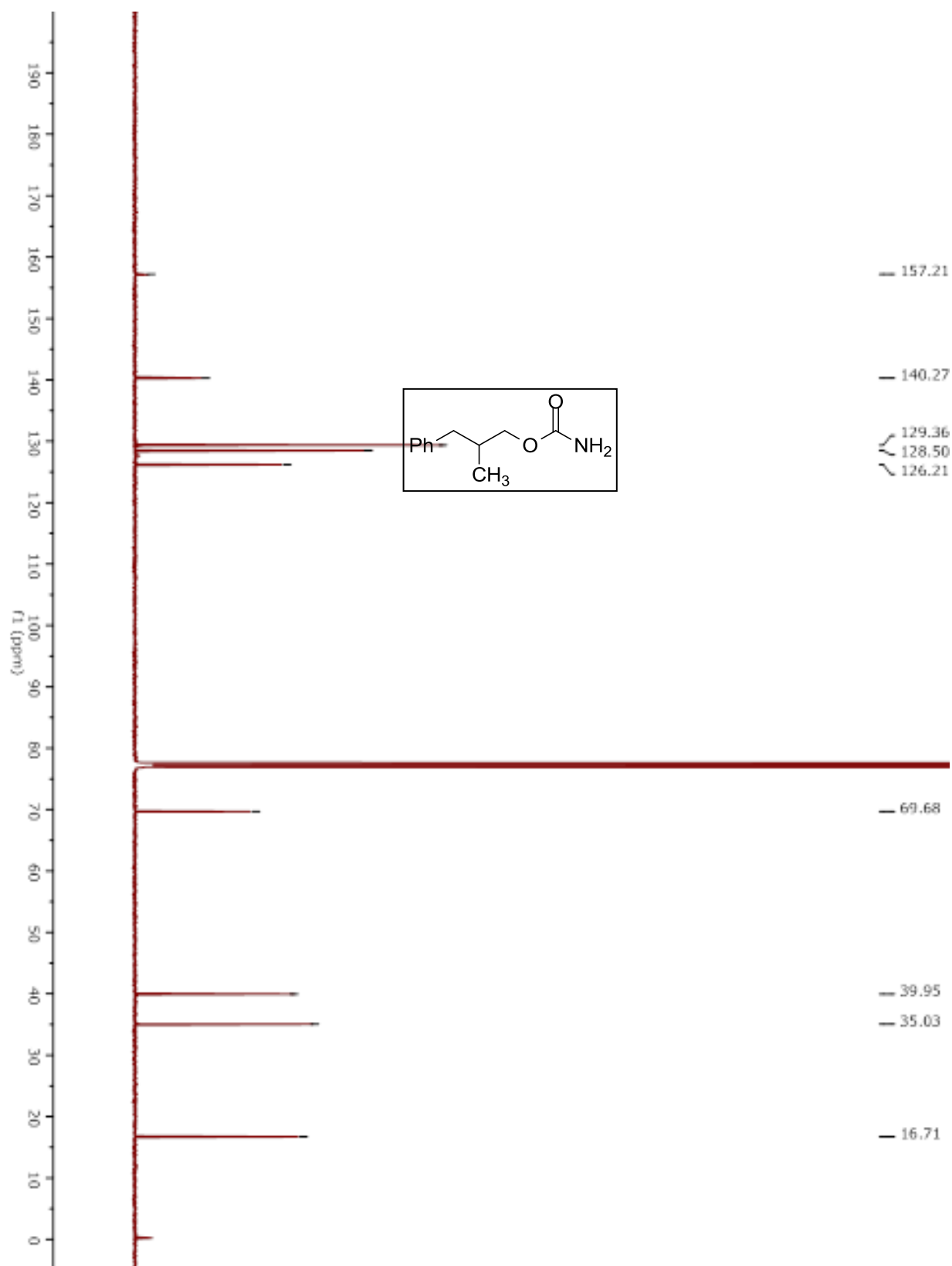
Compound 5.20e.



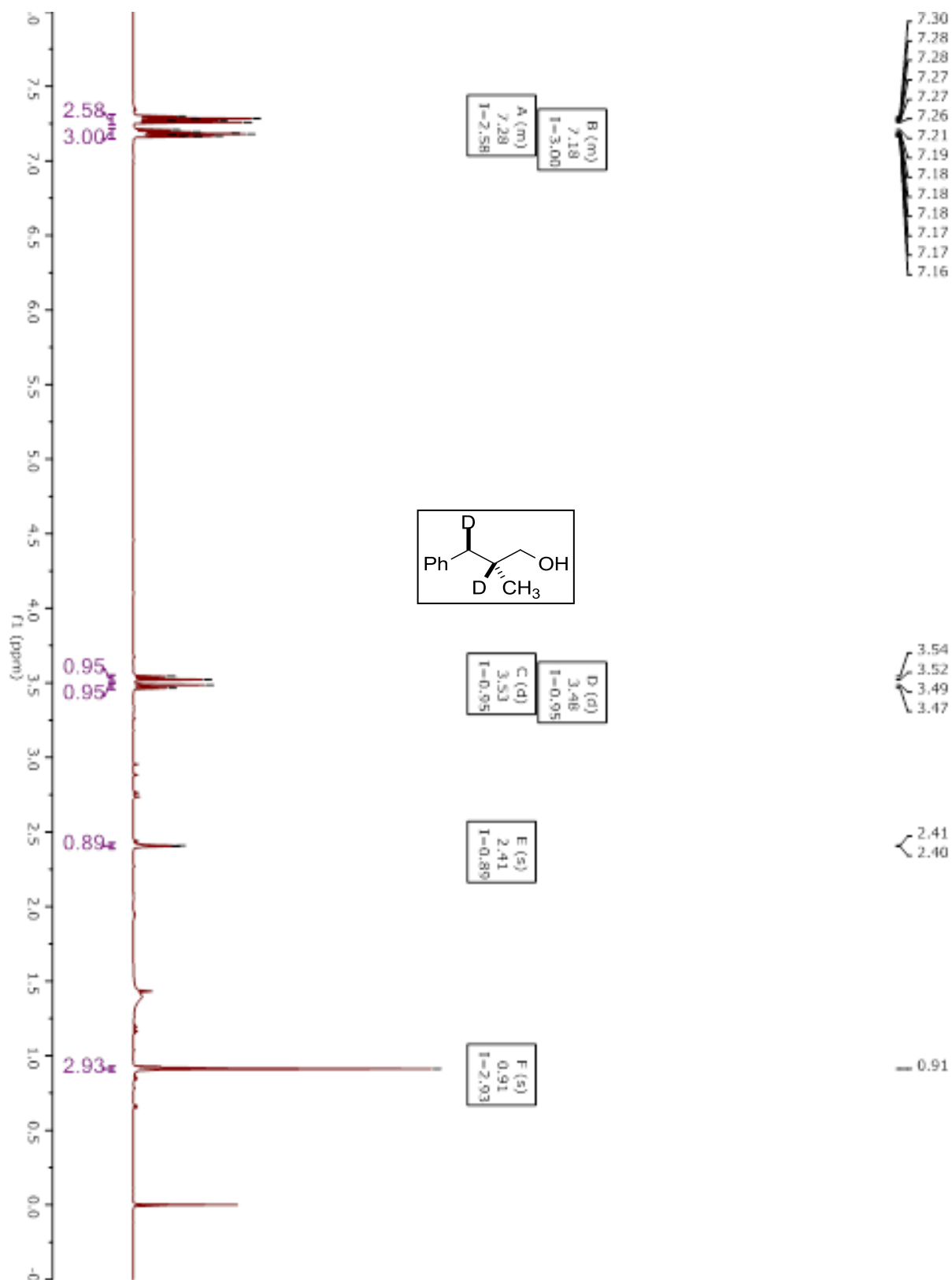
Compound 5.33-H.



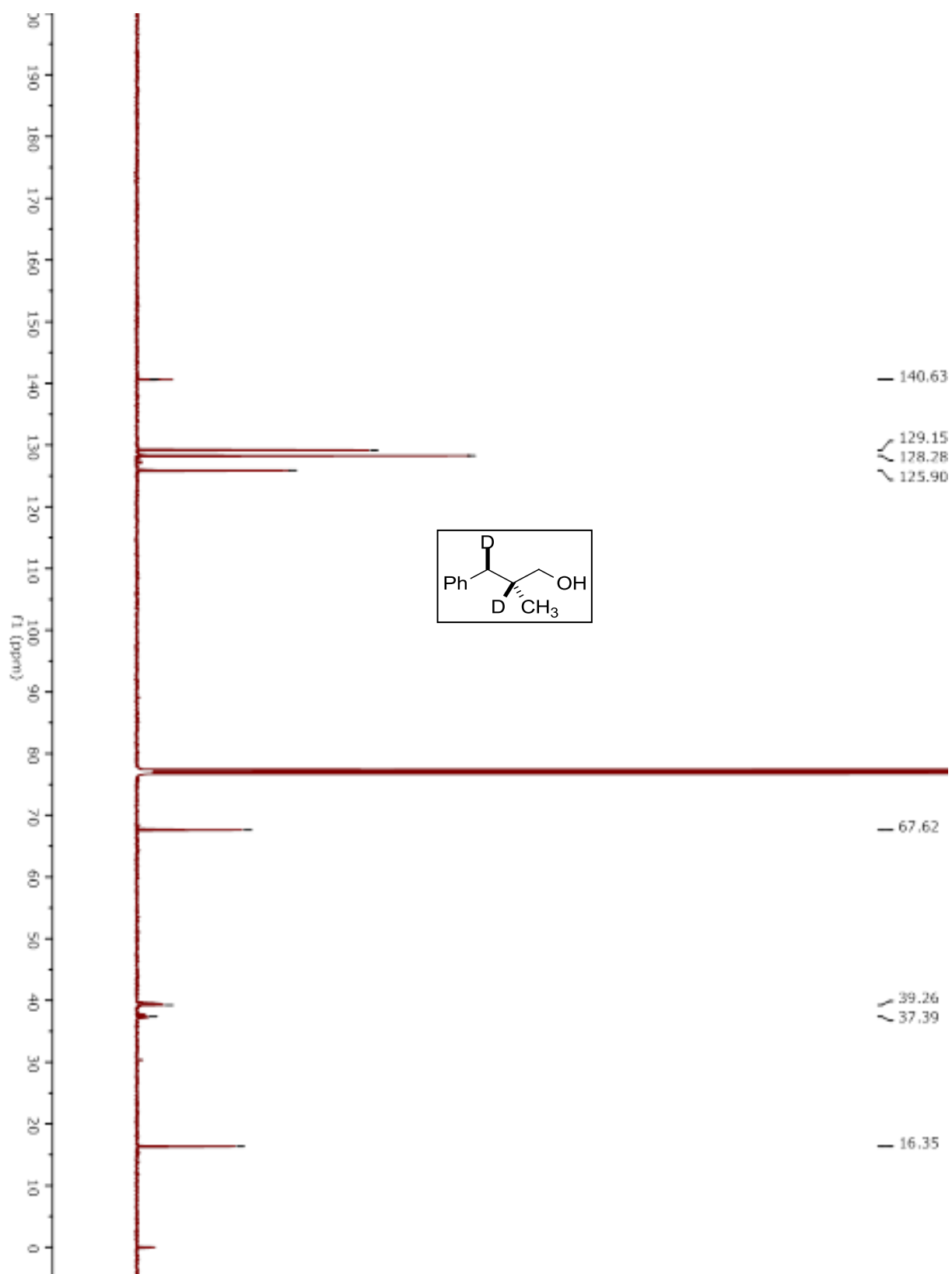
Compound 25-H.



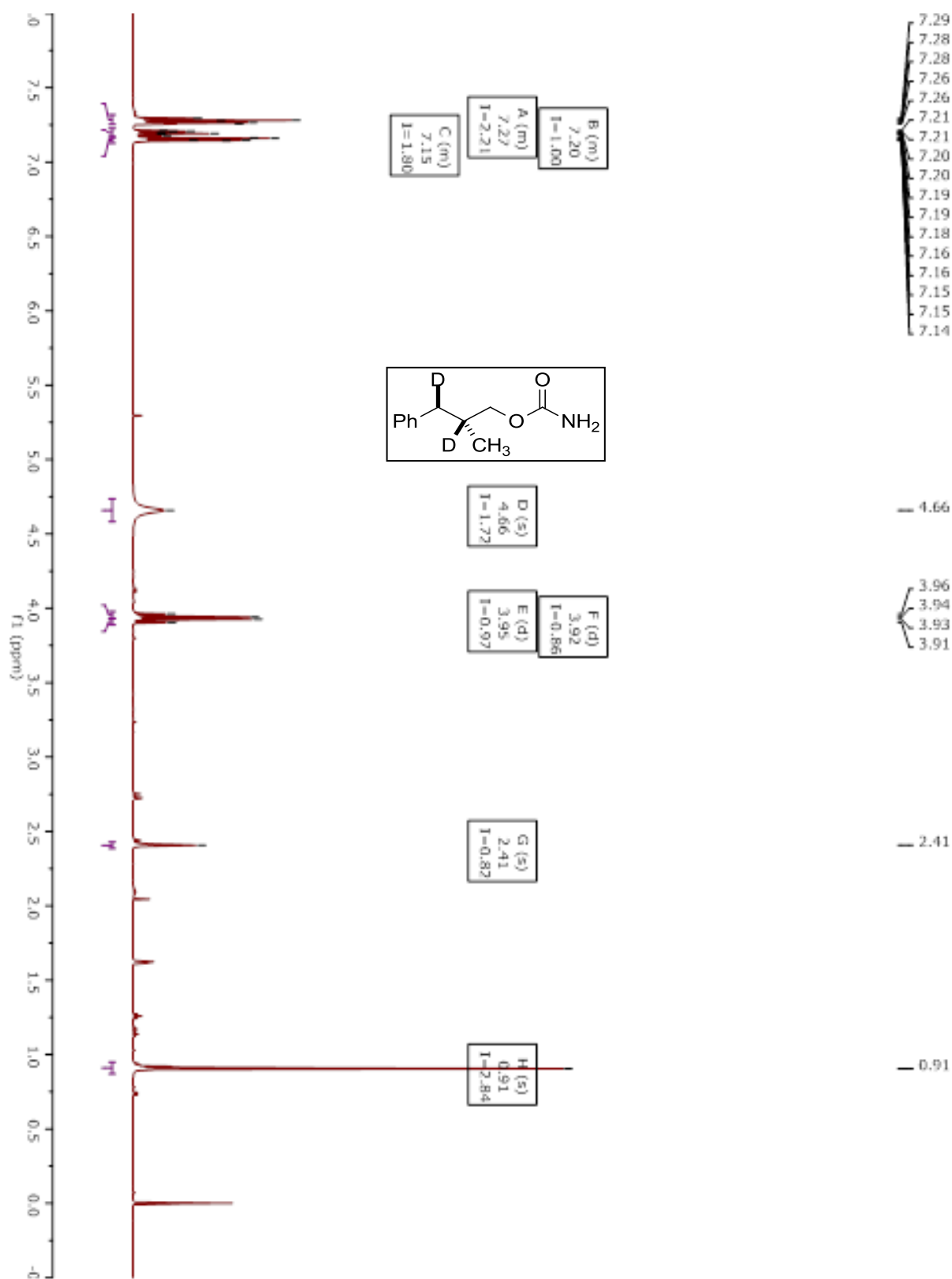
Compound S5.6-D.



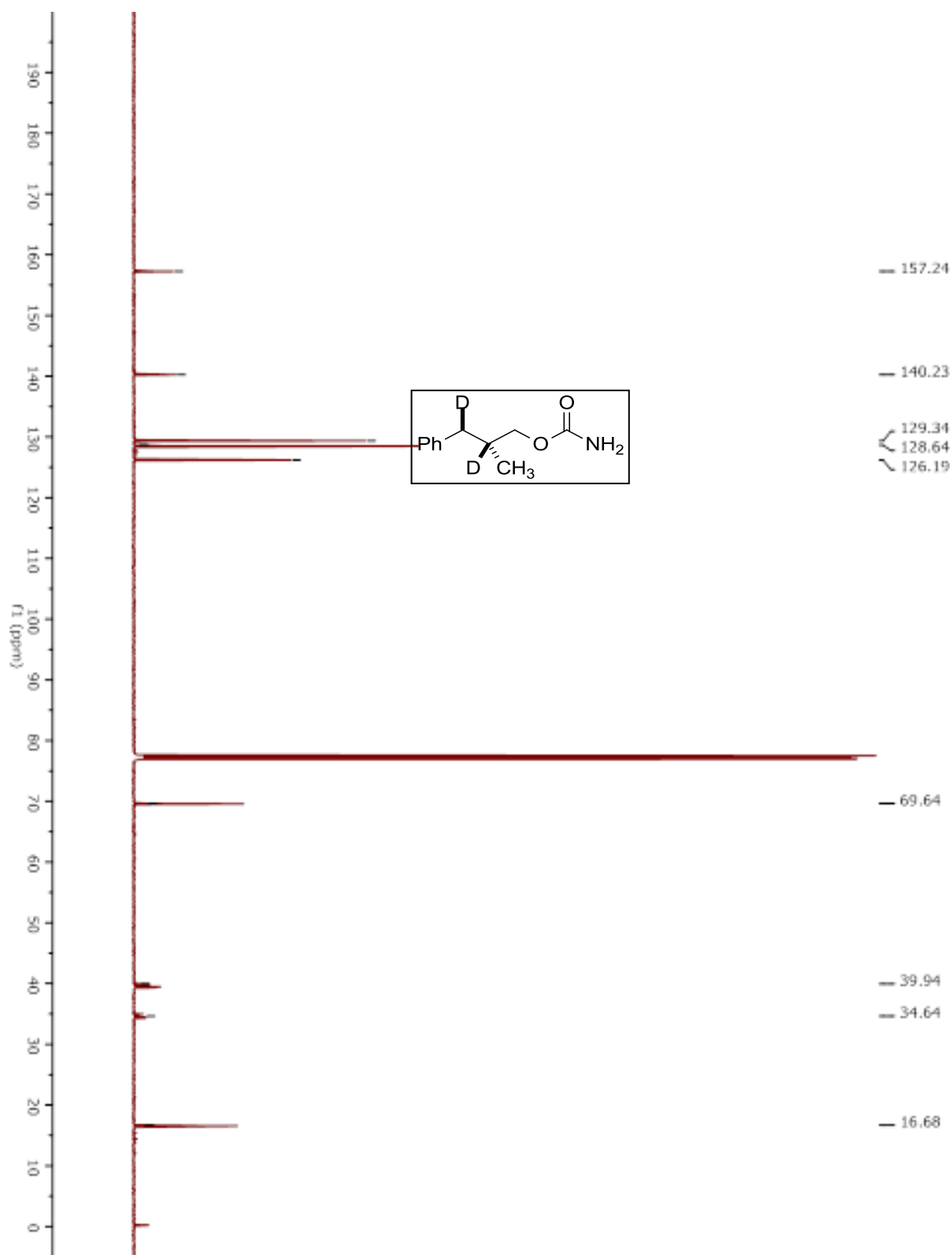
Compound S6-D.



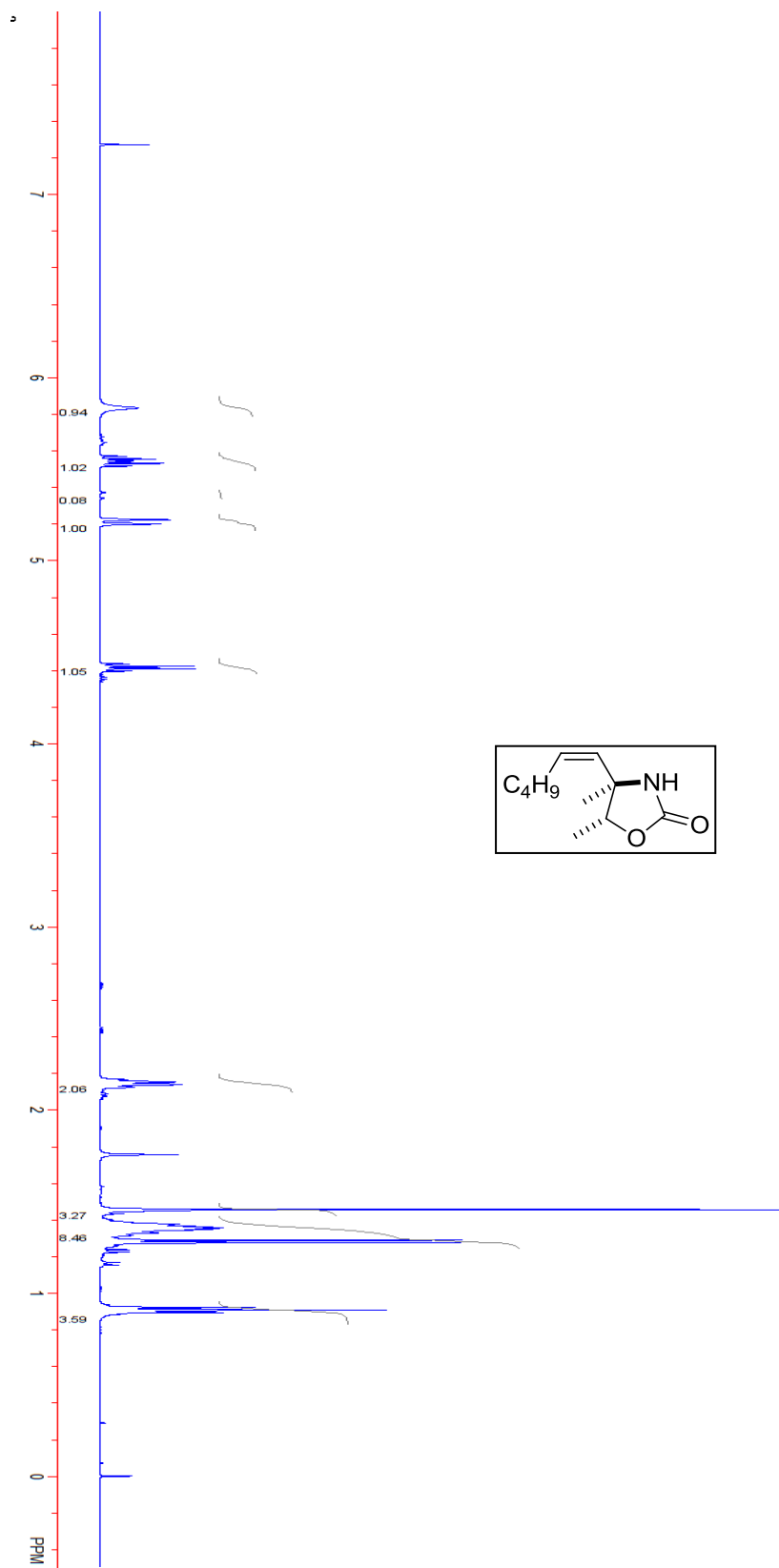
Compound 5.33-D.



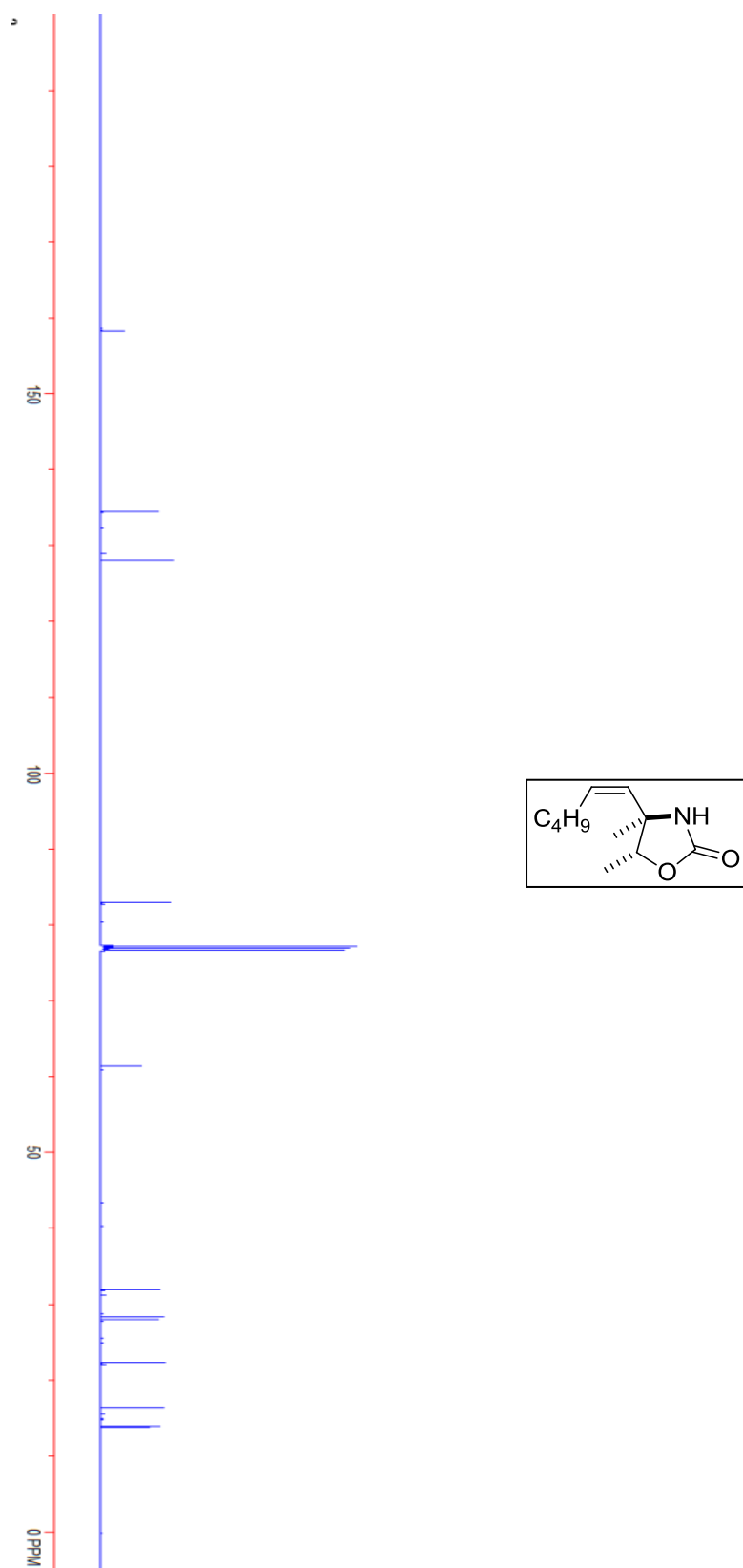
Compound 5.33-D.



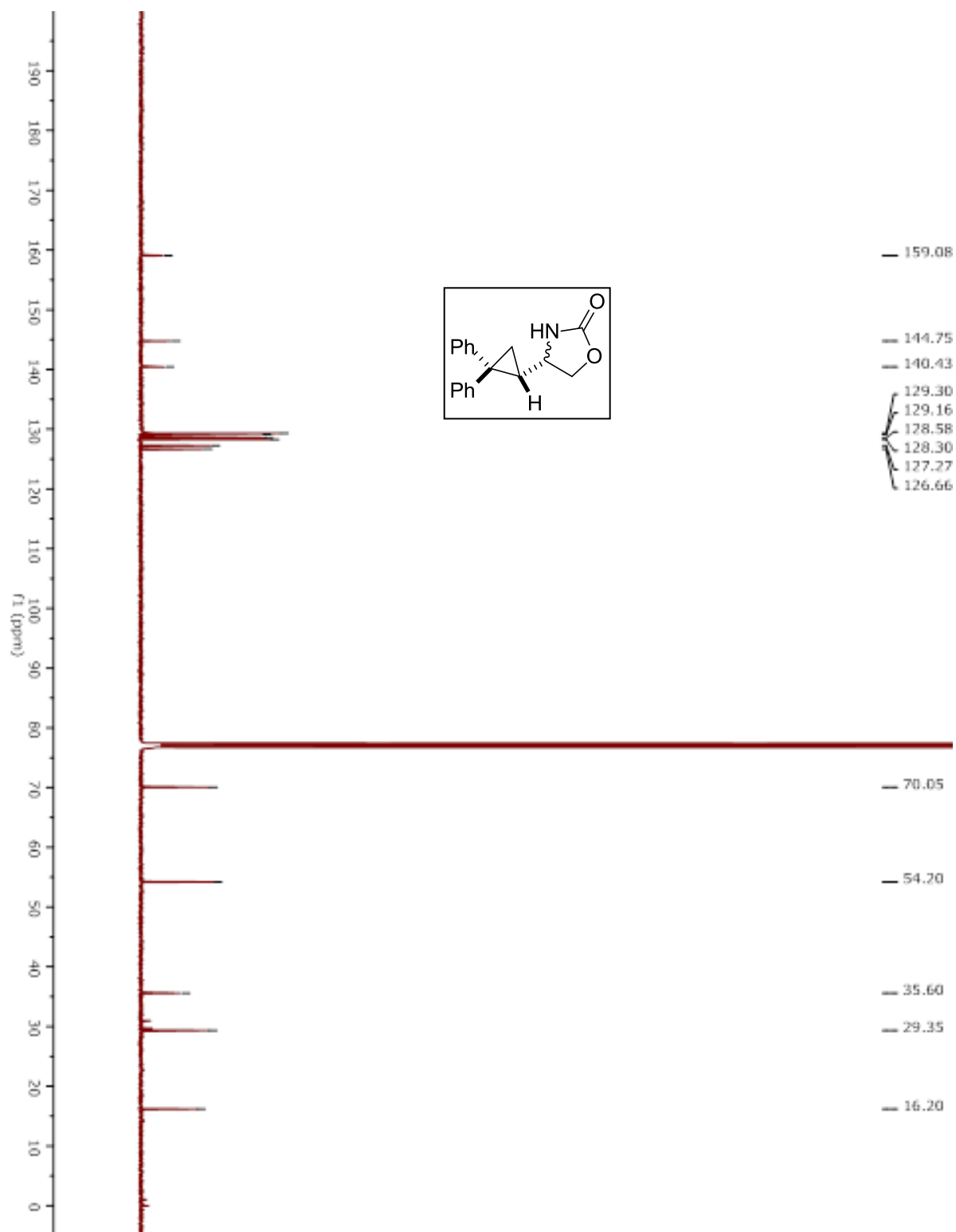
Compound 5.14a.



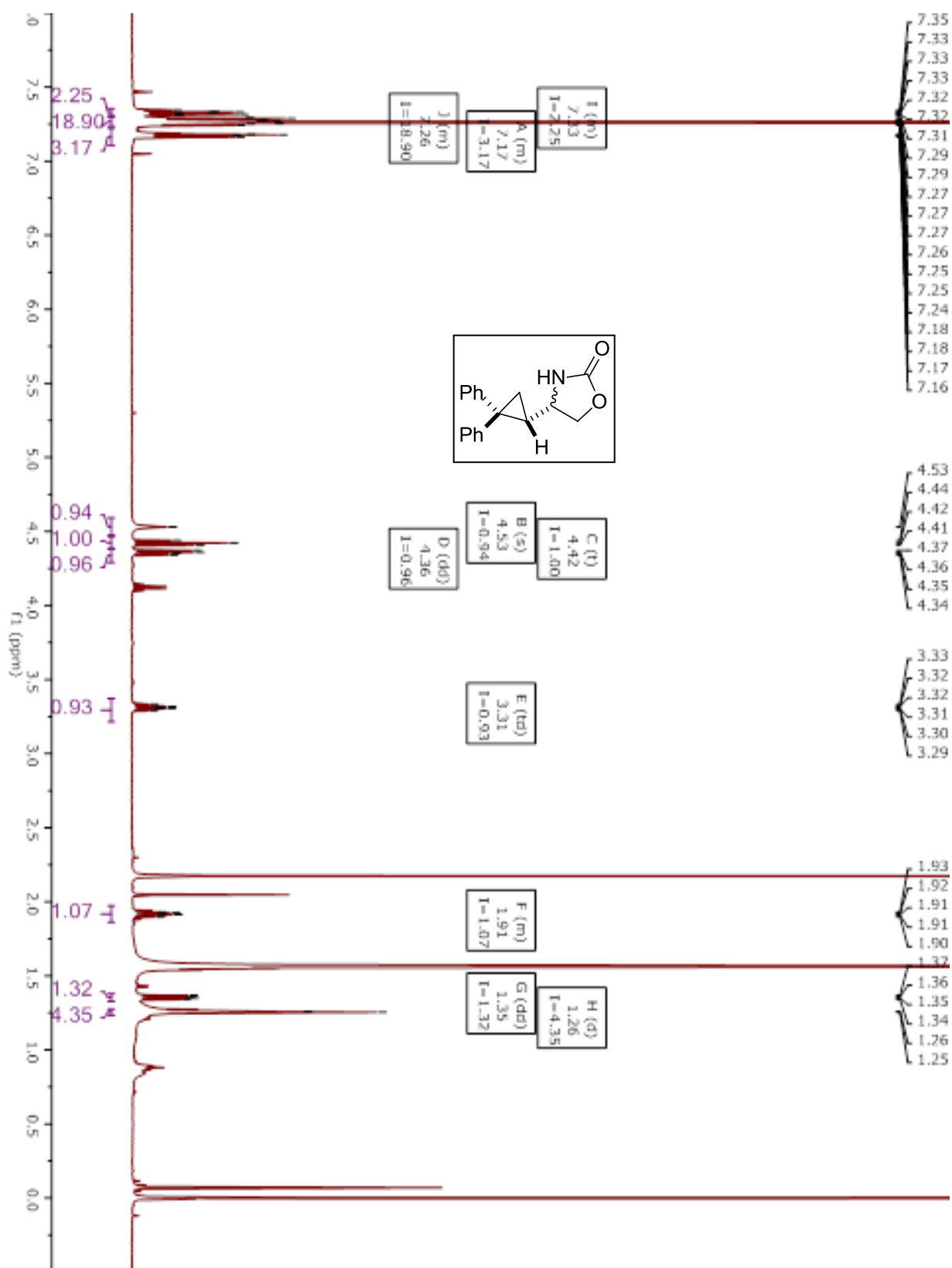
Compound 5.14a.



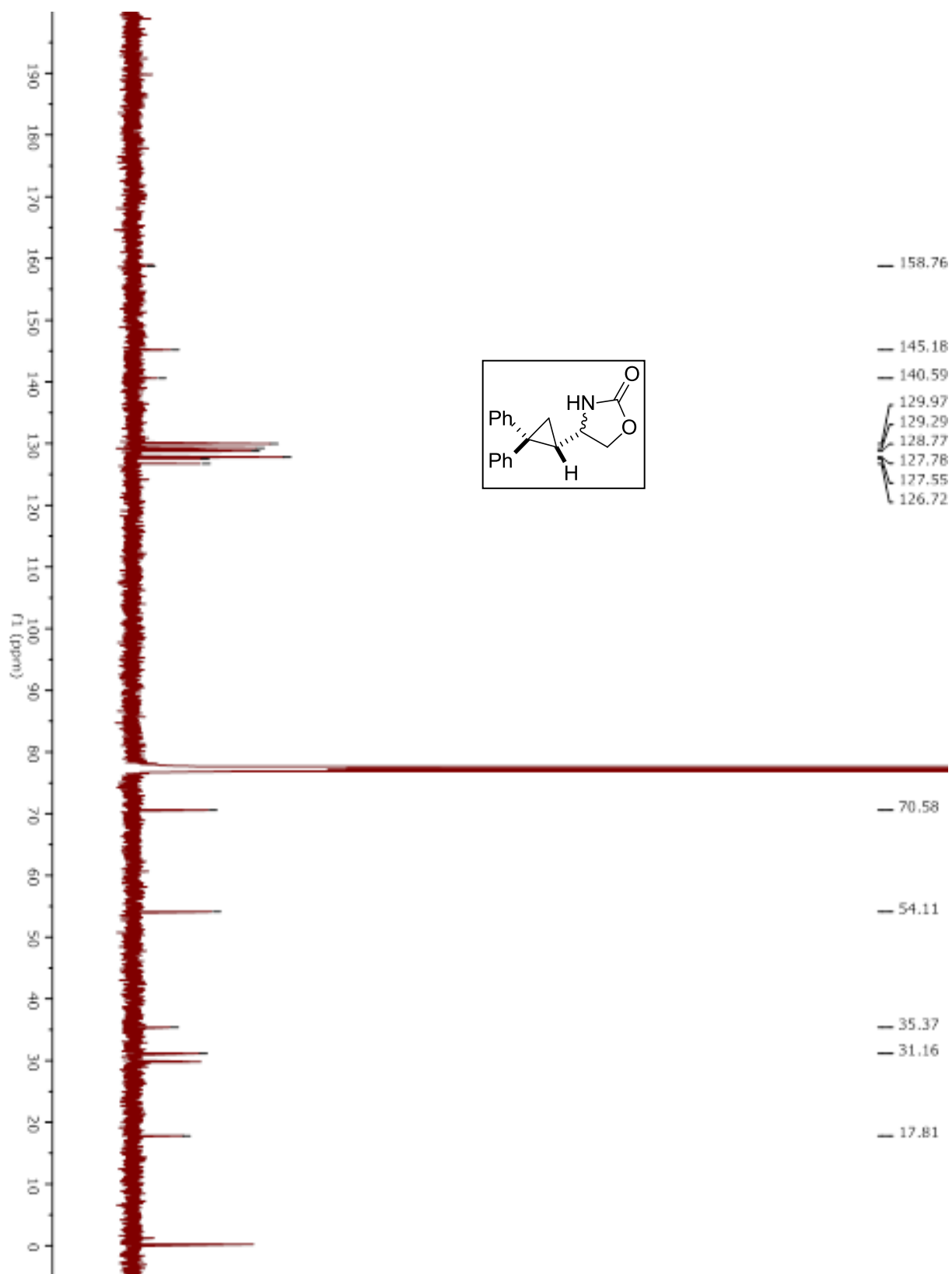
Compound 5.15. Major diastereomer.



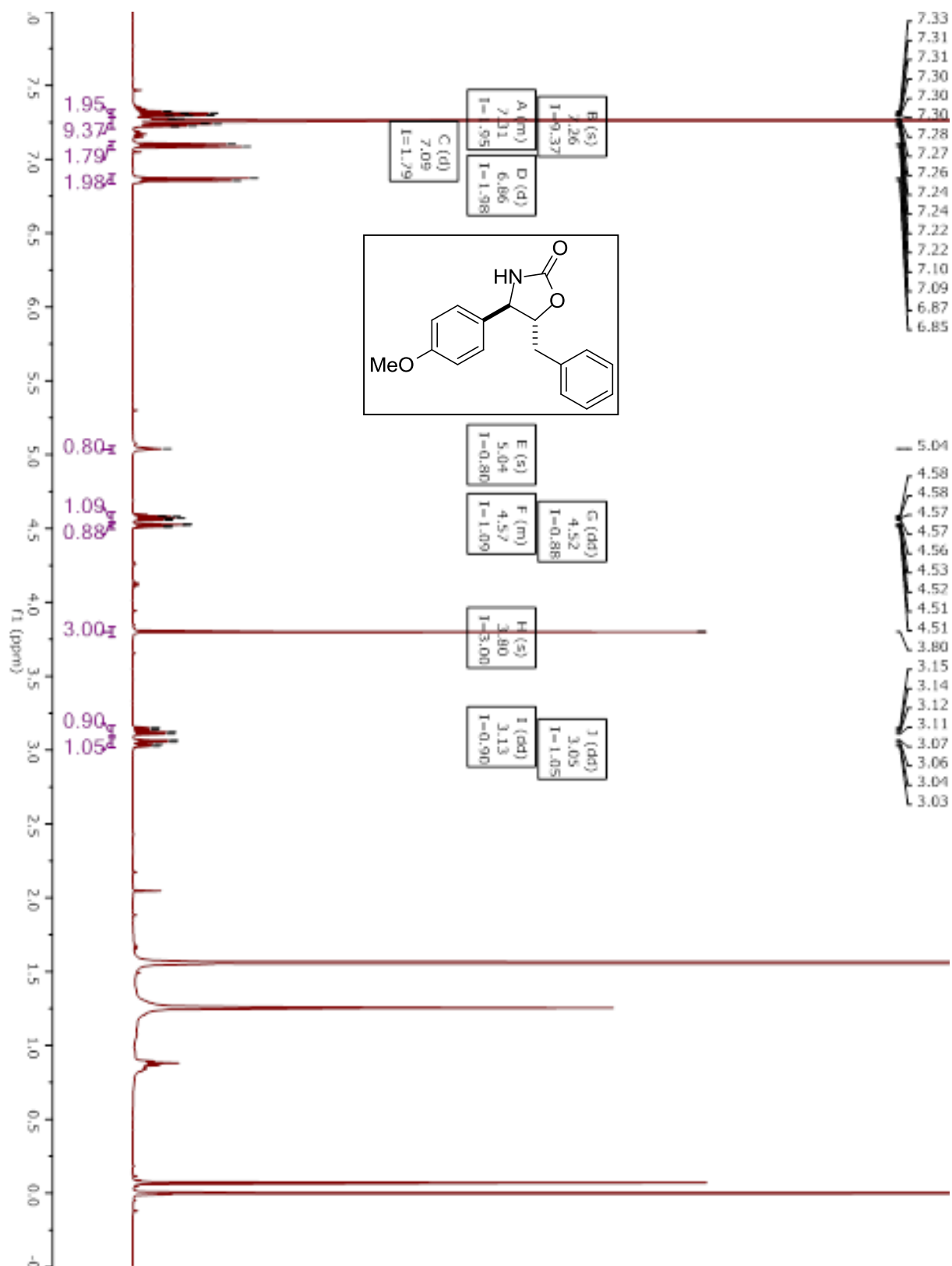
Compound 5.15. Minor diastereomer.



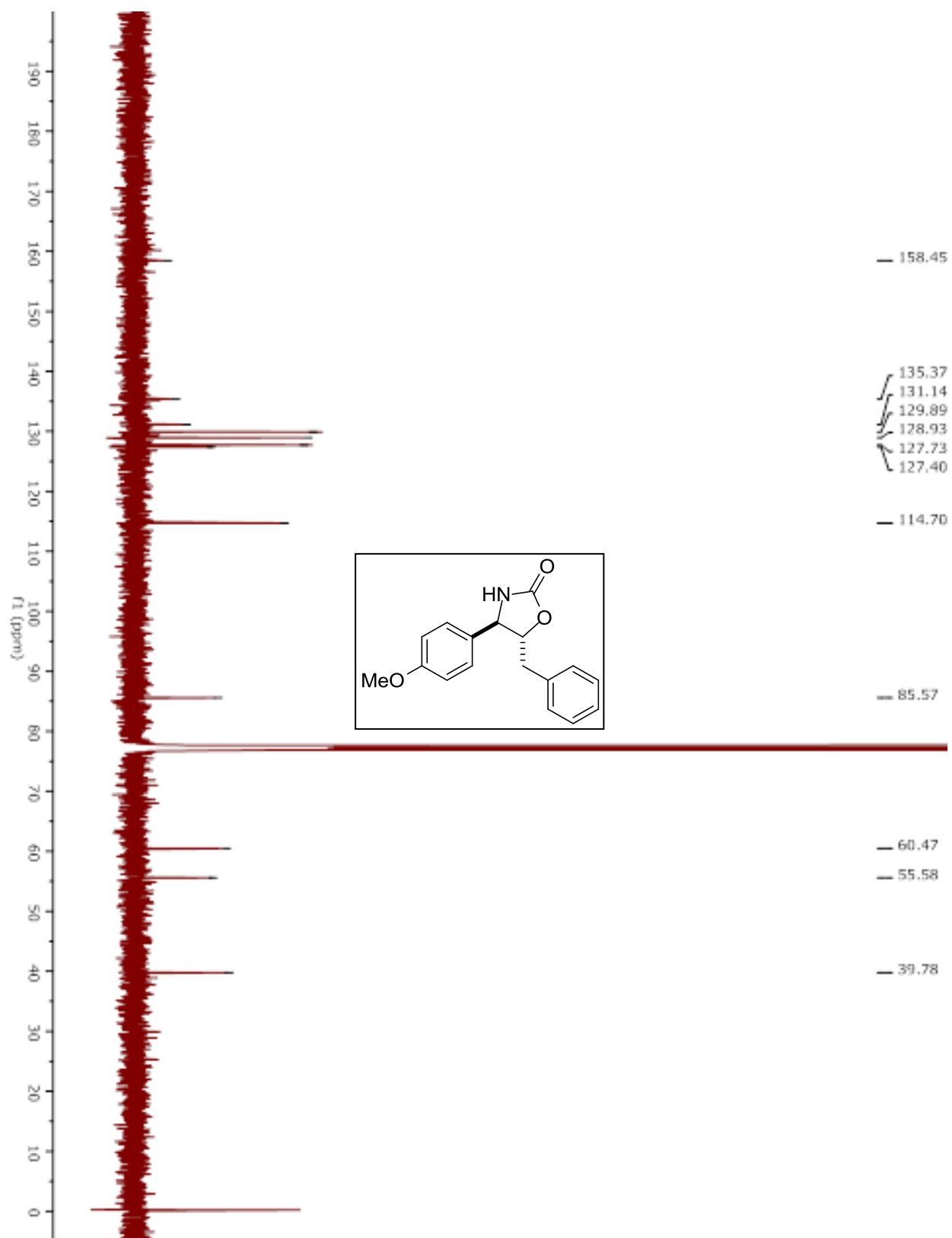
Compound 5.15. Minor diastereomer.



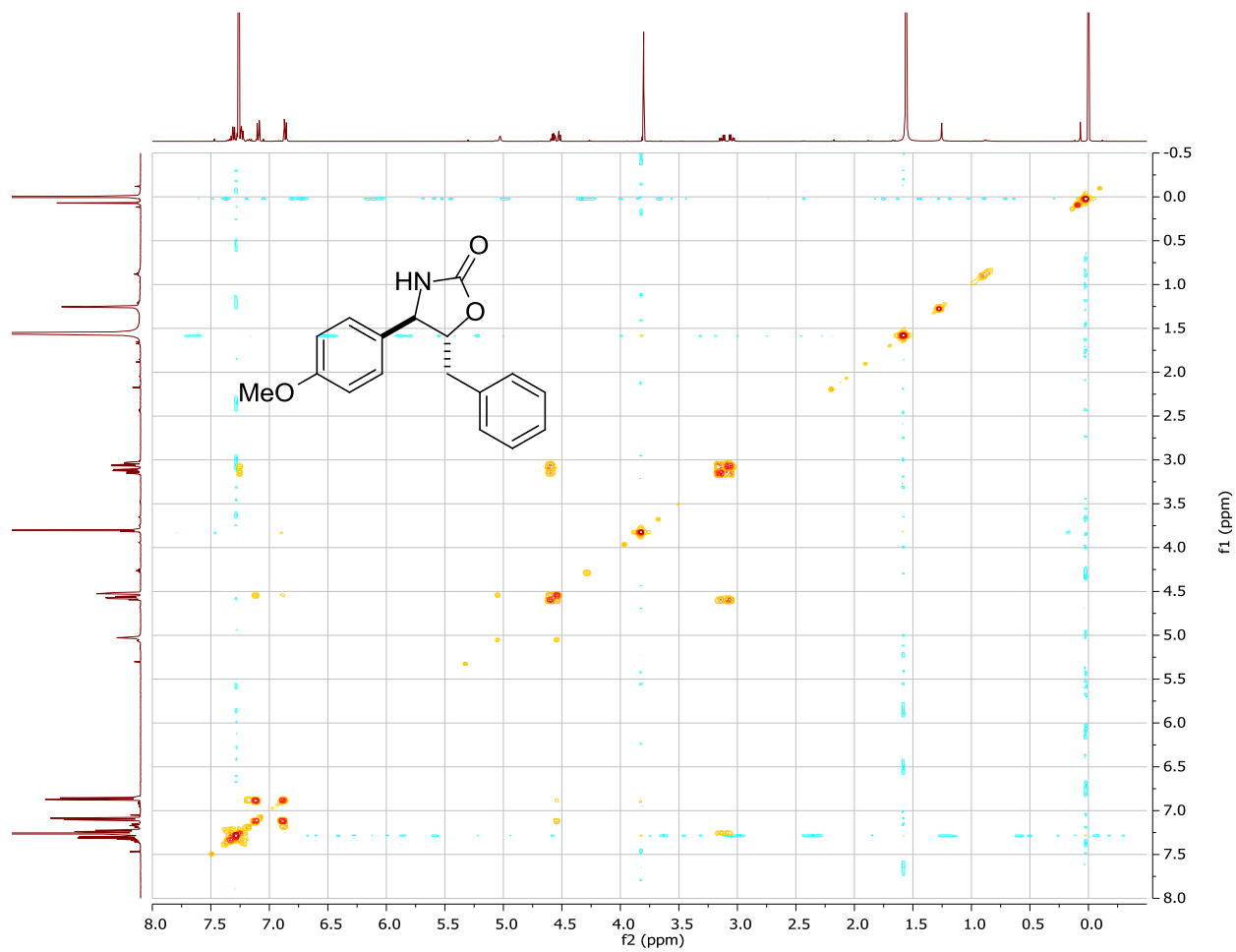
Compound 5.22aa.



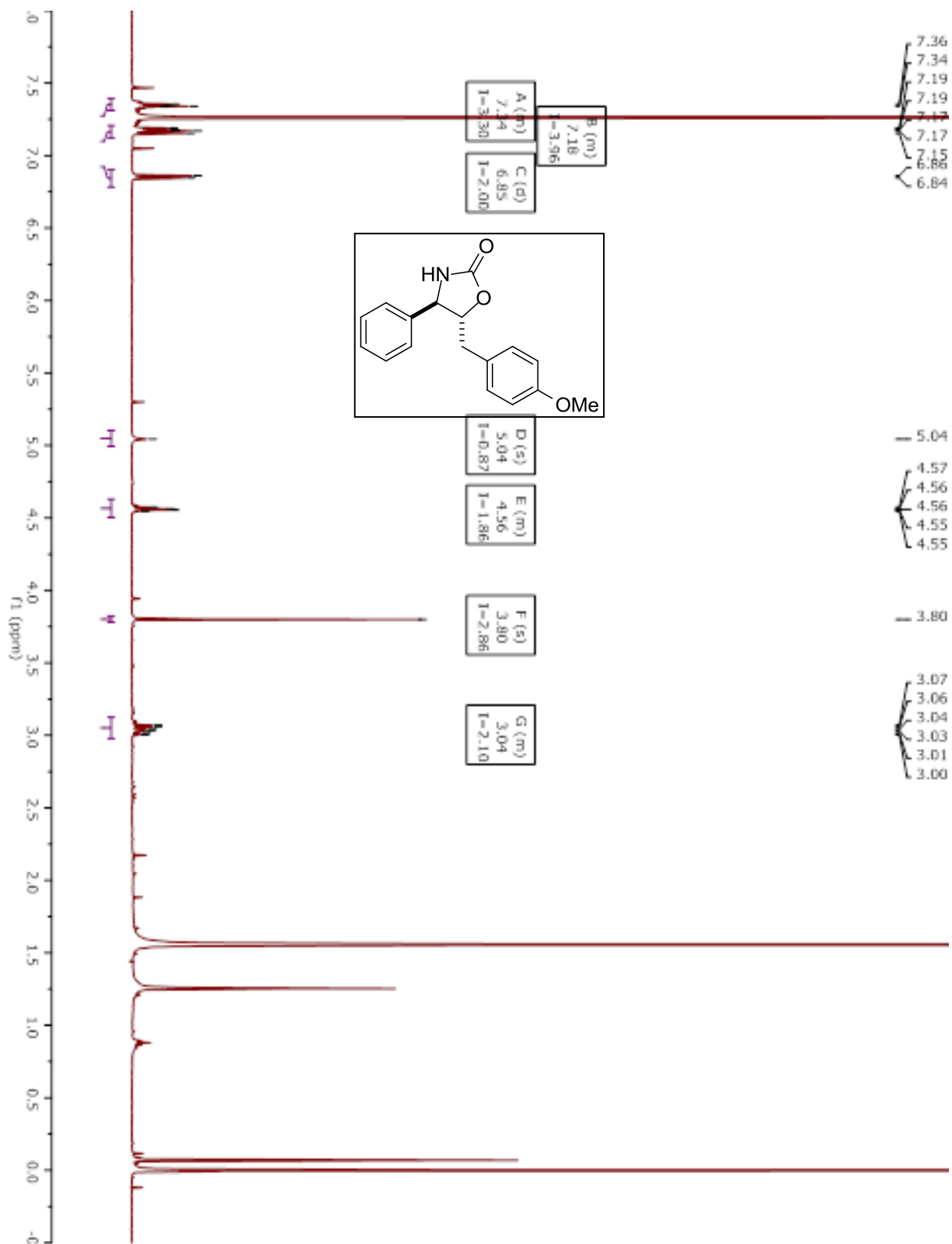
Compound 5.22aa.



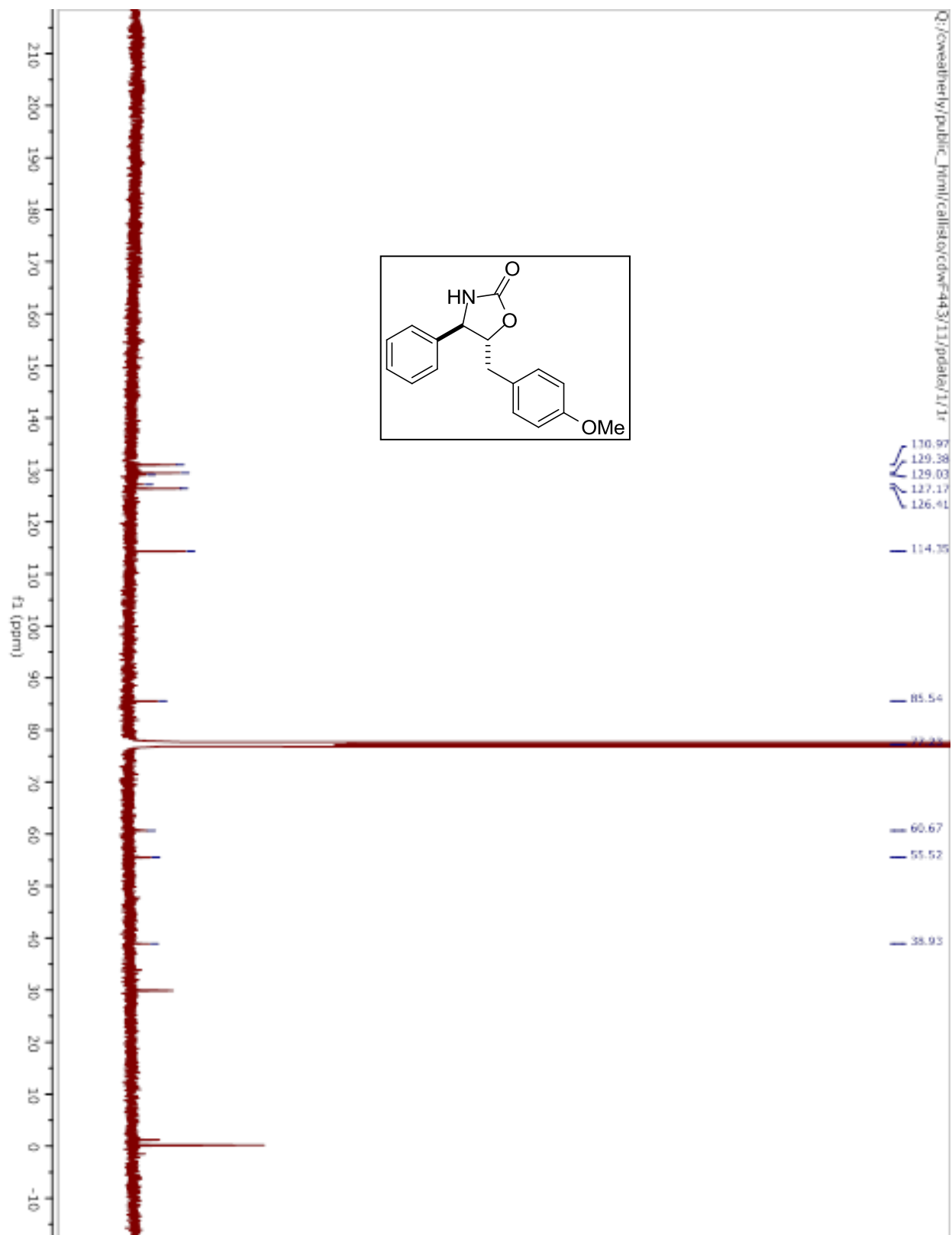
Compound 5.22aa.



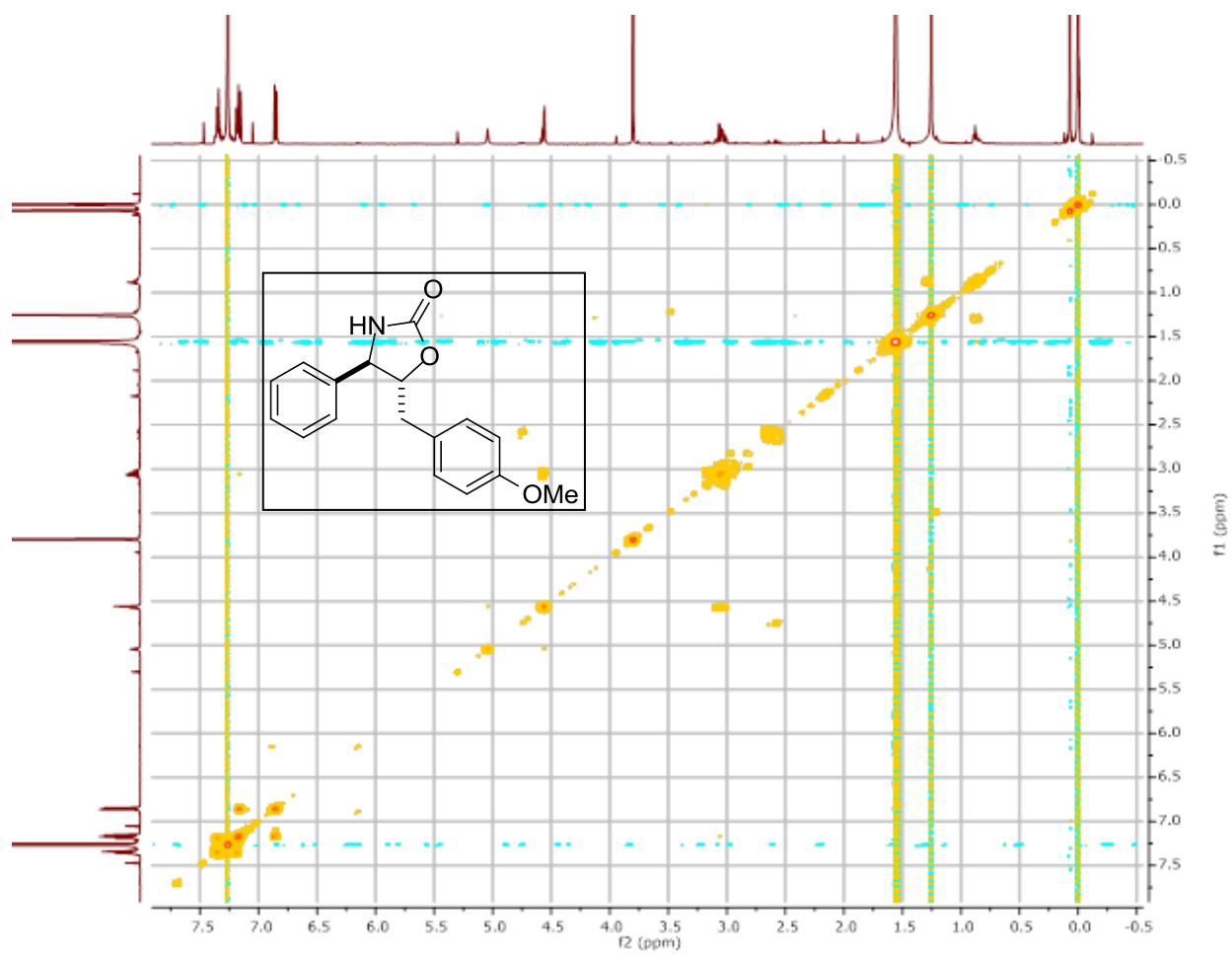
Compound 5.21a.



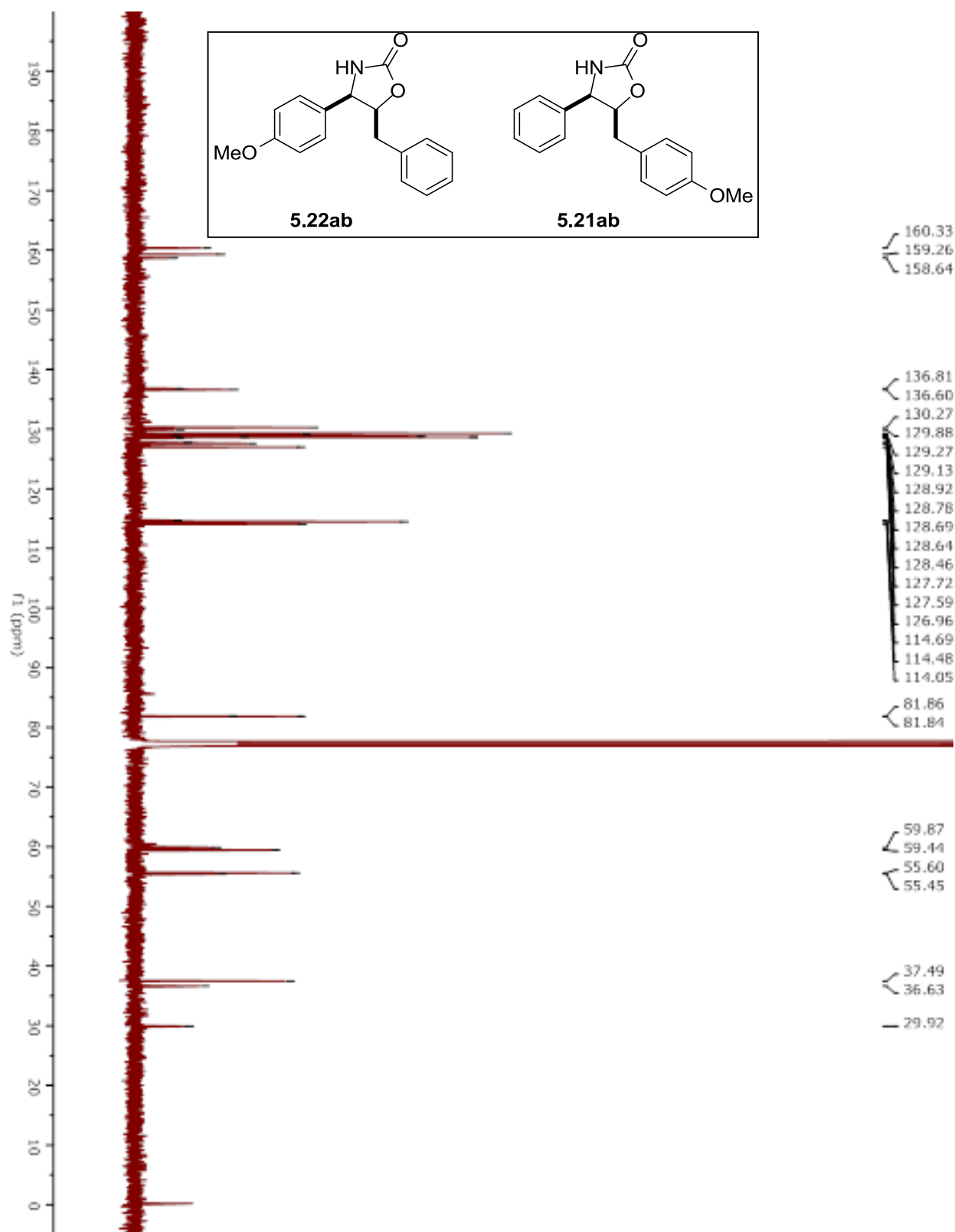
Compound 5.21aa.

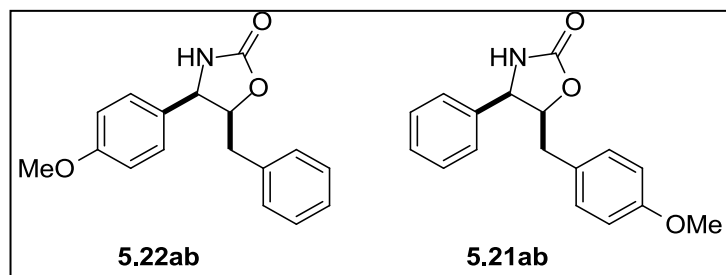
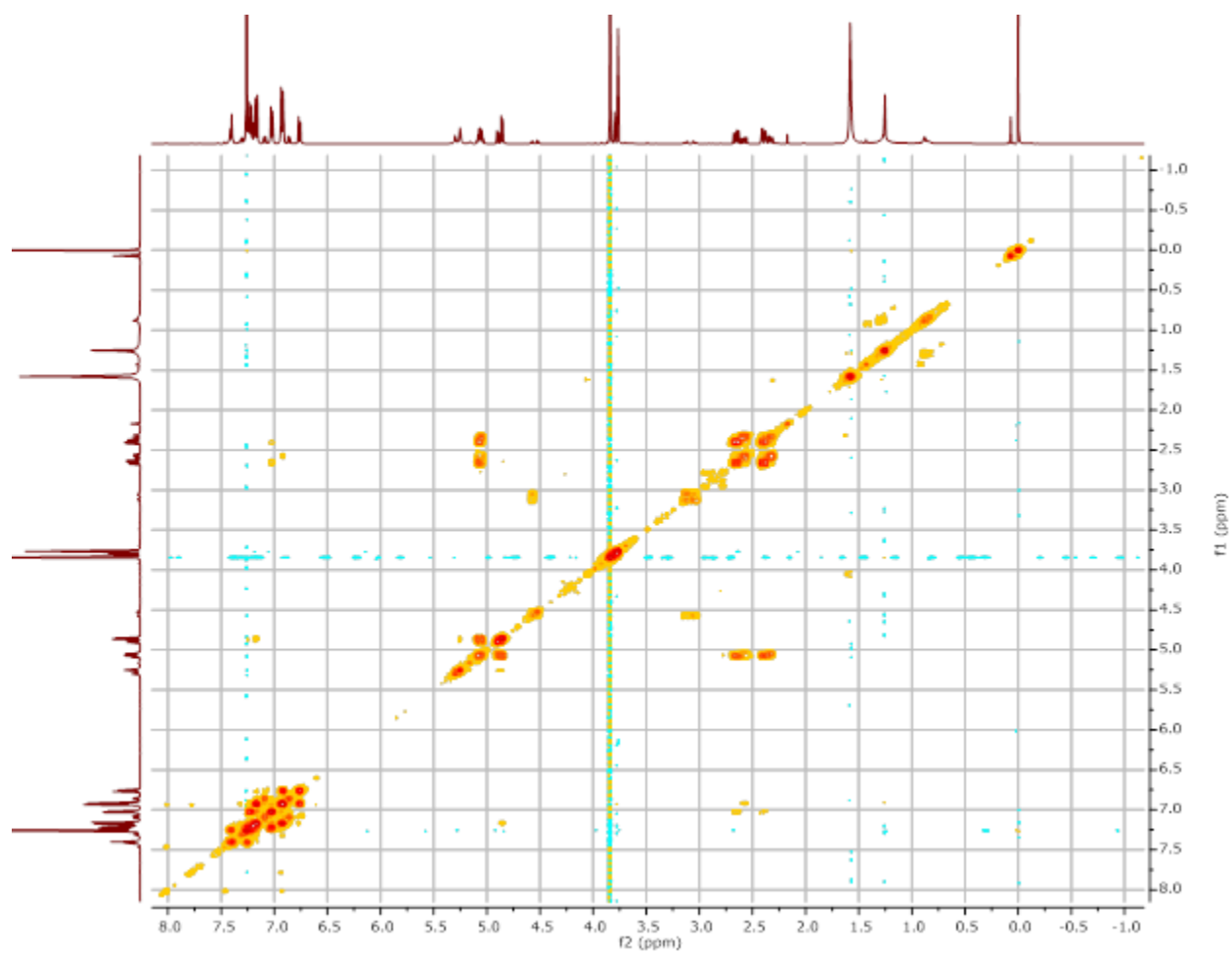


Compound 5.21aa.

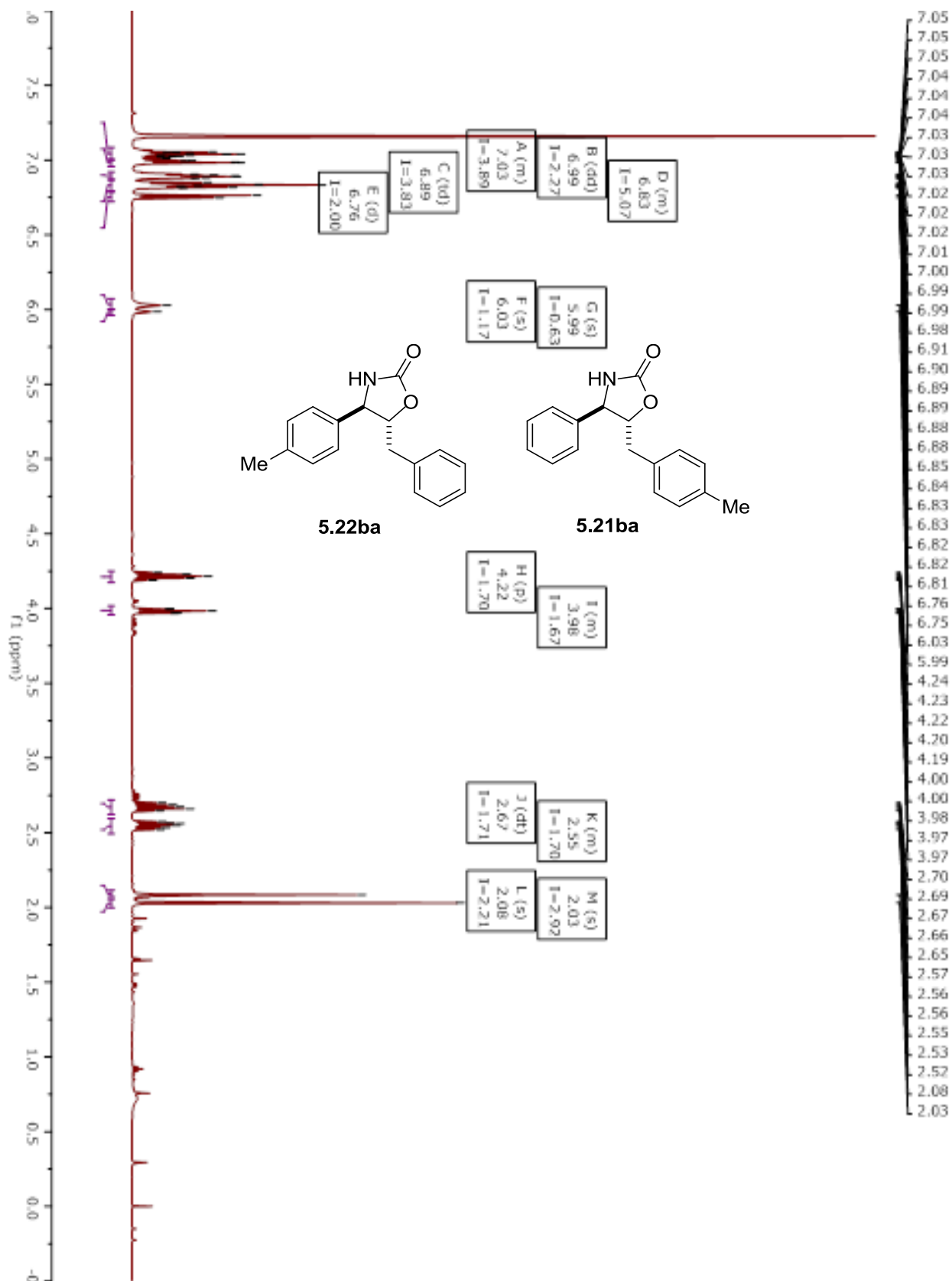


Compounds 5.21ab and 5.22ab. (mixture of regioisomers).

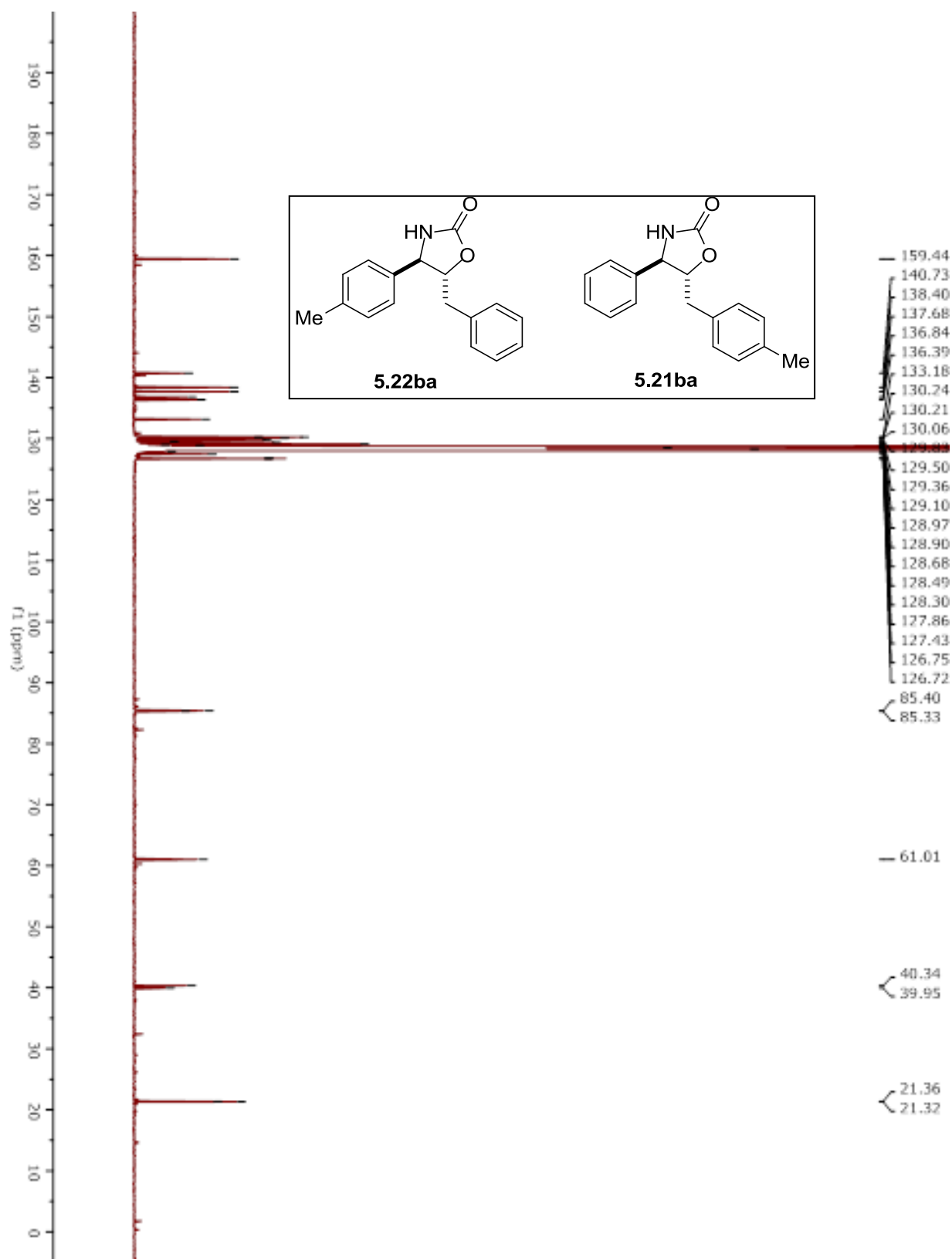


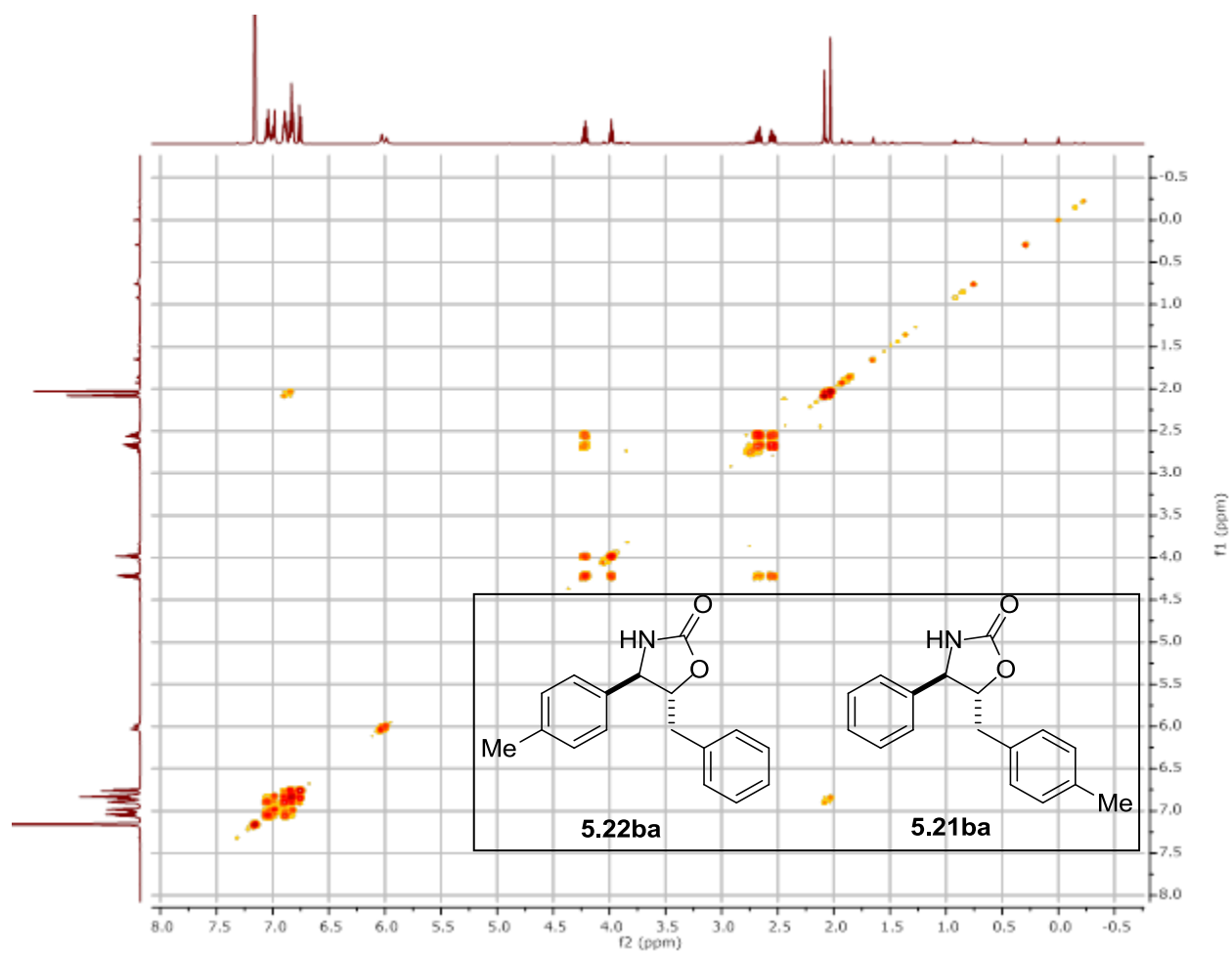
Compounds 5.21ab and 5.22ab. (mixture of isomers).

Compounds 5.21ba and 5.22ba. (mixture of regioisomers).

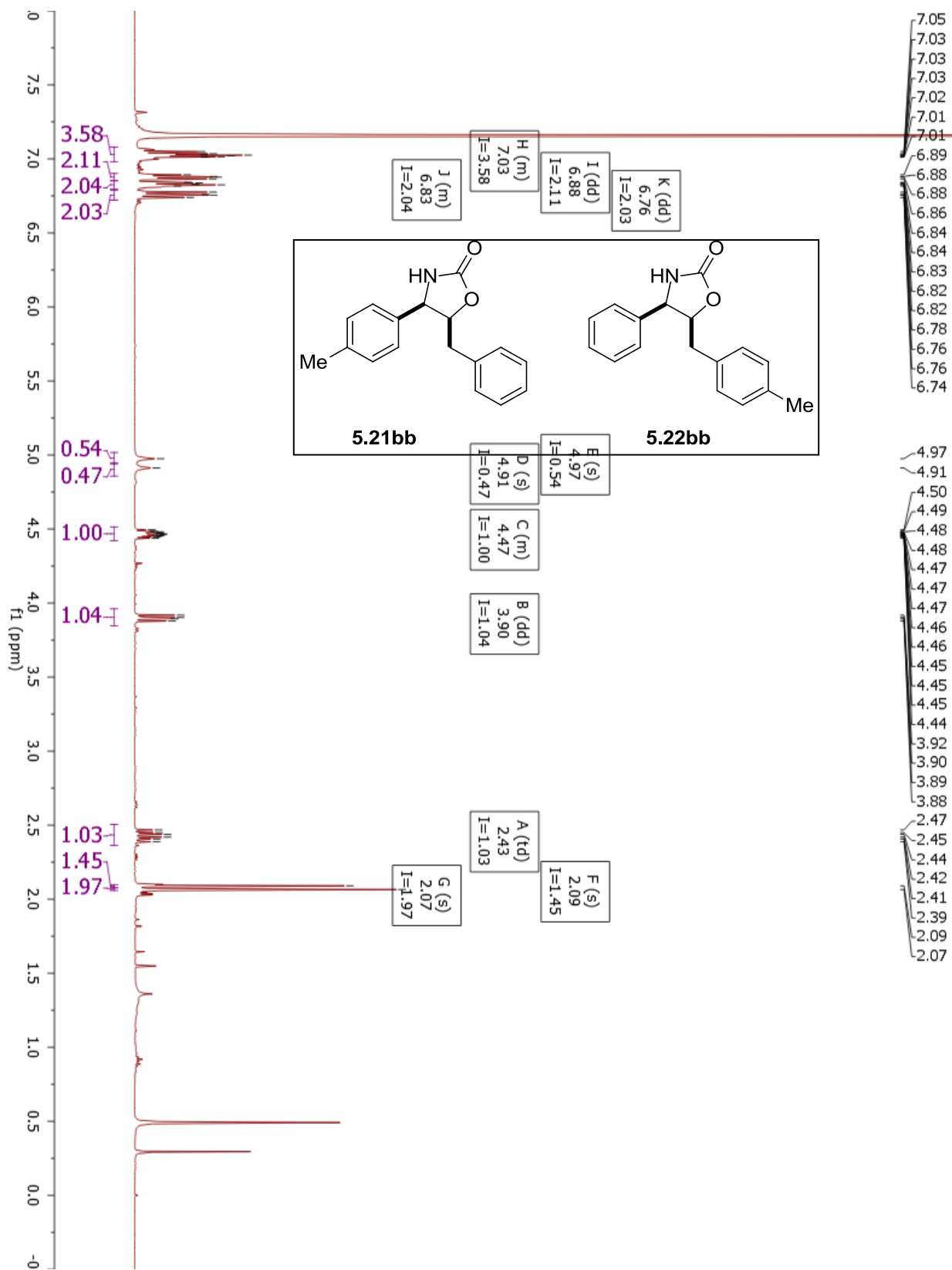


Compounds 5.21ba and 5.22ba. (mixture of regioisomers).

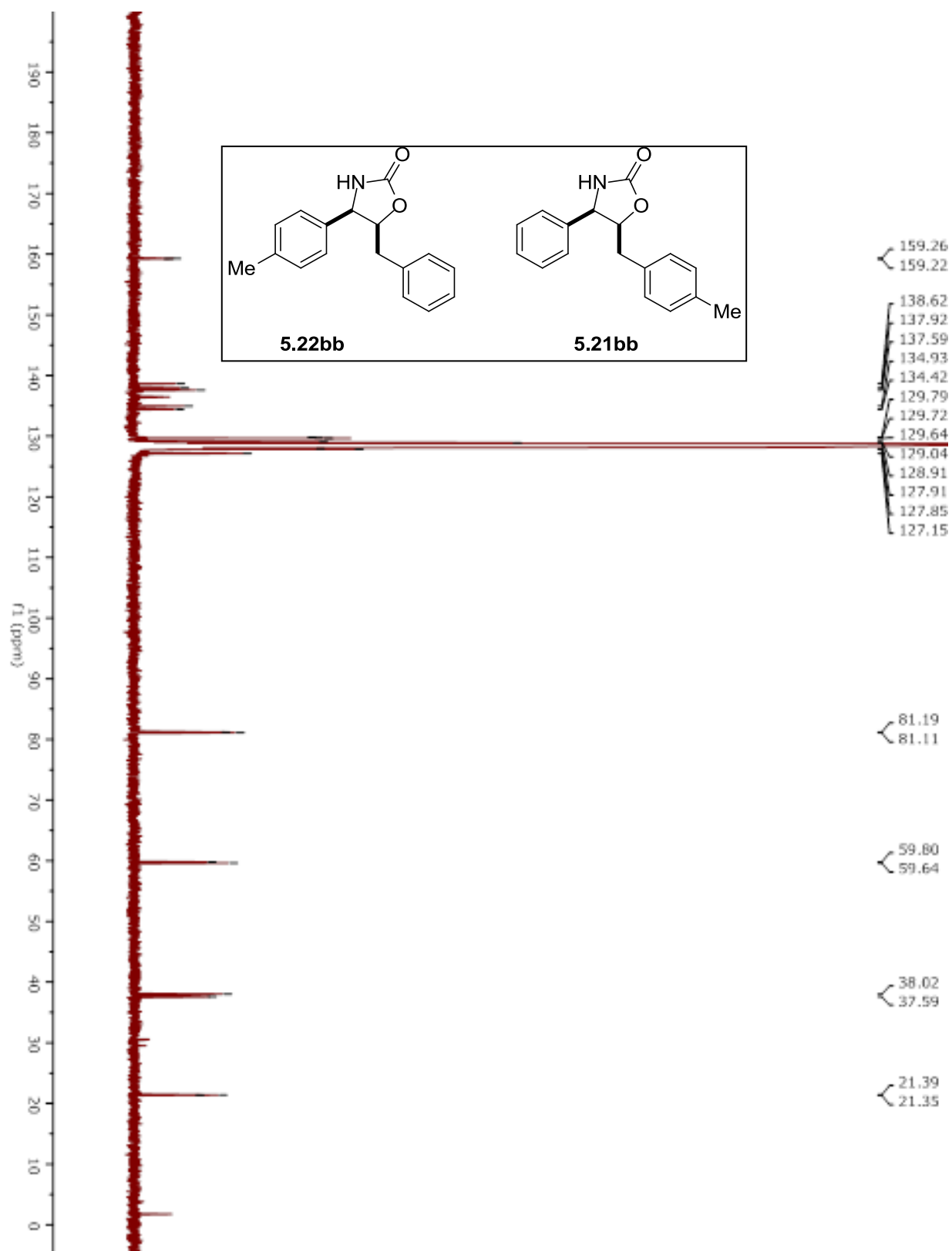


Compounds 5.21ba and 5.22ba. (mixture of regioisomers).

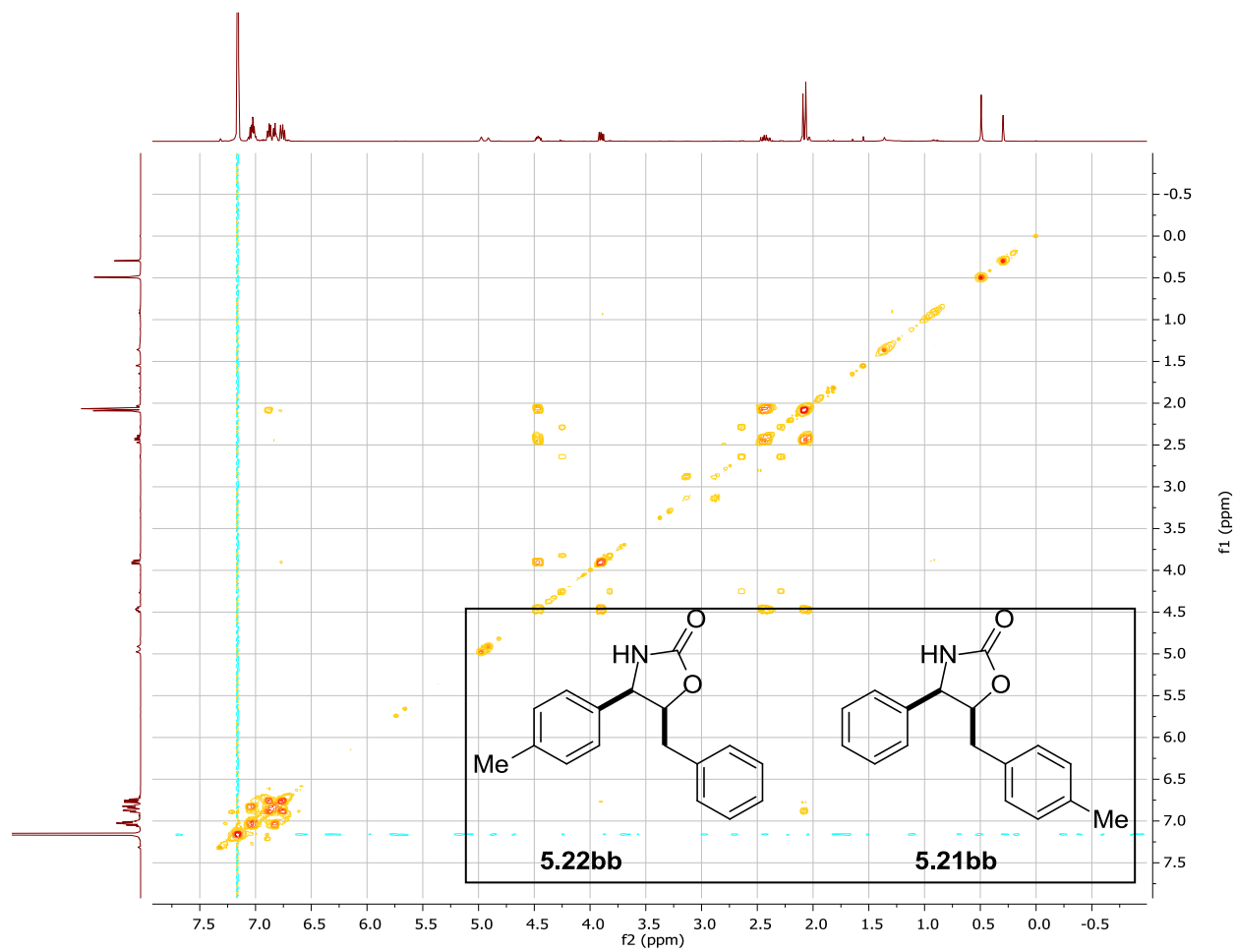
Compound 5.21bb and 5.22bb. (mixture of regioisomers).



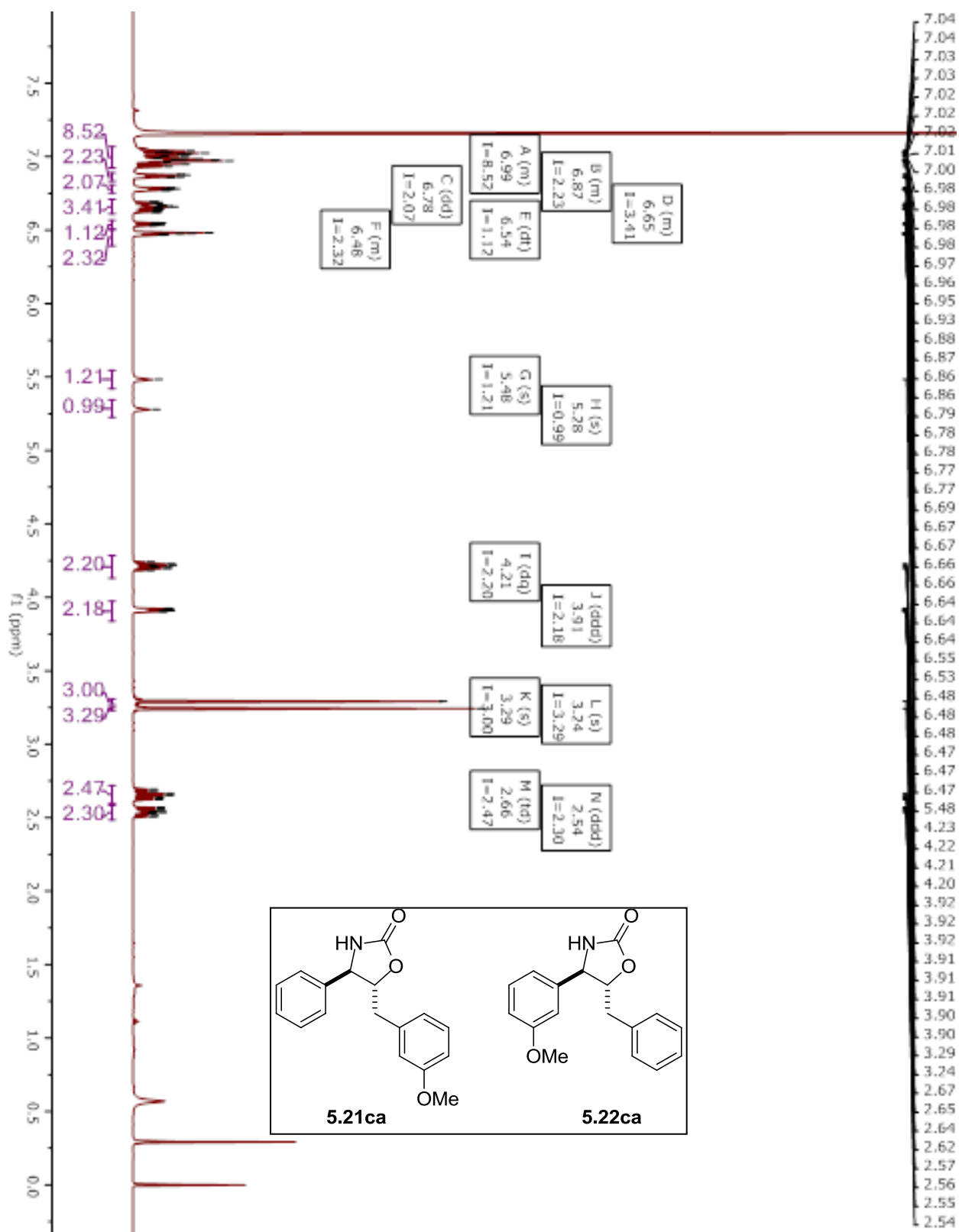
Compound 5.21bb and 5.22bb. (mixture of regioisomers).



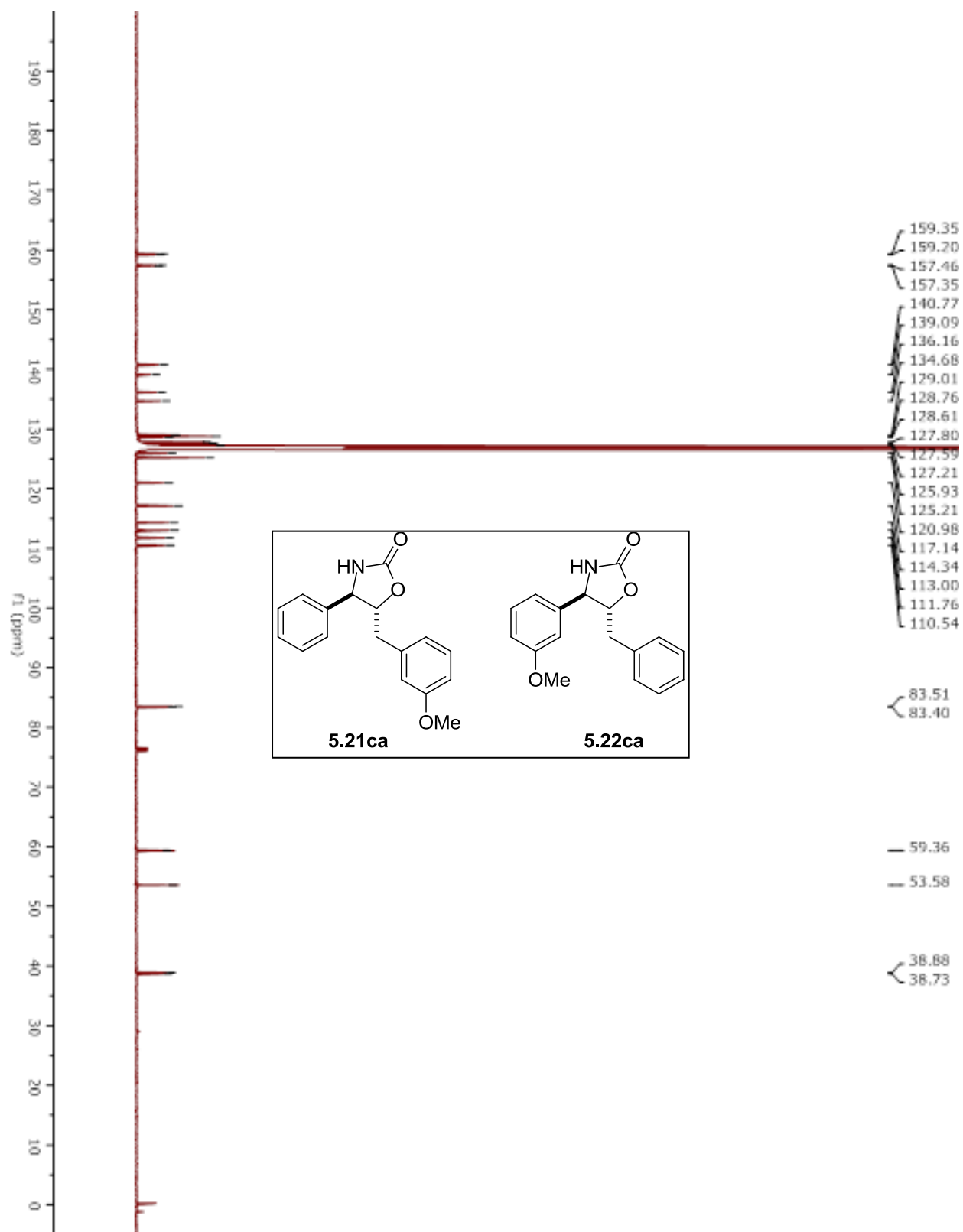
Compounds 5.21bb and 5.22bb. (mixture of regioisomers).



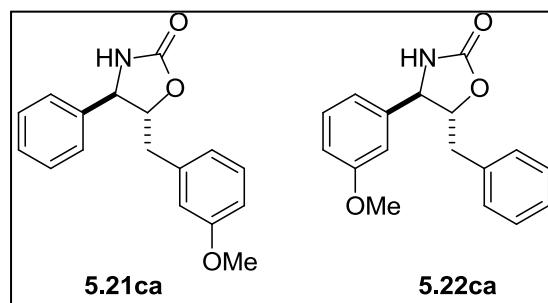
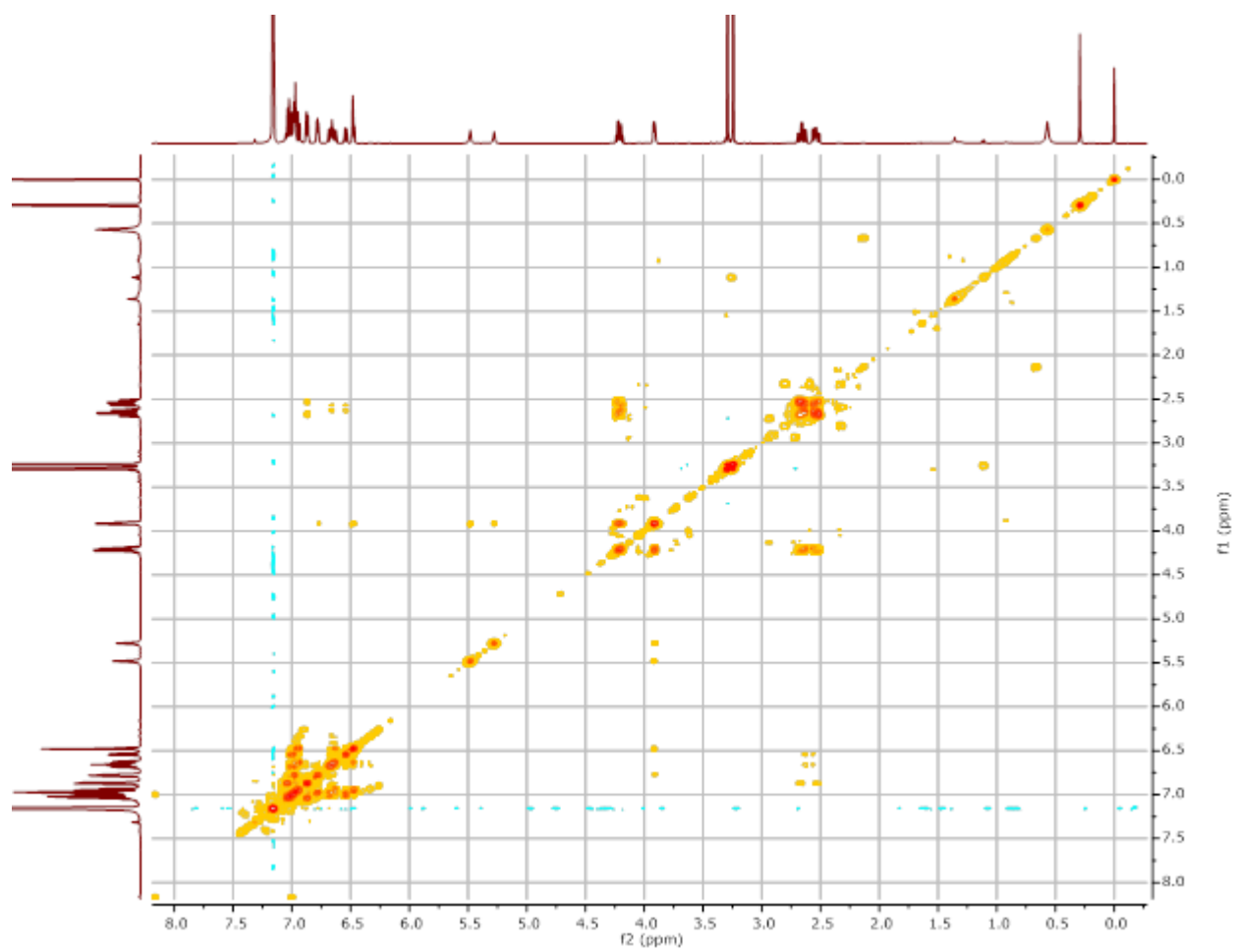
Compounds 5.21ca and 5.22ca.



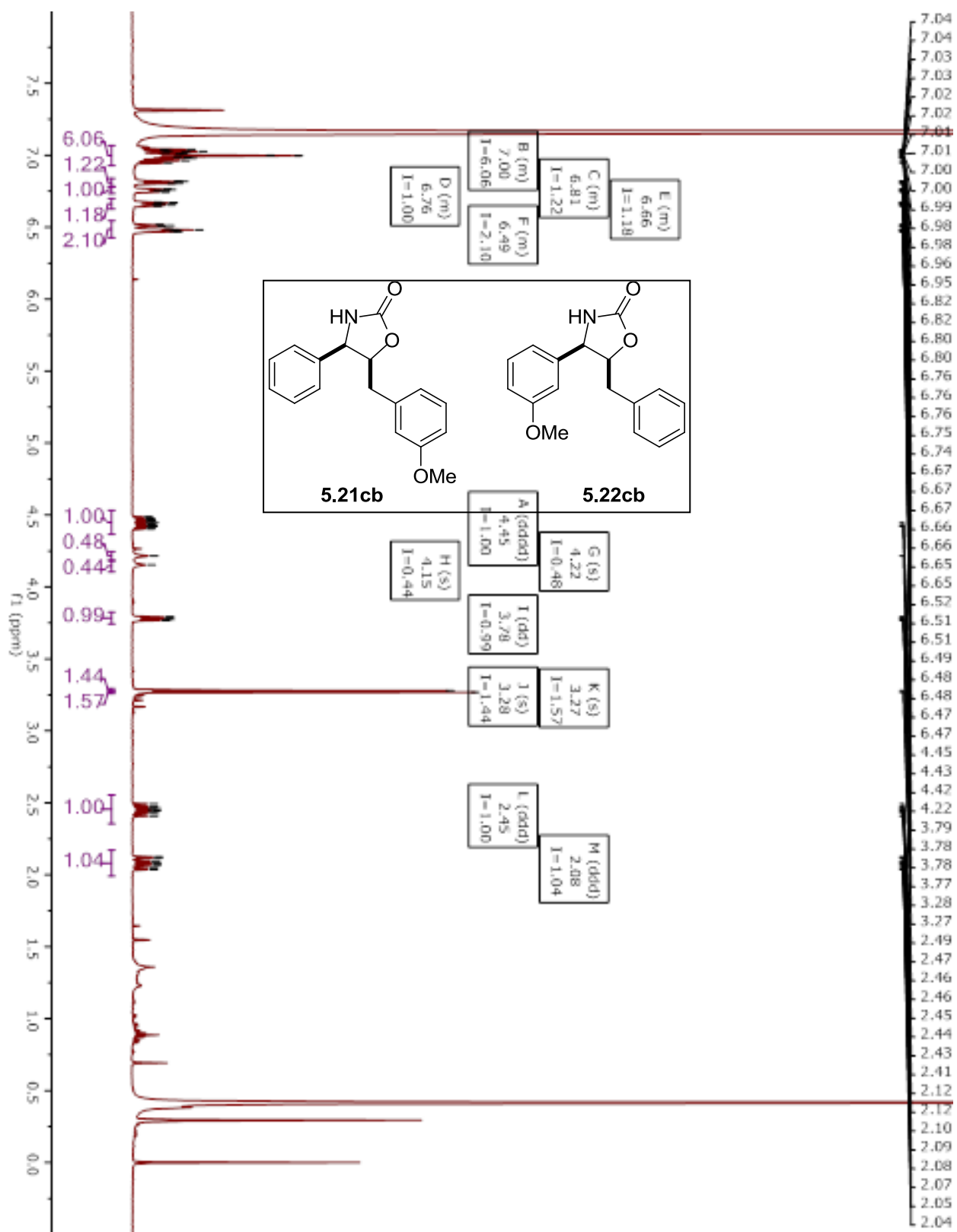
Compounds 5.21ca and 5.22ca.



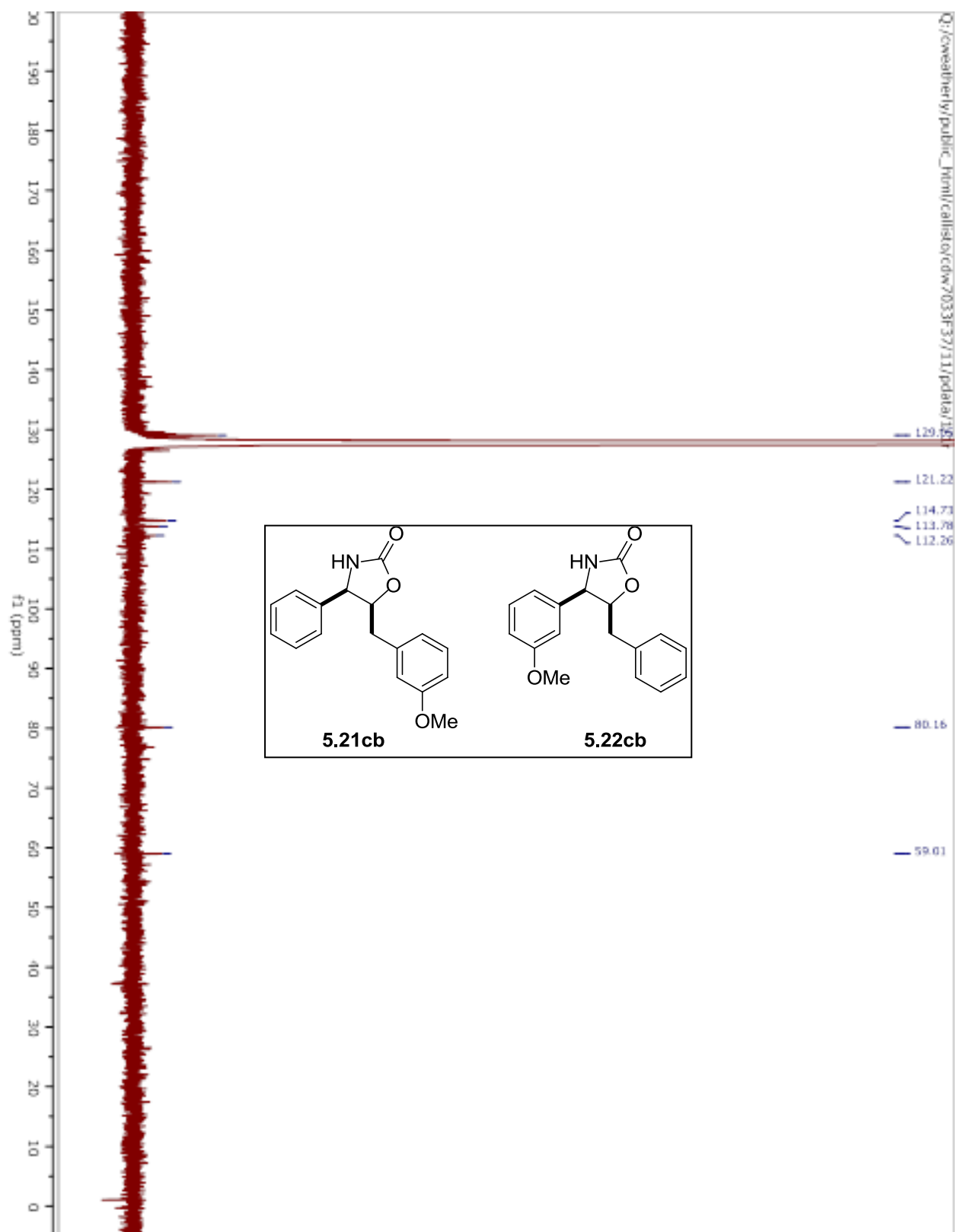
Compounds 5.21ca and 5.22ca.



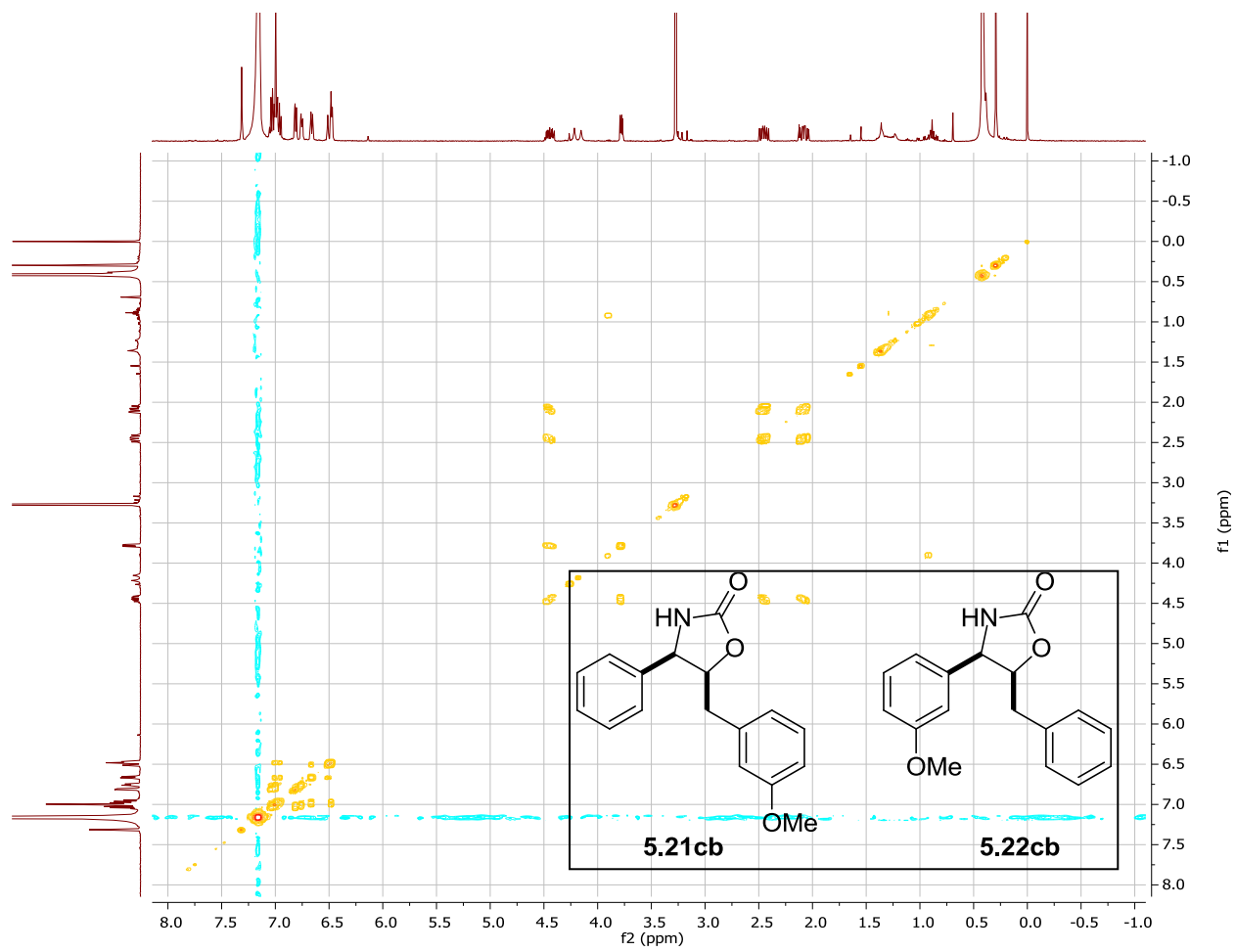
Compounds 5.21cb and 5.22cb.



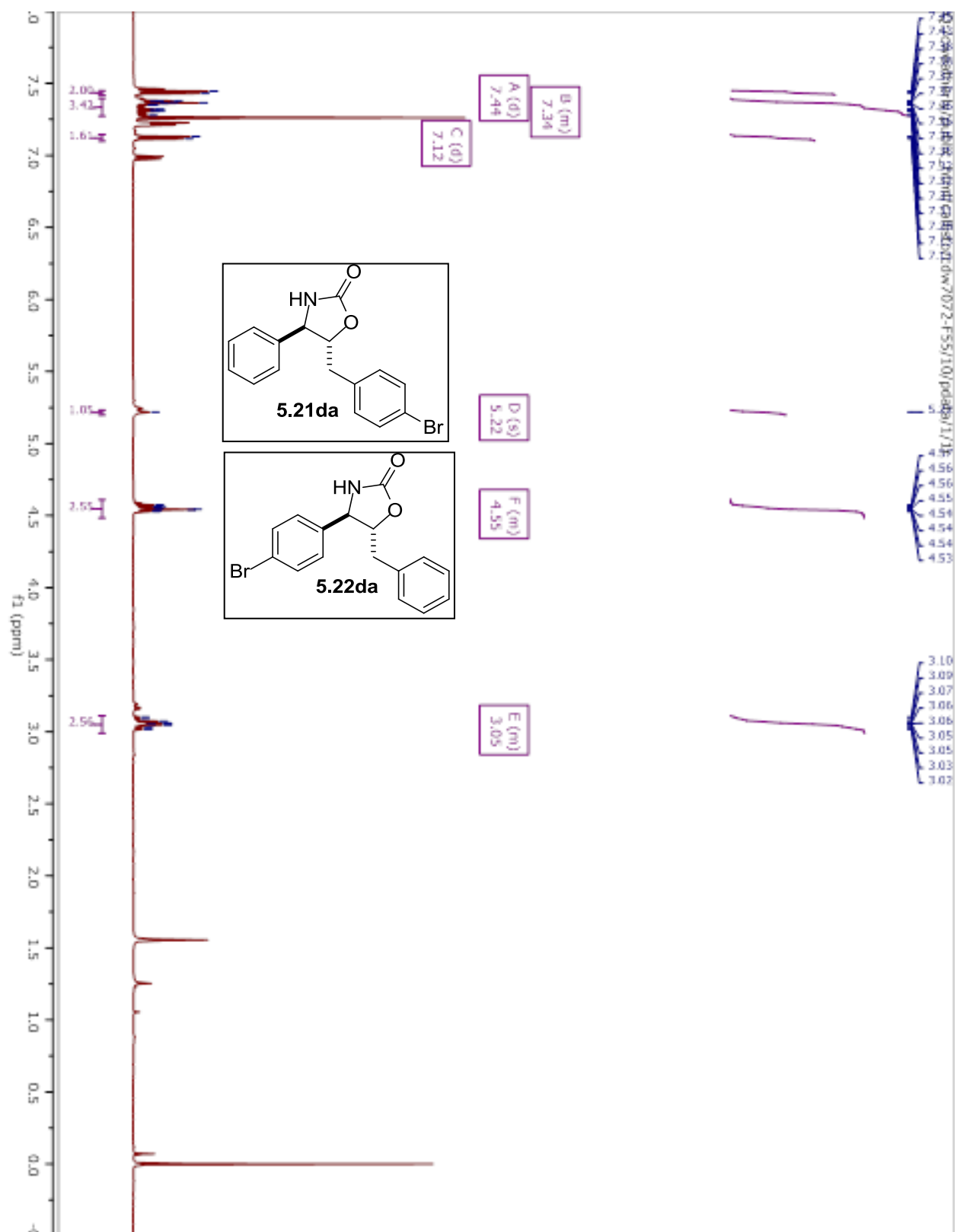
Compounds 5.21cb and 5.22cb.



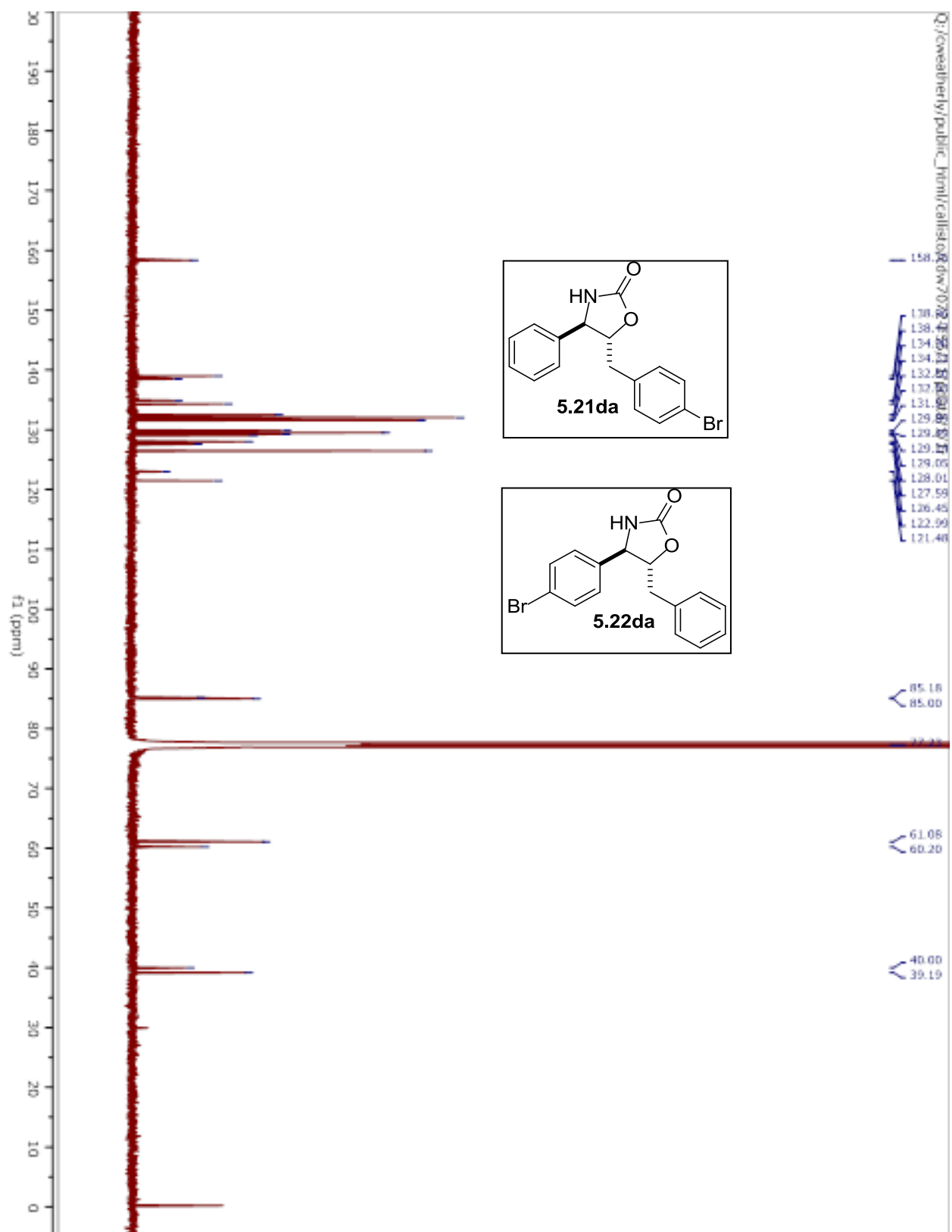
Compounds 5.21cb and 5.22cb.



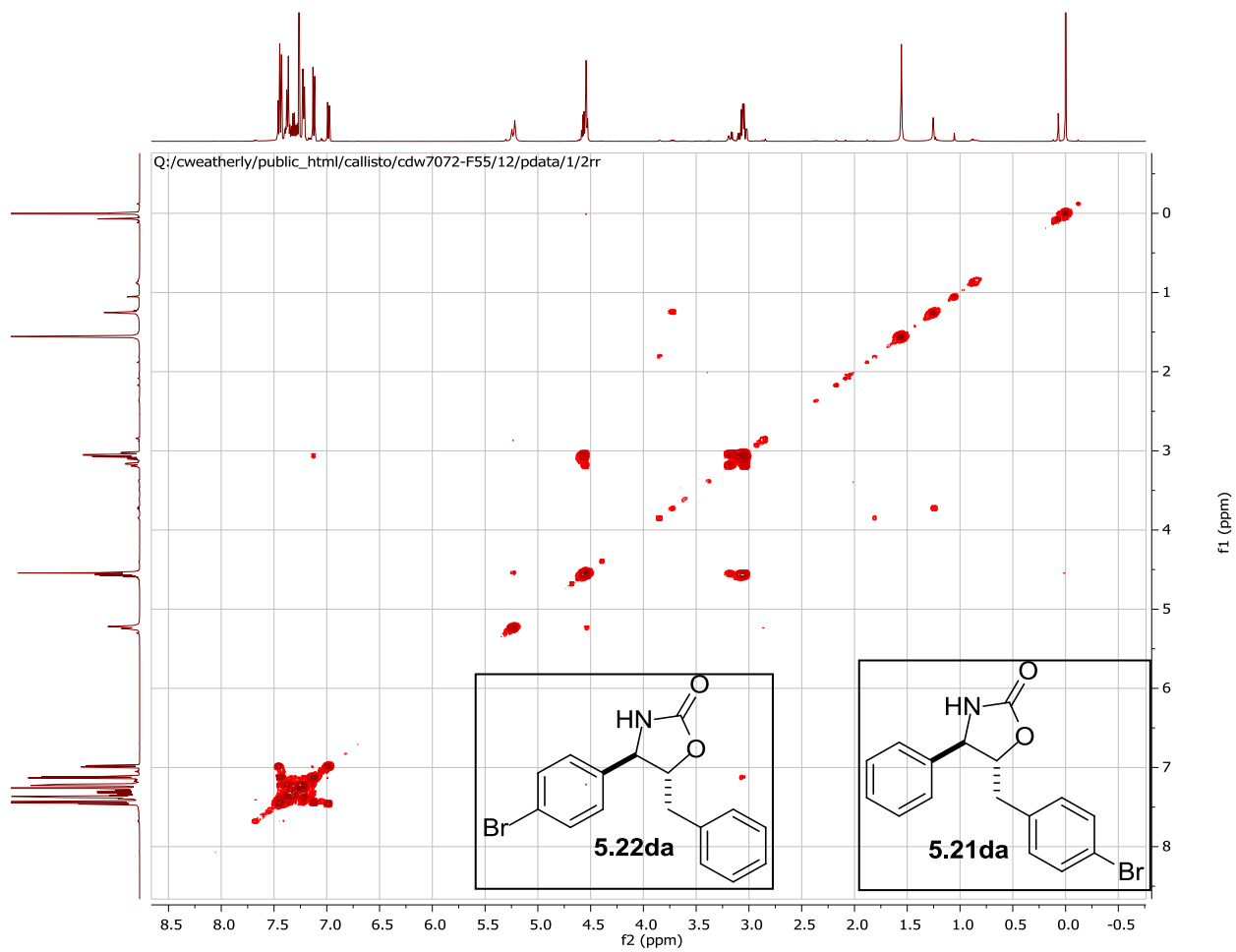
Compounds **5.21da** and **5.22da**. Only peaks assigned to **5.21da** are integrated.



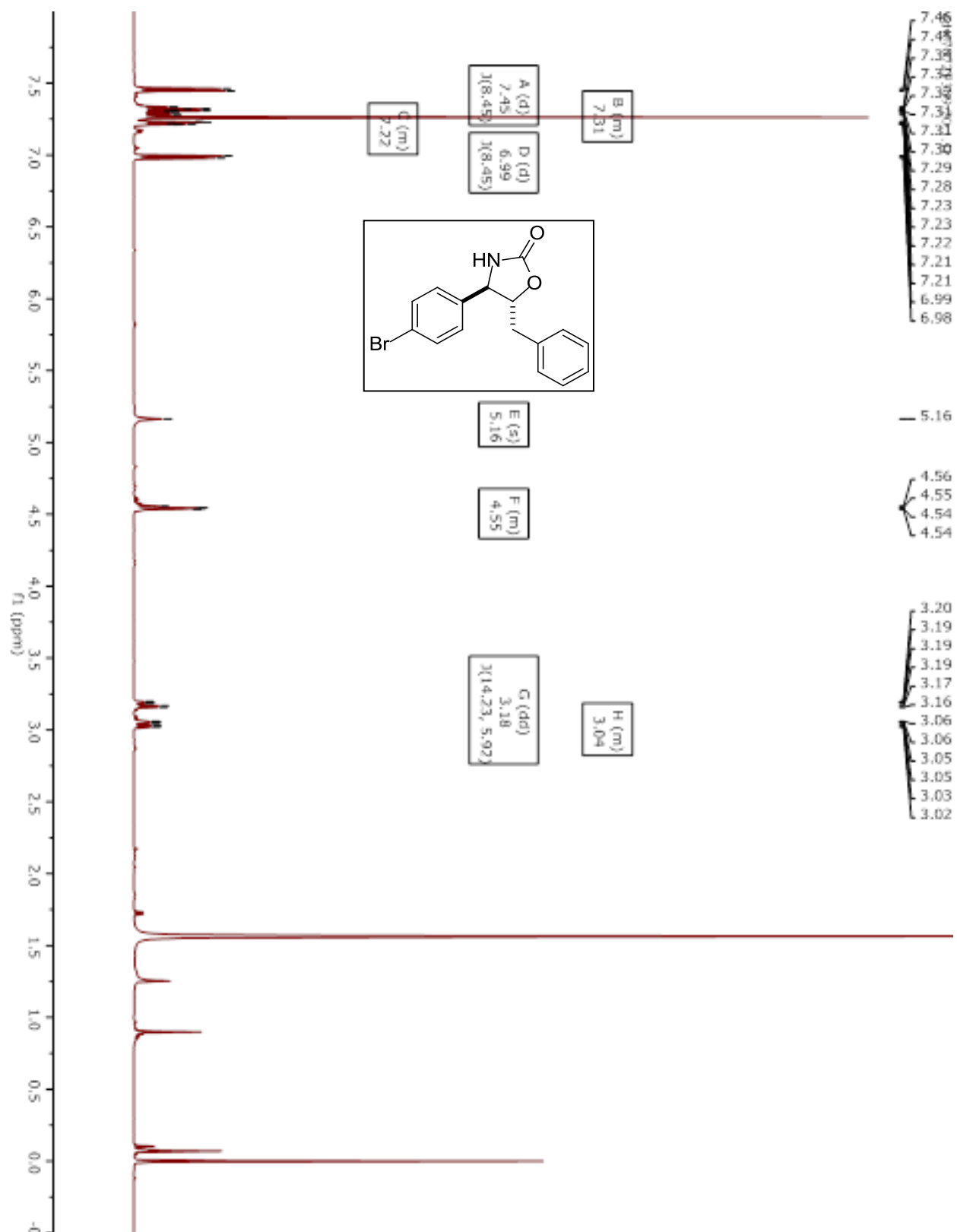
Compounds 5.21da and 5.22da.



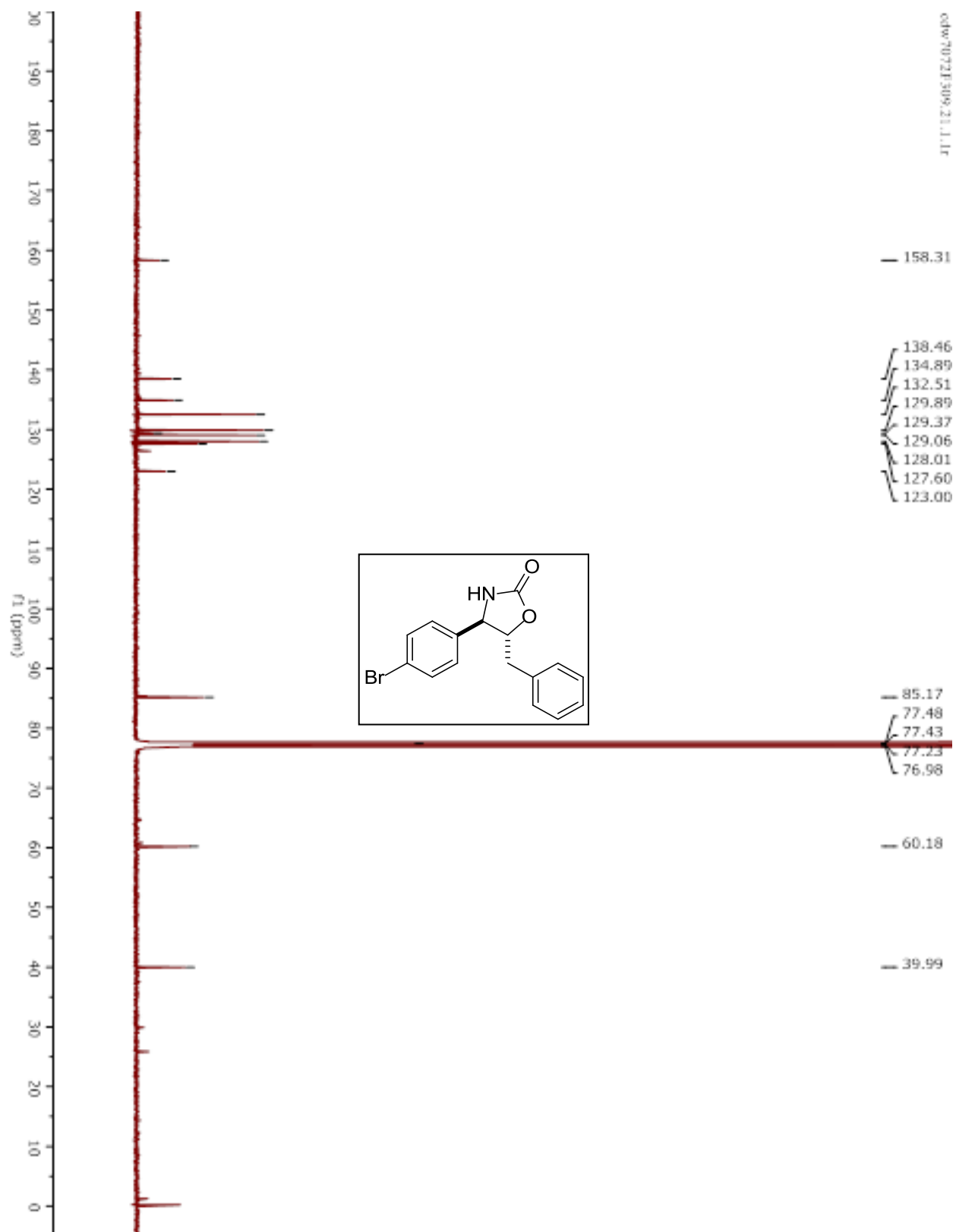
Compounds 5.21da and 5.22da.



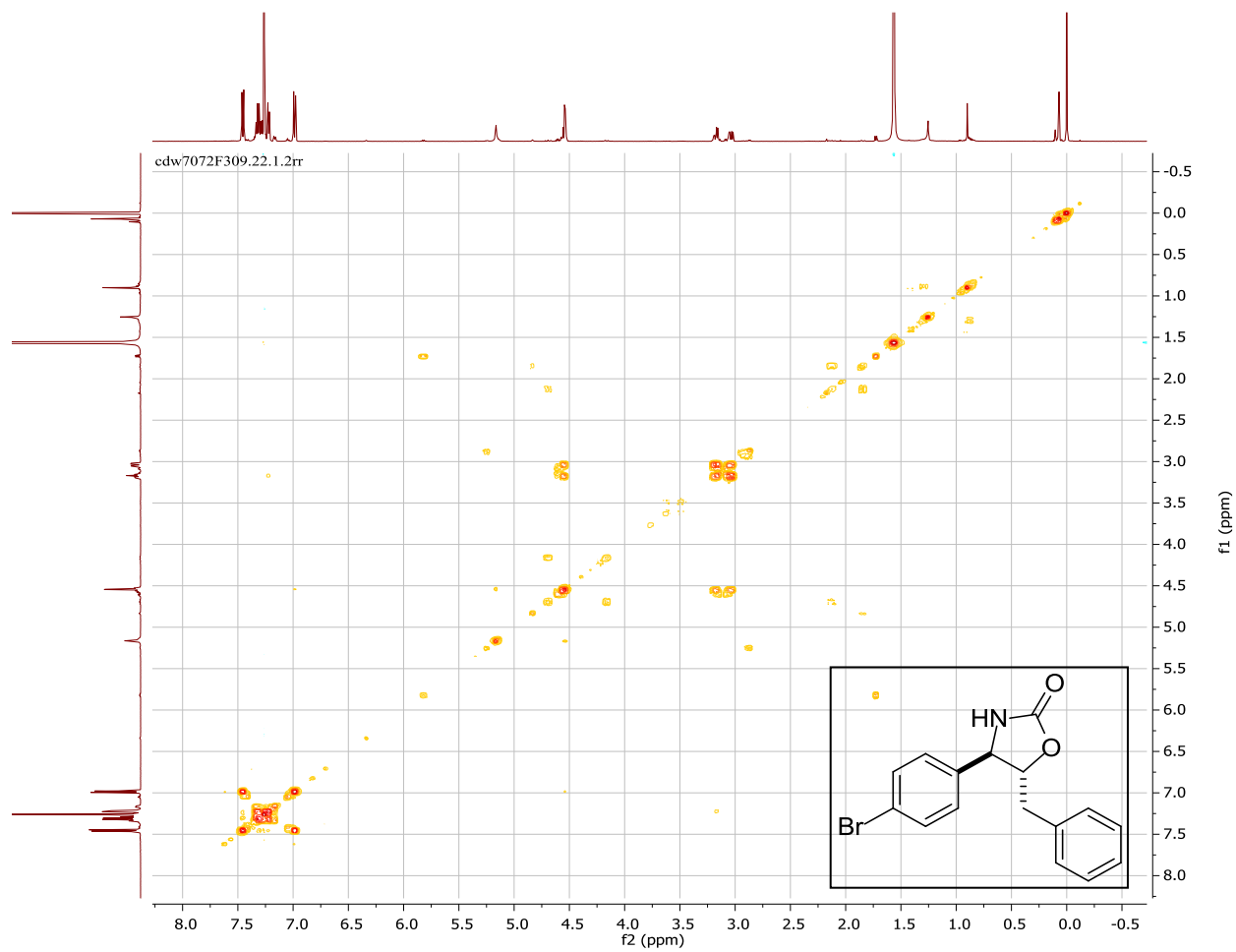
Compound 5.22da.



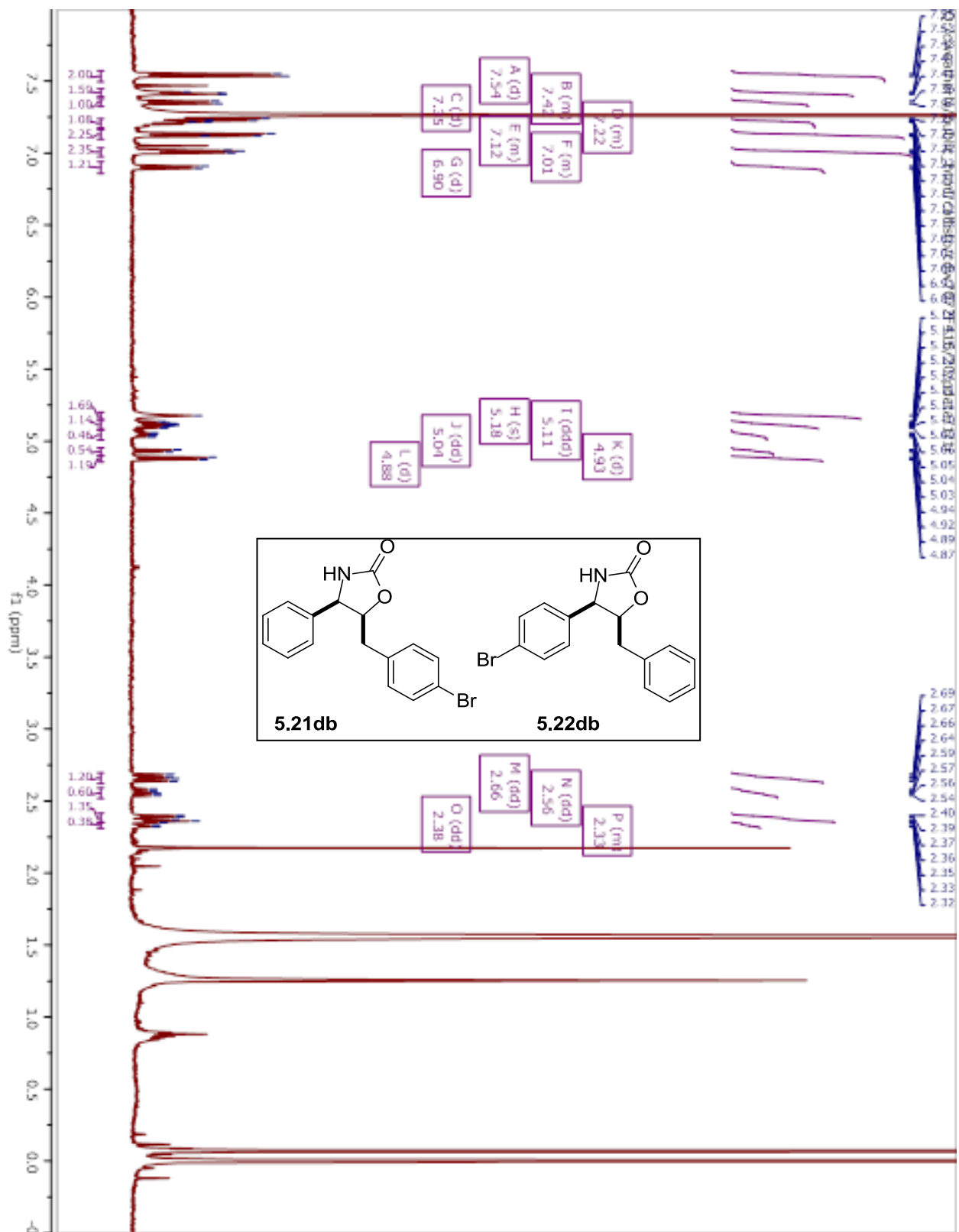
Compound 5.22da.



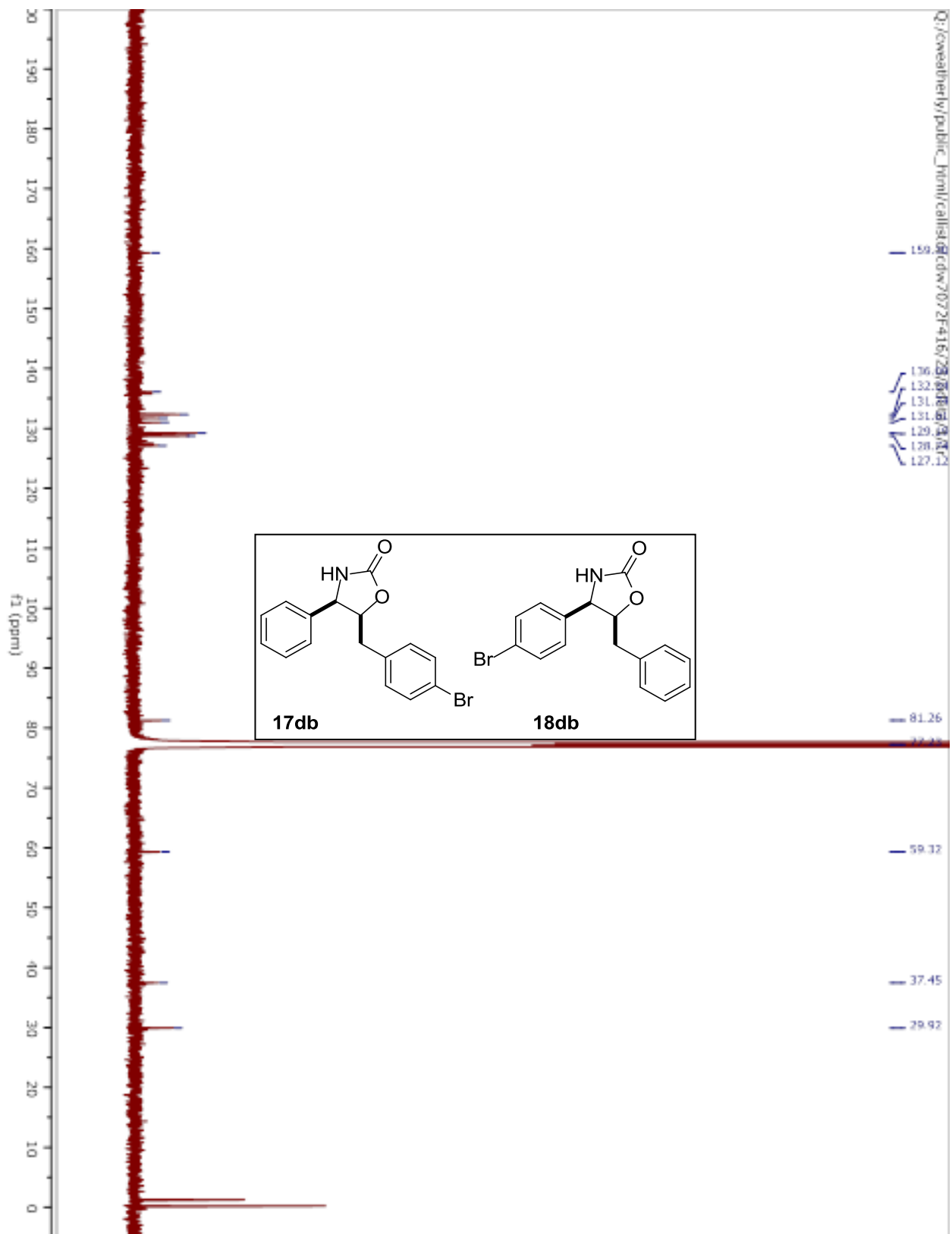
Compound 5.22da.



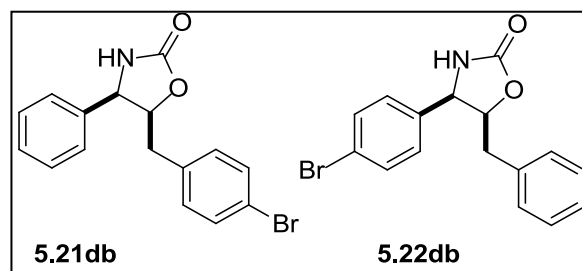
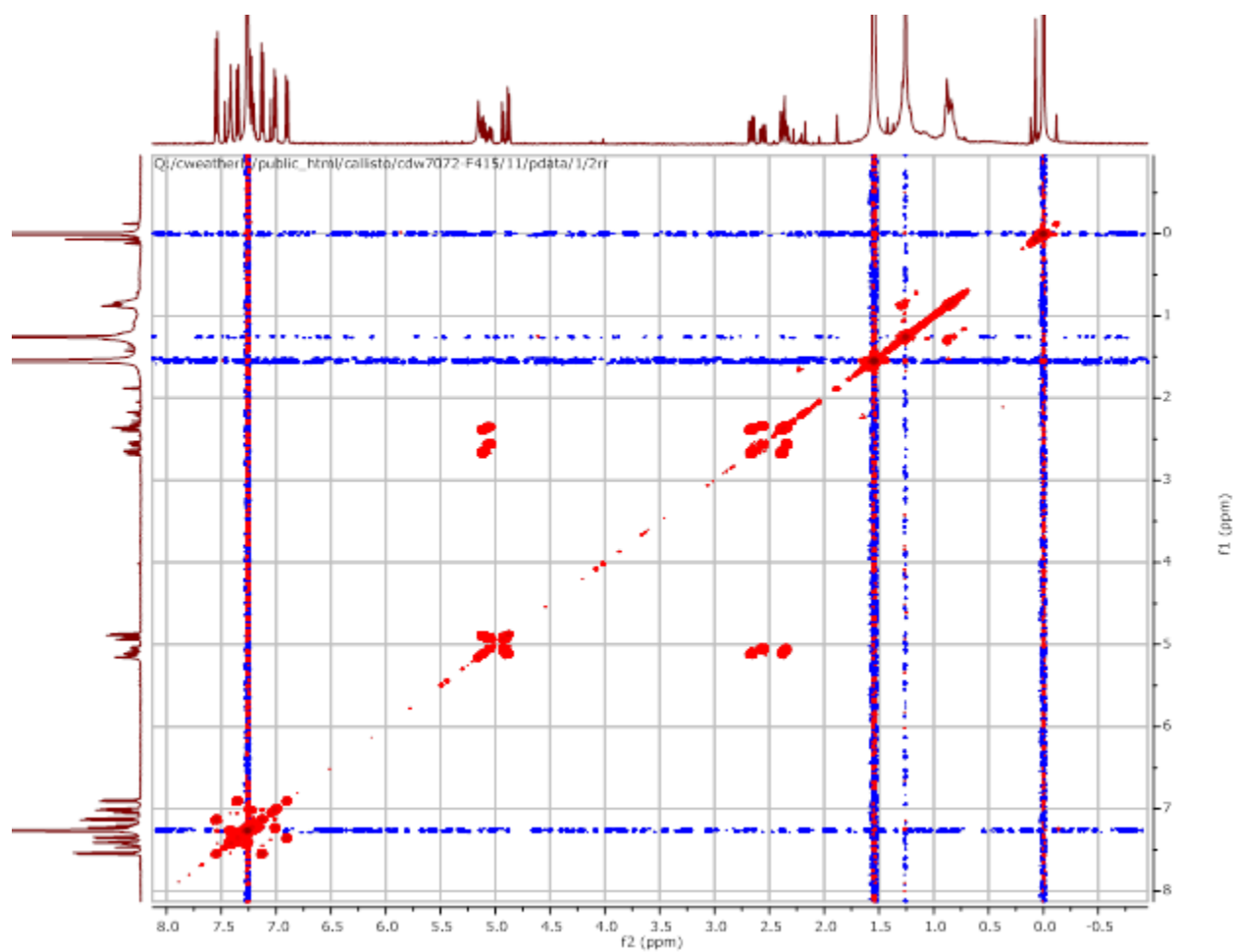
Compounds 5.21db and 5.22db.



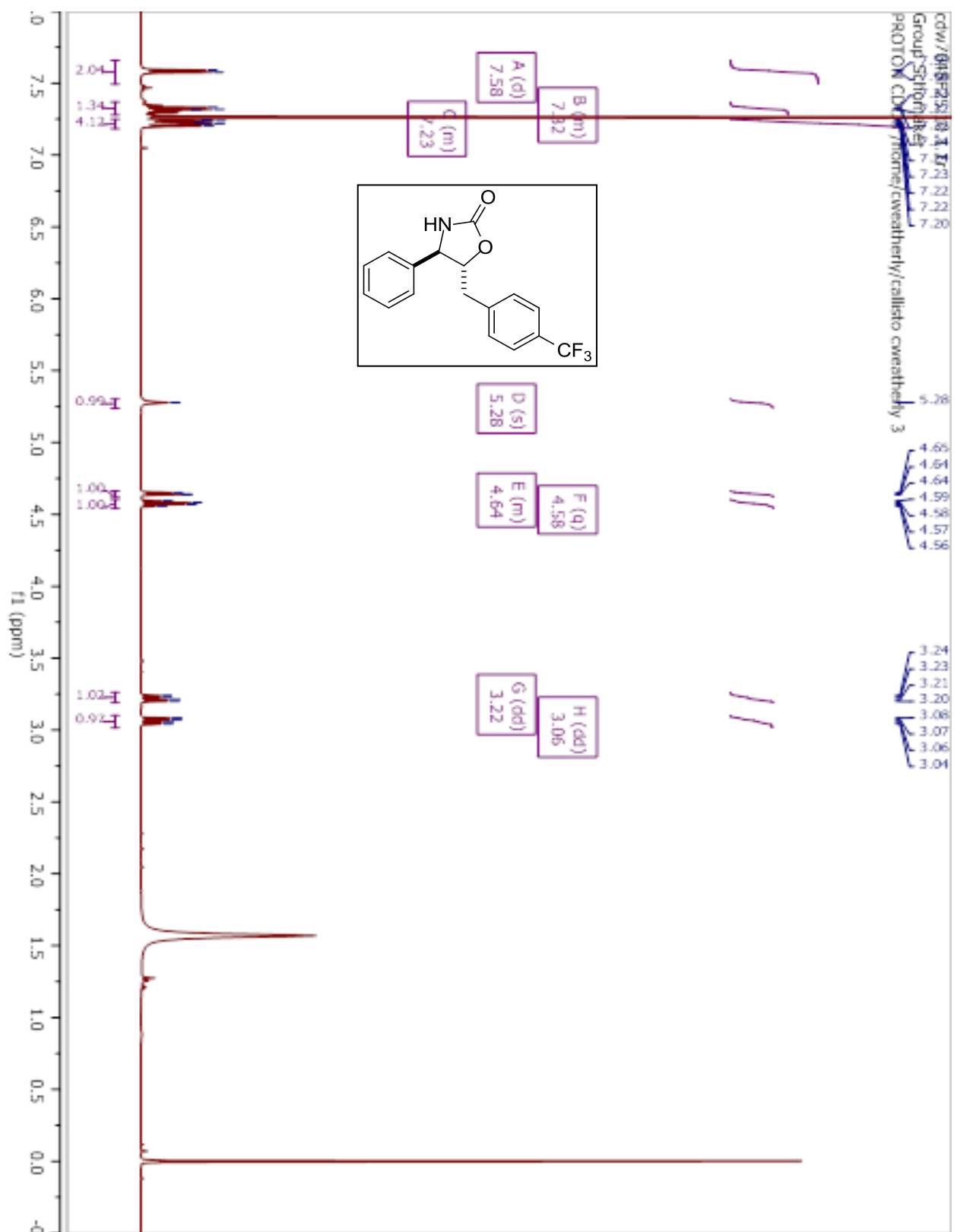
Compounds 5.21db and 5.22db.



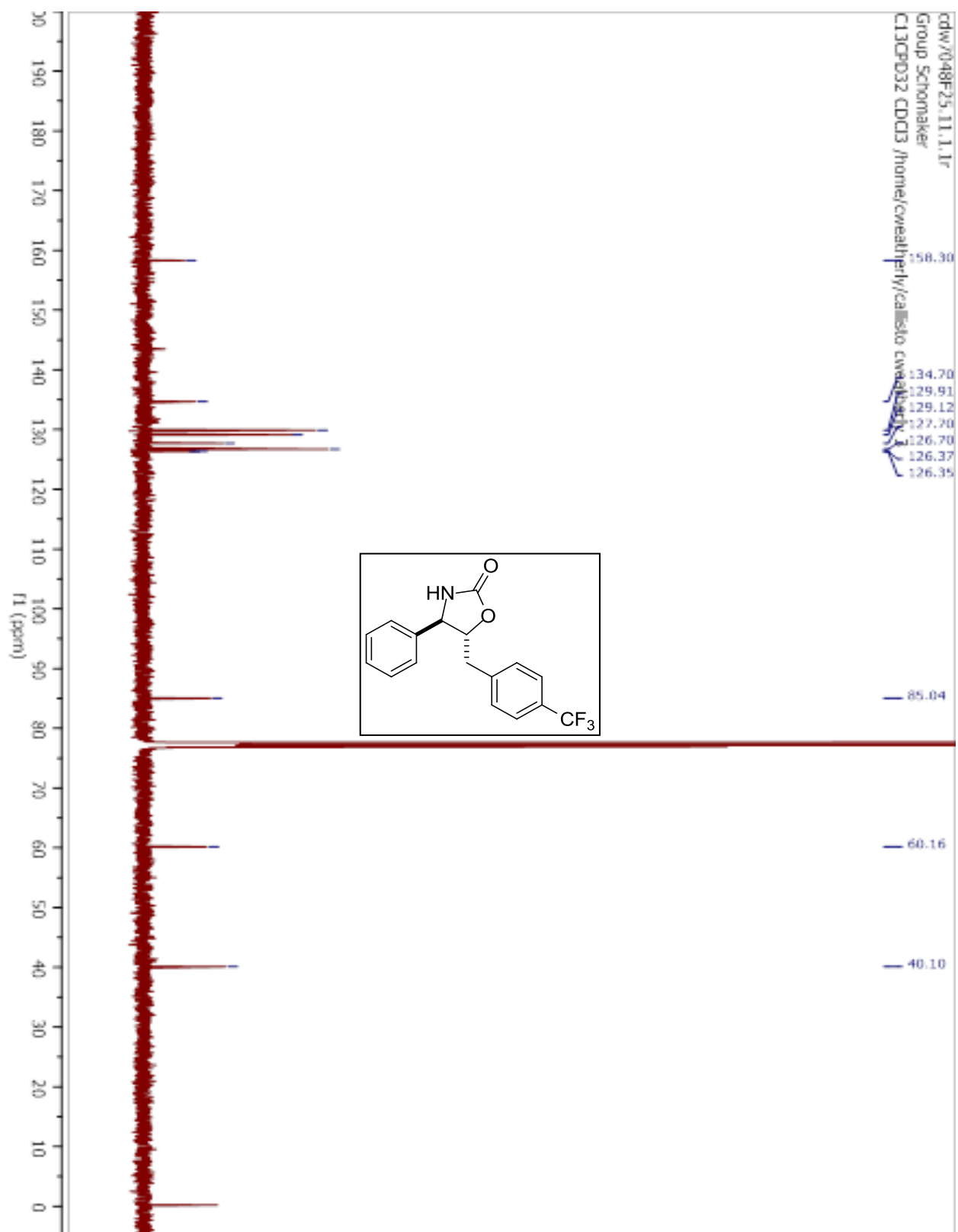
Compounds 5.21db and 5.22db.



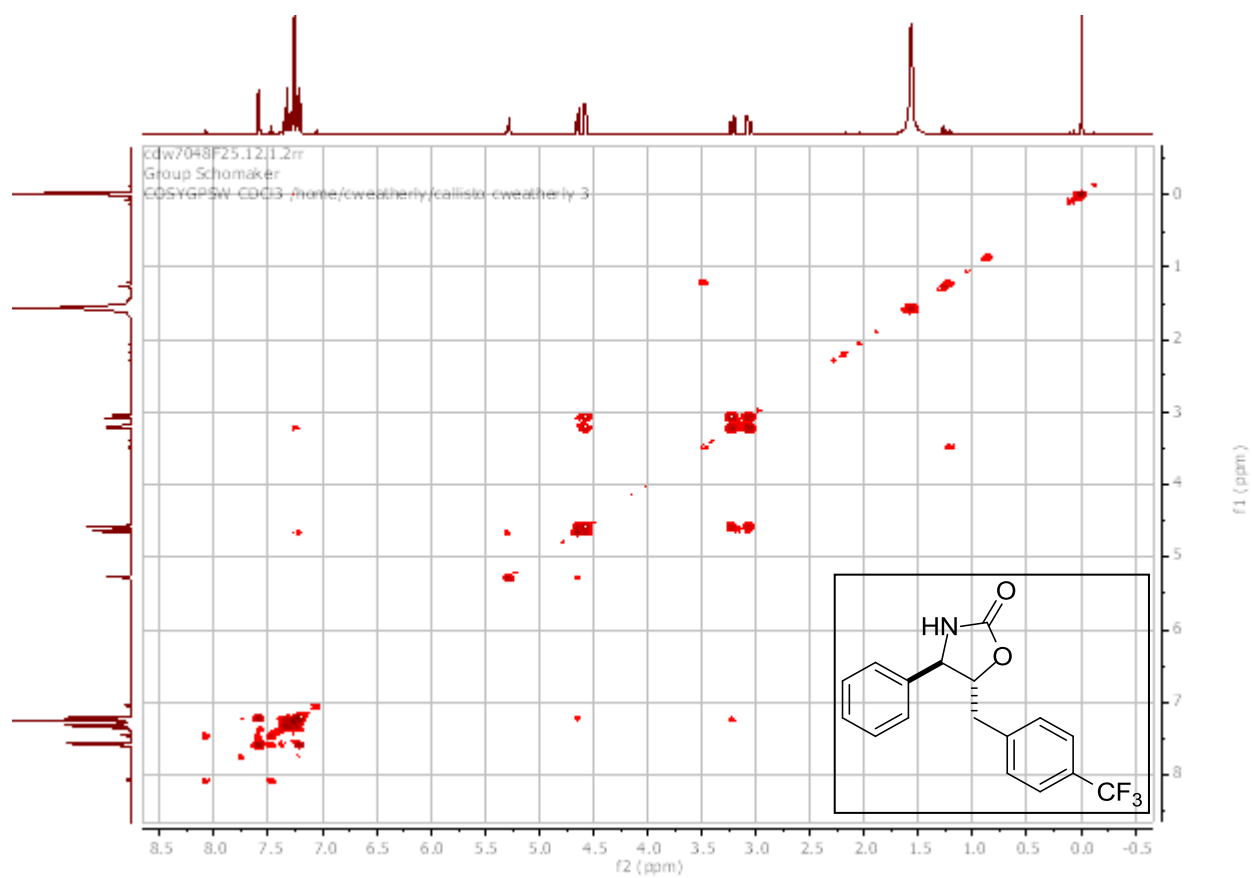
Compound 5.21ea.



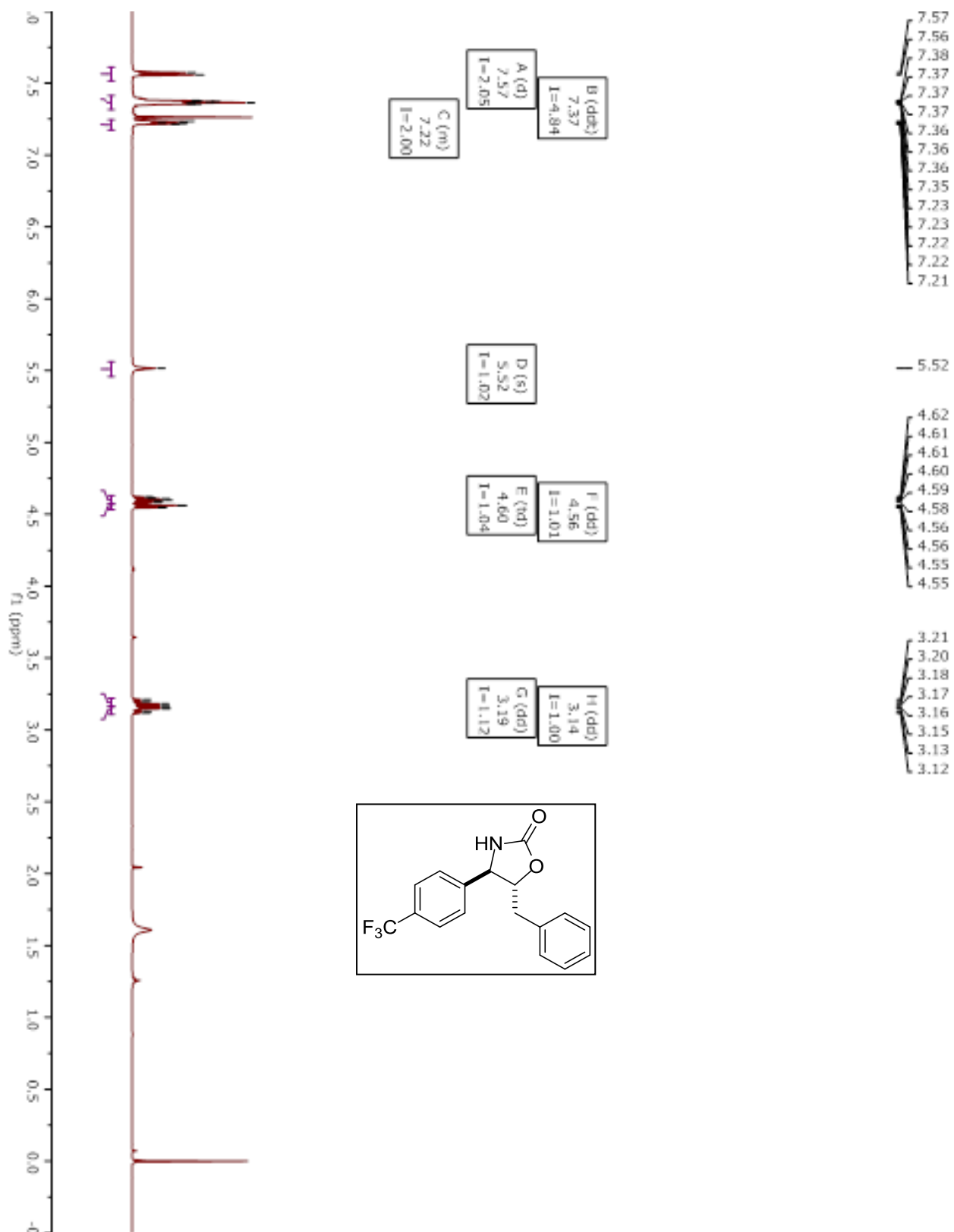
Compound 5.21ea.



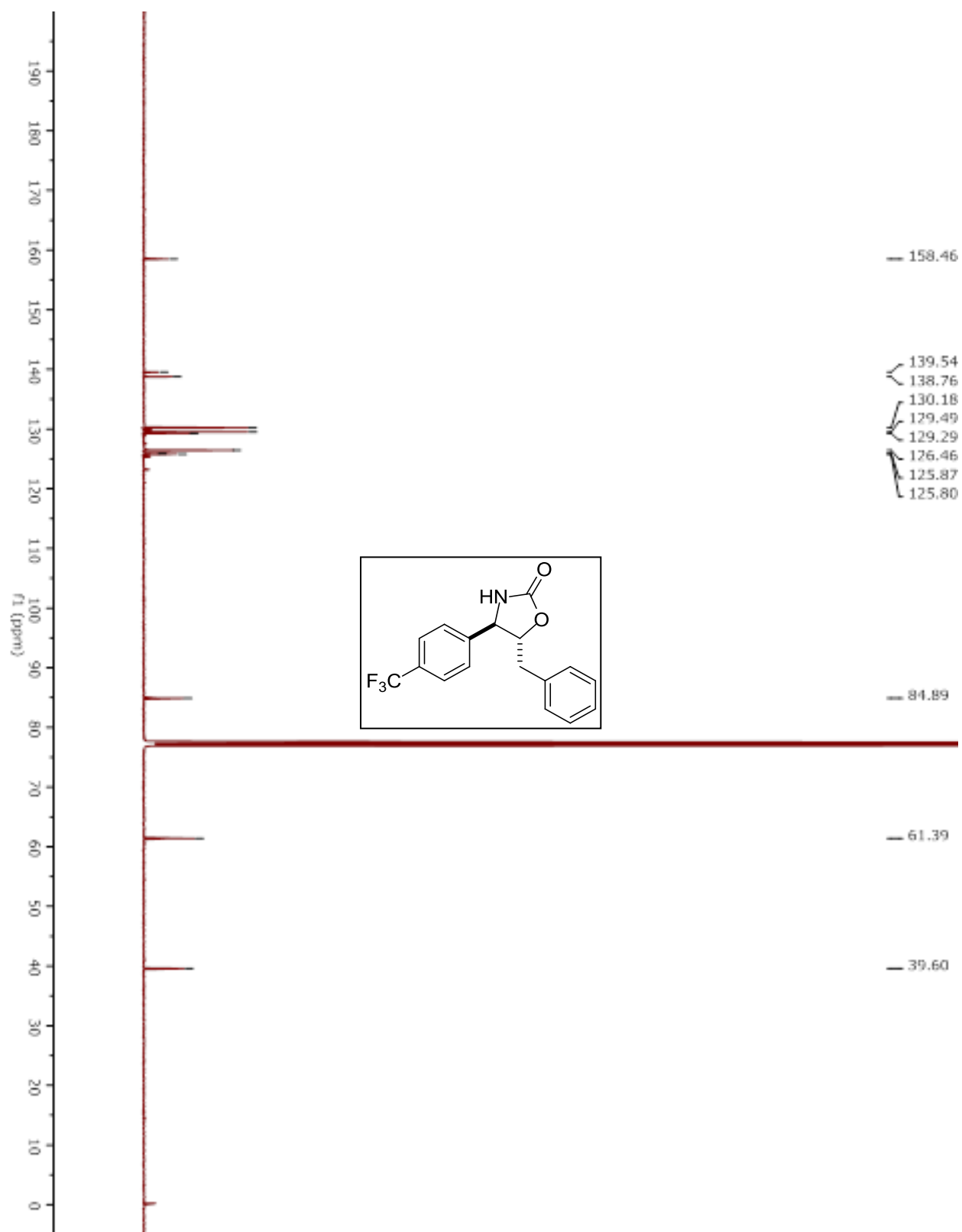
Compound 5.21ea.



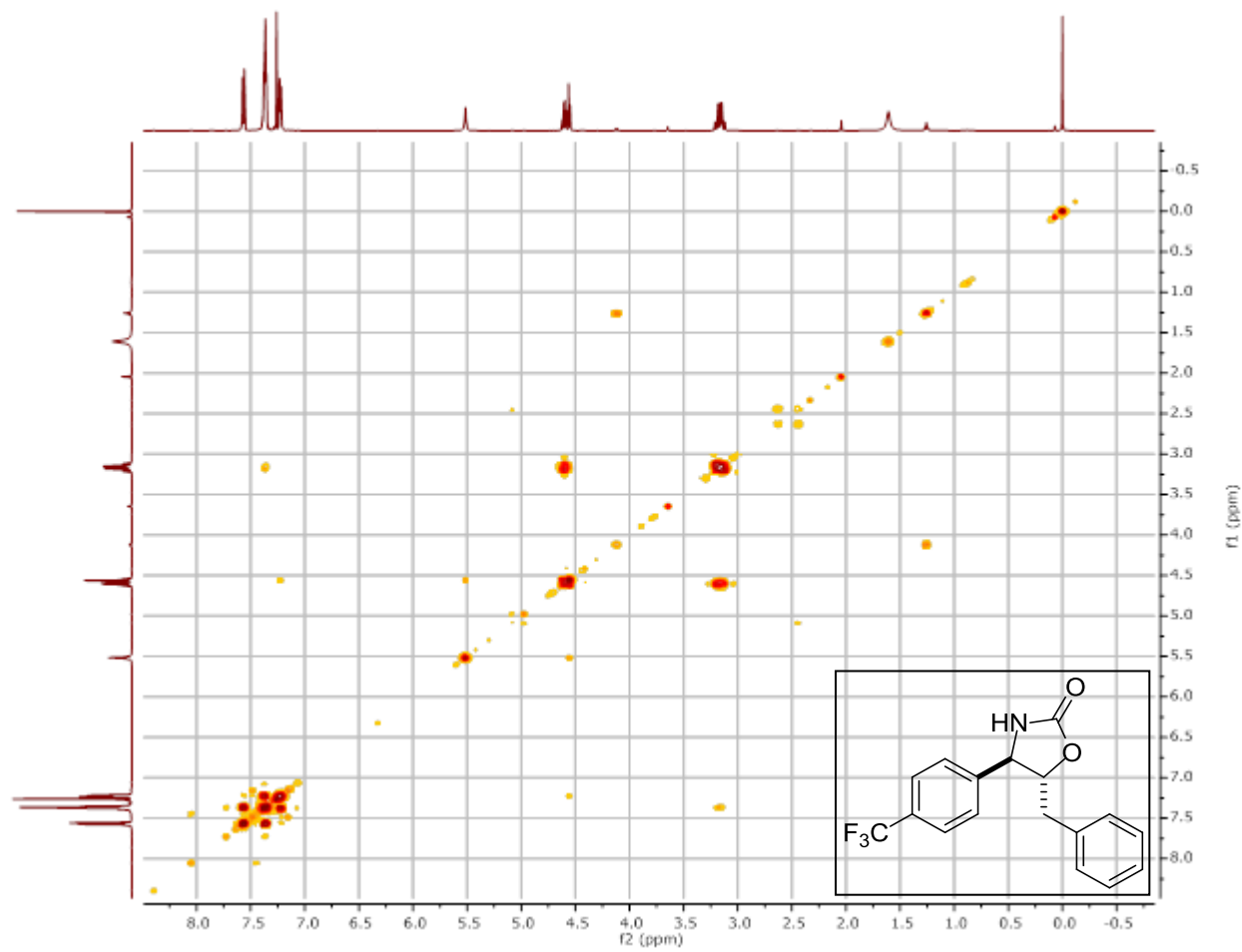
Compound 5.22ea major diastereomer.



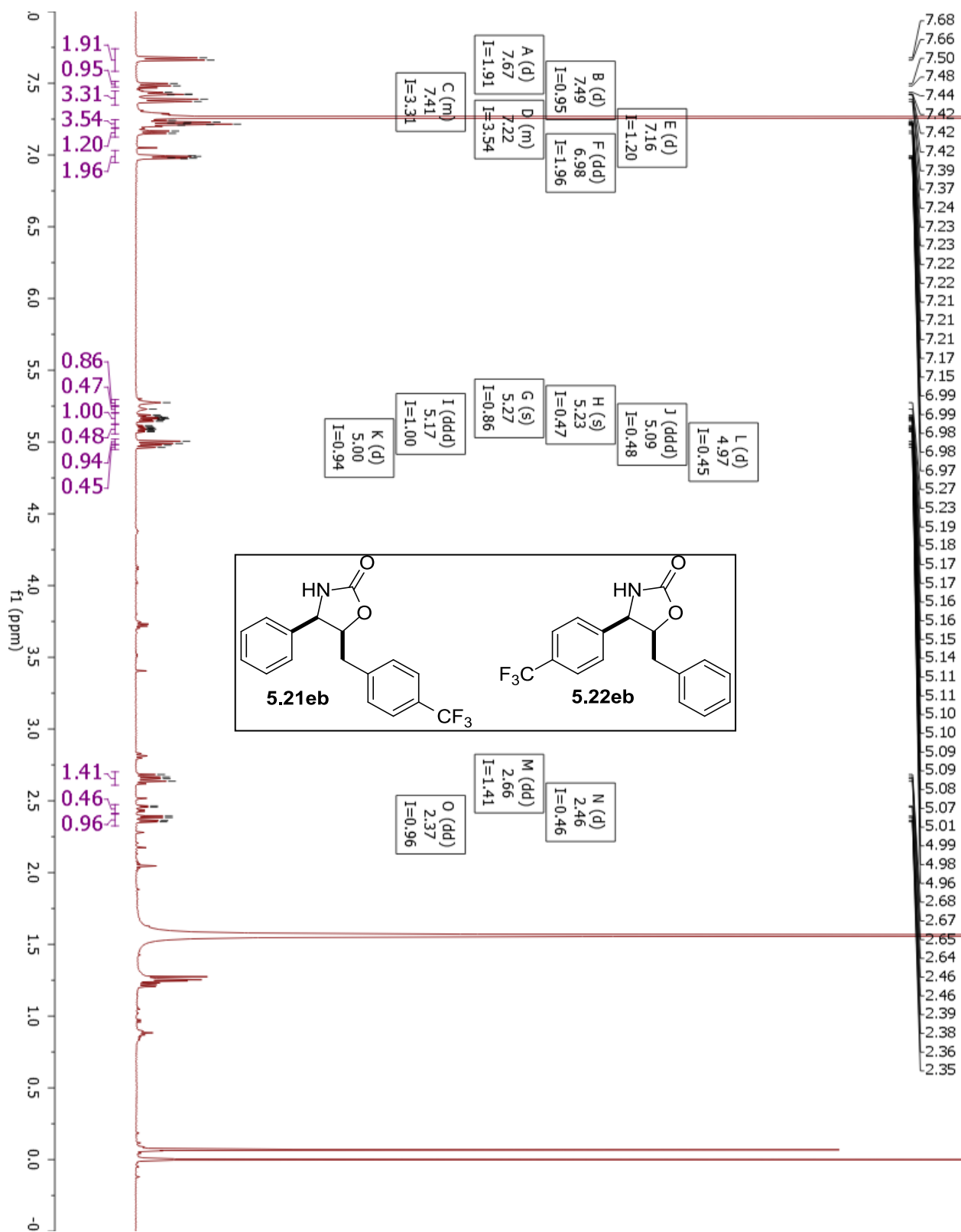
Compound 5.22ea major diastereomer.



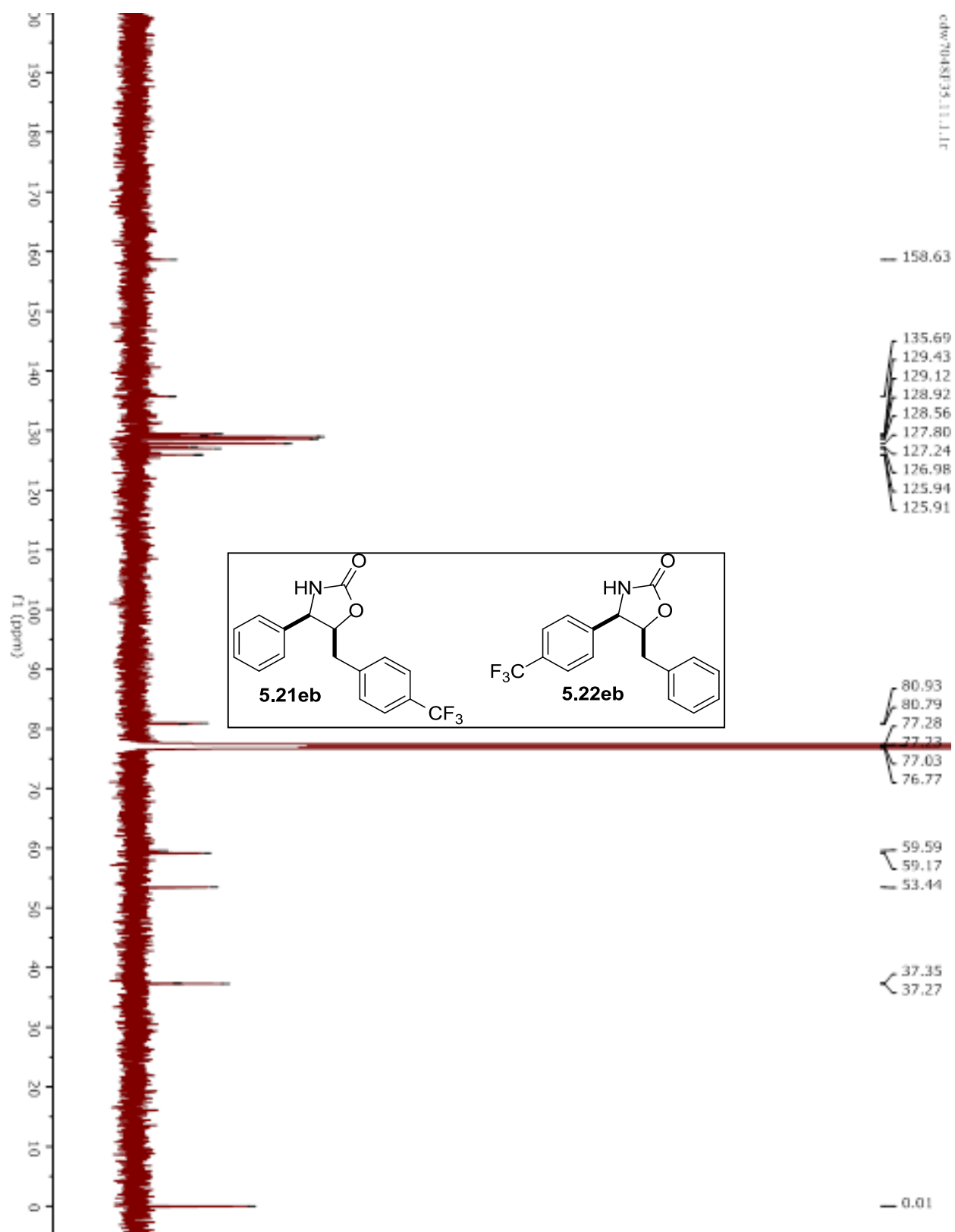
Compound 5.22ea major diastereomer.



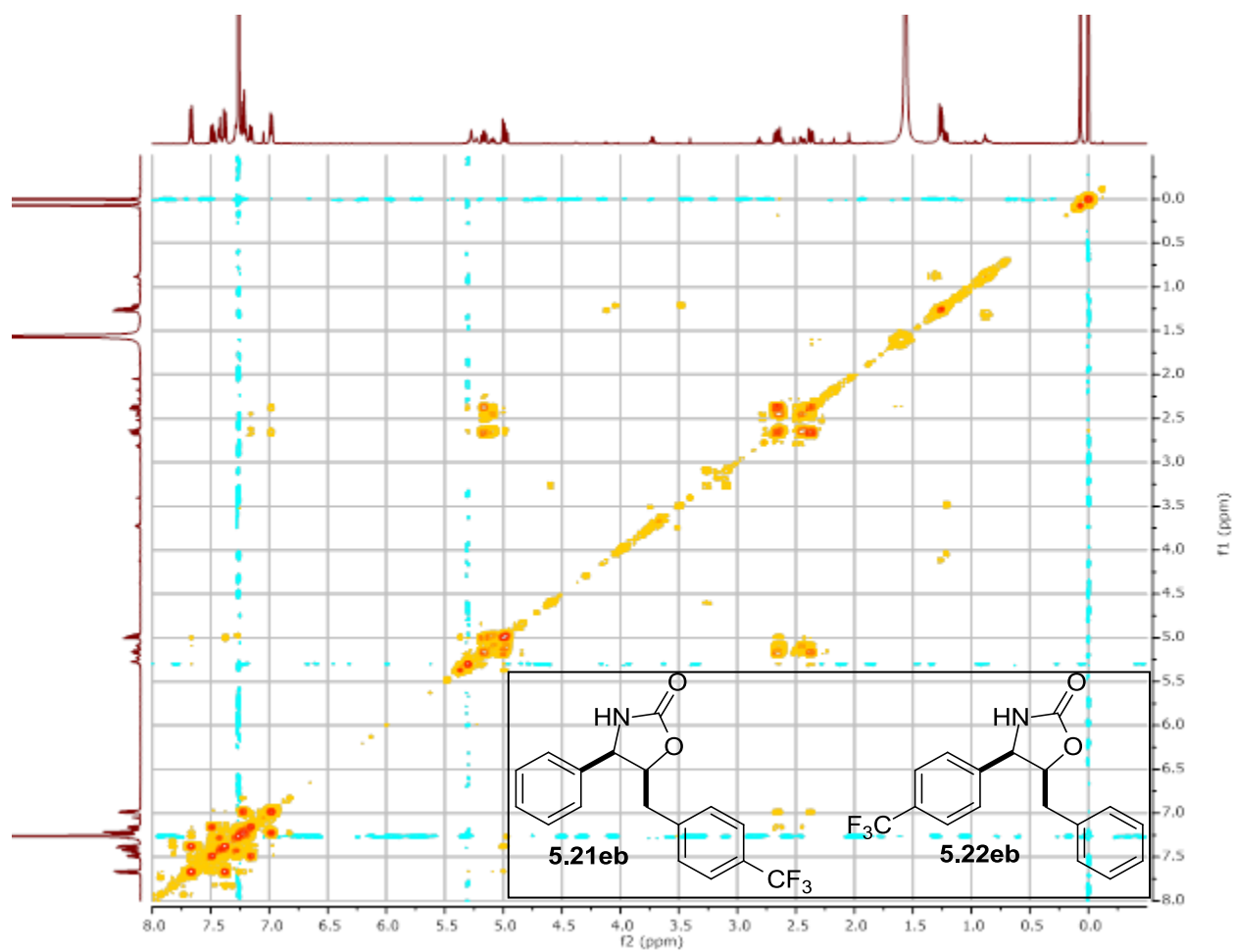
Compounds 5.21eb and 5.22eb.



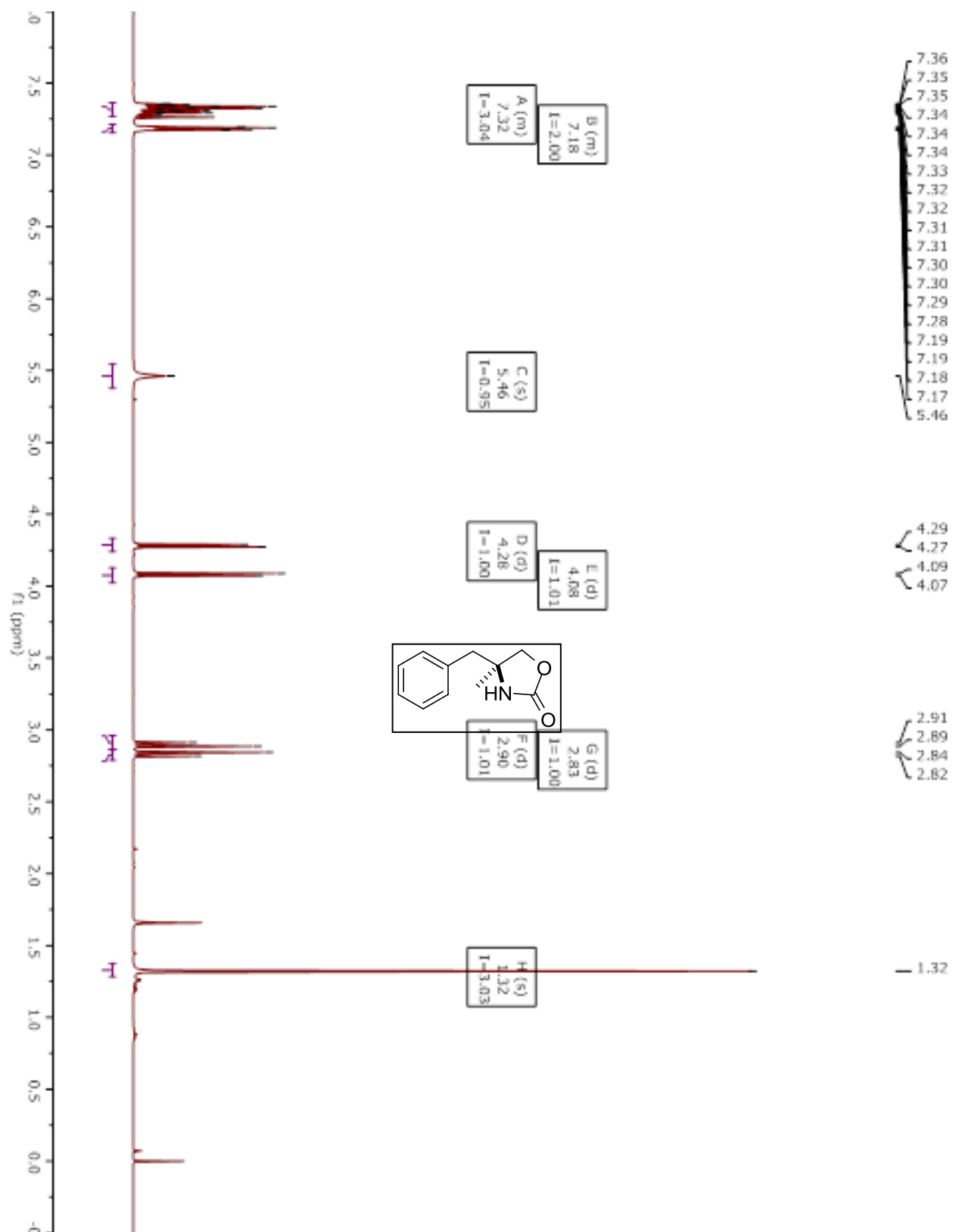
Compounds 5.21eb and 5.22eb.



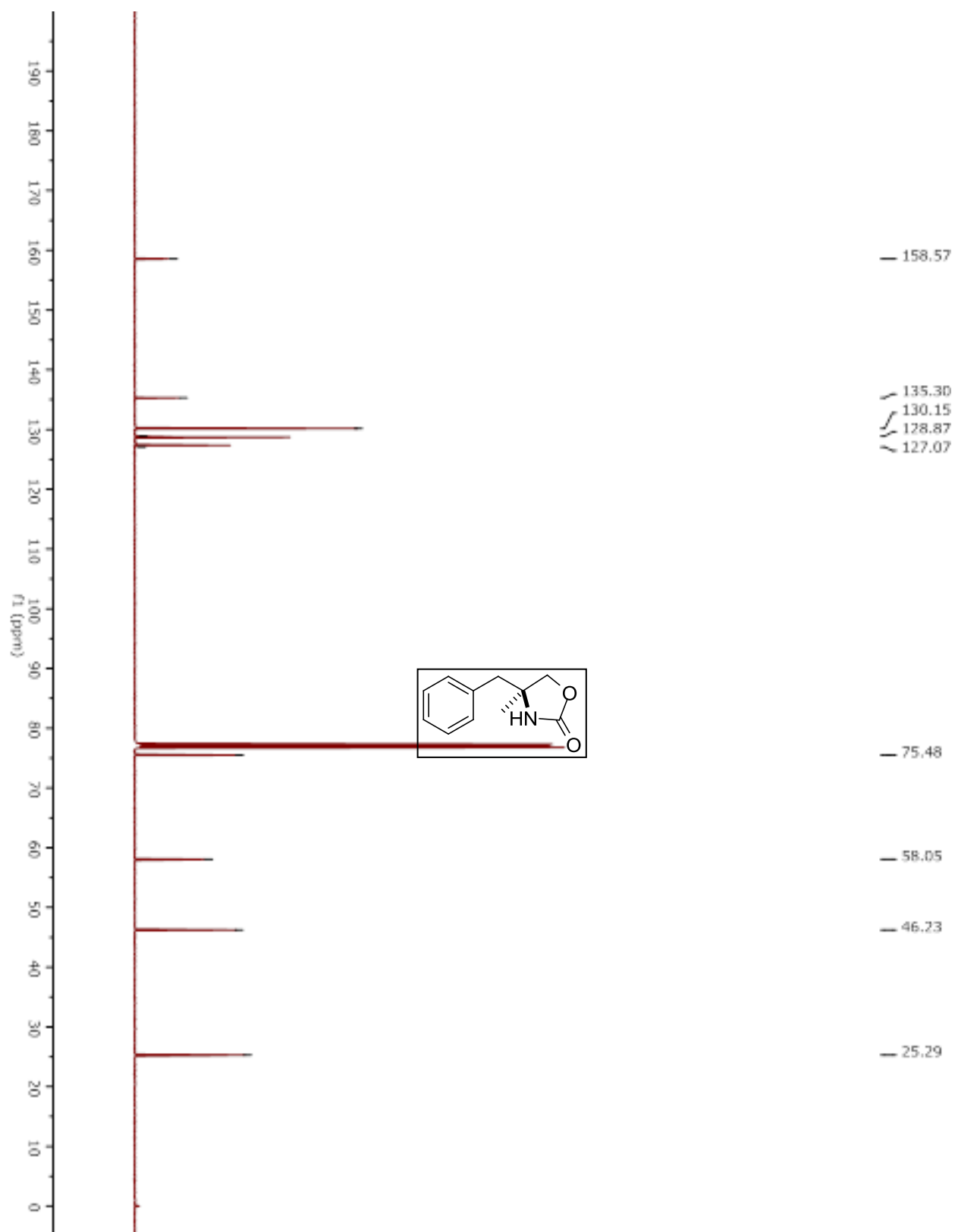
Compounds 5.21eb and 5.22eb.



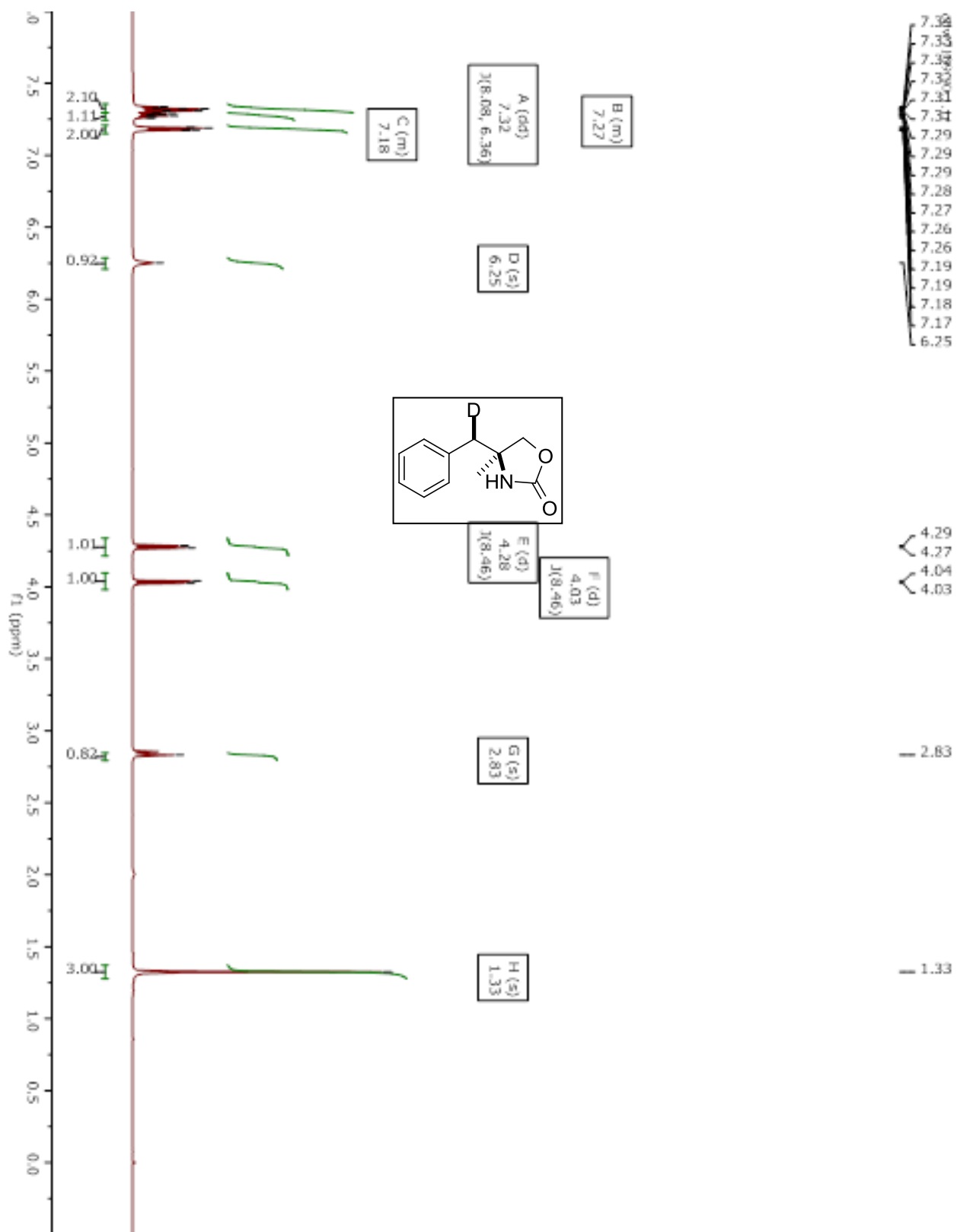
Compound 5.34-H.



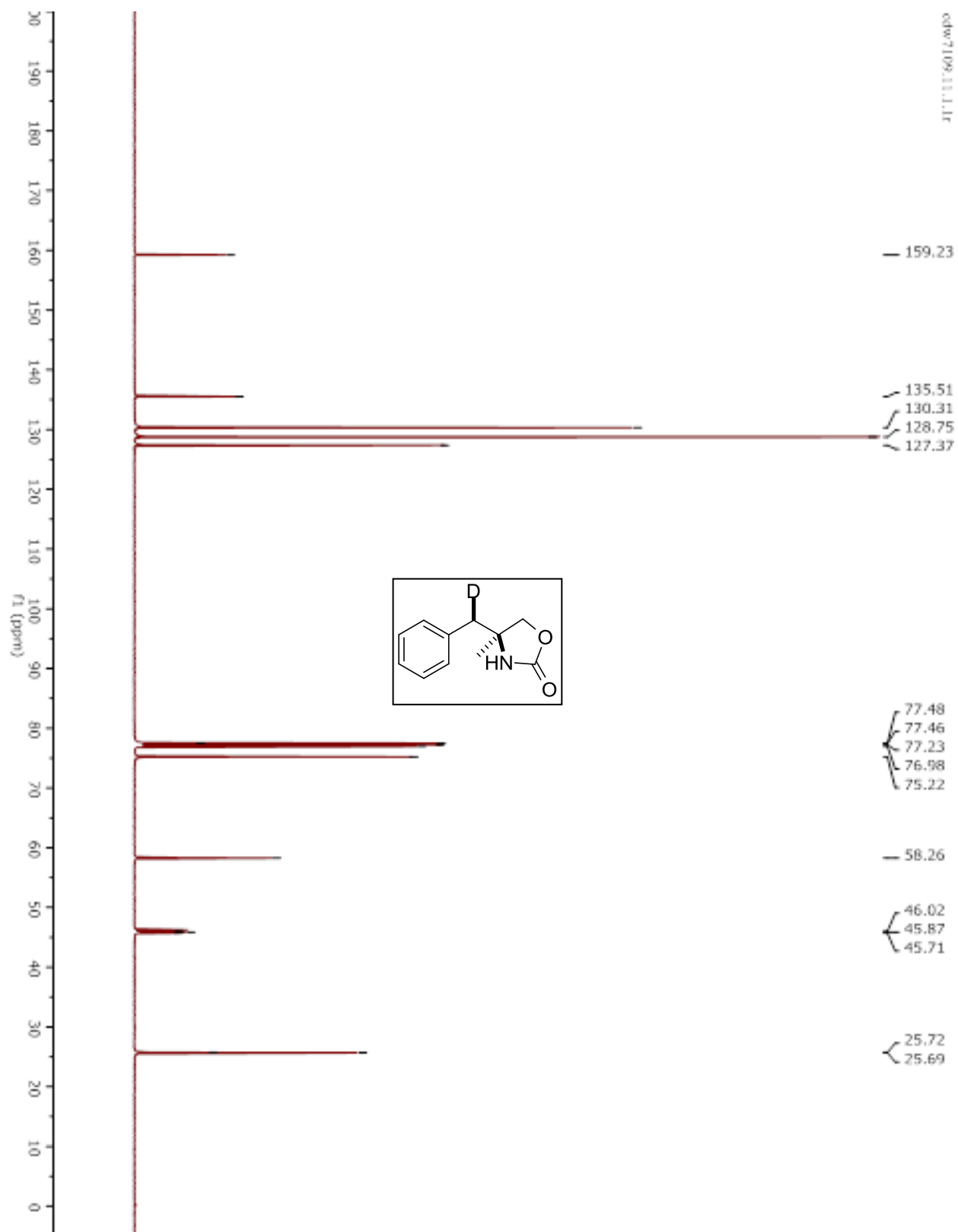
Compound 5.34-H.



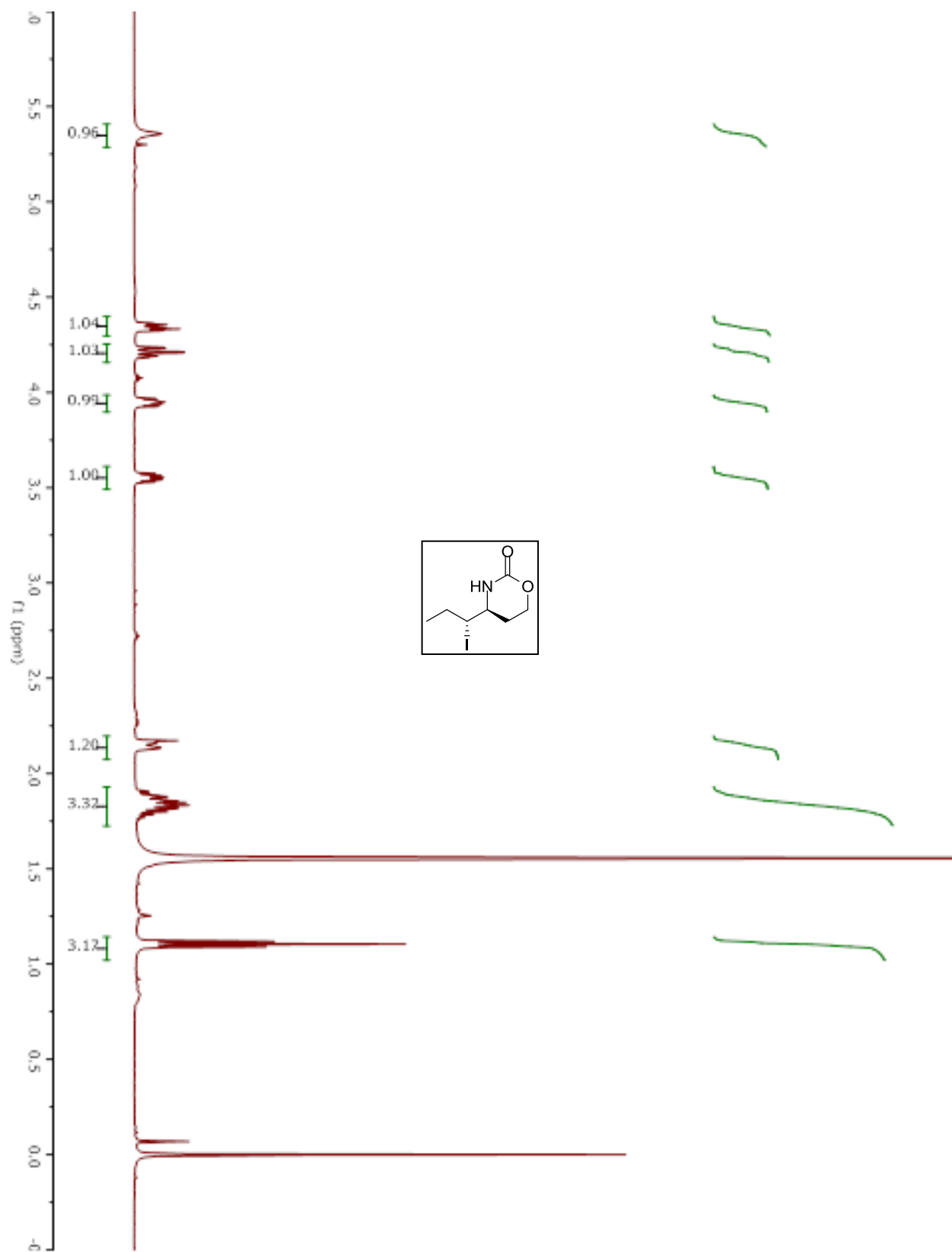
Compound 5.34-D.



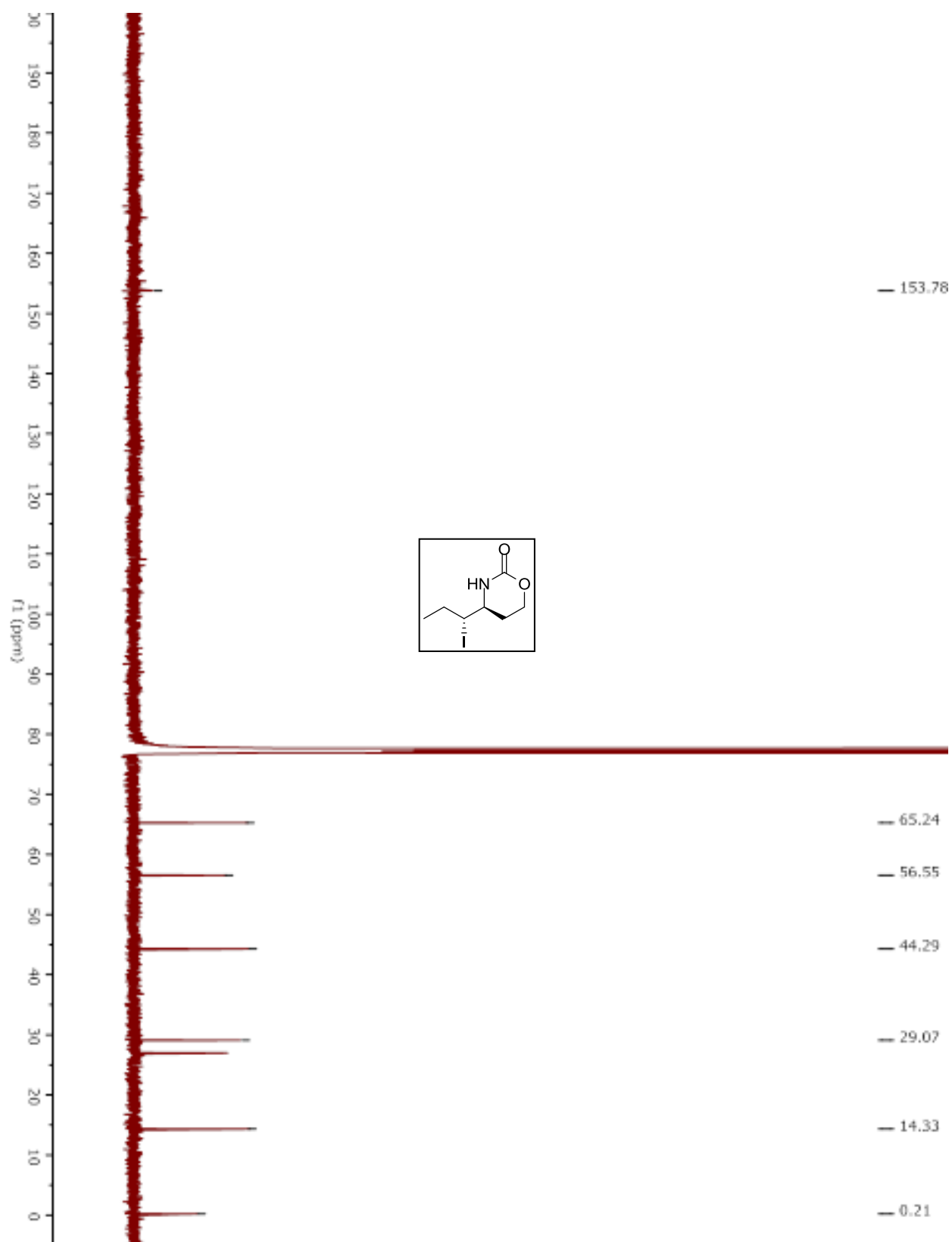
Compound 5.34-D.



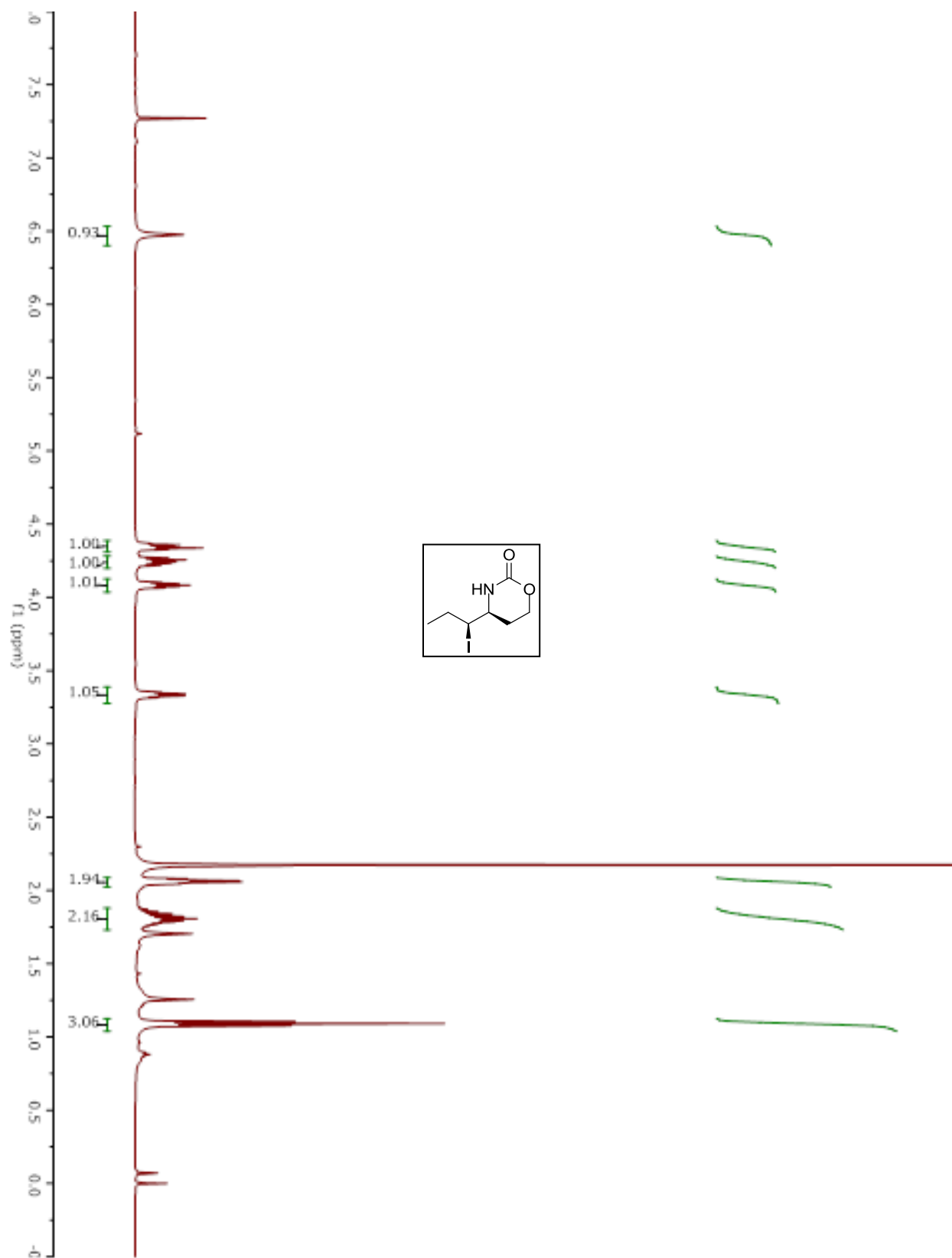
Compound S6.1.



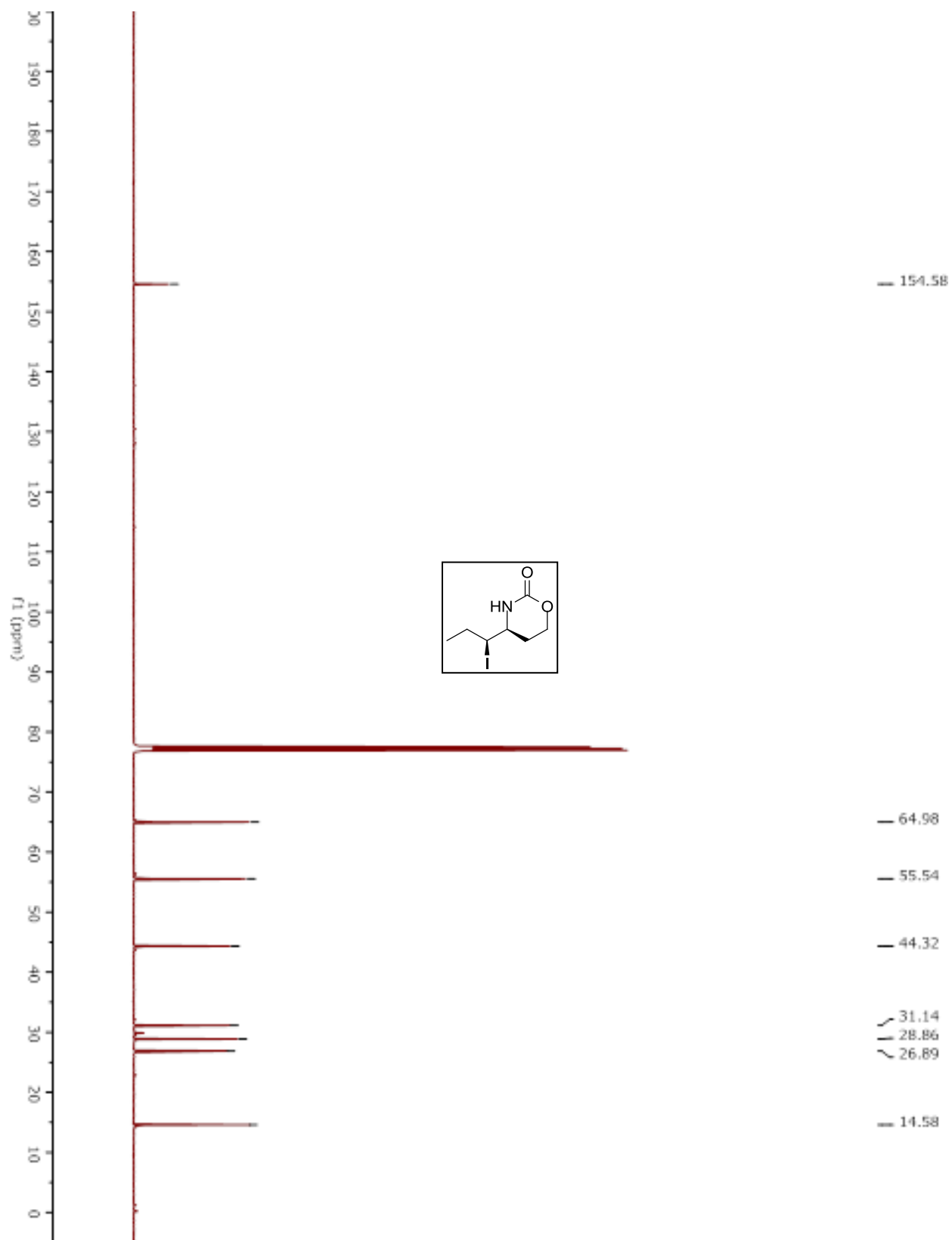
Compound S6.1.



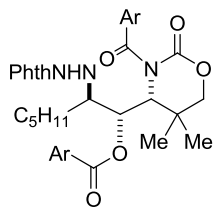
Compound S6.2.



Compound S6.2.



Appendix B. X-ray Crystallographic Data.



Data Collection

A pale yellow crystal with approximate dimensions 0.38 x 0.33 x 0.18 mm³ was selected under oil under ambient conditions and attached to the tip of a MiTeGen MicroMount[®]. The crystal was mounted in a stream of cold nitrogen at 100(1) K and centered in the X-ray beam by using a video camera.

The crystal evaluation and data collection were performed on a Bruker SMART APEXII diffractometer with Cu K_α ($\lambda = 1.54178 \text{ \AA}$) radiation and the diffractometer to crystal distance of 4.03 cm.

The initial cell constants were obtained from three series of ω scans at different starting angles. Each series consisted of 41 frames collected at intervals of 0.6° in a 25° range about ω with the exposure time of 5 seconds per frame. The reflections were successfully indexed by an automated indexing routine built in the APEXII program. The final cell constants were calculated from a set of 9922 strong reflections from the actual data collection.

The data were collected by using the full sphere data collection routine to survey the reciprocal space to the extent of a full sphere to a resolution of 0.82 Å. A total of 24547 data were harvested by collecting 19 sets of frames with 0.5° scans in ω with an exposure time 15/40 sec per frame. These highly redundant datasets were corrected for Lorentz and polarization effects. The absorption correction was based on fitting a function to the empirical transmission surface as sampled by multiple equivalent measurements. [1]

Structure Solution and Refinement

The systematic absences in the diffraction data were consistent for the space groups $P\bar{1}$ and $P1$. The E -statistics strongly suggested the centrosymmetric space group $P\bar{1}$ that yielded chemically reasonable and computationally stable results of refinement [2-4].

A successful solution by the direct methods provided most non-hydrogen atoms from the *E*-map. The remaining non-hydrogen atoms were located in an alternating series of least-squares cycles and difference Fourier maps. All non-hydrogen atoms were refined with anisotropic displacement coefficients. All hydrogen atoms were included in the structure factor calculation at idealized positions and were allowed to ride on the neighboring atoms with relative isotropic displacement coefficients.

The crystal selected for the single-crystal X-ray diffraction experiment proved to be a non-merohedral twin with a 18.7(2)% second component contribution. The twin components are related by a 180.0° rotation about reciprocal axis [001].

The crystal contains a racemate. The relative configuration of the three chiral centers (in the arbitrary selected molecule depicted in Figure 1) is SSS.

The final least-squares refinement of 468 parameters against 24547 data resulted in residuals *R* (based on F^2 for $I \geq 2\sigma$) and *wR* (based on F^2 for all data) of 0.0441 and 0.1488, respectively. The final difference Fourier map was featureless.

The molecular diagram is drawn with 30% probability ellipsoids.

References.

- [1] Bruker-AXS. (2007-2011) APEX2, SADABS, and SAINT Software Reference Manuals. Bruker-AXS, Madison, Wisconsin, USA.
- [2] Sheldrick, G. M. (2008) SHELXL. *Acta Cryst.* **A64**, 112-122.
- [3] Dolomanov, O.V.; Bourhis, L.J.; Gildea, R.J.; Howard, J.A.K.; Puschmann, H. "OLEX2: a complete structure solution, refinement and analysis program". *J. Appl. Cryst.* (2009) **42**, 339-341.
- [4] Guzei, I.A. (2006-2011). Internal laboratory computer programs "G1", "ResIns", "FCF_filter", "Modicifer".

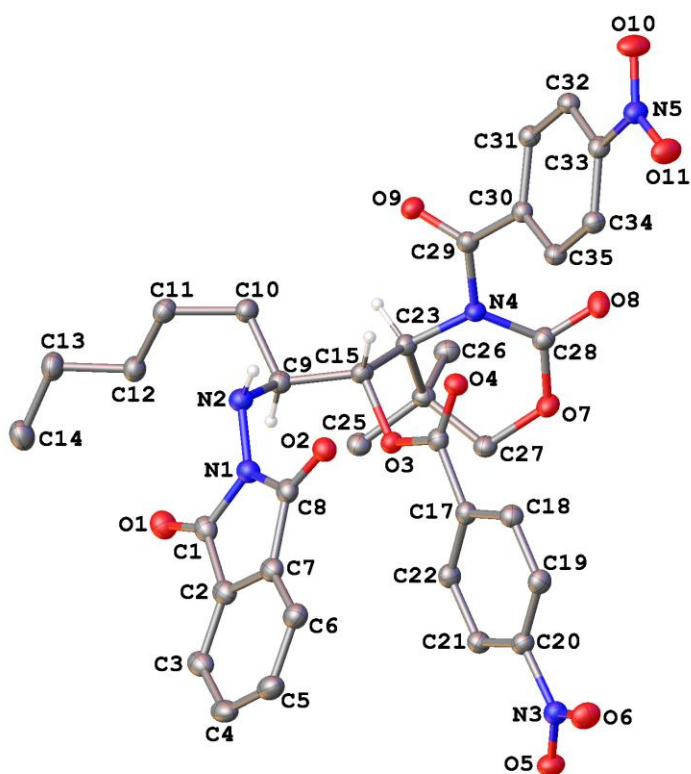


Figure 1. A molecular drawing of Schomaker11. All H atoms except on atom N2 and chiral C atoms are omitted.

Table 1. Crystal data and structure refinement for schomaker11.

Identification code	schomaker11	
Empirical formula	C ₃₅ H ₃₅ N ₅ O ₁₁	
Formula weight	701.68	
Temperature	100(1) K	
Wavelength	1.54178 Å	
Crystal system	triclinic	
Space group	$P\bar{1}$	
Unit cell dimensions	a = 11.5843(11) Å	$\alpha = 73.125(7)^\circ$.
	b = 12.0276(13) Å	$\beta = 78.428(9)^\circ$.
	c = 12.9101(15) Å	$\gamma = 73.353(5)^\circ$.
Volume	1635.6(3) Å ³	
Z	2	
Density (calculated)	1.425 Mg/m ³	
Absorption coefficient	0.902 mm ⁻¹	
F(000)	736	
Crystal size	0.38 x 0.33 x 0.18 mm ³	
Theta range for data collection	3.61 to 70.05°.	
Index ranges	-14 ≤ h ≤ 14, -14 ≤ k ≤ 14, -15 ≤ l ≤ 15	
Reflections collected	24547	
Independent reflections	24547 [R(int) = 0.0495]	
Completeness to theta = 67.00°	97.1 %	

Absorption correction	Numerical with SADABS
Max. and min. transmission	0.8545 and 0.7255
Refinement method	Full-matrix least-squares on F ²
Data / restraints / parameters	24547 / 0 / 468
Goodness-of-fit on F ²	0.979
Final R indices [I > 2σ(I)]	R1 = 0.0441, wR2 = 0.1349
R indices (all data)	R1 = 0.0517, wR2 = 0.1488
Largest diff. peak and hole	0.202 and -0.203 e.Å ⁻³

Table 2. Atomic coordinates ($\times 10^4$) and equivalent isotropic displacement parameters ($\text{\AA}^2 \times 10^3$) for schomaker11. $U(\text{eq})$ is defined as one third of the trace of the orthogonalized U^{ij} tensor.

	x	y	z	$U(\text{eq})$
O(1)	5892(2)	5748(2)	3385(1)	45(1)
O(2)	5062(1)	3716(1)	1236(1)	36(1)
O(3)	2813(1)	5702(1)	1780(1)	30(1)
O(4)	2658(1)	4907(1)	440(1)	34(1)
O(5)	1008(2)	988(2)	5617(1)	42(1)
O(6)	1388(2)	-5(2)	4379(1)	45(1)
O(7)	-314(1)	7120(2)	1540(1)	36(1)
O(8)	-630(2)	7410(2)	-154(1)	42(1)
O(9)	2394(1)	8386(1)	-1365(1)	35(1)
O(10)	1339(2)	6101(2)	-5160(1)	51(1)
O(11)	1087(2)	4519(2)	-3909(1)	47(1)
N(1)	5342(2)	5005(2)	2130(2)	34(1)
N(2)	5318(2)	6018(2)	1250(2)	34(1)
N(3)	1341(2)	893(2)	4671(2)	35(1)
N(4)	1203(2)	7567(2)	106(1)	29(1)
N(5)	1204(2)	5546(2)	-4200(2)	36(1)
C(1)	5687(2)	4935(2)	3136(2)	37(1)
C(2)	5725(2)	3690(2)	3788(2)	36(1)
C(3)	5974(2)	3136(2)	4849(2)	42(1)
C(4)	6021(2)	1921(2)	5226(2)	45(1)
C(5)	5827(2)	1286(2)	4559(2)	45(1)
C(6)	5564(2)	1848(2)	3494(2)	41(1)
C(7)	5509(2)	3057(2)	3132(2)	36(1)
C(8)	5269(2)	3900(2)	2050(2)	34(1)
C(9)	4211(2)	6997(2)	1262(2)	32(1)
C(10)	4526(2)	8120(2)	439(2)	35(1)
C(11)	5687(2)	8374(2)	589(2)	37(1)
C(12)	5647(2)	8593(2)	1701(2)	38(1)
C(13)	6773(2)	8920(2)	1825(2)	45(1)
C(14)	6876(3)	8805(3)	3008(2)	52(1)
C(15)	3106(2)	6750(2)	959(2)	30(1)
C(16)	2612(2)	4851(2)	1397(2)	30(1)
C(17)	2302(2)	3830(2)	2293(2)	30(1)
C(18)	2140(2)	2876(2)	1972(2)	33(1)
C(19)	1848(2)	1905(2)	2753(2)	34(1)
C(20)	1705(2)	1909(2)	3841(2)	32(1)
C(21)	1842(2)	2845(2)	4185(2)	34(1)
C(22)	2157(2)	3810(2)	3395(2)	33(1)
C(23)	1945(2)	7794(2)	816(2)	30(1)
C(24)	1114(2)	8132(2)	1828(2)	31(1)
C(25)	1824(2)	8145(2)	2707(2)	35(1)
C(26)	273(2)	9389(2)	1475(2)	36(1)
C(27)	349(2)	7232(2)	2333(2)	33(1)
C(28)	50(2)	7368(2)	463(2)	33(1)
C(29)	1650(2)	7793(2)	-1020(2)	30(1)
C(30)	1323(2)	7232(2)	-1787(2)	29(1)
C(31)	1312(2)	7878(2)	-2877(2)	30(1)
C(32)	1233(2)	7344(2)	-3670(2)	32(1)
C(33)	1186(2)	6152(2)	-3351(2)	31(1)
C(34)	1177(2)	5492(2)	-2272(2)	33(1)
C(35)	1233(2)	6045(2)	-1486(2)	31(1)

Table 3. Bond lengths [Å] and angles [°] for schomaker11.

O(1)-C(1)	1.209(3)	C(12)-H(12A)	0.9900
O(2)-C(8)	1.215(3)	C(12)-H(12B)	0.9900
O(3)-C(16)	1.351(3)	C(13)-C(14)	1.519(4)
O(3)-C(15)	1.467(3)	C(13)-H(13A)	0.9900
O(4)-C(16)	1.209(3)	C(13)-H(13B)	0.9900
O(5)-N(3)	1.233(2)	C(14)-H(14A)	0.9800
O(6)-N(3)	1.227(2)	C(14)-H(14B)	0.9800
O(7)-C(28)	1.341(3)	C(14)-H(14C)	0.9800
O(7)-C(27)	1.453(3)	C(15)-C(23)	1.555(3)
O(8)-C(28)	1.209(3)	C(15)-H(15)	1.0000
O(9)-C(29)	1.209(3)	C(16)-C(17)	1.495(3)
O(10)-N(5)	1.228(2)	C(17)-C(22)	1.392(3)
O(11)-N(5)	1.222(2)	C(17)-C(18)	1.398(3)
N(1)-C(8)	1.391(3)	C(18)-C(19)	1.379(3)
N(1)-N(2)	1.402(3)	C(18)-H(18)	0.9500
N(1)-C(1)	1.407(3)	C(19)-C(20)	1.382(3)
N(2)-C(9)	1.473(3)	C(19)-H(19)	0.9500
N(2)-H(2)	0.90(3)	C(20)-C(21)	1.383(3)
N(3)-C(20)	1.473(3)	C(21)-C(22)	1.389(3)
N(4)-C(28)	1.388(3)	C(21)-H(21)	0.9500
N(4)-C(29)	1.415(3)	C(22)-H(22)	0.9500
N(4)-C(23)	1.500(3)	C(23)-C(24)	1.543(3)
N(5)-C(33)	1.476(3)	C(23)-H(23)	1.0000
C(1)-C(2)	1.483(3)	C(24)-C(27)	1.513(3)
C(2)-C(3)	1.387(3)	C(24)-C(25)	1.535(3)
C(2)-C(7)	1.389(3)	C(24)-C(26)	1.541(3)
C(3)-C(4)	1.388(4)	C(25)-H(25A)	0.9800
C(3)-H(3)	0.9500	C(25)-H(25B)	0.9800
C(4)-C(5)	1.390(4)	C(25)-H(25C)	0.9800
C(4)-H(4)	0.9500	C(26)-H(26A)	0.9800
C(5)-C(6)	1.397(4)	C(26)-H(26B)	0.9800
C(5)-H(5)	0.9500	C(26)-H(26C)	0.9800
C(6)-C(7)	1.378(3)	C(27)-H(27A)	0.9900
C(6)-H(6)	0.9500	C(27)-H(27B)	0.9900
C(7)-C(8)	1.493(3)	C(29)-C(30)	1.505(3)
C(9)-C(15)	1.538(3)	C(30)-C(35)	1.394(3)
C(9)-C(10)	1.543(3)	C(30)-C(31)	1.397(3)
C(9)-H(9)	1.0000	C(31)-C(32)	1.386(3)
C(10)-C(11)	1.521(3)	C(31)-H(31)	0.9500
C(10)-H(10A)	0.9900	C(32)-C(33)	1.385(3)
C(10)-H(10B)	0.9900	C(32)-H(32)	0.9500
C(11)-C(12)	1.522(3)	C(33)-C(34)	1.388(3)
C(11)-H(11A)	0.9900	C(34)-C(35)	1.386(3)
C(11)-H(11B)	0.9900	C(34)-H(34)	0.9500
C(12)-C(13)	1.515(3)	C(35)-H(35)	0.9500
C(16)-O(3)-C(15)	116.36(17)	O(6)-N(3)-O(5)	123.58(19)
C(28)-O(7)-C(27)	123.39(17)	O(6)-N(3)-C(20)	117.9(2)
C(8)-N(1)-N(2)	124.19(19)	O(5)-N(3)-C(20)	118.55(19)
C(8)-N(1)-C(1)	112.10(19)	C(28)-N(4)-C(29)	120.31(18)
N(2)-N(1)-C(1)	122.57(19)	C(28)-N(4)-C(23)	123.46(18)
N(1)-N(2)-C(9)	116.00(18)	C(29)-N(4)-C(23)	115.19(17)
N(1)-N(2)-H(2)	106.6(18)	O(11)-N(5)-O(10)	123.6(2)
C(9)-N(2)-H(2)	112.7(17)	O(11)-N(5)-C(33)	118.19(19)

O(10)-N(5)-C(33)	118.18(19)	C(13)-C(14)-H(14B)	109.5
O(1)-C(1)-N(1)	125.4(2)	H(14A)-C(14)-H(14B)	109.5
O(1)-C(1)-C(2)	129.1(2)	C(13)-C(14)-H(14C)	109.5
N(1)-C(1)-C(2)	105.5(2)	H(14A)-C(14)-H(14C)	109.5
C(3)-C(2)-C(7)	121.2(2)	H(14B)-C(14)-H(14C)	109.5
C(3)-C(2)-C(1)	130.4(2)	O(3)-C(15)-C(9)	107.84(17)
C(7)-C(2)-C(1)	108.3(2)	O(3)-C(15)-C(23)	109.91(17)
C(2)-C(3)-C(4)	117.6(2)	C(9)-C(15)-C(23)	117.44(18)
C(2)-C(3)-H(3)	121.2	O(3)-C(15)-H(15)	107.1
C(4)-C(3)-H(3)	121.2	C(9)-C(15)-H(15)	107.1
C(5)-C(4)-C(3)	121.0(2)	C(23)-C(15)-H(15)	107.1
C(5)-C(4)-H(4)	119.5	O(4)-C(16)-O(3)	124.2(2)
C(3)-C(4)-H(4)	119.5	O(4)-C(16)-C(17)	123.3(2)
C(4)-C(5)-C(6)	121.3(2)	O(3)-C(16)-C(17)	112.44(19)
C(4)-C(5)-H(5)	119.4	C(22)-C(17)-C(18)	120.4(2)
C(6)-C(5)-H(5)	119.4	C(22)-C(17)-C(16)	123.2(2)
C(7)-C(6)-C(5)	117.2(2)	C(18)-C(17)-C(16)	116.4(2)
C(7)-C(6)-H(6)	121.4	C(19)-C(18)-C(17)	119.7(2)
C(5)-C(6)-H(6)	121.4	C(19)-C(18)-H(18)	120.2
C(6)-C(7)-C(2)	121.6(2)	C(17)-C(18)-H(18)	120.2
C(6)-C(7)-C(8)	130.2(2)	C(18)-C(19)-C(20)	118.8(2)
C(2)-C(7)-C(8)	108.1(2)	C(18)-C(19)-H(19)	120.6
O(2)-C(8)-N(1)	124.4(2)	C(20)-C(19)-H(19)	120.6
O(2)-C(8)-C(7)	129.9(2)	C(21)-C(20)-C(19)	122.9(2)
N(1)-C(8)-C(7)	105.65(19)	C(21)-C(20)-N(3)	118.4(2)
N(2)-C(9)-C(15)	114.09(18)	C(19)-C(20)-N(3)	118.6(2)
N(2)-C(9)-C(10)	106.66(18)	C(20)-C(21)-C(22)	117.9(2)
C(15)-C(9)-C(10)	109.64(18)	C(20)-C(21)-H(21)	121.0
N(2)-C(9)-H(9)	108.8	C(22)-C(21)-H(21)	121.0
C(15)-C(9)-H(9)	108.8	C(21)-C(22)-C(17)	120.2(2)
C(10)-C(9)-H(9)	108.8	C(21)-C(22)-H(22)	119.9
C(11)-C(10)-C(9)	114.14(19)	C(17)-C(22)-H(22)	119.9
C(11)-C(10)-H(10A)	108.7	N(4)-C(23)-C(24)	109.36(17)
C(9)-C(10)-H(10A)	108.7	N(4)-C(23)-C(15)	108.46(17)
C(11)-C(10)-H(10B)	108.7	C(24)-C(23)-C(15)	120.02(18)
C(9)-C(10)-H(10B)	108.7	N(4)-C(23)-H(23)	106.0
H(10A)-C(10)-H(10B)	107.6	C(24)-C(23)-H(23)	106.0
C(10)-C(11)-C(12)	113.4(2)	C(15)-C(23)-H(23)	106.0
C(10)-C(11)-H(11A)	108.9	C(27)-C(24)-C(25)	107.84(18)
C(12)-C(11)-H(11A)	108.9	C(27)-C(24)-C(26)	109.24(19)
C(10)-C(11)-H(11B)	108.9	C(25)-C(24)-C(26)	108.35(18)
C(12)-C(11)-H(11B)	108.9	C(27)-C(24)-C(23)	109.19(18)
H(11A)-C(11)-H(11B)	107.7	C(25)-C(24)-C(23)	113.00(18)
C(13)-C(12)-C(11)	113.4(2)	C(26)-C(24)-C(23)	109.16(18)
C(13)-C(12)-H(12A)	108.9	C(24)-C(25)-H(25A)	109.5
C(11)-C(12)-H(12A)	108.9	C(24)-C(25)-H(25B)	109.5
C(13)-C(12)-H(12B)	108.9	H(25A)-C(25)-H(25B)	109.5
C(11)-C(12)-H(12B)	108.9	C(24)-C(25)-H(25C)	109.5
H(12A)-C(12)-H(12B)	107.7	H(25A)-C(25)-H(25C)	109.5
C(12)-C(13)-C(14)	112.5(2)	H(25B)-C(25)-H(25C)	109.5
C(12)-C(13)-H(13A)	109.1	C(24)-C(26)-H(26A)	109.5
C(14)-C(13)-H(13A)	109.1	C(24)-C(26)-H(26B)	109.5
C(12)-C(13)-H(13B)	109.1	H(26A)-C(26)-H(26B)	109.5
C(14)-C(13)-H(13B)	109.1	C(24)-C(26)-H(26C)	109.5
H(13A)-C(13)-H(13B)	107.8	H(26A)-C(26)-H(26C)	109.5
C(13)-C(14)-H(14A)	109.5	H(26B)-C(26)-H(26C)	109.5

O(7)-C(27)-C(24)	111.59(18)	C(32)-C(31)-C(30)	120.6(2)
O(7)-C(27)-H(27A)	109.3	C(32)-C(31)-H(31)	119.7
C(24)-C(27)-H(27A)	109.3	C(30)-C(31)-H(31)	119.7
O(7)-C(27)-H(27B)	109.3	C(31)-C(32)-C(33)	118.1(2)
C(24)-C(27)-H(27B)	109.3	C(31)-C(32)-H(32)	121.0
H(27A)-C(27)-H(27B)	108.0	C(33)-C(32)-H(32)	121.0
O(8)-C(28)-O(7)	119.3(2)	C(32)-C(33)-C(34)	122.7(2)
O(8)-C(28)-N(4)	122.9(2)	C(32)-C(33)-N(5)	118.5(2)
O(7)-C(28)-N(4)	117.85(19)	C(34)-C(33)-N(5)	118.7(2)
O(9)-C(29)-N(4)	118.9(2)	C(33)-C(34)-C(35)	118.5(2)
O(9)-C(29)-C(30)	118.4(2)	C(33)-C(34)-H(34)	120.7
N(4)-C(29)-C(30)	122.44(18)	C(35)-C(34)-H(34)	120.7
C(35)-C(30)-C(31)	119.9(2)	C(34)-C(35)-C(30)	120.1(2)
C(35)-C(30)-C(29)	122.2(2)	C(34)-C(35)-H(35)	119.9
C(31)-C(30)-C(29)	116.99(19)	C(30)-C(35)-H(35)	119.9

Symmetry transformations used to generate equivalent atoms:

Table 4. Anisotropic displacement parameters ($\text{\AA}^2 \times 10^3$) for schomaker11. The anisotropic displacement factor exponent takes the form: $-2\pi^2 [h^2 a^{*2} U^{11} + \dots + 2 h k a^* b^* U^{12}]$

	U ¹¹	U ²²	U ³³	U ²³	U ¹³	U ¹²
O(1)	46(1)	46(1)	46(1)	-18(1)	-8(1)	-9(1)
O(2)	36(1)	40(1)	34(1)	-11(1)	-4(1)	-9(1)
O(3)	33(1)	30(1)	29(1)	-7(1)	-3(1)	-11(1)
O(4)	39(1)	36(1)	29(1)	-8(1)	-5(1)	-12(1)
O(5)	53(1)	45(1)	30(1)	-7(1)	-2(1)	-19(1)
O(6)	58(1)	33(1)	45(1)	-11(1)	-2(1)	-16(1)
O(7)	37(1)	46(1)	30(1)	-11(1)	2(1)	-18(1)
O(8)	33(1)	62(1)	37(1)	-20(1)	0(1)	-17(1)
O(9)	38(1)	39(1)	30(1)	-8(1)	-1(1)	-17(1)
O(10)	83(1)	51(1)	26(1)	-8(1)	-3(1)	-30(1)
O(11)	70(1)	40(1)	38(1)	-12(1)	-2(1)	-26(1)
N(1)	34(1)	35(1)	32(1)	-8(1)	-5(1)	-7(1)
N(2)	35(1)	35(1)	32(1)	-8(1)	-2(1)	-9(1)
N(3)	36(1)	35(1)	35(1)	-7(1)	-6(1)	-10(1)
N(4)	32(1)	32(1)	24(1)	-8(1)	-2(1)	-10(1)
N(5)	43(1)	39(1)	30(1)	-10(1)	-2(1)	-16(1)
C(1)	30(1)	44(1)	37(1)	-16(1)	-4(1)	-4(1)
C(2)	28(1)	44(1)	34(1)	-11(1)	-2(1)	-4(1)
C(3)	35(1)	55(2)	34(2)	-14(1)	-1(1)	-6(1)
C(4)	39(1)	58(2)	31(2)	-3(1)	-1(1)	-9(1)
C(5)	41(1)	45(2)	42(2)	-1(1)	-2(1)	-11(1)
C(6)	36(1)	44(1)	41(2)	-8(1)	-3(1)	-11(1)
C(7)	29(1)	43(1)	34(1)	-10(1)	0(1)	-7(1)
C(8)	28(1)	39(1)	35(1)	-12(1)	-1(1)	-7(1)
C(9)	33(1)	35(1)	31(1)	-10(1)	-3(1)	-9(1)
C(10)	37(1)	36(1)	34(1)	-9(1)	-4(1)	-13(1)
C(11)	37(1)	38(1)	38(2)	-10(1)	0(1)	-14(1)
C(12)	36(1)	40(1)	41(2)	-11(1)	-5(1)	-14(1)
C(13)	41(1)	52(2)	51(2)	-15(1)	-7(1)	-19(1)
C(14)	51(2)	56(2)	56(2)	-14(1)	-17(1)	-17(1)
C(15)	35(1)	29(1)	28(1)	-6(1)	-2(1)	-12(1)
C(16)	26(1)	32(1)	33(1)	-10(1)	-4(1)	-5(1)
C(17)	27(1)	31(1)	33(1)	-9(1)	-4(1)	-7(1)
C(18)	35(1)	37(1)	30(1)	-11(1)	-2(1)	-9(1)
C(19)	36(1)	32(1)	37(1)	-11(1)	-3(1)	-10(1)
C(20)	31(1)	31(1)	33(1)	-5(1)	-3(1)	-8(1)
C(21)	35(1)	37(1)	29(1)	-8(1)	-5(1)	-10(1)
C(22)	34(1)	32(1)	36(1)	-10(1)	-6(1)	-9(1)
C(23)	32(1)	31(1)	28(1)	-8(1)	-5(1)	-10(1)
C(24)	36(1)	32(1)	26(1)	-7(1)	-3(1)	-9(1)
C(25)	39(1)	41(1)	29(1)	-12(1)	-2(1)	-12(1)
C(26)	40(1)	33(1)	33(1)	-9(1)	-2(1)	-7(1)
C(27)	35(1)	36(1)	27(1)	-8(1)	-2(1)	-9(1)
C(28)	33(1)	35(1)	32(1)	-11(1)	0(1)	-10(1)
C(29)	30(1)	29(1)	29(1)	-6(1)	-4(1)	-5(1)
C(30)	27(1)	32(1)	28(1)	-9(1)	-3(1)	-7(1)
C(31)	31(1)	31(1)	30(1)	-7(1)	-2(1)	-8(1)
C(32)	32(1)	36(1)	26(1)	-6(1)	-3(1)	-9(1)
C(33)	33(1)	36(1)	28(1)	-12(1)	-1(1)	-11(1)
C(34)	35(1)	32(1)	31(1)	-8(1)	-3(1)	-9(1)
C(35)	33(1)	34(1)	27(1)	-7(1)	-3(1)	-10(1)

Table 5. Hydrogen coordinates ($\times 10^4$) and isotropic displacement parameters ($\text{\AA}^2 \times 10^{-3}$) for schomaker11.

	x	y	z	U(eq)
H(2)	5480(20)	5750(20)	640(20)	45(8)
H(3)	6108	3572	5302	51
H(4)	6187	1518	5950	54
H(5)	5876	453	4833	55
H(6)	5428	1416	3039	49
H(9)	4001	7148	2007	39
H(10A)	4608	8021	-309	42
H(10B)	3843	8823	509	42
H(11A)	5838	9087	15	44
H(11B)	6377	7686	492	44
H(12A)	4927	9248	1818	46
H(12B)	5548	7861	2274	46
H(13A)	6752	9755	1403	54
H(13B)	7501	8391	1516	54
H(14A)	7574	9094	3042	78
H(14B)	6989	7963	3413	78
H(14C)	6132	9283	3333	78
H(15)	3369	6518	248	37
H(18)	2230	2897	1219	40
H(19)	1747	1245	2547	41
H(21)	1725	2828	4939	40
H(22)	2275	4459	3607	40
H(23)	2230	8525	387	36
H(25A)	2294	7331	3001	53
H(25B)	1254	8439	3296	53
H(25C)	2377	8673	2384	53
H(26A)	765	9974	1145	54
H(26B)	-262	9605	2115	54
H(26C)	-220	9385	942	54
H(27A)	882	6442	2633	39
H(27B)	-234	7486	2944	39
H(31)	1359	8690	-3077	37
H(32)	1211	7782	-4411	38
H(34)	1133	4679	-2077	39
H(35)	1211	5616	-741	38

Table 6. Torsion angles [°] for schomaker11.

C(8)-N(1)-N(2)-C(9)	109.5(2)	O(5)-N(3)-C(20)-C(21)	10.1(3)
C(1)-N(1)-N(2)-C(9)	-83.6(2)	O(6)-N(3)-C(20)-C(19)	12.6(3)
C(8)-N(1)-C(1)-O(1)	175.0(2)	O(5)-N(3)-C(20)-C(19)	-167.5(2)
N(2)-N(1)-C(1)-O(1)	6.8(4)	C(19)-C(20)-C(21)-C(22)	-1.0(3)
C(8)-N(1)-C(1)-C(2)	-5.5(2)	N(3)-C(20)-C(21)-C(22)	-178.52(19)
N(2)-N(1)-C(1)-C(2)	-173.75(19)	C(20)-C(21)-C(22)-C(17)	1.3(3)
O(1)-C(1)-C(2)-C(3)	1.6(4)	C(18)-C(17)-C(22)-C(21)	-0.5(3)
N(1)-C(1)-C(2)-C(3)	-177.8(2)	C(16)-C(17)-C(22)-C(21)	178.5(2)
O(1)-C(1)-C(2)-C(7)	-175.7(2)	C(28)-N(4)-C(23)-C(24)	-16.4(3)
N(1)-C(1)-C(2)-C(7)	4.8(3)	C(29)-N(4)-C(23)-C(24)	151.95(18)
C(7)-C(2)-C(3)-C(4)	1.1(4)	C(28)-N(4)-C(23)-C(15)	116.2(2)
C(1)-C(2)-C(3)-C(4)	-175.9(2)	C(29)-N(4)-C(23)-C(15)	-75.5(2)
C(2)-C(3)-C(4)-C(5)	0.2(4)	O(3)-C(15)-C(23)-N(4)	-79.2(2)
C(3)-C(4)-C(5)-C(6)	-0.9(4)	C(9)-C(15)-C(23)-N(4)	157.10(19)
C(4)-C(5)-C(6)-C(7)	0.3(4)	O(3)-C(15)-C(23)-C(24)	47.5(2)
C(5)-C(6)-C(7)-C(2)	1.0(3)	C(9)-C(15)-C(23)-C(24)	-76.3(3)
C(5)-C(6)-C(7)-C(8)	179.0(2)	N(4)-C(23)-C(24)-C(27)	48.9(2)
C(3)-C(2)-C(7)-C(6)	-1.8(4)	C(15)-C(23)-C(24)-C(27)	-77.3(2)
C(1)-C(2)-C(7)-C(6)	175.9(2)	N(4)-C(23)-C(24)-C(25)	168.95(17)
C(3)-C(2)-C(7)-C(8)	179.8(2)	C(15)-C(23)-C(24)-C(25)	42.7(3)
C(1)-C(2)-C(7)-C(8)	-2.5(3)	N(4)-C(23)-C(24)-C(26)	-70.4(2)
N(2)-N(1)-C(8)-O(2)	-7.2(3)	C(15)-C(23)-C(24)-C(26)	163.37(18)
C(1)-N(1)-C(8)-O(2)	-175.3(2)	C(28)-O(7)-C(27)-C(24)	25.2(3)
N(2)-N(1)-C(8)-C(7)	172.05(19)	C(25)-C(24)-C(27)-O(7)	-177.30(18)
C(1)-N(1)-C(8)-C(7)	4.0(2)	C(26)-C(24)-C(27)-O(7)	65.1(2)
C(6)-C(7)-C(8)-O(2)	0.3(4)	C(23)-C(24)-C(27)-O(7)	-54.2(2)
C(2)-C(7)-C(8)-O(2)	178.4(2)	C(27)-O(7)-C(28)-O(8)	-170.0(2)
C(6)-C(7)-C(8)-N(1)	-178.9(2)	C(27)-O(7)-C(28)-N(4)	10.0(3)
C(2)-C(7)-C(8)-N(1)	-0.8(2)	C(29)-N(4)-C(28)-O(8)	-2.1(3)
N(1)-N(2)-C(9)-C(15)	-75.0(3)	C(23)-N(4)-C(28)-O(8)	165.7(2)
N(1)-N(2)-C(9)-C(10)	163.78(18)	C(29)-N(4)-C(28)-O(7)	177.89(18)
N(2)-C(9)-C(10)-C(11)	-49.9(3)	C(23)-N(4)-C(28)-O(7)	-14.3(3)
C(15)-C(9)-C(10)-C(11)	-173.90(19)	C(28)-N(4)-C(29)-O(9)	152.4(2)
C(9)-C(10)-C(11)-C(12)	-60.8(3)	C(23)-N(4)-C(29)-O(9)	-16.4(3)
C(10)-C(11)-C(12)-C(13)	-176.5(2)	C(28)-N(4)-C(29)-C(30)	-33.4(3)
C(11)-C(12)-C(13)-C(14)	-164.5(2)	C(23)-N(4)-C(29)-C(30)	157.87(18)
C(16)-O(3)-C(15)-C(9)	-133.21(18)	O(9)-C(29)-C(30)-C(35)	134.8(2)
C(16)-O(3)-C(15)-C(23)	97.6(2)	N(4)-C(29)-C(30)-C(35)	-39.5(3)
N(2)-C(9)-C(15)-O(3)	62.3(2)	O(9)-C(29)-C(30)-C(31)	-34.6(3)
C(10)-C(9)-C(15)-O(3)	-178.11(17)	N(4)-C(29)-C(30)-C(31)	151.1(2)
N(2)-C(9)-C(15)-C(23)	-172.89(19)	C(35)-C(30)-C(31)-C(32)	-1.1(3)
C(10)-C(9)-C(15)-C(23)	-53.3(3)	C(29)-C(30)-C(31)-C(32)	168.56(19)
C(15)-O(3)-C(16)-O(4)	0.0(3)	C(30)-C(31)-C(32)-C(33)	-1.0(3)
C(15)-O(3)-C(16)-C(17)	-179.11(17)	C(31)-C(32)-C(33)-C(34)	2.1(3)
O(4)-C(16)-C(17)-C(22)	-174.9(2)	C(31)-C(32)-C(33)-N(5)	-175.01(19)
O(3)-C(16)-C(17)-C(22)	4.2(3)	O(11)-N(5)-C(33)-C(32)	-175.5(2)
O(4)-C(16)-C(17)-C(18)	4.1(3)	O(10)-N(5)-C(33)-C(32)	4.6(3)
O(3)-C(16)-C(17)-C(18)	-176.79(18)	O(11)-N(5)-C(33)-C(34)	7.3(3)
C(22)-C(17)-C(18)-C(19)	-0.7(3)	O(10)-N(5)-C(33)-C(34)	-172.6(2)
C(16)-C(17)-C(18)-C(19)	-179.8(2)	C(32)-C(33)-C(34)-C(35)	-0.9(3)
C(17)-C(18)-C(19)-C(20)	1.0(3)	N(5)-C(33)-C(34)-C(35)	176.2(2)
C(18)-C(19)-C(20)-C(21)	-0.1(3)	C(33)-C(34)-C(35)-C(30)	-1.3(3)
C(18)-C(19)-C(20)-N(3)	177.4(2)	C(31)-C(30)-C(35)-C(34)	2.3(3)
O(6)-N(3)-C(20)-C(21)	-169.9(2)	C(29)-C(30)-C(35)-C(34)	-166.8(2)

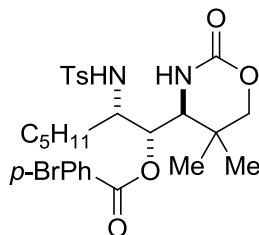
Table 7. Hydrogen bonds for schomaker11 [\AA and $^\circ$].

D-H...A	d(D-H)	d(H...A)	d(D...A)	$\angle(\text{DHA})$
N(2)-H(2)...O(2)#1	0.90(3)	2.48(3)	3.238(3)	142(2)
N(2)-H(2)...O(4)#1	0.90(3)	2.39(3)	3.059(3)	132(2)

Symmetry transformations used to generate equivalent atoms:

#1 $-x+1, -y+1, -z$

Crystallographic Experimental Section



Confirming the Absolute Stereochemistry of Compound A1. The 4-bromophenyl ester of the alcohol was prepared according to the following procedure and analyzed by X-ray crystallography: the alcohol (39 mg, 1.0 equiv), *N,N*-dimethylaminopyridine (10 mg, 0.8 equiv), 4-bromobenzoic acid (59 mg, 3.0) and dicyclohexylcarbodiimide (73 mg, 3.6 equiv) were added to a 10 ml flame-dried round bottomed flask with 2 ml dry dichloromethane and stirred 30 hours. Aqueous NH₄Cl (2 ml) was then added and the organic and aqueous layers were separated. The aqueous layer was extracted three times with dichloromethane and the combined organic layers were dried over Na₂SO₄ and concentrated *in vacuo*. The product was purified by flash chromatography using a hexanes/EtOAc gradient and recrystallized by diffusion of hexanes into a dichloromethane/Et₂O solution of the product at room temperature to yield colorless crystals.

Data Collection

A colorless crystal with approximate dimensions 0.4 x 0.3 x 0.2 mm³ was selected under oil under ambient conditions and attached to the tip of a MiTeGen MicroMount©. The crystal was mounted in a stream of cold nitrogen at 100(1) K and centered in the X-ray beam by using a video camera.

The crystal evaluation and data collection were performed on a Bruker Quazar SMART APEXII diffractometer with Mo K_α (λ = 0.71073 Å) radiation and the diffractometer to crystal distance of 4.96 cm.

The initial cell constants were obtained from three series of ω scans at different starting angles. Each series consisted of 12 frames collected at intervals of 0.5° in a 6° range about ω

with the exposure time of 10 seconds per frame. The reflections were successfully indexed by an automated indexing routine built in the APEXII program suite. The final cell constants were calculated from a set of 7705 strong reflections from the actual data collection.

The data were collected by using the full sphere data collection routine to survey the reciprocal space to the extent of a full sphere to a resolution of 0.70 Å. A total of 22130 data were harvested by collecting 6 sets of frames with 0.5° scans in ω and ϕ with exposure times of 4 sec per frame. These highly redundant datasets were corrected for Lorentz and polarization effects. The absorption correction was based on fitting a function to the empirical transmission surface as sampled by multiple equivalent measurements. [1]

Structure Solution and Refinement

The systematic absences in the diffraction data and E -statistics were consistent for the space groups $P3_1$ and $P3_2$. The latter space group $P3_2$ yielded chemically reasonable and computationally stable results of refinement with the molecules with the correct handedness [2-4].

A successful solution by the direct methods provided most non-hydrogen atoms from the E -map. The remaining non-hydrogen atoms were located in an alternating series of least-squares cycles and difference Fourier maps. All non-hydrogen atoms in the main molecules were refined with anisotropic displacement coefficients. All C-H hydrogen atoms were included in the structure factor calculation at idealized positions and were allowed to ride on the neighboring atoms with relative isotropic displacement coefficients. The amino H atoms were refined with N-H distance restraints but were not placed in idealized positions.

There are three $C_{27}H_{35}BrN_2O_6S$ molecules and three CH_2Cl_2 molecules in the asymmetric unit. All chiral centers have the R configuration.

There is extensive disorder in the organic molecules.

In molecule Br1 the aliphatic chain at C15 is disordered over two positions with the major component contribution of 82.9(10)%.

In molecule Br2 the ester chain at O8 is disordered over two positions with the major component contribution of 54.2(8)%, and the chain at C42 is disordered over two positions with the major component contribution of 53.0(14)%.

In molecule Br3 the large substituent at C69 is disordered over two positions with the major component contribution of 57.1(11)%, and atom C72 is disordered over two positions with the major component contribution of 80(2)%.

Two of the CH₂Cl₂ molecules are disordered over three positions each in ratios 63.1(3):23.7(4):13.1(4) and 53.2(3):32.9(3):14.0(3). Molecules C3s-C7s were refined isotropically.

Many atomic displacement and bond distance restraints and constraints were applied to all molecules to ensure a computationally stable refinement.

The final least-squares refinement of 1239 parameters against 19267 data resulted in residuals R (based on F^2 for $I \geq 2\sigma$) and wR (based on F^2 for all data) of 0.0534 and 0.1310, respectively. The final difference Fourier map was featureless.

Summary

Crystal Data for C₂₈H₃₇BrCl₂N₂O₆S ($M = 680.46$): trigonal, space group P3₂ (no. 145), $a = 23.982(9)$ Å, $c = 14.172(6)$ Å, $V = 7059(6)$ Å³, $Z = 9$, $T = 100.01$ K, $\mu(\text{Mo K}\alpha) = 1.589$ mm⁻¹, $D_{\text{calc}} = 1.441$ g/mm³, 74274 reflections measured ($3.396 \leq 2\theta \leq 52.794$), 19267 unique ($R_{\text{int}} = 0.0585$) which were used in all calculations. The final R_1 was 0.0534 ($I > 2\sigma(I)$) and wR_2 was 0.1310 (all data).

References

- [1] Bruker-AXS. (2009) APEX2, SADABS, and SAINT Software Reference Manuals. Bruker-AXS, Madison, Wisconsin, USA.
- [2] Sheldrick, G. M. (2008) SHELXL. *Acta Cryst.* **A64**, 112-122.
- [3] Dolomanov, O.V.; Bourhis, L.J.; Gildea, R.J.; Howard, J.A.K.; Puschmann, H. "OLEX2: a complete structure solution, refinement and analysis program". *J. Appl. Cryst.* (2009) **42**, 339-341.
- [4] Guzei, I.A. (2006-2008). Internal laboratory computer programs "ResIns", "FCF_filter", "Programs G1,2,3".

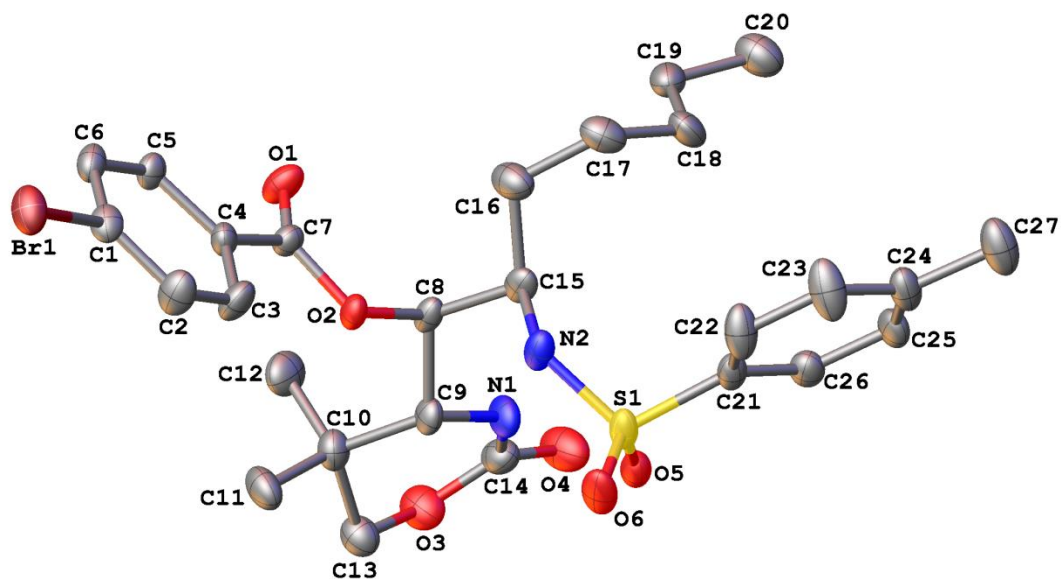


Figure 1. A molecular drawing of the first $C_{27}H_{35}BrN_2O_6S$ molecule shown with 50% probability ellipsoids. All H atoms and disordered parts are omitted.

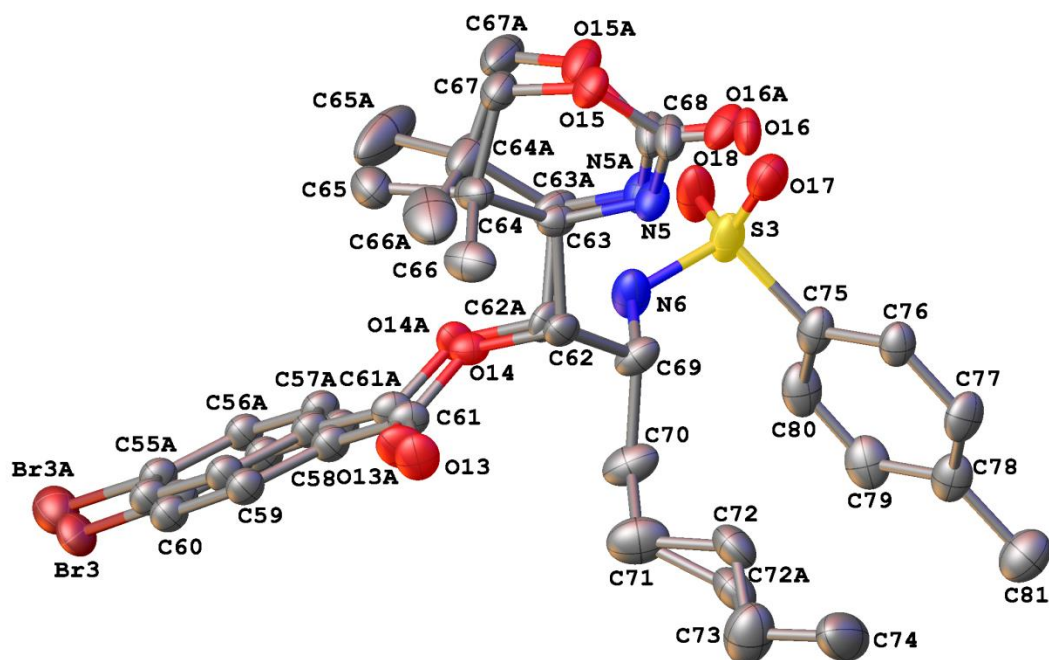


Figure 4. A molecular drawing of the third $C_{27}H_{35}BrN_2O_6S$ molecule shown with 50% probability ellipsoids. The disordered atoms are shown but all H atoms are omitted.

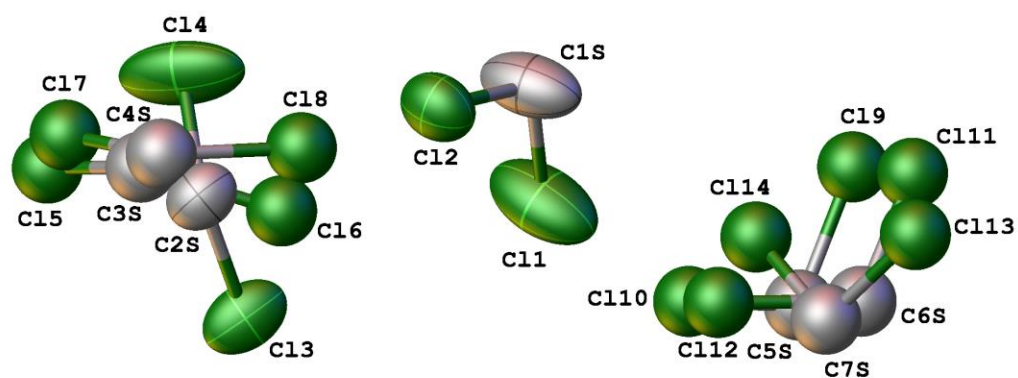


Figure 5. A molecular drawing of the three solvent molecules shown with 50% probability ellipsoids. Atoms shown as spheres were refined isotropically. The disordered atoms are shown but all H atoms are omitted.

Table 1 Crystal data and structure refinement for Schomaker19

Identification code	Schomaker19
Empirical formula	$C_{28}H_{37}BrCl_2N_2O_6S$
Formula weight	680.46
Temperature/K	100.01
Crystal system	trigonal
Space group	$P3_2$
$a/\text{\AA}$	23.982(9)
$b/\text{\AA}$	23.982(9)
$c/\text{\AA}$	14.172(6)
$\alpha/^\circ$	90
$\beta/^\circ$	90
$\gamma/^\circ$	120
Volume/ \AA^3	7059(6)
Z	9
$\rho_{\text{calc}}/\text{mg}/\text{mm}^3$	1.441
m/mm^{-1}	1.589
F(000)	3168.0
Crystal size/ mm^3	$0.4 \times 0.3 \times 0.2$
2θ range for data collection	3.396 to 52.794 $^\circ$
Index ranges	$-29 \leq h \leq 30, -28 \leq k \leq 29, -17 \leq l \leq 17$
Reflections collected	74274
Independent reflections	19267[R(int) = 0.0585]
Data/restraints/parameters	19267/2351/1239
Goodness-of-fit on F^2	1.021
Final R indexes [$I \geq 2\sigma(I)$]	$R_1 = 0.0534, wR_2 = 0.1205$
Final R indexes [all data]	$R_1 = 0.0752, wR_2 = 0.1310$
Largest diff. peak/hole / $e \text{\AA}^{-3}$	0.56/-0.90
Flack parameter	0.010(9)

Table 2 Fractional Atomic Coordinates ($\times 10^4$) and Equivalent Isotropic Displacement Parameters ($\text{\AA}^2 \times 10^3$) for Schomaker19. U_{eq} is defined as 1/3 of the trace of the orthogonalised U_{H} tensor.

Atom	<i>x</i>	<i>y</i>	<i>z</i>	$U(\text{eq})$
Br1	7904.2(3)	4185.9(4)	-3348.2(12)	34.76(18)
C1	7499(3)	4250(3)	-2235(4)	25.2(14)
C2	7537(4)	4827(3)	-2023(5)	34.5(16)
C3	7267(3)	4889(3)	-1196(4)	32.3(15)
C4	6955(3)	4365(3)	-592(4)	23.1(13)
C5	6911(3)	3782(3)	-825(4)	23.5(13)
C6	7182(3)	3720(3)	-1655(4)	26.6(14)
C7	6681(3)	4402(3)	332(4)	22.3(13)
O1	6448(2)	3972(2)	898(3)	32.4(11)
O2	6731(2)	4984.4(19)	468(3)	23.6(9)
C8	6561(3)	5124(3)	1381(4)	23.0(13)
S1	7609.9(8)	6875.0(8)	1493.5(16)	27.5(4)
O3	4821(2)	5072(3)	1854(4)	38.7(12)
O4	5199(3)	5418(3)	3281(4)	45.5(13)
O5	7041(2)	6785(2)	1943(3)	28.8(10)
O6	7814(3)	7235(2)	620(3)	37.9(12)
N1	5898(3)	5477(3)	2160(4)	30.2(13)
N2	7526(3)	6183(2)	1252(4)	26.2(12)
C9	6072(3)	5351(3)	1221(4)	24.3(13)
C10	5461(3)	4888(3)	675(5)	29.6(14)
C11	5565(4)	4932(4)	-389(5)	37.1(17)
C12	5154(3)	4184(3)	1015(6)	38.6(17)
C13	4985(3)	5123(4)	865(5)	32.9(15)
C14	5315(4)	5330(4)	2463(5)	33.1(15)
C15	7188(3)	5608(3)	1851(4)	25.8(13)
C16	7609(3)	5305(3)	2019(5)	36.8(17)
C17	8206(3)	5682(4)	2615(4)	35(2)
C18	8101(4)	5843(4)	3608(4)	35(2)
C19	7647(4)	5277(3)	4213(4)	32(2)
C20	7695(5)	5453(5)	5247(5)	44(2)
C17A	7670(20)	4889(15)	2765(14)	38(8)
C18A	7531(17)	5099(16)	3700(20)	33(6)
C19A	8069(19)	5735(17)	4060(20)	33(6)
C20A	8040(30)	5770(30)	5120(20)	44(2)

C21	8250(3)	7276(3)	2296(5)	25.7(14)
C22	8871(4)	7459(3)	2002(5)	38.4(18)
C23	9378(4)	7797(4)	2624(5)	46(2)
C24	9273(3)	7963(3)	3523(5)	32.0(15)
C25	8645(3)	7764(3)	3800(5)	31.1(15)
C26	8128(3)	7414(3)	3198(5)	29.1(14)
C27	9825(4)	8346(4)	4176(5)	46(2)
Br2	8776(2)	10021(2)	3327(2)	56.1(9)
C28	8850(5)	9650(4)	4459(5)	32.5(8)
C29	8358(4)	9050(4)	4751(5)	32.5(8)
C30	8412(4)	8791(4)	5600(6)	32.5(8)
C31	8958(5)	9130(4)	6156(6)	32.5(8)
C32	9450(4)	9729(4)	5864(6)	32.5(8)
C33	9395(4)	9989(4)	5016(6)	32.5(8)
C34	9016(6)	8892(7)	7098(10)	32.5(8)
O7	9445(3)	9167(3)	7643(5)	32.5(8)
O8	8516(2)	8315.1(19)	7282(3)	24.4(9)
C35	8451(3)	7993(3)	8168(4)	24.9(13)
Br2A	9124(3)	10319(2)	3569(2)	56.4(11)
C28A	9129(6)	9872(5)	4646(6)	32.5(8)
C29A	8612(5)	9258(5)	4809(6)	32.5(8)
C30A	8592(5)	8927(5)	5625(8)	32.5(8)
C31A	9090(5)	9209(5)	6278(7)	32.5(8)
C32A	9607(5)	9823(5)	6115(7)	32.5(8)
C33A	9627(5)	10154(4)	5299(8)	32.5(8)
C34A	9079(7)	8868(8)	7158(12)	32.5(8)
O7A	9549(5)	9094(5)	7649(8)	32.5(8)
S2	6679.4(8)	7124.0(8)	8355.2(17)	30.7(4)
O9	8633(2)	6334(2)	8293(3)	37.0(12)
O10	8357(2)	6289(2)	9781(4)	37.3(12)
O11	6829(2)	6666(2)	8767(4)	35.4(11)
O12	6322(2)	6976(2)	7485(4)	37.4(12)
N3	8230(3)	6972(3)	8827(4)	30.9(13)
N4	7338(3)	7777(3)	8141(4)	29.4(12)
C36	8280(3)	7303(3)	7926(5)	27.2(14)
C37	8763(4)	7238(4)	7290(5)	37.2(17)
C38	9459(4)	7651(4)	7593(6)	47(2)
C39	8673(4)	7344(4)	6239(5)	46(2)

C40	8572(4)	6531(3)	7346(5)	34.7(16)
C41	8403(3)	6529(3)	9000(5)	32.1(15)
C42	7924(3)	8044(3)	8716(4)	27.2(14)
C43	8153(3)	8747(3)	8967(4)	35.6(16)
C44	7746(6)	8854(6)	9679(6)	35(4)
C45	7743(9)	8608(10)	10666(7)	30(4)
C46	7336(6)	8715(6)	11374(6)	31(3)
C47	7313(8)	8416(7)	12322(7)	46(4)
C44A	7681(6)	8869(7)	9508(7)	43(5)
C45A	7555(6)	8638(12)	10522(7)	38(5)
C46A	8144(7)	8834(8)	11122(8)	45(5)
C47A	7983(10)	8708(9)	12161(8)	61(6)
C48	6232(2)	7282(2)	9192(3)	35.9(16)
C49	5925(3)	7617(3)	8915(3)	44.5(19)
C50	5553(3)	7727(3)	9558(4)	53(2)
C51	5488(2)	7503(3)	10478(4)	48(2)
C52	5795(3)	7168(2)	10755(3)	47(2)
C53	6167(2)	7057(2)	10112(3)	42.0(18)
C54	5068(5)	7621(5)	11161(8)	69(3)
Br3	2952.7(18)	5480.3(17)	786(3)	34.1(7)
C55	3448(5)	5889(5)	1883(6)	28.1(13)
C56	3955(5)	5792(5)	2121(6)	28.1(13)
C57	4323(5)	6086(6)	2919(7)	28.1(13)
C58	4183(5)	6476(6)	3479(6)	28.1(13)
C59	3676(6)	6574(6)	3241(7)	28.1(13)
C60	3308(5)	6280(6)	2443(7)	28.1(13)
C61	4540(11)	6785(16)	4343(13)	27(3)
O13	4330(15)	6962(19)	4988(14)	36(4)
O14	5132(8)	6860(12)	4334(13)	25(4)
C62	5504(9)	7040(10)	5206(15)	27(4)
C63	6115(7)	7698(6)	5011(10)	25(3)
C64	6020(6)	8267(6)	4766(11)	32(3)
C65	5765(6)	8229(7)	3759(10)	41(3)
C66	5593(6)	8367(6)	5478(11)	40(3)
C67	6680(6)	8853(6)	4801(10)	35(3)
O15	6958(6)	8966(6)	5726(8)	31(3)
C68	6910(20)	8458(8)	6231(17)	35(3)
O16	7160(20)	8565(14)	6998(16)	33(5)

N5	6505(14)	7869(9)	5891(15)	30(5)
Br3A	3040(3)	5515(2)	429(5)	45.9(11)
C55A	3519(6)	5912(8)	1534(8)	28.1(13)
C56A	4033(7)	5829(8)	1785(8)	28.1(13)
C57A	4379(7)	6110(9)	2605(9)	28.1(13)
C58A	4210(7)	6475(9)	3173(8)	28.1(13)
C59A	3696(8)	6558(9)	2922(9)	28.1(13)
C60A	3351(7)	6277(8)	2103(9)	28.1(13)
C61A	4551(15)	6750(20)	4064(19)	27(3)
O13A	4350(20)	6920(30)	4710(20)	41(6)
O14A	5142(12)	6811(19)	4079(18)	29(5)
C62A	5511(13)	7012(13)	4960(19)	28(5)
C63A	6190(11)	7584(9)	4741(14)	34(5)
C64A	6228(10)	8172(9)	4255(14)	53(5)
C65A	6120(14)	8047(13)	3172(13)	90(10)
C66A	5755(11)	8351(11)	4690(20)	65(7)
C67A	6906(10)	8730(10)	4353(15)	61(6)
O15A	7080(9)	8902(8)	5343(12)	44(4)
C68A	6870(30)	8420(12)	5990(20)	35(3)
O16A	7120(30)	8571(17)	6760(20)	36(7)
N5A	6528(19)	7819(12)	5660(20)	30(6)
S3	6566.9(10)	6279.4(11)	4859.4(16)	39.9(5)
O17	7020(3)	6834(3)	5375(4)	44.9(13)
O18	6748(3)	6122(3)	3977(4)	51.4(15)
N6	5951(3)	6358(4)	4621(4)	42.0(16)
C69	5586(4)	6455(3)	5368(5)	33.1(15)
C70	4944(4)	5836(4)	5503(6)	43.8(19)
C71	4508(4)	5838(4)	6263(6)	54(2)
C72	4744(5)	5895(7)	7242(5)	43(3)
C72A	4500(20)	5551(19)	7190(8)	43(3)
C73	4270(5)	5769(5)	8000(6)	62(3)
C74	4514(5)	5846(6)	8955(6)	68(3)
C75	6291(4)	5598(4)	5611(5)	33.6(15)
C76	6439(3)	5685(4)	6571(5)	31.5(15)
C77	6217(4)	5154(4)	7138(5)	35.8(17)
C78	5845(4)	4533(4)	6789(5)	37.8(17)
C79	5696(4)	4465(4)	5818(6)	41.7(18)
C80	5924(4)	4991(4)	5249(5)	40.4(17)

C8I	5608(5)	3953(4)	7404(6)	50(2)
Cl1	3108.4(17)	3713.0(18)	4035(4)	117.8(15)
Cl2	4372.1(13)	3840.1(13)	3751(2)	71.8(7)
C1S	3905(4)	4206(4)	3706(11)	94(4)
Cl3	2949.5(19)	2874(2)	6461(3)	72.5(13)
Cl4	4073(2)	4107(2)	6977(6)	120(3)
C2S	3778(4)	3372(5)	6411(12)	62(4)
Cl5	3743(6)	3531(6)	8181(9)	72.4(8)
Cl6	3362(7)	3462(7)	6171(9)	72.4(8)
C3S	3913(15)	3500(30)	6999(9)	72.4(8)
Cl7	3951(11)	3685(12)	7905(14)	72.4(8)
Cl8	3591(11)	3818(12)	6045(14)	72.4(8)
C4S	4020(30)	3560(40)	6718(16)	72.4(8)
Cl9	3094(3)	4067(2)	1239(4)	72.4(8)
Cl10	3251(3)	3014(3)	1708(4)	72.4(8)
C5S	2690(5)	3247(5)	1467(16)	72.4(8)
Cl11	3088(4)	4045(4)	614(7)	72.4(8)
Cl12	3277(5)	3006(5)	1369(7)	72.4(8)
C6S	2847(12)	3232(6)	640(20)	72.4(8)
Cl13	3529(10)	3446(9)	-515(12)	72.4(8)
Cl14	3271(10)	3477(10)	1447(12)	72.4(8)
C7S	3110(30)	2994(11)	458(18)	72.4(8)

Table 3 Anisotropic Displacement Parameters ($\text{\AA}^2 \times 10^3$) for Schomaker19. The Anisotropic displacement factor exponent takes the form: $-2\pi^2[h^2a^{*2}U_{11} + \dots + 2hka \times b \times U_{12}]$

Atom	U ₁₁	U ₂₂	U ₃₃	U ₂₃	U ₁₃	U ₁₂
Br1	28.8(4)	43.5(4)	27.6(3)	-9.0(3)	4.5(3)	14.7(3)
C1	19(3)	30(3)	26(3)	-5(3)	2(3)	12(3)
C2	46(4)	30(4)	23(3)	3(3)	9(3)	15(3)
C3	46(4)	20(3)	31(4)	0(3)	6(3)	17(3)
C4	28(3)	20(3)	19(3)	-4(2)	-5(2)	10(3)
C5	24(3)	17(3)	24(3)	-2(2)	1(3)	6(3)
C6	23(3)	25(3)	30(4)	-10(3)	-3(3)	11(3)
C7	27(3)	18(3)	23(3)	1(2)	1(3)	11(3)
O1	47(3)	24(2)	30(3)	6(2)	13(2)	20(2)
O2	34(2)	20(2)	16(2)	-3.0(17)	0.1(18)	12.7(19)
C8	35(3)	17(3)	16(3)	1(2)	5(3)	11(3)

S1	38.3(9)	20.6(8)	15.4(7)	-0.4(6)	-1.2(7)	8.5(7)
O3	38(3)	53(3)	31(3)	-1(2)	7(2)	27(3)
O4	55(3)	71(4)	27(3)	0(3)	6(2)	44(3)
O5	40(3)	24(2)	21(2)	-2.4(19)	-5(2)	15(2)
O6	59(3)	29(3)	15(2)	5.4(19)	-3(2)	14(2)
N1	35(3)	40(3)	18(3)	-9(2)	0(2)	21(3)
N2	36(3)	20(3)	16(3)	1(2)	5(2)	9(2)
C9	32(3)	25(3)	16(3)	-4(2)	2(2)	14(3)
C10	30(3)	28(3)	26(3)	-5(3)	-2(3)	11(3)
C11	39(4)	54(5)	24(3)	-10(3)	-7(3)	27(4)
C12	27(4)	30(4)	50(5)	-5(3)	-5(3)	8(3)
C13	32(4)	40(4)	27(3)	-1(3)	1(3)	19(3)
C14	44(4)	37(4)	27(4)	-2(3)	-1(3)	27(3)
C15	40(4)	24(3)	13(3)	4(2)	4(3)	16(3)
C16	44(4)	51(5)	27(4)	-1(3)	-2(3)	32(4)
C17	29(4)	44(5)	33(5)	9(4)	1(4)	19(4)
C18	41(5)	38(5)	27(4)	-1(4)	-13(4)	20(4)
C19	35(5)	33(5)	33(5)	-6(4)	-7(4)	21(4)
C20	46(7)	59(7)	32(4)	4(5)	-1(4)	31(6)
C17A	50(20)	24(17)	29(15)	8(11)	15(14)	11(14)
C18A	31(13)	45(15)	27(9)	-1(10)	-2(11)	21(11)
C19A	31(13)	45(15)	27(9)	-1(10)	-2(11)	21(11)
C20A	46(7)	59(7)	32(4)	4(5)	-1(4)	31(6)
C21	35(3)	17(3)	19(3)	0(2)	-1(3)	9(3)
C22	36(4)	31(4)	25(4)	-4(3)	6(3)	-1(3)
C23	35(4)	51(5)	24(4)	-3(3)	7(3)	0(4)
C24	36(4)	25(3)	22(3)	0(3)	-4(3)	6(3)
C25	43(4)	33(4)	16(3)	-3(3)	-6(3)	18(3)
C26	37(4)	26(3)	23(3)	2(3)	-1(3)	15(3)
C27	44(4)	46(5)	26(4)	-2(3)	-2(3)	5(4)
Br2	65.7(18)	59.8(19)	39.9(11)	30.2(12)	2.4(12)	29.2(17)
C28	26(2)	28.3(17)	37.7(17)	9.7(13)	3.5(14)	9.1(14)
C29	26(2)	28.3(17)	37.7(17)	9.7(13)	3.5(14)	9.1(14)
C30	26(2)	28.3(17)	37.7(17)	9.7(13)	3.5(14)	9.1(14)
C31	26(2)	28.3(17)	37.7(17)	9.7(13)	3.5(14)	9.1(14)
C32	26(2)	28.3(17)	37.7(17)	9.7(13)	3.5(14)	9.1(14)
C33	26(2)	28.3(17)	37.7(17)	9.7(13)	3.5(14)	9.1(14)
C34	26(2)	28.3(17)	37.7(17)	9.7(13)	3.5(14)	9.1(14)

O7	26(2)	28.3(17)	37.7(17)	9.7(13)	3.5(14)	9.1(14)
O8	26(2)	24(2)	15(2)	6.3(17)	6.6(17)	6.8(18)
C35	31(3)	23(3)	14(3)	2(2)	2(3)	8(3)
Br2A	84(3)	50.7(18)	31.6(13)	19.2(12)	9.4(14)	32(2)
C28A	26(2)	28.3(17)	37.7(17)	9.7(13)	3.5(14)	9.1(14)
C29A	26(2)	28.3(17)	37.7(17)	9.7(13)	3.5(14)	9.1(14)
C30A	26(2)	28.3(17)	37.7(17)	9.7(13)	3.5(14)	9.1(14)
C31A	26(2)	28.3(17)	37.7(17)	9.7(13)	3.5(14)	9.1(14)
C32A	26(2)	28.3(17)	37.7(17)	9.7(13)	3.5(14)	9.1(14)
C33A	26(2)	28.3(17)	37.7(17)	9.7(13)	3.5(14)	9.1(14)
C34A	26(2)	28.3(17)	37.7(17)	9.7(13)	3.5(14)	9.1(14)
O7A	26(2)	28.3(17)	37.7(17)	9.7(13)	3.5(14)	9.1(14)
S2	31.7(9)	26.0(8)	31.1(9)	0.5(7)	8.4(7)	12.0(7)
O9	45(3)	41(3)	30(3)	12(2)	12(2)	25(3)
O10	45(3)	44(3)	29(3)	17(2)	11(2)	27(3)
O11	37(3)	23(2)	44(3)	3(2)	9(2)	14(2)
O12	34(3)	33(3)	42(3)	-3(2)	3(2)	14(2)
N3	39(3)	35(3)	22(3)	10(2)	10(2)	21(3)
N4	31(3)	27(3)	27(3)	5(2)	7(2)	12(2)
C36	36(4)	24(3)	20(3)	4(3)	5(3)	14(3)
C37	43(4)	38(4)	34(4)	16(3)	20(3)	22(3)
C38	40(4)	49(5)	58(5)	22(4)	15(4)	27(4)
C39	69(6)	49(5)	26(4)	12(3)	20(4)	34(4)
C40	50(4)	37(4)	22(3)	8(3)	14(3)	26(3)
C41	35(4)	34(4)	27(4)	10(3)	9(3)	17(3)
C42	31(3)	27(3)	16(3)	-3(3)	2(3)	9(3)
C43	56(5)	23(3)	20(3)	-1(3)	0(3)	15(3)
C44	54(10)	24(9)	26(7)	-6(6)	0(7)	20(8)
C45	42(9)	28(8)	23(7)	4(6)	7(7)	19(7)
C46	38(7)	29(7)	32(7)	2(5)	5(6)	21(6)
C47	61(11)	50(9)	23(7)	-1(6)	9(7)	25(8)
C44A	71(14)	41(12)	16(8)	-1(8)	3(8)	28(11)
C45A	53(12)	38(9)	26(8)	0(8)	-1(7)	25(10)
C46A	53(10)	27(8)	38(8)	7(7)	-9(8)	8(8)
C47A	110(18)	42(11)	34(8)	-12(8)	-10(10)	41(12)
C48	29(4)	29(4)	43(4)	3(3)	13(3)	10(3)
C49	46(5)	46(5)	45(5)	6(4)	14(4)	25(4)
C50	49(5)	54(5)	64(5)	-1(4)	12(4)	32(4)

C51	33(4)	42(5)	50(5)	-14(4)	16(4)	5(3)
C52	44(5)	33(4)	46(5)	2(3)	22(4)	7(3)
C53	45(4)	29(4)	38(4)	1(3)	16(3)	8(3)
C54	50(5)	71(6)	79(7)	-19(5)	27(5)	25(5)
Br3	31.7(11)	34.3(10)	31.4(15)	-9.4(11)	-10.1(11)	12.8(8)
C55	29(2)	34.2(18)	21(4)	1(4)	4(3)	15.6(16)
C56	29(2)	34.2(18)	21(4)	1(4)	4(3)	15.6(16)
C57	29(2)	34.2(18)	21(4)	1(4)	4(3)	15.6(16)
C58	29(2)	34.2(18)	21(4)	1(4)	4(3)	15.6(16)
C59	29(2)	34.2(18)	21(4)	1(4)	4(3)	15.6(16)
C60	29(2)	34.2(18)	21(4)	1(4)	4(3)	15.6(16)
C61	29(4)	30(5)	21(11)	-3(9)	6(7)	15(3)
O13	41(7)	52(8)	26(10)	-6(10)	7(8)	31(6)
O14	24(5)	23(6)	23(10)	-3(7)	3(5)	8(4)
C62	25(6)	33(6)	18(10)	3(7)	4(6)	12(5)
C63	25(6)	25(6)	18(8)	-2(5)	3(5)	8(5)
C64	26(7)	29(6)	41(8)	8(6)	4(6)	14(5)
C65	33(7)	40(8)	44(8)	2(6)	-6(6)	14(6)
C66	36(7)	29(7)	57(9)	-2(6)	6(6)	17(6)
C67	35(7)	33(6)	30(7)	7(6)	-3(6)	12(5)
O15	40(6)	27(5)	30(6)	7(5)	2(5)	20(4)
C68	40(7)	29(4)	32(11)	0(6)	-15(11)	15(4)
O16	39(7)	37(7)	29(11)	2(7)	-12(10)	23(6)
N5	38(8)	24(6)	26(10)	1(6)	-5(8)	14(6)
Br3A	43.2(17)	41.4(14)	50(3)	-2.0(19)	-6.8(19)	18.9(12)
C55A	29(2)	34.2(18)	21(4)	1(4)	4(3)	15.6(16)
C56A	29(2)	34.2(18)	21(4)	1(4)	4(3)	15.6(16)
C57A	29(2)	34.2(18)	21(4)	1(4)	4(3)	15.6(16)
C58A	29(2)	34.2(18)	21(4)	1(4)	4(3)	15.6(16)
C59A	29(2)	34.2(18)	21(4)	1(4)	4(3)	15.6(16)
C60A	29(2)	34.2(18)	21(4)	1(4)	4(3)	15.6(16)
C61A	29(4)	30(5)	21(11)	-3(9)	6(7)	15(3)
O13A	36(9)	59(13)	27(14)	-8(13)	11(11)	23(8)
O14A	28(7)	44(11)	16(11)	-3(8)	2(6)	18(6)
C62A	39(9)	34(8)	12(13)	1(8)	2(8)	19(7)
C63A	38(9)	34(8)	19(9)	2(7)	5(8)	9(7)
C64A	60(11)	39(9)	37(9)	9(8)	-11(9)	7(7)
C65A	110(20)	61(15)	31(10)	9(9)	-21(11)	-7(14)

C66A	64(13)	31(11)	87(19)	-2(11)	-23(13)	13(10)
C67A	48(10)	51(11)	45(10)	22(9)	-14(9)	-4(9)
O15A	53(10)	35(7)	36(9)	7(7)	-8(8)	16(7)
C68A	40(7)	29(4)	32(11)	0(6)	-15(11)	15(4)
O16A	53(18)	25(9)	27(13)	4(9)	-3(12)	16(9)
N5A	39(10)	26(8)	26(13)	-1(7)	-3(10)	17(7)
S3	46.9(11)	67.2(13)	21.6(9)	10.4(9)	7.5(8)	40.4(11)
O17	47(3)	56(3)	34(3)	12(3)	5(2)	27(3)
O18	55(3)	102(5)	22(3)	10(3)	10(2)	58(4)
N6	45(4)	68(5)	28(3)	8(3)	7(3)	39(4)
C69	42(4)	29(3)	29(4)	6(3)	11(3)	18(3)
C70	52(5)	33(4)	45(4)	5(3)	18(4)	20(4)
C71	55(5)	51(5)	51(5)	-4(4)	18(4)	23(4)
C72	27(5)	51(8)	50(5)	-2(5)	-7(4)	18(5)
C72A	27(5)	51(8)	50(5)	-2(5)	-7(4)	18(5)
C73	76(7)	85(7)	43(5)	6(5)	7(4)	52(6)
C74	45(5)	91(8)	44(5)	7(5)	-4(4)	16(5)
C75	46(4)	45(4)	23(3)	2(3)	4(3)	33(4)
C76	38(4)	42(4)	22(3)	-1(3)	1(3)	26(3)
C77	54(5)	45(4)	16(3)	-3(3)	1(3)	30(4)
C78	47(4)	51(4)	30(4)	2(3)	7(3)	35(4)
C79	50(5)	51(5)	36(4)	-11(3)	-3(4)	34(4)
C80	52(5)	60(5)	24(4)	-9(3)	-4(3)	39(4)
C81	65(6)	46(5)	42(5)	2(4)	6(4)	30(4)
Cl1	92(2)	97(2)	178(4)	53(2)	70(3)	58(2)
Cl2	71.3(16)	63.4(15)	90.4(19)	7.2(14)	8.9(14)	40.9(14)
C1S	64(7)	61(7)	160(13)	18(7)	37(8)	33(6)
Cl3	55(2)	90(3)	77(3)	-33(2)	3(2)	40(2)
Cl4	72(3)	58(3)	231(8)	-42(4)	19(4)	32(2)
C2S	55(8)	70(9)	65(10)	-12(8)	0(7)	33(7)

Table 4. Bond Lengths for Schomaker19.

Atom	Atom	Length/Å	Atom	Atom	Length/Å
Br1	C1	1.899(5)	C46A	C47A	1.514(6)
C1	C2	1.375(7)	C48	C49	1.3900
C1	C6	1.379(7)	C48	C53	1.3900

C2	C3	1.382(7)	C49	C50	1.3900
C3	C4	1.390(7)	C50	C51	1.3900
C4	C5	1.387(7)	C51	C52	1.3900
C4	C7	1.489(7)	C51	C54	1.523(9)
C5	C6	1.388(7)	C52	C53	1.3900
C7	O1	1.202(7)	Br3	C55	1.904(7)
C7	O2	1.354(6)	C55	C56	1.3900
O2	C8	1.445(6)	C55	C60	1.3900
C8	C9	1.537(9)	C56	C57	1.3900
C8	C15	1.519(9)	C57	C58	1.3900
S1	O5	1.422(5)	C58	C59	1.3900
S1	O6	1.447(5)	C58	C61	1.464(13)
S1	N2	1.606(5)	C59	C60	1.3900
S1	C21	1.760(7)	C61	O13	1.218(15)
O3	C13	1.445(8)	C61	O14	1.339(14)
O3	C14	1.342(9)	O14	C62	1.458(16)
O4	C14	1.235(8)	C62	C63	1.549(16)
N1	C9	1.472(8)	C62	C69	1.53(3)
N1	C14	1.330(9)	C63	C64	1.533(17)
N2	C15	1.469(8)	C63	N5	1.488(16)
C9	C10	1.534(9)	C64	C65	1.537(18)
C10	C11	1.523(9)	C64	C66	1.54(2)
C10	C12	1.542(10)	C64	C67	1.503(16)
C10	C13	1.529(10)	C67	O15	1.434(16)
C15	C16	1.529(7)	O15	C68	1.363(19)
C16	C17	1.511(4)	C68	O16	1.208(15)
C16	C17A	1.511(4)	C68	N5	1.340(16)
C17	C18	1.513(4)	Br3A	C55A	1.895(10)
C18	C19	1.511(4)	C55A	C56A	1.3900
C19	C20	1.513(4)	C55A	C60A	1.3900
C17A	C18A	1.512(4)	C56A	C57A	1.3900
C18A	C19A	1.512(4)	C57A	C58A	1.3900
C19A	C20A	1.512(4)	C58A	C59A	1.3900
C21	C22	1.388(10)	C58A	C61A	1.468(16)
C21	C26	1.389(9)	C59A	C60A	1.3900
C22	C23	1.388(10)	C61A	O13A	1.206(18)
C23	C24	1.395(10)	C61A	O14A	1.350(18)
C24	C25	1.390(10)	O14A	C62A	1.465(19)

C24	C27	1.496(10)	C62A	C63A	1.55(2)
C25	C26	1.389(9)	C62A	C69	1.55(3)
Br2	C28	1.886(5)	C63A	C64A	1.53(2)
C28	C29	1.3900	C63A	N5A	1.491(19)
C28	C33	1.3900	C64A	C65A	1.56(2)
C29	C30	1.3900	C64A	C66A	1.53(3)
C30	C31	1.3900	C64A	C67A	1.51(2)
C31	C32	1.3900	C67A	O15A	1.46(2)
C31	C34	1.485(8)	O15A	C68A	1.36(2)
C32	C33	1.3900	C68A	O16A	1.207(19)
C34	O7	1.188(9)	C68A	N5A	1.34(2)
C34	O8	1.328(9)	S3	O17	1.428(6)
O8	C35	1.441(6)	S3	O18	1.436(5)
O8	C34A	1.351(10)	S3	N6	1.615(6)
C35	C36	1.532(9)	S3	C75	1.778(7)
C35	C42	1.539(9)	N6	C69	1.465(9)
Br2A	C28A	1.869(6)	C69	C70	1.526(10)
C28A	C29A	1.3900	C70	C71	1.502(11)
C28A	C33A	1.3900	C71	C72	1.479(8)
C29A	C30A	1.3900	C71	C72A	1.481(9)
C30A	C31A	1.3900	C72	C73	1.481(8)
C31A	C32A	1.3900	C72A	C73	1.481(9)
C31A	C34A	1.485(9)	C73	C74	1.448(13)
C32A	C33A	1.3900	C75	C76	1.395(9)
C34A	O7A	1.199(10)	C75	C80	1.369(11)
S2	O11	1.437(5)	C76	C77	1.369(10)
S2	O12	1.441(5)	C77	C78	1.389(11)
S2	N4	1.601(6)	C78	C79	1.411(11)
S2	C48	1.763(4)	C78	C81	1.491(11)
O9	C40	1.453(8)	C79	C80	1.361(11)
O9	C41	1.336(8)	Cl1	C1S	1.734(8)
O10	C41	1.226(8)	Cl2	C1S	1.735(8)
N3	C36	1.476(8)	Cl3	C2S	1.735(8)
N3	C41	1.340(9)	Cl4	C2S	1.732(8)
N4	C42	1.467(9)	Cl5	C3S	1.733(8)
C36	C37	1.535(10)	Cl6	C3S	1.733(8)
C37	C38	1.515(11)	Cl7	C4S	1.734(8)
C37	C39	1.544(10)	Cl7	Cl13 ¹	2.41(3)

C37	C40	1.523(10)	C18	C4S	1.733(8)
C42	C43	1.532(7)	C19	C5S	1.733(8)
C43	C44	1.513(6)	C110	C5S	1.732(8)
C43	C44A	1.513(6)	C111	C6S	1.734(8)
C44	C45	1.516(6)	C112	C6S	1.732(8)
C45	C46	1.509(6)	C113	C17 ²	2.41(3)
C46	C47	1.512(6)	C113	C7S	1.734(8)
C44A	C45A	1.514(6)	C114	C7S	1.733(8)
C45A	C46A	1.509(6)			

¹+X,+Y,1+Z; ²+X,+Y,-1+Z

Table 5 Bond Angles for Schomaker19.

Atom	Atom	Atom	Angle/°	Atom	Atom	Atom	Angle/°
C2	C1	Br1	118.9(4)	C43	C44	C45	115.3(7)
C2	C1	C6	121.8(5)	C46	C45	C44	115.1(7)
C6	C1	Br1	119.3(4)	C45	C46	C47	112.5(7)
C1	C2	C3	119.6(6)	C43	C44A	C45A	116.3(7)
C2	C3	C4	119.7(5)	C46A	C45A	C44A	115.8(8)
C3	C4	C7	122.8(5)	C45A	C46A	C47A	112.4(8)
C5	C4	C3	119.9(5)	C49	C48	S2	119.3(3)
C5	C4	C7	117.2(5)	C49	C48	C53	120.0
C4	C5	C6	120.4(5)	C53	C48	S2	120.7(3)
C1	C6	C5	118.5(5)	C48	C49	C50	120.0
O1	C7	C4	124.4(5)	C51	C50	C49	120.0
O1	C7	O2	123.8(5)	C50	C51	C54	118.8(6)
O2	C7	C4	111.9(5)	C52	C51	C50	120.0
C7	O2	C8	118.4(4)	C52	C51	C54	121.2(6)
O2	C8	C9	107.6(5)	C51	C52	C53	120.0
O2	C8	C15	106.5(5)	C52	C53	C48	120.0
C15	C8	C9	115.7(5)	C56	C55	Br3	119.0(5)
O5	S1	O6	119.1(3)	C56	C55	C60	120.0
O5	S1	N2	108.9(3)	C60	C55	Br3	121.0(5)
O5	S1	C21	107.6(3)	C55	C56	C57	120.0
O6	S1	N2	105.4(3)	C58	C57	C56	120.0
O6	S1	C21	106.5(3)	C57	C58	C59	120.0
N2	S1	C21	109.0(3)	C57	C58	C61	122.7(9)

C14	O3	C13	116.3(5)	C59	C58	C61	117.2(9)
C14	N1	C9	127.3(6)	C60	C59	C58	120.0
C15	N2	S1	124.9(4)	C59	C60	C55	120.0
N1	C9	C8	106.6(5)	O13	C61	C58	124.4(14)
N1	C9	C10	109.8(5)	O13	C61	O14	123.7(16)
C10	C9	C8	116.2(5)	O14	C61	C58	111.9(12)
C9	C10	C12	113.2(6)	C61	O14	C62	118.9(15)
C11	C10	C9	112.6(6)	O14	C62	C63	106.1(14)
C11	C10	C12	111.0(6)	O14	C62	C69	101.3(17)
C11	C10	C13	106.0(6)	C69	C62	C63	118.1(16)
C13	C10	C9	105.2(5)	C64	C63	C62	117.5(14)
C13	C10	C12	108.2(6)	N5	C63	C62	106.0(13)
O3	C13	C10	111.3(6)	N5	C63	C64	107.3(13)
O4	C14	O3	117.3(7)	C63	C64	C65	113.0(12)
O4	C14	N1	123.7(7)	C63	C64	C66	113.4(11)
N1	C14	O3	119.0(6)	C65	C64	C66	110.0(12)
C8	C15	C16	109.9(5)	C67	C64	C63	105.6(11)
N2	C15	C8	109.6(5)	C67	C64	C65	106.8(11)
N2	C15	C16	110.5(5)	C67	C64	C66	107.6(12)
C17	C16	C15	117.1(5)	O15	C67	C64	112.4(11)
C17A	C16	C15	136.9(14)	C68	O15	C67	119.0(11)
C16	C17	C18	116.4(5)	O16	C68	O15	118.2(18)
C19	C18	C17	115.9(6)	O16	C68	N5	124.5(18)
C18	C19	C20	112.3(6)	N5	C68	O15	116.7(16)
C16	C17A	C18A	106(2)	C68	N5	C63	127.9(15)
C17A	C18A	C19A	114(3)	C56A	C55A	Br3A	119.9(6)
C18A	C19A	C20A	111(3)	C56A	C55A	C60A	120.0
C22	C21	S1	118.9(5)	C60A	C55A	Br3A	120.1(6)
C22	C21	C26	121.4(6)	C55A	C56A	C57A	120.0
C26	C21	S1	119.6(5)	C58A	C57A	C56A	120.0
C23	C22	C21	118.9(7)	C57A	C58A	C59A	120.0
C22	C23	C24	121.0(7)	C57A	C58A	C61A	120.5(12)
C23	C24	C27	120.7(7)	C59A	C58A	C61A	119.4(11)
C25	C24	C23	118.6(6)	C58A	C59A	C60A	120.0
C25	C24	C27	120.7(6)	C59A	C60A	C55A	120.0
C26	C25	C24	121.4(6)	O13A	C61A	C58A	125.3(19)
C25	C26	C21	118.6(7)	O13A	C61A	O14A	122(2)
C29	C28	Br2	120.7(4)	O14A	C61A	C58A	112.5(16)

C29	C28	C33	120.0	C61A	O14A	C62A	119(2)
C33	C28	Br2	119.3(4)	O14A	C62A	C63A	108.3(19)
C28	C29	C30	120.0	O14A	C62A	C69	110(3)
C29	C30	C31	120.0	C69	C62A	C63A	108(2)
C30	C31	C32	120.0	C64A	C63A	C62A	117.3(19)
C30	C31	C34	121.8(5)	N5A	C63A	C62A	106.9(18)
C32	C31	C34	118.0(5)	N5A	C63A	C64A	106.1(16)
C33	C32	C31	120.0	C63A	C64A	C65A	109.9(18)
C32	C33	C28	120.0	C63A	C64A	C66A	111.6(18)
O7	C34	C31	126.4(7)	C66A	C64A	C65A	111.9(19)
O7	C34	O8	122.1(7)	C67A	C64A	C63A	108.5(16)
O8	C34	C31	111.5(7)	C67A	C64A	C65A	105.3(17)
C34	O8	C35	121.9(6)	C67A	C64A	C66A	109.6(19)
C34A	O8	C35	115.2(6)	O15A	C67A	C64A	111.5(16)
O8	C35	C36	106.4(5)	C68A	O15A	C67A	118.4(16)
O8	C35	C42	105.6(5)	O16A	C68A	O15A	116(2)
C36	C35	C42	114.3(5)	O16A	C68A	N5A	126(2)
C29A	C28A	Br2A	119.0(5)	N5A	C68A	O15A	117(2)
C29A	C28A	C33A	120.0	C68A	N5A	C63A	129.5(19)
C33A	C28A	Br2A	121.0(5)	O17	S3	O18	120.1(4)
C28A	C29A	C30A	120.0	O17	S3	N6	108.3(4)
C31A	C30A	C29A	120.0	O17	S3	C75	108.0(3)
C30A	C31A	C32A	120.0	O18	S3	N6	105.2(3)
C30A	C31A	C34A	121.1(6)	O18	S3	C75	107.6(4)
C32A	C31A	C34A	118.9(6)	N6	S3	C75	106.9(4)
C31A	C32A	C33A	120.0	C69	N6	S3	121.4(5)
C32A	C33A	C28A	120.0	N6	C69	C62	113.5(10)
O8	C34A	C31A	112.6(7)	N6	C69	C62A	101.8(13)
O7A	C34A	O8	128.4(9)	N6	C69	C70	109.1(6)
O7A	C34A	C31A	119.1(9)	C70	C69	C62	112.4(9)
O11	S2	O12	120.2(3)	C70	C69	C62A	112.9(11)
O11	S2	N4	108.9(3)	C71	C70	C69	116.9(7)
O11	S2	C48	107.6(3)	C72	C71	C70	116.0(8)
O12	S2	N4	104.6(3)	C72A	C71	C70	118.6(12)
O12	S2	C48	106.1(3)	C71	C72	C73	116.3(8)
N4	S2	C48	109.0(3)	C71	C72A	C73	116.1(8)
C41	O9	C40	117.0(5)	C74	C73	C72	115.6(9)
C41	N3	C36	127.7(6)	C74	C73	C72A	124.7(15)

C42	N4	S2	125.7(5)	C76	C75	S3	119.8(6)
C35	C36	C37	115.6(5)	C80	C75	S3	119.9(6)
N3	C36	C35	107.1(5)	C80	C75	C76	120.3(7)
N3	C36	C37	108.3(5)	C77	C76	C75	118.8(7)
C36	C37	C39	112.1(6)	C76	C77	C78	122.1(7)
C38	C37	C36	114.1(7)	C77	C78	C79	117.4(7)
C38	C37	C39	111.4(6)	C77	C78	C81	122.2(7)
C38	C37	C40	109.3(6)	C79	C78	C81	120.4(8)
C40	C37	C36	105.1(5)	C80	C79	C78	120.7(8)
C40	C37	C39	104.2(6)	C79	C80	C75	120.7(7)
O9	C40	C37	112.7(6)	Cl1	ClS	Cl2	114.5(5)
O9	C41	N3	119.0(6)	Cl4	C2S	Cl3	115.2(6)
O10	C41	O9	118.0(6)	Cl5	C3S	Cl6	118.0(12)
O10	C41	N3	123.0(6)	C4S	Cl7	Cl13 ¹	158(3)
N4	C42	C35	109.4(5)	Cl8	C4S	Cl7	110.1(12)
N4	C42	C43	110.4(5)	Cl10	C5S	Cl9	108.5(6)
C43	C42	C35	110.3(5)	Cl12	C6S	Cl11	116.5(9)
C44	C43	C42	115.8(6)	C7S	Cl13	Cl7 ²	159.1(13)
C44A	C43	C42	116.1(7)	Cl14	C7S	Cl13	111.0(12)

¹+X,+Y,1+Z; ²+X,+Y,-1+Z

Table 6 Hydrogen Bonds for Schomaker19.

D	H	A	d(D-H)/Å	d(H-A)/Å	d(D-A)/Å	D-H-A/°
N1	H1	O18	0.8799(16)	2.34(2)	3.165(8)	157(5)
N2	H2A	O10 ¹	0.8800(16)	1.929(9)	2.806(7)	175(6)
N3	H3	O6 ²	0.8799(15)	2.057(18)	2.914(8)	164(6)
N4	H4	O16	0.8799(15)	1.81(3)	2.68(3)	167(5)
N4	H4	O16A	0.8799(15)	2.09(3)	2.95(3)	167(6)
N5	H5	O12	0.88	2.16	2.991(19)	156.8
N5A	H5A	O12	0.88	2.34	3.16(3)	156.2
N6	H6	O4	0.8800(16)	2.02(4)	2.806(9)	148(7)

¹+X,+Y,-1+Z; ²+X,+Y,1+Z

Table 7 Torsion Angles for Schomaker19.

A	B	C	D	Angle/°	A	B	C	D	Angle/°
Br1	C1	C2	C3	-177.4(6)	C40	O9	C41	N3	-10.8(10)
Br1	C1	C6	C5	177.5(5)	C41	O9	C40	C37	45.1(8)
C1	C2	C3	C4	-0.6(11)	C41	N3	C36	C35	-144.1(7)
C2	C1	C6	C5	-1.7(10)	C41	N3	C36	C37	-18.7(9)
C2	C3	C4	C5	-0.6(10)	C42	C35	C36	N3	-65.4(7)
C2	C3	C4	C7	177.0(7)	C42	C35	C36	C37	173.7(6)
C3	C4	C5	C6	0.7(10)	C42	C43	C44	C45	66.2(15)
C3	C4	C7	O1	-174.6(7)	C42	C43	C44A	C45A	70.2(13)
C3	C4	C7	O2	4.5(9)	C43	C44	C45	C46	-179.9(13)
C4	C5	C6	C1	0.4(9)	C43	C44A	C45A	C46A	50(2)
C4	C7	O2	C8	-172.2(5)	C44	C43	C44A	C45A	-21(4)
C5	C4	C7	O1	3.1(10)	C44	C45	C46	C47	175.7(15)
C5	C4	C7	O2	-177.8(5)	C44A	C43	C44	C45	160(5)
C6	C1	C2	C3	1.8(11)	C44A	C45A	C46A	C47A	168.0(15)
C7	C4	C5	C6	-177.0(6)	C48	S2	N4	C42	82.2(6)
C7	O2	C8	C9	-127.4(5)	C48	C49	C50	C51	0.0
C7	O2	C8	C15	107.9(6)	C49	C48	C53	C52	0.0
O1	C7	O2	C8	6.9(9)	C49	C50	C51	C52	0.0
O2	C8	C9	N1	178.9(5)	C49	C50	C51	C54	-179.0(6)
O2	C8	C9	C10	56.3(7)	C50	C51	C52	C53	0.0
O2	C8	C15	N2	57.7(6)	C51	C52	C53	C48	0.0
O2	C8	C15	C16	-63.9(6)	C53	C48	C49	C50	0.0
C8	C9	C10	C11	-81.2(7)	C54	C51	C52	C53	178.9(6)
C8	C9	C10	C12	45.7(8)	Br3	C55	C56	C57	-180.0(6)
C8	C9	C10	C13	163.8(5)	Br3	C55	C60	C59	180.0(6)
C8	C15	C16	C17	-170.9(6)	C55	C56	C57	C58	0.0
C8	C15	C16	C17A	-85(2)	C56	C55	C60	C59	0.0
S1	N2	C15	C8	109.4(6)	C56	C57	C58	C59	0.0
S1	N2	C15	C16	-129.3(5)	C56	C57	C58	C61	178.2(17)
S1	C21	C22	C23	177.6(6)	C57	C58	C59	C60	0.0
S1	C21	C26	C25	-176.3(5)	C57	C58	C61	O13	-157(3)
O5	S1	N2	C15	-36.5(6)	C57	C58	C61	O14	24(3)
O5	S1	C21	C22	-175.9(5)	C58	C59	C60	C55	0.0
O5	S1	C21	C26	2.9(6)	C58	C61	O14	C62	-168(2)
O6	S1	N2	C15	-165.3(5)	C59	C58	C61	O13	21(5)
O6	S1	C21	C22	-47.1(6)	C59	C58	C61	O14	-157.6(19)

O6	S1	C21	C26	131.6(5)	C60	C55	C56	C57	0.0
N1	C9	C10	C11	157.8(6)	C61	C58	C59	C60	-178.3(16)
N1	C9	C10	C12	-75.2(7)	C61	O14	C62	C63	-119(3)
N1	C9	C10	C13	42.8(7)	C61	O14	C62	C69	117(3)
N2	S1	C21	C22	66.1(6)	O13	C61	O14	C62	13(5)
N2	S1	C21	C26	-115.1(5)	O14	C62	C63	C64	62(2)
N2	C15	C16	C17	68.1(7)	O14	C62	C63	N5	-178(2)
N2	C15	C16	C17A	154(2)	O14	C62	C69	C62A	33(6)
C9	C8	C15	N2	-61.8(7)	O14	C62	C69	N6	62.7(14)
C9	C8	C15	C16	176.6(5)	O14	C62	C69	C70	-61.8(14)
C9	N1	C14	O3	-4.5(11)	C62	C63	C64	C65	-74.3(17)
C9	N1	C14	O4	175.6(7)	C62	C63	C64	C66	51.7(17)
C9	C10	C13	O3	-63.5(7)	C62	C63	C64	C67	169.3(14)
C11	C10	C13	O3	177.0(6)	C62	C63	N5	C68	-150(4)
C12	C10	C13	O3	57.9(7)	C62	C69	C70	C71	-54.7(13)
C13	O3	C14	O4	164.8(6)	C63	C62	C69	C62A	-82(7)
C13	O3	C14	N1	-15.2(9)	C63	C62	C69	N6	-52.7(17)
C14	O3	C13	C10	50.8(8)	C63	C62	C69	C70	-177.2(12)
C14	N1	C9	C8	-138.7(7)	C63	C64	C67	O15	-63.0(16)
C14	N1	C9	C10	-12.1(9)	C64	C63	N5	C68	-23(4)
C15	C8	C9	N1	-62.1(7)	C64	C67	O15	C68	44(3)
C15	C8	C9	C10	175.2(5)	C65	C64	C67	O15	176.5(12)
C15	C16	C17	C18	59.0(9)	C66	C64	C67	O15	58.4(15)
C15	C16	C17A	C18A	-35(4)	C67	O15	C68	O16	178(4)
C16	C17	C18	C19	55.6(10)	C67	O15	C68	N5	-11(6)
C16	C17A	C18A	C19A	-75(4)	O15	C68	N5	C63	1(7)
C17	C16	C17A	C18A	72(2)	O16	C68	N5	C63	172(5)
C17	C18	C19	C20	165.8(7)	N5	C63	C64	C65	166.5(16)
C17A	C16	C17	C18	-73.8(14)	N5	C63	C64	C66	-67.5(18)
C17A	C18A	C19A	C20A	-155(4)	N5	C63	C64	C67	50.2(19)
C21	S1	N2	C15	80.7(6)	Br3A	C55A	C56A	C57A	-178.9(8)
C21	C22	C23	C24	-1.2(12)	Br3A	C55A	C60A	C59A	178.9(8)
C22	C21	C26	C25	2.4(10)	C55A	C56A	C57A	C58A	0.0
C22	C23	C24	C25	2.2(12)	C56A	C55A	C60A	C59A	0.0
C22	C23	C24	C27	-177.9(8)	C56A	C57A	C58A	C59A	0.0
C23	C24	C25	C26	-0.9(11)	C56A	C57A	C58A	C61A	177(2)
C24	C25	C26	C21	-1.4(10)	C57A	C58A	C59A	C60A	0.0
C26	C21	C22	C23	-1.2(11)	C57A	C58A	C61A	O13A	-160(5)

C27	C24	C25	C26	179.2(7)	C57A	C58A	C61A	O14A	23(5)
Br2	C28	C29	C30	-178.3(8)	C58A	C59A	C60A	C55A	0.0
Br2	C28	C33	C32	178.3(8)	C58A	C61A	O14A	C62A	-173(3)
C28	C29	C30	C31	0.0	C59A	C58A	C61A	O13A	17(7)
C29	C28	C33	C32	0.0	C59A	C58A	C61A	O14A	-160(3)
C29	C30	C31	C32	0.0	C60A	C55A	C56A	C57A	0.0
C29	C30	C31	C34	175.7(15)	C61A	C58A	C59A	C60A	-177(2)
C30	C31	C32	C33	0.0	C61A	O14A	C62A	C63A	-129(4)
C30	C31	C34	O7	-175.2(17)	C61A	O14A	C62A	C69	112(4)
C30	C31	C34	O8	4(2)	O13A	C61A	O14A	C62A	9(7)
C31	C32	C33	C28	0.0	O14A	C62A	C63A	C64A	56(3)
C31	C34	O8	C35	-177.8(10)	O14A	C62A	C63A	N5A	174(3)
C31	C34	O8	C34A	141(14)	O14A	C62A	C69	C62	-145(8)
C32	C31	C34	O7	1(3)	O14A	C62A	C69	N6	62(2)
C32	C31	C34	O8	-179.8(12)	O14A	C62A	C69	C70	-55(2)
C33	C28	C29	C30	0.0	C62A	C63A	C64A	C65A	-81(3)
C34	C31	C32	C33	-175.8(14)	C62A	C63A	C64A	C66A	43(3)
C34	O8	C35	C36	-132.2(14)	C62A	C63A	C64A	C67A	164(2)
C34	O8	C35	C42	106.0(14)	C62A	C63A	N5A	C68A	-134(6)
C34	O8	C34A	C31A	-33(11)	C62A	C69	C70	C71	-69.1(16)
C34	O8	C34A	O7A	149(15)	C63A	C62A	C69	C62	96(6)
O7	C34	O8	C35	2(3)	C63A	C62A	C69	N6	-56.3(18)
O7	C34	O8	C34A	-40(11)	C63A	C62A	C69	C70	-173.2(14)
O8	C35	C36	N3	178.4(5)	C63A	C64A	C67A	O15A	-62(3)
O8	C35	C36	C37	57.5(7)	C64A	C63A	N5A	C68A	-8(6)
O8	C35	C42	N4	55.4(6)	C64A	C67A	O15A	C68A	38(5)
O8	C35	C42	C43	-66.2(6)	C65A	C64A	C67A	O15A	-180(2)
C35	O8	C34A	C31A	-174.3(13)	C66A	C64A	C67A	O15A	60(2)
C35	O8	C34A	O7A	7(3)	C67A	O15A	C68A	O16A	167(6)
C35	C36	C37	C38	47.4(8)	C67A	O15A	C68A	N5A	1(8)
C35	C36	C37	C39	-80.4(8)	O15A	C68A	N5A	C63A	-18(10)
C35	C36	C37	C40	167.1(6)	O16A	C68A	N5A	C63A	179(7)
C35	C42	C43	C44	-167.4(7)	N5A	C63A	C64A	C65A	160(3)
C35	C42	C43	C44A	180.0(7)	N5A	C63A	C64A	C66A	-76(3)
Br2A	C28A	C29A	C30A	-177.3(9)	N5A	C63A	C64A	C67A	45(3)
Br2A	C28A	C33A	C32A	177.3(9)	S3	N6	C69	C62	127.4(9)
C28A	C29A	C30A	C31A	0.0	S3	N6	C69	C62A	134.0(10)
C29A	C28A	C33A	C32A	0.0	S3	N6	C69	C70	-106.3(7)

C29A C30A C31A C32A 0.0	S3	C75	C76	C77	179.4(5)
C29A C30A C31A C34A 179.5(18)	S3	C75	C80	C79	-178.5(6)
C30A C31A C32A C33A 0.0	O17	S3	N6	C69	-56.7(7)
C30A C31A C34A O8 -7(3)	O17	S3	C75	C76	10.7(7)
C30A C31A C34A O7A 171.4(18)	O17	S3	C75	C80	-170.4(6)
C31A C32A C33A C28A 0.0	O18	S3	N6	C69	173.7(6)
C32A C31A C34A O8 172.2(14)	O18	S3	C75	C76	141.8(6)
C32A C31A C34A O7A -9(3)	O18	S3	C75	C80	-39.3(7)
C33A C28A C29A C30A 0.0	N6	S3	C75	C76	-105.6(6)
C34A O8 C35 C36 -125.8(15)	N6	S3	C75	C80	73.3(7)
C34A O8 C35 C42 112.3(15)	N6	C69	C70	C71	178.4(7)
C34A C31A C32A C33A -179.5(17)	C69	C62	C63	C64	174.8(13)
S2 N4 C42 C35 110.8(5)	C69	C62	C63	N5	-65(2)
S2 N4 C42 C43 -127.6(5)	C69	C62A	C63A	C64A	175.2(17)
S2 C48 C49 C50 177.9(4)	C69	C62A	C63A	N5A	-66(3)
S2 C48 C53 C52 -177.9(4)	C69	C70	C71	C72	-66.1(12)
O11 S2 N4 C42 -34.8(6)	C69	C70	C71	C72A	-99(2)
O11 S2 C48 C49 -168.3(3)	C70	C71	C72	C73	-168.3(9)
O11 S2 C48 C53 9.6(4)	C70	C71	C72A	C73	158(2)
O12 S2 N4 C42 -164.6(5)	C71	C72	C73	C72A	65.8(16)
O12 S2 C48 C49 -38.4(4)	C71	C72	C73	C74	-178.2(11)
O12 S2 C48 C53 139.5(3)	C71	C72A	C73	C72	-65.4(16)
N3 C36 C37 C38 -72.8(7)	C71	C72A	C73	C74	-146(2)
N3 C36 C37 C39 159.5(6)	C72	C71	C72A	C73	65.5(16)
N3 C36 C37 C40 47.0(7)	C72A	C71	C72	C73	-65.7(16)
N4 S2 C48 C49 73.8(4)	C75	S3	N6	C69	59.4(7)
N4 S2 C48 C53 -108.3(4)	C75	C76	C77	C78	-0.4(11)
N4 C42 C43 C44 71.6(8)	C76	C75	C80	C79	0.3(11)
N4 C42 C43 C44A 59.0(8)	C76	C77	C78	C79	-0.6(11)
C36 C35 C42 N4 -61.3(7)	C76	C77	C78	C81	179.3(7)
C36 C35 C42 C43 177.1(5)	C77	C78	C79	C80	1.5(11)
C36 N3 C41 O9 -2.1(11)	C78	C79	C80	C75	-1.4(11)
C36 N3 C41 O10 178.3(7)	C80	C75	C76	C77	0.5(11)
C36 C37 C40 O9 -62.7(8)	C81	C78	C79	C80	-178.4(7)
C38 C37 C40 O9 60.1(8)	CI7 ¹	CI13	C7S	CI14	173(5)
C39 C37 C40 O9 179.3(6)	CI13 ²	CI7	C4S	CI8	94(5)
C40 O9 C41 O10 168.9(6)					

${}^1+X,+Y,-1+Z; {}^2+X,+Y,1+Z$

 Table 8 Hydrogen Atom Coordinates ($\text{\AA}\times 10^4$) and Isotropic Displacement Parameters ($\text{\AA}^2\times 10^3$) for Schomaker19.

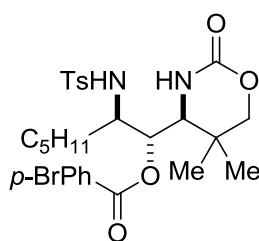
Atom	x	y	z	U(eq)
H2	7748	5182	-2442	41
H3A	7295	5287	-1041	39
H5B	6693	3424	-414	28
H6A	7151	3321	-1819	32
H8	6354	4720	1765	28
H1	6210(20)	5740(30)	2540(30)	36
H2A	7780(20)	6190(30)	790(30)	31
H9	6294	5767	868	29
H11A	5755	5382	-589	56
H11B	5152	4671	-708	56
H11C	5857	4772	-554	56
H12A	5426	4006	826	58
H12B	4726	3929	731	58
H12C	5114	4171	1704	58
H13A	5178	5578	663	39
H13B	4589	4864	490	39
H15	7089	5737	2472	31
H16A	7339	4881	2322	44
H16B	7744	5226	1397	44
H16C	7550	5058	1432	44
H16D	8051	5678	1978	44
H17A	8495	6090	2284	42
H17B	8432	5433	2654	42
H18A	8524	6070	3929	42
H18B	7934	6145	3569	42
H19A	7746	4926	4135	38
H19B	7199	5116	3995	38
H20A	7677	5850	5316	66
H20B	8103	5518	5502	66
H20C	7336	5104	5592	66
H17C	8112	4951	2763	45
H17D	7361	4429	2647	45

H18C	7441	4762	4175	40
H18D	7138	5131	3629	40
H19C	8033	6092	3771	40
H19D	8489	5784	3875	40
H20D	7596	5487	5336	66
H20E	8175	6216	5309	66
H20F	8324	5639	5411	66
H22	8947	7354	1387	46
H23	9804	7916	2434	55
H25	8568	7869	4414	37
H26	7700	7273	3399	35
H27A	9789	8084	4728	69
H27B	9816	8732	4380	69
H27C	10231	8473	3848	69
H29	7985	8819	4371	39
H30	8076	8381	5799	39
H32	9823	9961	6245	39
H33	9731	10398	4816	39
H35	8866	8214	8524	30
H29A	8271	9065	4363	39
H30A	8239	8507	5736	39
H32A	9948	10016	6561	39
H33A	9980	10573	5188	39
H3	8070(20)	7080(30)	9300(30)	37
H4	7220(20)	7994(19)	7780(30)	35
H36	7849	7083	7612	33
H38A	9606	8103	7448	71
H38B	9726	7514	7254	71
H38C	9494	7602	8273	71
H39A	8213	7159	6103	69
H39B	8850	7134	5845	69
H39C	8899	7807	6102	69
H40A	8121	6263	7132	42
H40B	8849	6451	6912	42
H42	7828	7789	9311	33
H43A	8598	8944	9216	43
H43B	8171	8979	8380	43
H43C	8552	8914	9345	43

H43D	8266	9000	8375	43
H44A	7297	8641	9445	42
H44B	7902	9322	9717	42
H45A	7587	8141	10629	37
H45B	8192	8822	10901	37
H46A	6893	8529	11124	37
H46B	7512	9184	11457	37
H47A	7117	7948	12250	69
H47B	7055	8510	12762	69
H47C	7751	8594	12569	69
H44C	7266	8659	9165	51
H44D	7842	9338	9505	51
H45C	7293	8802	10823	46
H45D	7294	8162	10519	46
H46C	8450	9298	11028	54
H46D	8357	8593	10914	54
H47D	7894	8273	12319	91
H47E	7603	8746	12301	91
H47F	8349	9024	12536	91
H49	5969	7771	8285	53
H50	5343	7956	9368	64
H52	5750	7014	11384	56
H53	6376	6828	10302	50
H54A	5306	8067	11387	104
H54B	4953	7326	11698	104
H54C	4676	7547	10838	104
H56	4051	5525	1739	34
H57	4670	6019	3082	34
H59	3581	6840	3623	34
H60	2962	6346	2280	34
H62	5249	7081	5731	32
H63	6365	7641	4492	30
H65A	5977	8074	3328	62
H65B	5856	8658	3559	62
H65C	5299	7932	3748	62
H66A	5155	7997	5457	60
H66B	5584	8760	5317	60
H66C	5769	8409	6115	60

H67A	6965	8798	4351	42
H67B	6652	9234	4601	42
H5	6467	7544	6229	36
H56A	4148	5579	1397	34
H57A	4730	6053	2776	34
H59A	3581	6808	3311	34
H60A	2999	6334	1931	34
H62A	5289	7147	5429	34
H63A	6428	7424	4350	41
H65D	6438	7946	2918	134
H65E	6167	8433	2861	134
H65F	5686	7685	3058	134
H66D	5381	8206	4271	98
H66E	5967	8820	4764	98
H66F	5613	8144	5305	98
H67C	7210	8614	4064	73
H67D	6945	9107	4010	73
H5A	6496	7516	6048	36
H6	5670(30)	5974(15)	4400(50)	50
H69	5836	6534	5967	40
H69A	5837	6588	5970	40
H70A	4707	5732	4897	53
H70B	5034	5484	5640	53
H71A	4430	6200	6141	65
H71B	4089	5435	6212	65
H71C	4623	6291	6373	65
H71D	4063	5610	6014	65
H72A	5113	6336	7329	52
H72B	4908	5592	7321	52
H72C	4947	5646	7331	52
H72D	4230	5077	7138	52
H73A	4096	6063	7911	75
H73B	3908	5323	7928	75
H73C	4324	6191	7816	75
H73D	3801	5467	8041	75
H74A	4861	6291	9048	103
H74B	4680	5552	9060	103
H74C	4165	5748	9403	103

H76	6691	6106	6826	38
H77	6320	5212	7791	43
H79	5435	4048	5558	50
H80	5827	4937	4593	48
H81A	5312	3569	7044	75
H81B	5382	3998	7949	75
H81C	5974	3913	7621	75
H1SA	4100	4588	4124	113
H1SB	3916	4360	3054	113
H2SA	3984	3142	6693	75
H2SB	3909	3454	5740	75
H3SA	3968	3124	6906	87
H3SB	4333	3890	6859	87
H4SA	4480	3795	6531	87
H4SB	3854	3093	6604	87
H5SA	2398	3150	2013	87
H5SB	2427	3008	912	87
H6SA	2389	2991	828	87
H6SB	2872	3097	-16	87
H7SA	2638	2774	323	87
H7SB	3224	2661	584	87



Confirming the Absolute Stereochemistry of Compound A2. The 4-bromophenyl ester of the corresponding alcohol was prepared according to the following procedure and analyzed by X-ray crystallography: the alcohol (13 mg, 1.0 equiv), *N,N*-dimethylaminopyridine (3 mg, 0.8 equiv), 4-bromobenzoic acid (20 mg, 3.0) and dicyclohexylcarbodiimide (24 mg, 3.6 equiv) were added to a 10 ml flame-dried round bottomed flask with 1.2 ml dry dichloromethane and stirred 30 hours. Aqueous NH_4Cl (1.2 ml) was then added and the organic and aqueous layers were

separated. The aqueous layer was extracted three times with dichloromethane and the combined organic layers were dried over Na_2SO_4 and concentrated *in vacuo*. The product was purified by flash chromatography using a hexanes/EtOAc gradient and recrystallized by diffusion of hexanes into a dichloromethane/ Et_2O solution of the product at room temperature to yield colorless crystals.

Crystallographic Experimental Section

Data Collection

A colorless crystal with approximate dimensions $0.20 \times 0.09 \times 0.04 \text{ mm}^3$ was selected under oil under ambient conditions and attached to the tip of a MiTeGen MicroMount[®]. The crystal was mounted in a stream of cold nitrogen at 150(1) K and centered in the X-ray beam by using a video camera.

The crystal evaluation and data collection were performed on a Bruker Quazar SMART APEXII diffractometer with $\text{Mo K}\alpha$ ($\lambda = 0.71073 \text{ \AA}$) radiation and the diffractometer to crystal distance of 4.96 cm.

The initial cell constants were obtained from three series of ω scans at different starting angles. Each series consisted of 12 frames collected at intervals of 0.5° in a 6° range about ω with the exposure time of 10 seconds per frame. The reflections were successfully indexed by an automated indexing routine built in the APEXII program suite. The final cell constants were calculated from a set of 9973 strong reflections from the actual data collection.

The data were collected by using the full sphere data collection routine to survey the reciprocal space to the extent of a full sphere to a resolution of 0.70 \AA . A total of 68821 data were harvested by collecting 5 sets of frames with 0.5° scans in ω and ϕ with exposure times of 30 sec per frame. These highly redundant datasets were corrected for Lorentz and polarization effects. The absorption correction was based on fitting a function to the empirical transmission surface as sampled by multiple equivalent measurements. [1]

Structure Solution and Refinement

The systematic absences in the diffraction data and the *E*-statistics were uniquely consistent for the space group *C2/c* that yielded chemically reasonable and computationally stable results of refinement [2-4].

A successful solution by the direct methods provided most non-hydrogen atoms from the *E*-map. The remaining non-hydrogen atoms were located in an alternating series of least-squares cycles and difference Fourier maps. All non-hydrogen atoms were refined with anisotropic displacement coefficients unless otherwise specified. All hydrogen atoms were included in the structure factor calculation at idealized positions and were allowed to ride on the neighboring atoms with relative isotropic displacement coefficients.

The lattice contains two diastereomers, RSS and SSR.

The Br1 atoms is disordered over two position with the major component contribution of 81.6(4)%. The propyl group at C17 is disordered over two positions in a 60.4(2):39.6(2) ratio. The methyl group of the major component is further disordered in a 37.2(2):23.2(2) ratio. The disorder was modeled with constraints and restraints and atoms C18/C18a, C19/C19a, C20/C20a/C20b were refined isotropically.

There was one peak of electron density in the unit cell void. It was modeled with an idealized geometry as a 21.0(5)% occupied water molecule disordered over a crystallographic two-fold axes. The water oxygen atom O7 was refined isotropically with a fixed displacement parameter.

The final least-squares refinement of 356 parameters against 9219 data resulted in residuals *R* (based on F^2 for $I \geq 2\sigma$) and *wR* (based on F^2 for all data) of 0.0422 and 0.1093, respectively. The final difference Fourier map was featureless.

References

- [1] Bruker-AXS. (2009) APEX2, SADABS, and SAINT Software Reference Manuals. Bruker-AXS, Madison, Wisconsin, USA.
- [2] Sheldrick, G. M. (2008) SHELXL. *Acta Cryst.* **A64**, 112-122.
- [3] Dolomanov, O.V.; Bourhis, L.J.; Gildea, R.J.; Howard, J.A.K.; Puschmann, H. "OLEX2: a complete structure solution, refinement and analysis program". *J. Appl. Cryst.* (2009) **42**, 339-341.

[4] Guzei, I.A. (2013). Internal laboratory computer programs Gn.

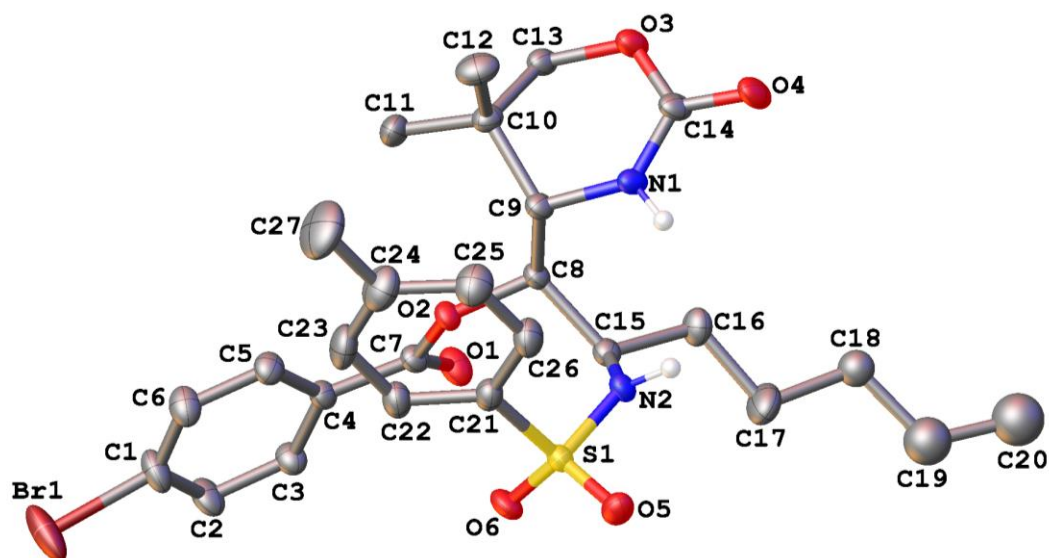


Figure 1. A molecular drawing of Schomaker24 shown with 50% probability ellipsoids. All aliphatic and aromatic H atoms and minor components of the disordered parts are omitted.

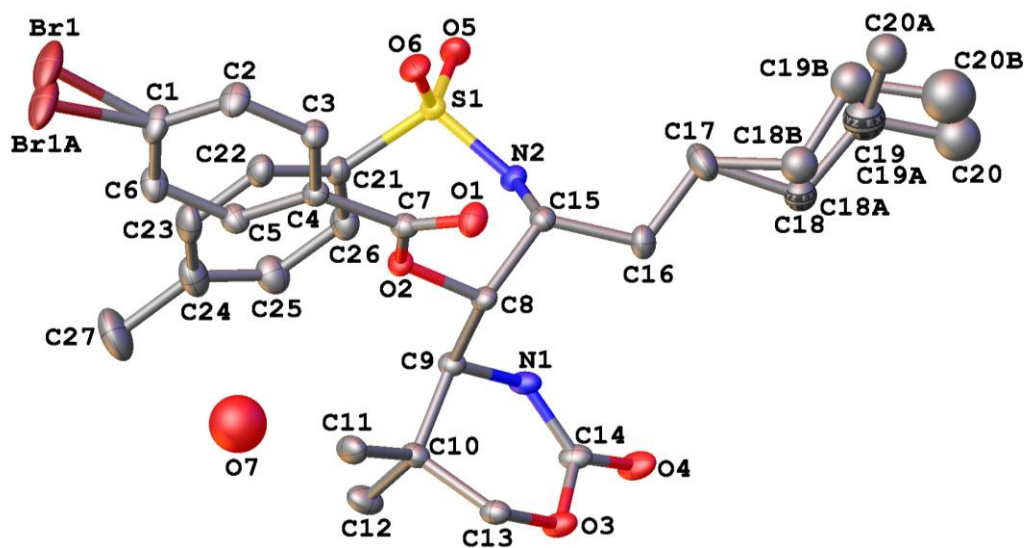


Figure 1. A molecular drawing of Schomaker24 shown with 40% probability ellipsoids. All H atoms are omitted but all disordered moieties are shown. Atoms C18 and C18a (and C19 and C19a) share the same sites which is indicated with “bands”.

Table 1. Crystal data and structure refinement for schomaker24.

Identification code	schomaker24	
Empirical formula	$C_{27} H_{35} Br N_2 O_6 S \times 0.21 H_2O$	
Formula weight	599.30	
Temperature	150 K	
Wavelength	0.71073 Å	
Crystal system	Monoclinic	
Space group	C2/c	
Unit cell dimensions	$a = 25.123(10) \text{ \AA}$	$\alpha = 90^\circ$.
	$b = 15.632(5) \text{ \AA}$	$\beta = 122.18(2)^\circ$.
	$c = 18.184(7) \text{ \AA}$	$\gamma = 90^\circ$.
Volume	6044(4) Å ³	
Z	8	
Density (calculated)	1.317 Mg/m ³	
Absorption coefficient	1.470 mm ⁻¹	
F(000)	2497	
Crystal size	0.2 x 0.09 x 0.04 mm ³	
Theta range for data collection	1.617 to 30.549°.	
Index ranges	-35 ≤ h ≤ 35, -22 ≤ k ≤ 22, -25 ≤ l ≤ 25	
Reflections collected	68821	
Independent reflections	9219 [R(int) = 0.0557]	
Completeness to theta = 25.0°	99.7 %	
Absorption correction	Numerical with SADABS	
Max. and min. transmission	0.6478 and 0.5701	
Refinement method	Full-matrix least-squares on F ²	
Data / restraints / parameters	9219 / 20 / 356	
Goodness-of-fit on F ²	1.015	
Final R indices [I > 2σ(I)]	R1 = 0.0422, wR2 = 0.0978	
R indices (all data)	R1 = 0.0702, wR2 = 0.1093	
Largest diff. peak and hole	0.548 and -0.548 e.Å ⁻³	

Table 2. Atomic coordinates ($\times 10^4$) and equivalent isotropic displacement parameters ($\text{\AA}^2 \times 10^3$) for schomaker24. $U(\text{eq})$ is defined as one third of the trace of the orthogonalized U_{ij} tensor.

	x	y	z	$U(\text{eq})$
Br(1)	475(1)	1883(1)	-203(1)	55(1)
Br(1A)	396(1)	1702(2)	15(2)	55(1)
S(1)	2127(1)	6273(1)	2310(1)	22(1)
O(1)	157(1)	5448(1)	1728(1)	29(1)
O(2)	1164(1)	5096(1)	2696(1)	20(1)
O(3)	1694(1)	6187(1)	5537(1)	27(1)
O(4)	2236(1)	7343(1)	5678(1)	34(1)
O(5)	2553(1)	6841(1)	2256(1)	30(1)
O(6)	1585(1)	5957(1)	1528(1)	30(1)
N(1)	2070(1)	6404(1)	4640(1)	24(1)
N(2)	1888(1)	6758(1)	2861(1)	21(1)
C(1)	504(1)	2788(1)	521(1)	33(1)
C(2)	38(1)	3402(1)	142(1)	31(1)
C(3)	77(1)	4102(1)	630(1)	25(1)
C(4)	577(1)	4186(1)	1490(1)	21(1)
C(5)	1033(1)	3548(1)	1861(1)	25(1)
C(6)	996(1)	2842(1)	1376(1)	31(1)
C(7)	598(1)	4972(1)	1967(1)	21(1)
C(8)	1227(1)	5842(1)	3219(1)	20(1)
C(9)	1810(1)	5626(1)	4118(1)	21(1)
C(10)	1709(1)	4978(1)	4671(1)	23(1)
C(11)	1318(1)	4195(1)	4174(1)	31(1)
C(12)	2357(1)	4671(1)	5418(1)	34(1)
C(13)	1359(1)	5438(1)	5028(1)	23(1)
C(14)	2005(1)	6666(1)	5286(1)	25(1)
C(15)	1273(1)	6646(1)	2764(1)	21(1)
C(16)	1093(1)	7474(1)	3034(1)	28(1)
C(17)	1080(1)	8258(1)	2533(2)	42(1)
C(18)	974(2)	9071(2)	2931(3)	33(1)
C(19)	963(2)	9889(3)	2474(3)	55(1)
C(20)	891(4)	10707(5)	2777(6)	66(2)
C(18A)	974(2)	9071(2)	2931(3)	33(1)
C(19A)	963(2)	9889(3)	2474(3)	55(1)
C(20A)	440(5)	10038(7)	1599(6)	49(3)
C(18B)	842(3)	9079(3)	2590(5)	42(1)
C(19B)	864(4)	9814(4)	2079(5)	52(2)
C(20B)	648(5)	10622(6)	2241(7)	90(3)
C(21)	2583(1)	5399(1)	2949(1)	24(1)

C(22)	2425(1)	4570(1)	2643(1)	29(1)
C(23)	2784(1)	3902(1)	3175(2)	37(1)
C(24)	3298(1)	4048(1)	4008(2)	41(1)
C(25)	3452(1)	4889(1)	4298(1)	38(1)
C(26)	3100(1)	5564(1)	3776(1)	31(1)
C(27)	3682(2)	3309(2)	4587(2)	64(1)
O(7)	141(7)	2610(8)	2779(8)	100

Table 3. Bond lengths [\AA] and angles [$^\circ$] for schomaker24.

Br(1)-C(1)	1.9067(19)	C(10)-C(13)	1.521(2)
Br(1A)-C(1)	1.880(3)	C(11)-H(11A)	0.9800
S(1)-O(5)	1.4349(14)	C(11)-H(11B)	0.9800
S(1)-O(6)	1.4346(14)	C(11)-H(11C)	0.9800
S(1)-N(2)	1.6044(15)	C(12)-H(12A)	0.9800
S(1)-C(21)	1.7650(18)	C(12)-H(12B)	0.9800
O(1)-C(7)	1.207(2)	C(12)-H(12C)	0.9800
O(2)-C(7)	1.346(2)	C(13)-H(13A)	0.9900
O(2)-C(8)	1.4599(19)	C(13)-H(13B)	0.9900
O(3)-C(13)	1.451(2)	C(15)-H(15)	1.0000
O(3)-C(14)	1.328(2)	C(15)-C(16)	1.537(2)
O(4)-C(14)	1.233(2)	C(16)-H(16A)	0.9900
N(1)-H(1)	0.8800	C(16)-H(16B)	0.9900
N(1)-C(9)	1.464(2)	C(16)-C(17)	1.519(3)
N(1)-C(14)	1.334(2)	C(17)-H(17A)	0.9900
N(2)-H(2)	0.8800	C(17)-H(17B)	0.9900
N(2)-C(15)	1.470(2)	C(17)-H(17C)	0.9900
C(1)-C(2)	1.382(3)	C(17)-H(17D)	0.9900
C(1)-C(6)	1.381(3)	C(17)-H(17E)	0.9900
C(2)-H(2A)	0.9500	C(17)-H(17F)	0.9900
C(2)-C(3)	1.378(2)	C(17)-C(18)	1.555(4)
C(3)-H(3)	0.9500	C(17)-C(18B)	1.443(5)
C(3)-C(4)	1.395(2)	C(18)-H(18A)	0.9900
C(4)-C(5)	1.393(2)	C(18)-H(18B)	0.9900
C(4)-C(7)	1.488(2)	C(18)-C(19)	1.518(4)
C(5)-H(5)	0.9500	C(19)-H(19A)	0.9900
C(5)-C(6)	1.385(3)	C(19)-H(19B)	0.9900
C(6)-H(6)	0.9500	C(19)-C(20)	1.441(7)
C(8)-H(8)	1.0000	C(20)-H(20A)	0.9800
C(8)-C(9)	1.544(2)	C(20)-H(20B)	0.9800
C(8)-C(15)	1.543(2)	C(20)-H(20C)	0.9800
C(9)-H(9)	1.0000	C(20A)-H(20D)	0.9800
C(9)-C(10)	1.540(2)	C(20A)-H(20E)	0.9800
C(10)-C(11)	1.529(2)	C(20A)-H(20F)	0.9800
C(10)-C(12)	1.540(3)	C(18B)-H(18C)	0.9900

C(18B)-H(18D)	0.9900	C(23)-H(23)	0.9500
C(18B)-C(19B)	1.497(6)	C(23)-C(24)	1.389(3)
C(19B)-H(19E)	0.9900	C(24)-C(25)	1.392(3)
C(19B)-H(19F)	0.9900	C(24)-C(27)	1.513(3)
C(19B)-C(20B)	1.464(8)	C(25)-H(25)	0.9500
C(20B)-H(20G)	0.9800	C(25)-C(26)	1.380(3)
C(20B)-H(20H)	0.9800	C(26)-H(26)	0.9500
C(20B)-H(20I)	0.9800	C(27)-H(27A)	0.9800
C(21)-C(22)	1.382(2)	C(27)-H(27B)	0.9800
C(21)-C(26)	1.391(3)	C(27)-H(27C)	0.9800
C(22)-H(22)	0.9500	O(7)-H(7A)	0.9583
C(22)-C(23)	1.383(3)	O(7)-H(7B)	0.9580
O(5)-S(1)-N(2)	106.98(8)	C(5)-C(6)-H(6)	120.6
O(5)-S(1)-C(21)	106.05(9)	O(1)-C(7)-O(2)	123.52(15)
O(6)-S(1)-O(5)	119.66(9)	O(1)-C(7)-C(4)	123.94(15)
O(6)-S(1)-N(2)	107.98(8)	O(2)-C(7)-C(4)	112.54(14)
O(6)-S(1)-C(21)	109.02(9)	O(2)-C(8)-H(8)	109.5
N(2)-S(1)-C(21)	106.45(8)	O(2)-C(8)-C(9)	103.12(13)
C(7)-O(2)-C(8)	116.54(13)	O(2)-C(8)-C(15)	108.26(12)
C(14)-O(3)-C(13)	118.85(13)	C(9)-C(8)-H(8)	109.5
C(9)-N(1)-H(1)	116.4	C(15)-C(8)-H(8)	109.5
C(14)-N(1)-H(1)	116.4	C(15)-C(8)-C(9)	116.54(13)
C(14)-N(1)-C(9)	127.22(14)	N(1)-C(9)-C(8)	110.38(14)
S(1)-N(2)-H(2)	117.0	N(1)-C(9)-H(9)	107.6
C(15)-N(2)-S(1)	125.93(11)	N(1)-C(9)-C(10)	107.12(13)
C(15)-N(2)-H(2)	117.0	C(8)-C(9)-H(9)	107.6
C(2)-C(1)-Br(1)	117.46(14)	C(10)-C(9)-C(8)	116.27(14)
C(2)-C(1)-Br(1A)	121.35(16)	C(10)-C(9)-H(9)	107.6
C(6)-C(1)-Br(1)	120.32(15)	C(9)-C(10)-C(12)	108.44(14)
C(6)-C(1)-Br(1A)	114.57(17)	C(11)-C(10)-C(9)	114.68(14)
C(6)-C(1)-C(2)	122.12(17)	C(11)-C(10)-C(12)	108.48(16)
C(1)-C(2)-H(2A)	120.7	C(13)-C(10)-C(9)	107.52(14)
C(3)-C(2)-C(1)	118.68(17)	C(13)-C(10)-C(11)	107.15(15)
C(3)-C(2)-H(2A)	120.7	C(13)-C(10)-C(12)	110.57(15)
C(2)-C(3)-H(3)	119.7	C(10)-C(11)-H(11A)	109.5
C(2)-C(3)-C(4)	120.62(17)	C(10)-C(11)-H(11B)	109.5
C(4)-C(3)-H(3)	119.7	C(10)-C(11)-H(11C)	109.5
C(3)-C(4)-C(7)	117.56(15)	H(11A)-C(11)-H(11B)	109.5
C(5)-C(4)-C(3)	119.48(15)	H(11A)-C(11)-H(11C)	109.5
C(5)-C(4)-C(7)	122.96(15)	H(11B)-C(11)-H(11C)	109.5
C(4)-C(5)-H(5)	119.9	C(10)-C(12)-H(12A)	109.5
C(6)-C(5)-C(4)	120.28(16)	C(10)-C(12)-H(12B)	109.5
C(6)-C(5)-H(5)	119.9	C(10)-C(12)-H(12C)	109.5
C(1)-C(6)-C(5)	118.78(17)	H(12A)-C(12)-H(12B)	109.5
C(1)-C(6)-H(6)	120.6	H(12A)-C(12)-H(12C)	109.5

H(12B)-C(12)-H(12C)	109.5	C(20)-C(19)-C(18)	120.5(5)
O(3)-C(13)-C(10)	112.55(14)	C(20)-C(19)-H(19A)	107.2
O(3)-C(13)-H(13A)	109.1	C(20)-C(19)-H(19B)	107.2
O(3)-C(13)-H(13B)	109.1	C(19)-C(20)-H(20A)	109.5
C(10)-C(13)-H(13A)	109.1	C(19)-C(20)-H(20B)	109.5
C(10)-C(13)-H(13B)	109.1	C(19)-C(20)-H(20C)	109.5
H(13A)-C(13)-H(13B)	107.8	H(20A)-C(20)-H(20B)	109.5
O(3)-C(14)-N(1)	119.98(15)	H(20A)-C(20)-H(20C)	109.5
O(4)-C(14)-O(3)	117.77(15)	H(20B)-C(20)-H(20C)	109.5
O(4)-C(14)-N(1)	122.24(16)	H(20D)-C(20A)-H(20E)	109.5
N(2)-C(15)-C(8)	114.05(14)	H(20D)-C(20A)-H(20F)	109.5
N(2)-C(15)-H(15)	106.5	H(20E)-C(20A)-H(20F)	109.5
N(2)-C(15)-C(16)	109.38(14)	C(17)-C(18B)-H(18C)	107.6
C(8)-C(15)-H(15)	106.5	C(17)-C(18B)-H(18D)	107.6
C(16)-C(15)-C(8)	113.24(14)	C(17)-C(18B)-C(19B)	119.0(5)
C(16)-C(15)-H(15)	106.5	H(18C)-C(18B)-H(18D)	107.0
C(15)-C(16)-H(16A)	108.8	C(19B)-C(18B)-H(18C)	107.6
C(15)-C(16)-H(16B)	108.8	C(19B)-C(18B)-H(18D)	107.6
H(16A)-C(16)-H(16B)	107.7	C(18B)-C(19B)-H(19E)	108.9
C(17)-C(16)-C(15)	113.75(16)	C(18B)-C(19B)-H(19F)	108.9
C(17)-C(16)-H(16A)	108.8	H(19E)-C(19B)-H(19F)	107.7
C(17)-C(16)-H(16B)	108.8	C(20B)-C(19B)-C(18B)	113.5(7)
C(16)-C(17)-H(17A)	109.8	C(20B)-C(19B)-H(19E)	108.9
C(16)-C(17)-H(17B)	109.8	C(20B)-C(19B)-H(19F)	108.9
C(16)-C(17)-H(17C)	109.8	C(19B)-C(20B)-H(20G)	109.5
C(16)-C(17)-H(17D)	109.8	C(19B)-C(20B)-H(20H)	109.5
C(16)-C(17)-H(17E)	106.5	C(19B)-C(20B)-H(20I)	109.5
C(16)-C(17)-H(17F)	106.5	H(20G)-C(20B)-H(20H)	109.5
C(16)-C(17)-C(18)	109.5(2)	H(20G)-C(20B)-H(20I)	109.5
H(17A)-C(17)-H(17B)	108.2	H(20H)-C(20B)-H(20I)	109.5
H(17C)-C(17)-H(17D)	108.2	C(22)-C(21)-S(1)	120.95(14)
H(17E)-C(17)-H(17F)	106.5	C(22)-C(21)-C(26)	120.83(17)
C(18)-C(17)-H(17A)	109.8	C(26)-C(21)-S(1)	118.21(14)
C(18)-C(17)-H(17B)	109.8	C(21)-C(22)-H(22)	120.5
C(18B)-C(17)-C(16)	123.4(3)	C(21)-C(22)-C(23)	119.09(18)
C(18B)-C(17)-H(17E)	106.5	C(23)-C(22)-H(22)	120.5
C(18B)-C(17)-H(17F)	106.5	C(22)-C(23)-H(23)	119.3
C(17)-C(18)-H(18A)	109.0	C(22)-C(23)-C(24)	121.30(19)
C(17)-C(18)-H(18B)	109.0	C(24)-C(23)-H(23)	119.3
H(18A)-C(18)-H(18B)	107.8	C(23)-C(24)-C(25)	118.52(19)
C(19)-C(18)-C(17)	113.0(3)	C(23)-C(24)-C(27)	120.7(2)
C(19)-C(18)-H(18A)	109.0	C(25)-C(24)-C(27)	120.8(2)
C(19)-C(18)-H(18B)	109.0	C(24)-C(25)-H(25)	119.5
C(18)-C(19)-H(19A)	107.2	C(26)-C(25)-C(24)	121.0(2)
C(18)-C(19)-H(19B)	107.2	C(26)-C(25)-H(25)	119.5
H(19A)-C(19)-H(19B)	106.8	C(21)-C(26)-H(26)	120.4

C(25)-C(26)-C(21)	119.24(18)	H(27A)-C(27)-H(27B)	109.5
C(25)-C(26)-H(26)	120.4	H(27A)-C(27)-H(27C)	109.5
C(24)-C(27)-H(27A)	109.5	H(27B)-C(27)-H(27C)	109.5
C(24)-C(27)-H(27B)	109.5	H(7A)-O(7)-H(7B)	104.4
C(24)-C(27)-H(27C)	109.5		

Symmetry transformations used to generate equivalent atoms:

Table 4. Anisotropic displacement parameters ($\text{\AA}^2 \times 10^3$) for schomaker24. The anisotropic displacement factor exponent takes the form: $-2 \sum_{i,j} h^i a^i b^j U^{ij} + \dots + 2 \sum_i h^i k^i a^i b^i U^{ii}$

	U11	U22	U33	U23	U13	U12
Br(1)	48(1)	52(1)	39(1)	-26(1)	6(1)	15(1)
Br(1A)	48(1)	52(1)	39(1)	-26(1)	6(1)	15(1)
S(1)	31(1)	19(1)	19(1)	-3(1)	15(1)	-3(1)
O(1)	23(1)	31(1)	25(1)	-8(1)	7(1)	1(1)
O(2)	21(1)	19(1)	16(1)	-4(1)	6(1)	-2(1)
O(3)	33(1)	31(1)	20(1)	-8(1)	15(1)	-12(1)
O(4)	43(1)	35(1)	23(1)	-14(1)	18(1)	-19(1)
O(5)	41(1)	25(1)	36(1)	0(1)	28(1)	-3(1)
O(6)	38(1)	30(1)	17(1)	-7(1)	13(1)	-2(1)
N(1)	28(1)	26(1)	16(1)	-4(1)	11(1)	-11(1)
N(2)	24(1)	20(1)	17(1)	-6(1)	10(1)	-4(1)
C(1)	30(1)	29(1)	31(1)	-13(1)	10(1)	1(1)
C(2)	27(1)	34(1)	22(1)	-9(1)	5(1)	0(1)
C(3)	23(1)	25(1)	20(1)	-1(1)	7(1)	2(1)
C(4)	22(1)	21(1)	18(1)	-4(1)	9(1)	-4(1)
C(5)	23(1)	24(1)	21(1)	-2(1)	6(1)	-2(1)
C(6)	26(1)	26(1)	30(1)	-3(1)	7(1)	3(1)
C(7)	22(1)	23(1)	16(1)	-2(1)	8(1)	-4(1)
C(8)	23(1)	20(1)	15(1)	-4(1)	9(1)	-3(1)
C(9)	22(1)	22(1)	15(1)	-2(1)	8(1)	-4(1)
C(10)	24(1)	23(1)	18(1)	2(1)	9(1)	-2(1)
C(11)	44(1)	21(1)	30(1)	-1(1)	22(1)	-7(1)
C(12)	30(1)	41(1)	27(1)	12(1)	12(1)	7(1)
C(13)	25(1)	24(1)	17(1)	-2(1)	10(1)	-7(1)
C(14)	25(1)	31(1)	15(1)	-4(1)	8(1)	-8(1)
C(15)	22(1)	21(1)	17(1)	-2(1)	8(1)	-1(1)
C(16)	28(1)	22(1)	35(1)	-1(1)	16(1)	3(1)
C(17)	54(1)	25(1)	38(1)	6(1)	17(1)	5(1)
C(21)	28(1)	19(1)	28(1)	-1(1)	17(1)	0(1)
C(22)	34(1)	22(1)	32(1)	-5(1)	18(1)	-3(1)
C(23)	43(1)	19(1)	52(1)	-4(1)	27(1)	-1(1)

C(24)	39(1)	29(1)	53(1)	7(1)	24(1)	8(1)
C(25)	32(1)	35(1)	38(1)	2(1)	12(1)	2(1)
C(26)	31(1)	23(1)	34(1)	-4(1)	14(1)	-3(1)
C(27)	63(2)	37(1)	75(2)	16(1)	25(2)	20(1)

Table 5. Hydrogen coordinates ($\times 10^4$) and isotropic displacement parameters ($\text{\AA}^2 \times 10^3$) for schomaker24.

	x	y	z	U(eq)
H(1)	2293	6734	4513	28
H(2)	2150	7124	3257	25
H(2A)	-303	3344	-443	37
H(3)	-239	4530	379	30
H(5)	1370	3597	2449	30
H(6)	1304	2402	1628	37
H(8)	849	5887	3265	24
H(9)	2137	5384	4022	25
H(11A)	1520	3895	3912	46
H(11B)	895	4378	3715	46
H(11C)	1287	3809	4574	46
H(12A)	2601	5162	5774	51
H(12B)	2582	4396	5177	51
H(12C)	2302	4260	5779	51
H(13A)	940	5614	4537	27
H(13B)	1295	5037	5395	27
H(15)	959	6570	2128	25
H(16A)	672	7399	2949	34
H(16B)	1397	7573	3662	34
H(17A)	738	8203	1915	51
H(17B)	1484	8307	2561	51
H(17C)	738	8203	1915	51
H(17D)	1484	8307	2561	51
H(17E)	1519	8355	2692	51
H(17F)	839	8096	1911	51
H(18A)	570	9014	2900	39
H(18B)	1313	9111	3552	39
H(19A)	1360	9910	2482	66
H(19B)	617	9834	1858	66
H(20A)	863	11158	2383	99
H(20B)	1255	10815	3362	99

H(20C)	507	10705	2791	99
H(19C)	983	10376	2836	66
H(19D)	1353	9905	2463	66
H(20D)	468	9646	1200	73
H(20E)	452	10630	1432	73
H(20F)	44	9938	1572	73
H(18C)	1077	9249	3209	51
H(18D)	398	8998	2411	51
H(19E)	1301	9887	2226	62
H(19F)	598	9677	1452	62
H(20G)	190	10662	1860	134
H(20H)	843	11101	2123	134
H(20I)	767	10644	2849	134
H(22)	2074	4462	2075	35
H(23)	2677	3331	2967	44
H(25)	3805	4999	4863	46
H(26)	3210	6136	3979	37
H(27A)	4105	3327	4685	97
H(27B)	3478	2768	4305	97
H(27C)	3710	3354	5144	97
H(7A)	94	2292	2298	150
H(7B)	310	2205	3247	150

Table 6. Torsion angles [$^{\circ}$] for schomaker24.

Br(1)-C(1)-C(2)-C(3)	-174.51(16)	N(1)-C(9)-C(10)-C(12)	-70.50(18)
Br(1)-C(1)-C(6)-C(5)	174.23(16)	N(1)-C(9)-C(10)-C(13)	49.08(17)
Br(1A)-C(1)-C(2)-C(3)	165.0(2)	N(2)-S(1)-C(21)-C(22)	121.09(15)
Br(1A)-C(1)-C(6)-C(5)	-166.2(2)	N(2)-S(1)-C(21)-C(26)	-57.60(17)
S(1)-N(2)-C(15)-C(8)	79.98(17)	N(2)-C(15)-C(16)-C(17)	56.7(2)
S(1)-N(2)-C(15)-C(16)	-152.07(13)	C(1)-C(2)-C(3)-C(4)	-0.1(3)
S(1)-C(21)-C(22)-C(23)	-177.96(15)	C(2)-C(1)-C(6)-C(5)	-2.0(3)
S(1)-C(21)-C(26)-C(25)	177.87(16)	C(2)-C(3)-C(4)-C(5)	-1.3(3)
O(2)-C(8)-C(9)-N(1)	160.83(12)	C(2)-C(3)-C(4)-C(7)	178.15(17)
O(2)-C(8)-C(9)-C(10)	-76.93(17)	C(3)-C(4)-C(5)-C(6)	1.2(3)
O(2)-C(8)-C(15)-N(2)	-75.76(16)	C(3)-C(4)-C(7)-O(1)	15.5(3)
O(2)-C(8)-C(15)-C(16)	158.29(14)	C(3)-C(4)-C(7)-O(2)	-164.33(15)
O(5)-S(1)-N(2)-C(15)	149.96(14)	C(4)-C(5)-C(6)-C(1)	0.5(3)
O(5)-S(1)-C(21)-C(22)	-125.22(15)	C(5)-C(4)-C(7)-O(1)	-165.02(18)
O(5)-S(1)-C(21)-C(26)	56.09(16)	C(5)-C(4)-C(7)-O(2)	15.1(2)
O(6)-S(1)-N(2)-C(15)	19.95(16)	C(6)-C(1)-C(2)-C(3)	1.8(3)
O(6)-S(1)-C(21)-C(22)	4.85(18)	C(7)-O(2)-C(8)-C(9)	160.13(13)
O(6)-S(1)-C(21)-C(26)	-173.84(14)	C(7)-O(2)-C(8)-C(15)	-75.81(17)
N(1)-C(9)-C(10)-C(11)	168.11(15)	C(7)-C(4)-C(5)-C(6)	-178.31(17)

C(8)-O(2)-C(7)-O(1)	1.5(2)
C(8)-O(2)-C(7)-C(4)	-178.67(13)
C(8)-C(9)-C(10)-C(11)	44.2(2)
C(8)-C(9)-C(10)-C(12)	165.56(15)
C(8)-C(9)-C(10)-C(13)	-74.87(17)
C(8)-C(15)-C(16)-C(17)	-174.89(16)
C(9)-N(1)-C(14)-O(3)	2.4(3)
C(9)-N(1)-C(14)-O(4)	-178.80(17)
C(9)-C(8)-C(15)-N(2)	39.83(19)
C(9)-C(8)-C(15)-C(16)	-86.11(18)
C(9)-C(10)-C(13)-O(3)	-57.79(17)
C(11)-C(10)-C(13)-O(3)	178.46(13)
C(12)-C(10)-C(13)-O(3)	60.42(19)
C(13)-O(3)-C(14)-O(4)	173.25(16)
C(13)-O(3)-C(14)-N(1)	-7.9(2)
C(14)-O(3)-C(13)-C(10)	37.1(2)
C(14)-N(1)-C(9)-C(8)	102.61(19)
C(14)-N(1)-C(9)-C(10)	-24.9(2)
C(15)-C(8)-C(9)-N(1)	42.40(19)
C(15)-C(8)-C(9)-C(10)	164.64(14)
C(15)-C(16)-C(17)-C(18)	-173.2(2)
C(15)-C(16)-C(17)-C(18B)	171.2(4)
C(16)-C(17)-C(18)-C(19)	179.3(3)
C(16)-C(17)-C(18B)-C(19B)	178.8(5)
C(17)-C(18)-C(19)-C(20)	-177.8(5)
C(17)-C(18B)-C(19B)-C(20B)	-176.0(7)
C(18)-C(17)-C(18B)-C(19B)	129.9(13)
C(18B)-C(17)-C(18)-C(19)	-42.5(9)
C(21)-S(1)-N(2)-C(15)	-96.99(15)
C(21)-C(22)-C(23)-C(24)	0.2(3)
C(22)-C(21)-C(26)-C(25)	-0.8(3)
C(22)-C(23)-C(24)-C(25)	-0.9(3)
C(22)-C(23)-C(24)-C(27)	179.3(2)
C(23)-C(24)-C(25)-C(26)	0.7(3)
C(24)-C(25)-C(26)-C(21)	0.1(3)
C(26)-C(21)-C(22)-C(23)	0.7(3)
C(27)-C(24)-C(25)-C(26)	-179.4(2)

Symmetry transformations used to generate equivalent atoms: #1 $-x+1/2, -y+3/2, -z+1$

Table 7. Hydrogen bonds for schomaker24 [\AA and $^\circ$].

D-H...A	d(D-H)	d(H...A)	d(D...A)	$\angle(\text{DHA})$
N(1)-H(1)...O(4)#1	0.88	2.01	2.880(2)	169.7
N(2)-H(2)...O(4)#1	0.88	1.91	2.766(2)	164.3

Symmetry transformations used to generate equivalent atoms:

#1 $-x+1/2, -y+3/2, -z+1$

Appendix C. Select HPLC Traces for Enantioselective Aziridination.

Compound S6.1 racemate.

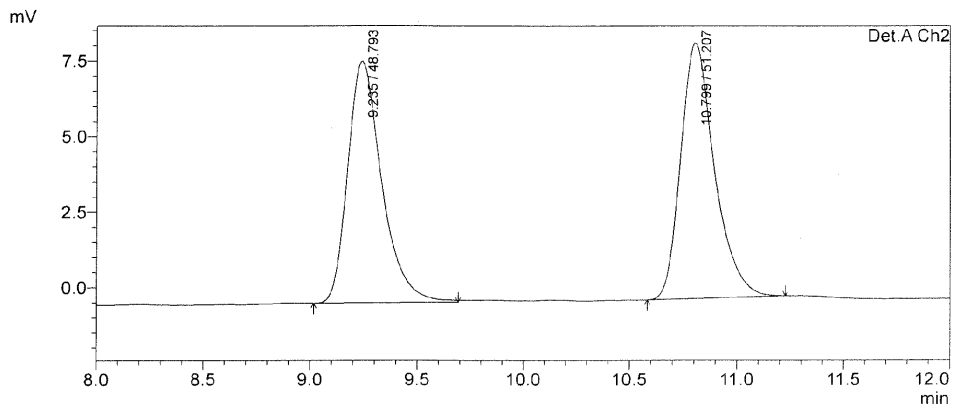
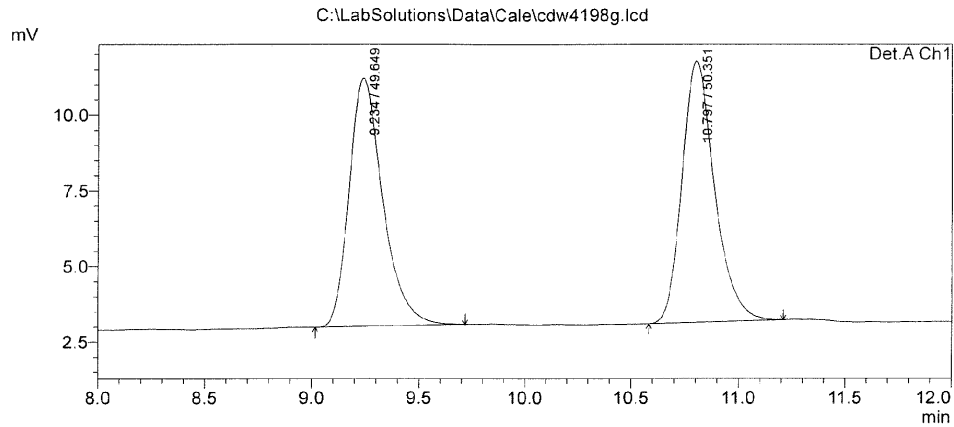
5/9/2015 19:34:51 1 / 1

==== Shimadzu LcSolutionAnalysis Report ====

C:\LabSolutions\Data\Cale\cdw4198g.lcd

Acquired by : Admin
Sample Name : cdw4198
Sample ID :
Tray# : 1
Vial # : 19
Injection Volume : 1 uL
Data File Name : cdw4198g.lcd
Method File Name : ROalkyl iodide.lcm
Batch File Name : cdw4198i.lcb
Report File Name : Default.lcr
Data Acquired : 4/23/2013 2:47:19 PM
Data Processed : 4/23/2013 3:02:20 PM

<Chromatogram>

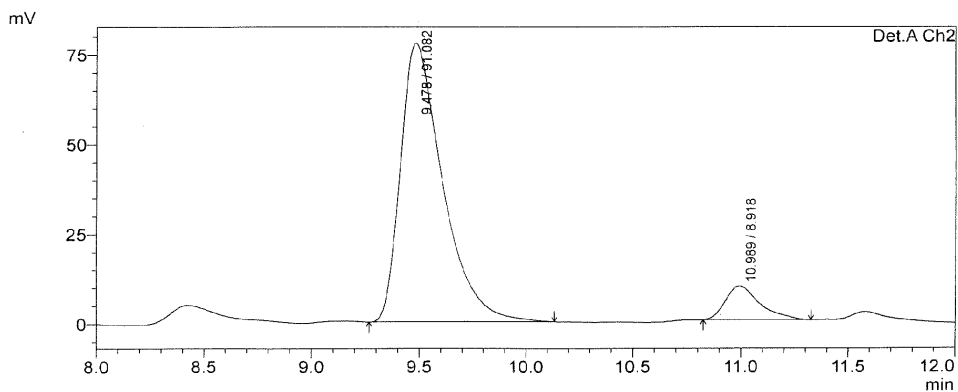
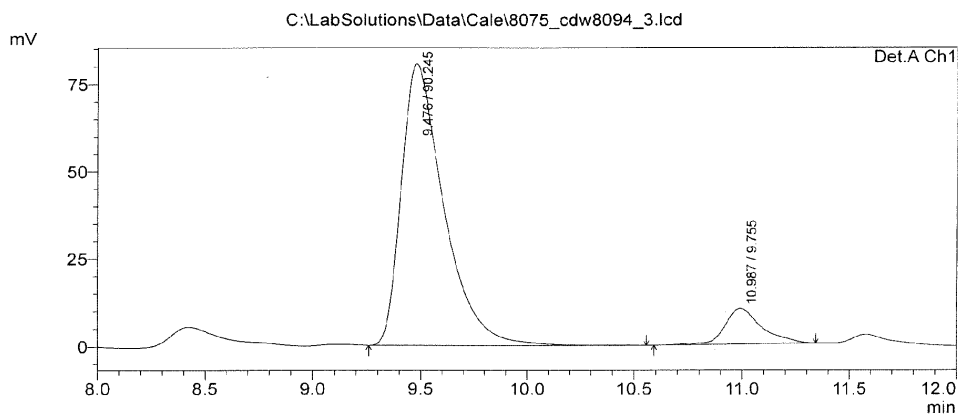


1 Det.A Ch1/260nm
2 Det.A Ch2/255nm

Compound S6.1 enantioenriched.

5/9/2015 19:48:49 1 / 1

C:\LabSolutions\Data\Cale\8075_cdw8094_3.lcd
Acquired by : Admin
Sample Name : cdw8094
Sample ID :
Tray# : 1
Vial # : 2
Injection Volume : 5 uL
Data File Name : 8075_cdw8094_3.lcd
Method File Name : ROalkyl iodide.lcm
Batch File Name : 8075.lcb
Report File Name : Default.lcr
Data Acquired : 3/18/2015 7:35:24 PM
Data Processed : 5/9/2015 7:45:52 PM

<Chromatogram>

1 Det. A Ch1/260nm
2 Det. A Ch2/255nm

Compound S6.2 racemate.

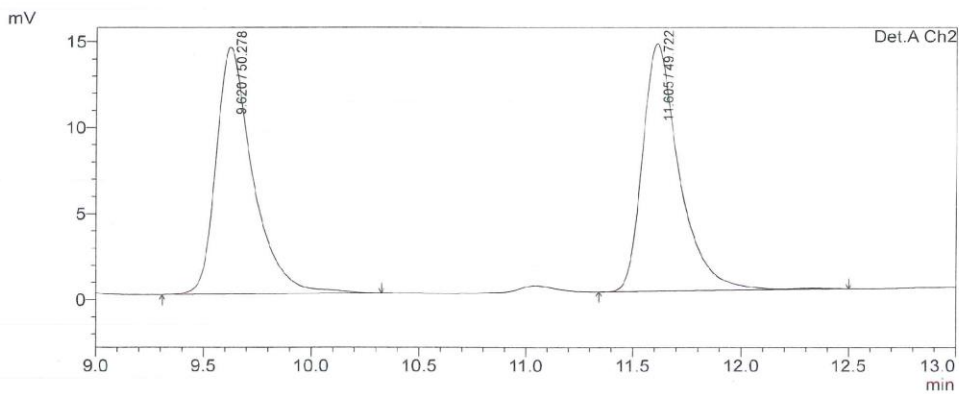
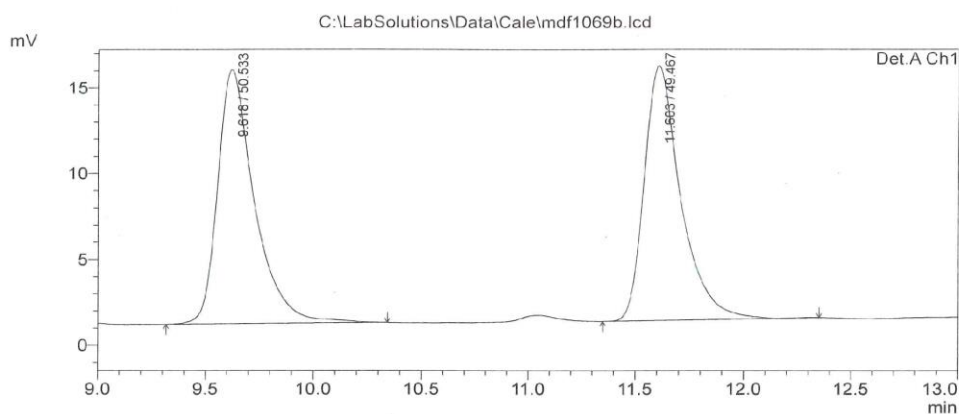
5/9/2015 19:51:43 1 / 1

==== Shimadzu LCsolution Analysis Report ====

C:\LabSolutions\Data\Cale\mdf1069b.lcd

Acquired by	: Admin
Sample Name	: mdf1069
Sample ID	:
Tray#	: 1
Vial #	: 37
Injection Volume	: 1 uL
Data File Name	: mdf1069b.lcd
Method File Name	: ROalkyl iodide.lcm
Batch File Name	: mdfrans.lcb
Report File Name	: Default.lcr
Data Acquired	: 5/16/2013 2:35:48 PM
Data Processed	: 5/16/2013 2:49:50 PM

<Chromatogram>



1 Det. A Ch1/260nm
2 Det. A Ch2/255nm

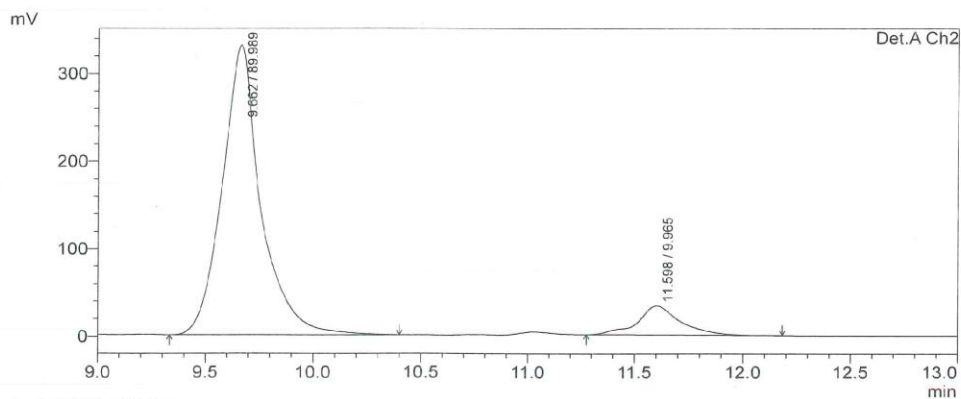
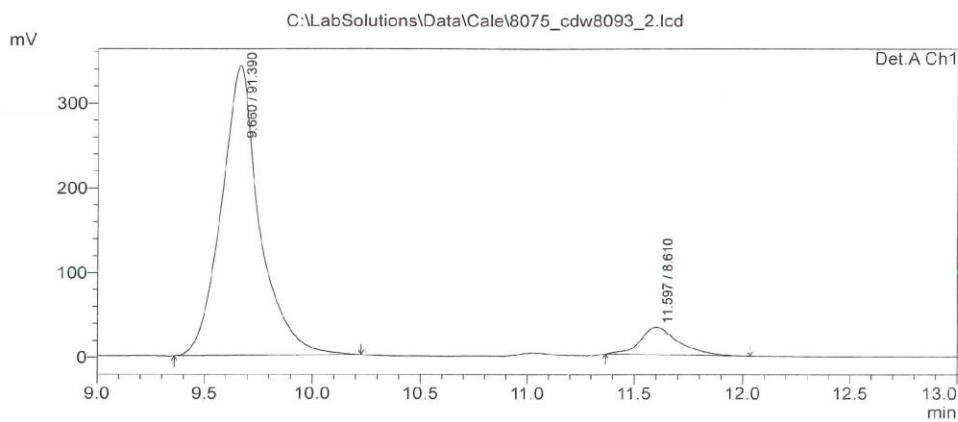
Compound S6.2 enantioenriched.

5/9/2015 19:53:56 1 / 1

C:\LabSolutions\Data\Cale\8075_cdw8093_2.lcd

Acquired by : Admin
Sample Name : cdw8093
Sample ID :
Tray# : 1
Vial # : 1
Injection Volume : 5 uL
Data File Name : 8075_cdw8093_2.lcd
Method File Name : ROalkyl iodide.lcm
Batch File Name : 8075.lcb
Report File Name : Default.lcr
Data Acquired : 3/18/2015 7:20:59 PM
Data Processed : 3/18/2015 7:35:01 PM

<Chromatogram>



1 Det.A Ch1/260nm
2 Det.A Ch2/255nm

